International Journal of Hygiene and Environmental Health 239 (2022) 113876

Contents lists available at ScienceDirect

International Journal of Hygiene and Environmental Health

journal homepage: www.elsevier.com/locate/ijheh

A new measure of hygiene inequality applied to urban-rural comparison

Alejandro Quispe-Coica *, Agustí Pérez-Foguet

Department of Civil and Environmental Engineering (DECA), Engineering Sciences and Global Development (EScGD), Barcelona School of Civil Engineering, Universitat Politècnica de Catalunya BarcelonaTech, Barcelona, Spain

ARTICLE INFO

Keywords:
Global monitoring
Ternary diagram
Sustainable development goals (SDGs)
Handwashing
COVID-19

ABSTRACT

Access to hygiene services remains one of the most urgent challenges facing countries, especially low-income ones. This has become much more critical in the current context of the COVID-19 pandemic. The WHO/UNICEF Joint Monitoring Program globally monitors access to hygiene service levels. As data are in three parts with a constant sum and a positive value, they are compositional data. Inequality is monitored in disaggregated data; in the urban–rural case, this is done through a simple difference between the urban and rural service levels. However, this simple form of calculation does not take into account the characteristics of the data, which can lead to erroneous interpretations of the results. Therefore, we propose an alternative measure of inequality that uses a ternary diagram and does not infringe on the data properties.

The results of the new urban–rural inequality measure show spatial heterogeneity. The highest inequality occurs in Colombia, with a value of 37.1 percentage points, and the lowest in Turkmenistan, with a value of zero. Our results also show that 73 of the 76 countries evaluated have higher basic hygiene services in urban areas than in rural areas. This means that urban households have more availability of a handwashing facility on-premises with soap and water than rural households. Likewise, by subdividing the ternary diagram into ternary parcels, we could group and rank the countries based on hygiene service conditions in a hierarchical order using tripartite information. Finally, our study finds that a multivariate measure of inequality can be important for the public policies of the sector with a general vision, which underscores the value of making evidence-based decisions.

1. Introduction

The 2030 Agenda is an ambitious action plan promoted by the United Nations and has the spirit of "leaving no one behind" (United Nations General Assembly, 2015). The inclusion of all people to reach the global goal in 2030 is the engine that drives all adhering countries. It addresses 17 sustainable development goals (SDGs); this study addresses SDG 6, and specifically, the section on hygiene in SDG 6.2.

Hand hygiene with soap and water is a high-impact, low-tech practice that correlates with good quality of public health and is a simple and effective way to reduce diseases. The reported benefits of handwashing are broad; for instance, as it can: reduce the transmission of viruses that cause common diseases; reduce the risk and incidence of diarrheal diseases (Shahid et al., 1996; Curtis and Cairncross, 2003); reduce the risk of respiratory infection (Rabie and Curtis, 2006); and provide economic benefits (Townsend et al., 2017). It acquires more relevance due to the novel severe acute respiratory syndrome coronavirus-2 (SARS-CoV-2), which caused the COVID-19 pandemic in 2020 (Pal et al., 2020; Synowiec et al., 2021). Currently, one of the main recommendations for reducing the risk of SARS-CoV-2 infection (besides vaccination) is the continuous practice of handwashing with soap and water (World Health Organization [WHO], 2020a). The remaining uncertainties about the transmission routes of SARS-CoV-2 (airborne in aerosol, surface contact, fecal-oral transmission (Heller et al., 2020; Pandey et al., 2021), etc.), and the fact that asymptomatic persons can have a high viral shedding (e.g., be infectious), underscores the importance of using handwashing as an essential measure (WHO, 2020b). For instance, a study under laboratory conditions shows that SARS-CoV-2 can remain viable and infectious in aerosols for hours, and on surfaces for up to days, depending on the spilled inoculum (van Doremalen et al., 2020).

Global monitoring of hygiene services has been incorporated into SDG 6.2 and has been carried out since 2015. The aim of Goal 6.2 is "by 2030, to achieve access to adequate and equitable sanitation and hygiene services for all … ". Proper hygiene is related to households having handwashing facilities with soap and water. The WHO/UNICEF Joint Monitoring Program (JMP) conducts global monitoring of households

* Corresponding author.
E-mail addresses: filimon.alejandro.quispe@upc.edu (A. Quispe-Coica), agusti.perez@upc.edu (A. Pérez-Foguet).

https://doi.org/10.1016/j.ijheh.2021.113876
Received 11 June 2021; Received in revised form 13 October 2021; Accepted 20 October 2021
Available online 29 October 2021

with or without handwashing facilities and classifies them into the three categories of the so-called handwashing ladder: basic, limited, and no facilities. The number of cases in each category is counted in a given household set (e.g., a country), after which three numerical variables are calculated; once divided by the total number of households, these form a constant sum proportion of one (or 100% if they are percentages); these are therefore compositional data (Aitchison, 1986; Egozcue and Pawlowsky-Glahn, 2011; Filzmoser et al., 2018; van den Boogaart and Tolosana-Delgado, 2013a).

The separate analysis of each percentage corresponds to the univariate analysis and is very common in the sector. The joint analysis of the three variables is a multivariate analysis. As the three hygiene variables have a constant sum constraint and are implicitly related to a predefined total or complementary parts, no variable can be interpreted independently of the others; rather, they must be interpreted as compositions (van den Boogaart and Tolosana-Delgado, 2013b). In global monitoring, the application of statistical techniques for compositional data in water, sanitation, and hygiene (WASH) began with Pérez-Foguet et al. (2017) and was expanded by Ezbakhe and Pérez-Foguet (2019), who incorporate the uncertainty of data into the analysis; however, its practical application to the global data set was not possible until Quispe-Coica and Pérez-Foguet (2020) introduced data preprocessing with zero values, missing data, and outliers. These analyzes have also recently been extended to the health domain related to child mortality (Ezbakhe and Pérez-Foguet, 2020).

Inequality of access to any service is one of the main obstacles to universal coverage. Therefore, as for water and sanitation, the JMP also monitors urban–rural inequality in hygiene. This information can help national and international actors in the sector to target interventions. In this sense, experts have recommended disaggregating the information and measuring inequalities from different aspects (Economic and Council, 2016; WHO/UNICEF, 2015). Hence, JMP currently monitors WASH inequality on data disaggregated by wealth quintiles, urban and rural residence, sub-national regions, and ladder service levels (see https://washdata.org/monitoring/inequalities). The wealth quintiles are based on an analysis of household assets, and the final result expressed in proportions is also represented by place of residence. Therefore, in any of the follow-up alternatives described, a measure of urban–rural inequality can be applied.

The current alternative used by the JMP for global reporting is to use the simple difference between the ratio of urban and rural service levels. For hygiene, this is carried out in the three categories of the handwashing ladder (WHO/UNICEF, 2016), giving three measures of inequality. This implies that, in an inequality ranking, countries are likely to have different positions depending on the category of analysis. As compositional data have a constant sum, a part or the rest will also be affected if one of the parts varies. Consequently, when interpreting a category, the rest of the categories must also be taken into account. In fact, the compositional data are multivariate by nature (van den Boogaart and Tolosana-Delgado, 2013b), thus reinforcing the idea of interpreting one category by considering the rest.

Knowing the space in which these data operate is also an important part, as it allows us to calculate inequality by selecting among the different multivariate alternatives that exist, using the one that best adapts to the data. The sample space in which the compositional data operates is the simplex S^D, and the vector space structure is called Aitchison geometry or the Aitchison simplex (which is a different geometric frame from the Euclidean vector space). Therefore, before applying any classical statistical technique, it is first necessary to perform log-ratio transformations (Aitchison, 1982, 1986; Egozcue et al., 2003). However, when data are in three or four parts, it is possible to represent them graphically in the same simplex space. If data are in three parts, the graphical representation in simplex is made through a ternary diagram; if in four parts, through a regular tetrahedron. If data are greater than four parts, the graphical representation in simplex is not possible; however, everything related to the operations, definitions, and interpretations of compositional data are valid for any number of parts (Pawlowsky-Glahn and Egozcue, 2006; Von Eynatten et al., 2002). It is also possible to reduce the number (n) of parts, independently of the dimensions, by an amalgamation process, a particular case being the dichotomous analysis, where the n parts are reduced to two.

That said, when the information is tripartite with a constant sum and is positive, as in the case of hygiene data, there are few multivariate alternatives that allow us to calculate urban–rural inequality in the simplex sample space. For our purpose, information is limited to the ternary diagram. Recall that everything ternary can be amalgamated and converted to binary, to then compare the inequality between two populations through arithmetic differences, a common practice carried out by the JMP to compare dichotomous variables (WHO/UNICEF, 2019a). The application of the ternary diagram to graphically represent data is very common in other areas of science, including the earth sciences, geochemistry, and chemistry (Miller, 2002; Graham et al., 2020; Verma, 2020). Lately, it has also been applied in epidemiology (Dumuid et al., 2020) and waste management, for both dynamic and static visualization (Bartl, 2014; Pomberger et al., 2017). Other studies present proposals for ternary graphical representation in centered data, which allows the graphical visualization and interpretation of the data structure to be improved (Von Eynatten et al., 2002).

On the other hand, in the literature in the WASH sector, it is very common to use univariate thematic maps of any of the categories of services accessed by the population, grouping (by color) those that are within a certain range (we will call this “amplitude” in this study). The global reports carried out by WHO/UNICEF are a clear example that the reading and interpretation of results are also univariate (WHO/UNICEF, 2019a, 2020). However, if the country data points are represented on the ternary diagram, each point represents a three-part composition, and they will have one reading or another, depending on their location on the ternary diagram.

A main objective of this study is to propose a multivariate measure of urban–rural inequality, taking into account the compositional characteristics of the data. For this, we first discretized the ternary diagram to represent the urban and rural data points in it, and then we calculated the distance between the two points as an overall measure of inequality. Another aim is to represent tripartite information on a thematic map. Finally, we applied this to a global data set on hygiene in urban and rural settings.

2. Materials and methods

2.1. Data analysis: input

For this study, the information was obtained from the JMP platform (www.washdata.org). Countries with data from 2017 were filtered, as they were the most up-to-date. As a result, the analysis is limited to data from 77 countries in the rural residence area, and the data from 76 countries in the urban residence area. The difference of one unit between urban and rural is due to Peru, which only presents information for rural and non-urban hygiene facilities. The breakdown of the number of countries by region (of a total of 76) is: 10 countries of the Central and Southern Asia (CSA) region, 9 countries of the Eastern and South-Eastern Asia (ESEA) region, 12 countries of Latin America and the Caribbean (LAC) region, 8 countries of the Northern Africa and Western Asia (NAWA) region, 3 countries of the Oceania region, and 34 countries of the Sub-Saharan Africa (SSA) region. Note that countries in several regions (Australia, New Zealand, Europe, and Northern America) were not included in the analysis, as no hygiene information for 2017 was found on the JMP website.

The information source provides disaggregated data on the presence or absence of a handwashing facility in the three levels of service: basic service (BS), limited service (LS), and no facility (NF). The BS level refers to the availability of an on-premise handwashing facility with soap and water; LS refers to the availability of an on-premise handwashing facility

lacking soap and/or water; and NF refers to no on-premise handwashing facility. This information is represented in a three-part composition vector $S^{D=3} = \{x = (x_1, x_2, x_3) : \forall x_i > 0, \ \sum_{i=1}^{3} x_i = 100\}$, which is subsequently represented in the ternary diagram.

2.2. Ternary diagram basics concepts

The ternary diagram is a diagram that graphically represents the proportions of the three compositions in an equilateral triangle. The mathematical basis of the equilateral triangle is the well-known Viviani theorem (Abboud, 2010), and it has the potential to express the compositional data of three parts as one. This is advantageous when doing a multivariate analysis of tripartite information.

Location of the data points on the ternary diagram can be determined in several ways. Here, we illustrate two ways. The first option is to draw lines parallel to the basis of the ternary diagram opposite the vertex (Fig. 1A). In the depicted example, a random value of 30% for BS, and of 20% for NF, is given. The first step is to plot the BS value with a straight line whose value is 30% (solid blue line in Fig. 1A); the NF value is then drawn with a solid black line whose value is 20%. The intersection of these two lines will be the location of data point "A" (BS = 30%, NF = 20%) on the ternary diagram. It should be noted that it is not necessary to draw the third line (dashed red line) to locate the data point of "A"; as there is a closing value of 100%, the result of LS will simply be a difference (i.e., LS = 100 - NF–BS). Consequently, it is possible to plot two-dimensional observations within a triangle.

The second option is related to the conversion between the ternary diagram and the XY coordinates (see Pomberger et al. (2017)). Briefly, the three-part composition must be converted to XY coordinates using Eq. (1) and Eq. (2); this transformation allows the distance between two points to be calculated in a classical way (Fig. 1B and C).

$$x' = NF + BS/2 \tag{1}$$

$$y' = BS \times \sqrt{3}/2 \tag{2}$$

The Pomberger et al. (2017) procedure is followed to construct the ternary diagram from the cited alternatives. The main justification is to ease capturing the data points in the ternary diagram through computational calculations; additionally, this allows the distance between two points ($d_{\overrightarrow{UR}}$) to be easily calculated.

2.3. Plotting and reading a ternary parcel

The construction of a colored thematic map, like the univariate ones, requires the underlying data to be ordered. This is accomplished by first discretizing the ternary diagram into the ternary parcel.

Ternary parcels can have different amplitudes. For example, if the ternary diagram is not delimited, the amplitude of the ternary parcel will be 100 (see Fig. 1A), and therefore the ternary reading would be BS $\leq$ 100, LS $\leq$ 100, and NF $\leq$ 100. If we limit the amplitude of the ternary parcel to 50, the number of ternary parcels will be 4, and the ternary reading of the plot located in the ternary center would be BS $\geq$ 50, LS $\leq$ 50, and NF $\leq$ 50. If we limit the amplitude of the ternary parcel to 20, the number of ternary parcels will be 25 (such as shown in Fig. 2A), and the reading of one of the ternary parcels will be BS $>$ 80, LS $<$ 20, and NF $<$ 20 (see reading of Q1, Fig. 2A). If the amplitude of the ternary parcel is 10, the number of ternary parcels that will be formed will be 100. The ternary parcel's amplitude is related to the precision of the reading. In this study, we selected an initial amplitude of 20 to analyze data, which represented an equilibrium between reading and ordering the parcels. We discuss the influence of the amplitude and the relationship with reading precision in the next sections.

On the other hand, to order the groups of countries (parcels), we define countries that have values close to the BS vertex as those that have a high coverage of handwashing facilities with soap and water on-premises as the ones in the best position. Countries that have values close to the NF vertex are those that have a high percentage of households that do not have handwashing facility and are shown as the last ones. Note that the order may have the four different classification alternatives (shown in Fig. 2):

i) the first classification alternative is the one shown in subfigure A. It follows the logic of classifying countries with a high degree of coverage of basic hygiene services facilities, and then from left to right to prioritize access to limited hygiene services, and finally closing with the worst group of countries in Q25;
ii) in the second alternative (subfigure B), the groups are arranged vertically from top to bottom, giving a higher value to countries that have a high coverage of basic hygiene services, and then from left to right to prioritize access to services of limited hygiene, and finally closing with the most unfavorable group of countries in Q25;
iii) in the third alternative (subfigure C), the groups are ordered diagonally from top to bottom and by levels. The first level is when NF $\leq$ 20, and the last level, when 80 $<$ NF. This order follows the criterion of first classifying countries with a low level of NF coverage (i.e., Q1 to Q9) and ending the classification with the group of countries with high NA values (i.e., Q25). Internally, for N = 1, it goes in descending order, giving priority to the basic level and ending in the LS vertex;
iv) the fourth alternative (subfigure D) is a variant of the third alternative; the only change is the internal order of each level (first the white ternary parcels, and then the colored ones). The criterion used to define the order at each level is used to give a higher value to the group of countries with the lowest NF, and diagonally from higher BS to lower BS, both in the white ternary parcel and in the gray ternary parcel.

For this analysis, we chose the fourth alternative (Fig. 2D), which ensures that the first five ranking orders (i.e., Q1-Q5) include the value of zero for NF compared to the other alternatives. In the first and second

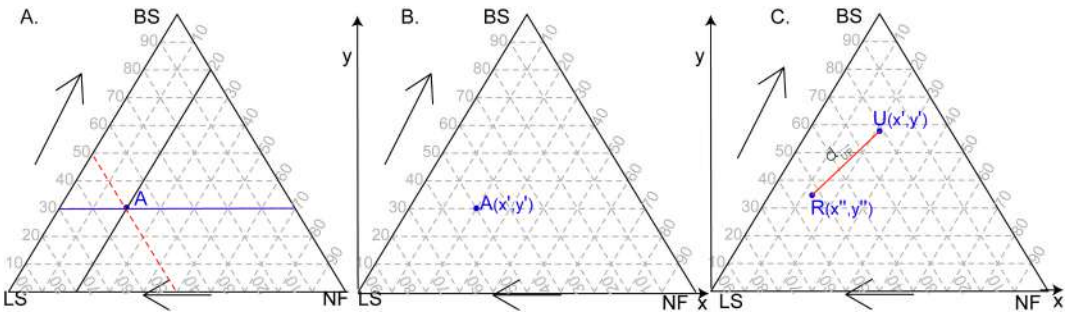

Fig. 1. Location of data points on the ternary diagram (plots A, B) and distance measurement (plot B). Plot A: BS value on solid blue line, NF value on solid black line, and LS value on dashed red line. (For interpretation of the references to color in this figure legend, the reader is referred to the Web version of this article.)

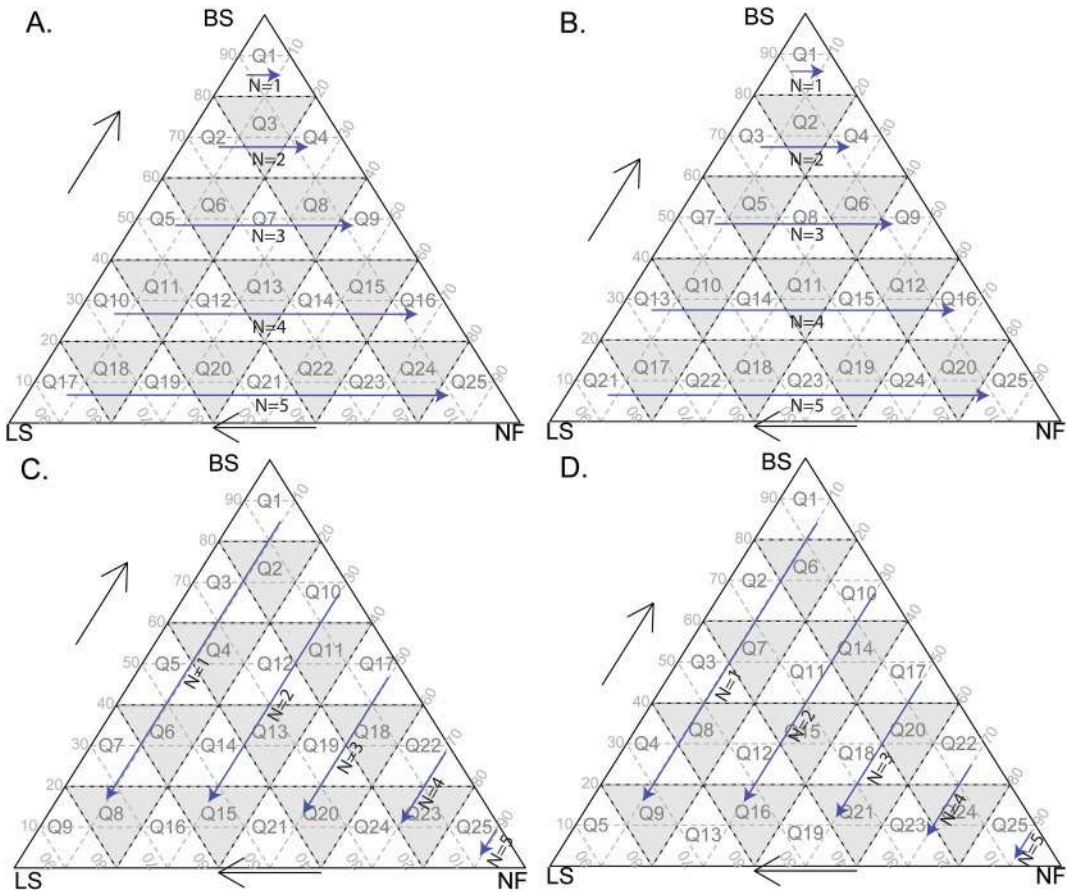

Fig. 2. (A–C) Three alternative routes to classify countries by groups: horizontally from left to right (A), vertically from top to bottom, with priority at shaded areas and then the white areas, from left to right (B), and diagonally from right to left, and diagonally from top to bottom with priority at white areas and then the shaded areas (C). N: level number.

alternatives, the group of countries captured by Q4 are those that do not have an NF value of zero; for the third alternative, countries that have a value of zero are more likely to be in Q3 or Q5 than in Q2 or Q4. In summary, by selecting the fourth (Fig. 2D), we place the group of countries with the lowest NF value in the first eight ranking orders (i.e., N = 1), and the group of countries with the highest NF value (i.e., N = 5) in the last order. This criterion is related to the vision of the 2030 Agenda of "leaving no one behind."

2.4. Urban–rural inequality in a ternary diagram

Urban–rural inequality is measured through distances $d_{\overrightarrow{UR}}$ in the ternary diagram through Eq. (3). The greatest inequality will be presented by the countries with the greatest distance, and the lowest inequality, by the countries with the least distance. A value of zero indicates that there is no urban–rural inequality, while a value of 100 percentage points (p.p.) indicates a maximum inequality between urban–rural.

$$d_{\overrightarrow{UR}} = \sqrt{(x' - x'')^2 + (y' - y'')^2} \quad (3)$$

where x ', y' are the values of the urban residence area, and x '', y '' are the values of the rural residence area.

The proposal is compared with the standard way of measure of inequality, i.e., one inequality value calculated with Eq. (3) versus three inequality values calculated through the absolute value of the urban–rural difference in terms of the proportion for each dimension; this strategy is currently being used by WHO/UNICEF as part of the comparison of the proportion of the population with access to WASH services between urban and rural areas and reported in global reports (WHO/UNICEF, 2019a). The ternary amalgamated in two gives a result of differences between urban and rural that is exactly proportional to the differences between the magnitudes of the dichotomous variables (see Appendix B).

Finally, a graphical representation of thematic maps, ternary diagrams, and box plots was built into the R Core Team (2020) (v.4.0.3) platform, for which the following R packages were used: ggplot2 (v3.3.5; Wickham, 2016), tidyverse (v1.3.1; Wickham et al., 2019), and pgirmess (v1.7.0; Giraudoux et al., 2021) for building the ternary diagram; and tmap (v3.3–2; Tennekes, 2018) and sf (v1.0-1; Pebesma, 2018) for thematic maps. The database and R scripts are presented in Quispe-Coica and Pérez-Foguet (2021).

3. Results

3.1. Ternary classification of the hygiene service ladders in urban and rural

The countries' information on access to hygiene facilities is presented in Figs. 3 and 4 for urban and rural residences, respectively. Twenty-five ternary parcels are used, with no information given for six ternary parcels in the urban area, and four in the rural area. The ternary diagrams and the corresponding classification in ternary parcels are presented in subfigure A and as thematic map in subfigure B. The univariate thematic map of the three hygiene categories is shown in subfigures C, D and E. The list with the classification of all the countries is presented in Table A1, and the summary of the number of countries found in each ternary parcel is shown in Table 1.

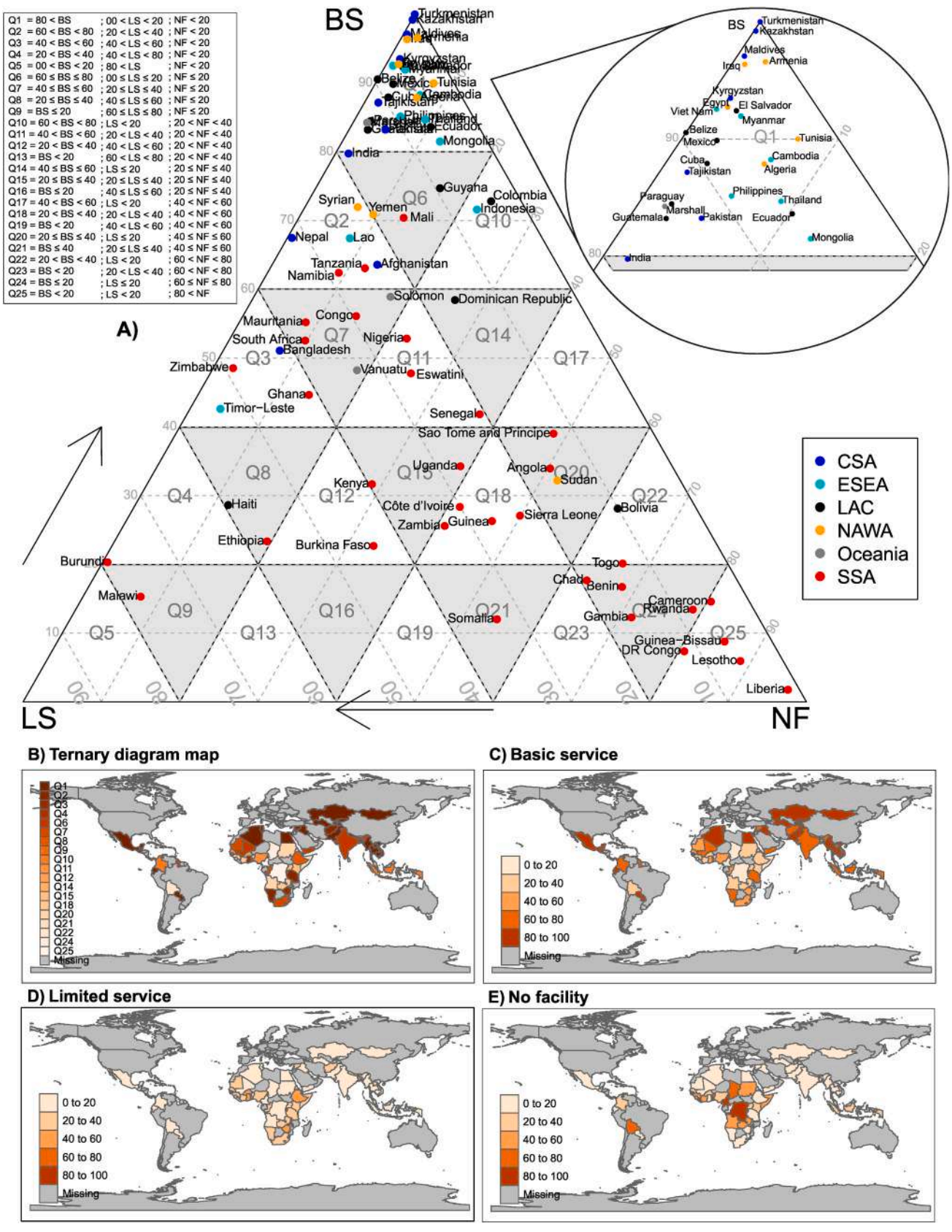

Fig. 3. Access to urban hygiene services in 2017. A: diagram ternary. B: ternary diagram map. C–E: univariate diagram.

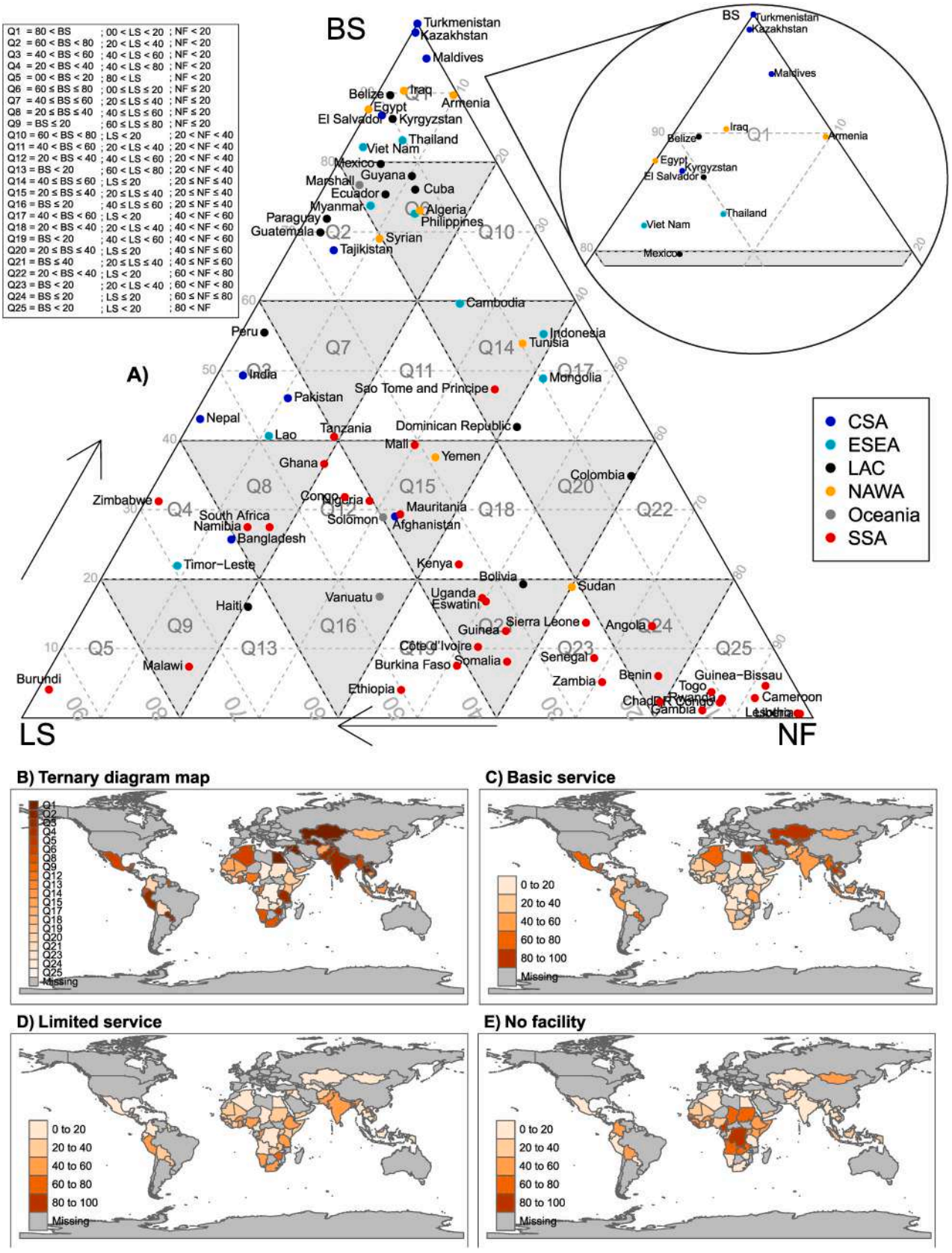

Fig. 4. Access to rural hygiene services in 2017. A: diagram ternary. B: ternary diagram map. C–E: univariate diagram.

Table 1
Quantification of the number of countries according to their classification in the ternary parcel. N, level number of Fig. 2D; Qn, ternary parcel of order n.

N	Qn	Urban							Rural						
		Global	Regional						Global	Regional					
			CSA	ESEA	LAC	NAWA	Oceania	SSA		CSA	ESEA	LAC	NAWA	Oceania	SSA
1	Q1	25	6	6	7	5	1		11	4	2	2	3		
	Q2	6	2	1		1		2	4	1		2	1		
	Q3	4	1	1				2	6	3	1	1			1
	Q4	1						1	3	1	1				1
	Q5								1						1
	Q6	4	1		1	1		1	8		2	4	1	1	
	Q7	5					2	3							
	Q8	2			1			1	3						3
	Q9	1						1	1						1
2	Q10	2		1	1										
	Q11	3						3							
	Q12	1						1	2						2
	Q13								1			1			
	Q14	1			1				4		2		1		1
	Q15	2						2	5	1			1	1	2
	Q16								1					1	
3	Q17								2		1	1			
	Q18	4						4	1						1
	Q19								2						2
	Q20	3				1		2	1			1			
	Q21	1						1	6			1			5
4	Q22	2			1			1							
	Q23								4				1		3
	Q24	4						4	3						3
5	Q25	5						5	8						8
	Total	76	10	9	12	8	3	34	77	10	9	13	8	3	34

Our classification method grouped 25 countries for urban residence, and 11 countries for rural residence, in Q1. The regional breakdown of Q1 shows that 7 LAC countries, 6 ESEA and CSA countries, 5 NAWA countries, and 1 Oceania country corresponded to urban residence, and 4 CSA countries, 3 NAWA countries, 2 LAC countries, and 2 ESEA countries corresponded to rural residence. No country from the SSA region appeared in this group, but they did from Q2 onwards.

The group of countries in the ternary parcel Q1 (i.e., 80 < BS, LS < 20, and NF < 20) are characterized by having the best conditions for on-site handwashing practice, as they have high coverage of basic services (BS > 80), low coverage of households with limited services (LS < 20), and low coverage of households without handwashing facilities (NF < 20). Their representation on the thematic map has the most intense color, and the intensity decreases in the order from Q1 to Q25. The difference between urban and rural in the number of countries captured by Q1 shows that there is a higher probability of having better handwashing conditions in urban residence than in rural residence, both in the total and in the regional breakdown.

The group of countries from Q2 to Q9 are characterized by having relatively better conditions for handwashing practice, as they have low coverage of households without on-site handwashing facilities (i.e., NF ≤ 20%), BS ≤ 80%, and LS from 0 to 100%. Note that rural Burundi is the only country in Q5 and is very close to the LS vertex, which implies that it has high coverage of LS (>80%), low coverage of BS (<20%), and low coverage of households with NF (<20%). Also noteworthy is the appearance for the first time of two countries in the SSA region in urban Q2 (Tanzania and Namibia).

The ternary parcels captured 9 urban countries and 13 rural ones in Q10 to Q16. This group of countries is characterized by having NF values that are within the range of 20%–40%, while the BS and LS values are between zero and 80%. Compared to Q1 to Q9, there is a higher concentration of rural than urban in Q10–Q16, with 13 vs. 9 countries, respectively; this pattern is observed also in the following classification levels (from N3 to N5).

Following the sequence, the group of countries that were classified in Q17 to Q21 have the common characteristic of having NF values from 40% to 60%, and BS and LS values from 0 to 60%. In the regional breakdown, there is a predominance of countries in the SSA region over the rest. For urban cases, there are 7 countries in SSA as compared to 1 in NAWA. For rural cases, there are 8 countries in SSA as compared to 3 in LAC and 1 in ESEA.

In the following order of classification, from Q22 to Q24, the situation is similar to the previous one: there is a predominance of countries from the SSA region over the rest. This is more drastic in the ternary parcel Q24, which contained only SSA countries, both in the urban and the rural categories.

The last sorting order corresponds to Q25. As for Q24, all the countries captured by this ternary parcel belong to the SSA region. The group of countries that are in this ternary parcel are characterized by low coverage of households with BS (<20), low coverage of LS (<20), and high coverage of households with NF (>80). Their representation on the thematic map has the lowest color in intensity, which means that countries in this group (of the total of countries analyzed) have the most unfavorable conditions for handwashing.

On the other hand, we note that interpreting the univariate thematic map can lead to an erroneous interpretation of the information. Using Burundi as an example, if we only interpret the BS value (of 4.1%) expressed in the thematic map in Fig. 4C, we observe that it is represented with the lowest color in intensity, giving the impression that Burundi has very unfavorable conditions for handwashing. However, in our classification alternative, Burundi is in Q5 and is represented in the thematic map in Fig. 4B with the most intense color. This means that it has relatively better conditions for handwashing, as it has a high value of LS (94.5%) and a low value of NF (1.4%). Consequently, a univariate analysis does not show what is going on in the other parts, highlighting the value of using an alternative way of exploring closed data with a ternary thematic map.

Finally, when crossing the classification of the countries with their

income level (Figure A3), we observe that in the order of classification from Q1 to Q9, there is a greater concentration of upper-middle-income countries than of lower and lower-middle-income countries, both in the urban and rural categories. This decreases in the higher levels; for example, at level 2 (i.e., N2; from Q10 to Q16), there are only three upper-middle-income countries in the urban residence areas, and only one in rural; at the next level (N3; from Q17 to Q21), there are only two upper-middle-income countries in rural areas and none in urban. At the highest levels, ternary parcels have not captured any upper-middle-income countries. In general, the results show that the upper-middle-income countries are concentrated at the top of the ternary diagram, and the lower-middle-income and low-income countries, at the bottom.

3.2. Urban–rural inequality in access to hygiene facilities

The results of the urban–rural inequality vectors are shown in the ternary diagram of Fig. 5A and spatially in Fig. 5B. The vectors use the urban residence area as the starting point, and the rural residence area as the end point. The distance between these two points, the module of the vector, represents urban–rural inequality.

In the ternary diagram, the vector directions do not have a defined order, indicating a differentiated behavior of inequality between countries; further, expressed as a thematic map, the results show spatial heterogeneity (Fig. 5B). However, common patterns are repeated in 73/76 countries, such as the direction of the vector from top to bottom (diagonally to the right or to the left). This indicates that there is a higher level of BS in urban than rural settings. In contrast, in Sao Tome and Principe and Guyana, the direction is from bottom to top (diagonally to the left), which means that the level of BS is higher in the rural than in the urban setting (see also Fig. 6B).

For LS, the urban–rural difference has a negative value in 57/76 countries, indicating that households in the rural residence area have greater coverage of hygiene facilities lacking soap or water than households in the urban residence area. Finally, in the case of NF, the urban–rural difference has a negative value in 68/76 countries, which means that households in the rural residence area have greater NF coverage than those in the urban ones.

The urban–rural inequality result expressed in terms of distance is shown in Fig. 6A and the summary statistics by quartiles in Table 2 (boxplot in Figure A1). We complement the inequality value illustrated

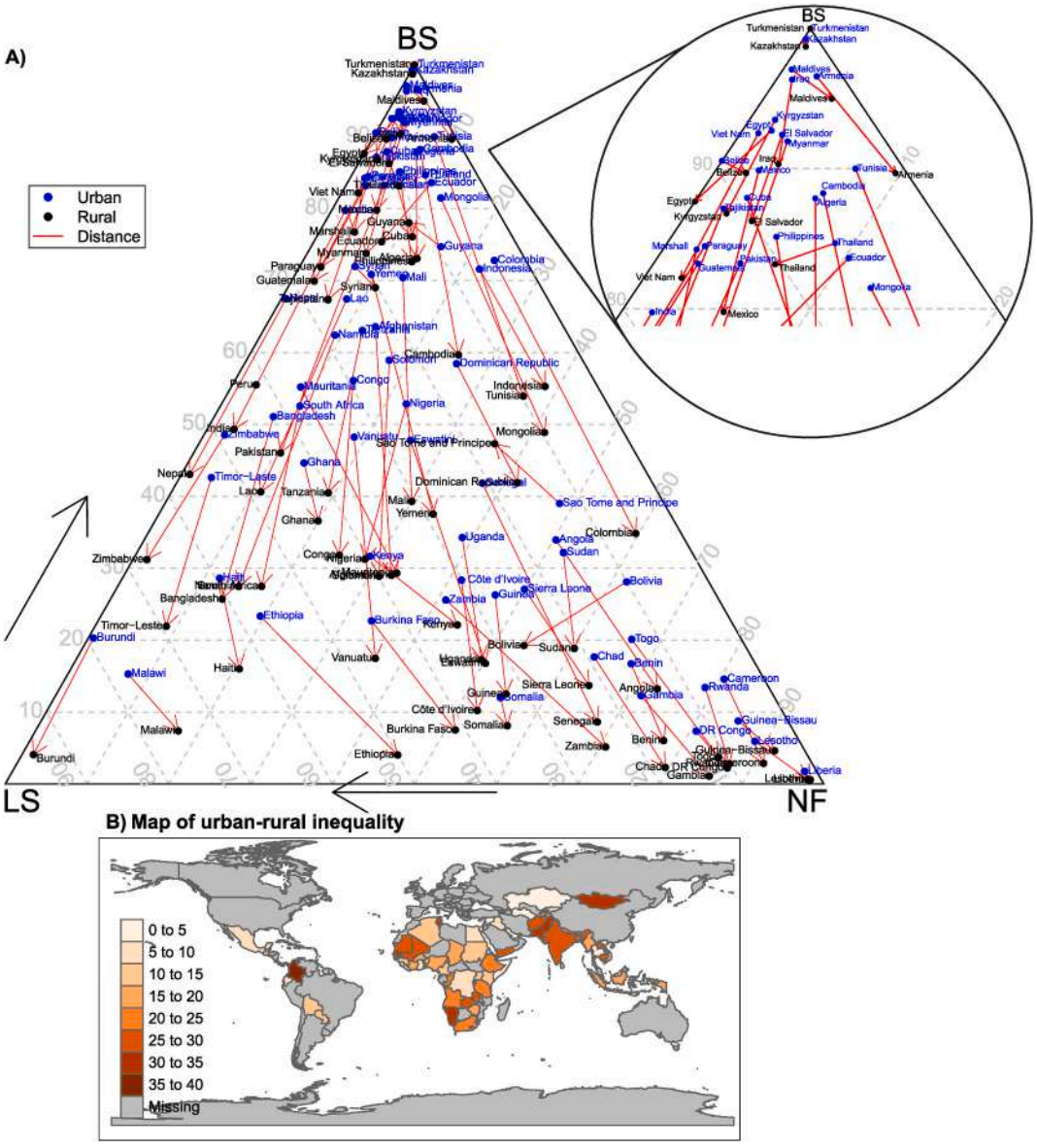

Fig. 5. Urban–rural inequality of the ternary diagram, expressed as distance (A) or map (B). The starting point of the vector is the urban position, and the ending point of the vector is the rural position.

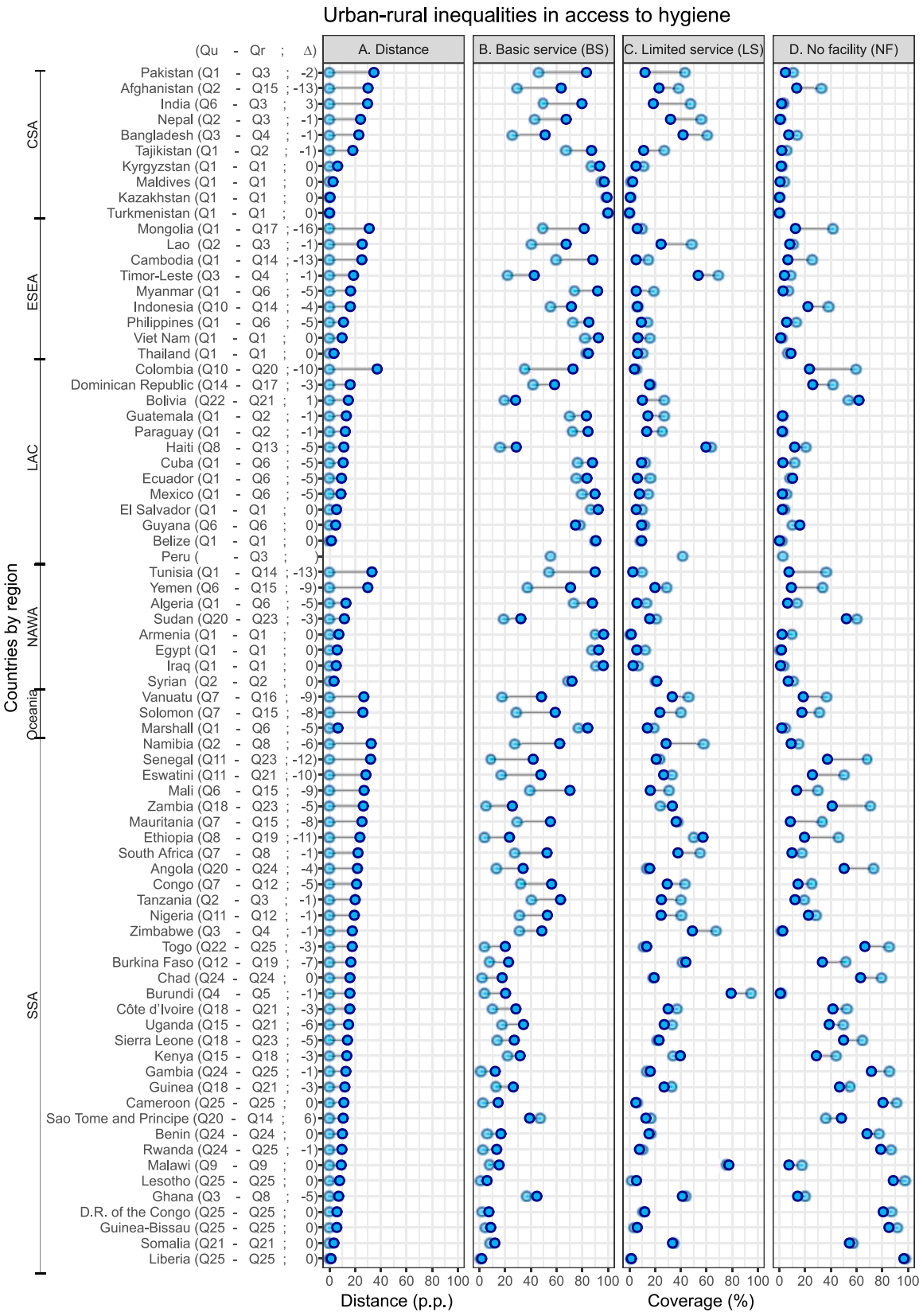

Fig. 6. A) A measure of inequality expressed in terms of distance. The blue circle represents the upper limit of the distance of the ternary diagram. B–D: Urban–rural inequality graph used by UNICEF and WHO (2020). A blue circle denotes urban, and a light blue circle, rural. Δ indicates the change of order between urban (Qu) and rural (Qr) in the ternary parcel (e.g., in Pakistan $\Delta = Q_{u=1} - Q_{r=3} = -2$). (For interpretation of the references to color in this figure legend, the reader is referred to the Web version of this article.)

Table 2
Statistical summary of the measure of inequality by quartiles. Values are expressed as a percentage and rounded to one decimal place.

Region	Minimum (p.p.)	Quartile 1 (p.p.)	Quartile 2 (p.p.)	Quartile 3 (p.p.)	Maximum (p.p.)
Central and Southern Asia (CSA)	0	3.7	20.5	28.3	34.6
Eastern and South-Eastern Asia (ESEA)	3.5	10.9	16.4	25.2	31.0
Latin America and the Caribbean (LAC)	1.5	8.1	11.0	13.5	37.1
Northern Africa and Western Asia (NAWA)	3.6	5.7	9.5	21.3	33.1
Oceania	6.6	16.3	26.0	26.4	26.8
Sub-Saharan Africa (SSA)	1.2	10.2	15.8	21.6	32.5
Global	0	8.7	14.4	23.1	37.1

in Fig. 6A with the results obtained from the urban (Qu) and rural (Qr) classification in the ternary diagram. The uppercase delta value (Δ) indicates a change of order between urban and rural in the ternary parcel (i.e., Δ = Qu - Qr). A negative value of Δ means that, in the classification, urban is in a higher order than rural; a positive value of Δ indicates the reverse process. A value of Δ equal to zero means that there is no change and, therefore, urban and rural are in the same ternary parcel.

Globally, 19/76 countries were identified as belonging to the first quartile with inequality distances ≤8.7 p.p. (with a minimum value of zero in Turkmenistan), and with inequality distances >8.7 p.p. in 75% of the remaining countries. In the third quartile, the inequality distances are ≤23.1 p.p. for 75% of the countries, and >23.1 p.p. for the remaining 25% of the countries, with a maximum value of 37.1 p.p. in Colombia. The zero-value found in Turkmenistan is based on having both NF and LS equal to null, with the BS service category at 100%; therefore, when applying Eq. (3), a vector with null distance is obtained. The meaning of the zero value is that there is equality between urban and rural in access to the hygiene service facilities and, in the particular case of Turkmenistan, the hygiene facilities also have soap and water.

From a regional perspective, the inequality measures show high heterogeneity. In the LAC region, Colombia is the country with the highest urban–rural inequality (with a value of 37.1 p.p.), and Belize is the country with the lowest inequality (with a value of 1.5 p.p.) (Fig. 6A). Colombia's inequality value deviates greatly from the normal behavior of the region, where 75% of the countries have inequality distances ≤13.5 p.p.; therefore, it is considered an atypical behavior. The LAC region also has the lowest interquartile range (IQR; 5.4 p.p.) with respect to the rest of the regions, which translates into less dispersion of data.

In contrast, the CSA region has the highest IQR value, of 24.6 p.p., which translates into a greater dispersion of data. Likewise, in CSA, 75% of the countries have an inequality distance of ≤28.3 p.p., with a value of zero in Turkmenistan; the remaining 25% the distances have an inequality distance of >28.3 p.p., with a maximum value of 34.6 p.p. in Pakistan.

In the ESEA region, 7/9 countries have inequality distances ≤25.2 p.p., with a minimum value of 3.5 p.p. in Thailand; in the remaining two countries, the inequality distances are >25.2 p.p., with a maximum value of 31.0 p.p. in Mongolia. In the Oceania region, distances could only be calculated for three countries; the minimum value is 6.6% in Marshall, and the maximum value is 26.8 p.p. in Vanuatu. In the SSA region, 75% of the countries have an inequality distance ≤21.6 p.p., with a minimum value of 1.2 p.p. in Liberia, and the remaining 25% of countries have distances >21.6 p.p., with a maximum value of 32.5 p.p. in Namibia.

Note that a low value in the inequality measure does not necessarily imply that the best conditions are present for handwashing with soap and water. For example, in the CSA, ESEA, LAC, and NAWA regions, a delta with a zero value corresponds to the countries with less inequality but is also present when urban and rural are in the same ternary parcel of Q1, Q2, or Q6. Q1 countries have the best conditions for handwashing with soap and water. However, in the SSA region, the four countries with the lowest inequality are in Q21 or Q25, yet at the same time have a Δ value equal to zero, which translates into countries with the most unfavorable conditions for handwashing with soap and water; indeed, they present high NF values (>80% in Q25, and between 40% and 60% in Q21). Consequently, to avoid an erroneous interpretation of the value of inequality, it is necessary that this magnitude be accompanied by the ternary classification.

Our results also show that the multivariate measure of inequality has a dual behavior with respect to BS hygiene: it has a direct relationship in the SSA region (i.e., the magnitude of inequality decreases and the average of the urban and-rural BS also decreases), and an inverse relationship in the remaining regions (i.e., the magnitude of inequality decreases, while the average of the urban-rural BS increases). This affirmation is supported by the result of the linear fit between the inequality measure obtained and the average urban and rural BS, which has a negative slope in the CSA, ESEA, LAC, NAWA, and Oceania regions, while the SSA region has a positive slope (see Figure A4).

The univariate graphs in Fig. 6B–D allow a very intuitive visualization of urban–rural inequality in access to hygiene services, facilitating the reading of each category. However, it is not possible to know the level of inequality in the country as a whole, since the three categories contain information on inequality and can score better or worse depending on the category of analysis. For instance, ordering the absolute value of inequality in descending order (e.g., with the highest inequality in the first order, and the lowest in the last order) leads to India being ranked 12th based only on the BS category, ranked 3rd based only on the LS category, and ranked 64th based on the NF category. However, the unique measure proposed in this study give India a value of 29.7 p.p., placing it in 9th place.

Another detail to take into account is that the sum of the inequality values of the three categories results in a value of zero (i.e., 30.4 p.p. (BS) – 28.8 p.p. (LS) – 1.6 p.p. (NF) = 0). This is because, for both urban and rural areas of residence, the sum of the parts has a constant value of 100% and, therefore, the difference between urban and rural results in zero. The constant closing value is a peculiarity of composition data, and it is also one of the reasons why it requires a particular statistical approach.

Finally, it can be inferred from the results obtained that access to basic service facilities —such as to hygiene facilities with soap and water— is a privilege of mainly households located in urban areas. Sao Tome, Principe, and Guyana are the only cases in which basic service was higher in rural than in urban areas. Meanwhile, limited hygiene and NF service are higher in rural than in urban areas.

4. Discussion

4.1. Urban–rural inequality in a ternary diagram

We constructed twenty-five ternary parcels with a reading precision of twenty, which allowed us to group the countries with similar behaviors in order from the ternary parcel Q1 to the ternary parcel Q25. We obtained results that show a greater concentration of countries with urban households (e.g., 25/76 countries in Q1) than rural (e.g., 11/77 countries in Q1) in the BS vertex. This translates into greater availability of handwashing facilities with soap and water in urban households than in rural ones. In contrast, countries in the ternary parcels Q24 and Q25, both urban and rural, correspond only to countries belonging to the SSA region.

For some country analyses, the amplitude of twenty was not beneficial, as it generates misleading results in the ranking order. For example, in the urban residence area (Fig. 3A), Kenya (BS = 31.7%, LS = 39.6%, NF = 28.7%) has better indicators than Burkina (BS = 22.7%, LS = 43.9%, NF = 33.4%) and is therefor, better; nonetheless, according to our ranking, it is at Q15, while Burkina is at Q12. However, if we adjust the reading precision to a magnitude of ten, Kenya would rank at Q48, and Burkina at Q56, in the new classification. This allows us to affirm that one of the limitations of the method has to do with the adequate selection of the reading precision.

The method is also limited when the data point is very close to the boundary of the subdivided ternary parcel or to its vertices; by not taking into account the uncertainty of the data, they are very likely to be in either one or both. Taking the same previous case above as an example, the Kenyan data point is very close between the limit of Q12 and Q15 (the limit between both has the value of 40 in LS), so if we add the uncertainty of the data, it is very likely that Kenya is doubly classified. Another more drastic case is shown for rural Tanzania: the data point is very close to one of the vertices of Q3, implying that if its uncertainty is added, it could also be in any of these (Q7, Q8, Q11, Q12, or Q15). This underscores the need to incorporate data uncertainty (Ezbakhe and Pérez-Foguet, 2019) to obtain greater precision in the order of classification.

Further, the values of the service stairs have a tendency to go to the upper limit of one, which expressed in the ternary diagram, indicates that the data points are very close to the vertices. This is relevant as SDG 6.2 seeks " … *by 2030, achieve access to adequate and equitable sanitation and hygiene for all and end open defecation* … ". Therefore, as the BS progress rate increases, the data points of the countries will tend to the BS vertex. This implies that it will be more relevant to capture data points when they are in Q1 under multivariate behavior.

Our method allows adjustments to the new conditions to be made, giving a more accurate reading. For this, it will only be necessary to adjust the amplitude of the ternary parcel to a value lower than twenty, which generates an increase in the number of subdivided ternary parcels.

However, an excessive increase in the breadth may not be beneficial to the grouping and ranking order of countries. To illustrate this situation, we carried out a Q1 zoom of the urban residence area (Fig. 3A) and then subdivided it into ternary parcels with three levels of reading precision (of 10, 5, and 2.5; Fig. 7A–C). Here, subfigure A was subdivided from a ternary parcel with an amplitude of twenty, to four ternary parcels with an amplitude of ten. The order of the classification follows the same logic outlined in Fig. 2D and goes from S1 as the best, to S4 as the least favorable. We also intuitively delimited three possible similar groups (colored red, green, and blue; Fig. 7), which should capture the following subdivisions as the reading precision increases.

By increasing the reading precision to five (Fig. 7B), the group of countries shown in red and blue are perfectly captured by the ternary parcels S1 and S7, respectively, while S2 captures the group of countries shown in green and has added Belize. If we continue to increase the reading accuracy to a 2.5 ternary delimitation, as shown in Fig. 7C, there is a greater dispersion of the group of intuitively delimited points: the group of countries in green is now distributed in S3, S11, and S18; the groups of countries in red and blue also have multiple distributions. The order of classification is also altered as the ternary reading amplitude increases, as seen for Myanmar (BS = 91.95%, LS = 5.25%, and NF = 2.80%) and El Salvador (BS = 92.41%, LS = 5.31%, and NF = 2.28%), shown in green. Both countries are in the same ternary parcel in subfigure A and B; in subfigure C, however, Myanmar is in S18 and El Salvador in S11, despite having very close data points.

Therefore, an excessive increase in the reading precision has a dispersion effect in the group of countries, which is not beneficial for the grouping or ordering of classification, in addition to the order uncertainty previously mentioned. Therefore, the precision of the ternary reading has to be limited, taking into account data uncertainty and the desired level of clustering of the final results.

Along the same lines as SDG 6.2, which seeks to end open defecation (OD) and provide adequate hygiene, our method allows us to explore the relationship between levels of hygiene service and a sanitation service category. For this, we used a boxplot to cross the ternary classification obtained for each country with the proportion of people who continue open defecation (Fig. 8). The boxplot shows that OD rate is lower for countries in Q1, and higher for those in Q25; this trend is more drastic in rural areas than in the urban ones. This shows that there is a relationship to a greater or lesser extent between those without handwashing facilities with soap and water and OD; i.e., households with sanitation facilities that do not practice OD are more likely to also have handwashing facilities with soap and water.

The countries in Q23, Q24 and Q25 belong mainly to the SSA region; according to Fig. 8, this group of countries has high values of OD and NF (NF > 60%). These conditions in the SSA region lead to diseases related

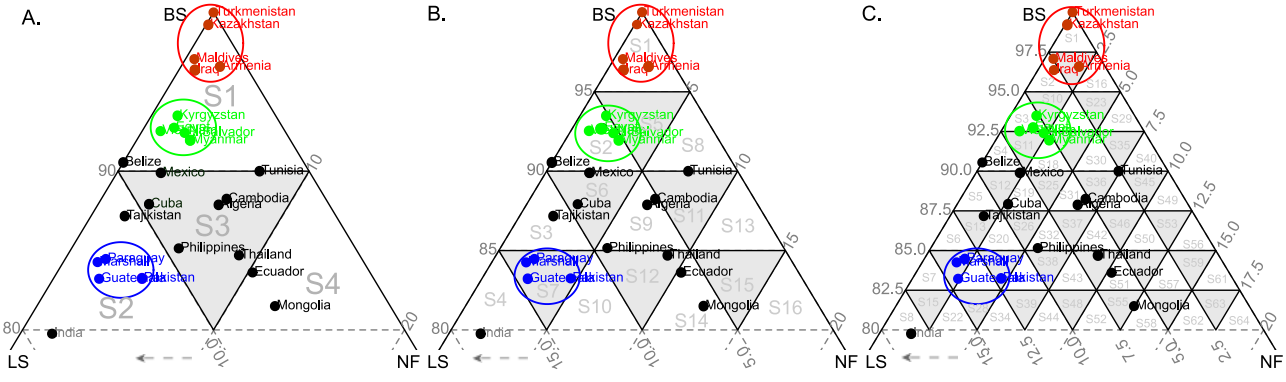

Fig. 7. Zoom of Q1 in the urban residential area subdivided into ternary parcels with different reading precision measures. Left: When the reading precision is 10, the subdivision of Q1 results in 4 ternary parcels. Center: When the reading precision is 5, the subdivision of Q1 results in 16 ternary parcels. Right: When the reading precision is 2.5, the subdivision of Q1 results in 64 ternary parcels. (Note that, to reduce confusion, the internal subdivisions are indicated with Sn).

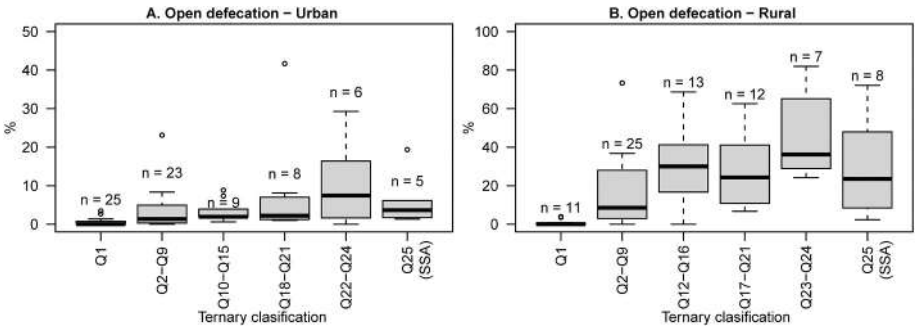

Fig. 8. Ternary classification vs open defecation, both in urban and rural areas. Open defecation (OD) refers to the disposal of human faeces in fields, forests, bushes, open bodies of water, beaches, other open spaces, or with solid waste. In rural regions, Syria was excluded from the analysis, as it did not have information from OD.

to inadequate WASH services, with diarrhea the main one. In SSA, improvements in sanitation were responsible for a reduction of more than 10% in the mortality rate from diarrhea in children under 5 years of age (Troeger et al., 2018). In the same region, Zerbo et al. (2021) found that 7.75% (5.99–9.7%) of all deaths due to diarrheal diseases are attributed to unsafe WASH. Systemic review of the effect of handwashing with soap on the risk of diarrhea in the community found that handwashing with soap can reduce the risk of diarrheal diseases by 42–47% (Curtis and Cairncross, 2003). Therefore, an intervention aimed at reducing OD and NF in households in the SSA region will have a positive effect on their public health.

SDG 6.2 also seeks equitable access; in that sense, our method gives an integrated measure of a three-part service ladder. The measure is for analyzing the difference between urban and rural, which allows the public policies of the sector to be differentiated with a general vision. This differs from the simple difference between the proportion of urban and rural that the JMP performs (WHO/UNICEF, 2016), which has also been used in other studies. Our methodology also incorporates calculations of common distances, which facilitates the understanding of each result obtained, allows comparison between countries (either on a thematic map or in distance measures), and allows an inequality ranking of urban–rural inequality of the countries.

However, expressing inequality in a single, multidimensional measure hides information from the parties, which does not allow for specific sectoral interventions. This is one of the main disadvantages of a comprehensive measure, as noted in other studies (Giné-Garriga et al., 2017; Giné-Garriga and Pérez-Foguet, 2010; Hsiao et al., 2005). Therefore, the obtained inequality measure is further strengthened if it is also accompanied by the usual measure of the simple difference between urban and rural between the parties or with the ternary classification obtained. For example, an inequality value of 3.5 p.p. in Thailand is not the same as a value of 3.5 p.p. in Somalia. This can be better visualized by adding the ternary parcel to which they belong: Thailand is in Q1 (i.e., it has $80 < BS$, $LS < 20$, $NF < 20$), and Somalia is in Q21 (i.e., it has $BS \leq 20$, $20 \leq LS \leq 40$, $40 \leq NF \leq 60$). This will help to provide a global magnitude for policies with a general vision and disaggregated magnitudes for targeted interventions.

In this study, we could not calculate urban–rural inequality for some countries due to a lack of information. However, for countries with available information, our results show that urban–rural inequalities can differ in magnitude from one country to another, from a minimum value of zero to a maximum value of 37.1 p.p. With regional geographic variation, the urban–rural inequality in CSA has a minimum value of zero and a maximum value of 34.6 p.p.; in ESEA, the minimum value of 3.5 p.p. and a maximum value of 31.0 p.p.; in LAC, a minimum of 1.5 p.p. and a maximum of 37.1 p.p.; and in NAWA, a minimum of 3.6 p.p. and a maximum of 33.1 p.p., in Oceania, the minimum is 6.6 p.p. and the maximum is 26.8 p.p., and in SSA, the minimum is 1.2 p.p. and the maximum is 32.5 p.p. The inequality measures obtained justify differentiated management strategies for both urban and rural areas, with greater emphasis on rural households as well as on the countries that are in the Q25 ternary parcel, which are the countries with the highest proportions of NF.

4.2. Hygiene facilities and COVID

Our results are based on information from 2017. However, we consider that the analysis by ternary parcels with an amplitude of twenty helps to compensate the brief changes that have been generated to date in analysis, which allows us to cross the information obtained from hygiene with the data of cases and death due to the COVID-19 disease. Hygiene cross-information corresponds only to countries that with urban and rural in the same ternary parcel or in the classification range of ternary parcels (e.g., in Fig. 6, Ghana has urban in Q3 and rural in Q8 and therefore is considered in the classification from Q2 to Q9); countries that do not meet this condition were excluded from this analysis. In any case, this discussion is informative for helping national and international actors to understand the link between hygiene and public health.

We were not able to calculate urban–rural inequality or the realities of some countries in terms of hygiene. The main reason is little or no information. It is more drastic in high-income regions, such as Europe, Northern America, Australia, and New Zealand, for which there is no ternary hygiene information for the year 2017. A recent study by Brauer et al. (2020) reaffirms the hypothesis that there is little global data on hygiene. Even so, with complementary information, they were able to estimate the proportion of the population with no facilities for washing hands with soap and water for the year 2019. They show that high-income countries have low levels of the proportion of the population without access to a handwashing station with soap and water. Having almost all basic services covered is probably one of the reasons why information gathering is taking a back seat. However, most of these countries also have the highest number of confirmed cases and deaths from COVID-19 according to the WHO (see Figure A2). The case of the USA is the most illustrative, especially as the estimates by Brauer et al. (2020) suggested that the proportion of the population without access to a handwashing station with soap and water was 0.4% value [lower = 0.3%, upper = 0.5%] in 2019. However, as of 15 March 2021, the USA is in the 9th place in the ranking of confirmed COVID-19 cases per 100,000 population and in the 13th place in the ranking of deaths from COVID-19 per 100,000 population.

Notably, Ahmad et al. (2020) showed that counties with a higher

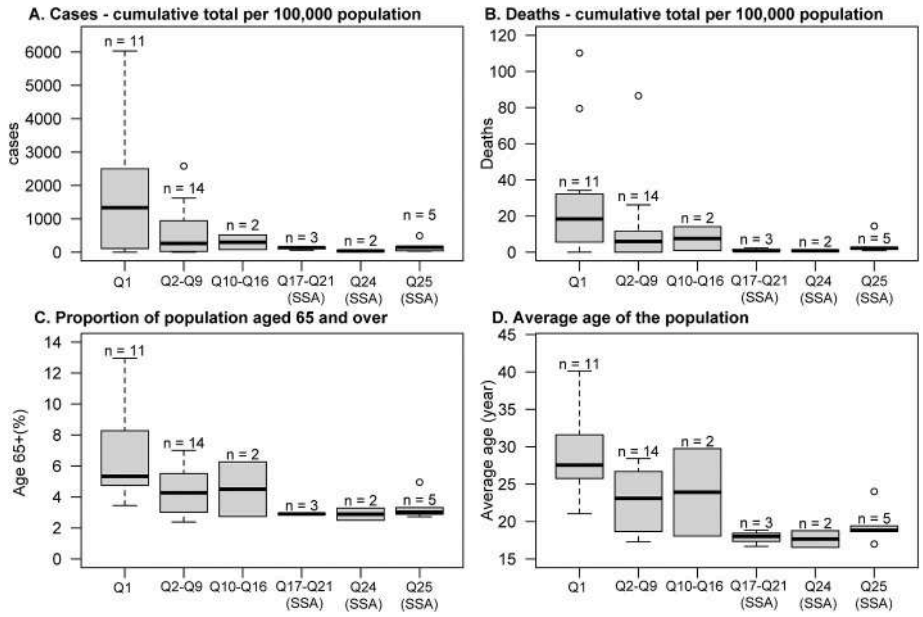

Fig. 9. A–D) Graphs based on level of service, e.g., countries in Q1 to Q9 belong to Level 1 (N1 to N5; see also Fig. 2D). Cases (A) and deaths (B) from COVID-19 per 100,000 population. Proportion of population that is ≥ 65-years old (C) and average age of the population (D); information obtained from United Nations Department of Economic and Social Affairs Population Division (2019).

percentage of substandard housing households had a higher incidence and mortality associated with COVID-19. Homes that have any of the following four problems are considered precarious conditions: overcrowding, high housing cost burden, incomplete kitchen facilities, and incomplete plumbing facilities. Incomplete plumbing is related to homes that lack hot and cold running water, a flushing toilet, or a bath/shower. The scarcity of water, lack of water, or water insecurity at homes (Stoler et al., 2021) makes hand hygiene difficult, which translates into an increased risk of infection by the SARS-COV2 virus. That said, it is likely that in homes without the necessary conditions to practice hand hygiene, there will be a greater increase in infection rate. Therefore, obtaining data, even if it is only low amounts of data, is still relevant for targeting interventions.

For the results obtained by crossing our ternary classification with confirmed cases and deaths from COVID-19, the median of the countries that are within the Q1 group is higher than the median of the rest of the groups in both confirmed cases and deaths from COVID-19 (Fig. 9A and B). This means that some countries that have higher rated levels of hygiene service (i.e., belong to 80 < BS, LS < 20, NF < 20) and have higher confirmed cases and deaths from COVID-19 (cumulative total per 100,000 population; as of 15 March 2021). In turn, the lowest values of the median of confirmed cases and deaths from COVID-19 are presented in the range of ternary parcels from Q17 to Q25 and, at the same time, the countries that are in this range of ternary parcels all belong to the SSA region.

It is paradoxical that, with low levels of BS hygiene, there is also a low rate of confirmed cases and deaths from COVID-19 (per 100,000 population). It would be expected that lower proportions of BS would lead to a higher contagion rate. We further assume that available figures represent the actual number of deaths more or less approximately, but with the same accuracy regardless of the country; however, some international news at the time of writing this research casts doubts about this hypothesis (ANDINA, 2021; GESTION, 2021). Nonetheless, possible explanations are emerging in the literature about this phenomenon, which is occurring in some countries of the SSA region. One explanation is that SSA countries have younger populations, which could act as a protective factor against COVID-19. Another possible explanation is related to the low proportion of older adults in SSA, given that older adults have a higher risk of hospitalization or death when contracting the COVID-19 disease (CDC, 2019; Shahid et al., 2020). According to the Centers for Disease Control and Prevention (CDC), as compared with 5–17-year-olds, the rate of hospitalization is 40 times higher in 65–74-year-olds, 65 times higher in 75–84-year-old, and 95 times higher in ≥85-year-olds (CDC, 2019). To contrast these statements, we crossed the classification of the countries into ternary parcels obtained with the average age of the population and the proportion of the population aged ≥65-year-olds (Fig. 9C and D). The results show that the median age in SSA is lower than the median age of the countries that are in the ternary parcel Q1; the same occurs for the proportion of the population aged ≥65-year-olds.

Other explanations have been suggested in the literature, such as the role of climate (Adedokun et al., 2020; Huang et al., 2020), vaccination against Bacillus Calmette-Guerin (BCG) (that might have a protective role against COVID-19) (Curtis et al., 2020; Miller et al., 2020), population density (Tcheutchoua et al., 2020), and others (Lalaoui et al., 2020; Mbow et al., 2020; Tcheutchoua et al., 2020). Of these, the most prominent is probably the lessons learned from dealing with diseases, such as ebola, malaria, HIV, and others, given that the infrastructures built and the response management systems in place have rapidly adapted to cope with the current pandemic (Lumu, 2020; Nachega et al., 2020; Payne, 2020).

All this could partly explain that even being in the ternary parcels from Q17 to Q25, some countries in the SSA region have low values of confirmed cases and deaths from COVID-19. The most striking thing is that the countries that are in Q25, such as Cameroon, Lesotho, DR Congo, Guinea-Bissau, and Liberia, also have low values of confirmed

cases and deaths from COVID-19 and, at the same time, represent the countries with the conditions most unfavorable for practicing hand hygiene, i.e., BS < 20, 80 < NF, LS < 20.

Finally, it is highly possible that, despite having access to a facility, handwashing with soap and water is being practiced poorly (Wolf et al., 2019), thus further increasing the likelihood of contracting COVID-19 disease.

5. Conclusions

To our knowledge, this is the first time that a measure of inequality was applied to the hygiene sector that takes into consideration the multivariate characteristics of the data. Furthermore, this is also the first attempt to classify the countries into ternary parcels that can later be represented on a thematic map, with the potential application of a spatial analysis.

The construction of the thematic map with each ternary parcel (Qn) offers a better visualization and interpretation of the results, either grouped by region or individually for each country. It is necessary that each ternary parcel (Qn) is read as ternary delimitations, or (in the individual case of a country represented by data in the ternary diagram) as data with tripartite information. Omitting any of the categories in the reading can contribute to inaccuracies in the interpretation of the results. Consequently, in this article, we provide another way to explore and interpret hygiene data in its space, which is the simplex.

Likewise, we propose an alternative measure of urban–rural inequality when the characteristic of the data is compositional and ternary, without infringing on the properties of the data (i.e., scale invariance, subcompositional coherence). This new measure of inequality is different from the simple urban–rural difference that is widely used in global monitoring of household access to drinking water and sanitation services. It has the potential to be applied to the monitoring of urban-rural inequality of the JMP service ladders on estimates of water, sanitation, hygiene, waste management and environmental cleaning in health care facilities (WHO/UNICEF, 2019b), which have tripartite information (basic service, limited service, and no service). It can also be used to monitor urban-rural inequality in the JMP service ladders on drinking water, sanitation, and hygiene in schools (UNICEF and WHO, 2020), which also has tripartite information.

The results we obtained highlight the need to continue to make efforts in rural households, in order to reduce the urban–rural gap that was evidenced in 2017, as they have less availability of basic facilities for handwashing than urban households. This translates into *leaving no one behind*. On the other hand, Colombia is proof that an upper-middle-income country is not necessarily a guarantee of equality in access to on-premise handwashing facilities, given that we identified it as the country with the greatest inequality in 2017.

Achieving universal access to hygiene facilities with soap and water by 2030 will continue to be a challenge, mainly in the countries of the SSA region that were classified in the ternary parcel Q24 (urban: Chad, Benin, Gambia, Rwanda; rural: Angola, Benin, Chad) and Q25 (urban: Cameroon, DR Congo, Guinea-Bissau, Lesotho, Liberia; rural: Cameroon, DR Congo, Guinea-Bissau, Lesotho, Liberia, Togo, Rwanda, Gambia), as they are within the ternary parcels with the worst conditions. In addition, the current pandemic has highlighted the need for households to have facilities to wash their hands with soap and water; continuous hand hygiene will act as a protective barrier, thus reducing the risk of contagion of the SARS-CoV-2 virus or other common diseases.

Finally, it is possible to explore and measure the urban–rural inequality of the compositional data in the ternary diagram when these are tripartite data. When they are in four parts, it can also be calculated in the regular tetrahedron, a subject that is not addressed in this study. For five or more parts, it is necessary first to perform logarithmic ratio transformations to apply any usual statistical technique, a topic that is also not addressed in this research. Therefore, future research should address new methodologies to measure urban–rural inequality when compositional data has four or more parts. We recommend that greater emphasis be placed on the five-part inequality measures, as SDGs 6.1 and 6.2 have five levels of service in the water and sanitation ladders.

Acknowledgements

This research was developed within the framework of a grant from the Peruvian government (Reference PRONABEC-President of the Republic Scholarship), through a full scholarship awarded to Alejandro Quispe Coica, and was partially funded by the Ministry of Science, Innovation and Universities of Spain (Ref: RTI2018-095518-B-C22) and by the Agència de Gestió d'Ajuts Universitaris i de Recerca de la Generalitat de Catalunya (Ref. 2017 SGR 1496).

Appendix A

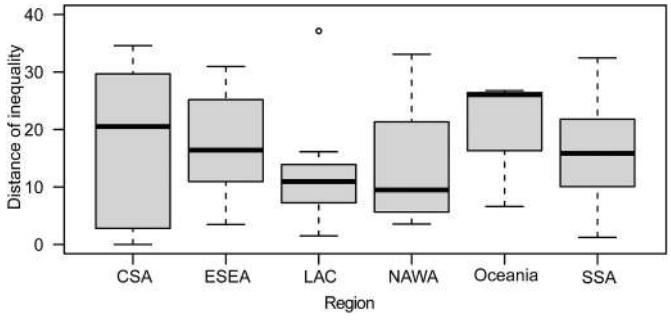

Fig. A1. Boxplot of urban–rural inequality by region

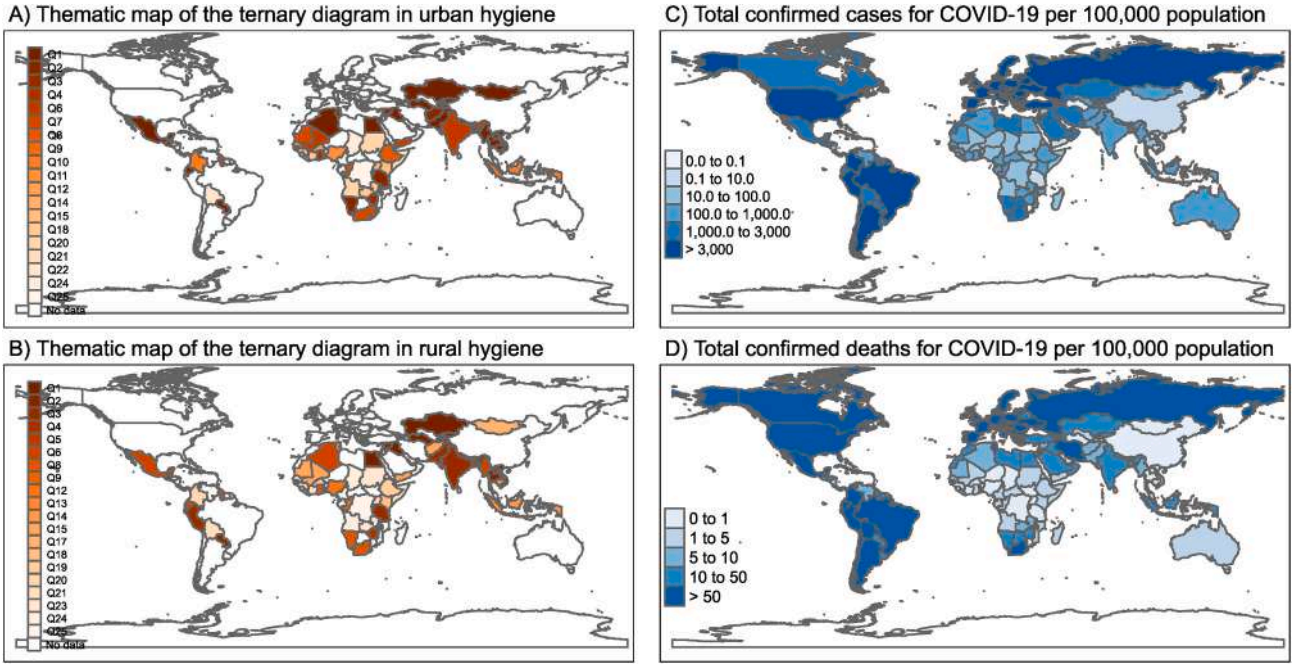

Fig. A2. Urban (A) and rural (B) hygiene service of 2017. Thematic map of confirmed cases (C) and deaths (D) from COVID-19, obtained March 15, 2021 from the WHO platform (see https://covid19.who.int/)

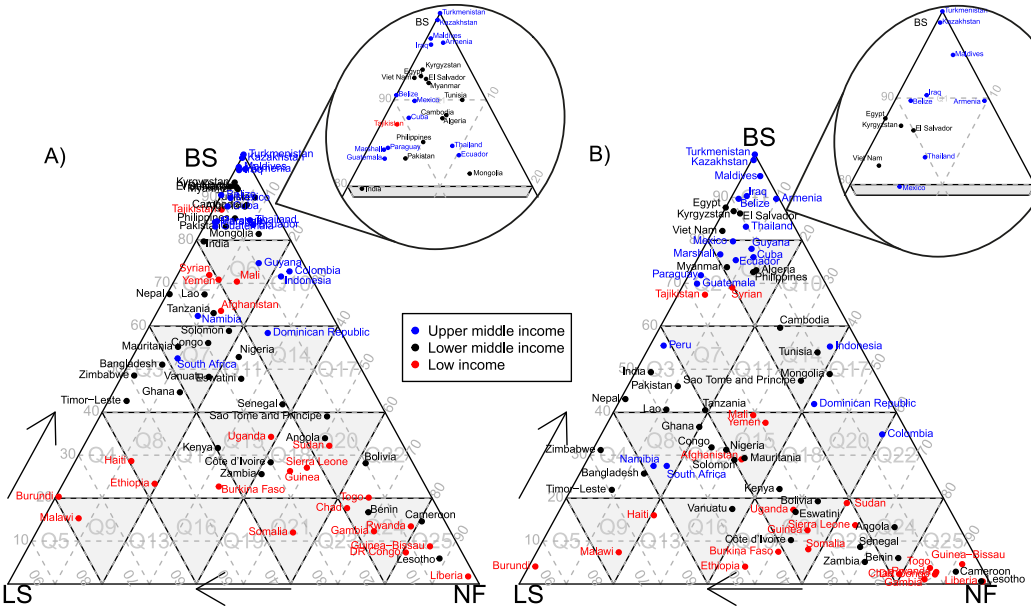

Fig. A3. Urban (left) and rural (right) graphical representation of the countries in the ternary diagram by income. Information on the classification of countries according to their level of wealth was obtained from World Bank (2021).

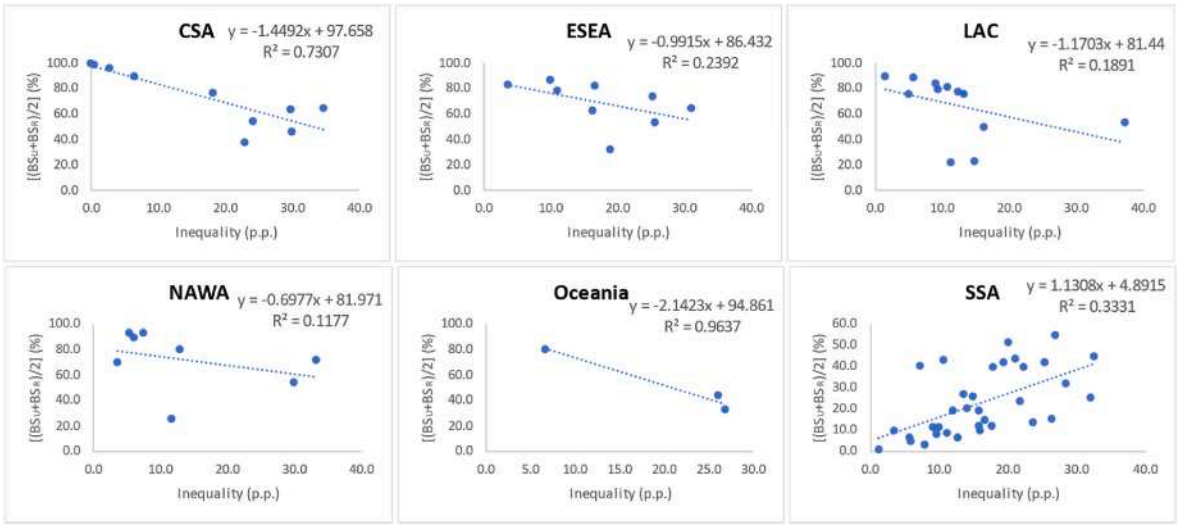

Fig. A4. Linear fit, in the six regions analyzed, between the inequality measure obtained and the average urban and rural BS. The CSA, ESEA, LAC, NAWA and Oceania regions have a negative slope, while the SSA region has a positive slope.

Table A1
Urban and rural classification of countries in the ternary diagram

ID	Urban	Rural
Q1	Algeria, Armenia, Belize, Cambodia, Cuba, Ecuador, Egypt, El Salvador, Guatemala, Iraq, Kazakhstan, Kyrgyzstan, Maldives, Marshall, Mexico, Mongolia, Myanmar, Pakistan, Paraguay, Philippines, Tajikistan, Thailand, Tunisia, Turkmenistan and Vietnam	Armenia, Belize, Egypt, El Salvador, Iraq, Kazakhstan, Kyrgyzstan, Maldives, Thailand, Turkmenistan and Vietnam
Q2	Afghanistan, Laos, Namibia, Nepal, Syria and Tanzania	Guatemala, Paraguay, Syria and Tajikistan
Q3	Bangladesh, Ghana, Timor-Leste, Zimbabwe	India, Laos, Nepal, Pakistan and Tanzania
Q4	Burundi	Bangladesh, Timor-Leste and Zimbabwe
Q5		Burundi
Q6	Guyana, India, Mali and Yemen	Algeria, Cuba, Ecuador, Guyana, Marshall, Mexico, Myanmar and Philippines
Q7	Congo, Mauritania, Solomon, South Africa and Vanuatu	
Q8	Ethiopia and Haiti	Ghana, Namibia and South Africa
Q9	Malawi	Malawi
Q10	Colombia and Indonesia	
Q11	Eswatini, Nigeria and Senegal	
Q12	Burkina Faso	Congo and Nigeria
Q13		Haiti
Q14	Dominican Republic	Cambodia, Indonesia, Sao Tome and Principe and Tunisia
Q15	Kenya and Uganda	Afghanistan, Mali, Mauritania, Solomon and Yemen
Q16		Vanuatu
Q17		Dominican Republic and Mongolia
Q18	Côte d'Ivoire, Guinea, Sierra Leone and Zambia	Kenya
Q19		Burkina Faso and Ethiopia
Q20	Angola, Sao Tome and Principe and Sudan	Colombia
Q21	Somalia	Bolivia, Côte d'Ivoire, Eswatini, Guinea, Somalia and Uganda
Q22	Bolivia and Togo	
Q23		Senegal, Sierra Leone, Sudan and Zambia
Q24	Benin, Chad, Gambia and Rwanda	Angola, Benin and Chad
Q25	Cameroon, DR Congo, Guinea-Bissau, Lesotho and Liberia	Cameroon, DR Congo, Gambia, Guinea-Bissau, Lesotho, Liberia, Rwanda and Togo

Appendix B

As is known, the n parts of the composition can only be represented geometrically in the simplex when they are three and four parts. It is also possible to do a bivariate analysis, for this it is necessary to first merge the n parts of the composition into two as shown in Eq. (B.1). In statistical analysis of compositional data, this procedure is called amalgamation (Greenacre, 2020; Greenacre et al., 2021; Mateu-Figueras and Daunis-i-Estadella, 2008).

$$S^n = \left\{ x = (x_1, x_2, \ldots, x_n) : \forall x_i > 0, \quad \sum_{i=1}^{n} x_i = 100 \right\} \rightarrow S^2 = \{ x = (x_1, x_2) : \forall x_i > 0, \quad x_1 + x_2 = 100 \} \tag{B.1}$$

The geometric figure is a 45° isosceles right triangle. In this geometry, the percentages of the categories can be directly compared and this is a common practice in the WASH sector. To be more explicit, we illustrate the dichotomous variable in Figure B1. The graph has been constructed with a series of dichotomous points that have a constant sum with a value of one. The data points are on the hypotenuse of the triangle.

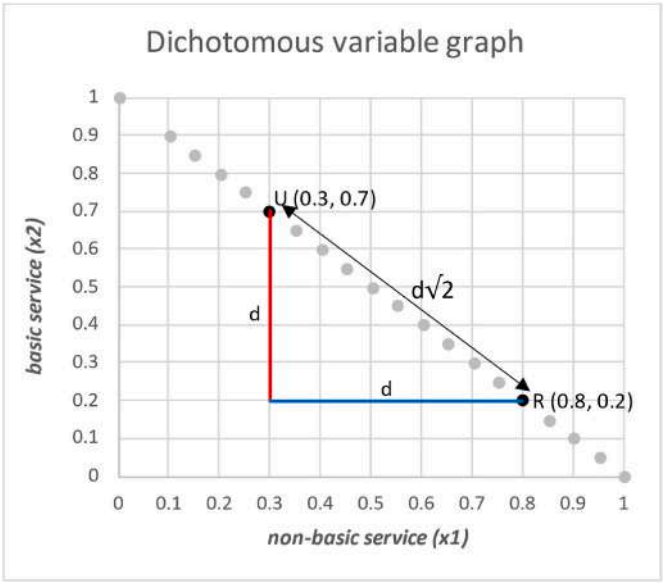

Fig. B.1. d: distance measurement. U: urban. R: rural.

The inequality is calculated by the difference between the vector $\overrightarrow{U}_{(x1,\,x2)}$ and $\overrightarrow{R}_{(x1,\,x2)}$, the result of which is shown in Table B1. The result of the vector difference always gives the same value (i.e., $|U_{x1} - R_{x1}| = |U_{x2} - R_{x2}|$). As an example, we compare the two dichotomous points and the result in both is equal to 0.5 (see Table B1).

Table B.1
Comparison of the urban-rural inequality measure for a dichotomous variable. |Δ|: Absolute value of the urban-rural difference

Urban ($\overrightarrow{U}_{(x1,\,x2)}$)		Rural ($\overrightarrow{R}_{(x1,\,x2)}$)		Δ (Urban - Rural)	
U_{x1}	U_{x2}	R_{x1}	R_{x2}	$\lvert U_{x1} - R_{x1} \rvert$	$\lvert U_{x2} - R_{x2} \rvert$
0.3	0.7	0.8	0.2	0.5	0.5

Now, if we take into account the distance between the two points as a measure of inequality (i.e., $d\sqrt{2}$), we can observe that when normalizing the measure of inequality between the value of zero and one (i.e., divide $d\sqrt{2}$ by $\sqrt{2}$, a result is obtained $d \in [0–1]$), in magnitude, the result is equal to that obtained by the simple difference between the dichotomous variables of urban and rural.

In summary, for dichotomous variables, obtaining a single measure of inequality according to our approach is equal to the simple difference between the parts, as the JMP already does. The interpretation is also the same as that commonly done in the WASH sector. Therefore, in this paper we have focused on the ternary diagram because there was not yet an alternative way of measuring inequality in tripartite data that was consistent with the definitions of compositional data.

References

Abboud, E., 2010. Viviani's theorem and its extension. Coll. Math. J. 41, 203–211. https://doi.org/10.4169/074683410X488683.

Adedokun, K.A., Olarinmoye, A.O., Olarinmoye, A.O., Mustapha, J.O., Kamorudeen, R. T., 2020. A close look at the biology of SARS-CoV-2, and the potential influence of weather conditions and seasons on COVID-19 case spread. Infect. Dis. Poverty 9, 1–5. https://doi.org/10.1186/s40249-020-00688-1.

Ahmad, K., Erqou, S., Shah, N., Nazir, U., Morrison, A.R., Choudhary, G., Wu, W.-C., 2020. Association of poor housing conditions with COVID-19 incidence and mortality across US counties. PLoS One 15, e0241327. https://doi.org/10.1371/journal.pone.0241327.

Aitchison, J., 1986. The Statistical Analysis of Compositional Data (Monographs on Statistics and Applied Probability), first ed. Chapman & Hall, Ltd., London, United Kingdom.

Aitchison, J., 1982. The statistical analysis of compositional data. J. R. Stat. Soc. Ser. B 44, 139–160.

ANDINA, 2021. Perú es el primer país en el mundo en sincerar sus cifras de fallecidos por covid-19. ANDINA: Agencia Peruana de Noticias. https://andina.pe/agencia/noticia-peru-es-primer-pais-el-mundo-sincerar-sus-cifras-fallecidos-covid19-847490.aspx. (Accessed 2 June 2021).

Bartl, A., 2014. Moving from recycling to waste prevention: a review of barriers and enables. Waste Manag. Res. https://doi.org/10.1177/0734242X14541986.

Brauer, M., Zhao, J.T., Bennitt, F.B., Stanaway, J.D., 2020. Global access to handwashing: implications for COVID-19 control in low-income countries. Environ. Health Perspect. 128, 057005 https://doi.org/10.1289/EHP7200.

Curtis, N., Sparrow, A., Ghebreyesus, T.A., Netea, M.G., 2020. Considering BCG vaccination to reduce the impact of COVID-19. Lancet. https://doi.org/10.1016/S0140-6736(20)31025-4.

CDC, 2019. Older Adults and COVID-19. Centers for Disease Control and Prevention. https://www.cdc.gov/coronavirus/2019-ncov/need-extra-precautions/older-adults.html. (Accessed 17 April 2021).

Curtis, V., Cairncross, S., 2003. Effect of washing hands with soap on diarrhoea risk in the community: a systematic review. Lancet Infect. Dis. https://doi.org/10.1016/S1473-3099(03)00606-6.

Dumuid, D., Pedišić, Ž., Palarea-Albaladejo, J., Martín-Fernández, J.A., Hron, K., Olds, T., 2020. Compositional data analysis in time-use epidemiology: what, why, how. Int. J. Environ. Res. Publ. Health 17, 2220. https://doi.org/10.3390/ijerph17072220.

Economic, U.N., Council, S., 2016. Report of the inter-agency and expert group on sustainable development goal indicators. E/CN.3/2016/2/Rev.1. Stat. Comm 13.

Egozcue, J.J., Pawlowsky-Glahn, V., 2011. Basic Concepts and Procedures, en: Compositional Data Analysis: Theory and Applications. John Wiley & Sons, Ltd, Chichester, UK, pp. 12–28. https://doi.org/10.1002/9781119976462.ch2.

Egozcue, J.J., Pawlowsky-Glahn, V., Mateu-Figueras, G., Barceló-Vidal, C., 2003. Isometric logratio transformations for compositional data analysis. Math. Geol. 35, 279–300. https://doi.org/10.1023/A:1023818214614.

Ezbakhe, F., Pérez-Foguet, A., 2020. Child mortality levels and trends: a new compositional approach. Demogr. Res. 43, 1263–1296. https://doi.org/10.4054/DEMRES.2020.43.43.

Ezbakhe, F., Pérez-Foguet, A., 2019. Estimating access to drinking water and sanitation: the need to account for uncertainty in trend analysis. Sci. Total Environ. 696, 133830. https://doi.org/10.1016/j.scitotenv.2019.133830.

Filzmoser, P., Hron, K., Templ, M., 2018. Compositional Data as a Methodological Concept, en: Applied Compositional Data Analysis. Springer Nature, Switzerland, pp. 1–16. https://doi.org/10.1007/978-3-319-96422-5_1.

GESTION, 2021. COVID-19: tasa de letalidad se dispara de 3.5% a 9.4% tras sinceramiento de número de muertos. Diario Gestión. https://gestion.pe/peru/covid-19-en-peru-tasa-de-letalidad-se-dispara-de-35-a-94-tras-sinceramiento-de-cifra-de-muertos-nndc-noticia/. (Accessed 2 June 2021).

Giné-Garriga, R., Flores-Baquero, Ó., Jiménez Fdez de Palencia, A., Pérez-Foguet, A., 2017. Monitoring sanitation and hygiene in the 2030 Agenda for Sustainable Development: a review through the lens of human rights. Sci. Total Environ. 580, 1108–1119. https://doi.org/10.1016/j.scitotenv.2016.12.066.

Giné-Garriga, R., Pérez-Foguet, A., 2010. Improved method to calculate a water poverty index at local scale. J. Environ. Eng. 136, 1287–1298. https://doi.org/10.1061/(ASCE)EE.1943-7870.0000255.

Giraudoux, Patrick, Antonietti, Jean-Philippe, Beale, Colin, Lancelot, Renaud, Pleydell, David, Mike, Treglia, 2021. Pgirmess: Spatial Analysis and Data Mining for Field Ecologists. R package version. https://cran.r-project.org/package=pgirmess. (Accessed 13 June 2021).

Graham, T.R., Gorniak, R., Dembowski, M., Zhang, X., Clark, S.B., Pearce, C.I., Clark, A. E., Rosso, K.M., 2020. Solid-state recrystallization pathways of sodium aluminate hydroxy hydrates. Inorg. Chem. 59, 6857–6865. https://doi.org/10.1021/acs.inorgchem.0c00258.

Greenacre, M., 2020. Amalgamations are valid in compositional data analysis, can be used in agglomerative clustering, and their logratios have an inverse transformation. Appl. Comput. Geosci. 5, 100017. https://doi.org/10.1016/J.ACAGS.2019.100017.

Greenacre, M., Grunsky, E., Bacon-Shone, J., 2021. A comparison of isometric and amalgamation logratio balances in compositional data analysis. Comput. Geosci. 148, 104621. https://doi.org/10.1016/J.CAGEO.2020.104621.

Heller, L., Mota, C.R., Greco, D.B., 2020. COVID-19 faecal-oral transmission: are we asking the right questions? Sci. Total Environ. 729, 138919. https://doi.org/10.1016/j.scitotenv.2020.138919.

Hsiao, C., Shen, Y., Fujiki, H., 2005. Aggregate vs. disaggregate data analysis—a paradox in the estimation of a money demand function of Japan under the low interest rate policy. J. Appl. Econom. 20, 579–601. https://doi.org/10.1002/jae.806.

Huang, Z., Huang, J., Gu, Q., Du, P., Liang, H., Dong, Q., 2020. Optimal temperature zone for the dispersal of COVID-19. Sci. Total Environ. 736, 139487. https://doi.org/10.1016/j.scitotenv.2020.139487.

Lalaoui, R., Bakour, S., Raoult, D., Verger, P., Sokhna, C., Devaux, C., Pradines, B., Rolain, J.M., 2020. What could explain the late emergence of COVID-19 in Africa? New Microbes New Infect. https://doi.org/10.1016/j.nmni.2020.100760.

Lumu, I., 2020. COVID-19 response in sub-saharan Africa: lessons from Uganda. Disaster Med. Public Health Prep. 14, e46–e48. https://doi.org/10.1017/dmp.2020.248.

Mateu-Figueras, G., Daunis-i-Estadella, J., 2008. Compositional Amalgamations and Balances: a Critical Approach. en: CODAWORK'08, Girona (Spain).

Mbow, M., Lell, B., Jochems, S.P., Cisse, B., Mboup, S., Dewals, B.G., Jaye, A., Dieye, A., Yazdanbakhsh, M., 2020. COVID-19 in Africa: dampening the storm? Science 369, 624–626.

Miller, A., Reandelar, M.J., Fasciglione, K., Roumenova, V., Li, Y., Otazu, G.H., 2020. Correlation between Universal BCG Vaccination Policy and Reduced Mortality for COVID-19. medRxiv. https://doi.org/10.1101/2020.03.24.20042937.

Miller, W.E., 2002. Revisiting the geometry of a ternary diagram with the half-taxi metric. Math. Geol. 34, 275–290. https://doi.org/10.1023/A:1014842906442.

Nachega, J.B., Mbala-Kingebeni, P., Otshudiema, J., Mobula, L.M., Preiser, W., Kallay, O., Michaels-Strasser, S., Breman, J.G., Rimoin, A.W., Nsio, J., Ahuka-Mundeke, S., Zumla, A., Tam-Fum, J.J.M., 2020. Responding to the challenge of the dual Covid-19 and ebola epidemics in the democratic republic of Congo'priorities for achieving control. Am. J. Trop. Med. Hyg. https://doi.org/10.4269/ajtmh.20-0642.

Pal, M., Berhanu, G., Desalegn, C., Kandi, V., 2020. Severe acute respiratory syndrome coronavirus-2 (SARS-CoV-2): an update. Cureus 12. https://doi.org/10.7759/cureus.7423.

Pandey, D., Verma, S., Verma, P., Mahanty, B., Dutta, K., Daverey, A., Arunachalam, K., 2021. SARS-CoV-2 in wastewater: challenges for developing countries. Int. J. Hyg Environ. Health. https://doi.org/10.1016/j.ijheh.2020.113634.

Pawlowsky-Glahn, V., Egozcue, J.J., 2006. Compositional data and their analysis: an introduction. Geol. Soc. London, Spec. Publ. 264, 1–10. https://doi.org/10.1144/GSL.SP.2006.264.01.01.

Payne, C., 2020. COVID-19 in Africa. Nat. Hum. Behav. 4, 436–437. https://doi.org/10.1038/s41562-020-0870-5.

Pebesma, E., 2018. Simple features for R: standardized support for spatial vector data. RIO J. 10, 439–446. https://doi.org/10.32614/RJ-2018-009.

Pérez-Foguet, A., Giné-Garriga, R., Ortego, M.I.I., 2017. Compositional data for global monitoring: the case of drinking water and sanitation. Sci. Total Environ. 590–591, 554–565. https://doi.org/10.1016/j.scitotenv.2017.02.220.

Pomberger, R., Sarc, R., Lorber, K.E., 2017. Dynamic visualisation of municipal waste management performance in the EU using Ternary Diagram method. Waste Manag. 61, 558–571. https://doi.org/10.1016/j.wasman.2017.01.018.

Quispe-Coica, A., Pérez-Foguet, A., 2020. Preprocessing alternatives for compositional data related to water, sanitation and hygiene. Sci. Total Environ. 743, 140519. https://doi.org/10.1016/j.scitotenv.2020.140519.

Quispe-Coica, Alejandro, Pérez-Foguet, Agustí, 2021. Multivariate measure of urban-rural inequality of hygiene facilities (R code). Zenodo. https://doi.org/10.5281/zenodo.5593837.

R Core Team, 2020. R: A Language and Environment for Statistical Computing.

Rabie, T., Curtis, V., 2006. Handwashing and risk of respiratory infections: a quantitative systematic review. Trop. Med. Int. Health. https://doi.org/10.1111/j.1365-3156.2006.01568.x.

Shahid, N.S., Greenough III, W.B., Samadi, A.R., Huq, M.I., Rahman, N., 1996. Hand washing with soap reduces diarrhoea and spread of bacterial pathogens in a Bangladesh village. J. Diarrhoeal Dis. Res. 85–89.

Shahid, Z., Kalayanamitra, R., McClafferty, B., Kepko, D., Ramgobin, D., Patel, R., Aggarwal, C.S., Vunnam, R., Sahu, N., Bhatt, D., Jones, K., Golamari, R., Jain, R., 2020. COVID-19 and older adults: what we know. J. Am. Geriatr. Soc. 68, 926–929. https://doi.org/10.1111/jgs.16472.

Stoler, J., Miller, J.D., Brewis, A., Freeman, M.C., Harris, L.M., Jepson, W., Pearson, A.L., Rosinger, A.Y., Shah, S.H., Staddon, C., Workman, C., Wutich, A., Young, S.L., Adams, E., Ahmed, F., Alexander, M., Asiki, G., Balogun, M., Boivin, M.J., Carrillo, G., Chapman, K., Cole, S., Collins, S.M., Eini-Zinab, H., Escobar-Vargas, J., Ghattas, H., Ghorbani, M., Hagaman, A., Hawley, N., Jamaluddine, Z., Krishnakumar, D., Maes, K., Mathad, J., Maupin, J., Owuor, P.M., Melgar-Quiñonez, H., Morales, M.M., Moran, J., Omidvar, N., Rasheed, S., Samayoa-Figueroa, L., Sánchez-Rodriguez, E.C., Santoso, M.V., Schuster, R.C., Sheikhi, M., Srivastava, S., Sullivan, A., Tesfaye, Y., Triviño, N., Trowell, A., Tshala-Katumbay, D., Tutu, R., 2021. Household water insecurity will complicate the ongoing COVID-19 response: evidence from 29 sites in 23 low- and middle-income countries. Int. J. Hyg Environ. Health 234, 113715. https://doi.org/10.1016/j.ijheh.2021.113715.

Synowiec, A., Szczepański, A., Barreto-Duran, E., Lie, L.K., Pyrc, K., 2021. Severe acute respiratory syndrome coronavirus 2 (SARS-CoV-2): a systemic infection. Clin. Microbiol. Rev. 34 https://doi.org/10.1128/cmr.00133-20.

Tcheutchoua, D.N., Tankeu, A.T., Wouna Angong, D.L., Agoons, B.B., Yanwou Nguemnang, N.Y., Nana Djeunga, H.C., Kamgno, J., 2020. Unexpected low burden of coronavirus disease 2019 (COVID-19) in sub-Saharan Africa region despite disastrous predictions: reasons and perspectives. Pan Afr. Med. J. 37 https://doi.org/10.11604/pamj.2020.37.352.25254.

Tennekes, M., 2018. Tmap: thematic maps in R. J. Stat. Software 84, 1–39. https://doi.org/10.18637/jss.v084.i06.

Townsend, J., Greenland, K., Curtis, V., 2017. Costs of diarrhoea and acute respiratory infection attributable to not handwashing: the cases of India and China. Trop. Med. Int. Health 22, 74–81. https://doi.org/10.1111/tmi.12808.

Troeger, C., Blacker, B.F., Khalil, I.A., Rao, P.C., Cao, S., Zimsen, S.R., Albertson, S.B., Stanaway, J.D., Deshpande, A., Abebe, Z., Alvis-Guzman, N., Amare, A.T., Asgedom, S.W., Anteneh, Z.A., Antonio, C.A.T., Aremu, O., Asfaw, E.T., Atey, T.M., Atique, S., Avokpaho, E.F.G.A., Awasthi, A., Ayele, H.T., Barac, A., Barreto, M.L., Bassat, Q., Belay, S.A., Bensenor, I.M., Bhutta, Z.A., Bijani, A., Bizuneh, H., Castañeda-Orjuela, C.A., Dadi, A.F., Dandona, L., Dandona, R., Do, H.P., Dubey, M., Dubljanin, E., Edessa, D., Endries, A.Y., Eshrati, B., Farag, T., Feyissa, G.T., Foreman, K.J., Forouzanfar, M.H., Fullman, N., Gething, P.W., Gishu, M.D., Godwin, W.W., Gugnani, H.C., Gupta, R., Hailu, G.B., Hassen, H.Y., Hibstu, D.T., Ilesanmi, O.S., Jonas, J.B., Kahsay, A., Kang, G., Kasaeian, A., Khader, Y.S., Khan, E. A., Khan, M.A., Khang, Y.H., Kissoon, N., Kochhar, S., Kotloff, K.L., Koyanagi, A., Kumar, G.A., Magdy Abd El Razek, H., Malekzadeh, R., Malta, D.C., Mehata, S., Mendoza, W., Mengistu, D.T., Menota, B.G., Mezgebe, H.B., Mlashu, F.W., Murthy, S., Naik, G.A., Nguyen, C.T., Nguyen, T.H., Ningrum, D.N.A., Ogbo, F.A., Olagunju, A.T., Paudel, D., Platts-Mills, J.A., Qorbani, M., Rafay, A., Rai, R.K., Rana, S.M., Ranabhat, C.L., Rasella, D., Ray, S.E., Reis, C., Renzaho, A.M., Rezai, M. S., Ruhago, G.M., Safiri, S., Salomon, J.A., Sanabria, J.R., Sartorius, B., Sawhney, M., Sepanlou, S.G., Shigematsu, M., Sisay, M., Somayaji, R., Sreeramareddy, C.T., Sykes, B.L., Taffere, G.R., Topor-Madry, R., Tran, B.X., Tuem, K.B., Ukwaja, K.N., Vollset, S.E., Walson, J.L., Weaver, M.R., Weldegwergs, K.G., Werdecker, A., Workicho, A., Yenesew, M., Yirsaw, B.D., Yonemoto, N., El Sayed Zaki, M., Vos, T., Lim, S.S., Naghavi, M., Murray, C.J., Mokdad, A.H., Hay, S.I., Reiner, R.C., 2018. Estimates of the global, regional, and national morbidity, mortality, and aetiologies of diarrhoea in 195 countries: a systematic analysis for the Global Burden of Disease Study 2016. Lancet Infect. Dis. 18, 1211–1228. https://doi.org/10.1016/S1473-3099(18)30362-1.

UNICEF and WHO, 2020. Progress on Drinking Water, Sanitation and Hygiene in School: Special Focus on COVID-19. UNICEF, New York.

United Nations Department of Economic and Social Affairs Population Division, 2019. World Population Prospects, Online Edition. Rev. 1.

United Nations General Assembly, 2015. General Assembly Resolution A/RES/70/1. Transforming Our World: the 2030 Agenda for Sustainable Development.

van den Boogaart, K.G., Tolosana-Delgado, R., 2013a. Fundamental concepts of compositional data analysis, en: Analyzing Compositional Data with R. Springer, Berlin Heidelberg, pp. 13–50. https://doi.org/10.1007/978-3-642-36809-7_2.

van den Boogaart, K.G., Tolosana-Delgado, R., 2013b. Introduction, en: Analyzing Compositional Data with R. Springer, Berlin Heidelberg, pp. 1–12. https://doi.org/10.1007/978-3-642-36809-7_1.

van Doremalen, N., Bushmaker, T., Morris, D.H., Holbrook, M.G., Gamble, A., Williamson, B.N., Tamin, A., Harcourt, J.L., Thornburg, N.J., Gerber, S.I., Lloyd-Smith, J.O., de Wit, E., Munster, V.J., 2020. Aerosol and surface stability of SARS-CoV-2 as compared with SARS-CoV-1. N. Engl. J. Med. 382, 1564–1567. https://doi.org/10.1056/nejmc2004973.

Verma, S.P., 2020. Multidimensional Techniques for Compositional Data Analysis, en: Road from Geochemistry to Geochemometrics. Springer Singapore, pp. 441–479. https://doi.org/10.1007/978-981-13-9278-8_11.

Von Eynatten, H., Pawlowsky-Glahn, V., Egozcue, J.J., 2002. Understanding perturbation on the simplex: a simple method to better visualize and interpret compositional data in ternary diagrams. Math. Geol. 34, 249–257. https://doi.org/10.1023/A:1014826205533.

WHO/UNICEF, 2020. Hygiene Baselines Pre-COVID-19. JMP.

WHO/UNICEF, 2019a. Progress on Household Drinking Water, Sanitation and Hygiene 2000-2017: Special Focus on Inequalities, WHO. United Nations Children's Fund (UNICEF) and World Health Organization, New York.
WHO/UNICEF, 2019b. WASH in Health Care Facilities: Global Baseline Report 2019. World Health Organization, Geneva.
WHO/UNICEF, 2016. Inequalities in sanitation and drinking water in Latin America and the Caribbean, en: Inequalities in sanitation and drinking water in Latin America and the Caribbean, p. 12.
WHO/UNICEF, 2015. Task Force on Monitoring Inequalities for the 2030 Sustainable Development Agenda Meeting Report. WHO/UNICEF, New York, NY, USA.
WHO, 2020a. Recommendations to Member States to Improve Hand Hygiene Practices to Help Prevent the Transmission of the COVID-19 Virus: Interim Guidance, 1 April 2020. World Health Organization, Geneva PP - Geneva.
WHO, 2020b. Transmission of SARS-CoV-2: Implications for Infection Prevention Precautions: Scientific Brief, 09 July 2020. World Health Organization, Geneva PP - Geneva.
Wickham, H., 2016, 2.[a] ed. ggplot2: Elegant Graphics for Data Analysis. Use R! Springer Nature, New York. https://doi.org/10.1007/978-3-319-24277-4.
Wickham, H., Averick, M., Bryan, J., Chang, W., McGowan, L.D., François, R., Grolemund, G., Hayes, A., Henry, L., Hester, J., Kuhn, M., Pedersen, T.L., Miller, E., Bache, S.M., Müller, K., Ooms, J., Robinson, D., Seidel, D.P., Spinu, V., Takahashi, K., Vaughan, D., Wilke, C., Woo, K., Yutani, H., 2019. Welcome to the tidyverse. J. Open Source Softw. 4, 1686. https://doi.org/10.21105/joss.01686.
Wolf, J., Johnston, R., Freeman, M.C., Ram, P.K., Slaymaker, T., Laurenz, E., Prüss-Ustün, A., 2019. Handwashing with soap after potential faecal contact: global, regional and country estimates. Int. J. Epidemiol. 48, 1204–1218. https://doi.org/10.1093/ije/dyy253.
World Bank, 2021. GDP per capita (current US$) | Data. World Bank Open Data. https://data.worldbank.org/indicator/NY.GDP.PCAP.CD. (Accessed 9 March 2018).
Zerbo, A., Castro Delgado, R., Arcos González, P., 2021. Water sanitation and hygiene in Sub-Saharan Africa: coverage, risks of diarrheal diseases, and urbanization. J. Biosaf. Biosecurity 3, 41–45. https://doi.org/10.1016/J.JOBB.2021.03.004.

International Journal of Hygiene and Environmental Health 239 (2022) 113864

Contents lists available at ScienceDirect

International Journal of Hygiene and Environmental Health

journal homepage: www.elsevier.com/locate/ijheh

Climate variability and seasonal patterns of paediatric parainfluenza infections in the tropics: An ecological study in Singapore

Stacy Soh [a], Liat Hui Loo [b,c], Natasha Jamali [d], Matthias Maiwald [b,c,e], Joel Aik [a,f,*]

[a] Environmental Epidemiology and Toxicology Division, National Environment Agency, 40 Scotts Road, Environment Building, #13-00, 228231, Singapore
[b] Department of Pathology and Laboratory Medicine, KK Women's and Children's Hospital, 100 Bukit Timah Road, 229899, Singapore
[c] Duke-NUS Graduate Medical School, 8 College Road, 169857, Singapore
[d] Environmental Monitoring and Modelling Division, National Environment Agency, 40 Scotts Road, #13-00, 228231, Singapore
[e] Department of Microbiology and Immunology, Yong Loo Lin School of Medicine, NUHS Tower Block, 1E Kent Ridge Road Level 11, 119228, Singapore
[f] Pre-Hospital & Emergency Research Centre, Duke-NUS Medical School, 8 College Road, 169857, Singapore

ARTICLE INFO

Keywords:
Parainfluenza virus
Paediatric
Time series
Singapore
Climate variability

ABSTRACT

Objectives: Evidence of the relationship between climate variability, air pollution and human parainfluenza virus (HPIV) infections has been inconsistent. We assessed this in a paediatric population from a highly urbanized tropical city-state.

Methods: We analysed all reports of HPIV infections in children <5 years old obtained from a major specialist women and children's hospital in Singapore. Assuming a negative binomial distribution and using multivariable fractional polynomial modelling, we examined the relations between climate variability, air quality and the risk of HPIV infections, adjusting for time-varying confounders.

Results: We identified 6393 laboratory-confirmed HPIV infections from 2009 to 2019. Every 1 °C decline in temperature was associated with a 5.8% increase (RR: 0.943, 95% Confidence Interval [95% CI]: 0.903–0.984) in HPIV infection risk 6 days later. Every 10% decrease in relative humidity was associated with a 15.8% cumulative increase in HPIV risk over the next 6 days (cumulative RR: 0.842, 95% CI: 0.771–0.919). Rainfall was positively associated with HPIV risk 2 days later (RR: 1.021, 95% CI: 1.000–1.043). A within-year seasonal rise of HPIV was driven by HPIV-3 and HPIV-1 and preceded by a seasonal decline in temperature. Gender was an effect modifier of the climate-HPIV relationship. Air quality was not associated with HPIV risk.

Conclusions: This study demonstrates a close association between HPIV infection risk and tropical climate variability. The climate dependence and seasonal predictability of HPIV can inform the timing of community campaigns aimed at reducing infection risk and the development of hospital resources and climate adaption plans.

1. Introduction

Human parainfluenza viruses (HPIVs) are a common cause of respiratory infections in infants and children worldwide. HPIVs are the second leading cause of hospitalizations associated with lower respiratory illness in children under 5 years of age, following respiratory syncytial virus (RSV) (Schmidt et al., 2011). In addition to local HPIV circulation within Vietnam, new HPIV lineages from different geographical regions have been detected as well (Linster et al., 2018). HPIV has been found to manifest with acute lower respiratory illness, which has been reported as a main cause of hospitalization in Malaysia (Khor et al., 2012). HPIV symptoms vary by both the serotype and host and are associated with a spectrum of illness (Schomacker et al., 2012). HPIV-1 and -2 are most often associated with croup (Frost et al., 2014) while HPIV-3 occurs endemically throughout the year and is more often associated with bronchiolitis, bronchitis and pneumonia (Henrickson, 2003). Despite ongoing developmental efforts, a licensed vaccine is not yet available (Schmidt et al., 2011).

While all HPIVs are responsible for infections throughout the year, several studies have documented distinct seasonal trends for HPIV-1, -2

* Corresponding author. Environmental Epidemiology and Toxicology Division, National Environment Agency, 40 Scotts Road, Environment Building, #13-00, 228231, Singapore.
E-mail addresses: stacy_soh@nea.gov.sg (S. Soh), loo.liat.hui@kkh.com.sg (L.H. Loo), Natasha_Jamali@nea.gov.sg (N. Jamali), matthias.maiwald@singhealth.com.sg (M. Maiwald), joel_aik@nea.gov.sg (J. Aik).

https://doi.org/10.1016/j.ijheh.2021.113864
Received 25 July 2021; Received in revised form 9 October 2021; Accepted 14 October 2021
Available online 28 October 2021

and -3 in the northern hemisphere (Price et al., 2019; Swamy et al., 2016). HPIV-3 activity peaks annually in the spring and summer months, while HPIV-1 peaks biennially during the fall months in the United States (Fry et al., 2006). Different environments with varying climatic factors influence the interaction of the pathogens with the host, affecting the probability of exposure and infection (du Prel et al., 2009). Studies have reported inconsistent associations between climate variability and HPIV infections. Temperature and rainfall were found to be positively correlated with paediatric reports of HPIV (Yan et al., 2015) in one study, while another study found an inverse correlation between HPIV and temperature (du Prel et al., 2009). Similarly, other studies have reported opposing associations of HPIV with relative humidity (Price et al., 2019; Cheon et al., 2019).

Unlike RSV and Influenza infections, the relationship between climate variability with HPIV is less well documented, with most studies being carried out in temperate climates and few in tropical settings. In this study, we aimed to quantify the effect of climate variability on paediatric HPIV infections in tropical Singapore.

2. Methods

2.1. Ethics statement

This study was granted approval by the Environmental Health Institute of the National Environment Agency (NEA), Singapore.

2.2. Research setting

Singapore is a small, heavily urbanized city-state located within the tropics of Southeast Asia. Situated near the equator, Singapore experiences a tropical climate with high humidity, abundant rainfall and high temperatures all year round. The largest referral centre in Singapore dedicated to women's and children's healthcare is KK Women's and Children's Hospital (KKH), an 830-bed hospital specializing in obstetrics, gynaecology, paediatrics and neonatology.

2.3. Outcome measure

We included all daily reports of laboratory-confirmed serotype- and gender-specific paediatric HPIV infections under 5-years of age from KKH from 2009 to 2019. Duplicate positive samples from the same patients were excluded before analysis. Multiplex reverse-transcriptase polymerase chain reaction (RT-PCR) and immunofluorescence (IF) testing was used to confirm the presence of HPIV in nasopharyngeal swab samples obtained from hospital patients. Specimens were collected on flocked swabs, submitted in universal transport medium and tested within 12 h (h). Viral RNA was extracted following the manufacturer's instructions. Between 2009 and August 2012, the hospital used the Seeplex RV12 OneStep ACE multiplex PCR detection kit, then the Seeplex RV15 OneStep ACE detection kit (both Seegene Inc., South Korea) (Seegene Inc. Seeplex®15, 2021). This was replaced in March 2018 with the Biofire Respiratory Panel 1.0 multiplex PCR, and in July 2019 with the Biofire Respiratory Panel 2.0 (both BioFire Diagnostics, Inc. Salt Lake City, Utah) (Biofire DiagnosticsC., 2021). Respiratory virus direct IF testing (D3 Double Duet DFA Respiratory Virus immunofluorescence kit, Diagnostic Hybrids, Athens, OH, USA) (Quidel Corporation, 2021) was performed during the entire period 2009–2019. Testing was based on physician requests. The Seeplex PCRs targeted 12 (including HPIV-1, -2, -3) and 15 (including HPIV-1, -2, -3, -4) different respiratory viruses, the Biofire Respiratory Panel 1.0 and 2.0 targeted 17 and 18 different pathogens, respectively (both including HPIV-1, -2, -3 -4), and the Double Duet IF kit targeted 8 different viruses (including HPIV-1, -2, -3). All primer and probe sequences and IF antibodies were of a proprietary nature, supplied by the kit manufacturers.

3. Climate and air quality data

We obtained contemporaneous climate data comprising mean temperature, relative humidity and rainfall from the 11 weather monitoring stations located across Singapore from the Meteorological Services Singapore (MSS). We computed the arithmetic mean of each meteorological factor across all weather stations to derive daily national mean measures of temperature, relative humidity and rainfall. We obtained from NEA daily measures of nitrogen dioxide (NO_2), carbon monoxide (CO), sulphur dioxide (SO_2), ozone (O_3), particulate matter of aerodynamic diameter of <2.5 μm ($PM_{2.5}$) and <10 μm (PM_{10}) averaged across the island.

3.1. Statistical analyses

We analysed the short-term associations between paediatric reports of HPIV with meteorological factors on a daily timescale. We assumed a negative binomial distribution to account for over-dispersion in the outcome measure. In the core model, we accounted for the long-term trend and within-year seasonal patterns of HPIV infections. We modelled seasonal patterns using Fourier terms that captured periodic annual and 6-monthly cycles of infections. We also included a day-of-the week categorical term to capture within-week variations in infections. As an offset, we fitted the logged daily population estimates of those under 5 years of age interpolated from the annual mid-year population census data. We used a categorical variable to account for the potential change in HPIV trends following the switches in diagnostic test methods.

The incubation period of HPIV infections has been reported to be between 2 and 6 days (d) (Lessler et al., 2009), with a potential for fomite transmission of up to 4 and 10 h after deposition on absorptive and non-absorptive surfaces, respectively (Brady et al., 1990). We therefore made an *a priori* assumption that changes in climate effects up to 7 d before the detection of HPIV could potentially be causally associated with an infection. We used multivariable fractional polynomial modelling to investigate non-linear associations between HPIV and climate and air quality parameters up to a maximum 7-day lag period. We simultaneously included the immediate and lagged effects of each of these factors into the core model and used backward elimination to obtain the most parsimonious penultimate model by retaining terms at a 10% level of significance. Finally, we examined the autocorrelation function plots of the penultimate model before adding lags of its deviance residuals to adjust for any observed serial correlation. We used the Likelihood Ratio Test (LRT) to evaluate the statistical significance of pairs of Fourier terms as well as any categorical terms retained in the model. We assessed model fit by using the Akaike Information Criterion (AIC) (Akaike, 1974). Air quality parameters were not significantly included in our final model. Non-significant weather terms were also excluded. The final multivariable regression model is described in Equation (1):

$$\begin{aligned}\log E(Y_t) = {} & \beta_0 + \beta_1 t \\ & + \sum_{m=1}^{2}\left\{\beta_{2(m)}\sin\left(\frac{2\pi m t}{365.25}\right) + \beta_{3(m)}\cos\left(\frac{2\pi m t}{365.25}\right)\right\} \\ & + \beta_{4d} DOW_{d=1\,to\,7} + \beta_5 temperature_{i=6} + \beta_6 humidity_{i=1} + \beta_7 humidity_{i=6} \\ & + \beta_8 rainfall_{i=2} + \beta_{9_p} period_{p=1\,to\,4} + \beta_{10_i} devres_{i=2,3,4,5,7,8,9,13,15,16} \\ & + \log(N_t)\end{aligned} \tag{1}$$

Where $E(Y_t)$ represents the expected number of paediatric reports of HPIV at day t. β_o denotes the model intercept, t represents the linear function of time and m refers to the number of full oscillation cycles within the year. *DOW* is a categorical variable denoting the day of the week. *temperature*, *humidity* and *rainfall* represent the mean ambient air temperature, relative humidity and cumulative rainfall, respectively,

and *i* corresponds to the lag day of the indicated numeral. *period* distinguishes the time periods between the previous and new multiplex PCR systems that were used for laboratory confirmation. *devres* represents the deviance residuals derived from the penultimate model and *i* corresponds to the lag day of the indicated numeral. β_1 to β_{10i} each represent the effect of the respective independent variables. $log(N_t)$ represents the child population offset term.

We fitted separate models for each gender to investigate effect modification of the climate-HPIV infection association. We examined the seasonal components of HPIV infections from the final model with the seasonal components of each individual HPIV type and the climate variables for trend consistency. In sensitivity analysis, we assessed the robustness of our main results in relation to the degree of seasonal control by adding Fourier terms that modelled higher cyclical frequency disease patterns.

3.2. Software

All statistical analyses were carried out using STATA 12.1 software (StataCorp, USA). In the final model, statistical significance was evaluated at the 5% level.

4. Results

4.1. Descriptive statistics

Over the study period from 2009 to 2019, there were 6393 paediatric reports of laboratory-confirmed HPIV infections, with an average of 1.59 reports per day. HPIV-3 (61.0%) and HPIV-1 (29.0%) were most frequently detected (Table 1). Among all HPIV reports, 1491 (23.3%) were confirmed by RT-PCR and 4901 (76.7%) were confirmed by IF testing. The mean age of children with HPIV infections was 1.42 years (SD: 1.13 years). Eight repeat positive results from the same patients were excluded. There were 38 individuals with at least two HPIV co-infections. There were more infections among males than among females. Mean daily ambient temperature did not vary considerably from the daily mean, and mean daily relative humidity was generally high throughout the year. Rainfall levels were higher at the end of the year.

Table 1
Summary of reported HPIV infections and climatic factors in Singapore, 2009 to 2019.

Variable	Counts/ N (%)	Daily Measures				
		Mean ± SD	Median	IQR	Min	Max
Paediatric HPIV	6393 (100%)	1.59 ± 1.64	1	0–2	0	12
Age (in years)	6393 (100%)	1.42 ± 1.13	1.13	0.51–2.05	0.02	5.0
Type						
HPIV-1	1852 (29.0%)	0.46 ± 0.78	0	0–1	0	6
HPIV-2	405 (6.3%)	0.10 ± 0.33	0	0–0	0	4
HPIV-3	3897 (61.0%)	0.97 ± 1.23	0	0–2	0	9
HPIV-4	239 (3.7%)	0.06 ± 0.30	0	0–0	0	5
Gender						
Male	3640 (56.9%)	0.91 ± 1.13	1	0–1	0	9
Female	2753 (43.1%)	0.69 ± 0.98	0	0–1	0	7
Climatic Factors						
Mean Temperature (°C)	4017 (100%)	27.9 ± 1.1	27.9	27.1–28.7	22.8	30.8
Relative Humidity (%)	4017 (100%)	79.2 ± 5.4	79.1	75.3–83.0	59.2	96.9
Rainfall (mm)	4017 (100%)	5.3 ± 12.5	0	0–4	0	216.2
Air Quality						
$PM_{2.5}$ ($\mu g/m^3$)	4017 (100%)	18.3 ± 12.6	15.8	12.6–20.4	5.1	274.4
PM_{10} ($\mu g/m^3$)	4017 (100%)	30.2 ± 15.5	27.5	23.0–33.6	9.7	335.9
O_3 ($\mu g/m^3$)	4017 (100%)	24.4 ± 10.1	22.6	17.3–30.2	4.4	76.0
NO_2 ($\mu g/m^3$)	4017 (100%)	23.9 ± 7.2	23.3	18.8–28.5	6.8	53.4
SO_2 ($\mu g/m^3$)	4017 (100%)	10.5 ± 6.0	9.8	5.4–14.0	2.0	45.0
CO (mg/m^3)	4017 (100%)	0.5 ± 0.2	0.5	0.4–0.6	0.2	3.3

HPIV, human parainfluenza virus; SD, standard deviation; IQR, interquartile range.

4.2. Multivariable regression modelling

4.2.1. Long-term trend and cyclical patterns

There was a general increase in the number of HPIV ($p<0.001$) infections over the study duration, even after accounting for population changes, with distinct 12- and 6-monthly cycles (see Supplementary Material, Table S1). Relative to Mondays, the daily number of HPIV infections declined as the week progressed (see Fig. 1). Changes in the multiplex PCR system from Seeplex RV12 to Seeplex RV15, Biofire RP1.0 and Biofire RP2.0 were independently associated with increases in detected HPIV infections (see Fig. 1).

4.2.2. Meteorological and air quality effects

A 1°C decrease in ambient air temperature on the present day was associated with a 5.7% increase in HPIV infections 6 d later (RR: 0.943, 95% CI: 0.903 to 0.984). A 10% decrease in mean relative humidity on the present day was associated with an independent, subsequent increase in HPIV risk 1 d (RR: 0.933, 95% CI: 0.882–0.983) and 6 d later (RR: 0.902, 95% CI: 0.829–0.973). This was equivalent to a cumulative 15.8% increase in HPIV risk (RR: 0.842, 95% CI: 0.771–0.919) due to the decline in humidity. We observed evidence of a positive rainfall effect (RR: 1.021, 95% CI: 1.000–1.043). Multivariable fractional polynomial modelling did not reveal any non-linear meteorological relations with HPIV (see Supplementary Material, Annex 1). There was no evidence that relative humidity altered the relationship between temperature and HPIV risk 6 d later ($p=0.494$). Air quality was not associated with HPIV risk (Table S2).

There was no residual autocorrelation in our final model (see Supplementary Material, Annex 2). The AIC value for our final model improved from 3.05 to 3.02, indicating a better model fit after accounting for meteorological effects and autocorrelation. In period-stratified sensitivity analysis, the weather-HPIV risk estimates were similar when the Seeplex RV12 and RV15 were used (Table S3). There was insufficient study power to assess the weather-HPIV risk estimates in the periods where the Biofire RP1.0 and Biofire RP2.0 systems were used.

4.2.3. Gender effect modification

We observed a gender difference in meteorologically-driven HPIV risk. Female HPIV risk was driven by mean ambient air temperature ($RR_{Females}$: 0.927, 95% CI: 0.868–0.992) and relative humidity ($RR_{Females}$: 0.779, 95% CI: 0.681–0.891) while male HPIV-risk was driven by rainfall (RR_{Males}: 1.028, 95% CI: 1.002–1.059) (see Fig. 2).

4.3. Seasonal component analysis

HPIV infections peaked in April and declined until September and then rose again. The within-year seasonal decline in ambient air temperature occurred prior to the seasonal rise in HPIV infections (Fig. 3). The seasonal components for relative humidity and rainfall and the relationship to HPIV incidence were less conclusive (Supplementary

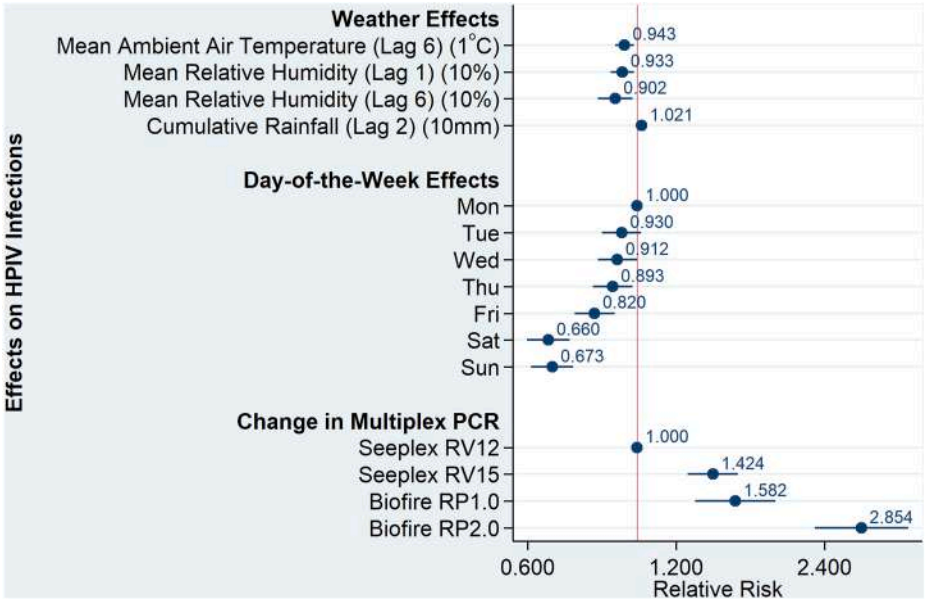

Fig. 1. Independent effects of meteorological factors and day-of-the-week on HPIV infections. The solid navy circles represent the point estimates of the independent effects, while the horizontal navy lines represent the 95% confidence intervals. The number of days between the respective meteorological exposure and the subsequent observed change in HPIV risk is indicated in brackets (i.e. lag X). The vertical solid red line represents the null effect. For the weather effects, the average measurements were set as relative risk of 1. For the day-of-the-week effects, Monday, and for the multiplex PCRs, the Seeplex RV12 were set as 1, respectively.

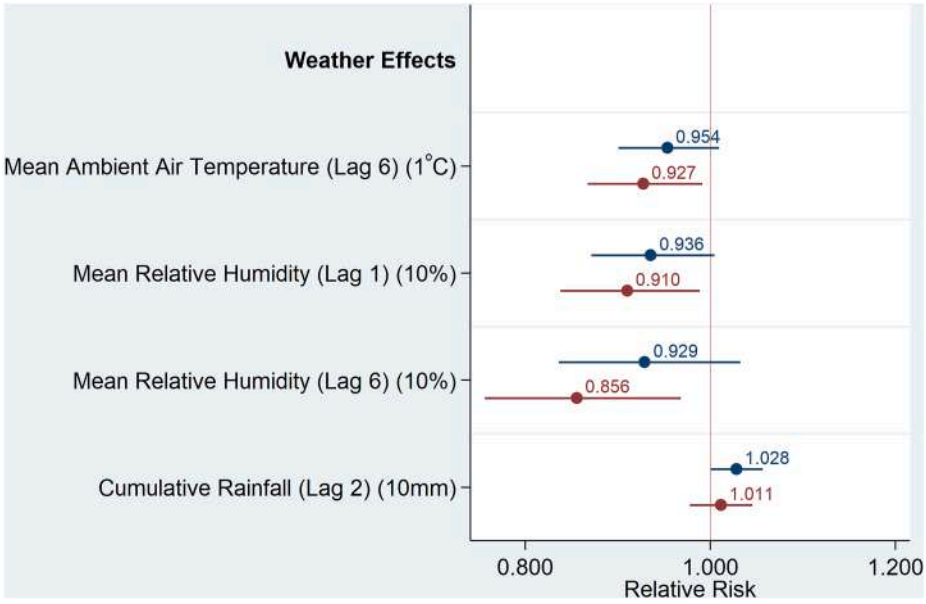

Fig. 2. Independent effects of meteorological factors on HPIV infections by gender. The solid navy and maroon circles represent the point estimates of the independent effects for males and females, respectively. The number of days between the respective meteorological exposures and the subsequent observed change in HPIV risk is indicated in brackets (i.e. lag X). The horizontal navy and maroon lines represent the 95% confidence intervals for males and females, respectively. The vertical solid red line represents the null effect.

Material, Annex 3). The seasonal patterns of HPIV-1 and HPIV-3 followed closely with that of all HPIV infections (Fig. 4) but that for HPIV-2 and HPIV-4 appeared to be inversely related.

4.3.1. Sensitivity analysis

Including additional terms to represent higher within-year frequency seasonal patterns of HPIV did not alter our effect estimates to an important degree (see Supplementary Material, Annex 4).

5. Discussion

In this study, we sought to determine the associations between meteorological parameters and air pollution with paediatric HPIV risk in the tropics. We found that HPIV infections were independently associated with climate parameters, with gender being an effect modifier. Furthermore, the within-year seasonal pattern in overall HPIV infections was closely synchronized with that of HPIV-1 and HPIV-3 infections, which were the two most commonly detected among the four HPIV types.

Meteorological factors are likely to modulate HPIV risk through the direct influence on respiratory virus survival as well as the indirect influence of human behaviour and consequently infection risk. The inverse relationship between temperature and HPIV risk observed in our study was consistent with a previous study undertaken in Germany (du Prel et al., 2009). RNA-containing enveloped viruses, such as HPIV, are susceptible to heat degradation arising from increased temperatures (Tang, 2009). Higher temperatures have also been found to reduce viral replication (Yamaya et al., 2019). Colder temperatures enhance respiratory viral survival in the environment (Lowen and Steel, 2014), thus prolonging the duration over which they can remain viable and thus increasing the infection risk of individuals that come into contact with them.

Evidence on the effect of relative humidity on HPIV infections is mixed, with one study in Edinburgh, Scotland, reporting a positive

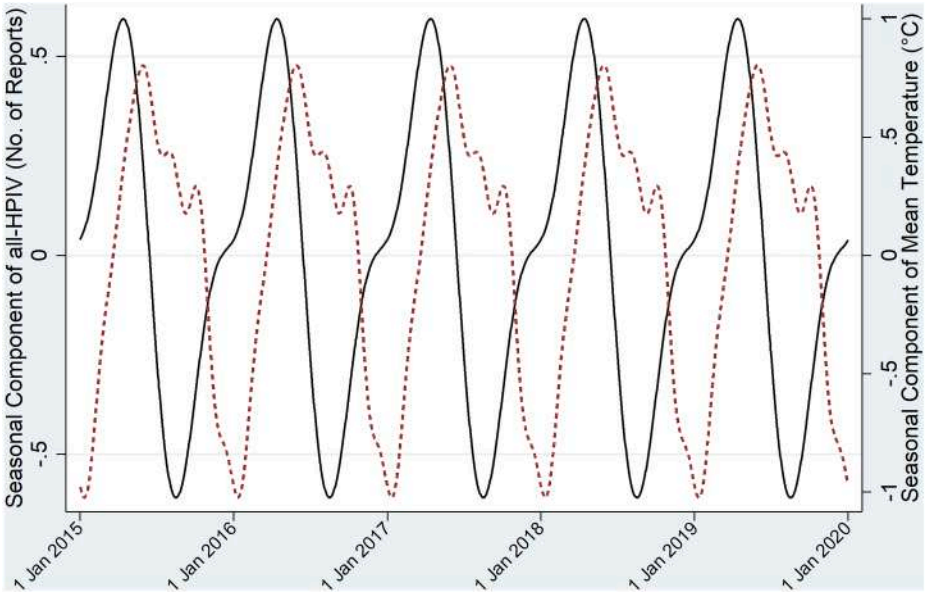

Fig. 3. Seasonal components of all-HPIV infections and ambient air temperature in Singapore demonstrated for 5 years (2015 to 2019).
The solid black line represents the change in the number of HPIV reports each day attributable to the seasonal pattern of HPIV while the dotted red line represents the change in temperature each day attributable to its seasonal pattern. The horizontal line centred at the value of 0 represents the neutral effect of seasonality on HPIV infections and ambient temperature.

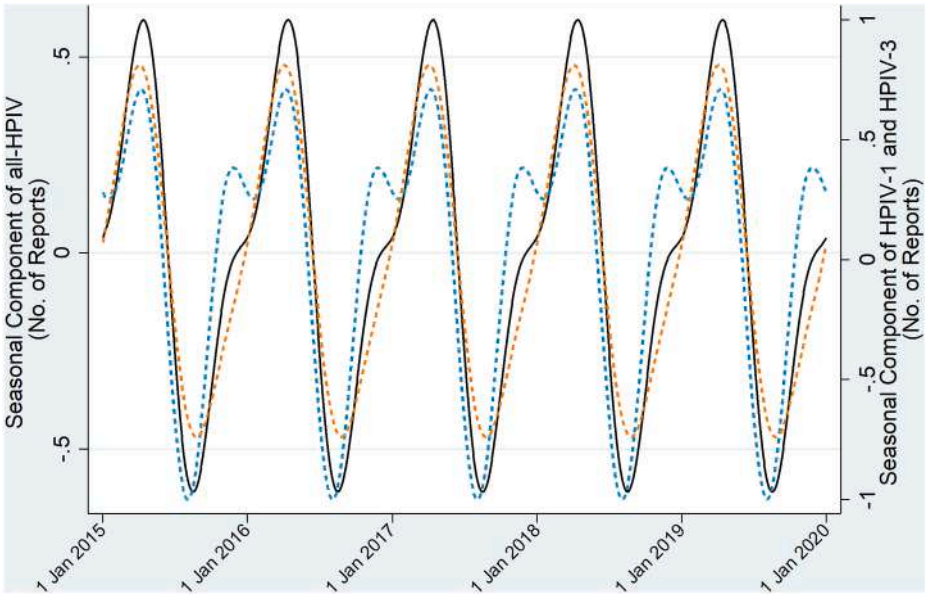

Fig. 4. Seasonal components of all-HPIV, HPIV-1 and HPIV-3 infections in Singapore demonstrated for 5 years (2015 to 2019).
The lines depict the change in the number of reported HPIV (solid black line), HPIV-1 (blue dotted line) and HPIV-3 (orange dotted line) infections each day attributable to their respective seasonal patterns. The horizontal line centred at the value of 0 represents the neutral effect of seasonality on HPIV infections.

relationship between HPIV-3 and relative humidity (Price et al., 2019), and two others undertaken in the Republic of Korea and Sweden, reporting an inverse relationship between HPIV risk and relative humidity (Cheon et al., 2019; Sundell et al., 2016). The observed inverse relationship between HPIV risk and humidity in our study was consistent with these two studies and a previous one in Singapore which reported the same observation (Loh et al., 2011). Lower relative humidity levels facilitate the evaporation of aerosolized virus particles, allowing prolonged circulation in the airborne environment which can lead to increased viral transmission (Sundell et al., 2016). In addition, lipid-enveloped viruses such as HPIV and Influenza are able to survive longer at lower relative humidity levels (Tang, 2009), thus increasing the probability of infection risk of individuals exposed during these conditions.

The positive effect of rainfall on HPIV in our study was consistent with a study in China which reported a positive correlation between HPIV rates and monthly total rainfall (Yan et al., 2015). There may be an increased tendency for individuals to seek shelter during rain events, thus increasing the probability of exposure to indoor spaces where human density may be higher and conditions optimal for droplet and fomite transmission.

In our study, females appeared to be more vulnerable to HPIV infections at lower temperatures and humidity levels, while males appeared to be relatively more susceptible to rainfall effects. To the best of our knowledge, no previous studies have reported gender differences in these climate exposures on HPIV. We recommend that further research be undertaken to confirm these findings and elucidate the biological mechanisms behind these gender-differentiated effects.

Differences in host susceptibility, predominance of HPIV-serotypes and climates between study settings may have contributed to the

differences in the climate-HPIV relationships reported in previous studies. In temperate settings, cyclical HPIV-1 peaks during the fall and HPIV-3 peaks in the spring and summer months (Fry et al., 2006; Weinberg, 2006; Knott et al., 1994). In tropical settings, these cyclical patterns are less pronounced, with no distinct seasonality detected in some studies (Fé et al., 2008; Chew et al., 1998). However, a previous study in Singapore found that the most commonly detected parainfluenza virus (HPIV-3) peaked between February and May (Chew et al., 1998). This was similar to the pattern reported in a study in Kuala Lumpur, Malaysia, which also found that HPIV-1 and HPIV-3 peaked from March to May (Khor et al., 2012). A study on hospitalizations for acute paediatric respiratory infections in Nha Trang, Vietnam, found that HPIV-3 peaked in January and February, although the finding did not reach statistical significance (Althouse et al., 2018). The distinct seasonal rise in HPIV infections from January to April in our study was consistent with the above-mentioned studies conducted in South-East Asia. The seasonal rise in our study appeared to be driven primarily by HPIV-3 and HPIV-1 infections. This may suggest in part the role of periodic regional travel patterns in HPIV circulation, as well as the influence of common weather patterns on HPIV infection experienced across the region.

We used laboratory-confirmed HPIV infections, thus minimizing the risk of case misclassification. Though nationally reported HPIV infections were not available, we included all reports from a major children's hospital, and therefore the observed seasonal rises in HPIV and its climate dependence were likely to reflect the general patterns in the wider community. Ours was an ecological study and therefore the findings were not generalizable to individuals. Nasopharyngeal swab testing was based on ordering by attending clinicians and is likely to reflect symptomatic infections rather than mild or asymptomatic cases. Thus, selection bias is possible. We accounted for the immediate and lagged effects of climate factors and conducted sensitivity analysis for seasonal control to provide reassurance on the accuracy of our model estimates.

While our study findings might not have any direct implications for clinical management, hospital administrators can use the predictable seasonal rise in HPIV infections to prioritize the within-year allocation of healthcare resources to manage surges in HPIV infections. In addition, policy makers and public health practitioners could reinforce good personal hygiene practices prior to anticipated periods of lower temperature and humidity to reduce fomite-driven transmission risk. In addition, avoiding crowded indoor spaces prior to and during peak infection periods could help reduce HPIV transmission.

Our study suggests that climate variability played an important role in shaping paediatric HPIV trends in a tropical-city setting. The within-year seasonal predictability of HPIV infections, together with periods of lower temperature and relative humidity can inform the timing of mitigation measures aimed at improving personal hygiene and reducing potential exposure, as well as the development of primary healthcare and hospital resource plans aimed at managing increases in HPIV infections.

Transparency declaration

The authors declare that they have no competing interests. This research did not receive any specific grant from funding agencies in the public, commercial, or not-for-profit sectors.

Acknowledgements

Note. We thank the KK Women's and Children's Hospital Laboratory System Administrator (Ms. Fadhillah Binte Ami) and the Microbiology Laboratory staff for providing the HPIV data, and the Meteorological Services Singapore for providing the weather data for our study. We are appreciative of the advice and feedback provided by Dr Ng Lee Ching, Group Director (Environmental Health Institute) (NEA). The information and opinions expressed reflect solely those of the authors.

Appendix A. Supplementary data

Supplementary data to this article can be found online at https://doi.org/10.1016/j.ijheh.2021.113864.

Authors' contributions

SS and JA conceptualized the study, led the writing of the article and analysed the data.

SS, LLH, MM and JA contributed to the interpretation of results and to the revision of the article drafts.

All authors critically revised the article for important intellectual content and approved all components of the final draft.

Availability of data and material

The HPIV and weather data underlying the results presented in our study are owned by a third party. They are available upon reasonable request.

References

Akaike, H., 1974. A new look at the statistical model identification. IEEE Trans. Automat. Control 19 (6), 716–723.

Althouse, B.M., Flasche, S., Minh, L.N., Thiem, V.D., Hashizume, M., Ariyoshi, K., et al., 2018. Seasonality of respiratory viruses causing hospitalizations for acute respiratory infections in children in Nha Trang, Vietnam. Int. J. Infect. Dis. 75, 18–25.

Biofire Diagnostics LLC. Biofire Film Array System Documents, 2021. https://www.biofiredx.com/support/documents/#toggle-id-3.

Brady, M.T., Evans, J., Cuartas, J., 1990. Survival and disinfection of parainfluenza viruses on environmental surfaces. Am. J. Infect. Control 18 (1), 18–23.

Cheon, J.M., Yang, Y.J., Yoon, Y.S., Lee, E.S., Lee, J.H., Huh, Y., et al., 2019. Influence of fine particulate dust particulate matter 10 on respiratory virus infection in the Republic of Korea. Korean J. Fam. Pract. 9 (5), 454–459.

Chew, F.T., Doraisingham, S., Ling, A.E., Kumarasinghe, G., Lee, B.W., 1998. Seasonal trends of viral respiratory tract infections in the tropics. Epidemiol. Infect. 121 (1), 121–128.

du Prel, J.-B., Puppe, W., Gröndahl, B., Knuf, M., Weigl, F., Schaaff, F., et al., 2009. Are meteorological parameters associated with acute respiratory tract infections? Clin. Infect. Dis. 49 (6), 861–868.

Fé, M.M.M., Monteiro, A.J., Moura, F.E.A., 2008. Parainfluenza virus infections in a tropical city: clinical and epidemiological aspects. Braz. J. Infect. Dis. 12, 192–197.

Frost, H.M., Robinson, C.C., Dominguez, S.R., 2014. Epidemiology and clinical presentation of parainfluenza type 4 in children: a 3-year comparative study to parainfluenza types 1–3. J. Infect. Dis. 209 (5), 695–702.

Fry, A.M., Curns, A.T., Harbour, K., Hutwagner, L., Holman, R.C., Anderson, L.J., 2006. Seasonal trends of human parainfluenza viral infections: United States, 1990–2004. Clin. Infect. Dis. 43 (8), 1016–1022.

Henrickson, K.J., 2003. Parainfluenza viruses. Clin. Microbiol. Rev. 16 (2), 242–264.

Khor, C.-S., Sam, I.C., Hooi, P.-S., Quek, K.-F., Chan, Y.-F., 2012. Epidemiology and seasonality of respiratory viral infections in hospitalized children in Kuala Lumpur, Malaysia: a retrospective study of 27 years. BMC Pediatr. 12 (1), 32.

Knott, A.M., Long, C.E., Hall, C.B., 1994. Parainfluenza viral infections in pediatric outpatients: seasonal patterns and clinical characteristics. Pediatr. Infect. Dis. J. 13 (4).

Lessler, J., Reich, N.G., Brookmeyer, R., Perl, T.M., Nelson, K.E., Cummings, D.A.T., 2009. Incubation periods of acute respiratory viral infections: a systematic review. Lancet Infect. Dis. 9 (5), 291–300.

Linster, M., Do, L.A.H., Minh, N.N.Q., Chen, Y., Zhe, Z., Tuan, T.A., et al., 2018. Clinical and molecular epidemiology of human parainfluenza viruses 1–4 in children from Viet Nam. Sci. Rep. 8 (1), 6833.

Loh, T.P., Lai, F.Y.L., Tan, E.S., Thoon, K.C., Tee, N.W.S., Cutter, J., et al., 2011. Correlations between clinical illness, respiratory virus infections and climate factors in a tropical paediatric population. Epidemiol. Infect. 139 (12), 1884–1894.

Lowen, A.C., Steel, J., 2014. Roles of humidity and temperature in shaping influenza seasonality. J. Virol. 88 (14), 7692–7695.

Price, R.H.M., Graham, C., Ramalingam, S., 2019. Association between viral seasonality and meteorological factors. Sci. Rep. 9 (1), 929.

Quidel Corporation, 2021. Double Duet DFA (direct fluorescent antibody) respiratory virus screening & ID kit. https://www.quidel.com/sites/default/files/product/documents/PI2000000EN00.pdf.

Schmidt, A.C., Schaap-Nutt, A., Bartlett, E.J., Schomacker, H., Boonyaratanakornkit, J., Karron, R.A., et al., 2011. Progress in the development of human parainfluenza virus vaccines. Expert Rev. Respir. Med. 5 (4), 515–526.

Schomacker, H., Schaap-Nutt, A., Collins, P.L., Schmidt, A.C., 2012. Pathogenesis of acute respiratory illness caused by human parainfluenza viruses. Curr. Opin. Virol. 2 (3), 294–299.

Seegene Inc. Seeplex®RV15 OneStep ACE Detection, 2021. https://www.seegene.com/assays/seeplex_rv15_onestep_ace_detection.

Sundell, N., Andersson, L.-M., Brittain-Long, R., Lindh, M., Westin, J., 2016. A four year seasonal survey of the relationship between outdoor climate and epidemiology of viral respiratory tract infections in a temperate climate. J. Clin. Virol. 84, 59–63.

Swamy, M.A., Malhotra, B., Reddy, P.V.J., Kumar, N., Tiwari, J.K., Gupta, M.L., 2016. Distribution and trends of human parainfluenza viruses in hospitalised children. Indian J. Pediatr. 83 (10), 1109–1113.

Tang, J.W., 2009. The effect of environmental parameters on the survival of airborne infectious agents. J. R. Soc. Interface 6, S737–S746.

Weinberg, G.A., 2006. Parainfluenza viruses: an underappreciated cause of pediatric respiratory morbidity. Pediatr. Infect. Dis. J. 25 (5), 447–448.

Yamaya, M., Nishimura, H., Lusamba Kalonji, N., Deng, X., Momma, H., Shimotai, Y., et al., 2019. Effects of high temperature on pandemic and seasonal human influenza viral replication and infection-induced damage in primary human tracheal epithelial cell cultures. Heliyon 5 (2) e01149.

Yan, Hua-Jie, He, Dong-Ping, Sheng, Jun, Dong, Wei, Liu, Jia, Shao, Jie, 2015. Association between parainfluenza virus infection and climatic factors in children. CJCP 17 (12), 1297–1300.

International Journal of Hygiene and Environmental Health

doi: 10.1016/S1438-4639(21)00205-4

International Journal of Hygiene and Environmental Health 239 (2022) 113866

Contents lists available at ScienceDirect

International Journal of Hygiene and Environmental Health

journal homepage: www.elsevier.com/locate/ijheh

Effect of a combined household-level piped water and sanitation intervention on reported menstrual hygiene practices and symptoms of urogenital infections in rural Odisha, India

Belen Torondel [a,*,1], Jane Ferma [a,1], Suzanna C. Francis [a], Bethany A. Caruso [b,c], Parimita Routray [a], Heather Reese [b], Thomas Clasen [b]

[a] London School of Hygiene and Tropical Medicine, Kepple Street, WC1E 7HT, London, UK
[b] Gangarosa Department of Environmental Health, Rollins School of Public Health, Emory University, 201 Dowman Dr, Atlanta, GA, 30322 Atlanta, GA, USA
[c] Hubert Department of Global Health, Rollins School of Public Health, Emory University, 201 Dowman Dr, Atlanta, GA, 30322, Atlanta, GA, USA

ARTICLE INFO

Keywords:
Menstruation
WASH intervention
Urogenital symptoms
Odisha
India

ABSTRACT

Adequate menstrual hygiene management (MHM) requires access to water and sanitation and can be challenging for many women and girls living in resource-poor settings. Inadequate MHM has been associated with urogenital infections. The aim of this study is to assess the impact of a combined household-level piped water and sanitation intervention on MHM practices and urogenital infection symptoms (UGS) among women living in rural communities of Odisha (India). This study was nested within a pair-matched cohort study designed to assess impact of the Gram Vikas MANTRA program, which provided household-level piped water, bathing areas and latrine to all households in intervention villages, on diarrheal disease (primary outcome). The program did not specifically promote menstrual hygiene practices. Forty-five intervention villages were randomly selected from a list of those where implementation was previously completed at least five years before and matched to 45 control villages. Data for the main study was collected in four rounds from June 2015 to October 2016. For the MHM sub study, household surveys were administered in round four to randomly selected women aged 18 or older among study households from the 90 villages, to assess self-reported MHM practicesand urogenital infections symptoms. MHM practices were deemed adequate if they met some of the criteria developed on the basis of international monitoring that the GV program could modify (adequate frequency of absorbent change, washing the body with soap and privacy for managing menstruation). Multilevel mixed-effects logistic regression with a random effect distribution at the level of the pair and village was used to estimate the effect of the intervention on adequate MHM practices (primary outcome) and reported UGS (secondary outcome). A total of 1045 women (517 from intervention and 528 from control) were included in the study. Women who lived in the villages receiving the intervention, were more likely to report adequate MHM practices than those in control villages (Adjusted OR (AOR) 3.54, 95% Confidence Interval (CI): 1.86–6.78). 14.51% and 15.53% of women living in the control and intervention villages reported having at least one UGS. There was no evidence of an intervention effect on reported UGS (AOR = 0.97, 95%CI: 0.64–1.46). While household latrines or bathing areas with access to piped water improve the environment that enable MHM practices related to privacy, the provision of such facilities alone had only a moderate impact in adequate MHM and did not have an effect on self-reported UGS. More targeted inventions that include behavior change strategies and that address other barriers may be necessary to improve MHM practices.

1. Introduction

Every day, more than 300 million girls and women between the ages of 15 and 49 are menstruating(George, 2013). Menstrual hygiene practices are influenced by factors at the individual, family, and community level. The ability of girls and women to adequately manage their

* Corresponding author.
E-mail address: belen.torondel@lshtm.ac.uk (B. Torondel).
[1] Sharing first authorship.

https://doi.org/10.1016/j.ijheh.2021.113866
Received 29 May 2021; Received in revised form 21 September 2021; Accepted 17 October 2021
Available online 23 October 2021

menstruation hygienically and with dignity is crucial to their health and well-being, and is a public health issue(Plesons et al., 2021; Sommer et al., 2015). A working definition of adequate menstrual hygiene management (MHM) was established by the WHO/UNICEF Joint Monitoring Programme on Water and Sanitation (JMP) in 2012 to inform global monitoring. MHM was defined as 'Women and adolescent girls using a clean menstrual management material to absorb or collect blood that can be changed in privacy as often as necessary for the duration of the menstruation period, using soap and water for washing the body as required, and having access to facilities to dispose of used menstrual management materials'(Sommer and Sahin, 2013). The definition includes different aspects of the physical requirements for having adequate MHM, and it is increasingly being used among researchers and practitioners; however, a unified or standardized definition has not been achieved yet. Based on the WHO definition, Hennegan and colleagues developed a tool to quantify the different aspects of MHM and creating a single estimated that measure adequate MHM. Using this tool, they estimated the prevalence of adequate MHM among Ugandan school girls and found 90.5% of girls failed to meet available criteria for adequate MHM(Hennegan et al., 2016). Qualitative research in rural Odisha, India, which examined women's detailed accounts of menstruation at various life stages, proposed a revised definition of adequate MHM that captured voiced needs more comprehensively for women in the population(MacRae, Clasen, Dasmohapatra and Caruso, 2019b). Most of the components of the MHM definition—both the JMP's and revised versions—require appropriate resources and access to water and sanitation facilities to promote and facilitate adequate hygienic and comfortable menstrual practices. However, access to household sanitation and water remains a global challenge. As of 2015, 2.3 billion people lacked even basic sanitation services, with 860 million using unimproved facilities and another 890 million practicing open defecation—with a high proportion residing in India(World Health Organization, 2019). Due to this situation, government of India has made big investments in different sanitation campaigns during the last decade (World Bank, 2010) being the main focus toilet construction, with fewer resources availed for sustained coverage and use and without much attention to women needs (Garn et al., 2017). Despite finding good coverage levels of improved community water sources around rural India, the amount of water provided may be insufficient to fulfill the different needs that women face when managing their menstruation (Sebastian et al., 2013). Making water available into households, especially closer to the sanitation facilities may help to meet the needs that women require during menstruation (Routray et al., 2015; Schmidt et al., 2009). Several studies conducted in rural India have also emphasized that the lack of adequate sanitation at home influences women's experiences of safety and privacy(Caruso et al., 2015; Hulland et al., 2015; Sahoo et al., 2015; Sclar et al., 2018), and may impact mental health(Caruso et al., 2017, 2018).

Although water and sanitation are important for all women, the need for water, sanitation and hygiene (WASH) facilities in India is particularly urgent for those menstruating, including for personal washing and changing, and to meet the needs of the large number of women who use reusable materials that require washing. In India, between 43% and 88% of women wash and reuse cotton cloths rather than use disposable pads (Dasgupta and Sarkar, 2008; Narayan et al., 2001). However, reusable material may not be well sanitized because cleaning is often done without soap and with unclean water. Above it, the social taboos and restrictions force drying indoors, or covered by other clothing, away from direct sunlight and open air(MacRae, Clasen, Dasmohapatra and Caruso, 2019a; Sahoo et al., 2015). Unhygienic washing, drying and storing practices are particularly common in rural areas of Odisha state and amongst women and girls in lower socio-economic groups(Caruso et al., 2017; Das et al., 2015; MacRae et al., 2019b; Torondel et al., 2018) and have been associated with urogenital infections (Das et al., 2015; Torondel et al., 2018).

Two hospital-based studies conducted by our group in Odisha in 2015 and 2018, showed that women diagnosed with vulvovaginal yeast infection were more likely to use reusable absorbent material and practice lower frequency of personal washing than those who were not diagnosed with vulvovaginal yeast infections. And among women reusing absorbent material, vulvovaginal yeast infections were more frequent in women who dried their menstrual material inside their house and who stored the cloth hidden in the toilet compartment(Torondel et al., 2018). Compared to women diagnosed with bacterial vaginosis (BV), women without BV were more likely to practice personal washing more frequently and change absorbent material in a toilet facility and report higher frequency of absorbent change (Das et al., 2015; Torondel et al., 2018).

Urogenital tract infections which comprise reproductive tract infections (RTI) and urinary tract infections (UTIs) are a major public health concern worldwide and are particularly common in low-income settings(Lanfranco and Alangaden, 2016; Wasserheit et al., 1989). RTIs can result in pelvic inflammatory diseases, infertility, adverse pregnancy outcomes, and increased susceptibility to HIV(Nagarkar and Mhaskar, 2015). UTIs are a significant cause of morbidity in females of all ages. Serious sequelae include frequent recurrences, pyelonephritis with sepsis, pre-term birth and complications caused by frequent antimicrobial use(Flores-Mireles et al., 2015). The prevalence of reported symptoms of RTI in different population-based studies in Indian women varied from (13%–55%) (Baker et al., 2017; Bhilwar et al., 2015; Krupp et al., 2007; Sciences, 2006). A study to determine the prevalence of community acquired-UTIs in rural Odisha, showed that prevalence in females was 45.2%(Dash et al., 2013).

Studies on the role of WASH in the context of MHM have focused primarily on girls and the school environment and access to menstrual hygiene products (van Eijk et al., 2016), and there is less information on, and attention to the needs of women and girls outside the school environment and the influence of having appropriate WASH into MHM practices (Hennegan et al., 2018; Sommer et al., 2016). Our previous studies in India assessing the relationship between WASH access, MHM and urogenital infections showed that places where women can manage menstruation-related washing in privacy and comfort are important for adequate MHM(Das et al., 2015; Torondel et al., 2018). This was affected by having access to WASH facilities at the household.

As mentioned earlier, Indian Government's efforts to improve shortfalls in rural water and sanitation have been focused on constructions of community water sources and toilets for selected households. However, deficiencies in water quality, quantity and coverage at the household and community levels, and low use of toilets inspired a novel approach to WASH delivery led by Gram Vikas, a local non-governmental organization in Odisha, India. Their approach provides household-level piped water connections contingent on full community-level toilet coverage(Reese et al., 2017). In other words, once all in the community have a toilet, Gram Vikas 'turns on' water that is piped to all households and toilets. Our group conducted an evaluation to assess the impact of the Gram Vikas program on diarrhea (primary outcome) and other health outcomes(Reese et al., 2019; Sinharoy et al., 2021). Although the program addressed two potential drivers for appropriate menstrual hygiene practices, such as access to water and privacy, it did not specifically focus on improving the menstrual health among women in the community. To date, no research has assessed the impact of a household-level WASH intervention on menstrual hygiene practices and the potential urogenital symptoms that could result from poor hygiene.

We nested an MHM study within the evaluation of the Gram Vikas MANTRA program in rural Odisha, India. The objectives of this nested study were 1) Investigate the impact of WASH intervention on adequate MHM, 2) Investigate the relationship between adequate MHM and reported UGS and 3) Investigate the impact of WASH intervention on reported UGS. We also investigated the determinants of adequate MHM and reported urogenital symptoms (see Fig. 1).

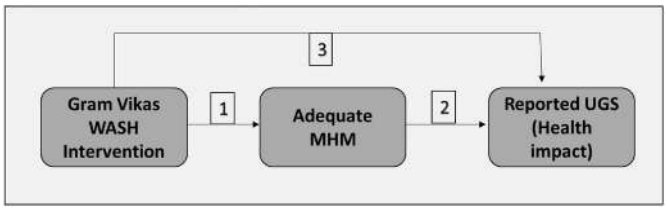

Fig. 1. Theoretical model for the association between WASH, Adequate menstrual hygiene management (MHM) and reported urogenital infection symptoms (UGS). Objective 1 is to investigate the impact of WASH intervention on adequate MHM. Objective 2 is to investigate the association between adequate MHM and reported UGS. Objective 3 is to investigate the impact of WASH intervention on reported UGS.

2. Methods

2.1. The WASH intervention and evaluation

The MANTRA program (Movement and Action Network for the Transformation of Rural Areas), developed by Gram Vikas (Reese et al., 2017), consisted of: 1) a household pour-flush toilet with dual soak-away pits, 2) an attached bathing room, and 3) household piped water connections in the toilet, bathing room, and kitchen(Reese et al., 2017). For a village to be eligible to receive the program, every household must have committed to the construction of their own toilet and bathing room. Gram Vikas assisted with the development of a piped water system, which was connected after every household completed toilet construction, and the village assumed responsibility for the ongoing operation and maintenance costs.

The evaluation was of 45 matched villages with one intervention and one control village in each pair (90 total). The primary objective of the main study was to assess the long-term impact of the WASH intervention on diarrheal disease (Reese et al., 2019). The 45 intervention villages were randomly selected using a computer generated sequence from a list provided by Gram Vikas of villages with completed interventions in Ganjam and Gajapati districts, restricted to those with an intervention start date of 2003–2006. The intervention took an average of 3 years to be fully implemented; the latest year that a selected intervention village completed the implementation was in 2010(Reese et al., 2017). Between April–September of 2015, 45 control villages from the same districts, that had not received the Gram Vikas MANTRA WASH intervention, were matched retrospectively to the 45 intervention villages through a multi-step restriction, matching, and exclusion process to reduce potential bias due to baseline differences. We used an iterative multivariate matching scheme (R Matching package, version 4.9–2) to match villages on pre-intervention characteristics from the Government of India Census (2001) and Below Poverty Line Survey 2002, including demographic, socioeconomic, sanitation and water access characteristics, among others; balance was achieved on all variables(Reese et al., 2017). These village-level matching variables were selected due to their theorised association with the primary outcome, diarrhoeal diseases, as well as data availability. Villages were exact matched on district to limit any political or large-scale geographic variation between district populations (Diamond and Sekhon, 2013; Reese et al., 2017). Within each village, up to 40 households with children less than 5 years of age were randomly selected to be enrolled in the main evaluation study. The evaluation was carried out between June 2015 and October 2016 and consisted of four study rounds. Data collected in each round is described in Supplementary Fig. 1. Household and individual level data were collected during rounds 1 and 4 and included educational attainment of head of the household and primary caregiver, household wealth, health information of all the members of the house, and household access to sanitation and water (Supplementary Fig. 2).

2.2. MHM sub-study

The MHM sub-study was carried out during round four (July–Oct 2016). Sixteen households were randomly selected per village (1440 total), with one woman aged 18 years or older randomly selected to participate per household. Randomization of households and women was done using a computer generated sequence. Women were eligible to participate in the sub-study if they had experienced menstruation in the previous six months. The male and/or female household head provided written informed consent for the household and each participant consented before completing the MHM questionnaire. Individual level data for MHM practices and urogenital symptoms were collected in round four by female field workers in face-to-face interviews (Supplementary Fig. 3). Data included marital status, age, menstrual practices (related to all the different domains captured in the MHM definition, including participant's body hygiene practices, type of absorbent used, and hygiene practices related to management of absorbent material), sanitation practices and urogenital symptoms. The questionnaire was adapted from a validated questionnaire that was used in a previous hospital based study conducted in Odisha to assess the association of different menstrual practices and urogenital infections(Torondel et al., 2018).

2.2.1. Sample size

The sample size was based on objective 3, the effect of the WASH intervention on reported UGS. Our population-based study in Odisha showed that 13% of women reported at least one of the 4 urogenital symptoms used in our definition of UGS (Baker et al., 2017), and our hospital-based study in Odisha that investigated the effect of different household WASH characteristics on urogenital infections found that women whose water source was outside their home were 1.46 more likely to be a case of urogenital infection (defined with symptomatology) and 2.1 more likely to be laboratory diagnosed with BV or UTI infections compared with women who had the water source inside their home (95%CI 1.0–2.2) and (95%CI 1.3–3.4), respectively(Torondel et al., 2018). Therefore, we assumed that the WASH intervention could have an effect size of 0.55 on participants' reported symptoms of UGS. For objective 3, if 13% had a reported urogenital symptom in the control group, with an effect size of 0.55, 80% power and 0.05 significance level, then at least 448 would be needed in each arm. We targeted 16 women per village (total 1440) to account for non-responses (due to not fitting into the eligibility criteria or refuse to participate) or absence the day of the visit.

2.3. Data management and analysis

Survey data was collected on mobile phones using the Open Data Kit (available from https://opendatakit.org/).

2.3.1. Definitions of the outcomes and other covariates

The primary outcome for this study was 'adequate MHM' which was modified *a priori* from the Hennegan tool to quantify adequate MHM based on the working definition of MHM developed by WHO and UNICEF Joint Monitoring Programme (Sommer and Sahin, 2013) (Hennegan et al., 2016). The tool includes the domains of access to clean absorbents including (when relevant) sufficient washing, drying, storage and wrapping of reusable absorbents; adequate frequency of absorbent change; washing the body with soap and water; adequate disposal, and privacy for managing menstruation. However, the Gram Vikas WASH intervention could only affect certain domains of the definition, because it did not provide menstrual hygiene materials such as disposable pads or menstrual cups or methods for absorbent disposal. Therefore, we modified the tool to include only the domains from the MHM definition that the intervention could impact, such as adequate frequency of absorbent change; washing the body with soap and privacy for managing menstruation (Supplementary Table 1).

The secondary outcome was reported urogenital symptoms. After

conducting a literature search of the most common symptoms used to diagnose RTIs (Balamurugan and Bendigeri, 2012; García et al., 2004; Prabha et al., 2012) and UTIs(Schmiemann et al., 2010), we selected four symptoms to assess reported urogenital symptoms: abnormal vaginal discharge; burning or itching in the genitalia; urinate more frequently; and burning or itching while urinating. Women were asked about current symptoms at the time of interview. If a woman reported at least one of the symptoms, then she was defined as having reported UGS positive(Das et al., 2015).

Potential confounding covariates were identified *a priori* based on the literature. Other variables we included were limited to what was collected in the overall evaluation of the WASH intervention. They included wealth index, healthcare decisions (who usually makes decisions about healthcare for yourself: you, someone else, or you and someone else decide jointly?), market access (How often do you go to the market/haat/bazaar?) and experience of stigma (Worried about being treated as untouchable by others). A wealth index variable was created(Reese et al., 2019). We used principal components analysis (R psych package, version 1.6.12) to construct the household wealth index from 15 variables, including household asset ownership, housing characteristics, agricultural land acreage, and below poverty line status (Bassani et al., 2014; Filmer and Pritchett, 2001). We extracted the component which explained the most variability as the wealth index (Kolenikov and Angeles, 2004).

2.3.2. Statistical analysis

All analysis was conducted in STATA 15.1. Participant characteristics, MHM practices, and reported UGS were analyzed to provide descriptive statistics of the analytic sample.

To investigate the determinants of adequate MHM and reported UGS, two multilevel mixed-effects logistic regression models were carried out using methods for a matched-pair cluster randomised controlled trial (Hayes and Moulton, 2017). Unadjusted results were calculated for selected characteristics. The adjusted analysis included age *a priori* with other variables that were associated with the outcome using a p-value cut-off of 0.05 in the unadjusted analysis. Also, the effect of clustering and multicollinearity was assessed by evaluating the standard errors in each of the models.

To assess the impact of the WASH intervention on adequate MHM (Objective 1) we used the same multilevel mixed-effects logistic regression methods described above(Hayes and Moulton, 2017). While villages were exact matched by district and pre-intervention demographic, socioeconomic, sanitation and water access characteristics (Reese et al., 2017), there was likely to be confounding at the individual level. A crude estimate was calculated. Then an adjusted model was developed using age as a forced variable and adding each potential confounder identified in the determinant's analysis described above one by one (confounder + exposure + outcome). Effect estimates were compared to the crude estimates, and potential confounders were included in the final adjusted model if there was a 10% change from the crude estimate. The effect of clustering and multicollinearity was assessed by evaluating the standard errors in each of the models.

A similar analysis was used to assess the relationship between adequate MHM and reported UGS (Objective 2), and the effect of the WASH intervention with reported UGS (Objective 3).

Missing data were explored to investigate patterns and difference between the intervention groups using Chi square (Supplementary Table 2). In all the multivariate models, data was missing by design which resulted in excluded data in the analysis. Specifically, data was missing because some data was collected in the household portion of the survey, yet not all women responded to the HH portion of the survey because it targeted the mother or primary caregiver of the youngest child <5. Therefore, the women who responded to the MHM survey may not have responded to the HH survey. Thus data was missing at random (MAR).

Ethical approval

The study was approved by LSHTM, U.K (No. 9071) and the Kalinga Institute of Medical Sciences of KIIT University, Bhubaneswar, India ethics committees (KIMS/KIIT/IEC/053/2015). The study was registered at ClinicalTrials.gov (NCT02441699).

3. Results

3.1. Characteristics of the study population

A total of 1440 women were visited in the 90 villages, and 395 were excluded from the study: 240 (16.6%) had reached menopause, 52 (3.6%) were pregnant, and 102 (7.0%) just gave birth. A total of 1045 women were included in this study, 528 were from control villages and 517 were from intervention villages. Table 1 presents participant sociodemographic characteristics. The mean age of the sample was 27 years (SD: 6.1) with most women aged 25–29 in both the control villages (35.2%) and intervention villages (38.3%). A higher proportion of women living in both the control (96.8%) and intervention (97.9%) villages were married. Ninety-eight percent of the sample were Hindu, with the remaining 2% Christian. Women living in the intervention villages were similar to women living in the control villages in regard to most sociodemographic variables. However, women in the intervention arm were wealthier than those in the control arm (24.4% vs 15.7%, respectively) and more women in the intervention arm had completed secondary school than those in the control arm (59.8% vs 44.3%, respectively). Women in the control arm were more likely to be caregivers who completed primary school or below than those living in the intervention arm (40.3% vs 30.0%, respectively). Women in the control arm reported having experienced stigma when menstruating more often

Table 1
Socio-demographic characteristics of women participating in the MHM study (N = 1045).

Characteristics		Women living in control villages *(n = 528)*		Women living in intervention villages *(n = 517)*	
		n[a]	%[a]	n[a]	%[a]
Age (years) *(n = 957)*	18–24	144	27.27	144	27.85
	25–29	187	35.42	198	38.30
	30 +	148	28.03	136	26.31
Religion *(n = 915)*	Christian/other	7	1.33	8	1.55
	Hindu	449	85.04	451	87.23
Marital Status *(n = 1045)*	Single	14	2.65	7	1.35
	Married	511	96.78	506	97.87
	Widowed	3	0.57	4	0.77
Wealth Index *(n = 832)*	Poor/Middle	323	61.17	300	58.03
	Rich	83	15.72	126	24.37
Caregiver Education Attainment *(n = 911)*	Primary or less	213	40.34	155	29.98
	Secondary or above	234	44.32	309	59.77
Experience Stigma[b] *(n = 1039)*	No	329	62.31	360	69.63
	Yes	194	36.74	156	30.17
Market Access [c] *(n = 908)*	No	109	20.64	121	23.40
	Yes	343	64.96	335	64.80
Healthcare Decision [d] *(n = 909)*	Self	133	25.19	124	23.98
	Someone else	152	28.79	154	29.79
	Self and someone else (joint)	167	31.63	179	34.62

[a] Numbers/percentages do not add up to 100% due to missing values. For further information on missing values see Supplementary Table 2.
[b] Menstruating women who experienced stigma from others during the last two menstruation cycles.
[c] The number of times menstruating women have attended the market. This indicates access to resources such as absorbents.
[d] Independence on healthcare decision making. This indicates ease of access to healthcare for women.

than those in the intervention (36.7% vs 30.2%, respectively).

Missing data were identified and presented in Supplementary Table 2. The exposure of interest (WASH) and outcome of interest (UGS and MHM) had no missing data, however, MHM criterion variables consisted of some missing observations. Variables with more than 10% missing data were wealth index (20.4%), female caregiver education attainment (12.8%), healthcare decisions (13.0%), market access (13.1%) and religion (12.4%). Women living in the control villages vs. women living in the intervention villages were missing more data on wealth index (23.1% vs 17.6% $p < 0.001$), female caregiver attainment (15.3% vs 10.3% $p < 0.0001$) and experience of taboo (1% vs 0.2% $p = 0.02$).

3.2. A description of MHM practices

Table 2 shows the prevalence of the different menstrual hygiene practices, distributed in the five domains used by WHO to define MHM, among women from control and intervention arms.

3.2.1. Clean absorbents

The type of menstrual absorbent most commonly used during the last six cycles in this community was a reusable cloth/towel. More women living in the control arm used reusable materials than women living in the intervention arm (89.6% vs 81.6%), and disposable sanitary pads were more commonly used in intervention arm than in control arm. Among women reusing cloths/towels, more women in the control arm washed them with soap and water and dried them in the sun or in an open space compared with women from intervention arm (85% vs 78.1% and 81.6% vs 74.3%, respectively). More women in the control arm stored their cloth in a changing room or hidden inside the house or hidden at a place outside the house than the intervention arm (47.5% vs 35.6% and 34.9% vs 31.1%, respectively). The proportion of women reporting storing their reusable cloth/towel with other clothes was very low in both arms (0.4% and 0.4%, respectively). More women living in the control arms wrapped their cloth in polythene when they stored their reusable cloth than women living in the intervention arms (83.9% vs 78.1%).

3.2.2. Adequate frequency of absorbent change

Adequate frequency of absorbent change is defined as women who change their absorbent three times or more per day on their heaviest day (Das et al., 2015). There was no evidence of a difference in frequency of absorbent change between the women living in the intervention and control arms (45.2% and 48.2%, respectively).

3.2.3. Washing the body practices

Three quarters of women reported that they practice full body washing during menstruation and a third reported only doing a vaginal wash. Most women reported washing with water and soap during their menstruation with no evidence of a difference of these practices between women living in the control and intervention arms (94.9% vs 98.9%). Most women reported washing more than once every day during their menstruation and no difference was found between women living in the control and intervention arms (76.7% and 76.9%, respectively).

3.2.4. Difficulty with disposal

Most women reported that they did not have difficulty in finding a place to dispose the cloth or pad during the last two menstrual periods. There was no evidence of a difference between women living in control and intervention arms (92.2% vs 93.8%).

3.2.5. Privacy for managing menstruation

The location where women changed their absorbents differed between control and intervention arm. A higher proportion of women in the control arm reported changing their absorbent material in a private room in the house compared to women living in the intervention villages

Table 2
Self-reported MHM practices by study arm among women in Odisha, India during July–October 2016 (N = 1045).

Survey question	Survey responses	Women living in control villages *(n = 528)*		Women living in intervention villages *(n = 517)*	
		n[a]	%[12]	n[a]	%[a]
MHM Criteria 1: Clean absorbents					
What was the most commonly absorbent material used during the last 6 cycles? *(n = 1039)*	Disposable sanitary pads	48	9.09	92	17.79
	Reusable cloths/ towel	473	89.58	422	81.62
	Nothing	1	0.19	1	0.19
	Other	1	0.19	1	0.19
With what do you wash your cloth? *(n = 870)**	Water only	8	1.52	7	1.35
	Water and soap	449	85.04	404	78.14
	Other	1	0.19	1	0.19
After washing it, how do you dry the cloth? *(n = 870)**	Dry it in the sun or open space	431	81.63	384	74.27
	Dry it inside the house	26	4.92	28	5.42
	Other	1	0.19	0	0.00
Where do you normally store the cloth for use next time? *(n = 870)**	With my clothes	2	0.38	2	0.39
	In some place in the toilet	16	3.03	61	11.80
	Changing room or hidden place inside house	251	47.54	184	35.59
	In hidden place outside house	184	34.85	161	31.14
	Other	5	0.95	4	0.77
Do you wrap cloth in anything when storing? *(n = 870)**	Yes, polythene	443	83.90	404	78.14
	Yes, other material	11	2.08	3	0.58
	No	4	0.76	5	0.97
MHM Criteria 2: Adequate frequency of absorbent change					
How often do you change your absorbent material on your heaviest day? *(n = 1039)*	1x per day	21	3.98	30	5.80
	2x per day	247	46.78	252	48.74
	3x per day	165	31.25	151	29.21
	4x per day	59	11.17	50	9.67
	5+ times per day	31	5.87	33	6.38
MHM Criteria 3: Washing the body practices					
What type of washing do you practice during menstruation? *(n = 1039)*	Only vaginal wash	178	33.71	165	31.91
	Bath of full body	341	64.58	349	67.50
	I don't wash myself	4	0.76	2	0.39
How often do you wash yourself (bath or vaginal wash) during menstruation? *(n = 1032)*	Only the first day of my cycle	14	2.65	21	4.06
	A few times throughout the cycle	79	14.96	74	14.31
	At least once every day	20	3.79	21	4.06
	More than once everyday	405	76.70	398	76.98
What do you use to wash yourself during menstruation? *(n = 1031)*	Water only	16	3.03	17	3.29
	Water and soap/ detergent	501	94.89	496	98.94
	Other	1	0.19	0	0.00
MHM Criteria 4: Difficulty with disposal					
Had difficulty finding a place to dispose of cloth or pad during your last two menstrual periods? *(n = 1039)*	Never	487	92.23	485	93.81
	Sometimes	17	3.22	19	3.68
	Always	19	3.60	12	2.32
MHM Criteria 5: Privacy for managing menstruation					
Where do you most often change your absorbent	In household toilet	26	4.92	141	27.27
	Bathing room	22	4.17	100	19.34

(*continued on next page*)

Table 2 (*continued*)

Survey question	Survey responses	Women living in control villages (*n = 528*)		Women living in intervention villages (*n = 517*)	
		n[a]	%[12]	n [a]	% [a]
material when at home? (*n = 1039*)	In toilet of neighbour/ relative	0	0.00	1	0.19
	In private room in the house	405	76.70	253	48.94
	Outside (field/ rive/pond etc)	59	11.17	20	3.87
	Other	11	2.08	1	0.19
Where do you wash the absorbent materials you reuse? (*n = 870*)*	Inside toilet stall	24	4.55	222	42.94
	Bathroom	14	2.65	38	7.35
	At private tube well/tap in yard or house	17	3.22	5	0.97
	At public tube well/tap in village	8	1.52	0	0.00
	In pond/river	353	66.86	116	22.44
	I do not wash it/ NA	1	0.19	0	0.00
	Other	41	7.77	31	6.00

[a] Numbers/percentages do not add up to 100% due to missing values for further information on missing values see Supplementary Table 2 *Answered only by women who said that reusable cloth was the most common material used in the last 6 months.

(76.7% vs 48.9%). Fewer women in the control villages changed their absorbent material in the household toilet or bathing room compared to women in the intervention arm (4.9% vs 27.3% and 4.2% vs 19.3%, respectively). More women living in the control arm changed their absorbent outside (hiding behind a bush/tree in the open field/river/ pond etc) than women living in the intervention arm (11.2% vs 3.9%).

More women in the intervention arm washed their absorbent inside the toilet stall or bathroom than women living in control arm (42.9% vs 4.6% and 7.4% vs 2.7%, respectively). More women living in the control arm wash their absorbents in a pond/river than women living in the intervention arm (66.9% vs 22.4%, respectively).

3.3. Prevalence and determinants of adequate MHM

Using the modified definition of adequate MHM, 10.1% of participants had adequate MHM: 4.7% among women living in control arm; and 15.7% living in the intervention arm. Supplementary Table 3 displays the results of the unadjusted and adjusted analyses of selected characteristics and the adequate MHM definition. The adjusted analysis showed that wealth index and female caregiver education attainment were independently associated with adequate MHM. Women who were wealthier had 1.88 times the odds of adequate MHM compared to women who were poorer (95% CI:1.08–3.26). Women whose caregiver completed education at the secondary school level and above, had 2.33 times the odds of adequate MHM compared to women whose caregiver completed education at primary level and below (95% CI:1.20–4.53). There was a weak association with the experience of stigma and MHM; women who had experienced stigma had 1.65 times the odds of adequate MHM than women who did not experience stigma (95% CI:0.96–2.85). No other variables were independently associated with the relaxed definition of MHM.

3.4. Prevalence and determinants of reported UGS

Supplementary Table 4 describes the prevalence of reported urogenital symptoms in the MHM sub-study. Abnormal vaginal discharge was the most reported symptom (9%). Women in the intervention villages had less burning or itching in the genitalia two weeks prior to the survey than women in the control villages (2.9% vs 5.7%, p = 0.03). There was no evidence of other differences in reported UGS between women living in control and intervention villages.

Based on the combined reported UGS variable (having at least one symptom), 15.0% women reported symptoms of diseases pertaining to a urogenital infection. Supplementary Table 5 displays the results of the unadjusted and adjusted analyses of selected characteristics and the UGS outcome. Based on univariate and multivariate analysis none of the characteristics showed strong evidence of an association with the combined UGS variable. There was no evidence of multicollinearity in the multivariable models.

3.5. The effect of the WASH intervention on adequate MHM

Table 3 displays the effect of the WASH intervention on adequate MHM. Women living in intervention villages had 3.82 times the odds of adequately managing their menstruation compared to women living in the control villages (95% CI: 2.25–6.50) in the unadjusted analysis. After adjusting for age, caregiver education attainment, experience of stigma and wealth index, women living in the intervention villages had 3.54 times the adjusted odds of adequately managing their menstruation compared to women living in the control villages (95% CI: 1.86–6.78).

3.6. The effect of the WASH intervention on reported UGS

14.51% and 15.53% of women living in the control and intervention villages reported having at least one symptom of UGS. Women living in intervention villages had 0.92 times the odds of a reported UGS compared to women living in the control villages (95% CI: 0.66–1.37) in the unadjusted analysis (Table 4). After adjusting for experience of stigma and caregiver education attainment, women in the intervention villages had 0.97 times the odds of self-reporting symptoms (95% CI: 0.64–1.46; p = 0.9) than women living in the intervention villages. Having adequate MHM practice was not associated with UGS symptoms (0.81; 95%CI: 0.39–1.68 p = 0.6) when adjusted by age (Table 4).

4. Discussion

To the best of our knowledge, this is the first study to evaluate the effect of an intervention designed to improve water and sanitation at the household level on MHM practices and urogenital symptoms. The study findings support the hypothesis that the Gram Vikas WASH MANTRA intervention is associated with better MHM practices. Women living in the intervention villages reported more adequate MHM practices related to privacy aspects of changing and washing compared to women living in control villages. More women living in the intervention villages changed the absorbent in the household toilet and bathing room; whereas more women living in the control villages changed the absorbent outside (e.g. field, river, pond). Among women who reused the cloth, women in control villages washed their material in the pond or river three times more than women in intervention villages, whilst women in intervention villages washed their menstrual absorbents five times more often inside the toilet stall or bathing room compared to women in control villages. All these differences can be explained by the novelty of this intervention in providing toilets and bathrooms with piped water, which is not typical of WASH interventions in India or elsewhere.

Interestingly, a fifth of women in intervention villages still use ponds to wash their material, despite having a toilet or bathroom constructed at home. A similar result was observed in a qualitative study conducted in another rural district from the same state, which showed that only 20% of the interviewed women washed their absorbent in the latrines (MacRae et al., 2019b). The persistence of these washing practices could be explained by the socializing habits that women from rural communities have when going to open defecation, especially in the evening,

Table 3
The effect of the WASH intervention on adequate MHM among menstruating women living in Odisha, India July–October 2016 (N = 1045).

	Adequate MHM [a]				
		Unadjusted [b] *(n = 1045)*		Adjusted [c] *(n = 743)*	
n event/N (%)		**Odds Ratio (95% CI)**	**P-value [d]**	**Odds Ratio (95%CI)**	**P-value [d]**
Women living in control villages	25/528 (4.7)	1	<0.001	1	<0.001
		–		–	
Women living in intervention villages	81/517 (15.7)	3.82 (2.25–6.50)		3.54 (1.86–6.78)	

[a] Adequate menstrual hygiene practices definition: Adequate frequency of absorbent change, Wash body with soap and water (frequency and type of washing only) and privacy for managing menstruation.
[b] Adjusted for clustering at the pair and village level.
[c] The model was adjusted for clustering at the pair and village level, age and for variables that changed the OR by >10% in bivariate models including wealth index, female caregiver education attainment and experience of stigma (Supplementary Table 1). Sample size decreased due to missing data in the confounder variables. Data was missing because not all women responded to the HH survey as the HH survey targeted the mother or primary caregiver of the youngest child <5. Missing data were explored to investigate patterns and difference between the intervention groups using Chi square (Supplementary Table 2).
[d] P-values derived from nested likelihood ratio tests.

Table 4
The effect of the WASH intervention on reported urogenital symptoms (UGS) and effect of adequate MHM on UGS among menstruating women living in Odisha, India July–October 2016 (N = 1045).

		The combined UGS variable [a]					
			Univariate [b] *(n = 1045)*		Multivariate [c]		
		n event/N (%)	**Odds Ratio (95% CI)**	**P-value [d]**	**N[e]**	**Odds Ratio (95%CI)**	**P-value [d]**
WASH	Women living in control villages	82/528 (15.5)	1	0.8	901	1	0.9
			–			–	
	Women living in Intervention villages	75/517 (14.5)	0.92 (0.66–1.37)			0.97 (0.64–1.46)	
MHM [f]	Women who have inadequate MHM	143/939 (15.2)	1	0.6	957	1	0.6
			–			–	
	Women who have adequate MHM	14/106 (13.2)	0.84 (0.45–1.55)			0.81 (0.39–1.68)	

[a] The combined UGS variable consists of self-reported symptoms in the past two weeks of abnormal vaginal discharge, burning or itching in the genitalia, burning or itching when urinating and urinating frequently.
[b] Adjusted for clustering at the pair and village level.
[c] The model was adjusted for clustering at the pair and village level, age and variables that changed the OR by >10% in bivariate models. For the WASH variable this includes: Experience of stigma and female caregiver education. For the MHM variable there were no identified confounders to adjust for (Appendix 5).
[d] P-values derived from nested likelihood ratio tests.
[e] Total number of women in the final model.
[f] Adequate MHM definition: Wash body with soap and water and privacy for managing menstruation.

which is a rare opportunity for them to leave their houses and be free from household chores and responsibilities(Routray et al., 2015). Open defecation (OD) normally happens next to ponds and women probably change and wash their absorbent after practicing OD.

Similar practices were reported for adequate frequency of absorbent change and for washing the body with soap and water among both groups, suggesting that our intervention did not impact these aspects of MHM. We could hypothesize that having a private toilet and bathing area would increase the frequency of changes of absorbents; however, there was no difference in the frequency of absorbent change, indicating that this behavior could be influenced more by the type of material used, which the Gram Vikas MANTRA intervention did not attempt to change, and not much by the physical environment.

Therefore, privacy for managing menstruation appeared to be the biggest driver in the definition of adequate MHM. The findings of this study are consistent with previous studies that have shown that women who have access to WASH facilities have higher odds of adequately managing their menstruation than women who do not(Das et al., 2015; Hennegan et al., 2018). A qualitative study conducted in the same state reported that inadequate menstruation ranked as one of the most stressful sanitation behaviors for women', forcing them to navigate social and physical barriers during their daily sanitation routines(Hulland et al., 2015). Still, follow-on research in Odisha found that women who lacked access to a functional latrine, an enclosed bathing space, or a water source within their compound, had significantly higher overall 'Menstrual Insecurity' scores—indicating greater insecurity—than those with these facilities(Caruso et al., 2020). These findings suggest that WASH infrastructure has inherent benefits to menstruators, even if fully adequate MHM may not be realized. As such, intervention that address components of the WASH environment alone, like the Gran Vikas MANTRA intervention may be impactful and necessary in changing menstrual practices, even if not sufficient to enable adequate MHM.

Even though there was evidence that the intervention improved MHM, the proportion with adequate MHM practices in the intervention arm was still low (16%), suggesting that other factors such as type of material used, or cultural and traditional habits related to changing and washing can influence some of the practices that infrastructure cannot change alone. In fact, another qualitative study conducted in the same state to understand women's menstruation-related concerns, indicated that in order to improve menstrual experiences more is needed than facilities that change the physical environment alone(Caruso et al., 2017). Efforts to enable urinating, defecating and managing menstruation independently, comfortably, safely, hygienically, privately, healthily, with dignity and as needed require transformative approaches that also address the gendered, sociocultural and social environments that impact women despite facility access.

There were several other independent predictors of adequate MHM. Women who were wealthier and who had educated caregivers were more likely to have adequate MHM, suggesting the importance of knowledge and resource access. Several studies conducted in India have also showed similar results(Kansal et al., 2016; Khanna et al., 2005), indicating that wealth and education of the mother are important predictors for following hygienic practices during menstruation. There was a weak association with the experience of stigma and increase adequate MHM. One potential explanation is that women that experience stigma could change their practices, which could lead to better hygienic

practices.

The relationship between the WASH intervention, MHM and urogenital symptoms was less clear. Women living in the intervention villages reported less genital burning or itching compare to women living in control villages. This finding could be related to the type of menstrual material used, as women living in control villages used more reusable cloths. Previous studies conducted in Odisha, India found that women who use reusable pads were more likely to have urogenital symptoms than women who were using disposable sanitary pads(Das et al., 2015; Torondel et al., 2018). These previous studies also showed an association between changing in a toilet and reduced UGS. Our study did not find any association between reported urogenital symptoms between women living in the control or intervention villages, nor any association between women with adequate MHM and urogenital symptoms; however, we were limited by measuring reported symptoms only, genital symptoms can be poorly predictive of the urogenital infections(Anderson et al., 2004). More studies using laboratory diagnosed urogenital infections are needed to better understand health outcomes related to MHM and WASH interventions.

A growing number of studies in India have shown how access to sanitation may influence health beyond disease, particularly for women and girls(Caruso et al., 2018; Sclar et al., 2018). Different studies indicate that inadequate sanitation may put women and girls at greater risk of experiencing violence(World Health Organization, 2013). For example, an ethnographic study in urban slums in Pune and Jaipur documented the harassment and violence that women regularly face when going for open defecation(Kulkarni, O'Reilly and Bhat, 2017). Therefore, access to appropriate WASH when menstruating is very important for safety and mental health.

The strength of this study includes its design, a large matched-cohort that have received the WASH intervention since 2004. The match design provides rigorous means for estimating causal effects given that randomization to the intervention group was not feasible due to the several year implementation process(Arnold et al., 2010; Reese et al., 2017). While there are limitations inherent to observational studies, the matched study design and multivariable modelling analysis plan reduce the potential for confounding, and robust analytical methods were used to generate effect estimates(Reese et al., 2017). Another strength is that interviewers were women field workers and surveys were conducted in private spaces of the houses, which assured a relaxed environment to discuss a stigmatized topic.

There are several limitations. Firstly, the study outcomes of adequate MHM and symptoms were based on self-reported responses from the survey, which is subject to social desirability bias and recall bias. Secondly, the fact that we used a pool estimate to describe MHM, required to establish a predefined criterion to establish what was a good or bad practice for each component of the definition, which was based on very limited literature. The need for a pool estimate could be also questioned, as we believe it is useful to establish the state of MHM in different populations and use this data for advocacy, but other studies have argued that the definition did not capture other factors such as menstrual taboos or social support that can impact menstrual practices but are not captured in the definition(Hennegan et al., 2016; MacRae et al., 2019b). Hennegan also suggested that until evidence guidelines are developed, and comparable measures of MHM have been tested and used across studies, it is not advised to present only pooled estimates; it would be more informative to present the individual aspects that make up MHM to be able to understand relationships with outcomes(Hennegan et al., 2016). During the last years, the MHM definition has continued to evolve, and future studies should test other definitions to inspire how to assess adequacy(Hennegan et al., 2021; MacRae et al., 2019b). Thirdly, the study design presented certain limitations. As the main aim of the primary study aimed to asses longer-term effects, a study design in which the intervention status was not randomly assigned was employed (Reese et al., 2019). Despite both study arms being well balanced at the village-level after matching on pre-intervention characteristics, we still cannot rule out potential for residual confounding (Reese et al., 2019). In addition, we did not have available pre-intervention urogenital infections prevalence that could be used for the matching process. Another limitation is that we could not assess immediate impacts on the intervention of our outcomes of interest, due to the time lapse between intervention completion and study initiation (Reese et al., 2019). Finally, there are limitations to generalizability. Interventions study villages were randomly selected from those where the implementation was complete, however there were villages who refuse to participate when approached first time by Gram Vikas during their motivation visit. Despite these villages being excluded from the list of potential control villages, non-participating villages may be different from participating villages in their awareness of health risks, collective efficacy, or other characteristics, thus introducing selection bias(Reese et al., 2019). Therefore, this study cannot conclude that the Gram Vikas intervention can have the same impact observed in this study across all villages in this setting or elsewhere (Reese et al., 2019).

5. Conclusion

In conclusion, this study provides evidence that a combined intervention, where provision of household piped water connections were combined with community sanitation coverage, is important to improve environment that enable adequate MHM practices among women living in these communities. However, in order to achieve a higher impact on adequate MHM among women in these communities, more targeted interventions towards addressing other barriers to improve MHM are needed.

Declaration of competing interest

This research does not contain any conflict of interests.

Acknowledgments

We would like to acknowledge all the participants of the study, the field workers and everyone involved in data collection. We would also like to thank Helen Weiss, Clare Tanton and Richard Hayes for their advice in different aspects of the manuscript analysis.

Appendix A. Supplementary data

Supplementary data to this article can be found online at https://doi.org/10.1016/j.ijheh.2021.113866.

Funding

This work was supported by the Bill & Melinda Gates Foundation (OPP1008048).

Data statement

The datasets used and/or analyzed during the current study are available from the corresponding author on reasonable request.

References

Anderson, M.R., Klink, K., Cohrssen, A., 2004. Evaluation of vaginal complaints. Jama 291 (11), 1368–1379.

Arnold, B.F., Khush, R.S., Ramaswamy, P., London, A.G., Rajkumar, P., Ramaprabha, P., Colford, J.M., 2010. Causal inference methods to study nonrandomized, preexisting development interventions. In: Proceedings of the National Academy of Sciences, vol. 107, pp. 22605–22610, 52.

Baker, K.K., Padhi, B., Torondel, B., Das, P., Dutta, A., Sahoo, K.C., Freeman, M.C., 2017. From menarche to menopause: a population-based assessment of water, sanitation, and hygiene risk factors for reproductive tract infection symptoms over life stages in rural girls and women in India. PLoS One 12 (12).

Balamurugan, S.S., Bendigeri, N., 2012. Community-based study of reproductive tract infections among women of the reproductive age group in the urban health training centre area in hubli, Karnataka. Indian J. Community Med. 37 (1), 34–38. https://doi.org/10.4103/0970-0218.94020.
Bassani, D.G., Corsi, D.J., Gaffey, M.F., Barros, A.J., 2014. Local distributions of wealth to describe health inequalities in India: a new approach for analyzing nationally representative household survey data, 1992–2008. PLoS One 9 (10), e110694.
Bhilwar, M., Lal, P., Sharma, N., Bhalla, P., Kumar, A., 2015. Prevalence of reproductive tract infections and their determinants in married women residing in an urban slum of North-East Delhi, India. J. Nat. Sci. Biol. Med. 6 (Suppl. 1), S29.
Caruso, B.A., Clasen, T.F., Hadley, C., Yount, K.M., Haardörfer, R., Rout, M., Cooper, H. L., 2017. Understanding and defining sanitation insecurity: women's gendered experiences of urination, defecation and menstruation in rural Odisha, India. BMJ global health 2 (4), e000414.
Caruso, B.A., Cooper, H.L., Haardörfer, R., Yount, K.M., Routray, P., Torondel, B., Clasen, T., 2018. The association between women's sanitation experiences and mental health: a cross-sectional study in Rural, Odisha India. SSM-population health 5, 257–266.
Caruso, B.A., Portela, G., McManus, S., Clasen, T., 2020. Assessing women's menstruation concerns and experiences in rural India: development and validation of a menstrual insecurity measure. Int. J. Environ. Res. Publ. Health 17 (10), 3468.
Caruso, B.A., Sevilimedu, V., Fung, I.C.-H., Patkar, A., Baker, K.K., 2015. Gender disparities in water, sanitation, and global health. Lancet 386 (9994), 650–651.
Das, P., Baker, K.K., Dutta, A., Swain, T., Sahoo, S., Das, B.S., Bilung, B., 2015. Menstrual hygiene practices, WASH access and the risk of urogenital infection in women from Odisha, India. PLoS One 10 (6), e0130777.
Dasgupta, A., Sarkar, M., 2008. Menstrual hygiene: how hygienic is the adolescent girl? Indian J. Community Med.: official publication of Indian Association of Preventive & Social Medicine 33 (2), 77.
Dash, M., Padhi, S., Mohanty, I., Panda, P., Parida, B., 2013. Antimicrobial resistance in pathogens causing urinary tract infections in a rural community of Odisha, India. Journal of family & community medicine 20 (1), 20.
Diamond, A., Sekhon, J.S., 2013. Genetic matching for estimating causal effects: a general multivariate matching method for achieving balance in observational studies. Rev. Econ. Stat. 95 (3), 932–945.
Filmer, D., Pritchett, L.H., 2001. Estimating wealth effects without expenditure data—or tears: an application to educational enrollments in states of India. Demography 38 (1), 115–132.
Flores-Mireles, A.L., Walker, J.N., Caparon, M., Hultgren, S.J., 2015. Urinary tract infections: epidemiology, mechanisms of infection and treatment options. Nat. Rev. Microbiol. 13 (5), 269–284.
García, P.J., Chavez, S., Feringa, B., Chiappe, M., Weili, L., Jansen, K.U., Holmes, K.K., 2004. Reproductive tract infections in rural women from the highlands, jungle, and coastal regions of Peru. Bull. World Health Organ. 82, 483–492.
Garn, J.V., Sclar, G.D., Freeman, M.C., Penakalapati, G., Alexander, K.T., Brooks, P., Clasen, T.F., 2017. The impact of sanitation interventions on latrine coverage and latrine use: a systematic review and meta-analysis. Int. J. Hyg Environ. Health 220 (2), 329–340.
George, R., 2013. Celebrating womanhood: how better menstrual hygiene management is the path to better health, dignity and business: water Supply and Sanitation Collaborative Council.
Hayes, R.J., Moulton, L.H., 2017. Cluster randomised trials: Chapman and Hall/CRC.
Hennegan, J., Dolan, C., Wu, M., Scott, L., Montgomery, P., 2016. Measuring the prevalence and impact of poor menstrual hygiene management: a quantitative survey of schoolgirls in rural Uganda. BMJ open 6 (12), e012596.
Hennegan, J., Winkler, I.T., Bobel, C., Keiser, D., Hampton, J., Larsson, G., Mahon, T., 2021. Menstrual health: a definition for policy, practice, and research. Sexual and Reproductive Health Matters 29 (1), 1911618.
Hennegan, J., Zimmerman, L., Shannon, A., Exum, N., OlaOlorun, F., Omoluabi, E., Schwab, K., 2018. The relationship between household sanitation and women's experience of menstrual hygiene: findings from a cross-sectional survey in Kaduna State, Nigeria. Int. J. Environ. Res. Publ. Health 15 (5), 905.
Hulland, K.R., Chase, R.P., Caruso, B.A., Swain, R., Biswal, B., Sahoo, K.C., Dreibelbis, R., 2015. Sanitation, stress, and life stage: a systematic data collection study among women in Odisha, India. PLoS One 10 (11), e0141883.
International Institute for Population Sciences (IIPS), 2010. District level household and facility survey (DLHS-3), 2007–08: India, Orissa. Mumbai: International Institute for Population Studies (IIPS).
Kansal, S., Singh, S., Kumar, A., 2016. Menstrual hygiene practices in context of schooling: a community study among rural adolescent girls in Varanasi. Indian J. Community Med.: official publication of Indian Association of Preventive & Social Medicine 41 (1), 39.
Khanna, A., Goyal, R., Bhawsar, R., 2005. Menstrual practices and reproductive problems: a study of adolescent girls in Rajasthan. J. Health Manag. 7 (1), 91–107.
Kolenikov, S., Angeles, G., 2004. The use of discrete data in PCA: theory, simulations, and applications to socioeconomic indices. In: Chapel Hill: carolina Population Center. University of North Carolina, pp. 1–59.
Krupp, K., Madhivanan, P., Karat, C., Chandrasekaran, V., Sarvode, M., Klausner, J., Reingold, A., 2007. Novel recruitment strategies to increase participation of women in reproductive health research in India. Global Publ. Health 2 (4), 395–403.
Kulkarni, S., O'Reilly, K., Bhat, S., 2017. No relief: lived experiences of inadequate sanitation access of poor urban women in India. Gend. Dev. 25 (2), 167–183.
Lanfranco, O.A., Alangaden, G.J., 2016. Genitourinary tract infections. Diagnostic microbiology of the immunocompromised host 569–611.
MacRae, E.R., Clasen, T., Dasmohapatra, M., Caruso, B.A., 2019a. 'It's like a burden on the head': redefining adequate menstrual hygiene management throughout women's varied life stages in Odisha, India. PLoS One 14 (8).
MacRae, E.R., Clasen, T., Dasmohapatra, M., Caruso, B.A., 2019b. 'It's like a burden on the head': redefining adequate menstrual hygiene management throughout women's varied life stages in Odisha, India. PLoS One 14 (8), e0220114.
Nagarkar, A., Mhaskar, P., 2015. A systematic review on the prevalence and utilization of health care services for reproductive tract infections/sexually transmitted infections: evidence from India. Indian J. Sex. Transm. Dis. 36 (1), 18.
Narayan, K., Srinivasa, D., Pelto, P., Veerammal, S., 2001. Puberty rituals reproductive knowledge and health of adolescent schoolgirls in south India. Asia Pac. Popul. J. 16 (2), 225–238.
Plesons, M., Patkar, A., Babb, J., Balapitiya, A., Carson, F., Caruso, B.A., Jahangir, A., 2021. The state of adolescent menstrual health in low-and middle-income countries and suggestions for future action and research. Reprod. Health 18 (1), 1–13.
Prabha, M., Sasikala, G., Bala, S., 2012. Comparison of syndromic diagnosis of reproductive tract infections with laboratory diagnosis among rural married women in Medak district, Andhra Pradesh. Indian J. Sex. Transm. Dis. 33 (2), 112.
Reese, H., Routray, P., Torondel, B., Sclar, G., Delea, M.G., Sinharoy, S.S., Chang, H.H., 2017. Design and rationale of a matched cohort study to assess the effectiveness of a combined household-level piped water and sanitation intervention in rural Odisha, India. BMJ open 7 (3), e012719.
Reese, H., Routray, P., Torondel, B., Sinharoy, S.S., Mishra, S., Freeman, M.C., Clasen, T., 2019. Assessing longer-term effectiveness of a combined household-level piped water and sanitation intervention on child diarrhoea, acute respiratory infection, soil-transmitted helminth infection and nutritional status: a matched cohort study in rural Odisha, India. Int. J. Epidemiol. 48 (6), 1757–1767.
Routray, P., Schmidt, W.-P., Boisson, S., Clasen, T., Jenkins, M.W., 2015. Socio-cultural and behavioural factors constraining latrine adoption in rural coastal Odisha: an exploratory qualitative study. BMC Publ. Health 15 (1), 880.
Sahoo, K.C., Hulland, K.R., Caruso, B.A., Swain, R., Freeman, M.C., Panigrahi, P., Dreibelbis, R., 2015. Sanitation-related psychosocial stress: a grounded theory study of women across the life-course in Odisha, India. Soc. Sci. Med. 139, 80–89.
Schmidt, W.-P., Cairncross, S., Barreto, M.L., Clasen, T., Genser, B., 2009. Recent diarrhoeal illness and risk of lower respiratory infections in children under the age of 5 years. Int. J. Epidemiol. 38 (3), 766–772.
Schmiemann, G., Kniehl, E., Gebhardt, K., Matejczyk, M.M., Hummers-Pradier, E., 2010. The diagnosis of urinary tract infection: a systematic review. Deutsches Ärzteblatt International 107 (21), 361.
Sciences, I.I.f.P., 2006. District level household survey (DLHS-2), 2002–04: IIPS. Mumbai, India.
Sclar, G., Penakalapati, G., Caruso, B., Rehfuess, E.A., Garn, J., Alexander, K., Clasen, T., 2018. Exploring the relationship between sanitation and mental and social well-being: a systematic review and qualitative synthesis. Soc. Sci. Med. 217, 121–134.
Sebastian, A., Hoffmann, V., Adelman, S., 2013. Menstrual management in low-income countries: needs and trends. Waterlines 32 (2), 135–153.
Sinharoy, S.S., Reese, H.E., Praharaj, I., Chang, H.H., Clasen, T., 2021. Effects of a combined water and sanitation intervention on biomarkers of child environmental enteric dysfunction and associations with height-for-age z-score: a matched cohort study in rural Odisha, India. PLoS Neglected Trop. Dis. 15 (3), e0009198.
Sommer, M., Chandraratna, S., Cavill, S., Mahon, T., Phillips-Howard, P., 2016. Managing menstruation in the workplace: an overlooked issue in low-and middle-income countries. Int. J. Equity Health 15 (1), 86.
Sommer, M., Hirsch, J.S., Nathanson, C., Parker, R.G., 2015. Comfortably, safely, and without shame: defining menstrual hygiene management as a public health issue. Am. J. Publ. Health 105 (7), 1302–1311.
Sommer, M., Sahin, M., 2013. Overcoming the taboo: advancing the global agenda for menstrual hygiene management for schoolgirls. Am. J. Publ. Health 103 (9), 1556–1559.
Torondel, B., Sinha, S., Mohanty, J.R., Swain, T., Sahoo, P., Panda, B., Cumming, O., 2018. Association between unhygienic menstrual management practices and prevalence of lower reproductive tract infections: a hospital-based cross-sectional study in Odisha, India. BMC Infect. Dis. 18 (1), 473.
van Eijk, A.M., Sivakami, M., Thakkar, M.B., Bauman, A., Laserson, K.F., Coates, S., Phillips-Howard, P.A., 2016. Menstrual hygiene management among adolescent girls in India: a systematic review and meta-analysis. BMJ open 6 (3), e010290.
Wasserheit, J.N., Harris, J.R., Chakraborty, J., Kay, B.A., Mason, K.J., 1989. Reproductive tract infections in a family planning population in rural Bangladesh. Stud. Fam. Plann. 20 (2), 69–80.
World Bank, 2010. A decade of the total sanitation campaign : rapid assessment of processes and outcomes, 2. Annexes. Retrieved from Washington, DC. http://hdl.handle.net/10986/17287.
World Health Organization, 2013. Global and regional estimates of violence against women: prevalence and health effects of intimate partner violence and non-partner sexual violence. World Health Organization.
World Health Organization, 2019. Progress on household drinking water, sanitation and hygiene 2000-2017: special focus on inequalities. World Health Organization.

International Journal of Hygiene and Environmental Health 239 (2022) 113879

Contents lists available at ScienceDirect

International Journal of Hygiene and Environmental Health

journal homepage: www.elsevier.com/locate/ijheh

Effects of SNPs in *SOD2* and *SOD3* interacted with fluoride exposure on the susceptibility of dental fluorosis

Yuhui Du [a], Xiaoli Fu [a], Jing Jin [b], Zhiyuan Li [a], Kaihong Xu [a], Meng Guo [a], Xiangbo Hou [a], Zichen Feng [a], Limin Ding [a], Yongxiang Gong [a], Bin Liu [a], Fangfang Yu [a], Guoyu Zhou [a], Yue Ba [a,*]

[a] School of Public Health, Zhengzhou University, Zhengzhou, Henan, 450001, China
[b] Houzhai Center Hospital, Erqi District, Zhengzhou, Henan, 450001, China

ARTICLE INFO

Keywords:
Fluoride
Single nucleotide polymorphism
SOD2 gene
SOD3 gene
Dental fluorosis

ABSTRACT

A total of 649 children aged 7–13 years of age were recruited in a cross-sectional study in Tongxu County, China (2017) to assess the effects of interaction between single nucleotide polymorphisms (SNPs) in *SOD2* and *SOD3* gene and fluoride exposure on dental fluorosis (DF) status. Associations between biomarkers and DF status were evaluated. Logistic regression suggested that the risk of DF in children with rs10370 GG genotype and rs5746136 TT genotype was 1.89-fold and 1.72-fold than that in children with TT/CC genotype, respectively. Increased T-SOD activity was associated with a lower risk of DF (*OR* = 0.99). The rs2855262*rs10370*UF model was regarded as the optimal interaction model in generalized multifactor dimensionality reduction analyses. Our findings suggested that rs4880 and rs10370 might be useful genetic markers for DF, and there might be interactions among rs10370 in *SOD2*, rs2855262 in *SOD3,* and fluoride exposure on DF status.

1. Introduction

Multiple elements exposure in the environment might affect human health (Ceballos et al., 2021; Soler-Blasco et al., 2020; Wan et al., 2021). Excessive ingestion of fluoride can induce fluorosis. Dental fluorosis (DF) is one of the typical clinical features and is regarded as the first discovery of a clinical feature, suggesting the association between fluoride exposure and human health (Jha et al., 2011). DF is characterized by mottling, chalky spots (or stripes, plaques), yellowish to black stains, and even pitting defect on tooth or enamel surfaces. Considering its role as a biomarker of other health lesions caused by fluoride and effects on mental health, DF is an important clinical symptom (Molina-Frechero et al., 2017; Yu et al., 2018).

Excessive intake of fluoride during tooth formation has been confirmed as the main risk factor for DF (Moller, 1982; Pendrys and Stamm, 1990). The effects of fluoride on teeth are mediated through several ways. Fluoride reacts with calcium, depositing calcium fluoride in the developing tooth structure, disturbing normal mineralization of enamel, and causing anomalous spherical structure in the normal crystalline structure, with increased porosity and opacity (Everett, 2011). The mechanism of odontoblasts apoptosis induced by sodium fluoride (NaF) has also been confirmed in vitro (Li et al., 2013). In addition, fluoride exposure might have detrimental effects on transitional, early-secretory, and maturation stages of ameloblasts and the developing enamel matrix (DenBesten and Thariani, 1992; Lyaruu et al., 2006), significantly impacting fluoride-induced tooth damage. Oxidative stress, as an important mode of fluoride toxicity (Chouhan et al., 2010; Garcia-Montalvo et al., 2009; Zhang et al., 2007), might be responsible for several mechanisms above. Previous studies have confirmed that fluoride exposure induces oxidative stress, activating apoptotic pathway in cementoblasts and ameloblasts (Li et al., 2017; Ni et al., 2018; Wang et al., 2016). Superoxide dismutase isozymes (SODs), an important family of the oxidative stress system, are essential to protect the body from effects of O_2^-, including SOD1, SOD2 and SOD3. SOD1, also called Cu/Zn-SOD, is almost exclusively found in intracellular cytoplasmic spaces. SOD2 (Mn-SOD) and SOD3 (extracellular Cu/Zn-SOD) can allbe found in serum (Zelko et al., 2002). It has been reported that mutations in genes might be associated with changes in phenotypes and mutations in *SOD2*, and *SOD3* genes appear to be associated with changes in serum SOD activity (Lewandowski et al., 2020). The SOD activity is believed to be involved in several

* Corresponding author.
E-mail addresses: 694078176@qq.com (Y. Du), xlfu66@126.com (X. Fu), 670030787@qq.com (J. Jin), lizhiyuan@zzu.edu.com (Z. Li), kaihhongong@163.com (K. Xu), 15754307599@163.com (M. Guo), 1142077913@qq.com (X. Hou), 2313888516@qq.com (Z. Feng), 1617738851@qq.com (L. Ding), 1610991676@qq.com (Y. Gong), 2507656299@qq.com (B. Liu), yufangfang@zzu.edu.cn (F. Yu), zhouguoyu@zzu.edu.cn (G. Zhou), byyue@zzu.edu.cn (Y. Ba).

https://doi.org/10.1016/j.ijheh.2021.113879
Received 11 August 2021; Received in revised form 11 October 2021; Accepted 28 October 2021
Available online 2 November 2021

Abbreviation

DF	dental fluorosis
SNPs	single nucleotide polymorphisms
GMDR	generalized multifactor dimensionality reduction analyses
SODs	Superoxide dismutase isozymes
AMBN	*ameloblastin*
TFIP11	*tuftelin interacting protein 11*
TUFT1	*tuftelin*
COL1A2	*type I collagen alpha 2 chain*
ESR	*estrogen receptor*
BMI	body mass index
CDC	Centers for Disease Control and Prevention
CV	coefficient of variant
T-SOD	total superoxide dismutase
UF	Urinary fluoride
UCr	urinary creatinine
OR	odds ratio
CI	confidence interval
TBA	testing balanced accuracy
CVC	cross-validation consistency

fluoride-induced health effects, including reproductive damage, neural impairment, and hepatic anomalies (Adelakun et al., 2021; Cao et al., 2019; Lu et al., 2017). A study of Li et al. (2017) indicated that SOD activity also played an important role in the mechanism of NaF-induced ameloblast apoptosis. Therefore, SOD activity might correlate with the DF status.

It is noteworthy that genetic factors, such as gene polymorphisms, have attracted considerable attention concerning DF susceptibility. Previous studies (Charone et al., 2019; Dalledone et al., 2019; Kuchler et al., 2018) found that the polymorphisms of *ameloblastin* (*AMBN*), *tuftelin interacting protein* 11 (*TFIP11*), *tuftelin* (*TUFT1*), *Ambn*、*Col14a1*, *Mmp20* and *estrogen receptor 1* (*ESR1*) might have a relationship with the risk of DF. Our previous studies showed that *type* I *collagen alpha* 2 *chain* (*COL1A2*) gene *Pvu*II and *ESR* gene polymorphisms were also related to DF development (Ba et al., 2011; Huang et al., 2008). Considering the important role of SOD activity in the DF process, variations in SOD genotypes would be associated with the prevalence of DF. Besides, a study demonstrated that the health effects of fluoride exposure had interactions with genetic factors (Ma et al., 2017). However, differential susceptibility of genetic factors to DF and the effects of interactions between fluoride exposure and genetic factors on DF development remains unclear.

Given the above, a cross-sectional study was conducted in a rural area located in Tongxu County of Henan Province. Five single nucleotide polymorphisms (SNPs) were selected from *SOD2* and *SOD3* genes to assess the effects of genetic polymorphisms and interactions with fluoride exposure on the prevalence of DF in school-age children to provide useful genetic marker for differential risk of DF and epidemiological evidence for prevention of DF.

2. Materials and methods

2.1. Location and subjects

As described in our previous study (Wang et al., 2021), a cross-sectional study was conducted in rural areas of Tongxu County of Henan province, China, an endemic fluorosis area of drinking water type due to natural geological structure in 2017. Four local primary schools were randomly selected according to fluoride concentration, one of which was located in the fluorosis area and the other three were located in the non-fluorosis area. Students in grades 2–6 from the four schools were selected by the cluster sampling method. From which we selected students who were born and resided locally. They did not expose to other fluoride sources from brick tea and industry dust. Children who were non-local residents or had received calcium and phosphorus supplements were excluded. Children with diseases affecting calcium and phosphorus metabolism, digestive diseases, thyroid-related disease, and neuropsychiatric disorders were also excluded. All the 649 children aged 7–13 years recruited in the study were boarding-school students and had similar living conditions, living habits and dietary patterns. There is no fluoride pollution from coal combustion and industry in the investigated area, and the local residents had no habit of drinking brick tea. Therefore, drinking water is the main source of fluoride exposure. Children and their guardians agreed to participate in the study and signed informed consent forms after being informed of the study procedure. The protocol of this research was approved by the Ethics Committee of Zhengzhou University (ZZUIRB, 2017–018).

2.2. Collection of general information

Demographic data were obtained through a structured questionnaire by a face-to-face interview, including age, gender, class, grade, health status, paternal and maternal information, etc. Both children and their guardians joined in and provided information.

The body mass index (BMI) was used to assess children's developmental status. All the subjects were examined by skilled medical professionals from Kaifeng Centers for Disease Control and Prevention (CDC) to measure height and weight. Height (cm) and weight (kg) were measured in duplicate by a standard measurement device (V. BODY HBF-371; OMRON, Kyoto, Japan). Precisions were 0.1 cm and 0.1 kg, respectively, and the mean value was used for calculation. The BMI was calculated using height and weight values with the formula: BMI (kg/m^2) = weight/height^2.

2.3. Assessment of dental fluorosis

DF was also examined by the public medical professionals from Kaifeng CDC. Prior to the examination, medical experts were trained in diagnostic criteria and achieved unified examination skills. Then the examinations were performed in a brightly lit room. After tooth cleaning and drying, all the buccal surfaces of permanent teeth were examined with the help of artificial lights. Dean's fluorosis index (WS/T 208–2011) was used to determine the presence of DF. Each child was examined twice by two independent medical professionals. The accordant results of double measurements were recorded. In case of disagreement, the third expert joined in and performed the third assessment, and the final diagnosis was recorded by collating the three diagnostic results.

2.4. Measurement of urinary fluoride and urinary creatinine

Urinary fluoride (UF) concentrations were determined as the internal exposure levels and urinary creatinine (UCr) levels were used to correct for variations in urine dilution, in this study. All the children provide more than 50 mL of early-morning urine samples for measuring UF and UCr concentrations. UF levels were measured by the fluoride ion-selective electrode method (Shanghai Exactitude Instrument, Shanghai, China), with 0.01 mg/L of the detection limit. All the samples were measured twice, and mean values were used. The coefficient of variant (CV) values of repeated determinations were all <10%. UCr contents were determined using the picric acid method and all the assays were performed according to the kit protocol (Creatinine Assay Kit C011-1-1, Jiancheng Bioengineering Institute, Nanjing, China), which were used to correct for variations in urine dilution (Bashash et al., 2017). Each sample was measured twice and average values were used. In addition, 15% of urine samples from different plates were randomly

selected to repeat the measurement. The CV values of repeated tests were <10%.

2.5. Assessment of SOD activity

Peripheral fasting blood samples were collected, and serums were separated. Each serum sample was used to assess the total superoxide dismutase (T-SOD) activity. All the assays were performed according to the manufacturer's instructions. Ten percent of serum samples were randomly selected for duplicate measurements. The CV coefficients ranges was <10%, and mean values of repeated measurement were ultimately used.

The T-SOD activity was assessed with the Xanthine Oxidase Method (Total SOD Assay Kit A001-1, Jiancheng Bioengineering Institute, Nanjing, China). In this method, the xanthine-xanthine oxidase system was used as a superoxide generator. SOD can inhibit the generation of nitrite by the reaction between hydroxylamine and superoxide. The reduction of absorbance at 550 nm was measured at room temperature (RT). One unit of SOD was defined as the amount of enzyme that causes 50% inhibition.

2.6. Identification of genotypes

Five SNPs in *SOD2* and *SOD3* were selected from Haploview software, meeting the following criteria: (1) The minor allele frequencies of these SNPs were all >0.1; (2) these SNPs were reported in previous studies; (3) The retained SNPs in the same gene was not strong in linkage disequilibrium (pairwise $r^2 < 0.8$). According to the criteria, 5 SNPs from the *SOD2* and *SOD3* genes were retrieved, including rs10370 (in *SOD2*), rs4880 (in *SOD2*), rs5746136 (in *SOD2*), rs13306703 (in *SOD3*) and rs2855262 (in *SOD3*) (see Table S1).

Genomic DNA miniprep kits (LifeFeng Biotechnology, Shanghai, China) were used to extract the genomic DNA from the peripheral blood samples. The genotyping of the 5 SNPs was performed by operators blinded to subjects' information using a custom-by-design 48-Plex SNPscan™ Kit (Cat#: G0104; Genesky Biotechnologies Inc., Shanghai, China). The kit was developed according to the patented SNP genotyping technology of Genesky Biotechnologies Inc., based on double ligation and multiplex fluorescence PCR. The reaction was carried out in an ABI2720 thermal cycler (Chen et al., 2012). Approximately 4% of the samples were repeatedly genotyped for quality control, and the consistency rate was >96%. The identified genotypes were TT/TG/GG for rs10370, GG/GA/AA for rs4880, CC/CT/TT for rs5746136, CC/CT/TT for rs13306703 and TT/TC/CC for rs2855262.

2.7. Statistical analyses

The dataset was created using the Epidata3.0 software (Epidata Association Odense, Denmark) and all data were put in independently by two operators.

Means and standard deviations were displayed for age, BMI, UCr concentration, UF levels, T-SOD activity, and percentages/proportions for gender, gene types, and allele types. The chi-square test and student's *t*-test were used for difference testing in continuous and categorical variables between children with and without DF. In trend testing, new variables were generated based on the UF concentrations and the T-SOD activity, taking the median value of each tertile range as every value in this tertile range. Multiple logistic regressions were employed to explore associations between DF and biomarkers, with or without covariates adjustments, and reported as the odds ratio (*OR*) with the 95% confidence interval (*CI*).

Furthermore, the associations between T-SOD activity and SNPs were also evaluated, reporting β value with the 95% *CI*. The statistical analyses above were performed by SPSS 21.0 (SPSS Inc., Chicago, USA). In addition, taking previous studies as references, multivariable linear or logistic regressions were adjusted by confounding factors such as age, gender, BMI and UCr (Abanto Alvarez et al., 2009; Narwaria and Saksena, 2013; Zhou et al., 2019a). To further explore the associations between interactions of genetic factors and fluoride exposure and the risk of DF, the generalized multifactor dimensionality reduction (GMDR) method was performed with 10-fold cross-validation. A dichotomous variable of fluoride exposure, generated by UF concentrations taking 1.4 mg/L as the cutoff value, was used in the GMDR analyses. The models were assessed by the testing balanced accuracy (TBA), cross-validation consistency (CVC) scores, and *P* values. The TBA was used to evaluate the accuracy of the interaction to predict DF status. The CVC scores are measures of the consistency degree defined as the times of a given combination regarded as the optimal model in a particular validated run. The *P* values were used to assess the significance of an identified model. The GMDR analyses were performed using GWAS-GMDR 1.0 beta software (http://ibi.zju.edu.cn/software) (Xu et al., 2016). The test was regarded statistically significant at $P < 0.05$.

3. Results

3.1. The distributions of general characteristics and biomarkers in children with and without DF

A total of 649 subjects aged 7–13 years were recruited in the present study dataset, including 337 (51.9%) girls and 312 (48.1%) boys. Totally, 178 (27.4%) children were suffering from DF. As shown in Table 1, the children were divided into two groups by DF status: the non-DF and DF groups. The mean ages in the DF group was significantly higher than in the non-DF group ($P = 0.026$). The gender, BMI and UCr in the DF group were comparable to the non-DF group. Compared with children in the non-DF group, children in the DF group exhibited higher UF concentrations and lower T-SOD levels. The DF prevalence in children with high fluoride exposure (UF > 1.4 mg/L) was 33.4%, while it was 22.6% in children with low fluoride exposure (UF ≤ 1.4 mg/L).

3.2. The associations between DF and biomarkers

The ancestral allele types are T for rs10370, G for rs4880, C for rs5746136, C for rs13306703 and T for rs2855262 (see Table S1). The genotype distributions of SNPs are presented in Table 2. We found that children with the GG genotype of rs10370 had a 1.89-fold (95%*CI* for *OR*: 1.20, 2.96) DF risk than children with the TT genotype, after adjusting for the control factors. An increased risk of DF was also observed in children carrying the TT genotype of rs5746136 (*OR*: 1.72, 95% *CI* for *OR*: 1.09, 2.69). In terms of alleles, compared with children carrying the T/C alleles, children carrying the G allele of rs10370 (*OR* = 1.31) or T allele rs5746136 (*OR* = 1.26) had a higher risk of DF.

The associations between UF and DF are presented in Table 3. The prevalence of DF showed an upward trend across tertiles of UF (all *P* <

Table 1
General characteristics of the study population.

variables	non-DF ($n = 471$)	DF ($n = 178$)	*t*/	*P* value
Age (year)[a]	9.96 ± 1.31	10.22 ± 1.26	2.230	**0.026**
Gender[b]			1.339	0.247
Boys	233(74.7)	79(25.3)		
Girls	238(70.6)	99(29.4)		
BMI (kg/m^2)[a]	17.65 ± 3.17	17.40 ± 2.34	1.087	0.278
UCr (mg/L)[a]	972.32 ± 660.51	1009.68 ± 679.68	0.630	0.529
UF (mg/L)[a]	1.31 ± 0.85	1.59 ± 0.88	3.634	**<0.001**
UF group[b]			9.550	**0.002**
UF ≤ 1.4 mg/L	278(77.4)	81(22.6)		
UF > 1.4 mg/L	193(66.6)	97(33.4)		
T-SOD (U/ml)[a]	115.56 ± 21.05	111.32 ± 20.61	2.324	**0.021**

Abbreviation: BMI, body mass index; DF, dental fluorosis; T-SOD, total superoxide dismutase; UCr, urinary creatinine; UF, urinary fluoride.

[a] Continuous variables were presented by mean ± standard deviation.

[b] Categorical variables were presented by number (proportion/percentage).

Table 2
The association between SNPs and the risk of DF.

SNPs	non-DF ($n = 471$)	DF ($n = 178$)	*OR* (95% *CI*)[a]	*P* value for genotypes	*P* value for alleles
SOD2					
rs10370				**0.008**	
TT	142 (30.1)	46 (25.8)	reference		
TG	241 (51.2)	81 (45.5)	1.07 (0.73,1.57)	0.741	
GG	88 (18.7)	51 (28.7)	1.89 (1.20,2.96)	**0.006**	
T	525 (55.7)	173 (48.6)	reference		
G	417 (44.3)	183 (51.4)	1.31 (1.04,1.64)		**0.021**
rs4880				0.496	
GG	13 (2.8)	4 (2.2)	reference		
GA	126 (26.8)	45 (25.3)	1.58 (0.48,5.17)	0.452	
AA	332 (70.5)	129 (72.5)	1.81 (0.57,5.74)	0.316	
G	152 (16.1)	53 (14.9)	reference		
A	790 (83.9)	303 (85.1)	1.17 (0.85,1.62)		0.333
rs5746136				**0.034**	
CC	134 (28.5)	42 (23.6)	reference		
CT	238 (50.5)	84 (47.2)	1.08 (0.73,1.60)	0.683	
TT	99 (21.0)	52 (29.2)	1.72 (1.09,2.69)	**0.019**	
C	506 (53.7)	168 (47.2)	reference		
T	436 (46.3)	188 (52.8)	1.26 (1.01,1.58)		**0.044**
SOD3					
rs13306703				0.646	
CC	326 (69.2)	125 (70.2)	reference		
CT	135 (28.7)	47 (26.4)	0.89 (0.62,1.29)	0.552	
TT	10 (2.1)	6 (3.4)	1.39 (0.52,3.71)	0.514	
C	787 (83.5)	297 (83.4)	reference		
T	155 (16.5)	59 (16.6)	0.97 (0.72,1.32)		0.858
rs2855262				0.460	
TT	198 (42.0)	81 (45.5)	reference		
TC	223 (47.3)	76 (42.7)	0.83 (0.59,1.16)	0.270	
CC	50 (10.6)	21 (11.8)	1.06 (0.62,1.81)	0.838	
T	619 (65.7)	238 (66.9)	reference		
C	323 (34.3)	118 (33.1)	0.98 (0.78,1.25)		0.893

[a] Adjusted by age, gender, BMI, UCr and UF.

0.05). Compared with children in tertile 1, children in tertile 2 and in tertile 3 had 1.85-fold and 2.47-fold DF risk, respectively. A 1.53-fold (95%*CI* for *OR*: 1.22, 1.93) risk of DF was observed for each 1 mg/L increment in UF concentrations after adjusting for potential confounding factors.

The associations between T-SOD activity and DF levels are presented in Table 4. The risk of DF showed upward trends across tertiles of T-SOD (*P* for trend <0.05) after adjusting for covariates. The risk of DF in children decreased 0.1% with an increase in per-unit T-SOD activity, suggesting that increased T-SOD activity was a protective factor for the incidence of DF.

Table 3
The association between UF and DF.

UF (mg/L)	DF			
	Crude, *OR* (95% *CI*)	*P* value	Adjusted, *OR* (95% *CI*)[a]	*P* value
Tertile 1(≤0.88)	Reference		Reference	
Tertile 2 (0.89–1.64)	1.72(1.10,2.69)	**0.018**	1.85(1.17,2.93)	**0.008**
Tertile 3(>1.64)	2.30(1.48,3.57)	**<0.001**	2.47(1.52,4.02)	**<0.001**
Trend test		**<0.001**		**<0.001**
Increase per 1 mg/L	1.43(1.18,1.74)	**<0.001**	1.53(1.22,1.93)	**<0.001**

[a] Adjusted by age, gender, BMI and UCr.

Table 4
The association between T-SOD and DF.

T-SOD (U/mL)	DF			
	Crude, *OR* (95% *CI*)	*P* value	Adjusted, *OR* (95% *CI*)[a]	*P* value
Tertile 1(≤105.37)	Reference		Reference	
Tertile 2 (105.38–123.35)	0.95(0.69,1.33)	0.778	1.01(0.71,1.46)	0.933
Tertile 3(>123.35)	0.60(0.42,0.85)	**0.004**	0.64(0.43,0.95)	**0.029**
Trend test		**0.005**		**0.034**
Increase per 1 mg/L	0.99(0.98,0.99)	**0.004**	0.99(0.98,0.99)	**0.014**

[a] Adjusted by age, gender, BMI, UCr and UF.

3.3. The associations between SNP types and T-SOD activity

Simple and multiple linear regressions were used to explore the associations between SNPs and T-SOD activity. After covariates adjustments, significant associations were observed between the T-SOD activity and polymorphisms of rs10370 and rs4880. Compared with children carrying the TT/GG genotypes, children with the GG genotype of rs10370 and the AA genotype of rs4880 exhibited 4.24 U/mL and 4.25 U/mL reductions in T-SOD activity, respectively. No associations were observed between rs5746136, rs13306703, and rs2855262 genotypes and the T-SOD activity. Compared with children carrying the T allele, children carrying the G allele of rs10370 exhibited significant reductions in T-SOD activity (adjusted $\beta = -3.87$, 95%*CI* for β: −6.03, −1.71), after adjusting for confounding factors. Similarly, children carrying the A allele of rs4880 and the T allele of rs5746136 also exhibited significantly reduced T-SOD activity compared to children carrying the G/C allele (Table 5).

3.4. The effects of interactions between gene types and fluoride exposure

GMDR analyses were performed to explore the effects of interactions between fluoride exposure and *SOD2* and *SOD3* polymorphisms on the risk of DF. The possible interaction models are summarized in Table 6. After covariate adjustments, the GMDR analyses suggested three interaction models of UF*rs10370, UF*rs2855262*rs10370, and UF*rs2855262*rs10370*rs4880 with statistically significant differentiation (all $P = 0.0107$), indicating potential gene-environment interactions among UF, rs10370, rs2855262, and rs4880. Based on TBA and CVC, UF*rs2855262*rs10370 model was regarded as the optimal model, showing a good CVC of 10/10 and TBA of 58.66%. The high-risk and low-risk distributions of the optimal model are illustrated in Fig. 1. We found the GG genotype of rs10370, higher UF concentrations (>1.4 mg/L) combined with the TT genotype of rs2855262 took the highest DF risk with the highest sum score in the optimal model. The combinations of rs10370 = GG*UF > 1.4 mg/L and rs4880 = AA*rs10370 = GG*UF ≤ 1.4 mg/L*rs2855262 = TT had the maximum risks in the other two statistically significant models (Figs. S1 and S2), respectively.

Table 5
The associations of SNPs and T-SOD activity.

SNPs	T-SOD activity			
	Crude β (95% *CI*)	*P*-value	Adjusted β (95% *CI*)[a]	*P*-value
SOD2				
rs10370				
TT	reference		reference	
TG	−2.06(−5.01,0.884)	0.170	−2.22(−5.29,0.84)	0.155
GG	−2.86(−6.53,0.82)	0.127	−4.24(−8.06,−0.43)	**0.029**
T	reference		reference	
G	−2.89(−4.97,−0.80)	**0.007**	−3.87(−6.03,−1.71)	**<0.001**
rs4880				
GG	reference		reference	
GA	−0.07(−10.41,10.26)	0.989	−5.77(−15.83,4.29)	0.259
AA	−3.82(−7.12, −0.52)	**0.023**	−4.25(−7.65, −0.84)	**0.015**
G	reference		reference	
A	−3.27(−6.20, −0.33)	**0.029**	−3.80(−6.80,−0.80)	**0.013**
rs5746136				
CC	reference		reference	
CT	−2.09(−5.04,0.85)	0.164	−2.39(−5.45,0.67)	0.126
TT	−2.17(−5.73,1.39)	0.231	−3.25(−6.97,0.46)	0.086
C	reference		reference	
T	−2.54(−4.62, −0.46)	**0.017**	−3.43(−5.59, −1.27)	**0.002**
SOD3				
rs13306703				
CC	reference		reference	
CT	1.67(−1.64,4.98)	0.322	1.77(−1.70,5.25)	0.317
TT	−10.05(−18.41, −1.68)	**0.019**	−3.91(−13.60,5.79)	0.429
C	reference		reference	
T	−0.72(-3.50,2.06)	0.611	−0.66(−2.26,3.59)	0.657
rs2855262				
TT	reference		reference	
TC	2.65(−0.30,5.60)	0.079	1.69(−1.38,4.76)	0.281
CC	−0.98(−5.84,3.88)	0.692	−1.37(−6.31,3.58)	0.588
T	reference		reference	
C	1.08(−1.13,3.29)	0.339	0.35(−1.93,2.63)	0.763

[a] Adjusted by age, gender, BMI, UCr and UF.

Table 6
The summary information for GMDR.

model	TBA	*P* value[a]	CVC
rs10370	0.5365	0.3770	8/10
UF*rs10370	0.5429	**0.0107**	9/10
UF*rs2855262*rs10370	0.5866	**0.0107**	10/10
UF*rs2855262*rs10370*rs4880	0.5497	**0.0107**	9/10
UF*13306703*rs2855262*rs10370*rs4880	0.5115	0.3770	9/10
UF*13306703*rs2855262*rs10370*rs4880*rs5746136	0.5056	0.8281	10/10

[a] Adjusted by age, gender, BMI and UCr.

4. Discussion

The relationships between biomarkers (UF, T-SOD, and SNPs) and DF were explored in the present study. The associations between T-SOD activity and SNPs in *SOD2* and *SOD3* genes were also tested. Then the associations between gene-environment interactions and the risk of DF were investigated with GMDR analyses. We found that children with the GG genotype of rs10370 and the TT genotype of rs5746136 had a 1.89-fold and 1.72-fold risk of DF, respectively, than children carrying the TT/CC gene types, and compared with children carrying the T/G/C alleles, children carrying the G allele of rs10370, the A allele of rs4880 or the T allele of rs5746136 had a higher risk of DF. In addition, increased T-SOD activity was associated with a lower risk of DF. Besides, interactions of rs2855262, rs10370 and UF were regarded as the optimal model in the risk of DF, in which, the children carrying the GG genotype of rs10370, the TT genotype of rs2855262 and having higher UF concentrations (>1.4 mg/L) had the highest risk of DF.

Given the number of DF cases and affected areas, the drinking water type endemic fluorosis is still a major public health concern in China, especially in the north-central region. There were still 1055 counties regarded as drinking water type endemic fluorosis regions, and 12.41 million suffered from dental fluorosis until the end of 2019 according to the National Health Commission of the P.R. China (http://www.nhc.gov.cn/guihuaxxs/s10748/202006/ebfe31f24cc145b198dd730603ec4442.shtml). Therefore, it is essential to identify the susceptible populations to prevent DF. Studies have widely investigated the importance of fluoride exposure, including the duration, ingested amount, and the stage of fluoride exposure, in the incidence of DF (DenBesten and Thariani, 1992; Robinson and Kirkham, 1990). Consistent with previous studies (Yu et al., 2018; Zhou et al., 2019a), the positive associations between the risk of DF and UF concentrations in children aged 7–13 years were also observed in this study. Recent researches have directed attention toward the importance of oxidative stress in the mechanisms of fluoride-induced DF (Li et al., 2017; Zhou et al., 2019b). A significant decrease in SOD activity in NaF-treated ameloblasts has been reported (Li et al., 2017). In this study, reductions in the risk of DF were associated with T-SOD activity, suggesting that increased T-SOD activity might be a protective factor for DF. Studies have shown that mutations in *SOD3* and *SOD2* gene might be associated with changes in corresponding SOD levels (Bresciani et al., 2015; Folz et al., 1994). The significant associations between mutations in *SOD2* gene and T-SOD activity observed in this study indicate that mutations in rs10370 and rs4880 in *SOD2* gene were correlated with decreased T-SOD activity in serum. The decreased T-SOD activity might lead to its impaired catalytic ability to convert the superoxide radical to hydrogen peroxide (Wang et al., 2018).

Genetic factors, especially gene polymorphisms, have been implicated in the mechanism of DF recently. Previous studies have explored the associations between *matrix metalloproteinases* (*MMPs*), *catalase* (*CAT*) rs769217, *paraoxonase 1* (*PON1*) rs662, vitamin D receptor gene CDX2, *COL1A2*, *osteocalcin*, *ESR* and *PTH Bst* BI polymorphisms and DF status, providing evidence of the associations between of *COL1A2, CAT* rs769217, *PON1* rs662 and *ESR* gene polymorphisms and the risk of DF in children with high-load fluoride (Ba et al., 2009, 2011; Huang et al., 2008; Liu et al., 2018, 2019; Romualdo et al., 2019; Wen et al., 2012; Zhang et al., 2010). Subsequently, Kuchler et al., 2017, 2018 suggested that the polymorphisms of *tissue inhibitors of metalloproteinase1*, *distal-less1, DLX2, AMBN, TFIP11*, and *TUFT1* genes involved in enamel development might be useful genetic markers for the differential risk of DF. Furthermore, the study conducted by Abbasoglu et al. (2020) indicated that the polymorphisms of rs4284505 in microRNA17 were associated with the DF status. In the present study, there were significant associations between polymorphisms of *SOD2* (rs10370 and rs5746136) and the risk of DF, which might be due to decreased T-SOD activity caused by mutations in the *SOD2* gene, resulting in impaired clearance of reactive oxygen species and then leading to oxidative stress. Then the imbalance in the oxidative and anti-oxidant system during oxidative stress might mediate the ameloblast apoptosis and other cellular events and ultimately cause DF (Li et al., 2012, 2017).

It is well established that the effects of a single gene on the phenotypic trait of DF might be too small to be noticed sometimes. For instance, Huang et al., Jarquin-Yneza et al., and Rahila et al. (Huang et al., 2008; Jarquin-Yneza et al., 2018; Rahila et al., 2019) reported significant associations between polymorphisms in *COL1A2 Pvu*II (rs214777) and the incidence of DF, whereas Escobar-Garcia et al. and Saha et al. (Escobar-Garcia et al., 2016; Saha et al., 2021) did not observe such associations. These differences do not appear to be explained only by regions, fluoride exposure, and race. The process of DF might result from a complex interaction of genetic aspects and environmental exposure. Interactions between fluoride exposure and genetic factors in phenotypes have been reported. Zhao et al. (2021)

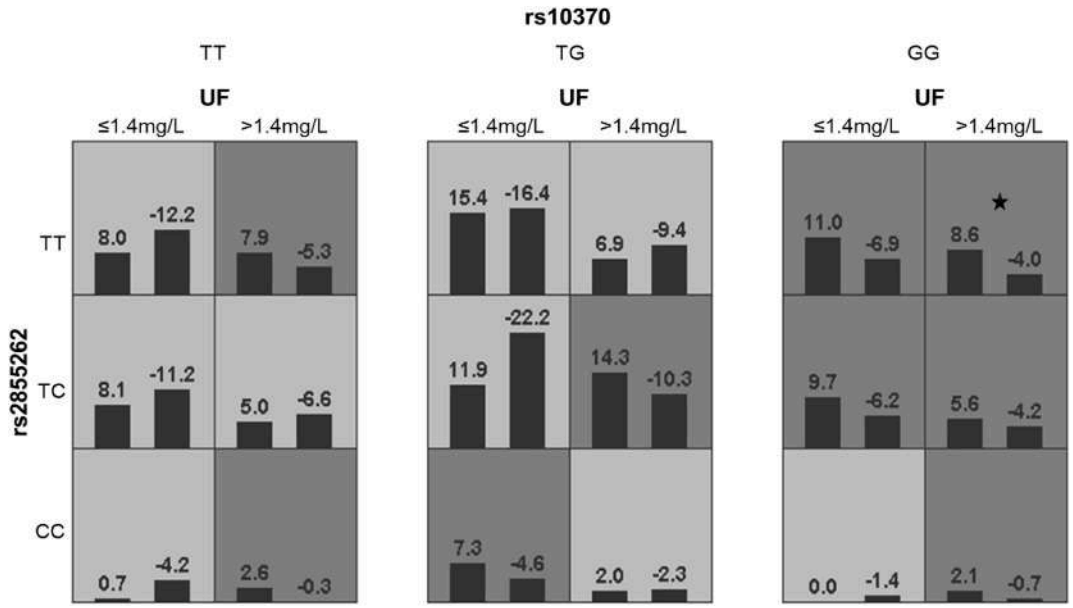

Fig. 1. The interaction pattern among rs10370, rs2855262 and UF. In each cell, the left bar represents a positive score, and the right bar a negative score. Dark and light gray cells correspond to the high-risk and low-risk interaction combinations, respectively. High-risk cells are indicated by dark shading, low-risk cells by light shading. White cells are unclassified. The ★ represents that the GG genotype of rs10370, higher UF concentrations (>1.4 mg/L) combined with the TT genotype of rs2855262 got the highest sum score in this model.

observed the effects of interactions between fluoride exposure and dopamine relative genes on intelligence. In our previous studies, the interactions between fluoride exposure and *ESR* alpha polymorphisms affected reproductive hormone concentrations and androgen binding protein levels (An et al., 2019; Ma et al., 2017). Here we observed that the interaction between fluoride exposure and polymorphisms of rs2855262 and rs103701 affected the risk of DF, suggesting that interactions between fluoride exposure and genetic polymorphisms were associated with the risk of DF. It might because alleles showing different sensitivities to fluoride exposure affected DF. John A. Eisman (1999) summarized previous research findings and suggested that this sensitivity might also be related to age because of the accumulation of age-related environmental exposures. Further studies are required to investigate the allelic effects of possible modifications in age-related fluoride accumulation on the risk of DF.

There are several advantages to the present study. Firstly, children recruited in this study are full-time accommodated students, with a similar dietary pattern, daily schedule and general demographic characteristics, resulting in fewer confounding factors. Secondly, The GMDR analyses were used in the present study, which can improve accuracy and reduce false-positive rate with the cross-validation test (Lou et al., 2007). However, there is also a limitation in the present study. We did not collect detailed information about fluoride exposure from food, drinking water and toothpaste, and we used urinary fluoride concentrations as the internal intake levels to deal with this issue.

5. Conclusion

In conclusion, rs4880 and rs10370 in *SOD2* might be useful genetic markers for DF, and interactions between rs10370 in *SOD2* and rs2855262 in *SOD3* and fluoride exposure might affect the risk of DF.

Notes

There are no competing financial interest among authors.

Funding

This study was supported by the National Natural Science Foundation of China (81972981 and 82003401) and Key Projects of Colleges and Universities of Henan Education Department (21A330006).

Acknowledgments

We are grateful to express our deep thanks to all of children recruited in this study, their guardian and their teachers. We thank all scientific and technological worker in the investigation for their hard work.

Appendix A. Supplementary data

Supplementary data to this article can be found online at https://doi.org/10.1016/j.ijheh.2021.113879.

References

Abanto Alvarez, J., Rezende, K.M., Marocho, S.M., Alves, F.B., Celiberti, P., Ciamponi, A. L., 2009. Dental fluorosis: exposure, prevention and management. Med. Oral, Patol. Oral Cirugía Bucal 14, E103–E107.

Abbasoglu, Z., Dalledone, M., Wambier, L.M., Pecharki, G., Baratto-Filho, F., Andrades, K.M.R., Scariot, R., Trevilatto, P.C., Brancher, J.A., Kuchler, E.C., 2020. Single nucleotide polymorphism rs4284505 in microRNA17 and risk of dental fluorosis. Acta Odontol. Scand. 78, 463–466.

Adelakun, S.A., Akintunde, O.W., Ogunlade, B., 2021. Fluoride-induced testicular degeneration and sperm quality deteriorations: salutary role of Cyperus esculentus tubers (tiger nut) extract in animal model. Rev. Int. Androl. 19 (3), 201–212. https://doi.org/10.1016/j.androl.2020.01.003.

An, N., Zhu, J., Ren, L., Liu, X., Zhou, T., Huang, H., Sun, L., Ding, Z., Li, Z., Cheng, X., Ba, Y., 2019. Trends of SHBG and ABP levels in male farmers: influences of environmental fluoride exposure and ESR alpha gene polymorphisms. Ecotoxicol. Environ. Saf. 172, 40–44.

Ba, Y., Huang, H., Yang, Y., Cui, L., Zhu, J., Zhu, C., Liu, J., Zhang, Y., 2009. The association between osteocalcin gene polymorphism and dental fluorosis among children exposed to fluoride in People's Republic of China. Ecotoxicol. Environ. Saf. 72, 2158–2161.

Ba, Y., Zhang, H., Wang, G., Wen, S., Yang, Y., Zhu, J., Ren, L., Yang, R., Zhu, C., Li, H., Cheng, X., Cui, L., 2011. Association of dental fluorosis with polymorphisms of estrogen receptor gene in Chinese children. Biol. Trace Elem. Res. 143, 87–96.

Bashash, M., Thomas, D., Hu, H., Martinez-Mier, E.A., Sanchez, B.N., Basu, N., Peterson, K.E., Ettinger, A.S., Wright, R., Zhang, Z., Liu, Y., Schnaas, L., Mercado-Garcia, A., Tellez-Rojo, M.M., Hernandez-Avila, M., 2017. Prenatal fluoride exposure

and cognitive outcomes in children at 4 and 6-12 Years of age in Mexico. Environ. Health Perspect. 125, 097017.
Bresciani, G., Cruz, I., González-Gallego, J., 2015. Manganese superoxide dismutase and oxidative stress modulation. Adv. Clin. Chem. 68, 87–130.
Cao, K., Xiang, J., Dong, Y.T., Xu, Y., Li, Y., Song, H., Zeng, X.X., Ran, L.Y., Hong, W., Guan, Z.Z., 2019. Exposure to fluoride aggravates the impairment in learning and memory and neuropathological lesions in mice carrying the APP/PS1 double-transgenic mutation. Alzheimer's Res. Ther. 11, 35.
Ceballos, D.M., Young, A.S., Allen, J.G., Specht, A.J., Nguyen, V.T., Craig, J.A., Miller, M., Webster, T.F., 2021. Exposures in nail salons to trace elements in nail polish from impurities or pigment ingredients - a pilot study. Int. J. Hyg Environ. Health 232, 113687.
Charone, S., Kuchler, E.C., Leite, A.L., Silva Fernandes, M., Taioqui Pela, V., Martini, T., Brondino, B.M., Magalhaes, A.C., Dionisio, T.J., C, F.S., Buzalaf, M.A.R., 2019. Analysis of polymorphisms in genes differentially expressed in the enamel of mice with different genetic susceptibilities to dental fluorosis. Caries Res. 53, 228–233.
Chen, X., Li, S., Yang, Y., Yang, X., Liu, Y., Liu, Y., Hu, W., Jin, L., Wang, X., 2012. Genome-wide association study validation identifies novel loci for atherosclerotic cardiovascular disease. J. Thromb. Haemostasis : JTH 10, 1508–1514.
Chouhan, S., Lomash, V., Flora, S.J., 2010. Fluoride-induced changes in haem biosynthesis pathway, neurological variables and tissue histopathology of rats. J. Appl. Toxicol. : JAT 30, 63–73.
Dalledone, M., Cunha, A.S., Ramazzotto, L.A., Pecharki, G.D., Nelson-Filho, P., Scariot, R., Trevilatto, P.C., Vieira, A.R., Kuchler, E.C., Brancher, J.A., 2019. Estrogen receptor gene is associated with dental fluorosis in Brazilian children. Clin. Oral Invest. 23, 3565–3570.
DenBesten, P.K., Thariani, H., 1992. Biological mechanisms of fluorosis and level and timing of systemic exposure to fluoride with respect to fluorosis. J. Dent. Res. 71, 1238–1243.
Eisman, J.A., 1999. Genetics of osteoporosis. Endocr. Rev. 20, 788–804.
Escobar-Garcia, D., Mejia-Saavedra, J., Jarquin-Yanez, L., Molina-Frechero, N., Pozos-Guillen, A., 2016. Collagenase 1A2 (COL1A2) gene A/C polymorphism in relation to severity of dental fluorosis. Community Dent. Oral Epidemiol. 44, 162–168.
Everett, E.T., 2011. Fluoride's effects on the formation of teeth and bones, and the influence of genetics. J. Dent. Res. 90, 552–560.
Folz, R.J., Peno-Green, L., Crapo, J.D., 1994. Identification of a homozygous missense mutation (Arg to Gly) in the critical binding region of the human EC-SOD gene (SOD3) and its association with dramatically increased serum enzyme levels. Hum. Mol. Genet. 3, 2251–2254.
Garcia-Montalvo, E.A., Reyes-Perez, H., Del Razo, L.M., 2009. Fluoride exposure impairs glucose tolerance via decreased insulin expression and oxidative stress. Toxicology 263, 75–83.
Huang, H., Ba, Y., Cui, L., Cheng, X., Zhu, J., Zhang, Y., Yan, P., Zhu, C., Kilfoy, B., Zhang, Y., 2008. COL1A2 gene polymorphisms (Pvu II and Rsa I), serum calciotropic hormone levels, and dental fluorosis. Community Dent. Oral Epidemiol. 36, 517–522.
Jarquin-Yneza, L., Alegria-Torres, J.A., Castillo, C.G., de Jesus Mejia-Saavedra, J., 2018. Dental fluorosis and a polymorphism in the COL1A2 gene in Mexican children. Arch. Oral Biol. 96, 21–25.
Jha, S.K., Mishra, V.K., Sharma, D.K., Damodaran, T., 2011. Fluoride in the environment and its metabolism in humans. Rev. Environ. Contam. Toxicol. 211, 121–142.
Kuchler, E.C., Dea Bruzamolin, C., Ayumi Omori, M., Costa, M.C., Antunes, L.S., Pecharki, G.D., Trevilatto, P.C., Vieira, A.R., Brancher, J.A., 2018. Polymorphisms in nonamelogenin enamel matrix genes are associated with dental fluorosis. Caries Res. 52, 1–6.
Kuchler, E.C., Tannure, P.N., Oliveira, D.S., Charone, S., Nelson-Filho, P., Silva, R.A., Costa, M.C., Antunes, L.S., Calasans Maia, M.D., Antunes, L.A., 2017. Polymorphisms in genes involved in enamel development are associated with dental fluorosis. Arch. Oral Biol. 76, 66–69.
Lewandowski, L., Kepinska, M., Milnerowicz, H., 2020. Alterations in concentration/activity of superoxide dismutases in context of obesity and selected single nucleotide polymorphisms in genes: SOD1, SOD2, SOD3. Int. J. Mol. Sci. 21.
Li, P., Xue, Y., Zhang, W., Teng, F., Sun, Y., Qu, T., Chen, X., Cheng, X., Song, B., Luo, W., Yu, Q., 2013. Sodium fluoride induces apoptosis in odontoblasts via a JNK-dependent mechanism. Toxicology 308, 138–145.
Li, W., Jiang, B., Cao, X., Xie, Y., Huang, T., 2017. Protective effect of lycopene on fluoride-induced ameloblasts apoptosis and dental fluorosis through oxidative stress-mediated Caspase pathways. Chem. Biol. Interact. 261, 27–34.
Li, X., Han, Y., Yuan, G., Liang, Z., Bai, C., Li, Y., 2012. Aluminum induces osteoblast apoptosis through the oxidative stress-mediated JNK signaling pathway. Biol. Trace Elem. Res. 150, 502–508.
Liu, J., Tao, N., Luo, M., Zhao, X., Yang, S., Zeng, R., Zhang, Y., Wang, K., 2018. Association between paraoxonase 1 rs662 polymorphism and dental fluorosis. Chin J Ctrl Endem Dis 33, 247–249.
Liu, J., Yang, S., Luo, M., Tao, N., Zhao, X., Zhang, Y., 2019. Association between catalase single nucleotide polymorphism and dental fluorosis. Journal of Fujian Medical University 53, 85–89.
Lou, X.Y., Chen, G.B., Yan, L., Ma, J.Z., Zhu, J., Elston, R.C., Li, M.D., 2007. A generalized combinatorial approach for detecting gene-by-gene and gene-by-environment interactions with application to nicotine dependence. Am. J. Hum. Genet. 80, 1125–1137.
Lu, Y., Luo, Q., Cui, H., Deng, H., Kuang, P., Liu, H., Fang, J., Zuo, Z., Deng, J., Li, Y., Wang, X., Zhao, L., 2017. Sodium fluoride causes oxidative stress and apoptosis in the mouse liver. Aging 9, 1623–1639.
Lyaruu, D.M., Bervoets, T.J., Bronckers, A.L., 2006. Short exposure to high levels of fluoride induces stage-dependent structural changes in ameloblasts and enamel mineralization. Eur. J. Oral Sci. 114 (Suppl. 1), 111–115 discussion 127-119, 380.
Ma, Q., Huang, H., Sun, L., Zhou, T., Zhu, J., Cheng, X., Duan, L., Li, Z., Cui, L., Ba, Y., 2017. Gene-environment interaction: does fluoride influence the reproductive hormones in male farmers modified by ERalpha gene polymorphisms? Chemosphere 188, 525–531.
Molina-Frechero, N., Nevarez-Rascon, M., Nevarez-Rascon, A., Gonzalez-Gonzalez, R., Irigoyen-Camacho, M.E., Sanchez-Perez, L., Lopez-Verdin, S., Bologna-Molina, R., 2017. Impact of dental fluorosis, socioeconomic status and self-perception in adolescents exposed to a high level of fluoride in water. Int. J. Environ. Res. Publ. Health 14.
Moller, I.J., 1982. Fluorides and dental fluorosis. Int. Dent. J. 32, 135–147.
Narwaria, Y.S., Saksena, D.N., 2013. Prevalence of dental fluorosis among primary school children in rural areas of karera block, Madhya Pradesh. Indian J. Pediatr. 80, 718–720.
Ni, J., Li, Y., Zhang, W., Shu, R., Zhong, Z., 2018. Sodium fluoride causes oxidative stress and apoptosis in cementoblasts. Chem. Biol. Interact. 294, 34–39.
Pendrys, D.G., Stamm, J.W., 1990. Relationship of total fluoride intake to beneficial effects and enamel fluorosis. J. Dent. Res. 69, 529–538 discussion 556-527.
Rahila, C., Aswath Narayanan, M.B., Ramesh Kumar, S.G., Leena Selvamary, A., Sujatha, A., John Kirubaharan, J., 2019. Association of COL1A2 (PvuII) gene polymorphism with risk and severity of dental fluorosis - a case control study. The Saudi dental journal 31, 463–468.
Robinson, C., Kirkham, J., 1990. The effect of fluoride on the developing mineralized tissues. J. Dent. Res. 69, 685–691 discussion 721.
Romualdo, P.C., Pucinelli, C.M., Tannure, P.N., Nelson-Filho, P., Segato, R.A.B., Brancher, J.A., Magalhaes, N.L., Costa, M.C., Antunes, L.A.A., Antunes, L.S., Buzalaf, M.A.R., Charone, S., Kuchler, E.C., 2019. Evaluation of genetic polymorphisms in MMP2, MMP9 and MMP20 in Brazilian children with dental fluorosis. Environ. Toxicol. Pharmacol. 66, 104–108.
Saha, D., Goswami, R., Majumdar, K.K., Sikdar, N., Pramanik, S., 2021. Evaluating the association between dental fluorosis and polymorphisms in bone development and mineralization genes among population from a fluoride endemic region of Eastern India. Biol. Trace Elem. Res. 199, 1–8.
Soler-Blasco, R., Murcia, M., Lozano, M., Gonzalez-Safont, L., Amoros, R., Ibarluzea, J., Broberg, K., Irizar, A., Lopez-Espinosa, M.J., Lertxundi, N., Marina, L.S., Ballester, F., Llop, S., 2020. Prenatal manganese exposure and neuropsychological development in early childhood in the INMA cohort. Int. J. Hyg Environ. Health 224, 113443.
Wan, H., Chen, S., Cai, Y., Chen, Y., Wang, Y., Zhang, W., Chen, C., Wang, N., Guo, Y., Lu, Y., 2021. Lead exposure and its association with cardiovascular disease and diabetic kidney disease in middle-aged and elderly diabetic patients. Int. J. Hyg Environ. Health 231, 113663.
Wang, A., Ma, Q., Gong, B., Sun, L., Afrim, F.K., Sun, R., He, T., Huang, H., Zhu, J., Zhou, G., Ba, Y., 2021. DNA methylation and fluoride exposure in school-age children: Epigenome-wide screening and population-based validation. Ecotoxicol. Environ. Saf. 223, 112612.
Wang, L., Zhu, Y., Wang, D., 2016. High-fluoride activates the FasL signalling pathway and leads to damage of ameloblast ultrastructure. Arch. Oral Biol. 71, 31–37.
Wang, Y., Branicky, R., Noe, A., Hekimi, S., 2018. Superoxide dismutases: dual roles in controlling ROS damage and regulating ROS signaling. J. Cell Biol. 217, 1915–1928.
Wen, S., Li, A., Cui, L., Huang, Q., Chen, H., Guo, X., Luo, Y., Hao, Q., Hou, J., Ba, Y., 2012. The relationship of PTH Bst BI polymorphism, calciotropic hormone levels, and dental fluorosis of children in China. Biol. Trace Elem. Res. 147, 84–90.
Xu, H.M., Xu, L.F., Hou, T.T., Luo, L.F., Chen, G.B., Sun, X.W., Lou, X.Y., 2016. GMDR: versatile software for detecting gene-gene and gene-Environ- ment interactions underlying complex traits. Curr. Genom. 17, 396–402.
Yu, X., Chen, J., Li, Y., Liu, H., Hou, C., Zeng, Q., Cui, Y., Zhao, L., Li, P., Zhou, Z., Pang, S., Tang, S., Tian, K., Zhao, Q., Dong, L., Xu, C., Zhang, X., Zhang, S., Liu, L., Wang, A., 2018. Threshold effects of moderately excessive fluoride exposure on children's health: a potential association between dental fluorosis and loss of excellent intelligence. Environ. Int. 118, 116–124.
Zelko, I.N., Mariani, T.J., Folz, R.J., 2002. Superoxide dismutase multigene family: a comparison of the CuZn-SOD (SOD1), Mn-SOD (SOD2), and EC-SOD (SOD3) gene structures, evolution, and expression. Free Radic. Biol. Med. 33, 337–349.
Zhang, M., Wang, A., He, W., He, P., Xu, B., Xia, T., Chen, X., Yang, K., 2007. Effects of fluoride on the expression of NCAM, oxidative stress, and apoptosis in primary cultured hippocampal neurons. Toxicology 236, 208–216.
Zhang, R., Li, S., Pan, L., Yue, L., Yu, C., 2010. Relationship between the polymorphisms of CDX2 binding site in vitamin D receptor gene and the children's dental fluorosis. Acta Univ. Med. Anhui 45, 241–243.
Zhao, L., Yu, C., Lv, J., Cui, Y., Wang, Y., Hou, C., Yu, J., Guo, B., Liu, H., Li, L., 2021. Fluoride exposure, dopamine relative gene polymorphism and intelligence: a cross-sectional study in China. Ecotoxicol. Environ. Saf. 209, 111826.
Zhou, G., Yang, L., Luo, C., Liu, H., Li, P., Cui, Y., Liu, L., Yu, X., Zeng, Q., Chen, J., Zhao, Q., Dong, L., Niu, Q., Zhang, S., Wang, A., 2019a. Low-to-moderate fluoride exposure, relative mitochondrial DNA levels, and dental fluorosis in Chinese children. Environ. Int. 127, 70–77.
Zhou, X., Chen, Z., Zhong, W., Yu, R., He, L., 2019b. Effect of fluoride on PERK-Nrf2 signaling pathway in mouse ameloblasts. Hum. Exp. Toxicol. 38, 833–845.

International Journal of Hygiene and Environmental Health 239 (2022) 113877

Contents lists available at ScienceDirect

International Journal of Hygiene and Environmental Health

journal homepage: www.elsevier.com/locate/ijheh

Exploring the relationship between metal exposure, BDNF, and behavior in adolescent males

Andrea Rodríguez-Carrillo [a,b,c], Vicente Mustieles [a,c,d], Shereen Cynthia D'Cruz [e], Louis Legoff [e], Fernando Gil [f], Pablo Olmedo [f], Iris Reina-Pérez [a,b,c], Antonio Mundo [b], Marina Molina [b], Fatima Smagulova [e], Arthur David [e], Carmen Freire [b,c,d,*], Mariana F. Fernández [a,b,c,d]

[a] Department of Radiology and Physical Medicine, School of Medicine, University of Granada, 18016, Granada, Spain
[b] Biomedical Research Center (CIBM), University of Granada, 18016, Granada, Spain
[c] Instituto de Investigación Biosanitaria de Granada (ibs.GRANADA), 18012, Granada, Spain
[d] Consortium for Biomedical Research in Epidemiology and Public Health (CIBERESP), Spain
[e] Univ Rennes, EHESP, INSERM, IRSET (Institut de Recherche en Santé, Environnement et Travail), UMR_S 1085, F-35000, Rennes, France
[f] Department of Legal Medicine, Toxicology and Physical Anthropology, School of Medicine, University of Granada, 18016, Granada, Spain

ARTICLE INFO

Keywords:
Metals
Brain-derived neurotrophic factor
Behavior
Human biomonitoring
Effect biomarker
HBM4EU
DNA methylation

ABSTRACT

Background: Brain-derived neurotrophic factor (BDNF) plays an important role in brain development by regulating multiple pathways within the central nervous system. In the Human Biomonitoring for Europe Project (HBM4EU), this neurotrophin is being implemented as a novel effect biomarker to evaluate the potential threats of environmental chemicals on neurodevelopment.

Objectives: To explore the relationships among exposure to environmental metals, BDNF biomarkers at two levels of biological complexity, and behavioral function in adolescent males.

Methods: Data were gathered from 125 adolescents on: spot urine sample total concentrations of the neurotoxic metal(oid)s arsenic (As), cadmium (Cd), mercury (Hg), and lead (Pb); serum BDNF protein concentrations; and concurrent behavioral functioning according to the Child Behavior Check List (CBCL/6–18). In 113 of the participants, information was also collected on blood BDNF DNA methylation at six CpGs. Associations were evaluated by multivariate linear regression analysis adjusted for confounders.

Results: As, Cd, Hg, and Pb were detected in 100%, 98.5%, 97.0%, and 89.5% of urine samples, respectively. Median serum BDNF concentration was 32.6 ng/mL, and total percentage of BDNF gene methylation was 3.8%. In the adjusted models, urinary As was non-linearly associated with more internalizing problems and Cd with more externalizing behaviors. The percentage BDNF DNA methylation at CPGs #5 and the mean percentage CpG methylation increased across As tertiles (p-trend = 0.04 and 0.03, respectively), while 2nd tertile and 3rd tertile of Cd concentrations were associated with lower serum BDNF and higher CpG3 methylation percentage. Additionally, when BDNF was categorized in tertiles, serum BDNF at the 3rd tertile was associated with fewer behavioral problems, particularly withdrawn (p-trend = 0.04), social problems (p-trend = 0.12), and thought problems (p-trend = 0.04).

Conclusion: Exposure to As and Cd was associated with BDNF gene DNA methylation BDNF gene and serum BDNF, respectively. Associations with DNA methylation may be attributable to a higher variability over time in circulating BDNF concentrations than in the methylation status of this gene. Caution should be taken when interpreting the results relating postnatal Pb and Hg to behavioral functioning. Further studies are needed to verify these findings.

1. Introduction

The human brain develops from week eight of gestation up to late adolescence and even early adulthood (Rice and Barone, 2000; Stiles and Jernigan, 2010), being considered fully developed at around 25 years of age (Stiles and Jernigan, 2010). Hence, children are especially

* Corresponding author. Biomedical Research Center (CIBM), University of Granada, 18016, Granada, Spain.
E-mail address: cfreire@ugr.es (C. Freire).

https://doi.org/10.1016/j.ijheh.2021.113877
Received 22 June 2021; Received in revised form 22 October 2021; Accepted 22 October 2021
Available online 28 October 2021

vulnerable to environmental neurotoxic compounds, including certain metals (Zhou et al., 2019). Current evidence suggests that exposure to environmental chemicals plays a major role in the so-called "silent pandemic of neurodevelopmental toxicity", *i.e.,* the rising incidence of behavioral and cognitive problems in children and adolescents, including autism spectrum disorders (ASDs) and attention-deficit hyperactivity disorder (ADHD) (Bellinger, 2009; Grandjean and Landrigan, 2014). However, although developmental susceptibility to environmental chemicals may extend into adolescence, the potential adverse health effects of environmental exposure in this age group have not been fully elucidated (Mustieles et al., 2020; Pfeifer and Allen, 2021).

Brain-derived neurotrophic factor (BDNF), a member of the neurotrophic family, has been associated with a wide range of neuropsychological processes, including neuro- and glio-synaptogenesis, synaptic plasticity, and neurite growth, among others (Kowiański et al., 2018; Sasi et al., 2017). This is largely explained by the characteristic pattern of BDNF synthesis, in which several biologically active isoforms interact with multiple receptors, thereby triggering, upregulating, or downregulating numerous signaling pathways (Kowiański et al., 2018). BDNF has been proposed as a biomarker of effect for brain functioning, allowing the exploration of potential causal pathways between exposure to particular endocrine disruptors (e.g., metals, bisphenol A, polycyclic aromatic hydrocarbons) and neurobehavioral outcomes in epidemiological studies (Kalia et al., 2017; Kundakovic et al., 2015; Mustieles et al., 2020; Perera et al., 2015; Tang et al., 2014). Exposure of humans to the neurotoxic environmental metals mercury (Hg) (particularly methyl-Hg), cadmium (Cd), lead (Pb), and arsenic (As) has been associated with disturbances in the pattern of BDNF synthesis, mainly detected as alterations in serum concentrations of total BDNF (Karim et al., 2019; Spulber et al., 2010; Y. Wang et al., 2016; Zhou et al., 2019; Zou et al., 2014). However, the biological meaning of BDNF gene DNA methylation patterns remain poorly understood. In a mouse study, Kundakovic et al. reported that blood BDNF gene methylation levels at six CpGs reflected the methylation profile and transcription levels in the hippocampus; they suggested that blood BDNF DNA methylation levels might be a surrogate marker of brain BDNF expression in humans (Kundakovic et al., 2015).

Humans are simultaneously exposed to multiple environmental chemicals. There are particular concerns about metallic/metalloid elements, which are ubiquitous in the environment, given that some of them are known to be neurodevelopmental toxicants, even at very low doses (Grandjean and Landrigan, 2006; Jakubowski, 2011; Rodríguez-Barranco et al., 2016; Schoeman et al., 2009). These elements are frequently detected in human urine, blood, and hair samples (Gil and Hernández, 2015). Chronic exposure of humans to As, Cd, Hg, and Pb has been implicated in various adverse effects (ATSDR 2020; 2016, 2012, 1999), and epidemiologists have increasingly addressed the effects of this exposure on neurodevelopment in relation to anxiety, depression, Alzheimer's disease, and ASD, among others (Freire et al., 2018; Jaishankar et al., 2014; Long et al., 2019; Mravunac et al., 2019; Sanders et al., 2014; Shah-Kulkarni et al., 2020; Yousef et al., 2011; Zhou et al., 2019). However, the behavioral effects of environmental metal exposure remain controversial, in part because fully standardized instruments are not available to assess the behavioral functioning of children and adolescents (Ciesielski et al., 2012; Khan et al., 2011; Lucchini et al., 2012; Roberts et al., 2013; Sanders et al., 2015).

Effect biomarkers based on toxicologic findings have been identified by the Human Biomonitoring for Europe Project (HBM4EU) after comprehensive searches of the literature (Baken et al., 2019; Mustieles et al., 2020; Steffensen et al., 2020). The most promising biomarkers are being tested in several European cohorts to assess their value as indicators of the potential adverse effects of environmental chemicals. BDNF has been highlighted as a brain development marker that might complement neuropsychological tests (Mustieles et al., 2020). The hypothesis of the present study was that BDNF is involved in the causal pathway between metal exposure and adverse effects on behavioral function and therefore serves as an adequate epidemiological biomarker to evaluate exposure-mediator-effect relationships. The study objectives were therefore: to assess the relationship between exposure to As, Cd, Pb, and/or Hg and behavioral functioning in adolescent males; and to investigate the role of the BDNF biomarker measured at two levels of biological organization (BDNF gene DNA methylation and serum protein concentration).

2. Material and methods

2.1. Study population

This study is part of the *INMA*-INfancia y Medio Ambiente (Environment and Childhood) Project, a multicenter population-based birth cohort study designed to investigate the effects of environmental exposures and diet during pregnancy and early life on fetal, child, and adolescent development in different parts of Spain (Guxens et al., 2012). The INMA-Granada cohort recruited 668 mother-son pairs in Granada, Southern Spain, in 2000–2002 (Fernandez et al., 2007). Randomly selected adolescents from the baseline cohort were re-contacted to seek their participation in clinical follow-ups at the ages of 4–5 (n = 220, 32.9%) and 9–11 years (n = 298, 44.6%). Participants who attended both follow-up sessions (n = 269) were invited to participate in the most recent follow-up at the age of 15–17 years (2017–2019) Agreement was obtained from 151 (56.13%) of these, who underwent physical examinations at the Pediatrics Unit of our third-level university hospital in Granada (Castiello et al., 2020). All 151 participants provided a urine sample, and 135 of them also provided a blood sample. The present study included the adolescents with available data on urinary metal concentrations, behavioral outcomes, serum total BDNF protein concentrations, and relevant covariates (n = 125); information on BDNF gene DNA methylation patterns was also available for 113 of these adolescents (see Fig. 1). The parents/guardians of the adolescents signed informed consent to their participation in the study, which was approved by the Biomedical Research Ethics Committee of Granada (Spain).

2.2. Analysis of urinary metal concentrations

A single spot urine sample was collected from the first morning void of each participant on the day of their hospital visit. Samples were stored at −80 °C until analysis. Urinary concentrations of total (both organic and inorganic) As, Cd, Hg, and Pb were measured at the laboratory of the Department of Legal Medicine, Toxicology and Physical Anthropology, University of Granada, using inductively coupled plasma mass spectrometry with an Agilent 8900 triple quadrupole ICP-MS (Agilent Technologies, Santa Clara, CA, USA) as previously described (Castiello et al., 2020). Quality control and quality assessment procedures included spiked samples with 400 μg/L of a multielement internal standard solution with Sc, Ge, Ir, and Rh; intermediate calibration standards; blanks; and the following certified reference materials (US National Institute of Standards and Technology): Trace Elements in Natural Water Standard Reference Material SRM 1640a and Seronorm (Sero, Billingstad, Norway), and Trace Elements Urine L1 and L2 (references 210605 and 210705, respectively)]. Limits of detection (LODs) were 0.60 μg/L for As, 0.01 μg/L for Cd, 0.05 μg/L for Hg, and 0.16 μg/L for Pb (Supplementary Material, Table S1). Urinary creatinine was measured by the Jaffle method in a Roche Cobas C-311 system using a commercial kit (Creatinine Jaffé Gen 2, CREJ2) and expressed as mg/dL.

2.3. Serum BDNF and whole blood BDNF gene DNA methylation

Peripheral venous blood samples were drawn from participants under non-fasting conditions between 5 p.m. and 7 p.m. on the same day as the collection of the urine sample. Blood samples were immediately processed to obtain serum and whole blood aliquots, which were

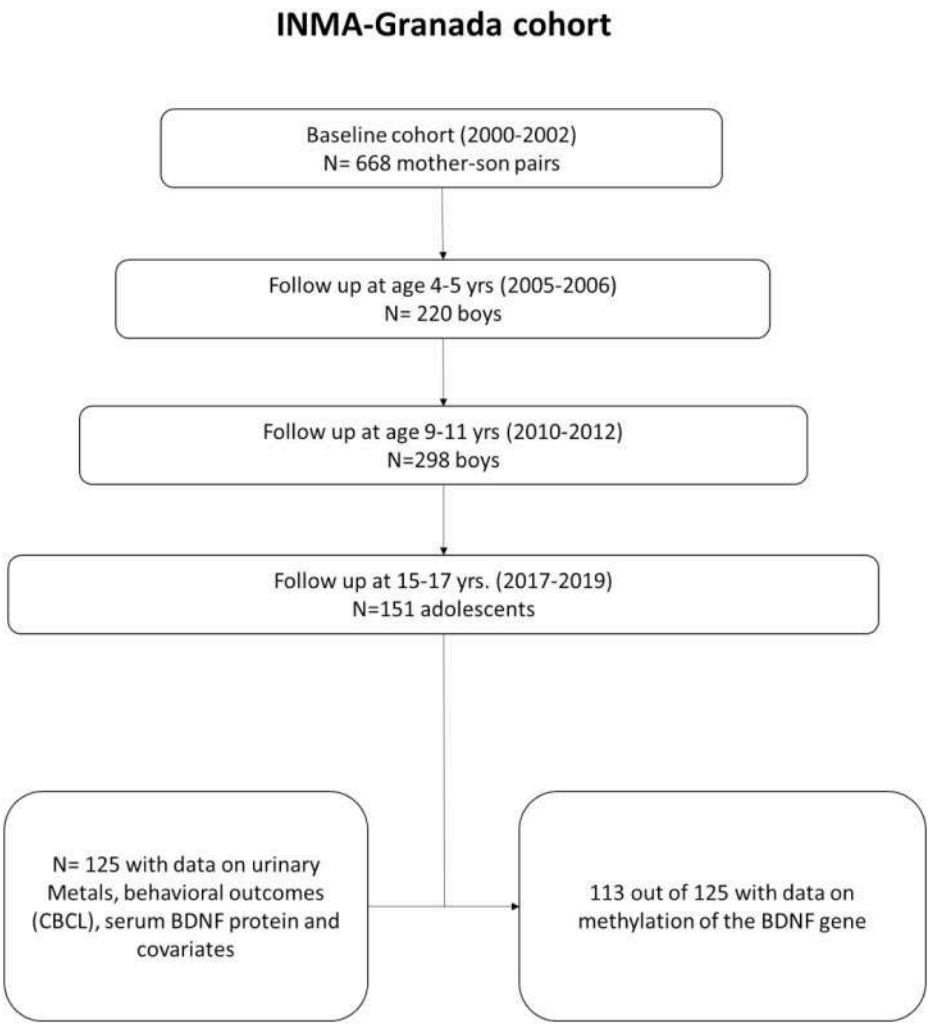

Fig. 1. Flow-chart showing the time-line of follow-ups conducted in the INMA-Granada cohort and the final sample of 15–17-year-old adolescents in the present study.

subsequently stored at −80 C°. Whole blood was sent in dry ice to the Human Genotyping Laboratory at the Spanish National Cancer Research Center, where genomic DNA was extracted using Maxwell® RSC equipment, quantified by PicoGreen assay, and diluted to 50 ng/μL. Extracted DNA was always stored at −80 °C until use.

Total serum BDNF concentrations (mature and immature isoforms of BDNF) were measured with an enzyme-linked immunosorbent assay using the commercial Quantikine® ELISA kit (R&D Systems, Minneapolis, MN, USA) at the Biomedical Research Center (CIBM), Granada, Spain. Briefly, samples were defrosted, vortexed, aliquoted in 10 μL, and diluted 100-fold. Next, 50 μL of diluted sample was tested in duplicate, placed in a 96-well plate coated with an anti-BDNF monoclonal antibody, and incubated at room temperature for 2 h. The plate was then washed four times with 400 μL wash buffer solution, followed by the addition of 200 μL BDNF-specific monoclonal antibody in each well. The plate was incubated for 1 h at room temperature and then washed as described above. Finally, 200 μL of a mixture containing stabilized hydrogen peroxide and tetramethylbenzidine was added to each well, and the plate was incubated for 30 min at room temperature protected from light. Then, 50 μL of Stop Solution (sulfuric acid) was added to each well, and samples were immediately read by luminometry at 450 nm wavelength. Serum total BDNF protein concentrations had intra- and inter-assay coefficients of variation of <5% and 15%, respectively.

DNA methylation of the BDNF gene was determined by bisulfite pyrosequencing analysis at the IRSET (Institut de Recherche en Santé, Environnement et Travail - INSERM UMR1085) in Rennes (France), as described in detail elsewhere (Mustieles et al., 2022). Genomic DNA levels were quantified using the QuantiFluor dsDNA system (Promega E2670). Successively, 500 ng of genomic DNA was bisulfite converted (BS) with Epitect Fast Bisulfite Conversion kit (Qiagen, 59826), and the concentration and purification were then remeasured with NanoDrop (Thermo Scientific NanoDrop 8000; RNA40 mode). Downstream PCR amplification (Biometra TProfessional Thermoycler, France) was performed using BDNF primers, 20 ng of BS-converted DNA, and Takara EpiTaq hot-start DNA polymerase at a final concentration of 0.6 U/25 μL (Takara, R110A) under the following conditions: initial denaturation at 98 °C for 30 s denaturation at 98 °C for 30 s, annealing at 55 °C for 30 s, and extension at 72 °C for 30 s, running a total of 40 cycles. Primers used for BDNF amplification (0.4 μM final concentration) are reported in Table S1, and the reverse primer was biotinylated. Exon IV of BDNF was the target region (genomic coordinates: chr11:27,723,070–27,723,280 retrieved from UCSC Genome Browser Human February 2009 (GRCh37/hg19), previously validated in rodents and humans (Kundakovic et al., 2015), which contains 6 CpGs, including a CREB-binding site (cAMP response element-binding site). After PCR amplification, the products were purified using the MinElute PCR purification kit (Qiagen, 28006) and then loaded on a 2% agarose gel to ensure amplification of a single BDNF product. Samples were sent to the LIGAN (Lille Integrated Genomics Advanced Network for personalized medicine) Genomic Platform in Lille (France) for pyrosequencing using

Pyromark Q4 Advanced Pyrosequencing technology. The methylation level at each CpG was expressed as percentage DNA methylation.

2.4. Behavioral functioning assessment

The validated Spanish version of the Child Behavior Checklist (CBCL/6–18) was used to evaluate the behavioral function of the participants (Sardinero García et al., 1997). This questionnaire was completed by the parents/guardians of each participant in relation to his behavior during the previous six months (Achenbach and Rescorla, 2013; Sardinero García et al., 1997). The CBCL contains 118 items rated on a three-point scale (not true, somewhat true, very/often true) and grouped in the following eight syndrome scales: anxious/depressed, withdrawn/depressed, somatic complaints, social problems, thought problems, attention problems, rule-breaking behavior, and aggressive behavior. These scales are summarized in three composite scales: internalizing problems (sum of anxious/depressed, withdrawn/depressed, and somatic complaints scale scores); externalizing problems (sum of rule-breaking behavior and aggressive behavior scale scores); and total problems (reported as sex and age-normalized T-scores). A higher scale score always indicates more behavioral problems (Achenbach and Rescorla, 2013).

2.5. Covariates

Data on sociodemographic characteristics and lifestyle factors were collected by administering *ad hoc* questionnaires to the participants and their parents/guardians. The weight, height, and body mass index (BMI) of participants were measured following standardized procedures, extensively detailed in Castiello et al. (2020). Covariates used in the present study included data collected at the 15- to 17-year-old follow up visit on the characteristics of the adolescents: age (in months, continuous), area of residence (categorized as urban or sub-urban/rural), annual family income (<25000, 25000–35000, or >35000 €), and passive smoking (yes or no); on the characteristics of their mothers: age (in years, continuous), intelligence (verbal reasoning measured by the similarities subtest of WAIS-III at the 9- to 10-year-old follow-up), marital status (stable partner: yes or no), schooling (up to primary, secondary, or university), current employment status (employed or unemployed) and alcohol consumption (yes or no). The adolescents also completed a validated food frequency questionnaire to obtain information on their overall fish consumption (monthly intake of <3 portions, 3–5 portions, or >5 portions) (Notario-Barandiaran et al., 2020).

2.6. Statistical analysis

Descriptive analyses were performed to summarize the sociodemographic and lifestyle characteristics of the study participants. Urine samples with undetected levels of As, Cd, Hg, and Pb were assigned a value of LOD/$\sqrt{2}$. Detection frequencies and/or percentiles were calculated for raw urinary metal concentrations (μg/L) and the effect biomarkers, i.e., serum BDNF and percentage DNA methylation at 6 CPIs of Exon-IV from the BDNF gene. Spearman's correlation analysis was conducted to assess relationships between metal levels concentrations, expressed as μg/L.

Multivariate linear regression models were performed for: i) the association of metal exposure with behavioral outcomes; ii) the association of metal exposure with the BDNF biomarkers of effect (serum BDNF and methylation profile of the BDNF gene) and iii) the association of these biomarkers with behavioral outcomes.

Urinary metal concentrations were left-skewed and therefore modeled as (natural) log-transformed variables. Associations with metals and effect biomarkers were considered as continuous variables and also categorized in tertiles to investigate possible non-linear relationships. Next, generalized additive models (GAM) were constructed for a more precise assessment of non-linear associations between metal exposure and behavioral outcomes. Confounders were carefully selected based on: i) substantive knowledge supporting their relevance for neurodevelopment and/or metals exposure; ii) their use in previous epidemiological studies; and iii) change in regression coefficient (beta) by more than 10%. Thus, two adjusted models were performed for all exposure-effects analyses. First model (Model 1) was adjusted for the age and BMI of adolescents, given that the age determines the stage of brain development and BMI is known to have an important impact on children's behavior (Hughes et al., 2020; Richards and Xie, 2015). We used unadjusted urinary metal concentrations and urinary creatinine concentrations as separate independent variables in accordance with previous observations reporting that this is a better approach to control for measurement error bias due to variability of urine concentrations (Barr et al., 2005; O'Brien et al., 2016). Because multiple metals may simultaneously affect behavioral functioning, regression models were mutually adjusted for all metals. In models with continuous exposure variable, all metals were introduced as continuous variables, whereas in models with categorical exposure variable, all metals were introduced categorized into tertiles. This approach was performed given that our sample size was not large enough to conduct advanced analysis of mixture effects. Model 1 was further adjusted by maternal schooling and intelligence, since these variables have their own influence on neurodevelopment and have been also extensively used in epidemiological studies evaluating neurodevelopmental outcomes (Patra et al., 2016; Wirt et al., 2015). Model 2 (fully-adjusted) was additionally controlled for adolescents' passive smoking and fish intake. Second-hand tobacco is a potential source of exposure to heavy metals, especially for Cd (Campbell et al., 2014; Navas-Acien, 2018; Spulber et al., 2010), while tobacco smoke has been negatively associated with the neurodevelopment of children (Chen et al., 2013; Lee et al., 2011; Spulber et al., 2010). Fish consumption was included because it is a major source of exposure to As, Hg, and Pb, although it has also been positively associated with neurodevelopment due to its content of fatty acids such as omega-3 (Gil and Gil, 2015; Mozaffarian and Rimm, 2006). Finally, multicollinearity was assessed in all regression models by calculating the variance inflation factor (VIF). Additionally, a sensitivity analysis was performed including one single element at a time to test the consistency across models. Associations showing $p < 0.05$ were considered significant. Nevertheless, given the relative small sample size, statistical significance was additionally evaluated based on internal validity, coherence and previous toxicological and epidemiological evidence of the observed associations (Amrhein et al., 2019). SPSS v26.0 (IBM, Chicago, IL) and R statistical software version 3.4.3 were used for data analyses.

3. Results

3.1. Descriptive analyses

Table 1 displays the general characteristics of the study participants and their mothers. The mean (standard deviation - SD) age of the adolescents was 16.9 (0.4) years and their mean BMI was 23.33 (4.99) kg/m^2. Almost three-quarters of the participants lived in urban areas, just under half were passive smokers, around one-third reported a monthly fish intake of less than 3 portions, and just over one-third had a family income of 25000–35000 €/year. Their mothers had a mean age of 39.5 years, almost all had a stable partner, just under one-third had a university education, more than three-quarters were employed, and around half of them regularly consumed alcohol (Table 1).

All urine samples contained quantifiable concentrations of As (median = 24.20 μg/L), 98.5% contained concentrations of Cd (median = 0.08 μg/L), 97.0% concentrations of Hg (median = 0.76 μg/L), and 89.5% concentrations of Pb (median = 0.42 μg/L) (Table 2). Significant positive correlations were found between As and Cd, Hg and Pb concentrations (Spearman's rho = 0.22, 0.52 and 0.19, respectively) and between Cd with Hg and Pb concentrations (Spearman's rho = 0.52 and

Table 1
General characteristics of study participants (n = 125).

Variables	Mean ± SD or n (%)
Adolescents	
Age (years)	16.6 ± 0.4
BMI (kg/m^2)	23.6 ± 5.2
Creatinine (mg/dL)	184.6 ± 57.6
Area of residence	
Urban	96 (72.2)
Sub-urban/rural	37 (27.8)
Passive smoking	
Yes	55 (41.4)
No	76 (57.1)
Fish consumption	
<3 portions per month	45 (33.8)
3–5 portions per month	40 (30.1)
>5 portions per month	43 (32.3)
Mothers	
Age (years)	39.6 ± 4.7
Schooling	
Up to primary	50 (40.0)
Secondary	44 (35.2)
University	31 (24.8)
Occupational status	
Employed	78 (62.4)
Unemployed	47 (37.6)
Marital status	
Stable partner	115 (92.0)
No stable partner	10 (8.0)
Alcohol consumption	
Yes	65 (52.0)
No	60 (48.0)
Annual family income (euros)	
<25000	48 (36.1)
25000-35000	59 (44.1)
>35000	29 (21.8)
Verbal reasoning*	15.6 ± 5.1

SD: Standard deviation; BMI: Body mass index.
*Verbal reasoning measured by similarities subtest of WAIS-III at 9-11-year follow-up.

0.36, respectively) but not between Hg and Pb concentrations (Supplementary Material, Table S2). The median concentration of serum BDNF was 32.6 ng/mL and the median percentage DNA methylation values for CpGs 1 to 6 were: 4.5%, 3.2%, 3.2%, 5.7%, 3.2%, and 2.4%, respectively; the median percentage total CpG methylation was 3.8% (Table 2). The distribution of CBCL T-scores is exhibited in Supplementary Material (Table S3). Globally, there was a lower prevalence of externalizing problems (16%) than of internalizing problems (32%) in this study population.

3.2. Metal exposure and adolescents' behavior

Table 3 displays the associations between tertiles of urinary metal concentrations and CBCL T-scores. The overall patterns pointed towards a non-linear relationship of urinary As and Cd concentrations with behavioral problems, with As exposure being associated with more internalizing problems, such as anxiety, somatic and thought problems; and Cd with more externalizing problems, such as social, attention problems and aggressive behavior. Further, second and third tertiles (intermediate and high levels) of urinary As and Cd levels were associated with greater anxiety and more somatic complaints, aggressive behaviors, and social and internalizing problems; however, some of these associations did not reach the statistical significance. These associations persisted but some were attenuated after adjustment for passive smoking and fish intake (Table 3). GAM analyses confirmed the presence of non-linear relationships for As and Cd (Supplementary Material, Figs. S1 and S2). Both Hg and Pb exposure showed associations with lower CBCL scores in several subscales, especially withdrawn, somatic complaints, and social and internalizing problems, which remained after adjustment for passive smoking and fish intake (Table 3).

Models considering continuous urinary metal concentrations showed associations of Cd with more social problems and aggressive behavior, although these relationships did not reach the statistically significance. However, Hg concentrations were significantly associated with fewer social problems (Table S4). The VIF was below 1.5 for each independent variable, ruling out multicollinearity. Finally, sensitivity analyses not showed substantial differences between models, neither in the direction of associations, and neither in overall patterns (Table S7).

3.3. Metal exposure and BDNF

The overall pattern showed lower serum BDNF levels across tertiles of urinary As and Cd concentrations, with significant associations between Cd and serum BDNF and between As and CpG5 and total CpGs methylation percentages. However, these associations were not observed for Hg and Pb (Table 4).

In relation to the BDNF gene methylation profile, concentrations of As in the third tertile (higher level) were associated with higher percentage methylation at CpGs #4, 5, and 6 and for total CpGs, with statistically significant results for CpG 5 and total DNA methylation. Associations were also found between urinary Cd in the second *versus* first tertile and lower BDNF gene methylation at CpGs #2 and 3 (Table 4). In the fully-adjusted model, the aforementioned associations remained and some became stronger (Table 4). Urinary Pb concentrations were positively but non-significantly associated with higher DNA methylation patterns, while urinary Hg showed associations with decreasing BDNF gene DNA methylation (Table 4). Models with continuous data showed non-significant associations of As with higher total CpG methylation and of Pb with higher methylation at CpG 1, whereas Cd was negatively but also non-significantly associated with methylation at CpG3 (Table S5). VIF values for each independent variable in all models were <1.5, ruling out multicollinearity. Sensitivity analyses showed an attenuation of associations between As and BDNF DNA methylation percentages, however, direction and overall tendencies were still observed (Table S8).

3.4. BDNF and adolescents' behavior

Continuous serum BDNF concentrations suggested association with a

Table 2
Distribution of urinary metal concentrations (μg/L), serum BDNF concentrations (ng/mL), and percentage of BDNF gene DNA methylation values at six CpGs (%).

		As		Cd		Hg		Pb	
% Detection (n = 125)		100		98.5		97.0		89.5	
Percentiles	**25**	8.26		0.05		0.29		0.27	
	50	24.20		0.08		0.76		0.42	
	75	44.07		0.12		1.02		0.70	
		Serum BDNF	**CpG1**	**CpG2**	**CpG3**	**CpG4**	**CpG5**	**CpG6**	**Total CpGs**
n		125	111	113	113	105	108	101	112
Percentiles	**25**	25.41	3.82	2.90	2.84	5.35	2.69	2.02	3.45
	50	32.59	4.46	3.20	3.21	5.70	3.16	2.34	3.77
	75	39.40	4.87	3.51	3.64	6.32	3.67	3.12	4.06

Table 3
Adjusted models for the association between tertiles of urinary metal concentrations and CBCL scores (n = 125).

CBCL scores	Model 1				Model 2			
	As tertiles (μg/g)							
	1st (0.58–6.19)	2nd (6.47–16.18)	3rd (16.35–465.4)	p-trend	1st (0.58–6.19)	2nd (6.47–16.18)	3rd (16.35–465.4)	p-trend
	Mean (SD)	β (95% CI)	β (95% CI)		Mean (SD)	β (95% CI)	β (95% CI)	
Syndrome scores								
Anxious depressed	53.9 (4.9)	3.38 (0.39;6.37)*	1.71 (−1.34;4.76)	0.32	54.0 (4.9)	4.0 (0.87;7.13)**	1.77 (−1.31;4.84)	0.34
Withdrawn	57.0 (6.1)	0.83 (−2.64;4.29)	1.15 (−2.38;4.69)	0.52	57.0 (6.2)	0.95 (−2.68;4.57)	1.44 (−2.12;4.99)	0.43
Somatic complaints	55.2 (6.1)	5.77 (2.08;9.46)**	3.06 (−0.70;6.82)†	0.15	55.3 (6.2)	5.58 (1.66;9.50)**	2.86 (−0.99;6.70)†	0.20
Social problems	55.0 (5.8)	0.79 (−2.2;3.78)	1.34 (−1.71;4.39)	0.38	54.8 (5.8)	1.1 (−2.05;4.24)	1.49 (−1.59;4.57)	0.34
Thought problems	53.3 (4.3)	2.61 (−0.25;5.46)†	1.43 (−1.49;4.34)	0.37	53.2 (4.3)	2.56 (−0.45;5.57)†	1.36 (−1.60;4.31)	0.42
Attention problems	54.6 (4.6)	2.48 (−0.36;5.31)†	0.65 (−2.25;3.54)	0.72	54.5 (4.6)	2.58 (−0.43;5.60)†	0.60 (−2.36;3.55)	0.79
Rule-breaking behavior	54.6 (5.8)	−0.53 (−3.16;2.11)	−1.29 (−3.98;1.41)	0.34	54.7 (5.9)	−0.31 (−2.95;2.34)	−1.34 (−3.94;1.25)	0.29
Aggressive behavior	55.7 (6.3)	0.22 (−2.81;3.24)	0.18 (−2.90;3.27)	0.91	55.5 (6.3)	1.01 (−2.09;4.12)	0.35 (−2.7;3.40)	0.85
Composite scores								
Internalizing problems	52.4 (10.4)	5.28 (0.25;10.31)*	4.16 (−0.98;9.29)†	0.13	52.4 (10.6)	5.87 (0.52;11.22)*	4.43 (−0.82;9.68)†	0.12
Externalizing problems	52.2 (9.9)	0.59 (−4.14;5.32)	−0.54 (−5.37;4.29)	0.81	52.0 (10.0)	1.96 (−2.82;6.74)	−0.22 (−4.91;4.47)	0.87
Total problems	52.3 (9.7)	3.12 (−1.52;7.76)	1.98 (−2.76;6.71)	0.43	52.1 (9.8)	3.88 (−0.97;8.73)†	2.20 (−2.56;6.96)	0.41
CBCL scores	Cd tertiles (μg/g)							
	1st (0.03–0.05)	2nd (0.04–0.05)	3rd (0.05–0.55)	p-trend	1st (0.01–0.03)	2nd (0.04–0.05)	3rd (0.05–0.55)	p-trend
	Mean (SD)	β (95% CI)	β (95% CI)		Mean (SD)	β (95% CI)	β (95% CI)	
Syndrome scores								
Anxious depressed	55.2 (5.2)	0.29 (−2.91;3.48)	0.89 (−2.22;4.01)	0.56	55.2 (5.2)	0.67 (−2.66;4.0)	1.37 (−1.88;4.61)	0.40
Withdrawn	56.9 (6.8)	1.71 (−1.89;5.32)	0.94 (−2.58;4.45)	0.63	56.9 (6.8)	1.57 (−2.15;5.28)	1.37 (−2.25;4.99)	0.47
Somatic complaints	59.6 (8.1)	−0.05 (−4.05;3.94)	−3.42 (−7.31;0.47)†	0.07	59.6 (8.1)	0.48 (−3.67;4.63)	−2.78 (−6.83;1.26)	0.160
Social problems	53.4 (4.8)	4.85 (1.85;7.85)*	3.05 (0.13;5.98)*	0.06	53.4 (4.8)	4.50 (1.37;7.63)**	2.85 (−0.20;5.90)†	0.10
Thought problems	53.7 (4.9)	1.83 (−1.19;4.85)	1.98 (−0.97;4.92)	0.06	53.7 (4.9)	2.38 (−0.75;5.50)†	2.47 (−0.57;5.51)†	0.12
Attention problems	54.5 (5.1)	2.84 (−0.11;5.79)†	0.66 (−2.22;3.53)	0.19	54.5 (5.1)	2.94 (−0.15;6.03)†	0.77 (−2.23;3.78)	0.69
Rule-breaking behavior	54.4 (5.6)	−1.10 (−3.83;1.67)	−0.56 (−3.24;2.12)	0.71	54.4 (5.6)	−0.70 (−3.42;2.01)	0.12 (−2.52;2.76)	0.90
Aggressive behavior	53.9 (5.61)	2.28 (−0.88;5.44)	3.97 (0.89;7.05)*	0.01	53.9 (5.6)	2.56 (−0.64;5.76)†	4.26 (1.14;7.38)**	0.01
Composite scores								
Internalizing problems	55.6 (10.3)	1.54 (−3.77;6.84)	−0.82 (−5.99;4.36)	0.72	55.6 (10.3)	1.65 (−3.92;7.22)	−0.19 (−5.62;5.24)	0.91
Externalizing problems	50.6 (9.4)	1.87 (−3.08;6.82)	3.18 (−1.64;8.01)	0.19	50.6 (9.4)	2.37 (−2.57.7.32)	3.87 (−0.95;8.68)†	0.11
Total problems	52.5 (9.0)	3.57 (−1.26;8.40)	1.66 (−3.05;6.37)	0.53	52.5 (9.0)	3.84 (−1.15;8.83)†	2.21 (−2.65;7.07)	0.41
CBCL scores	Hg tertiles (μg/g)							
	1st (0.02–0.23)	2nd (0.23–0.48)	3rd (0.49–3.24)	p-trend	1st (0.02–0.23)	2nd (0.23–0.48)	3rd (0.49–3.24)	p-trend
	Mean (SD)	β (95% CI)	β (95% CI)		Mean (SD)	β (95% CI)	β (95% CI)	
Syndrome scores								
Anxious depressed	55.9 (5.8)	−1.02 (−4.16;2.13)	−2.38 (−5.83;1.07)	0.17	56.3 (5.8)	−1.29 (−6.29;0.95)	−2.67 (−6.29;0.95)	0.14
Withdrawn	58.8 (8.2)	−3.04 (−6.59;0.51)†	−4.15 (−8.25;-0.26)*	0.04	59.0 (8.4)	−2.94 (−6.58;0.70)†	−4.57 (−8.62;-0.53)*	0.03
Somatic complaints	59.3 (7.8)	−3.36 (−7.22;0.51)†	−0.51 (−4.75;3.73)	0.87	59.5 (8.0)	−3.79 (−7.79;0.21)†	−1.25 (−5.70;3.20)	0.65
Social problems	56.6 (6.7)	−2.56 (−5.63;0.51)†	−5.37 (−8.73;-2.00)**	<0.001	56.3 (6.8)	−1.9 (−5.06;1.25)	−4.68 (−8.20–1.17)**	0.01
Thought problems	54.4 (5.1)	−0.73 (−3.71;2.25)	−1.61 (−4.88;1.64)	0.32	54.5 (5.3)	−1.10 (−4.17;1.97)	−2.35 (−5.76;1.07)	0.17
Attention problems	55.8 (5.3)	0.28 (−2.67;3.23)	−1.65 (−4.89;1.59)	0.29	55.5 (5.4)	0.49 (−2.58;3.56)	−1.51 (−4.92;1.91)	0.35
Rule-breaking behavior	54.9 (5.96)	−1.85 (−4.55;0.84)	−1.31 (−4.27;1.64)	0.40	55.1 (6.1)	−1.99 (−4.63;0.65)†	−1.77 (−4.71;1.17)	0.25
Aggressive behavior	56.0 (6.1)	−1.06 (−4.16;2.05)	−3.26 (−6.67;0.14)†	0.05	56.0 (6.2)	−0.94 (−4.06;2.19)	−3.28 (−6.76;0.20)†	0.06
Composite scores								
Internalizing problems	56.4 (10.9)	−3.18 (−8.39;2.04)	−2.51 (−8.23;3.21)	0.40	56.8 (11.1)	−3.20 (−8.64;2.25)	−2.95 (−9.01;3.11)	0.35
Externalizing problems	52.7 (9.66)	−1.57 (−6.43;3.30)	−2.47 (−7.81;2.87)	0.36	53.0 (9.7)	−1.47 (−6.30;3.37)	−2.74 (−8.12;2.64)	0.31
Total problems	54.6 (9.5)	−2.78 (−7.58;2.01)	−3.79 (−9.05;1.47)	0.15	54.7 (9.7)	−2.58 (−7.51;2.35)	−3.99 (−9.47;1.49)	0.15
CBCL scores	Pb tertiles (μg/g)							
	1st (0.01–0.18)	2nd (0.18–0.31)	3rd (0.31–2.64)	p-trend	1st (0.01–0.18)	2nd (0.18–0.31)	3rd (0.31–2.64)	p-trend
	Mean (SD)	β (95% CI)	β (95% CI)		Mean (SD)	β (95% CI)	β (95% CI)	
Syndrome scores								
Anxious depressed	55.5 (6.3)	0.31 (−2.7;3.31)	−2.28 (−5.25;0.69)†	0.14	55.7 (6.3)	0.20 (−2.92;3.33)	−2.30 (−5.42;0.82)	0.15
Withdrawn	57.4 (5.1)	−0.86 (−4.28;2.56)	−1.04 (−4.42;2.35)	0.54	57.4 (5.1)	−0.69 (−4.20;2.83)	−1.26 (−4.77;2.25)	0.48
Somatic complaints	60.3 (7.6)	−4.54 (−8.27;-0.81)*	−3.31 (−7.01;0.38)†	0.07	60.5 (7.6)	−4.62 (−8.50;-0.74)*	−3.37 (−7.24;0.51)†	0.09
Social problems	55.0 (5.7)	−0.17 (−3.12;2.78)	−0.76 (−3.68;2.16)	0.60	54.8 (5.7)	0.58 (−2.47;3.62)	−0.43 (−3.48;2.61)	0.78
Thought problems	54.8 (5.0)	−0.17 (−3.03;2.70)	−0.94 (−3.77;2.01)	0.51	54.8 (5.1)	−0.06 (−3.02;2.90)	−0.74 (−3.70;2.22)	0.62
Attention problems	55.9 (5.5)	−1.14 (−3.99;1.71)	−1.55 (−4.37;1.28)	0.27	55.8 (5.5)	−0.75 (−3.73;2.23)	−1.34 (−4.32;1.64)	0.37
Rule-breaking behavior	53.6 (4.4)	−0.27 (−2.88;2.33)	0.91 (−1.67;3.48)	0.49	53.7 (4.5)	0.31 (−2.25.2.88)	1.48 (−1.08;4.04)	0.25
Aggressive behavior	55.6 (5.7)	−0.11 (−3.10;2.88)	−0.84 (−3.8;2.12)	0.57	55.4 (5.7)	0.67 (−2.35;3.68)	0.01 (−3.00;3.03)	0.99
Composite scores								
Internalizing problems	57.5 (8.2)	−4.59 (−9.59;0.41)†	−4.19 (−9.14;0.76)†	0.09	57.7 (8.2)	−4.50 (−9.75;0.74)†	−4.32 (−9.57;0.92)†	0.10
Externalizing problems	52.7 (7.5)	−1.89 (−6.56;2.78)	−1.30 (−5.92;3.33)	0.57	52.5 (7.5)	−0.70 (−5.36;3.97)	0.05 (−4.62;4.71)	0.98
Total problems	55.3 (7.2)	−3.3 (−7.89;1.30)	−3.24 (−7.79;1.31)	0.15	55.2 (7.3)	−2.43 (−7.20;2.32)	−2.55 (−7.30;2.19)	0.28

Model 1: adjusted for adolescent's age and BMI, maternal schooling and intelligence, and for all metals simultaneously.
Model 2: additionally adjusted for passive tobacco smoking and total fish intake of adolescents.
For all subscales, higher score indicates more behavioral problems.
**p < 0.0; *p < 0.05; †p < 0.10.

lower score for the withdrawn subscale (β = −0.12, 95%CI = −0.27, 0.03) (Fig. 2A). Lower scores were obtained by adolescents in the second and third tertiles of serum BDNF concentrations than by those in the first (lowest) tertile in the withdrawn [(β_{T2} = −3.77, 95% CI = −7.00;-0.53), (β_{T3} = −3.49, 95% CI = −6.95; −0.02)], social problems (β_{T3} = −2.52, 95% CI = −5.69,0.65, and thought problems (β_{T3} = −2.88, 95% CI = −5.78; 0.01) subscales, observing a significant linear trend for both withdrawn (p-trend = 0.04) and thought problems (p-trend = 0.04) (Table S6). A lower score in the total problems scale was observed in participants in the second *versus* first tertile of serum BDNF concentrations (β = −3.85, 95% CI = −8.28; 0.58).

When total DNA methylation of the BDNF gene was considered as a continuous variable, no significant association was found with the behavior of the adolescents, although the percentage BDNF gene methylation appeared in general to be inversely related to the behavioral scores (Fig. 2). Similar results were obtained when tertiles of total BDNF gene DNA methylation were considered (data not shown).

4. Discussion

The results of this exploratory study among Spanish adolescent males (aged 15–17 years) suggest a relationship between urinary As and Cd exposure and behavioral problems, possibly through their effects on BDNF secretion patterns (serum BDNF protein levels and BDNF gene DNA methylation percentage). In these adolescents, intermediate urinary As and Cd concentrations were associated with more internalizing and externalizing problems, respectively. Furthermore, results suggest that serum BDNF protein concentrations were lower in adolescents exposed to moderate and high As and Cd levels. High As concentrations were also associated with increased percentage BDNF gene DNA methylation and moderate urinary Cd concentrations suggested associations with decreased BDNF gene DNA methylation percentages. Interestingly, increased serum BDNF levels were associated with fewer behavioral alterations (*i.e.,* withdrawn and social, thought, and total problems). Hg and Pb concentrations were found to be inversely related to behavioral functioning. No statistically significant relationships were found between Hg or Pb concentrations and percentage BDNF gene DNA methylation or serum BDNF protein concentrations.

4.1. Epidemiological evidence on the association of As and Cd exposure with neurobehavior

Urinary Cd concentrations were within the range reported for adolescents by the National Health and Nutrition Examination Survey (NHANES, 2009–2014) and the German Human Biomonitoring Commission (Sanders et al., 2019; Schulz et al., 2011). However, urinary As concentrations were higher in the present population. Previous epidemiological studies have assessed the potential harmful effects of postnatal exposure to As and Cd on neurobehavioral function, but the results have not been conclusive. On the one hand, two systematic reviews found no association between As exposure and behavioral outcomes in children between 5 and 15 years of age (Rodríguez-Barranco et al., 2013; Tolins et al., 2014). On the other hand, two epidemiological studies in children aged between 6 and 12 years reported that urinary As (total and inorganic) was associated with poorer attention (Rodríguez-Barranco et al., 2016) and with depressive problems (Lin et al., 2017), more in line with the present findings. In other epidemiological studies, postnatal newborn hair concentrations of Cd were associated with withdrawn and social and attention problems in 7- to 16-year-old Chinese children (Bao et al., 2009), and urinary Cd was related to worse prosocial behavior in 10-year-old children (Gustin et al., 2018). However, no significant association was found between blood Cd concentrations and more behavioral problems in children at 2, 5, or 7 years of age (Cao et al., 2009). In the present study, urinary Cd concentrations were associated with CBCL subscales for externalizing behaviors (*i.e.*, social problems and aggressive behavior) and for somatic and thought problems. These patterns seem to point towards an association of As and Cd exposure with altered behavioral functioning in adolescents.

The above comparisons with the present findings should be interpreted with caution. First, because most previous studies measured As and Cd prenatally or during early or late childhood, whereas the present study focused on adolescence. Neurological mechanisms and the susceptibility of behavioral functions to these compounds differ among developmental periods (Gore et al., 2018; Spear, 2000; Stiles and Jernigan, 2010); which may explain the absence of evidence on the association between metal exposure and behavioral domains during this period of development (Rodríguez-Barranco et al., 2013; Spear, 2000). Second, data on metal concentrations may differ according to the matrix used (*e.g.*, urine, blood, hair, or drinking water). Urine is a useful matrix for assessing chronic exposure to Cd in biomonitoring studies because of its long half-life, reflecting long-term exposure, whereas concentrations of As in urine correspond to acute exposure (Gil and Hernández, 2015). Finally, wide variations in the instruments used to assess behavioral functioning may also explain discrepancies among studies (Rodríguez-Carrillo et al., 2019).

4.2. Possible effects of As and Cd on neurobehavior through alteration of BDNF expression patterns

The suggestive association of As and Cd exposure with behavioral functioning might be explained by their binding to N-methyl-D-aspartate (NMDA) receptors in the hippocampus (Karri et al., 2016). This would lead to a reduction in BDNF concentrations and consequent behavioral and cognitive impairments, consistent with the adverse outcome pathways (AOPs) described by Mustieles et al. (2020) (Fig. 3). The hippocampus is responsible for the formation of emotional responses and the acquisition of memory and learning, which are both associated with social behavior (Ciranna, 2006). It is especially susceptible to exogenous and endogenous stressors, and the resulting changes in its structure and function can play a crucial role in the development of mood disorders (Zaletel et al., 2017).

Exposure to As may affect behavioral function through a direct action on the BDNF gene, given that As can alter DNA methylation patterns, possibly by interacting with transcription factor binding sites (TFBS) and inhibiting DNA repair mechanisms (Demanelis et al., 2019; Karim et al., 2019) (mechanisms of action shown in Fig. 3, numbers 1 and 2). This may explain the present findings of increased BDNF gene methylation in adolescents with higher urinary As concentrations (Fig. 3). The present mechanism is also consistent with experimental findings of an association between memory deficits and decreased hippocampal BDNF and CAMP responsive element binding protein 1 (CREB) in mice exposed to As (Sun et al., 2015). As can also exert an indirect effect on BDNF *via* the following pathways: first, by the inhibition of NMDA receptors, which play a key role in Ca^{+2} influx mechanisms, leading to reduced BDNF concentrations (Wang et al., 2016) (Fig. 3, number 3); second, through an imbalance of the oxidative stress homeostasis, thereby increasing reactive oxygen species (ROS) and reducing glutathione (GSH) (Karri et al., 2016; Mimouna et al., 2018), which favors cell injury or death and leads to neuroinflammation and ultimately to the degeneration of hippocampal brain cells, reducing the expression of BDNF (Karri et al., 2016) (Fig. 3, number 4); and, finally, by altering the metabolism of neurotransmitters such as GSH or serotonin, which play an important role in the expression and production of BDNF (Htway et al., 2019; Ramos-Chávez et al., 2015). For example, adult male mice prenatally exposed to As exhibited a down-regulation of BDNF expression and social isolation-like behavior, possibly mediated by an As-induced alteration of the serotonergic system (Htway et al., 2019). The present results indicate that greater exposure to As could be associated with higher DNA BDNF gene DNA methylation percentage at several CpGs. If so, it would reduce BDNF gene expression levels and protein concentrations, potentially generating more behavioral problems. Some of the associations found with BDNF gene methylation and

Table 4
Adjusted models for the association of tertiles of urinary metal concentration with serum BDNF (n = 125) and BDNF gene methylation (n = 113).

	Model 1				Model 2			
	As tertiles (μg/g)							
	1st (0.58–6.19)	2nd (6.47–16.18)	3rd (16.35–465.4)	p-trend	1st (0.58–6.19)	2nd (6.47–16.18)	3rd (16.35–465.4)	p-trend
	Mean (SD)	β (95% CI)	β (95% CI)		Mean (SD)	β (95% CI)	β (95% CI)	
sBDNF	35.2 (10.1)	−1.15 (−5.97;3.66)	−2.91 (−7.87;2.05)	0.25	35.1 (10.3)	−0.77 (−5.87;4.34)	−2.69 (−7.64;2.26)	0.27
metBDNF								
CpG 1	4.5 (0.6)	−0.09 (−0.37;0.55)	−0.10 (−0.58;0.37)	0.66	4.5 (0.6)	0.12 (−0.35;0.60)	−0.08 (−0.56;0.40)	0.73
CpG 2	3.1 (0.5)	0.17 (−0.11;0.45)	0.20 (−0.09;0.50)	0.16	3.1 (0.5)	0.12 (−0.18;0.41)	0.18 (−0.11;0.48)	0.22
CpG 3	3.2 (0.5)	0.15 (−0.17;0.47)	0.22 (−0.11;0.54)	0.18	3.2 (0.5)	0.10 (−0.22;0.42)	0.19 (−0.14;0.51)	0.24
CpG 4	5.8 (0.9)	0.25 (−0.39;0.90)	0.62 (−0.05;1.28)†	0.06	5.8 (0.9)	0.20 (−0.47;0.87)	0.60 (−0.10;1.27)†	0.07
CpG 5	3.0 (0.6)	0.33 (−0.09;0.76)†	0.54 (0.11;0.98)*	0.01	3.0 (0.6)	0.23 (−0.19;0.65)	0.49 (0.07;0.91)*	0.02
CpG 6	2.4 (0.5)	0.25 (−0.37;0.87)	0.74 (0.09;1.39)*	0.02	2.4 (0.8)	0.12 (−0.48;0.72)	0.67 (0.05;1.29)*	0.03
CpG t	3.6 (0.5)	0.25 (−0.09;0.58)	0.41 (0.06;0.75)*	0.02	3.7 (0.5)	0.19 (−0.15;0.52)	0.38 (0.04;0.72)*	0.02
	Cd tertiles(μg/g)							
	1st (0.01–0.03)	2nd (0.04–0.05)	3rd (0.05–0.55)	p-trend	1st (0.01–0.03)	2nd (0.04–0.05)	3rd(0.05–0.55)	p-trend
	Mean (SD)	β (95% CI)	β (95% CI)		Mean (SD)	β (95% CI)	β(95% CI)	
sBDNF	34.6 (9.0)	−0.78 (−5.80;4.20)	−2.14 (−7.14;2.87)	0.38	34.6 (9.0)	−1.20 (−6.42;4.02)	−3.00 (−8.25;2.25)	0.25
metBDNF								
CpG 1	4.6 (1.0)	−0.29 (−0.76;0.19)	−0.13 (−0.63;0.36)	0.62	4.6 (1.0)	−0.36 (−0.84;0.13)	−0.17 (−0.67;0.33)	0.55
CpG 2	3.4 (0.5)	−0.39 (−0.67;-0.10)*	−0.14 (−0.43;0.16)	0.43	3.4 (0.5)	−0.41 (−0.69;-0.20)*	−0.14 (−0.43;0.16)	0.46
CpG 3	3.4 (0.5)	−0.37 (−0.69;-0.10)*	−0.14 (−0.48;0.19)	0.46	3.4 (0.5)	−0.41 (−0.72;-0.10)*	−0.18 (−0.51;0.15)	0.34
CpG 4	6.1 (1.0)	−0.43 (−1.07;0.22)	0.06 (−0.62;0.74)	0.82	6.1 (1.0)	−0.43 (−1.09;0.24)	0.04 (−0.66;0.73)	0.85
CpG 5	3.3 (0.7)	−0.21 (−0.65;0.22)	0.17 (−0.28;0.62)	0.42	3.3 (0.7)	−0.22 (−0.65;0.21)	0.14 (−0.30;0.31)	0.48
CpG 6	2.6 (0.8)	0.00 (−0.67;0.67)	0.46 (−0.24;1.15)	0.16	2.6 (0.8)	0.04 (−0.62;0.69)	0.41 (−0.26;1.07)	0.20
CpG t	3.9 (0.5)	−0.29 (−0.62;0.10)†	−0.00 (−0.36;0.35)	0.95	3.9 (0.5)	−0.32 (−0.70;0.00)†	−0.05 (−0.40;0.29)	0.83
	Hg tertiles(μg/g)							
	1st (0.02–0.23)	2nd (0.23–0.48)	3rd (0.49–3.24)	p-trend	1st (0.02–0.23)	2nd(0.23–0.48)	3rd(0.49–3.24)	p-trend
	Mean (SD)	β (95% CI)	β (95% CI)		Mean (SD)	β(95% CI)	β(95% CI)	
sBDNF	34.9 (9.5)	−0.14 (−5.06;4.79)	−0.65 (−5.96;4.65)	0.80	34.7 (9.8)	0.34 (−4.79;5.47)	0.28 (−5.33;5.88)	0.92
metBDNF								
CpG 1	4.6 (1.0)	−0.28 (−0.73;0.17)	0.29 (−0.22;0.80)	0.31	4.6 (10.0)	−0.21 (−0.68;0.25)	0.37 (−0.17;0.91)	0.20
CpG 2	3.3 (0.5)	−0.14 (−0.43;0.14)	−0.13 (−0.45;0.20)	0.41	3.3 (0.5)	−0.17 (−0.47;0.12)	−0.15 (−0.49;0.19)	0.35
CpG 3	3.4 (0.6)	−0.16 (−0.48;0.16)	−0.20 (−0.56;0.17)	0.27	3.3 (0.6)	−0.19 (−0.51;0.14)	−0.17 (−0.54;0.20)	0.34
CpG 4	6.1 (1.1)	−0.35 (−0.99;0.29)	−0.42 (−1.16;0.32)	0.24	6.1 (1.1)	−0.43 (−1.08;0.23)	−0.46 (−1.23;0.31)	0.21
CpG 5	3.4 (0.8)	−0.39 (−0.72;0.14)	−0.46 (−0.95;0.0)†	0.06	3.3 (0.8)	−0.34 (−0.76;0.10)†	−0.44 (−0.93;0.0)†	0.06
CpG 6	2.7 (1.0)	−0.32 (−0.96;0.32)	−0.64 (−1.39;1.1)†	0.09	2.7 (1.0)	−0.40 (−1.03;0.20)	−0.56 (−1.30;0.2)†	0.12
CpG t	3.9 (0.6)	−0.19 (−0.53;0.14)	−0.20 (−0.59;0.18)	0.27	3.8 (0.6)	−0.24 (−0.57;0.09)	−0.21 (−0.59;0.17)	0.26
	Pb tertiles(μg/g)							
	1st (0.01–0.18)	2nd (0.18–0.31)	3rd (0.31–2.64)	p-trend	1st (0.01–0.18)	2nd (0.18–0.31)	3rd(0.31–2.64)	p-trend
	Mean (SD)	β (95% CI)	β (95% CI)		Mean (SD)	β (95% CI)	β(95% CI)	
sBDNF	34.1 (9.8)	−1.01 (−5.78;3.75)	0.36 (−4.34;5.06)	0.87	33.9 (9.9)	−0.72 (−5.70;4.27)	0.81 (−4.16;5.78)	0.73
metBDNF								
CpG 1	4.4 (0.7)	0.35 (−0.15;0.84)	0.18 (−0.28;0.64)	0.48	4.4 (0.7)	0.38 (−0.12;0.90)†	0.18 (−0.29;0.65)	0.51
CpG 2	3.1 (0.5)	0.23 (-0.08;0.5)†	−0.02 (−0.30;0.26)	0.78	3.1 (0.5)	0.23 (−0.07;0.50)†	−0.04 (−0.32;0.25)	0.70
CpG 3	3.2 (0.5)	0.18 (−0.17;0.52)	0.06 (−0.26;0.38)	0.75	3.2 (0.5)	0.12 (−0.22;0.46)	0.00 (−0.31;0.32)	0.96
CpG 4	5.7 (0.8)	0.46 (−0.24;1.16)	0.29 (−0.35;0.93)	0.39	5.7 (0.8)	0.42 (−0.29;1.13)	0.26 (−0.40;0.91)	0.46
CpG 5	3.2 (0.6)	0.16 (−0.31;0.62)	−0.1 (−0.52;0.33)	0.60	3.2 (0.6)	0.10 (−0.36;0.55)	−0.17 (−0.58;0.24)	0.38
CpG 6	2.5 (0.7)	0.31 (−0.40;1.01)	−0.01 (−0.64;0.63)	0.55	2.5 (0.7)	0.18 (−0.51;0.87)	−0.13 (−0.74;0.49)	0.62
CpG t	3.7 (0.4)	0.30 (−0.05;0.70)†	0.07 (−0.26;0.40)	0.78	3.7 (0.4)	0.26 (−0.09;0.60)†	0.02 (−0.30;0.34)	0.99

Model 1: adjusted for adolescent's age and BMI, maternal schooling and intelligence, and for all metals simultaneously.
Model 2: additionally adjusted for passive tobacco smoking and total fish intake of adolescents.
For all subscales, a higher score indicates more behavioral problems.
sBDNF: serum BDNF; metBDNF: BDNF gene methylation.
*$p < 0.05$; †$p < 0.10$.

protein levels may be in line with the effects described in the above animal models.

As in the case of As, the neurotoxic activity of Cd has also been implicated in the disruption of various pathways. It has been found to cross the blood-brain barrier, enter the CNS, and disrupt the hippocampal membrane function (Kumar et al., 1996; Wang and Du, 2013) (Fig. 3, number 5). In murine studies, Cd exposure was reported to inhibit acetylcholine esterase (AchE) and Na^{+}/K^{+}-ATP-ase pump, reducing neuronal activity in pups (Gupta et al., 1991), Cd-induced redox homeostasis imbalance increased neuronal death in rats (Wang and Du, 2013) (Figs. 3 and 5), and Cd was found to mimic the ubiquitous intracellular ion Ca^{+2}, thereby inhibiting its influx pathways (Xu et al., 2011) (Figs. 3 and 6). However, inadequate information is available to accurately determine whether these pathways have a direct or indirect effect on hippocampal BDNF expression. Some animal studies also found a downregulation of BDNF expression after Cd exposure (Kadry and Megeed, 2018; Mimouna et al., 2018). In the present investigation, adolescents with urinary Cd concentrations in the second tertile (intermediate level) showed associations with decreased serum BDNF concentrations and a tendency towards reduced BDNF gene DNA.

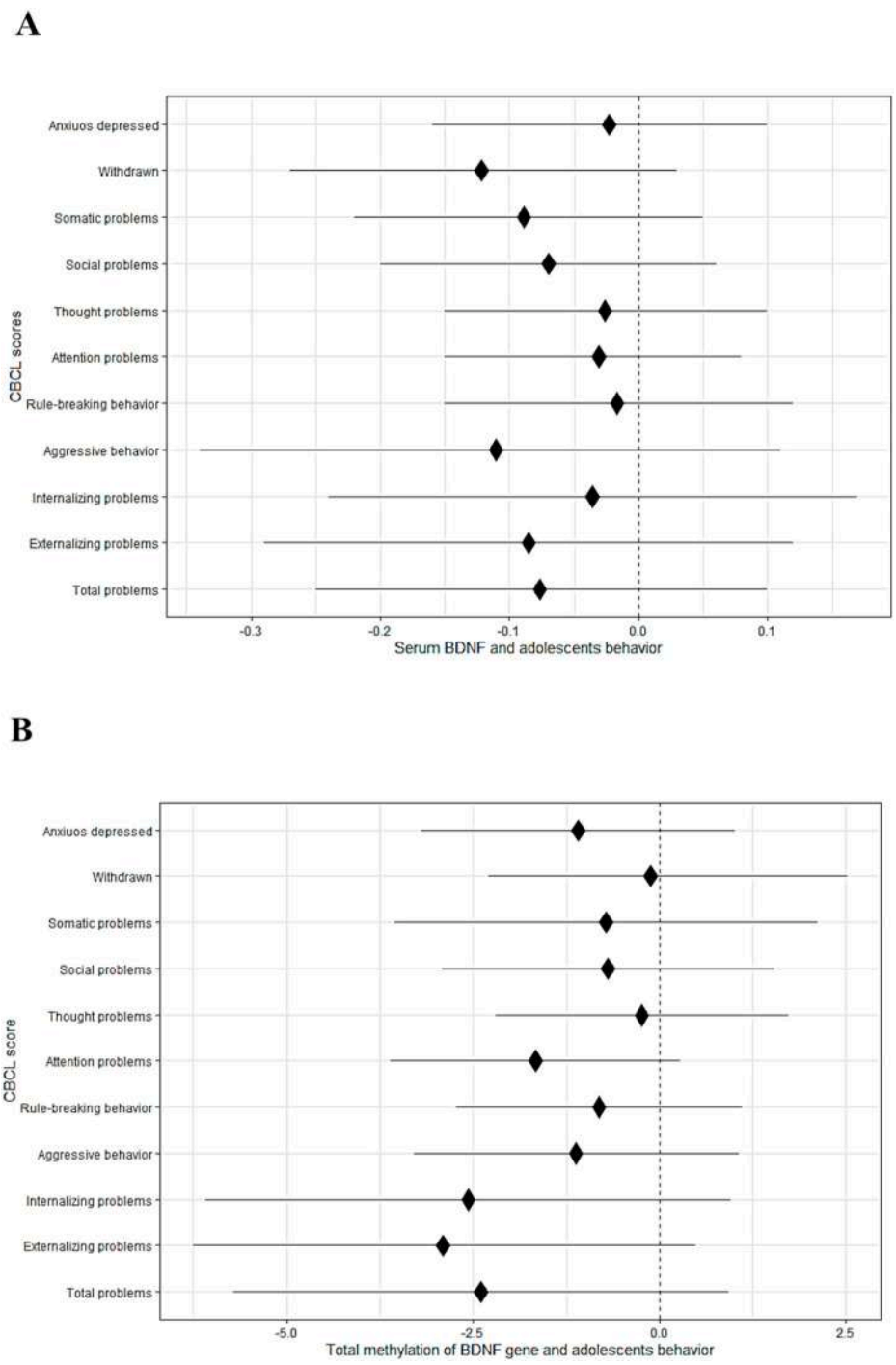

Fig. 2. Forest plot showing associations of serum BDNF concentrations (Fig. 2A) and total BDNF gene DNA methylation at six CpGs (Fig. 2B) with behavioral outcomes.

4.3. Hg and Pb exposure, adolescents' behavior and BDNF effect biomarker

Urinary Hg and Pb concentrations were also within the range described for adolescents by the National Health and Nutrition Examination Survey (NHANES, 2009–2014) and German Human Biomonitoring Commission (Sanders et al., 2019; Schulz et al., 2011). Unexpectedly, Hg and Pb concentrations were not associated with neurobehavioral problems in these adolescents. As anticipated, moderate urinary Pb concentrations tended to be associated with higher percentage DNA methylation at CpGs #1, 4 and with total CpG methylation, while urinary Hg concentrations were associated with lesser BDNF gene DNA methylation. No association was observed between serum BDNF protein concentrations and the studied metals.

Adverse effects of prenatal and postnatal exposure to Pb and Hg on cognitive function and intelligence are well documented in humans (Canfield et al., 2003; Cecil et al., 2008; Debes et al., 2006; Freire et al., 2018; Hu et al., 2006; Jusko et al., 2008; Lanphear et al., 2005; Llop et al., 2012; Wright et al., 2008). However, the potential impact of Hg and Pb on behavioral functioning remains unclear, although some studies found associations of postnatal exposure to Pb and Hg with anxiety, social problems, and ADHD (Debes et al., 2006; Liu et al., 2014;

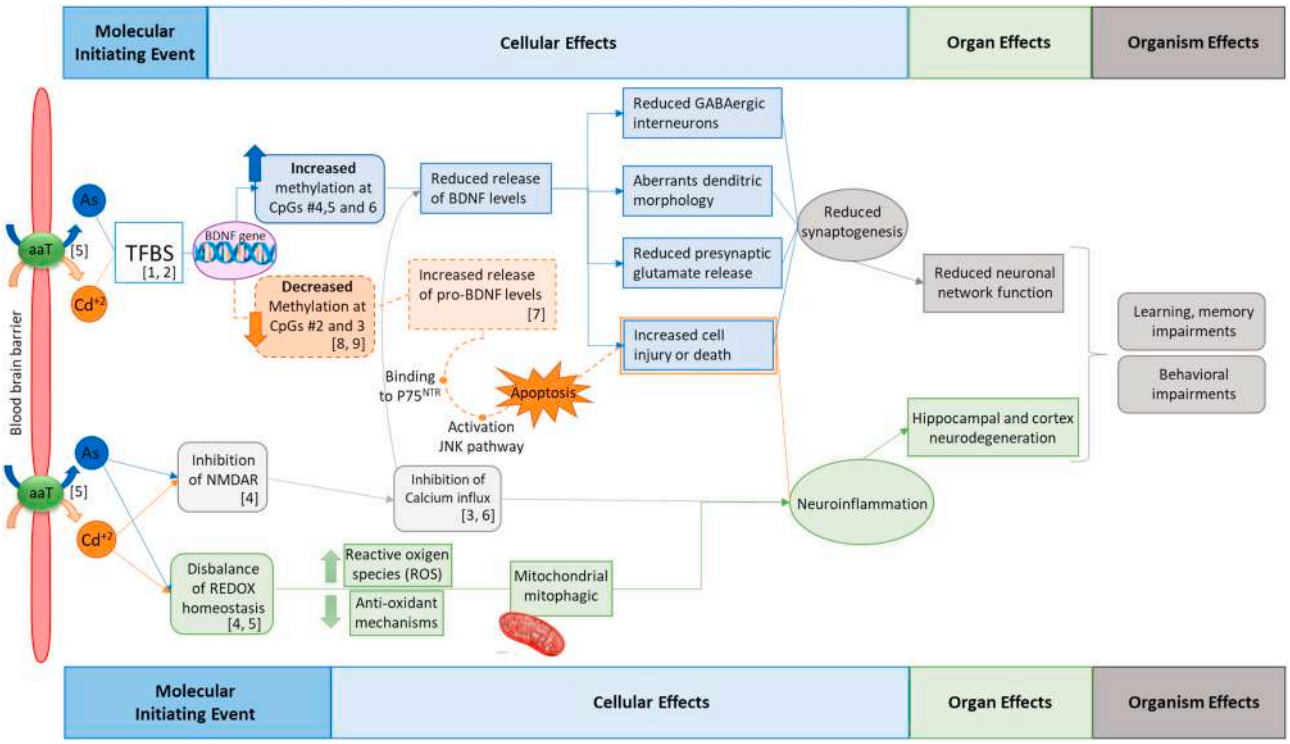

Fig. 3. Hypothesized adverse outcome pathway (AOP) based on the AOPs published by Mustieles et al. (2020) and other specific toxicological references for As (Demanelis et al., 2019; Karim et al., 2019; Karri et al., 2016; Wang et al., 2016) and Cd (Guan et al., 2019; Wang and Du, 2013; Xia et al., 2020; Xu et al., 2011; Zaletel et al., 2017). AOP followed by As and Cd in the hippocampus after crossing the blood brain barrier. As: Arsenic; aaT: amino acid transporter; BDNF: brain-derived neurotrophic factor; Cd: Cadmium; JNK: c-Jun N-terminal kinase; NMDAR: N-Methyl-D-aspartate receptors; pro-BDNF: immature isoform of BDNF; TFBS: Transcription factor binding sites. The observed downregulation of BDNF methylation might lead to higher concentrations of the immature BDNF isoform (pro-BDNF), known to activate cellular apoptosis by binding to P75 neurotrophin receptor (NTR) (Zaletel et al., 2017) [7], possibly explaining the suggested adverse association of Cd with behavior (Fig.3). Similar results were found in a zebrafish model showing increased BDNF expression after Cd exposure alongside locomotor alterations (Xia et al., 2020) [8] and in a genome-wide study finding that Cd exposure reduced global DNA methylation in drosophila melanogaster (Guan et al., 2019) [9]. However, further research is needed to verify this hypothesis, given the absence of published data on the effects of Cd on pro-BDNF secretion and fact that this BDNF form was not measured in the present study.

Roy et al., 2009). Caution should be taken in interpreting the present results on postnatal Pb and Hg and behavioral functioning, given that urinary concentrations of Hg and Pb may reflect short-term rather than long-term exposure (Gil and Hernández, 2015) and may not serve as appropriate biomarkers to evaluate potential effects on behavior. In addition, some of these apparently protective associations may be explained by dietary and lifestyle confounders. For instance, fish consumption is a potential source of toxic metals as well as beneficial nutrients for brain development (Cano-Sancho and Casas, 2021; Gil and Gil, 2015). Although fish consumption was controlled for in the present study, residual confounding or dietary misclassification cannot be ruled out.

4.4. Strengths and limitations

Study limitations include the small sample size, reducing the statistical power of analyses and preventing the assessment of the mixture effect of the selected metals on BDNF and behavioral function, as well as potential interactions among them. Instead, we simultaneously adjusted the models for all metals in order to assess the effect exerted by a single metal while accounting for the influence of the remaining elements. Future studies in larger populations would be needed to address the combined effect of metals mixtures on BDNF and neurodevelopment. The cross-sectional design also means that causal relationships could not be inferred. Furthermore, the study investigated the concentration of total As and Hg, with no speciation procedure. Recent data from the Environment and Childhood study show that the primary source of Hg exposure is fish (Signes-Pastor et al., 2017), where Hg is present as methyl-Hg, the most neurotoxic form. The source of exposure of As, however, remains unknown, although rice (inorganic As) and seafood (organic As) consumption seem to be major sources of As exposure in the Spanish population (Signes-Pastor et al., 2017). Therefore, it is not clear whether our study population is mostly exposed to inorganic or organic As. Nevertheless, this lack of specificity would tend to underestimate rather than overestimate As effects on neurodevelopment. Additionally, previous studies have also reported associations between urinary total As and behavioral function (Rodríguez-Barranco et al., 2016). While urinary Cd and As levels appear to be a straightforward choice, it may not be the best biomarker for Pb and Hg exposure, since their short biological half-lives makes them suitable biomarkers for current or recent exposure (Gil and Hernández, 2015). Conversely, urinary Cd levels are a suitable biomarker of long-term and lifetime exposure to this metal (Gil and Hernández, 2015; Järup and Åkesson, 2009). Urinary As is also considered as adequate biomarker of short-term exposure, since it concentrations remains relatively stable among individuals with consistent dietary patterns (Hughes, 2006; Marchiset-Ferlay et al., 2012). Therefore, results for Cd and As could be more reliable compared to those of Pb and Hg. Finally, spurious associations may have been identified due to the application of multiple analyses, although several significant associations are supported by toxicological and epidemiological studies and are unlikely to be the result of chance. Moreover, the estimated coefficients and confidence intervals should be taken as a global representation of the pattern of relationships between the study variables. Study strengths include the novel exploration approach of BDNF as biomarker of neurodevelopment, assessed at different levels of biological organization (DNA methylation and serum protein). In future

epidemiological studies, this approach could contribute to elucidate the neurodevelopmental effects of metals and metalloids, especially As and Cd. Another strength is the effort to characterize the effect of As and Cd on behavioral functioning, given the scant available evidence on the impact of these pollutants. Finally, there has been inadequate research of this type in adolescence, which is characterized by important changes in neurological mechanisms.

5. Conclusion

Within an epidemiological context, serum BDNF protein levels and BDNF gene DNA methylation profile might serve as effect biomarkers to characterize the relationship of postnatal exposure to toxic metals, such as As and Cd, with behavioral problems in adolescents. However, due to study limitations, our results need to be verified in future larger epidemiological studies on metal exposures during this and other critical windows of neurodevelopment. Biomarkers of brain function are needed in human biomonitoring studies to better address current gaps in knowledge between environmental exposures and neurodevelopmental disorders.

Declaration of Competing interest

The authors declare no actual or potential conflicts of interest. The funders had no role in the study design, data collection or analysis, decision to publish, or preparation of the manuscript.

Funding and acknowledgements

This research would not have been achieved without the selfless collaboration of the INMA-Granada adolescents and families who took part in the study. The authors also acknowledge the Human Genotyping Laboratory at the Spanish National Cancer Research Center, CeGen-PRB3, which is supported by grant no. PT17/0019, of the PE I+D+i 2013–2016, funded by the Instituto de Salud Carlos III (ISCIII) and ERDF. They thank the European Union's Horizon 2020 research and innovation program HBM4EU for financial support under Grant Agreement No. 733032. The study was also supported by the ISCIII with grant no. CP16/00085. The authors also acknowledge the funding received from the University of Granada for the open access publishing costs and the support of the Biomedical Research Networking Center-CIBER de Epidemiología y Salud Pública (CIBERESP), and the ISCIII (FIS 17/01526, FIS-PI16/01820 and FIS-PI16/01858). Vicente Mustieles and Shereen Cynthia D'Cruz were under contract with the HBM4EU project. A. Rodríguez-Carrillo received a predoctoral fellowship (FPU 16/03011) from the Spanish Ministry of Education and C. Freire (grant no. MS16/00085) received a grant under the Miguel Servet Type I program of the ISCIII "Fondo Europeo de Desarrollo Regional'' (ISCIII/FEDER). This article forms part of the doctoral thesis developed by Andrea Rodríguez-Carrillo in the context of the "Clinical Medicine and Public Health Program" of the University of Granada (Spain).

Appendix A. Supplementary data

Supplementary data to this article can be found online at https://doi.org/10.1016/j.ijheh.2021.113877.

References

Achenbach, T., Rescorla, L., 2013. Achenbach system of empirically based assessment. In: Encyclopedia of Autism Spectrum Disorders. Springer, New York, pp. 31–39. https://doi.org/10.1007/978-1-4419-1698-3_219.

Amrhein, V., Greenland, S., McShane, B., 2019. Scientists rise up against statistical significance. Nature. https://doi.org/10.1038/d41586-019-00857-9.

URL ATSDR - Toxicological Profile, 2016. Arsenic [WWW document], accessed 9.21.20. https://www.atsdr.cdc.gov/toxprofiles/tp.asp?id=22&tid=3.

n.d. ATSDR - Toxicological Profile. Cadmium [WWW document], URL, accessed 9.21.20. https://www.atsdr.cdc.gov/ToxProfiles/tp.asp?id=48&tid=15.

Baken, K.A., Lambrechts, N., Remy, S., Mustieles, V., Rodríguez-Carrillo, A., Neophytou, C.M., Olea, N., Schoeters, G., 2019. A strategy to validate a selection of human effect biomarkers using adverse outcome pathways: proof of concept for phthalates and reproductive effects. Environ. Res. 175 https://doi.org/10.1016/j.envres.2019.05.013.

Bao, Q.S., Lu, C.Y., Song, H., Wang, M., Ling, W., Chen, W.Q., Deng, X.Q., Hao, Y.T., Rao, S., 2009. Behavioural development of school-aged children who live around a multi-metal sulphide mine in Guangdong province, China: a cross-sectional study. BMC Publ. Health 9, 217. https://doi.org/10.1186/1471-2458-9-217.

Barr, D.B., Wilder, L.C., Caudill, S.P., Gonzalez, A.J., Needham, L.L., Pirkle, J.L., 2005. Urinary creatinine concentrations in the U.S. population: implications for urinary biologic monitoring measurements. Environ. Health Perspect. 113, 192–200. https://doi.org/10.1289/EHP.7337.

Bellinger, D.C., 2009. Interpreting epidemiologic studies of developmental neurotoxicity: conceptual and analytic issues. Neurotoxicol. Teratol. https://doi.org/10.1016/j.ntt.2009.06.006.

Campbell, R.C.J., Stephens, W.E., Meharg, A.A., 2014. Consistency of arsenic speciation in global tobacco products with implications for health and regulation. Tob. Induc. Dis. 12 https://doi.org/10.1186/s12971-014-0024-5.

Canfield, R.L., Henderson, C.R., Cory-Slechta, D.A., Cox, C., Jusko, T.A., Lanphear, B.P., 2003. Intellectual impairment in children with blood lead concentrations below 10 μg per deciliter. N. Engl. J. Med. 348, 1517–1526. https://doi.org/10.1056/NEJMoa022848.

Cano-Sancho, G., Casas, M., 2021. Interactions between environmental pollutants and dietary nutrients: current evidence and implications in epidemiological research. J. Epidemiol. Community Health. https://doi.org/10.1136/jech-2020-213789.

Cao, Y., Chen, A., Radcliffe, J., Dietrich, K.N., Jones, R.L., Caldwell, K., Rogan, W.J., 2009. Postnatal cadmium exposure, neurodevelopment, and blood pressure in children at 2, 5, and 7 Years of age. Environ. Health Perspect. 117, 1580–1586. https://doi.org/10.1289/ehp.0900765.

Castiello, F., Olmedo, P., Gil, F., Molina, M., Mundo, A., Romero, R.R., Ruíz, C., Gómez-Vida, J., Vela-Soria, F., Freire, C., 2020. Association of urinary metal concentrations with blood pressure and serum hormones in Spanish male adolescents. Environ. Res. 182, 108958 https://doi.org/10.1016/j.envres.2019.108958.

Cecil, K.M., Brubaker, C.J., Adler, C.M., Dietrich, K.N., Altaye, M., Egelhoff, J.C., Wessel, S., Elangovan, I., Hornung, R., Jarvis, K., Lanphear, B.P., 2008. Decreased brain volume in adults with childhood lead exposure. PLoS Med. 5, e112. https://doi.org/10.1371/journal.pmed.0050112.

Chen, R., Clifford, A., Lang, L., Anstey, K.J., 2013. Is exposure to secondhand smoke associated with cognitive parameters ofchildren and adolescents?-a systematic literature review. Ann. Epidemiol. https://doi.org/10.1016/j.annepidem.2013.07.001.

Ciesielski, T., Weuve, J., Bellinger, D.C., Schwartz, J., Lanphear, B., Wright, R.O., 2012. Cadmium exposure and neurodevelopmental outcomes in U.S. children. Environ. Health Perspect. 120, 758–763. https://doi.org/10.1289/ehp.1104152.

Ciranna, L., 2006. Serotonin as a modulator of glutamate- and GABA-mediated neurotransmission: implications in physiological functions and in pathology. Curr. Neuropharmacol. 4, 101–114. https://doi.org/10.2174/157015906776359540.

Debes, F., Budtz-Jørgensen, E., Weihe, P., White, R.F., Grandjean, P., 2006. Impact of prenatal methylmercury exposure on neurobehavioral function at age 14 years. Neurotoxicol. Teratol. 28, 363–375. https://doi.org/10.1016/j.ntt.2006.02.004.

Demanelis, K., Argos, M., Tong, L., Shinkle, J., Sabarinathan, M., Rakibuz-Zaman, M., Sarwar, G., Shahriar, H., Islam, T., Rahman, M., Yunus, M., Graziano, J.H., Broberg, K., Engström, K., Jasmine, F., Ahsan, H., Pierce, B.L., 2019. Association of arsenic exposure with whole blood DNA methylation: an epigenome-wide study of Bangladeshi adults. Environ. Health Perspect. 127, 057011 https://doi.org/10.1289/EHP3849.

Fernandez, M.F., Olmos, B., Granada, A., López-Espinosa, M.J., Molina-Molina, J.-M., Fernandez, J.M., Cruz, M., Olea-Serrano, F., Olea, N., 2007. Human exposure to endocrine-disrupting chemicals and prenatal risk factors for cryptorchidism and hypospadias: a nested case–control study. Environ. Health Perspect. 115, 8–14. https://doi.org/10.1289/ehp.9351.

Freire, C., Amaya, E., Gil, F., Fernández, M.F., Murcia, M., Llop, S., Andiarena, A., Aurrekoetxea, J., Bustamante, M., Guxens, M., Ezama, E., Fernández-Tardón, G., Olea, N., 2018. Prenatal co-exposure to neurotoxic metals and neurodevelopment in preschool children: the Environment and Childhood (INMA) Project. Sci. Total Environ. 621, 340–351. https://doi.org/10.1016/j.scitotenv.2017.11.273.

Gil, A., Gil, F., 2015. Fish, a Mediterranean source of n-3 PUFA: benefits do not justify limiting consumption. Br. J. Nutr. 113, S58–S67. https://doi.org/10.1017/S0007114514003742.

Gil, F., Hernández, A.F., 2015. Toxicological importance of human biomonitoring of metallic and metalloid elements in different biological samples. Food Chem. Toxicol. https://doi.org/10.1016/j.fct.2015.03.025.

Gore, A.C., Krishnan, K., Reilly, M.P., 2018. Endocrine-disrupting chemicals: effects on neuroendocrine systems and the neurobiology of social behavior. Horm. Behav. https://doi.org/10.1016/j.yhbeh.2018.11.006.

Grandjean, P., Landrigan, P., 2006. Developmental neurotoxicity of industrial chemicals. Lancet. https://doi.org/10.1016/S0140-6736(06)69665-7.

Grandjean, P., Landrigan, P.J., 2014. Neurobehavioural effects of developmental toxicity. Lancet Neurol. https://doi.org/10.1016/S1474-4422(13)70278-3.

Guan, D.L., Ding, R.R., Hu, X.Y., Yang, X.R., Xu, S.Q., Gu, W., Zhang, M., 2019. Cadmium-induced genome-wide DNA methylation changes in growth and oxidative metabolism in Drosophila melanogaster. BMC Genom. 20, 356. https://doi.org/10.1186/s12864-019-5688-z.

Gupta, Alka, Gupta, Amita, Chandra, S.V., 1991. Gestational cadmium exposure and brain development: a biochemical study. Ind. Health 29, 65–71. https://doi.org/10.2486/indhealth.29.65.

Gustin, K., Tofail, F., Vahter, M., Kippler, M., 2018. Cadmium exposure and cognitive abilities and behavior at 10 years of age: a prospective cohort study. Environ. Int. 113, 259–268. https://doi.org/10.1016/j.envint.2018.02.020.

Guxens, M., Ballester, F., Espada, M., Fernández, M.F., Grimalt, J.O., Ibarluzea, J., Olea, N., Rebagliato, M., Tardón, A., Torrent, M., Vioque, J., Vrijheid, M., Sunyer, J., INMA Project, 2012. Cohort profile: the INMA–INfancia y Medio ambiente–(environment and childhood) project. Int. J. Epidemiol. 41, 930–940. https://doi.org/10.1093/ije/dyr054.

Htway, S.M., Sein, M.T., Nohara, K., Win-Shwe, T.T., 2019. Effects of developmental arsenic exposure on the social behavior and related gene expression in C3H adult male mice. Int. J. Environ. Res. Publ. Health 16. https://doi.org/10.3390/ijerph16020174.

Hu, H., Téllez-Rojo, M.M., Bellinger, D., Smith, D., Ettinger, A.S., Lamadrid-Figueroa, H., Schwartz, J., Schnaas, L., Mercado-García, A., Hernández-Avila, M., 2006. Fetal lead exposure at each stage of pregnancy as a predictor of infant mental development. Environ. Health Perspect. 114, 1730–1735. https://doi.org/10.1289/ehp.9067.

Hughes, A., Ask, H., Tesli, T., Askeland, R., Reichborn-Kjennerud, T., Andreassen, O., Helgeland, Ø., Njølstad, P., Davies, N., Havdahl, A., 2020. OP96Thecausal effect of BMI on neurodevelopment: a within family mendelian randomization study using MoBa. J. Epidemiol. Community Health 74, A44–A45. https://doi.org/10.1136/JECH-2020-SSMABSTRACTS.94.

Hughes, M.F., 2006. Biomarkers of exposure: a case study with inorganic arsenic. Environ. Health Perspect. 114, 1790–1796. https://doi.org/10.1289/EHP.9058.

Jaishankar, M., Tseten, T., Anbalagan, N., Mathew, B.B., Beeregowda, K.N., 2014. Toxicity, mechanism and health effects of some heavy metals. Interdiscipl. Toxicol. https://doi.org/10.2478/intox-2014-0009.

Jakubowski, M., 2011. Low-level environmental lead exposure and intellectual impairment in children - the current concepts of risk assessment. Int. J. Occup. Med. Environ. Health. https://doi.org/10.2478/s13382-011-0009-z.

Järup, L., Åkesson, A., 2009. Current status of cadmium as an environmental health problem. Toxicol. Appl. Pharmacol. 238, 201–208. https://doi.org/10.1016/J.TAAP.2009.04.020.

Jusko, T.A., Henderson, C.R., Lanphear, B.P., Cory-Slechta, D.A., Parsons, P.J., Canfield, R.L., 2008. Blood lead concentration <10 μg/dL and child intelligence at 6 years of age. Environ. Health Perspect. 116, 243–248. https://doi.org/10.1289/ehp.10424.

Kadry, M.O., Megeed, R.A., 2018. Probiotics as a complementary therapy in the model of cadmium chloride toxicity: crosstalk of β-catenin, BDNF, and StAR signaling pathways. Biol. Trace Elem. Res. 185, 404–413. https://doi.org/10.1007/s12011-018-1261-x.

Kalia, V., Perera, F., Tang, D., 2017. Environmental pollutants and neurodevelopment: review of benefits from closure of a coal-burning power plant in tongliang, China. Glob. Pediatr. Heal. 4 https://doi.org/10.1177/2333794x17721609, 2333794X1772160.

Karim, Y., Siddique, A.E., Hossen, F., Rahman, M., Mondal, V., Banna, H.U., Hasibuzzaman, M.M., Hosen, Z., Islam, M.S., Sarker, M.K., Nikkon, F., Saud, Z.A., Xin, L., Himeno, S., Hossain, K., 2019. Dose-dependent relationships between chronic arsenic exposure and cognitive impairment and serum brain-derived neurotrophic factor. Environ. Int. 131, 105029. https://doi.org/10.1016/j.envint.2019.105029.

Karri, V., Schuhmacher, M., Kumar, V., 2016. Heavy metals (Pb, Cd, as and MeHg) as risk factors for cognitive dysfunction: a general review of metal mixture mechanism in brain. Environ. Toxicol. Pharmacol. 48, 203–213. https://doi.org/10.1016/j.etap.2016.09.016.

Khan, K., Factor-Litvak, P., Wasserman, G.A., Liu, X., Ahmed, E., Parvez, F., Slavkovich, V., Levy, D., Mey, J., van Geen, A., Graziano, J.H., 2011. Manganese exposure from drinking water and children's classroom behavior in Bangladesh. Environ. Health Perspect. 119, 1501–1506. https://doi.org/10.1289/ehp.1003397.

Kowiański, P., Lietzau, G., Czuba, E., Waśkow, M., Steliga, A., Moryś, J., 2018. BDNF: a key factor with multipotent impact on brain signaling and synaptic plasticity. Cell. Mol. Neurobiol. https://doi.org/10.1007/s10571-017-0510-4.

Kumar, R., Agarwal, A.K., Seth, P.K., 1996. Oxidative stress-mediated neurotoxicity of cadmium. Toxicol. Lett. 89, 65–69. https://doi.org/10.1016/S0378-4274(96)03780-0.

Kundakovic, M., Gudsnuk, K., Herbstman, J.B., Tang, D., Perera, F.P., Champagne, F.A., 2015. DNA methylation of BDNF as a biomarker of early-life adversity. Proc. Natl. Acad. Sci. Unit. States Am. 112, 6807–6813. https://doi.org/10.1073/pnas.1408355111.

Lanphear, B.P., Hornung, R., Khoury, J., Yolton, K., Baghurst, P., Bellinger, D.C., Canfield, R.L., Dietrich, K.N., Bornschein, R., Greene, T., Rothenberg, S.J., Needleman, H.L., Schnaas, L., Wasserman, G., Graziano, J., Roberts, R., 2005. Low-level environmental lead exposure and children's intellectual function: an international pooled analysis. Environ. Health Perspect. 113, 894–899. https://doi.org/10.1289/ehp.7688.

n.d. Lead Toxicological Profile ATSDR. [WWW document], accessed 2.12.21, URL. https://wwwn.cdc.gov/TSP/ToxProfiles/ToxProfiles.aspx?id=96&tid=22.

Lee, B.E., Hong, Y.C., Park, H., Ha, M., Hyeong Kim, J., Chang, N., Roh, Y.M., Kim, B.N., Kim, Y., Oh, S. y, Ju Kim, Y., Ha, E.H., 2011. Secondhand smoke exposure during pregnancy and infantile neurodevelopment. Environ. Res. 111, 539–544. https://doi.org/10.1016/j.envres.2011.02.014.

Lin, Y.C., Su, C.T., Shiue, H.S., Chen, W.J., Chen, Y.H., Choy, C.S., Chiou, H.Y., Han, B.C., Hsueh, Y.M., 2017. The methylation capacity of arsenic and insulin resistance are associated with psychological characteristics in children and adolescents. Sci. Rep. 7, 1–11. https://doi.org/10.1038/s41598-017-03084-2.

Liu, J., Liu, X., Wang, W., Mccauley, L., Pinto-Martin, J., Wang, Y., Li, L., Yan, C., Rogan, W.J., 2014. Blood lead levels and children's behavioral and emotional problems. A Cohort Study 168, 737–745. https://doi.org/10.1001/jamapediatrics.2014.332.

Llop, S., Guxens, M., Murcia, M., Lertxundi, A., Ramon, R., Riaño, I., Rebagliato, M., Ibarluzea, J., Tardon, A., Sunyer, J., Ballester, F., 2012. Prenatal exposure to mercury and infant neurodevelopment in a multicenter cohort in Spain: study of potential modifiers. Am. J. Epidemiol. 175, 451–465. https://doi.org/10.1093/aje/kwr328.

Long, M., Ghisari, M., Kjeldsen, L., Wielsøe, M., Nørgaard-Pedersen, B., Mortensen, E.L., Abdallah, M.W., Bonefeld-Jørgensen, E.C., 2019. Autism spectrum disorders, endocrine disrupting compounds, and heavy metals in amniotic fluid: a case-control study. Mol. Autism. 10, 1. https://doi.org/10.1186/s13229-018-0253-1.

Lucchini, R.G., Zoni, S., Guazzetti, S., Bontempi, E., Micheletti, S., Broberg, K., Parrinello, G., Smith, D.R., 2012. Inverse association of intellectual function with very low blood lead but not with manganese exposure in Italian adolescents. Environ. Res. 118, 65–71. https://doi.org/10.1016/j.envres.2012.08.003.

Marchiset-Ferlay, N., Savanovitch, C., Sauvant-Rochat, M.P., 2012. What is the best biomarker to assess arsenic exposure via drinking water? Environ. Int. 39, 150–171. https://doi.org/10.1016/J.ENVINT.2011.07.015.

Mimouna, S. Ben, Chemek, M., Boughammoura, S., Banni, M., Messaoudi, I., 2018. Early-life exposure to cadmium triggers distinct Zn-dependent protein expression patterns and impairs brain development. Biol. Trace Elem. Res. 184, 409–421. https://doi.org/10.1007/s12011-017-1201-1.

Mozaffarian, D., Rimm, E.B., 2006. Fish intake, contaminants, and human health evaluating the risks and the benefits. J. Am. Med. Assoc. https://doi.org/10.1001/jama.296.15.1885.

Mravunac, M., Szymlek-Gay, E.A., Daly, R.M., Roberts, B.R., Formica, M., Gianoudis, J., O'connell, S.L., Nowson, C.A., Cardoso, B.R., 2019. Greater circulating copper concentrations and copper/zinc ratios are associated with lower psychological distress, but not cognitive performance in a sample of australian older adults. Nutrients 11. https://doi.org/10.3390/nu11102503.

Mustieles, et al., 2022. BDNF as a potential mediator between childhood BPA exposure and behavioral function in adolescent boys from the INMA-Granada cohort. Sci. Total Environ. 803, 150014. https://doi.org/10.1016/J.SCITOTENV.2021.150014.

Mustieles, V., D'Cruz, S.C., Couderq, S., Rodríguez-Carrillo, A., Fini, J.-B., Hofer, T., Steffensen, I.-L., Dirven, H., Barouki, R., Olea, N., Fernández, M.F., David, A., 2020. Bisphenol A and its analogues: a comprehensive review to identify and prioritize effect biomarkers for human biomonitoring. Environ. Int. 144, 105811. https://doi.org/10.1016/j.envint.2020.105811.

Navas-Acien, A., 2018. Global tobacco use: old and new products. In: Annals of the American Thoracic Society. American Thoracic Society, pp. S69–S75. https://doi.org/10.1513/AnnalsATS.201711-874MG.

Notario-Barandiaran, L., Freire, C., García-de-la-Hera, M., Compañ-Gabucio, L.M., Torres-Collado, L., González-Palacios, S., Mundo, A., Molina, M., Fernández, M.F., Vioque, J., 2020. Reproducibility and validity of a food frequency questionnaire for dietary assessment in adolescents in a self-reported way. Nutrients 12, 2081. https://doi.org/10.3390/nu12072081.

O'Brien, K.M., Upson, K., Cook, N.R., Weinberg, C.R., 2016. Environmental chemicals in urine and blood: improving methods for creatinine and lipid adjustment. Environ. Health Perspect. 124, 220–227. https://doi.org/10.1289/EHP.1509693.

Patra, K., Greene, M.M., Patel, A.L., Meier, P., 2016. Maternal education level predicts cognitive, language, and motor outcome in preterm infants in the second year of life. Am. J. Perinatol. 33, 738–744. https://doi.org/10.1055/s-0036-1572532.

Perera, F., Phillips, D.H., Wang, Y., Roen, E., Herbstman, J., Rauh, V., Wang, S., Tang, D., 2015. Prenatal exposure to polycyclic aromatic hydrocarbons/aromatics, BDNF and child development. Environ. Res. 142, 602–608. https://doi.org/10.1016/j.envres.2015.08.011.

Pfeifer, J.H., Allen, N.B., 2021. Puberty initiates cascading relationships between neurodevelopmental, social, and internalizing processes across adolescence. Biol. Psychiatr. https://doi.org/10.1016/j.biopsych.2020.09.002.

Ramos-Chávez, L.A., Rendón-López, C.R.R., Zepeda, A., Silva-Adaya, D., Del Razo, L.M., Gonsebatt, M.E., 2015. Neurological effects of inorganic arsenic exposure: altered cysteine/glutamate transport, NMDA expression and spatial memory impairment. Front. Cell. Neurosci. 9 https://doi.org/10.3389/fncel.2015.00021.

Rice, D., Barone, S., 2000. Critical periods of vulnerability for the developing nervous system: evidence from humans and animal models. Environ. Health Perspect. 108, 511–533. https://doi.org/10.1289/ehp.00108s3511.

Richards, J.E., Xie, W., 2015. Brains for all the ages: structural neurodevelopment in infants and children from a life-span perspective. Adv. Child Dev. Behav. 48, 1–52. https://doi.org/10.1016/BS.ACDB.2014.11.001.

Roberts, A.L., Lyall, K., Hart, J.E., Laden, F., Just, A.C., Bobb, J.F., Koenen, K.C., Ascherio, A., Weisskopf, M.G., 2013. Perinatal air pollutant exposures and autism spectrum disorder in the children of nurses' health study II participants. Environ. Health Perspect. 121, 978–984. https://doi.org/10.1289/ehp.1206187.

Rodríguez-Barranco, M., Gil, F., Hernández, A.F., Alguacil, J., Lorca, A., Mendoza, R., Gómez, I., Molina-Villalba, I., González-Alzaga, B., Aguilar-Garduño, C., Rohlman, D.S., Lacasaña, M., 2016. Postnatal arsenic exposure and attention impairment in school children. Cortex 74, 370–382. https://doi.org/10.1016/j.cortex.2014.12.018.

Rodríguez-Barranco, M., Lacasaña, M., Aguilar-Garduño, C., Alguacil, J., Gil, F., González-Alzaga, B., Rojas-García, A., 2013. Association of arsenic, cadmium and manganese exposure with neurodevelopment and behavioural disorders in children:

a systematic review and meta-analysis. Sci. Total Environ. https://doi.org/10.1016/j.scitotenv.2013.03.047.

Rodríguez-Carrillo, A., Mustieles, V., Pérez-Lobato, R., Molina-Molina, J.M., Reina-Pérez, I., Vela-Soria, F., Rubio, S., Olea, N., Fernández, M.F., 2019. Bisphenol A and cognitive function in school-age boys: is BPA predominantly related to behavior? Neurotoxicology. https://doi.org/10.1016/j.neuro.2019.06.006.

Roy, A., Bellinger, D., Hu, H., Schwartz, J., Ettinger, A.S., Wright, R.O., Bouchard, M., Palaniappan, K., Balakrishnan, K., 2009. Lead exposure and behavior among young children in Chennai, India. Environ. Health Perspect. 117, 1607–1611. https://doi.org/10.1289/ehp.0900625.

Sanders, A.P., Claus Henn, B., Wright, R.O., 2015. Perinatal and childhood exposure to cadmium, manganese, and metal mixtures and effects on cognition and behavior: a review of recent literature. Curr. Environ. Heal. reports 2, 284–294. https://doi.org/10.1007/s40572-015-0058-8.

Sanders, A.P., Mazzella, M.J., Malin, A.J., Hair, G., Busgang, S.A., Saland, J.M., Curtin, P., 2019. Combined exposure to lead, cadmium, mercury, and arsenic and kidney health in adolescents age 12–19 in NHANES 2009–2014. Environ. Int. 131, 104993. https://doi.org/10.1016/j.envint.2019.104993.

Sanders, A.P., Smeester, L., Rojas, D., DeBussycher, T., Wu, M.C., Wright, F.A., Zhou, Y. H., Laine, J.E., Rager, J.E., Swamy, G.K., Ashley-Koch, A., Miranda, M.L., Fry, R.C., 2014. Cadmium exposure and the epigenome: exposure-associated patterns of DNA methylation in leukocytes from mother-baby pairs. Epigenetics 9, 212–221. https://doi.org/10.4161/epi.26798.

Sardinero García, E., Pedreira Massa, J.L., Muñiz Fernández, J., 1997. El cuestionario CBCL de Achenbach: Adaptación española y aplicaciones clínico-epidemiológicas, pp. 447–480. https://journals.copmadrid.org/clysa 8.

Sasi, M., Vignoli, B., Canossa, M., Blum, R., 2017. Neurobiology of local and intercellular BDNF signaling. Pflügers Archiv. https://doi.org/10.1007/s00424-017-1964-4.

Schoeman, K., Bend, J.R., Hill, J., Nash, K., Koren, G., 2009. Defining a lowest observable adverse effect hair concentrations of mercury for neurodevelopmental effects of prenatal methylmercury exposure through maternal fish consumption: a systematic review. Ther. Drug Monit. 31, 670–682. https://doi.org/10.1097/FTD.0b013e3181bb0ea1.

Schulz, C., Wilhelm, M., Heudorf, U., Kolossa-Gehring, M., 2011. Update of the reference and HBM values derived by the German human biomonitoring commission. Int. J. Hyg Environ. Health 215, 26–35. https://doi.org/10.1016/j.ijheh.2011.06.007.

Shah-Kulkarni, S., Lee, S., Jeong, K.S., Hong, Y.C., Park, H., Ha, M., Kim, Y., Ha, E.H., 2020. Prenatal exposure to mixtures of heavy metals and neurodevelopment in infants at 6 months. Environ. Res. 182 https://doi.org/10.1016/j.envres.2020.109122.

Signes-Pastor, A.J., Carey, M., Vioque, J., Navarrete-Muñoz, E.M., Rodríguez-Dehli, C., Tardón, A., Begoña-Zubero, M., Santa-Marina, L., Vrijheid, M., Casas, M., Llop, S., Gonzalez-Palacios, S., Meharg, A.A., 2017. Urinary arsenic speciation in children and pregnant women from Spain. Expo. Heal. 92 9, 105–111. https://doi.org/10.1007/S12403-016-0225-7, 2016.

Spear, L.P., 2000. The adolescent brain and age-related behavioral manifestations. Neurosci. Biobehav. Rev. 24, 417–463. https://doi.org/10.1016/S0149-7634(00)00014-2.

Spulber, S., Rantamäki, T., Nikkilä, O., Castrén, E., Weihe, P., Grandjean, P., Ceccatelli, S., 2010. Effects of maternal smoking and exposure to methylmercury on brain-derived neurotrophic factor concentrations in umbilical cord serum. Toxicol. Sci. 117, 263–269. https://doi.org/10.1093/toxsci/kfq216.

Steffensen, I.-L., Dirven, H., Couderq, S., David, A., D'Cruz, S., Fernández, M., Mustieles, V., Rodríguez-Carrillo, A., Hofer, T., 2020. Bisphenols and oxidative stress biomarkers—associations found in human studies, evaluation of methods used, and strengths and weaknesses of the biomarkers. Int. J. Environ. Res. Publ. Health 17, 3609. https://doi.org/10.3390/ijerph17103609.

Stiles, J., Jernigan, T.L., 2010. The basics of brain development. Neuropsychol. Rev. https://doi.org/10.1007/s11065-010-9148-4.

Sun, B.-F., Wang, Q.-Q., Yu, Z.-J., Yu, Y., Xiao, C.-L., Kang, C.-S., Ge, G., Linghu, Y., Zhu, J.-D., Li, Y.-M., Li, Q.-M., Luo, S.-P., Yang, D., Li, L., Zhang, W.-Y., Tian, G., 2015. Exercise prevents memory impairment induced by arsenic exposure in mice: implication of hippocampal BDNF and CREB. PLoS One 10, e0137810. https://doi.org/10.1371/journal.pone.0137810.

Tang, D., Lee, J., Muirhead, L., Li, T.Y., Qu, L., Yu, J., Perera, F., 2014. Molecular and neurodevelopmental benefits to children of closure of a coal burning power plant in China. PLoS One 9, e91966. https://doi.org/10.1371/journal.pone.0091966.

Tolins, M., Ruchirawat, M., Landrigan, P., 2014. The developmental neurotoxicity of arsenic: cognitive and behavioral consequences of early life exposure. Ann. Glob. Heal. 80, 303. https://doi.org/10.1016/j.aogh.2014.09.005.

Wang, B., Du, Y., 2013. Cadmium and its neurotoxic effects. Oxid. Med. Cell. Longev. https://doi.org/10.1155/2013/898034.

Wang, C., Li, Z., Han, H., Luo, G., Zhou, B., Wang, S., Wang, J., 2016. Impairment of object recognition memory by maternal bisphenol A exposure is associated with inhibition of Akt and ERK/CREB/BDNF pathway in the male offspring hippocampus. Toxicology 341–343, 56–64. https://doi.org/10.1016/j.tox.2016.01.010.

Wang, Y., Chen, L., Gao, Y., Zhang, Y., Wang, C., Zhou, Y., Hu, Y., Shi, R., Tian, Y., 2016. Effects of prenatal exposure to cadmium on neurodevelopment of infants in Shandong, China. Environ. Pollut. 211, 67–73. https://doi.org/10.1016/j.envpol.2015.12.038.

Wirt, T., Schreiber, A., Kesztyüs, D., Steinacker, J.M., 2015. Early life cognitive abilities and body weight: cross-sectional study of the association of inhibitory control, cognitive flexibility, and sustained attention with BMI percentiles in primary school children. J. Obes 1–10. https://doi.org/10.1155/2015/534651, 2015.

Wright, J.P., Dietrich, K.N., Ris, M.D., Hornung, R.W., Wessel, S.D., Lanphear, B.P., Ho, M., Rae, M.N., 2008. Association of prenatal and childhood blood lead concentrations with criminal arrests in early adulthood. PLoS Med. 5, e101 https://doi.org/10.1371/journal.pmed.0050101.

Xia, Y., Zhu, J., Xu, Y., Zhang, H., Zou, F., Meng, X., 2020. Effects of ecologically relevant concentrations of cadmium on locomotor activity and microbiota in zebrafish. Chemosphere 257, 127220. https://doi.org/10.1016/j.chemosphere.2020.127220.

Xu, B., Chen, S., Luo, Y., Chen, Z., Liu, L., Zhou, H., Chen, W., Shen, T., Han, X., Chen, L., Huang, S., 2011. Calcium signaling is involved in cadmium-induced neuronal apoptosis via induction of reactive oxygen species and activation of MAPK/mTOR Network. PLoS One 6, e19052. https://doi.org/10.1371/journal.pone.0019052.

Yousef, S., Adem, A., Zoubeidi, T., Kosanovic, M., Mabrouk, A.A., Eapen, V., 2011. Attention deficit hyperactivity disorder and environmental toxic metal exposure in the United Arab Emirates. J. Trop. Pediatr. 57, 457–460. https://doi.org/10.1093/tropej/fmq121.

Zaletel, I., Filipović, D., Puškaš, N., 2017. Hippocampal BDNF in physiological conditions and social isolation. Rev. Neurosci. https://doi.org/10.1515/revneuro-2016-0072.

Zhou, C.C., Gao, Z.Y., He, Y.Q., Wu, M.Q., Chen, F., Wang, J., Liu, J.X., Yan, C.H., 2019. Effects of lead, mercury, aluminium and manganese co-exposure on the serum BDNF concentration of pre-school children in Taizhou, China. Chemosphere 217, 158–165. https://doi.org/10.1016/j.chemosphere.2018.11.028.

Zou, Y., ZouQing, L., Zeng, X., Shen, Y., Zhong, Y., Liu, J., Li, Q., Chen, K., Lv, Y., Huang, D., HuangLiang, G., Zhang, W., Chen, L., Yang, Y., Yang, X., 2014. Cognitive function and plasma BDNF levels among manganese-exposed smelters. Occup. Environ. Med. 71, 189–194. https://doi.org/10.1136/oemed-2013-101896.

International Journal of Hygiene and Environmental Health 239 (2022) 113865

Contents lists available at ScienceDirect

International Journal of Hygiene and Environmental Health

journal homepage: www.elsevier.com/locate/ijheh

Exposure to the pesticide DDT and risk of diabetes and hypertension: Systematic review and meta-analysis of prospective studies

José Ángel Hernández-Mariano [a], Mary Carmen Baltazar-Reyes [b], Eduardo Salazar-Martínez [b], Lea A. Cupul-Uicab [b,*]

[a] School of Public Health of Mexico/National Institute of Public Health, Cuernavaca, Morelos, 62100, Mexico
[b] Center for Population Health Research, National Institute of Public Health, Cuernavaca, Morelos, 62100, Mexico

ARTICLE INFO

Keywords:
Diabetes mellitus
Dose-response
Hypertension
Meta-analysis
p,p'-DDE
p,p'-DDT
Type 2 diabetes

ABSTRACT

Background: Experimental evidence suggests that *p,p'*-DDE might be involved in the development of diabetes and hypertension (HTN); however, the evidence in humans is inconclusive.
Objective: To summarize the epidemiological evidence for the association of *p,p'*-DDT exposure and its breakdown products with the risk of diabetes and HTN from prospective studies.
Methods: We performed a systematic review and meta-analysis based on the Preferred Reporting Items for Systematic Reviews and Meta-analyses (PRISMA) statement. Eligible studies (prospective) were search in PubMed, Web of Science, EBSCO, and SciELO databases (July 11, 2020). Different search algorithms were used for diabetes and HTN. Pooled odds ratios (ORs) were estimated from meta-analysis with random effects for each exposure and outcome.
Results: A total of 23 prospective studies were included in this review, 16 assessed diabetes and seven HTN; very few measured *p,p'*-DDT. Exposure to *p,p'*-DDE was associated with a slightly increased risk of type 2 diabetes (T2D) (pooled OR = 1.44; 95%CI: 1.00, 2.07; $p = 0.049$) and HTN (pooled OR = 1.21; 95%CI: 1.07, 1.38). Dose-response meta-analysis suggested a non-linear relation between *p,p'*-DDE and T2D. Exposure to *p,p'*-DDE was not associated with gestational diabetes (pooled OR = 1.01; 95%CI: 0.94, 1.09); similarly, *p,p'*-DDT was not associated with T2D (pooled OR = 1.03; 95%CI: 0.79, 1.35).
Conclusions: Evidence from prospective studies suggests that exposure to *p,p'*-DDE, the main breakdown product of *p,p'*-DDT, might increase the risk of developing T2D; such increase may be apparent only at low levels. Exposure to *p,p'*-DDE may also increase the risk of having HTN; however, further evidence is required.

1. Introduction

In the last three decades, the number of people with type 2 diabetes (T2D) and hypertension (HTN) worldwide has increased substantially (Mills et al., 2016; Saeedi et al., 2019); both diseases are major risk factors for cardiovascular disease, representing an important burden on public health globally. Risk factors of T2D and HTN such as family history, ethnicity, obesity, unhealthy diet, lack of physical activity, tobacco, and alcohol consumption are well documented (Bellou et al., 2018; Oparil et al., 2018). Nonetheless, emerging evidence suggests that exposure to persistent organic pollutants (POPs) such as polychlorinated biphenyls and *p,p'*-DDT (1,1,1-trichloro-2,2-bis (4-chlorophenyl) ethane), may play a role in the etiology of cardiometabolic disorders including T2D and HTN (Andersson et al., 2011; Heindel et al., 2017; Thayer et al., 2012).

P,p'-DDT is an organochlorine pesticide widely used worldwide since the 1940s, mainly to exterminate pests in crops and for the control of vector-borne diseases such as malaria and typhus. The toxicity of *p,p'*-DDT on the wildlife lead to its generalized banning since the 1970s and 1980s (ATSDR, 2019). However, its use continues nowadays under close surveillance for malaria control and some regions of the world such as Latin America still have reserves of *p,p'*-DDT stored (van den Berg, 2009). The half-life of *p,p'*-DDT and *p,p'*-DDE in human serum is approximately 7 and (Woodruff et al., 1994) 10 years, respectively (Hunter et al., 1997). Therefore, it is still possible to detect residues of these compounds among people whom experienced some degree of exposure in the past (Turusov et al., 2002).

The underlying mechanisms associating *p,p'*-DDT exposure with the

* Corresponding author. Center for Population Health Research, National Institute of Public Health Cuernavaca, Morelos, 62100, Mexico.
E-mail addresses: lea.cupul@insp.mx, acuicab@hotmail.com (L.A. Cupul-Uicab).

https://doi.org/10.1016/j.ijheh.2021.113865
Received 24 March 2021; Received in revised form 10 October 2021; Accepted 17 October 2021
Available online 23 October 2021

risk of developing T2D and HTN are not fully elucidated yet. Studies using animal models suggest that exposure to *p,p'*-DDT might decrease pancreatic secretory activity leading to impaired insulin secretion (Yau and Mennear, 1977); *in vitro* evidence also suggest that *p,p'*-DDT and *p,p'*-DDE might impair glucose metabolism and induce insulin resistance possibly due to disruptions in lipid homeostasis (Ruzzin et al., 2010). Additionally, perinatal exposure to *p,p'*-DDT might disturb the regulation of thermogenesis, lipids, and glucose, which could lead to insulin resistance and metabolic alterations (La Merrill et al., 2014). The main mechanism from experimental data linking prenatal exposure to *p.p'-DDT* with hypertension is the reported over-activation of the renin angiotensin system (La Merrill et al., 2016).

Regardless of the experimental evidence, epidemiological data continues to be inconclusive. Some of the prior studies in humans have reported positive associations between exposure to *p,p'*-DDE and the risk of T2D and HTN (La Merrill et al., 2013; Rylander et al., 2015; Singh and Chan, 2017; Turyk et al., 2009; Van Larebeke et al., 2015; Zong et al., 2018), whereas others have reported null associations (Arrebola et al., 2015; Donat-Vargas et al., 2018; Jaacks et al., 2019; Rahman et al., 2019; Rignell-Hydbom et al., 2010; Smarr et al., 2016). Discrepancies between these findings could be accounted by different study designs, methods to determine the exposure (*e.g.,* directly with biomarkers or indirectly through questionnaires), and the availability of data to control for confounding factors, among others.

Meta-analysis summarizing previous studies have assessed the association between the exposure to POPs and the risk of T2D and HTN regardless of the study design, rather than focusing on the effect of *p,p'*-DDT and its breakdown products in prospective studies (Evangelou et al., 2016; Park et al., 2016; Tang et al., 2014). A prior meta-analysis from prospective studies estimated a non-statistically significant association between *p,p'*-DDE exposure and T2D based on five available studies almost a decade ago (Wu et al., 2013). Hence, integrating the recent evidence from observational prospective studies assessing the potential adverse effects of the pesticide DDT on metabolic-related outcomes through a systematic review and meta-analysis using standard guidelines, would provide useful evidence for decision making process in public health. Therefore, our objective was to systematically review and integrate the epidemiologic evidence regarding the association of *p,p'*-DDT exposure and its breakdown products with the risk of diabetes and HTN from prospective studies and to summarize the evidence quantitatively by conducting a meta-analysis.

2. Materials and methods

2.1. Data source and searching algorithms

The systematic review and meta-analysis was based on the *Preferred Reporting Items for Systematic Reviews and Meta-analyses* (PRISMA) statement (Liberati et al., 2009). Epidemiological evidence on the association of *p,p'*-DDT exposure with the risk of diabetes and HTN was identified by conducting electronic searches on PubMed, Web of Science, EBSCO, and SciELO databases. We constructed and performed independent searching algorithms for each health outcome (Supplemental Table 1); the search was limited to human studies published in English and Spanish up to July 11, 2020. The titles and abstracts of the retrieved documents were independently screened by two authors to assess their relevance to our research objective. Subsequently, authors examined the full text of all potentially relevant studies applying the eligibility criteria to select the studies for the qualitative data synthesis (*i.e.,* prospective studies with exposure measured in biological samples). All discrepancies between the authors who examined the full texts were resolved by consensus.

2.2. Study question and eligibility criteria

The eligibility criteria for the studies were formulated based on the components of the *PECOS* statement (population, exposure, comparators, outcome, and study design) (Morgan et al., 2018) to answer the following research question: "*Does exposure to p,p'-DDT and its breakdown products increases the risk diabetes and HTN in humans?*" (Table 1). Therefore, we included all studies that investigated any potential association of exposure to *p,p'*-DDT and its breakdown products with the risk of diabetes and hypertension without restrictions on the type of diabetes or HTN. Cross-sectional studies were excluded from the systematic review in order to avoid potential reverse causality when interpreting the results. When two or more eligible articles reported results from the same study cohort, same isomers of *p,p'*-DDT, and same exposure period, the most recent study was included.

2.3. Data extraction and quality assessment

The data from the eligible studies were extracted independently in Excel spreadsheet forms. We extracted the following information from each study: first author, year of publication and country where the study was conducted; study design and name of the cohort; sample size and sex of the participants; ages of the participants; health outcome and how it was ascertained; type of exposure (prenatal or postnatal) and biospecimen; median levels of exposure (as reported: wet weight or lipid adjusted); estimated effect and its confidence intervals; risk and reference categories of the exposure; covariates used for adjustment; and the length of the follow-up.

The risk of bias (RoB) of each study was examined using a modified version of the ROBINS-I (*Risk Of Bias In Non-randomised Studies - of Interventions*) instrument, proposed for non-randomized studies that assess the effects of environmental exposures on health outcomes (Morgan et al., 2019; Sterne et al., 2016). The RoB instrument has seven items that assess the strengths and limitations of each study: 1) bias due to confounding, 2) bias in selecting participants in the study, 3) bias in exposures classification, 4) bias due to departures from intended exposures, 5) bias due to missing data, 6) bias in measurement of outcomes, and 7) bias in selection of reported results. Each item and study is rated as: low RoB, moderate RoB, serious RoB, or critical RoB (Morgan et al., 2019); the criteria for the risk of bias evaluation is reported in Supplemental Table 2. These results were then integrated in the GRADE framework *(Grading of Recommendations Assessment, Development, and Evaluation*) (Guyatt et al., 2011) to assess the certainty of the evidence.

We also assessed the quality of the studies included in the systematic review using the *Newcastle-Ottawa Scale* (NOS) for observational studies (Wells et al., 2009). The NOS has eight items grouped in three domains: I) selection of study groups; II) comparability of the groups; and III) exposure or outcomes of interest. Each domain is scored with a maximum of four, two, and three stars, respectively; thus, the total score for the scale sums up to nine stars. Based on this scale, the studies were classified as high quality ($\geq$7 stars), moderate (4–6 stars), and low quality ($\leq$3 stars) (Xing et al., 2016). The discrepancies when rating the quality of the studies were resolved by consensus.

2.4. Statistical analysis

We conducted meta-analysis with random effects to consider both within-and-between study variations (DerSimonian and Laird, 1986). Pooled odds ratios (ORs) were estimated from the published ORs and its 95% confidence intervals (95%CI); there were not enough coefficients from linear regressions to combine in a meta-analysis. Few studies (n = 3) reported only risk ratios (RRs) with its corresponding 95%CI, these were combined with the ORs assuming that the latter is a valid estimator of the RR in nested case-control studies (Szklo and Nieto, 2007). For the studies with three or more exposure categories, we used the reported OR from the highest exposure category relative to the reference to estimate the pooled OR. We conducted separate meta-analysis for each exposure (*p,p'*-DDT and *p,p'*-DDE) and outcome (T2D, gestational diabetes [GDM] and HTN) when there were at least three available studies; very few

Table 1
PECO statement.

Population	Exposure	Comparators	Outcomes	Study type
Humans without any restriction on race, sex, spoken language, geographic region, or religion. Exposure and outcomes measured at all life-stages, except newborns.	Prenatal and/or postnatal exposure to *p,p'*-DDT and its isomers. Exposure measured directly by standardized methods in biological samples (*i.e.,* blood serum, adipose tissue, etc.). Exclusions: determinations by environmental data or other indirect methods (*i.e.,* self-administered questionnaires of lifestyles or dietary intake).	Subsets/categories or groups used as reference in the publications with the lowest levels of exposure to *p,p'*-DDT and its isomers, compared to those with the highest levels of exposure.	Diabetes: Glycated hemoglobin levels (glycosylated hemoglobin); plasma glucose levels; type 1 diabetes; type 2 diabetes; gestational diabetes; or any type of diabetes. Hypertension: Systolic and diastolic blood pressure in mmHg, hypertension, and gestational hypertension.	Prospective epidemiological studies (*i.e.,* cohort, nested case-control or case-cohort). Exclusions: reviews, commentaries, conference abstracts, books, letters to the Editor, and meta-analyses.

studies assessed *p,p'*-DDT, thus we only estimated a pooled ORs for this isomer with T2D. Most of the studies reported associations with the outcomes using different exposure scales for *p,p'*-DDE such as categories based on quantiles, log-transformed (*ln* or log10), per interquartile range (IQR) increase, and a standard deviation (SD) increase of the *ln*-transformed exposure. Therefore, for T2D we conducted separate meta-analysis for the studies that modeled *ln*-transformed and for those modeling categories based on quantiles of *p,p'-DDE* in order to have consistent estimates. Most of the studies categorized *p,p'-DDE* in quartiles (one used tertiles and another quintiles), these were pooled together because their estimates were consistently obtained for the population in the top percentiles of exposure compared to those in the lowest percentiles; thus, the main results are based on this meta-analysis. Such approach was not feasible for the other outcomes due to the limited number of studies. The presence of statistical heterogeneity among the selected studies was assessed using the *Q*-test and the I^2 statistic (range 0–100%) (Higgins et al., 2019). Based on the Cochrane's criteria, an I^2 <30% is not relevant, an I^2 between 30 and 60% indicates moderate heterogeneity, while an $I^2 \geq 75\%$ indicates considerable heterogeneity (Higgins et al., 2019). Therefore, we conducted subgroup meta-analysis in the presence of moderate heterogeneity to identify the potential sources of heterogeneity such as exposure units (lipid standardized or not), outcome definition (self-reported or not), length of follow-up, participant's age, sex (only women or both), and geographic region where the study was conducted.

Two-stage random-effect dose-response meta-analysis with weighted linear mixed models were conducted to assess the shape of the relation between *p,p'*-DDE exposure and T2D (Crippa et al., 2019; Orsini, 2021; Orsini et al., 2006) across studies with at least three exposure categories. We extracted the ORs and medians (or means) of each exposure category from the publications; for the studies without medians (or means) we assigned the midpoint of each exposure category and for the open categories we used half the width of the adjacent category. The potential non-linear dose-response relation was assessed using restricted cubic splines with three knots located at fixed percentiles of the overall distribution according to Harrell's method (Harrell, 2001); these spline terms were then included in the dose-response meta-analysis (using Stata algorithms: *drmeta, drmeta_graph, drmeta_gof*) (Orsini, 2021). The estimated dose-response model was plotted using as reference the lowest level of exposure from the studies included in this meta-analysis (*p,p'*-DDE = 2.5 ng/g lipids).

The small-study effect as an indicator of publication bias was assessed by visual inspection of the funnel plots to identify asymmetric patterns and was complemented with the Egger's test (*p-value* <0.05) (Harbord et al., 2006). Additionally, as sensitivity analysis, we explored the effect of a single study on the overall pooled OR (from the top vs lowest quantiles) by excluding one study at the time to re-estimate the pooled OR. For the association between *p,p'*-DDE and T2D, we also applied the methodology described by Chêne and Thompson (1996) to rescale the study-specific *ln*(ORs) in order to have consistent estimates to pool in a meta-analysis (Chêne and Thompson, 1996). Thus, using the available information extracted, the study-specific *ln*(ORs) were rescaled to estimate the risk associated to an interquartile range (IQR) increase in *p,p'*-DDE; additionally, the study-specific estimates were also rescaled using the IQR (1147.9 ng/g lipids) from one of the study populations reported by Wu et al. (2013). All analyses were conducted using Stata (version 15.1, release 2020; StataCorp, College Station, TX, USA).

3. Results

3.1. Meta-analysis for diabetes

We identified a total 1569 (Fig. 1) potentially relevant references from the search in all databases (PubMed, Web of Science, EBSCO, and SciELO); after removing 522 duplicated references, 1047 were left to screen the titles and abstracts for relevance. With the screening process, 21 references were selected for full-text review, of these, five were excluded after full-text review (four of them were cross-sectional), leaving 16 articles for data extraction.

The information extracted from these 16 studies is summarized in Table 2. Nine were nested case-control studies (Grice et al., 2017; Jaacks et al., 2019; Lee et al., 2010; Rignell-Hydbom et al., 2009, 2010; Rylander et al., 2015; Wolf et al., 2019; Wu et al., 2013; Zong et al., 2018) and seven were cohort studies (Lee et al., 2011; Rahman et al., 2019; Shapiro et al., 2016; Smarr et al., 2016; Turyk et al., 2015; Vafeiadi et al., 2017; Van Larebeke et al., 2015). Seven were conducted in Europe, eight in North America (Grice et al., 2017; Lee et al., 2010; Rahman et al., 2019; Shapiro et al., 2016; Smarr et al., 2016; Turyk et al., 2015; Wu et al., 2013; Zong et al., 2018), and one in Asia (Jaacks et al., 2019). The length of follow-up ranged from four (Wolf et al., 2019) to 27 (Rignell-Hydbom et al., 2010) years, four had a follow-up of 5 years or less (Grice et al., 2017; Jaacks et al., 2019; Lee et al., 2011; Rylander et al., 2015; Wolf et al., 2019) and five had more than 15 years of follow-up (Lee et al., 2010; Rignell-Hydbom et al., 2010; Turyk et al., 2015; Wu et al., 2013); for the studies that assessed GDM the length of follow-up ranged from 13 to 24 weeks (Rahman et al., 2019; Shapiro et al., 2016; Smarr et al., 2016; Vafeiadi et al., 2017). The sample size of each study ranged from 212 (Rylander et al., 2015) to 2294 (Rahman et al., 2019); the ages of the participants ranged from >18 to 80 years, seven assessing T2D as an outcome included participants ≥60 years old (Jaacks et al., 2019; Lee et al., 2011; Rylander et al., 2015; Turyk et al., 2015; Van Larebeke et al., 2015; Wolf et al., 2019); half of the studies included only women and the other half included men and women. All the studies determined the exposure postnatally, with the exception of one that reported prenatal exposure (Rignell-Hydbom et al., 2010). Levels of *p,p'*-DDE were measured in all studies, five also determined concentrations of *p,p*-DDT (Grice et al., 2017; Lee et al., 2010; Rahman et al., 2019; Smarr et al., 2016; Wu et al., 2013), only two studies measured *o,p'*-DDT (Grice et al., 2017) and *p,p'*-DDD (Rahman et al., 2019). Concentrations of DDT and its congeners were reported on a wet basis in eight studies (Grice et al., 2017; Lee et al., 2011; Rignell-Hydbom et al., 2009, 2010; Shapiro et al., 2016; Turyk et al., 2015; Vafeiadi et al., 2017; Wolf et al., 2019). Nine studies added serum lipids as adjusting variables into their models (*i.e.,* serum total lipids, total

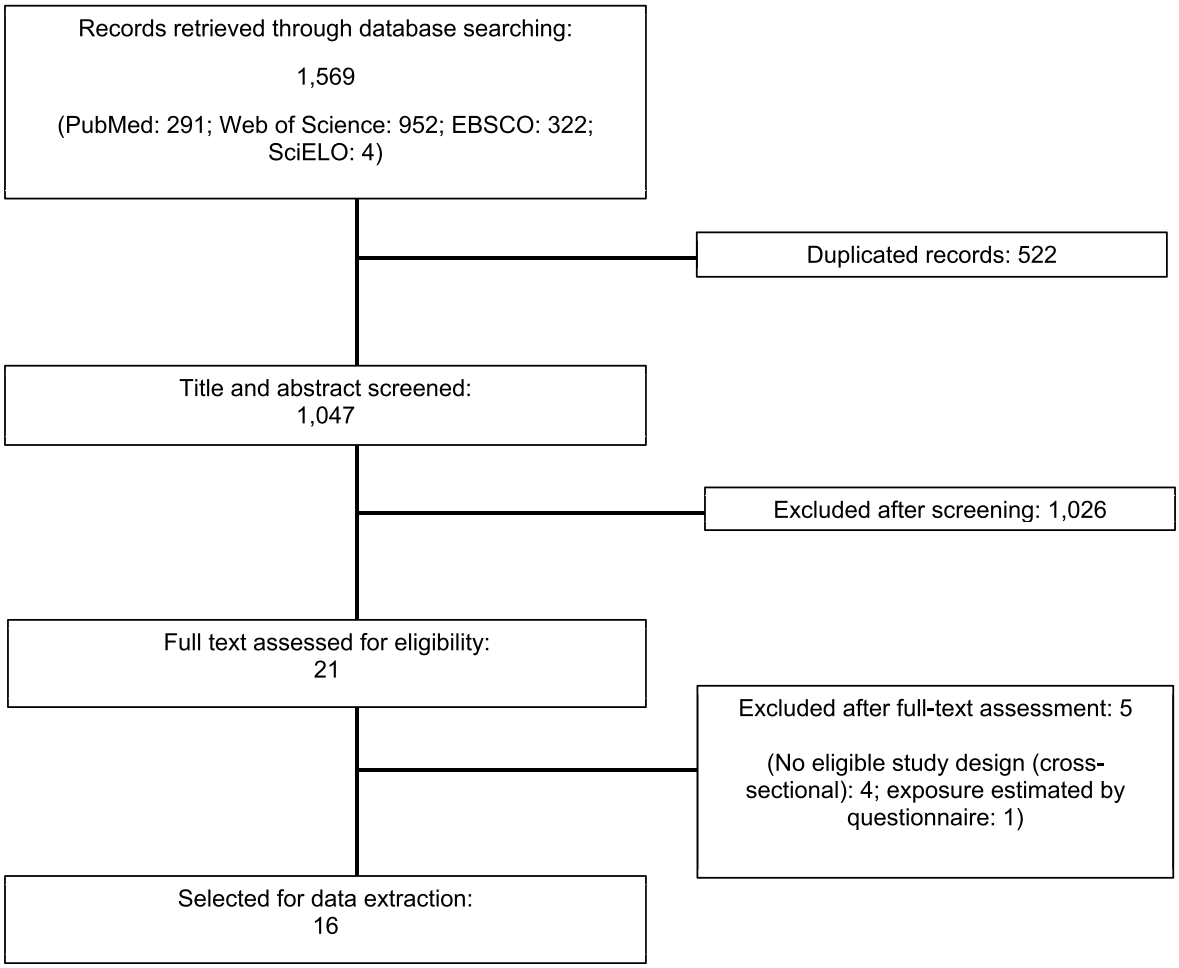

Fig. 1. Flow chart of the selection process of the studies assessing the association between *p,p'-DDT* exposure and risk of diabetes.

cholesterol, or triglycerides and cholesterol) (Grice et al., 2017; Jaacks et al., 2019; Lee et al., 2011; Rahman et al., 2019; Shapiro et al., 2016; Smarr et al., 2016; Turyk et al., 2015; Vafeiadi et al., 2017; Wolf et al., 2019); seven assessed the effect of lipid-standardized concentrations of DDT and its compounds; and two did not account for lipids at all (Rignell-Hydbom et al., 2009, 2010). Five studies log-transformed the exposure to estimate the ORs (Grice et al., 2017; Rahman et al., 2019; Turyk et al., 2015; Van Larebeke et al., 2015) and 11 categorized the exposure in quantiles. The type of diabetes was not clearly defined in two studies (Turyk et al., 2015; Van Larebeke et al., 2015), four assessed gestational diabetes as their main health outcome (Rahman et al., 2019; Shapiro et al., 2016; Smarr et al., 2016; Vafeiadi et al., 2017), one focused on type 1 diabetes (T1D) only (Rignell-Hydbom et al., 2010), and the remain focused on T2D as their main outcome. Two publications, Wolf et al. (2019) and Wu et al. (2013), reported ORs from two independent cohort studies. Potentially confounding factors considered in most studies included age, sex, education, body mass index (BMI), smoking, and alcohol consumption; studies that modeled non lipid-standardized concentrations of DDT and its compounds also adjusted for serum lipids, except two of them (Rignell-Hydbom et al., 2009, 2010); only one reported an OR adjusted for other POPs (*i.e.,* hexachlorobenzene, trans-Nonachlor & oxychlordane) (Smarr et al., 2016). Overall, based on the NOS quality assessment, all the studies included in this review have moderate to high quality (Supplemental Table 3).

A total of seven studies examined the association between *p,p'*-DDE (top vs lowest quantile) and T2D, one of them was multicenter, therefore it contributed with two ORs in the meta-analysis. We observed a slight increased risk of T2D (pooled OR = 1.44; 95%CI: 1.00, 2.07; $p = 0.049$) among those with the highest concentrations of *p,p'*-DDE relative to the lowest; there was evidence of moderate heterogeneity ($I^2 = 44.4\%$) (Fig. 3A). The meta-analysis based on the studies that modeled *ln*-transformed *p,p'*-DDE, showed results in the same direction (pooled OR = 1.28; 95%CI: 0.92, 1.78), but the observed heterogeneity ($I^2 = 67.8\%$) between-studies was higher (Fig. 3B). Because *p,p'*-DDE is a lipophilic pollutant, we conducted a meta-analysis (from Fig. 3A) limited to the studies that considered the effect of lipids (lipid standardization or adding lipids as a covariate in the regression models); only one study did not account for lipids (Rignell-Hydbom et al., 2009). The pooled OR from the studies that considered the effect of lipids was 1.60 (95%CI: 1.00, 2.55; $p = 0.049$; n = 6 studies) with moderate heterogeneity ($I^2 = 41.1\%$) (Supplemental Fig. 1). There were not enough studies to stratify by the approach used to take into account the effect of lipids, only two included serum lipids as a covariate in their regression models (Lee et al., 2010, 2011).

Stratified meta-analysis (Supplemental Table 4) showed stronger associations than those from Fig. 3A among studies that relied mostly on self-reported diagnosis of T2D (pooled OR = 2.12; 95%CI: 1.05, 4.26; n = 3 studies) and those conducted only among women (pooled OR = 1.62; 95%CI: 1.02, 2.58; n = 4 studies). The magnitude of the effect were similar for the studies with longer follow-up (≥10 years, pooled OR = 1.49; 95%CI: 1.12, 1.97; n = 3 studies) and those conducted in the American continent (pooled OR = 1.49; n = 3 studies) as these were estimated from the same three studies. Although the association between *p,p'*-DDE and T2D seem stronger among studies that included participants ≥60 years of age (pooled OR = 2.52), the estimate was

Table 2
Characteristics of the studies evaluating the association of *p,p'*-DDT and its breakdown products with diabetes.

First author, year & country	Study design (Cohort's name)	n (sex)	Age in years	Outcome & ascertainment	Type of exposure (sample)	Median of measured compounds	OR (95% IC)	Risk category	Adjusting variables	Follow-up time
Wolf et al. (2019). Germany	Nested case-control (CARLA)	231 (♂138; ♀93	45–83	T2D. Self-reported diabetes or HbA1c ≥ 6.5% or newly prescribed glucose-lowering medication.	Postnatal (serum)	*p,p'*-DDE: 838 ng/g[a] (IQR = 1169)	1.39 (1.01, 1.89)	Per interquartile range increase in exposure (IQR = 8.9 ng/mL).	BMI, alcohol, smoking, physical activity, parental diabetes, & total cholesterol.	~4 years
Wolf et al. 2019. Germany	Nested case-control (KORA).	165 (♂ 99; ♀ 66)	25–74	T2D. Self-reported diabetes & HbA1c ≥ 6.3%, or HbA1c >6.5% & OGTT; diagnosed diabetes.	Postnatal (serum)	*p,p'*-DDE: 337 ng/g[a] (IQR = 254)	1.28 (0.95, 1.72)	Per interquartile range increase in exposure (IQR = 2.5 ng/mL).	BMI, alcohol, smoking, physical activity, parental diabetes, & total cholesterol.	~7 years
Rahman et al. 2019. USA	Cohort (NICHD Fetal Grow Study).	2294 (♀)	18–44	GD. Test at 23–31 weeks: 100-g 3-hr OGTT or 75 g 2-h OGTT. At least 2-diagnostic plasma glucose measurements of: fasting ≥5.3 mmol/L; 1-hr, ≥10.0 mmol/L; 2-h, ≥8.6 mmol/L; 3-h, ≥7.8 mmol/L. The same thresholds for fasting, 1-h and 2-h glucose measurements were applied.	Postnatal (serum)	*p,p'*-DDE: 103 (99.2, 107.5) ng/g[b] *p,p'*-DDD: 1.2 ng/g[b] *p,p'*-DDT: 2.77 ng/g[b]	1.01 (0.94, 1.09)[c] 0.99 (0.89, 1.09)[c] 0.95 (0.79, 1.13)[c]	Per SD increase in exposure.	Age, BMI at enrollment, education, parity, race/ethnicity, history of T2D, & serum total lipids.	~14 weeks
Jaacks et al. 2019. India	Nested case-control (CARRS)	516 (♂ 222; ♀ 294)	≥20	T2D. Fasting plasma glucose ≥126 mg/dl, HbA1c ≥ 6.5%, or self-reported physician-diagnosed diabetes.	Postnatal (serum)	p,p'-DDE: 454.9 ± 665.3 ng/g[a,d]	0.87 (0.30, 2.55) 0.99 (0.83, 1.18)	Fourth *vs.* first quartile. Per one increase in the *ln*-transformed exposure.	Age, occupation, household income, ever use tobacco products, waist circumference, & fasting plasma glucose.	~5 years
Zong et al. 2018. USA	Nested case-control (NHSII)	1586 (♀)	32–55	T2D. Self-reported physician-diagnosed diabetes plus treatment with insulin or oral hypoglycemic medication or measurement of glucose concentration.	Postnatal (serum)	*p,p'*-DDE: 272 ng/g[a] (IQR = 331)	1.56 (1.14, 2.13)	Third *vs.* first tertile.	Age, ethnicity, time of sample collection, fasting status, menopausal status, post-menopausal hormone use, history of diabetes, oral contraceptive, lifetime breastfeeding, parity, state of residence, smoking, alcohol, & physical activity.	~11 years
Grice et al. 2017. USA	Nested case-control (NAGRIC)	300 (♂ 100; ♀ 200)	18–40	T2D. Plasma glucose concentration 2-hr post-load (2hrPG) ≥200 mg/dl; by clinical diagnosis between examinations.	Postnatal (serum)	*o,p'*-DDT: 126.3 ng/g[b] *p,p'*-DDT: 1949.7 ng/g[b] *p,p'*-DDE: 7417.2 (6998.36, 7861.07) ng/g[b]	1.12 (0.83, 1.50) 1.04 (0.78, 1.40) 0.92 (0.65, 1.30)	Per SD increase in the *ln*-transformed exposures.	Age, sex, BMI, sample water loss after thawing, serum storage time, cholesterol, & triglycerides.	~23 years
Vafeiadi et al. 2017. Greece	Cohort (Rhea)	939 (♀)	>16	GD. 100-g, 3-hr OGTT at 24–28 weeks: fasting ≥95 mg/dl; 1hr of ≥180 mg/dl; 2 h of ≥155 mg/dl; and 3 h ≥ 140 mg/dl.	Postnatal (serum)	*p,p'*-DDE: 2.03 ng/mL[a] (IQR = 2.4661)	0.65 (0.28, 1.47) 0.59 (0.23, 1.51)	Third vs. first tertile. Per log_{10} increase	Gestational age at sample collection, age, pre-pregnancy BMI, parity, education, smoking during pregnancy, gestational weight gain, serum triglycerides & cholesterol.	~ 13 weeks
Smarr et al. 2016. USA	Cohort (LIFE)	258 (♀)	18–40	GD. Physician report of high blood sugar at ≥24 weeks of gestation.	Postnatal (serum)	*p,p'*-DDE: 0.56 ng/g[a] (IQR = 0.39) *p,p'*-DDT: <LOD	1.20 (0.72, 2.02)	Per SD increase in the *ln*-transformed exposure.	Age, BMI, non-white race, smoking, sum of log-transformed and rescaled POPs (HCB, trans-Nonachlor & oxychlordane), & serum lipids.	~24 weeks

(*continued on next page*)

Table 2 (*continued*)

First author, year & country	Study design (Cohort's name)	n (sex)	Age in years	Outcome & ascertainment	Type of exposure (sample)	Median of measured compounds	OR (95% IC)	Risk category	Adjusting variables	Follow-up time
							1.01 (0.55, 1.85)			
Shapiro et al. 2016. Canada	Cohort (MIREC)	1274 (♀)	>18	GD. Test at 24–28 weeks: 100-g 3-hr OGTT. At least 2-plasma glucose measurements of: fasting, ≥5.3 mmol/L; 1-hr, ≥10.0 mmol/L; 2-h, ≥8.6 mmol/L; 3-h, ≥7.8 mmol/L.	Postnatal (serum)	*p,p′*-DDE: 0.32 ng/mL (IQR = 0.29)	1.1 (0.4, 2.9)	Fourth *vs.* first quartile.	Age, race, pre-pregnancy BMI, education, & total lipids.	~14 weeks
Rylander et al. 2015. Norway	Nested case-control (NOWAC)	212 (♀)	30–70	T2D. Self-reported diabetes diagnosis.	Posnatal (serum)	*p,p′*-DDE: 125 ng/g[a] (Range: 10.9–895)	11.3 (2.55, 49.9)	Fourth *vs.* first quartile.	BMI, breastfeeding, hypertension, & smoking.	~5 years
Turyk et al. 2015. USA	Cohort (GLCHAGL)	413 (♂ 313; ♀ 100)	25–76	Unspecified diabetes. Self-reported diabetes diagnosis & date of diagnosis.	Posnatal (serum)	*p,p′*-DDE: 2.0 (1.8, 2.1) ng/g[b]	2.63 (1.17, 5.89)	Per one increment in the *ln*-transformed exposure.	Age, BMI, gender, calcium channel blockers use, & serum lipids.	~16 years
Van Larebeke et al. 2015. Belgium	Cohort (FLEHS)	1583 (♂ 313; ♀ 100)	50–65	Unspecified diabetes. Self-reported diabetes.	Postnatal (serum)	*p,p'*-DDE: 486 ng/g (percentiles 10th = 147 & 90th = 1575)	1.72 (1.21, 2.42)	Per one increment in *ln*-transformed exposure.	BMI, exercise (min/week), education, alcohol (glass/week).	~7 years
Wu et al. 2013. USA	Nested case-control (Breast cancer study)	981 (♀)	30–55	T2D. Self-reported physician-diagnosis of diabetes plus treatment with insulin or oral hypoglycemic medication or measurement of glucose concentration.	Postnatal (serum)	*p,p'*-DDT: 53.5 ng/g[a] *p,p'*-DDE: 773 ng/g[a] (IQR = 762.3)	1.11 (0.38, 3.27) 1.59 (0.50, 5.03) 0.94 (0.57, 1.61)	Fourth *vs.* first quartile. Fourth *vs.* first quartile Per one increment *ln*-transformed exposure.	Age, baseline BMI in 1990, smoking, alcohol intake, physical activity, & history of diabetes.	~18 years
Wu et al. 2013. USA	Nested case-control (NHL study)	422 (♀)	30–55	T2D. Self-reported physician-diagnosis of diabetes plus treatment with insulin or oral hypoglycemic medication or measurement of glucose concentration.	Postnatal (serum)	*p,p'*-DDT: 43.5 ng/g[a] *p,p'*-DDE: 973.8 ng/g[a] (IQR = 1147.9)	1.01 (0.34, 3.02) 1.57 (0.49, 5.07) 1.15 (0.65, 2.01)	Fourth *vs.* first quartile. Fourth *vs.* first quartile. Per one increment *ln*-transformed exposure.	Age, baseline BMI in 1990, smoking, alcohol intake, physical activity, & history of diabetes.	~18 years
Lee et al. 2011. Sweden	Cohort (PIVUS)	725 (♂ 350; ♀ 375)	>70	T2D. Fasting glucose ≥6.2 mmol/L or use of insulin or oral hypoglycemic agents.	Postnatal (serum)	*p,p'-DDE*: NR (Range 0.011–23.271 ng/g (IQR = 3.58)	2.1 (0.7, 6.3)	Fifth *vs.* first quintile.	Sex, BMI, smoking, physical activity, alcohol, triglycerides, & total cholesterol.	~5 years
Rignell et al. 2010. Sweden	Nested case-control (Malmö)	300 (♂ 150; ♀ 150)	<27	T1D. Based on the diabetes incidence study from the Swedish registry.	Prenatal (maternal serum)	*p,p'*-DDE: 9.60 ng/mL[a] (IQR = 11.0)	0.64 (0.28, 1.46)	Fourth *vs.* first quartile.	Age, sex, preterm, high birth weight; maternal age & smoking in early pregnancy.	~27 years
Lee et al. 2010. USA	Nested case-control (CARDIA)	180 (♂ 72; ♀ 108)	18–30	Fasting glucose ≥126 mg/dL at 2+ examinations or use of antidiabetic drugs.	Postnatal (serum)	*p,p'*-DDE: 3.3130 ng/g *p,p′*-DDT: NR	0.70 (0.2, 1.9)	Fourth *vs.* first quartile.	Age, sex, race, & BMI.	~18 years

(*continued on next page*)

Table 2 (*continued*)

First author, year & country	Study design (Cohort's name)	n (sex)	Age in years	Outcome & ascertainment	Type of exposure (sample)	Median of measured compounds	OR (95% IC)	Risk category	Adjusting variables	Follow-up time
							0.90 (0.31, 2.65)			
Rignell et al. 2009. Sweden	Nested case-control (WHILA)	742 (♀)	50–59	T2D. Fasting glucose >6.1 mmol/l or 2-hr post challenge venous blood glucose level >10.0 mmol/l.	Postnatal (serum)	*p,p'*-DDE: 2.89 ng/mL[a] (Range: 0.063–34.86)	1.1 (0.76, 1.5)	Fourth vs. first quartile.	Age, calendar year, BMI, heredity, birth country, education, smoking, alcohol, hormone replacement therapy & physical activity.	~6 years

Symbols: ♂, males; ♀, females.

Abbreviations: CARDIA, Coronary Artery Risk Development in Young Adults; CARLA, Cardiovascular Disease, Living and Ageing in Halle. CARRS, Centre for Cardiometabolic Risk Reduction in South-Asia; FLEHS, Flemish Environment and Health Survey; IQR, interquartile range; GD, gestational diabetes; GLCHAGL, The Great Lakes Consortium for the Health Assessment of Great Lakes Sport Fish; HbA1c, glycosylated hemoglobin; hr, hours; KORA, Cooperative Health Research in the Region of Augsburg; LIFE, Investigation of Fertility and the Environment; LOD, limit of detection; *ln*, natural logarithm; MIREC, Maternal Infant Research on Environmental Chemicals; NAGRIC, Native American from the Gila River Indian Community; NHL, Non-Hodgkin lymphoma; NHSII, Nurses' Health Study II; NICHD, National Institute of Child Health and Human Development; NOWAC, Norwegian Women and Cancer study; ng/g, nanograms/gram of lipids; ng/mL, nanograms/milliliter; NR, Not reported; OGTT, oral glucose tolerance test; OR, odds ratio; PIVUS, Prospective Investigation of the Vasculature in Uppsala Seniors study; Rhea, The Mother-Child Cohort in Crete, Greece; SD, standard deviation; T1D, type 1 diabetes; T2D, type 2 diabetes; WHILA. Women's Health in the Lund Area.

[a] From the controls.

[b] Geometric mean (95%CI).

[c] Relative risks.

[d] Mean ± standard deviation.

imprecise with substantial heterogeneity (I^2 = 73.4%); however, the association remain among studies that included participants <60 years (OR = 1.32; 95%CI: 1.06, 1.65; n = 4 studies). The greatest attenuations were observed for the strata of studies that used fasting glucose or glycosylated hemoglobin as part of their outcome definition (pooled OR = 1.01; 95%CI: 0.80, 1.50; n = 4 studies) and for those that included both men and women (pooled OR = 1.09; 95%CI: 0.57, 2.09: n = 3 studies). However, some of these strata showed moderate to considerable heterogeneity, suggesting unaccounted sources of heterogeneity.

The two-stage random-effects dose-response meta-analysis included five studies with available data (Supplemental Table 5). Except for one study, none of the individual studies showed a linear relation between *p,p'*-DDE and T2D. According to the Akaike Information Criterion (AIC) and deviance, the shape of the dose-response relationship was not linear (Supplemental Table 6 and Supplemental Fig. 2). However, a 500 ng/g increase in *p,p'*-DDE exposure was associated with a slight increased risk of T2D (OR = 1.20; 95%CI: 1.04, 1.39; *p-linear trend* = 0.01). The dose-response meta-analysis using cubic splines suggests a non-linear relationship. The overall risk of T2D tended to increase with increasing levels of *p,p'*-DDE up to ~1100 ng/g of lipids (Fig. 4), whereas at higher levels of exposure the risk increase little and the estimates become imprecise as showed by the wide confidence intervals. The strongest association is observed with *p,p'*-DDE levels of ~950 ng/g (OR = 1.65; 95%CI: 1.07, 2.53).

Our results from the sensitivity analysis after omitting one study at the time, showed associations in the same direction and of similar magnitude as what we observed in Fig. 3A (Supplemental Table 7). The pooled OR ranged from 1.33 to 1.60, the greatest attenuation occurred after excluding the study by Rylander et al. (pooled OR = 1.33; 95%CI; 1.07, 1.64) and the greatest increase after excluding the study by Rignel-Hydbom et al. (pooled OR = 1.60; 95%CI; 1.00, 2.55); these exclusions changed the pooled ORs by 7.6% and 11.1%, respectively. As expected, the greatest attenuation was caused when excluding the study with the strongest association (OR = 11.3; 95%CI: 2.55, 49.99); interestingly, such exclusion practically eliminated the observed heterogeneity, suggesting that this single study was the main source of heterogeneity in our meta-analysis.

The results from the sensitivity analysis rescaling the *ln*(OR) of T2D in order to have consistent estimates for the exposure across studies, showed results in the same direction as those observed in Fig. 3A, but the magnitude of the associations observed were lessened. The risk of T2D increased little with an IQR increase in *p,p'*-DDE (pooled OR = 1.13; 95%CI: 1.05, 1.23; n = 5 studies) with no heterogeneity (Supplemental Fig. 3). When we rescaled the study-specific estimates using the IQR (1147.9 ng/g lipids) reported by Wu et al. (2013), the effect was similar to that observed in Fig. 3A (pooled OR = 1.41; 95%CI: 1.16, 1.71: n = 4 studies) with no heterogeneity (Supplemental Fig. 4). Overall, these results were also consistent with those from the dose-response meta-analysis.

We did not observe a statistically significant risk of GDM in relation to *p,p'*-DDE exposure, the estimated pooled ORs from four studies was 1.01 (95%CI: 0.94, 1.09) and there was no evidence of heterogeneity (I^2 = 0%) (Supplemental Fig. 5). No high risk of T2D with *p,p'*-DDT exposure (pooled OR = 1.03; 95%CI: 0.79, 1.35) was observed in a meta-analysis with four studies, and again, there was no evidence of heterogeneity (I^2 = 0%) (Supplemental Fig. 6).

3.2. Meta-analysis for hypertension

A total of 980 references (Fig. 2) were retrieve by the search in all databases (PubMed, Web of Science, EBSCO, and SciELO); of these, 427 duplicated references were removed leaving 533 to screen. With the screening of titles and abstracts, 15 references were selected for full-text review; of these, eight did not meet the inclusion criteria (six of them were cross-sectional) and were excluded after full-text review leaving seven relevant references for data extraction.

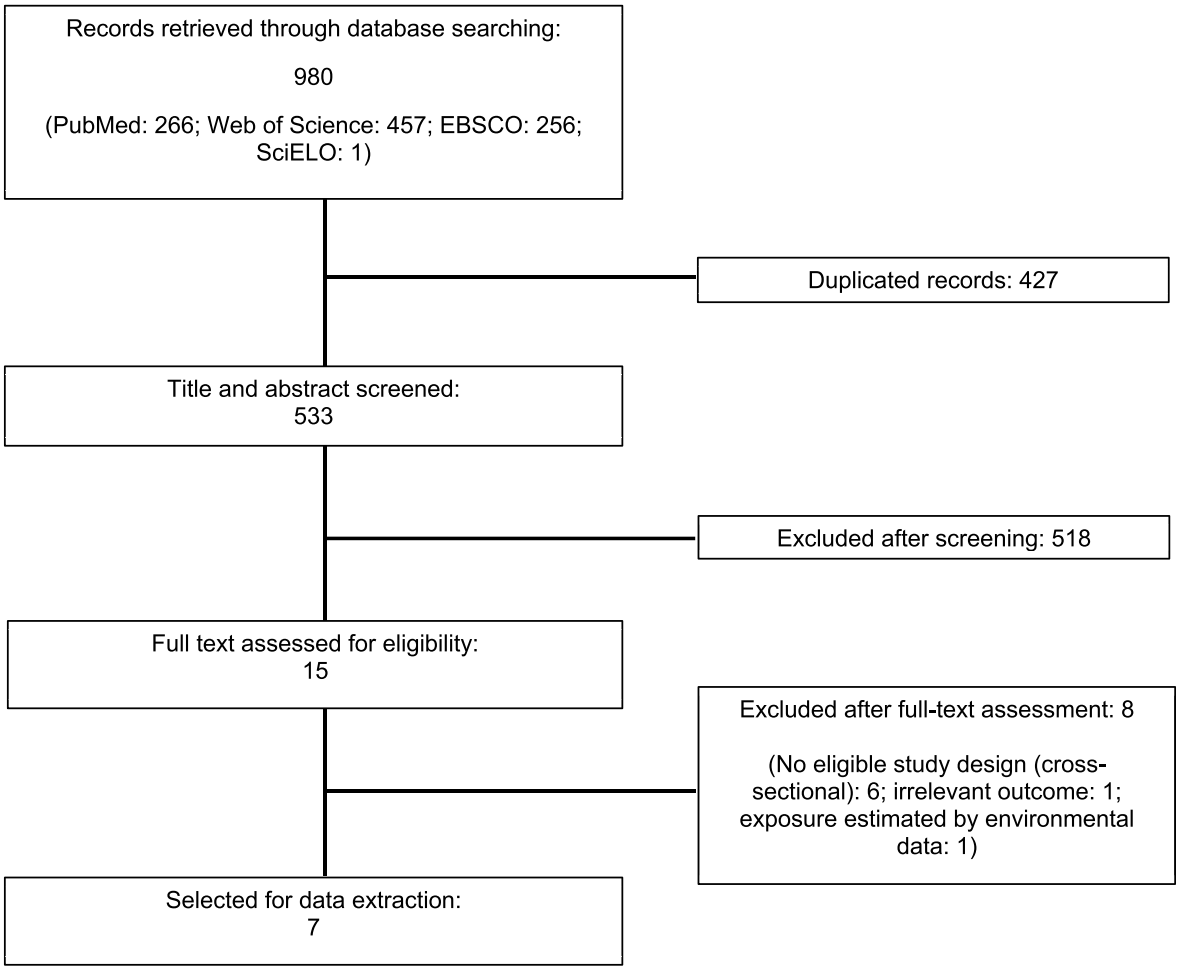

Fig. 2. Flow chart of the selection process of the studies assessing the association between *p,p'-DDT* exposure and risk of hypertension.

Data extracted from the selected studies is summarized in Table 3. All studies were cohorts, except for a nested case-control study; four were conducted in Europe (Arrebola et al., 2015; Donat-Vargas et al., 2018; Vafeiadi et al., 2015; Van Larebeke et al., 2015), two in North America (La Merrill et al., 2013; Smarr et al., 2016), and one in Asia (Lee et al., 2016). The sample sizes of the studies ranged from 214 (Lee et al., 2016) to 1583 (Van Larebeke et al., 2015); the length of follow-up ranged from one (Lee et al., 2016) to 47 years (La Merrill et al., 2013); the study that assessed gestational hypertension had a follow-up of ~24 weeks (Smarr et al., 2016). The ages of the participants ranged from 4 to 80 years, only two studies included participants older than 60 years of age (Arrebola et al., 2015; Van Larebeke et al., 2015); and most of the studies included men and women. As expected, all studies determined concentrations of *p,p'*-DDE in biological samples, three studies also measured *p,p*-DDT (La Merrill et al., 2013; Lee et al., 2016; Smarr et al., 2016) and one o,*p'*-DDT (La Merrill et al., 2013). Two studies assessed the exposure prenatally (La Merrill et al., 2013; Vafeiadi et al., 2015); four modeled lipid-standardized concentrations of DDT and its compounds (Arrebola et al., 2015; Donat-Vargas et al., 2018; Lee et al., 2016; Van Larebeke et al., 2015), two added serum lipids as adjusting variables into their models (*i.e.,* serum total lipids or triglycerides and cholesterol) (Smarr et al., 2016; Vafeiadi et al., 2015) and one did not considered lipids at all (La Merrill et al., 2013). Five studies log-transformed the exposure to estimate the ORs and two categorized the exposure in quantiles (Donat-Vargas et al., 2018; La Merrill et al., 2013). The outcome of interest in most studies was chronic hypertension (Arrebola et al., 2015, 2015, 2015; Donat-Vargas et al., 2018; La Merrill et al., 2013; Van Larebeke et al., 2015), one was focused on gestational hypertension (Smarr et al., 2016), and two studies conducted among children assessed the average change of systolic and diastolic blood pressure (mmHg) as their outcome (Lee et al., 2016; Vafeiadi et al., 2015). Similar to what we observed with T2D, potentially confounding factors considered varied by study, but most of them adjusted for age, sex, smoking, and BMI; one study also adjusted for other POPs (i.e., hexachlorobenzene, trans-Nonachlor & oxychlordane) (Smarr et al., 2016). Based on the NOS quality assessment, all the studies included in the review were scored with moderate to high quality (Supplemental Table 8).

Overall, we observed that the studies reporting higher risks of HTN or increased blood pressure also reported higher levels of exposure compared to the others with null findings (La Merrill et al., 2013; Vafeiadi et al., 2015; Van Larebeke et al., 2015) (Table 3). The number of studies with similar data to combine in meta-analysis were very few and limited to chronic hypertension in relation to *p,p'*-DDE exposure. We observed a slight increased risk of chronic HTN with increasing concentrations of *p,p'*-DDE (pooled OR = 1.21; 95%CI: 1.07, 1.38); there was no evidence of heterogeneity (I^2 = 9.3%), however, this meta-analysis included only four studies with different exposure scales (two categorized by tertiles and two *ln*-transformed *p,p'*-DDE) (Fig. 5). Due to the limited number of studies, were unable con conduct stratified analysis and dose-response meta-analysis. Results from the sensitivity analysis consisting in omitting one study at the time (Supplemental Table 9), showed results comparable to those from Fig. 5, the pooled OR ranged from 1.19 to 1.30. The greatest attenuation (1.7%) was observed when omitting the study by La Merrill et al. (2013) and the greatest increase (by 7.4%) when omitting the study by Van Larebeke et al. (2015).

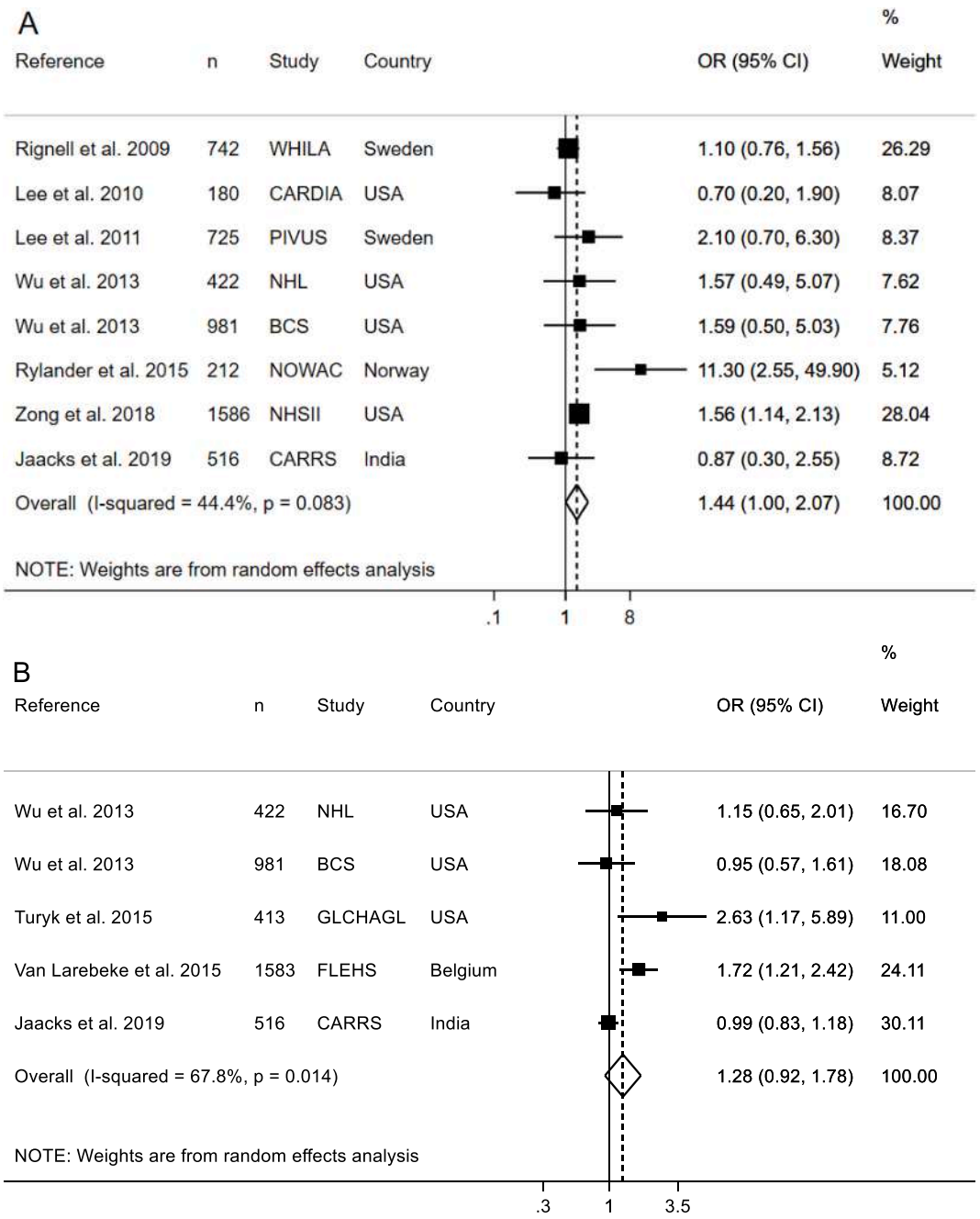

Fig. 3. Meta-analysis of studies assessing *p,p'*-DDE exposure and type 2 diabetes risk. ***A)*** Pooled OR from all studies estimating ORs for the top quantile compared to the lowest quantile. ***B)*** Pooled OR from all studies that reported *ln*-transformed *p,p'*-DDE.
All studies from panel A categorized the exposure into quartiles except the studies by Lee et al. (2011) and Zong et al. (2018) that used quintiles and the tertiles, respectively.

3.3. Assessment of publication bias

As mentioned before, evidence of publication bias was assessed using the funnel plots. No marked asymmetry (Supplemental Figs. 7–10) was observed for the meta-analysis that assessed the relationship between *p,p'*-DDE (top vs lowest quantiles, *ln*-transformed, rescaled estimators) and TD2 risk; moreover, the *Egger's* tests did not show statistically significant small-study effects ($p \geq 0.19$). As expected, the *Egger's* test was not statistically significant in the meta-analysis with non-statistically significant results (data not shown). Similarly, no marked asymmetry emerged in the meta-analysis of *p,p'*-DDE and risk of chronic HTN (Supplemental Fig. 11); the *Egger's* test did not show statistically significant small-study effects ($p = 0.14$).

Most of the studies included in the meta-analysis of T2D were rated with low to moderate risk of bias according to the RoB instrument (Supplemental Tables 10 and 11). The GRADE assessment also suggests high-certainty of the evidence for an increased risk of T2D associated to *p,p'*-DDE exposure (top vs lowest quantiles). The estimated effect for T2D had somewhat good precision as shown by the width of confidence interval; a non-linear dose response relationship was also evaluated. Exposure to *p,p'*-DDE was determined using standardized methods in biological samples, hence, indirectness was apparently not of concern. The risk of bias was not serious and no publication bias was detected (Supplemental Table 12). Similarly, the results from the RoB instrument rated the studies included in the meta-analysis of HTN with low to moderate risk of bias (Supplemental Tables 13 and 14). According to the

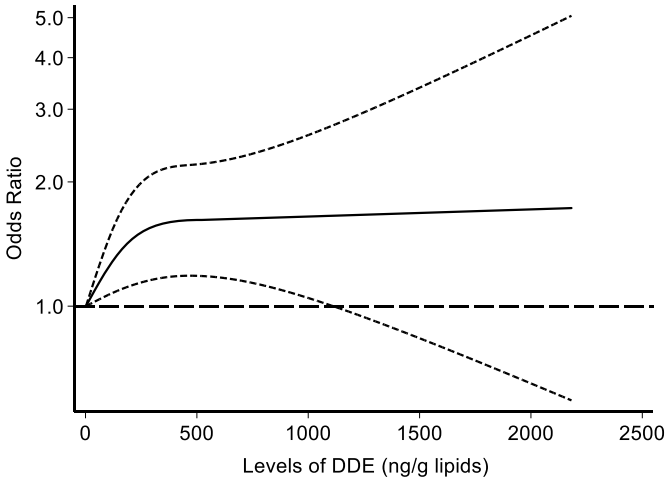

Fig. 4. Dose-response meta-analysis between *p,p'*-DDE exposure and type 2 diabetes: modeling the exposure using restricted cubic splines.
Perphaps it is unnecessary to add "Fig. 4 legend" if the legend will follow the title in the final version of the manuscript. OR's were estimated using as reference the lowest exposure level from one the studies included in the dose-response meta-analysis (2.15 ng/g lipids).

GRADE assessment, there is moderate certainty of the evidence for an association between *p,p'*-DDE exposure and hypertension (Supplemental Table 15). The risk of bias was not serious, inconsistency and indirectness were not of concern apparently, however, prospective studies were scarce, therefore potential publication bias cannot be disregarded; and we were unable to assess a dose-response gradient.

4. Discussion

Results from the present meta-analysis limited to prospective studies, suggest that exposure to *p,p'*-DDE, the main breakdown product of *p,p'*-DDT, might increase the risk of T2D; yet, the size of the effect remains uncertain and may be as little as 13%. Exposure to *p,p'*-DDE may also increase the risk of having chronic HTN, however, this result was based on few studies, thus more studies are warranted to confirm such association.

Most of the studies included in this review assessed the risk of developing T2D and chronic HTN in relation to postnatal exposure to *p,p'*-DDE, only three evaluated prenatal exposure. Our meta-analysis of chronic HTN included a study assessing prenatal exposure (La Merrill et al., 2013) to *p,p'*-DDE (on a wet-weight basis, Table 3) that reported a stronger association than the observed with postnatal exposure. However, the estimate obtained after excluding such study (pooled OR = 1.19; 95%CI: 1.06, 1.34) did not change our main conclusions. Further epidemiological studies are required before dismissing the potential adverse effect of prenatal exposure to *p,p'*-DDT and its breakdown products on the risk of T2D and HTN. Fetal development as a stage of greatest cellular plasticity, represents a vulnerable window for chemical exposure that can lead to epigenetic reprogramming that might influence the susceptibility of the exposed individual to develop metabolic disorders in later life (Barker et al., 2002; Wadhwa et al., 2009). Experimental evidence from animal studies suggests that prenatal exposure to *p,p'*-DDT and its breakdown products are capable to induce alterations in the programming of the offspring, which might lead to disease in adulthood (Bommarito et al., 2017; La Merrill et al., 2014; Schug et al., 2011).

As shown with the present review, few studies have focused on evaluating the effect of the *p,p'*-DDT isomer; only the study by La Merrill et al. (2013) reported a statistically significant association of this isomer with HTN (RR = 2.5; 95%CI: 1.2, 5.3) among adults. Detectable levels of *p,p'*-DDT represents ongoing exposure, whereas *p,p'*-DDE is an indicator of past exposure (Jaga and Dharmani, 2003) and therefore the most commonly measured across studies. Nevertheless, this review shows the importance to distinguish the effect between both compounds as well as to generate evidence related to active exposure to *p,p'*-DDT, especially in countries with ongoing use or manufacture.

Our results are consistent with a prior meta-analysis performed almost a decade ago (2012) limited to prospective studies as the present, though such study reported a non-statistically significant association between *p,p'*-DDE exposure and T2D (pooled OR = 1.25; 95%CI: 0.94, 1.66) based on five studies (Wu et al., 2013). The present meta-analysis based on seven studies (with eight ORs) showed a marginally significant association (*p-value* = 0.049). In agreement with our findings, no significant association between *p,p'*-DDT exposure and T2D risk was observed in the same review (pooled OR = 1.00; 95%CI: 0.54, 1.87) based on three studies (Wu et al., 2013). Also consistent with our findings, a previous meta-analysis of nine studies with various designs reported a somewhat stronger pooled OR between *p,p'*-DDE exposure and T2D (pooled OR = 1.65; 95%CI; 1.15, 2.37) than the estimated in the present (pooled OR = 1.44). However, associations of similar magnitude were observed from studies that accounted for lipids (pooled OR = 1.60; Supplemental Fig. 1) and those limited to women (pooled OR = 1.62; Supplemental Table 4). The main differences with this prior meta-analysis, besides the inclusion of cross-sectional and studies with indirect assessment of exposure, was the evidence of small-study effect as shown by their *Egger's* test (*p-value* <0.05) (Evangelou et al., 2016). A larger meta-analysis of 18 studies with various designs estimated a risk of T2D in relation to *p,p'*-DDE exposure (pooled OR = 1.33; 95%CI: 1.15, 1.54) that is comparable our estimate (Tang et al., 2014). However, the reported heterogeneity although moderate (I^2 = 56%) (Tang et al., 2014), was slightly higher than the observed in the present. The inclusion of cross-sectional studies in these previous meta-analyses is an important limitation when trying to establish a temporal association between the exposure and outcome of interest in order to avoid reverse causality.

Our stratified meta-analysis limited to studies that considered the effect of lipids (lipid-standardized *p,p'*-DDE or added total lipids as a covariate into their models) improve little the heterogeneity and showed stronger associations that were also marginally significant (Supplemental Fig. 1). Previous literature have showed that modeling *p,p'*-DDT and its compounds on a lipids-basis leads to more biased results than adding lipids as a covariate in the regression models (Schisterman et al., 2005). We were unable to conduct stratified analyses based on the approach used to take into account the effect of lipids due to the limited number of studies that adjusted for lipids, most studies modeled lipid-standardized *p,p'*-DDE concentrations. Nonetheless, one of the two studies that adjusted for lipids (as a covariate) reported a stronger association between *p,p'*-DDE and T2D (Lee et al., 2011) than the overall estimate (Fig. 3A). Because lipid concentrations (in serum or plasma) could be an intermediate variable in the association under study (Lee et al., 2007), this results suggest a direct effect of *p,p'*-DDE on T2D that is not explained by lipids.

We could not compare directly our results from the dose-response meta-analysis, to our knowledge this is the first attempt to assess the shape of the relation between *p,p'*-DDE exposure and T2D risk in a meta-analysis. Although based on five studies, our dose-response meta-analysis suggest a non-linear relationship between *p,p'*-DDE exposure and T2D; the confidence intervals at higher levels of exposure showed some degree of imprecision in the estimates. Nonetheless, this result is consistent with the hypothesis that exposure to persistent organic pollutant acting as endocrine disrupters show adverse effects at low-doses but not at higher doses (Lee et al., 2010; Vandenberg et al., 2012; Welshons et al., 2003).

In agreement with our findings, a previous meta-analysis of six studies reported a slight increased risk of hypertension with *p,p'*-DDE exposure (pooled OR = 1.10; 95%CI: 1.03, 1.18); no data on heterogeneity was reported (Park et al., 2016). However, a relevant limitations of

Table 3
Characteristics of the studies evaluating the association of *p,p'*-DDT and its breakdown products with hypertension.

First author, year & country	Study design (Cohort's name)	n (sex)	Age in years	Outcome & ascertainment	Type of exposure (sample)	Median of measured compounds	OR (95%IC)	Risk category	Adjusting variables	Follow-up time
Donat-Vargas et al. 2018. Sweden	Nested case-control (VIP)	427 (♂; ♀)	40–60	Hypertension. SBP>140 or DBP >90 mmHg or use of antihypertensive drugs or self-reported diagnosis of hypertension.	Postnatal (serum).	*p,p'*-DDE: 241 ± 198 ng/g[a,b]	1.59 (0.91, 2.82)	Third *vs.* first tertile.	Gender, age, year of sample collection, & pre-diabetic status.	~13 years
Van Larebeke et al. 2015. Belgium	Cohort (FLEHS)	1583 (♂ 77; ♀ 808)	50–65	Hypertension. Self-reported diagnosis of hypertension in last year.	Postnatal (serum).	*p,p'*-DDE: 486 ng/g (percentiles 10th = 147 & 90th = 1575)	1.23 (1.04, 1.45)	Per one increment in the *ln*-transformed exposure.	Gender, age, smoking, BMI, physical activity, education, & alcohol.	~7 years
Lee et al. 2016. South Korea	Cohort (EB&GC)	214 (♂ 106; ♀ 108)	8–10	DBP & SBP (relative change from baseline to follow-up). DBP & SBP in mmHg: average of 2 measurements.	Postnatal (serum).	*p,p'*-DDT: 3.03 ng/g *p,p'*-DDE: 43.46 ng/g	0.15 (−2.72, 241)[c] 1.70 (−1.89, 5.28)[d] 0.30 (−1.31, 1.92)[c] 1.61 (−0.64, 3.87)[d]	Per one increment in the *ln*-transformed exposure.	Sex, age, household income, & BMI change.	~1 year
Smarr et al. 2016. USA	Cohort (LIFE)	258 (♀)	18–40	Gestational hypertension. Physician report of gestational hypertension at ≥24 weeks of gestation.	Postnatal (serum).	*p,p'*-DDE: 0.56 ng/g[a] (IQR = 0.39) *p,p'*-DDT: <LOD	0.68 (0.33, 1.40) 0.27 (0.04, 1.73)	Per SD increase in the *ln*-transformed exposure.	Age, BMI, non-white race, smoking, sum of log-transformed and rescaled POPs (HCB, trans-Nonachlor & oxychlordane), & serum lipids.	NR
Vafeiadi et al. 2015. Greece	Cohort (Rhea)	689 (♂ 358; ♀ 331)	4	DBP & SBP. DBP & SBP in mmHg: average of 5 measurements.	Prenatal (maternal serum).	*p,p'*-DDE: 1.981 ng/mL (IQR = 2.24)	2.31 (−0.07, 4.69)[c] 1.79 (0.13, 3.46)[d]	Per log-10 increase in exposure.	Maternal: age, pre-pregnant BMI, parity, education, smoking during pregnancy, breastfeeding, triglycerides & cholesterol. Child: sex, birth weight, gestational age, & age at examination.	4 years
Arrebola et al. 2015. Spain	Cohort (Granada-Motril)	297 (♂ 131; ♀ 166)	>16	Hypertension. SBP>140 or DBP >90 mmHg or receipt of anti-hypertensive medication.	Postnatal (adipose tissue).	*p,p'*-DDE: 77.3 ng/g (IQR = 161.3)	1.11 (0.93, 1.33)[e]	Per one increment in the *ln*-transformed exposure.	Age, BMI, smoking, & alcohol.	~10 years
La Merril et al. 2013. USA	Cohort (CHDS)	527 (♀)	39–47	Hypertension. Self-reported physician-diagnosis of hypertension & use of antihypertensive medication.	Prenatal (maternal serum).	*p,p'*-DDT: NR 11.90 ng/mL[f] *o,p'*-DDT: NR 0.51 ng/mL[f] *p,p'*-DDE: NR 54.0 ng/mL[f]	2.5 (1.2, 5.3)[e] 1.2 (0.6, 2.2)[e] 1.7 (1.0, 3.0)[e]	Third *vs.* first tertile.	BMI, diabetes, menopausal status, race, & mother's race.	~39–47 years

Symbols: ♂, males; ♀, females.
Abbreviations: BMI, body mass index; CHDS, Child Health and Development Studies; DBP, diastolic blood pressure; EB&GC, the Ewha Birth & Growth cohort study; FLEHS, Flemish Environment and Health Survey; IQR, interquartile range; LIFE, Investigation of Fertility and the Environment; *ln*, natural logarithm; LOD, limit of detection; ng/g, nanograms/gram of lipids; ng/mL, nanograms/milliliter; NR, Not reported; OR, Odds ratio; PIVUS, Prospective Investigation of the Vasculature in Uppsala Seniors; Rhea, The Mother-Child Cohort in Crete, Greece; SBP, systolic blood pressure; SD, standard deviation; VIP, Ästerbotten Intervention Programme.
[a] From the controls.
[b] Values are means ± standard deviation.
[c] Beta coefficient for SBP (mmHg).
[d] Beta coefficient for DBP (mmHg).
[e] Relative risks.
[f] Levels from the upper tertiles.

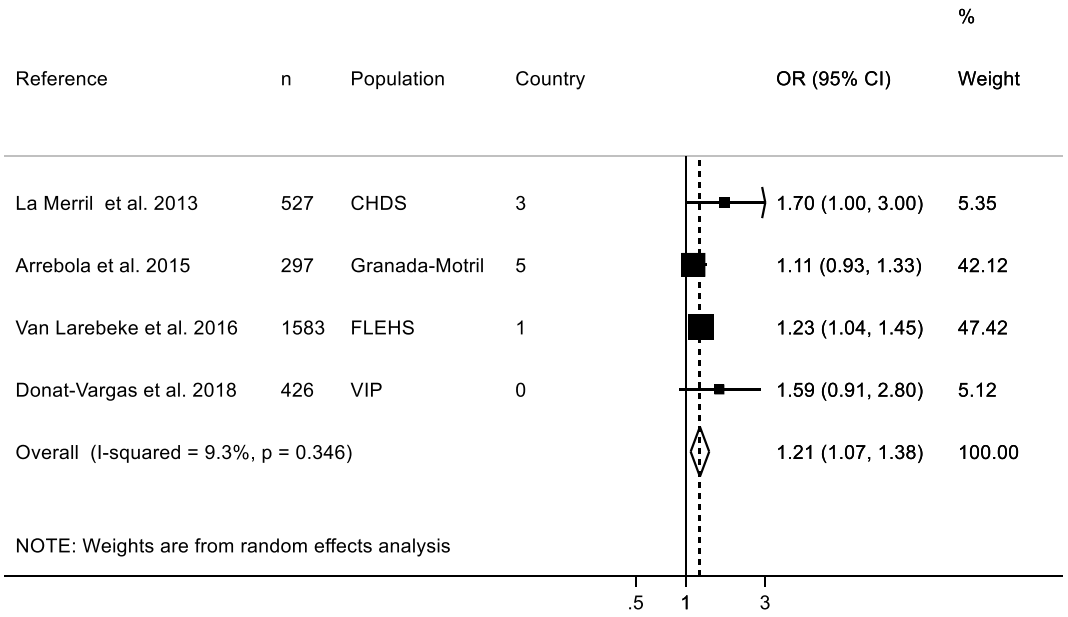

Fig. 5. Meta-analysis of studies assessing *p,p'*-DDE exposure and risk of hypertension.

such meta-analysis was the inclusion of cross-sectional studies (Park et al., 2016) unlike the present meta-analysis limited to prospective studies.

The biological mechanisms underlying the association of *p,p'*-DDT exposure with T2D and HTN risk have not been clearly elucidated yet. However, experimental evidence suggests that *p,p'*-DDT could inhibit the expression of glucose transporter proteins in the beta cells, decreasing the absorption of glucose in adipose tissue, liver, and pancreas, therefore limiting the access of glucose to glucokinase, which can prevent an adequate insulin secretion (Yau and Mennear, 1977). Additionally, *in vitro* evidence have showed the ability of *p,p'*-DDT and *p,p'*-DDE to impair glucose metabolism and induce insulin resistance, a plausible consequence of disrupted lipid homeostasis (Ruzzin et al., 2010). Results from animal models also suggests that perinatal exposure might disrupt the regulation of thermogenesis, lipids, and glucose, which could result in insulin resistance and metabolic alterations (La Merrill et al., 2014). Regarding hypertension, experimental evidence suggests that exposure to *p,p'*-DDT might cause an over-activation of the renin angiotensin system, which might produce a rise in blood pressure (La Merrill et al., 2016).

Some limitations of the present review include the scarcity of prospective epidemiological studies evaluating the associations of interest, which limited our ability to conduct meta-analysis for each metabolite of *p,p'*-DDT with each type of diabetes and hypertension. The effect of the exposure was not consistently assessed across all studies and not all studies had enough data to harmonize the scale of the exposure; therefore, we did attempt to rescale the estimates (ORs) using standard statistical methods (Chêne and Thompson, 1996) in order to have a consistent assessment of the exposure. Yet, we were unable to include all the selected studies in a single meta-analysis; but the overall results from our different meta-analyses were consistently in the same direction. Due to the limited number of studies, publication bias cannot be disregarded. We were unable to assess small-study effects in the meta-analysis of *p,p'*-DDE and HTN due to the limited number of studies, a preference to publish studies with positive results cannot be disregarded. The confounding factors selected to adjust the ORs varied among studies, therefore our pooled OR might be affected by residual confounding. Moreover, human populations are generally exposed to a mixture of chemicals including persistent organic pollutants highly correlated with *p,p'*-DDT, therefore our estimates might not reflect the effect of DDE alone but a mixture of chemicals. We were unable to conduct a dose-response meta-analysis for hypertension due to the limited number of studies.

Despite these limitations, important strengths of the present review includes the use of independent search algorithms for each outcome (diabetes and hypertension), therefore it is unlikely the exclusion of relevant publications as would have occur with a single search strategy for both outcomes. We only included prospective studies with the exposures determined in biospecimens, which contributed to the low risk of bias shown in the meta-analysis of DDE and T2D. Additionally, reverse causality is of little concern in the present review because only prospective studies were included. There is evidence that some metabolic disorders like diabetes might alter the metabolism of POPs in the body, such disorders may increase the chemicals' release from the adipose tissue or may slow its excretion from the body (Porta, 2006). Through this mechanism, diabetes may increase circulating levels of *p,p'*-DDT leading to a spurious association between higher levels of *p,p'*-DDT and higher risk of T2D in cross-sectional studies; nonetheless, this might be an unlikely explanation in the present study.

This revision reveals the need of more prospective evidence, especially considering other outcomes such as hypertension, GDM, and gestational hypertension. Future studies should also focused on the shape of the relationship, prenatal exposure, and mixtures of exposures. Prospective studies assessing the potential adverse effects of the *p,p'*-DDT isomer are scarce, but necessary when reconsidering the use of this pesticide.

4.1. Conclusion

The present meta-analysis limited to prospective studies in humans, provides evidence of the potential adverse effect of *p,p'*-DDE exposure, the main breakdown product of the pesticide *p,p'*-DDT. A slight increased risk of developing type 2 diabetes with *p,p'*-DDE exposure was consistently observed; the dose-response meta-analysis was suggestive of a non-linear relationship and the association with T2D was apparent at lower concentrations of *p,p'*-DDE. Despite a similar increased risk of developing hypertension was apparent, such result was based on very few studies that did not assessed *p,p'*-DDE exposure consistently, therefore confirmation is required before disregarding an adverse effect.

Source of funding

This work did not received funding.

Declaration of competing interest

None.

Acknowledgments

We thank the Mexican National Council of Science and Technology (CONACYT) for the scholarship granted to JAHM (628528) during his doctoral training at the School of Public Health from México.

Appendix A. Supplementary data

Supplementary data to this article can be found online at https://doi.org/10.1016/j.ijheh.2021.113865.

References

Andersson, H., Garscha, U., Brittebo, E., 2011. Effects of PCB126 and 17β-oestradiol on endothelium-derived vasoactive factors in human endothelial cells. Toxicology 285, 46–56. https://doi.org/10.1016/j.tox.2011.04.003.

Arrebola, J.P., Fernández, M.F., Martin-Olmedo, P., Bonde, J.P., Martín-Rodriguez, J.L., Expósito, J., Rubio-Domínguez, A., Olea, N., 2015. Historical exposure to persistent organic pollutants and risk of incident hypertension. Environ. Res. 138, 217–223. https://doi.org/10.1016/j.envres.2015.02.018.

ATSDR, 2019. Agency for toxic substances and disease Registry, US Department of health and human Services, Atlanta, GA. https://www.atsdr.cdc.gov/ToxProfiles/tp.asp?id=81&tid=20. (Accessed 17 September 2020).

Barker, D.J.P., Eriksson, J.G., Forsén, T., Osmond, C., 2002. Fetal origins of adult disease: strength of effects and biological basis. Int. J. Epidemiol. 31, 1235–1239. https://doi.org/10.1093/ije/31.6.1235.

Bellou, V., Belbasis, L., Tzoulaki, I., Evangelou, E., 2018. Risk factors for type 2 diabetes mellitus: an exposure-wide umbrella review of meta-analyses. PLoS One 13. https://doi.org/10.1371/journal.pone.0194127.

Bommarito, P.A., Martin, E., Fry, R.C., 2017. Effects of prenatal exposure to endocrine disruptors and toxic metals on the fetal epigenome. Epigenomics 9, 333–350. https://doi.org/10.2217/epi-2016-0112.

Chêne, G., Thompson, S.G., 1996. Methods for summarizing the risk associations of quantitative variables in epidemiologic studies in a consistent form. Am. J. Epidemiol. 144, 610–621. https://doi.org/10.1093/oxfordjournals.aje.a008971.

Crippa, A., Discacciati, A., Bottai, M., Spiegelman, D., Orsini, N., 2019. One-stage dose–response meta-analysis for aggregated data. Stat. Methods Med. Res. 28, 1579–1596. https://doi.org/10.1177/0962280218773122.

DerSimonian, R., Laird, N., 1986. Meta-analysis in clinical trials. Control. Clin. Trials 7, 177–188. https://doi.org/10.1016/0197-2456(86)90046-2.

Donat-Vargas, C., Åkesson, A., Tornevi, A., Wennberg, M., Sommar, J., Kiviranta, H., Rantakokko, P., Bergdahl, I.A., 2018. Persistent organochlorine pollutants in plasma, blood pressure, and hypertension in a longitudinal study. Hypertens. Dallas Tex 71, 1258–1268. https://doi.org/10.1161/HYPERTENSIONAHA.117.10691, 1979.

Evangelou, E., Ntritsos, G., Chondrogiorgi, M., Kavvoura, F.K., Hernández, A.F., Ntzani, E.E., Tzoulaki, I., 2016. Exposure to pesticides and diabetes: a systematic review and meta-analysis. Environ. Int. 91, 60–68. https://doi.org/10.1016/j.envint.2016.02.013.

Grice, B.A., Nelson, R.G., Williams, D.E., Knowler, W.C., Mason, C.C., Hanson, R.L., Bullard, K.M., Pavkov, M.E., 2017. Associations between persistent organic pollutants, type 2 diabetes, diabetic nephropathy, and mortality. Occup. Environ. Med. 74, 521–527. https://doi.org/10.1136/oemed-2016-103948.

Guyatt, G.H., Oxman, A.D., Vist, G., Kunz, R., Brozek, J., Alonso-Coello, P., Montori, V., Akl, E.A., Djulbegovic, B., Falck-Ytter, Y., Norris, S.L., Williams, J.W., Atkins, D., Meerpohl, J., Schünemann, H.J., 2011. GRADE guidelines: 4. Rating the quality of evidence–study limitations (risk of bias). J. Clin. Epidemiol. 64, 407–415. https://doi.org/10.1016/j.jclinepi.2010.07.017.

Harbord, R.M., Egger, M., Sterne, J.A.C., 2006. A modified test for small-study effects in meta-analyses of controlled trials with binary endpoints. Stat. Med. 25, 3443–3457. https://doi.org/10.1002/sim.2380.

Harrell, F., 2001. Regression modeling Strategies-with applications to linear models, logistic regression, and Survival analysis: Springer Series in statistics. Springer. https://doi.org/10.1007/978-1-4757-3462-1.

Heindel, J.J., Blumberg, B., Cave, M., Machtinger, R., Mantovani, A., Mendez, M.A., Nadal, A., Palanza, P., Panzica, G., Sargis, R., Vandenberg, L.N., Saal, F. vom, 2017. Metabolism disrupting chemicals and metabolic disorders. Reprod. Toxicol. Elmsford N 68, 3–33. https://doi.org/10.1016/j.reprotox.2016.10.001.

Higgins, J., Thomas, J., Chandler, J., Cumpston, M., Li, T., Page, M., Welch, V. (Eds.), 2019. Cochrane Handbook for Systematic Reviews of Interventions, second ed. John Wiley & Sons, Chichester (UK).

Hunter, D.J., Hankinson, S.E., Laden, F., Colditz, G.A., Manson, J.E., Willett, W.C., Speizer, F.E., Wolff, M.S., 1997. Plasma organochlorine levels and the risk of breast cancer. N. Engl. J. Med. 337, 1253–1258. https://doi.org/10.1056/NEJM199710303371801.

Jaacks, L.M., Yadav, S., Panuwet, P., Kumar, S., Rajacharya, G.H., Johnson, C., Rawal, I., Mohan, D., Mohan, V., Tandon, N., Barr, D.B., Narayan, K.M.V., Prabhakaran, D., 2019. Metabolite of the pesticide DDT and incident type 2 diabetes in urban India. Environ. Int. 133, 105089. https://doi.org/10.1016/j.envint.2019.105089.

Jaga, K., Dharmani, C., 2003. Global surveillance of DDT and DDE levels in human tissues. Int. J. Occup. Med. Environ. Health 16, 7–20.

La Merrill, M., Cirillo, P.M., Terry, M.B., Krigbaum, N.Y., Flom, J.D., Cohn, B.A., 2013. Prenatal exposure to the pesticide DDT and hypertension diagnosed in women before age 50: a longitudinal Birth cohort study. Environ. Health Perspect. 121, 594–599. https://doi.org/10.1289/ehp.1205921.

La Merrill, M., Karey, E., Moshier, E., Lindtner, C., La Frano, M.R., Newman, J.W., Buettner, C., 2014. Perinatal exposure of mice to the pesticide DDT impairs energy expenditure and metabolism in adult female offspring. PLoS One 9, e103337. https://doi.org/10.1371/journal.pone.0103337.

La Merrill, M.A., Sethi, S., Benard, L., Moshier, E., Haraldsson, B., Buettner, C., 2016. Perinatal DDT exposure induces hypertension and cardiac hypertrophy in adult mice. Environ. Health Perspect. 124, 1722–1727. https://doi.org/10.1289/EHP164.

Lee, D.-H., Lee, I.-K., Porta, M., Steffes, M., Jacobs, D.R., 2007. Relationship between serum concentrations of persistent organic pollutants and the prevalence of metabolic syndrome among non-diabetic adults: results from the National Health and Nutrition Examination Survey 1999-2002. Diabetologia 50, 1841–1851. https://doi.org/10.1007/s00125-007-0755-4.

Lee, D.-H., Lind, P.M., Jacobs, D.R., Salihovic, S., van Bavel, B., Lind, L., 2011. Polychlorinated biphenyls and organochlorine pesticides in plasma predict development of type 2 diabetes in the elderly. Diabetes Care 34, 1778–1784. https://doi.org/10.2337/dc10-2116.

Lee, D.-H., Steffes, M.W., Sjödin, A., Jones, R.S., Needham, L.L., Jacobs, D.R., 2010. Low dose of some persistent organic pollutants predicts type 2 diabetes: a nested case–control study. Environ. Health Perspect. 118, 1235–1242. https://doi.org/10.1289/ehp.0901480.

Lee, H.A., Park, S.H., Hong, Y.S., Ha, E.H., Park, H., 2016. The effect of exposure to persistent organic pollutants on metabolic health among Korean children during a 1-year follow-up. Int. J. Environ. Res. Publ. Health 13. https://doi.org/10.3390/ijerph13030270.

Liberati, A., Altman, D.G., Tetzlaff, J., Mulrow, C., Gøtzsche, P.C., Ioannidis, J.P.A., Clarke, M., Devereaux, P.J., Kleijnen, J., Moher, D., 2009. The PRISMA statement for reporting systematic reviews and meta-analyses of studies that evaluate health care interventions: explanation and elaboration. PLoS Med. 6, e1000100 https://doi.org/10.1371/journal.pmed.1000100.

Mills, K.T., Bundy, J.D., Kelly, T.N., Reed, J.E., Kearney, P.M., Reynolds, K., Chen, J., He, J., 2016. Global Disparities of hypertension prevalence and control: a systematic analysis of population-based studies from 90 countries. Circulation 134, 441–450. https://doi.org/10.1161/CIRCULATIONAHA.115.018912.

Morgan, R.L., Thayer, K.A., Santesso, N., Holloway, A.C., Blain, R., Eftim, S.E., Goldstone, A.E., Ross, P., Ansari, M., Akl, E.A., Filippini, T., Hansell, A., Meerpohl, J. J., Mustafa, R.A., Verbeek, J., Vinceti, M., Whaley, P., Schünemann, H.J., GRADE Working Group, 2019. A risk of bias instrument for non-randomized studies of exposures: a users' guide to its application in the context of GRADE. Environ. Int. 122, 168–184. https://doi.org/10.1016/j.envint.2018.11.004.

Morgan, R.L., Whaley, P., Thayer, K.A., Schünemann, H.J., 2018. Identifying the PECO: a framework for formulating good questions to explore the association of environmental and other exposures with health outcomes. Environ. Int. 121, 1027–1031. https://doi.org/10.1016/j.envint.2018.07.015.

Oparil, S., Acelajado, M.C., Bakris, G.L., Berlowitz, D.R., Cífková, R., Dominiczak, A.F., Grassi, G., Jordan, J., Poulter, N.R., Rodgers, A., Whelton, P.K., 2018. Hypertension. Nat. Rev. Dis. Primer 4, 18014. https://doi.org/10.1038/nrdp.2018.14.

Orsini, N., 2021. Weighted mixed-effects dose–response models for tables of correlated contrasts. STATA J. 21, 320–347. https://doi.org/10.1177/1536867X211025798.

Orsini, N., Bellocco, R., Greenland, S., 2006. Generalized least squares for trend estimation of summarized dose–response data. STATA J. 6, 40. https://doi.org/10.1177/1536867X0600600103.

Park, S.H., Lim, J.-E., Park, H., Jee, S.H., 2016. Body burden of persistent organic pollutants on hypertension: a meta-analysis. Environ. Sci. Pollut. Res. Int. 23, 14284–14293. https://doi.org/10.1007/s11356-016-6568-6.

Porta, M., 2006. Persistent organic pollutants and the burden of diabetes. Lancet Lond. Engl. 368, 558–559. https://doi.org/10.1016/S0140-6736(06)69174-5.

Rahman, M.L., Zhang, C., Smarr, M.M., Lee, S., Honda, M., Kannan, K., Tekola-Ayele, F., Buck Louis, G.M., 2019. Persistent organic pollutants and gestational diabetes: a multi-center prospective cohort study of healthy US women. Environ. Int. 124, 249–258. https://doi.org/10.1016/j.envint.2019.01.027.

Rignell-Hydbom, A., Elfving, M., Ivarsson, S.A., Lindh, C., Jönsson, B.A.G., Olofsson, P., Rylander, L., 2010. A nested case-control study of intrauterine exposure to persistent organochlorine pollutants in relation to risk of type 1 diabetes. PLoS One 5. https://doi.org/10.1371/journal.pone.0011281.

Rignell-Hydbom, A., Lidfeldt, J., Kiviranta, H., Rantakokko, P., Samsioe, G., Agardh, C.-D., Rylander, L., 2009. Exposure to p,p′-DDE: a risk factor for type 2 diabetes. PLoS One 4. https://doi.org/10.1371/journal.pone.0007503.

Ruzzin, J., Petersen, R., Meugnier, E., Madsen, L., Lock, E.-J., Lillefosse, H., Ma, T., Pesenti, S., Sonne, S.B., Marstrand, T.T., Malde, M.K., Du, Z.-Y., Chavey, C., Fajas, L., Lundebye, A.-K., Brand, C.L., Vidal, H., Kristiansen, K., Frøyland, L., 2010. Persistent organic pollutant exposure leads to insulin resistance syndrome. Environ. Health Perspect. 118, 465–471. https://doi.org/10.1289/ehp.0901321.

Rylander, C., Sandanger, T.M., Nøst, T.H., Breivik, K., Lund, E., 2015. Combining plasma measurements and mechanistic modeling to explore the effect of POPs on type 2

diabetes mellitus in Norwegian women. Environ. Res. 142, 365–373. https://doi.org/10.1016/j.envres.2015.07.002.

Saeedi, P., Petersohn, I., Salpea, P., Malanda, B., Karuranga, S., Unwin, N., Colagiuri, S., Guariguata, L., Motala, A.A., Ogurtsova, K., Shaw, J.E., Bright, D., Williams, R., 2019. Global and regional diabetes prevalence estimates for 2019 and projections for 2030 and 2045: results from the international diabetes federation diabetes atlas. Diabetes Res. Clin. Pract. 157 https://doi.org/10.1016/j.diabres.2019.107843 ninth ed.

Schisterman, E.F., Whitcomb, B.W., Louis, G.M.B., Louis, T.A., 2005. Lipid adjustment in the analysis of environmental contaminants and human health risks. Environ. Health Perspect. 113, 853–857. https://doi.org/10.1289/ehp.7640.

Schug, T.T., Janesick, A., Blumberg, B., Heindel, J.J., 2011. Endocrine disrupting chemicals and disease susceptibility. J. Steroid Biochem. Mol. Biol. 127, 204–215. https://doi.org/10.1016/j.jsbmb.2011.08.007.

Shapiro, G.D., Dodds, L., Arbuckle, T.E., Ashley-Martin, J., Ettinger, A.S., Fisher, M., Taback, S., Bouchard, M.F., Monnier, P., Dallaire, R., Morisset, A.-S., Fraser, W., 2016. Exposure to organophosphorus and organochlorine pesticides, perfluoroalkyl substances, and polychlorinated biphenyls in pregnancy and the association with impaired glucose tolerance and gestational diabetes mellitus: the MIREC Study. Environ. Res. 147, 71–81. https://doi.org/10.1016/j.envres.2016.01.040.

Singh, K., Chan, H.M., 2017. Persistent organic pollutants and diabetes among Inuit in the Canadian Arctic. Environ. Int. 101, 183–189. https://doi.org/10.1016/j.envint.2017.02.002.

Smarr, M.M., Grantz, K.L., Zhang, C., Sundaram, R., Maisog, J.M., Barr, D.B., Louis, G.M.B., 2016. Persistent organic pollutants and pregnancy complications. Sci. Total Environ. 551 (552), 285–291. https://doi.org/10.1016/j.scitotenv.2016.02.030.

Sterne, J.A., Hernán, M.A., Reeves, B.C., Savović, J., Berkman, N.D., Viswanathan, M., Henry, D., Altman, D.G., Ansari, M.T., Boutron, I., Carpenter, J.R., Chan, A.-W., Churchill, R., Deeks, J.J., Hróbjartsson, A., Kirkham, J., Jüni, P., Loke, Y.K., Pigott, T.D., Ramsay, C.R., Regidor, D., Rothstein, H.R., Sandhu, L., Santaguida, P.L., Schünemann, H.J., Shea, B., Shrier, I., Tugwell, P., Turner, L., Valentine, J.C., Waddington, H., Waters, E., Wells, G.A., Whiting, P.F., Higgins, J.P., 2016. ROBINS-I: a tool for assessing risk of bias in non-randomised studies of interventions. BMJ 355, i4919. https://doi.org/10.1136/bmj.i4919.

Szklo, M., Nieto, J., 2007. Epidemiology : beyond the Basics, second ed. Jones and Bartlett Publishers, Sudbury, Mass.

Tang, M., Chen, K., Yang, F., Liu, W., 2014. Exposure to organochlorine pollutants and type 2 diabetes: a systematic review and meta-analysis. PLoS One 9. https://doi.org/10.1371/journal.pone.0085556.

Thayer, K.A., Heindel, J.J., Bucher, J.R., Gallo, M.A., 2012. Role of environmental chemicals in diabetes and obesity: a National Toxicology Program workshop review. Environ. Health Perspect. 120, 779–789. https://doi.org/10.1289/ehp.1104597.

Turusov, V., Rakitsky, V., Tomatis, L., 2002. Dichlorodiphenyltrichloroethane (DDT): ubiquity, persistence, and risks. Environ. Health Perspect. 110, 125–128.

Turyk, M., Anderson, H., Knobeloch, L., Imm, P., Persky, V., 2009. Organochlorine exposure and incidence of diabetes in a cohort of Great Lakes Sport fish consumers. Environ. Health Perspect. 117, 1076–1082. https://doi.org/10.1289/ehp.0800281.

Turyk, M., Fantuzzi, G., Persky, V., Freels, S., Lambertino, A., Pini, M., Rhodes, D.H., Anderson, H.A., 2015. Persistent organic pollutants and biomarkers of diabetes risk in a cohort of Great Lakes Sport caught fish consumers. Environ. Res. 140, 335–344. https://doi.org/10.1016/j.envres.2015.03.037.

Vafeiadi, M., Georgiou, V., Chalkiadaki, G., Rantakokko, P., Kiviranta, H., Karachaliou, M., Fthenou, E., Venihaki, M., Sarri, K., Vassilaki, M., Kyrtopoulos, S. A., Oken, E., Kogevinas, M., Chatzi, L., 2015. Association of prenatal exposure to persistent organic pollutants with obesity and cardiometabolic traits in early childhood: the Rhea Mother–child cohort (Crete, Greece). Environ. Health Perspect. 123, 1015–1021. https://doi.org/10.1289/ehp.1409062.

Vafeiadi, M., Roumeliotaki, T., Chalkiadaki, G., Rantakokko, P., Kiviranta, H., Fthenou, E., Kyrtopoulos, S.A., Kogevinas, M., Chatzi, L., 2017. Persistent organic pollutants in early pregnancy and risk of gestational diabetes mellitus. Environ. Int. 98, 89–95. https://doi.org/10.1016/j.envint.2016.10.005.

van den Berg, H., 2009. Global status of DDT and its alternatives for Use in vector control to prevent disease. Environ. Health Perspect. 117, 1656–1663. https://doi.org/10.1289/ehp.0900785.

Van Larebeke, N., Sioen, I., Hond, E.D., Nelen, V., Van de Mieroop, E., Nawrot, T., Bruckers, L., Schoeters, G., Baeyens, W., 2015. Internal exposure to organochlorine pollutants and cadmium and self-reported health status: a prospective study. Int. J. Hyg Environ. Health 218, 232–245. https://doi.org/10.1016/j.ijheh.2014.11.002.

Vandenberg, L.N., Colborn, T., Hayes, T.B., Heindel, J.J., Jacobs, D.R., Lee, D.-H., Shioda, T., Soto, A.M., vom Saal, F.S., Welshons, W.V., Zoeller, R.T., Myers, J.P., 2012. Hormones and endocrine-disrupting chemicals: low-dose effects and Nonmonotonic dose responses. Endocr. Rev. 33, 378–455. https://doi.org/10.1210/er.2011-1050.

Wadhwa, P.D., Buss, C., Entringer, S., Swanson, J.M., 2009. Developmental origins of health and disease: brief history of the approach and current focus on epigenetic mechanisms. Semin. Reprod. Med. 27, 358–368. https://doi.org/10.1055/s-0029-1237424.

Wells, G., Shea, B., O'Connell, D., Peterson, J., Welch, v, Losos, M., Tugwell, P., 2009. The Newcastle–Ottawa Scale (NOS) for assessing the quality if nonrandomized studies in meta-analyses. http://www.ohri.ca/programs/clinical_epidemiology/oxford.asp. (Accessed 17 September 2020).

Welshons, W.V., Thayer, K.A., Judy, B.M., Taylor, J.A., Curran, E.M., vom Saal, F.S., 2003. Large effects from small exposures. I. Mechanisms for endocrine-disrupting chemicals with estrogenic activity. Environ. Health Perspect. 111, 994–1006. https://doi.org/10.1289/ehp.5494.

Wolf, K., Bongaerts, B.W.C., Schneider, Alexandra, Huth, C., Meisinger, C., Peters, A., Schneider, Andrea, Wittsiepe, J., Schramm, K.-W., Greiser, K.H., Hartwig, S., Kluttig, A., Rathmann, W., 2019. Persistent organic pollutants and the incidence of type 2 diabetes in the CARLA and KORA cohort studies. Environ. Int. 129, 221–228. https://doi.org/10.1016/j.envint.2019.05.030.

Woodruff, T., Wolff, M.S., Davis, D.L., Hayward, D., 1994. Organochlorine exposure estimation in the study of cancer etiology. Environ. Res. 65, 132–144. https://doi.org/10.1006/enrs.1994.1026.

Wu, H., Bertrand, K.A., Choi, A.L., Hu, F.B., Laden, F., Grandjean, P., Sun, Q., 2013. Persistent organic pollutants and type 2 diabetes: a prospective analysis in the Nurses' health study and meta-analysis. Environ. Health Perspect. 121, 153–161. https://doi.org/10.1289/ehp.1205248.

Xing, D., Xu, Y., Liu, Q., Ke, Y., Wang, B., Li, Z., Lin, J., 2016. Osteoarthritis and all-cause mortality in worldwide populations: grading the evidence from a meta-analysis. Sci. Rep. 6 https://doi.org/10.1038/srep24393.

Yau, D.T., Mennear, J.H., 1977. The inhibitory effect of DDT on insulin secretion in mice. Toxicol. Appl. Pharmacol. 39, 81–88. https://doi.org/10.1016/0041-008x(77)90179-x.

Zong, G., Valvi, D., Coull, B., Göen, T., Hu, F.B., Grandjean, P., Sun, Q., 2018. Persistent organic pollutants and risk of type 2 diabetes: a prospective investigation among Middle-aged women in Nurses' health study II. Environ. Int. 114, 334–342. https://doi.org/10.1016/j.envint.2017.12.010.

International Journal of Hygiene and Environmental Health 239 (2022) 113861

Contents lists available at ScienceDirect

International Journal of Hygiene and Environmental Health

journal homepage: www.elsevier.com/locate/ijheh

Impact of heat waves and cold spells on cause-specific mortality in the city of São Paulo, Brazil

Sara Lopes de Moraes [a,b,*], Ricardo Almendra [c], Ligia Vizeu Barrozo [a,b]

[a] Department of Geography, School of Philosophy, Literature and Human Sciences of the University of São Paulo, São Paulo, SP, Brazil
[b] Institute of Advanced Studies, of the University of São Paulo, São Paulo, SP, Brazil
[c] Centre of Studies on Geography and Spatial Planning (CEGOT), Department of Geography and Tourism, University of Coimbra, Coimbra, Portugal

ARTICLE INFO

Keywords:
Heat wave
Cold spell
Mortality
Extreme air temperature event
Elderly

ABSTRACT

The impact of heat waves and cold spells on mortality has become a major public health problem worldwide, especially among older adults living in low-to middle-income countries. This study aimed to investigate the effects of heat waves and cold spells under different definitions on cause-specific mortality among people aged ≥65 years in São Paulo from 2006 to 2015. A quasi-Poisson generalized linear model with a distributed lag model was used to investigate the association between cause-specific mortality and extreme air temperature events. To evaluate the effects of the intensity under different durations, we considered twelve heat wave and nine cold spell definitions. Our results showed an increase in cause-specific deaths related to heat waves and cold spells under several definitions. The highest risk of death related to heat waves was identified mostly at higher temperature thresholds with longer events. We verified that men were more vulnerable to die from cerebrovascular diseases and ischemic stroke on cold spells and heat waves days than women, while women presented a higher risk of dying from ischemic heart diseases during cold spells and tended to have a higher risk of chronic obstructive pulmonary disease than men during heat waves. Identification of heat wave- and cold spell-related mortality is important for the development and promotion of public health measures.

1. Introduction

Extreme weather events, such as heat waves, cold spells, and droughts, have always occurred worldwide. However, in the past few decades, the occurrence of these extreme events has increased owing to the current climate change (IPCC et al, 2014). In the near future, extreme air temperature events (ETEs), particularly events related to heat will be more frequent, longer, and intense (Meehl and Tebaldi, 2004; Perkins et al., 2012).

The definitions of ETEs are inconsistent in the literature, and no standard criteria have been established because of the differences in geographical locations, climate variability across regions, and population acclimatization (Robinson, 2001). However, ETEs are generally defined as periods of extremely high or low daily temperatures (mean, maximum, or minimum) outside the normal relative or absolute threshold, which last for consecutive days (Guo et al., 2017; Monteiro et al., 2013; Robinson, 2001). The study of various ETE definitions and different combinations may support the establishment of the best predictor to quantify the impact of ETEs on human health.

Several epidemiologic studies (Chen et al., 2020; Wang et al., 2016; Yang et al., 2019) have reported that the intensity and duration of ETEs influence mortality and morbidity, making it a current public health concern. A recent study found that heat wave-related increase in deaths is projected to be higher in Brazil and other tropical and subtropical areas than in the US and European countries, especially if no mitigation and adaptation strategies are applied to reduce the effects of heat waves on human health (Guo et al., 2018). Although in recent years, most studies have investigated the effects of heat waves and heat events on mortality, the high risk of deaths related to cold events is also expected to remain in some areas (Gasparrini et al., 2015, 2017).

Extremely high and low temperatures can induce substantial physiological stress in the human body. Furthermore, exposure to direct or indirect extreme cold and heat can trigger cardiovascular and respiratory symptoms, particularly in older adults, which is the most vulnerable group. Older people present physiological and socioeconomic limitations and are at a higher risk of death from cardiovascular and respiratory diseases (Anderson and Bell, 2009; Chen et al., 2019; Song et al.,

* Corresponding author. Department of Geography, School of Philosophy, Literature and Human Sciences, University of São Paulo, Cidade Universitária, Avenida Professor Lineu Prestes, 338, Zip code: 05508-000, São Paulo, SP, Brazil.
E-mail addresses: sara.moraes@usp.br (S.L. Moraes), ricardoalmendra85@gmail.com (R. Almendra), lija@usp.br (L.V. Barrozo).

https://doi.org/10.1016/j.ijheh.2021.113861
Received 27 July 2021; Received in revised form 30 September 2021; Accepted 12 October 2021
Available online 20 October 2021

Abbreviations

ETE	Extreme air temperature events
CI	confidence interval
COPD	chronic obstructive pulmonary disease
CVD	cardiovascular disease
df	degrees of freedom
ICD-10	International Classification of Diseases, 10th Revision
ns	natural cubic spline
PM_{10}	particulate matter with an aerodynamic diameter of <10 μm
RH	relative humidity
RR	relative risk
RRR	relative risk ratio
SEADE	São Paulo State System for Data Analysis Foundation
T	daily mean air temperature

2018; Vasconcelos et al., 2013; Wang et al., 2016).

Statistically significant associations between ETEs and the risk of mortality among people aged ≥65 years have been widely reported (Chen et al., 2019; Wang et al., 2016; Yang et al., 2019; Yin et al., 2018). In the summer of 2003, a severe heat wave event caused 70,000 excess deaths across European countries, affecting mainly older adults in France, Portugal, Luxemburg, and Italy (Robine et al., 2008). The excess mortality during extreme ETEs among older individuals occurred not only in Europe but also in Asia, Australia, and the United States over the years (Anderson and Bell, 2009; Tong et al., 2013; Yang et al., 2019). Most recently, in June 2021, an exceptional early hot summer condition occurred in the northwest and western Canada. Approximately 500 people may have died from heat wave events, especially older adults living alone in the greater Vancouver area (Cecco, 2021). In the same week, extremely cold temperatures were recorded for several days in the south and southwest of Brazil (INMET, 2021a).

Nonetheless, there is a lack of knowledge on the association between ETEs and excess mortality among the vulnerable population, particularly in Latin American cities. São Paulo is the most populated city in Latin America, with a significant level of socioeconomic inequalities, environmental disparities, and a large aging population. According to the São Paulo State System for Data Analysis Foundation (SEADE), the number of people aged ≥65 years is expected to be 2.8 million by 2050, representing about 22.9% of the population and an increase of 2% per year. Therefore, this study aimed to investigate the effects of heat waves and cold spells under different definitions on cause-specific mortality among people aged ≥65 years in São Paulo from 2006 to 2015.

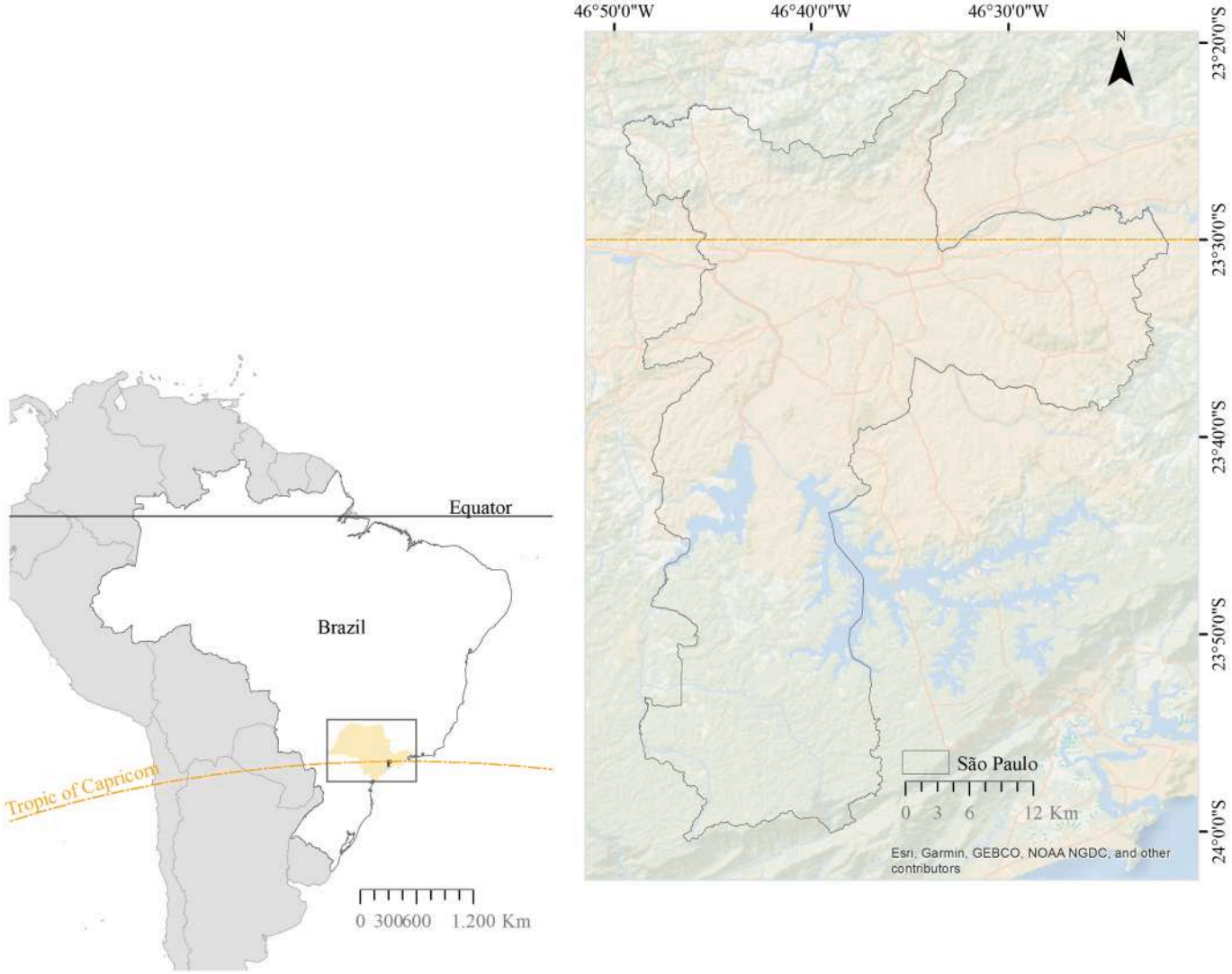

Fig. 1. City of São Paulo in Southeast Brazil.

2. Material and methods

2.1. Study area

The city of São Paulo is located in southeast Brazil (Fig. 1), with an estimated population of approximately 12.3 million and average population density of 7,398.26 hab/km^2 in 2020 (IBGE, 2020). According to the Köppen–Geiger classification, the study area has a humid subtropical climate, characterized by hot and wet summers and dry winters. The average monthly temperatures vary between 16.7 °C and 23.2 °C (INMET, 2021b).

2.2. Data collection

The daily mortality data of individuals aged ≥65 years from 2006 to 2015 were provided by the Information Improvement Program of the Municipality of São Paulo. For this study, we selected deaths due to cardiovascular diseases (CVD; International Classification of Diseases, 10th Revision [ICD-10]: I00–I99), respiratory diseases (ICD-10: J00–J99), and the following selected specific causes of death within these groups: ischemic heart disease (ICD-10: I20–I25), cerebrovascular diseases (ICD-10: I60–I69), ischemic stroke (ICD10: I63 and I65–I66), hemorrhagic stroke (ICD-10: I60–I62), and chronic obstructive pulmonary disease (COPD; ICD-10: J40–J44 and J47). Additionally, we divided the daily deaths by sex (female and male) for each cause of mortality.

Daily mean air temperature (T; °C) and relative humidity (RH; %) data for the study period were collected from the meteorological station of the Institute of Astronomy, Geophysics, and Atmospheric Sciences at University of São Paulo.

To adjust the effects of air pollution on the model, data on daily average concentrations of particulate matter with an aerodynamic diameter of <10 μm (PM_{10}) were obtained from the Environmental Company of the State of São Paulo.

2.3. Extreme air temperature event definitions

The T was assessed to classify the ETEs. The warm period was between September and March and the cold period between April and August. In this study, we analyzed heat wave events according to four relative thresholds (above the 90th, 92.5th, 95th, and 97.5th percentiles) and durations over 2, 3, or 4 consecutive days. Cold spells were defined by three relative thresholds (below the 3rd, 5th, and 10th percentiles) and over 2, 3, or 4 consecutive days. Therefore, twelve heat wave and nine cold spell definitions were individually assessed.

2.4. Statistical analyses

To analyze the association between daily mortality and the different ETE definitions presented, we applied a quasi-Poisson generalized linear model with a distributed linear lag model to capture the lag effects, as shown in previous studies (Chen et al., 2019; Yin et al., 2018; Zhao et al., 2019). We conducted a separate analysis of the heat wave and cold spell models. The general form of the model is as follows:

$$Log\ (\mu_t) = \alpha + cb(ETE_t,\ lag) + ns(RH_t,\ df) + ns(PM_{10t},\ df) + ns(time_t,\ df*10) + ns\left(Dos_t, df\right) + \gamma Dow_t + \delta Holiday_t$$

where μ_t is the daily number of deaths on day t of observation; α is the intercept; ETE is a binary variable that represents the heat wave and cold spell event on day t (1 = heat wave/cold spell days, and 0 = non-heat wave/cold spell days); *cb* is the *crossbasis* with a linear function and a natural cubic spline function (*ns*) (Chen et al., 2019; Gao et al., 2019; Wang et al., 2016; Lee et al., 2018) with two degrees of freedom (*df*) for lagged effects on mortality in the heat wave model and 3 df in the cold spell models, placed at equally spaced values in the log scale. Based on several studies (Chen et al., 2019; Guo et al., 2017; Yang et al., 2019), we used 10 lag days for heat waves and 27 lag days for cold spells.

Potential confounders, such as RH and PM_{10}, were controlled in the overall ETE model through the ns function. For the heat wave model, the RH and PM_{10} were controlled with 2 df. The models were also adjusted for long-term trends (time) of 2 df per year. Seasonality was controlled using the ns function with 2 df for the day of the season (Dos). Public holidays (Holiday) and the day of the week (Dow) were added to the model as categorical variables, which were in accordance with recent investigations (Guo et al., 2017; Yin et al., 2018).

Furthermore, in the second stage, we included the daily mean temperature in the previous model to verify the added effects of ETE on mortality. The daily mean temperature was controlled using the ns function and 2 df.

We assessed the cumulative relative risk (RR) with its 95% confidence interval (CI) for cold spell days compared to non-cold spell days and for heat wave days compared to non-heat wave days separately for each ETE definition, cause-specific death, and sex.

A sensitivity analysis was conducted to calibrate the model parameters by changing the df for: RH (2–4); air pollution (2–4); T (2–4); seasonality and long-term trends (1–4). We also tested different lagged effects for ETE (heat waves: 0–7 and 0–10 days; cold spells: 0–21 and 0–27 days). The model parameters were selected in this phase; preference was given to the lower values of the Akaike information criterion for quasi-Poisson regression.

In addition, we calculated the relative risk ratio (RRR) through a two-stage analysis based on Altman and Band, (2003) approach to assess the differences across relative risks of cause-specific mortality stratified by sex. The differences of RRs among males and females were already estimated in similar studies (Chen et al., 2019; Yang et al., 2019).

All statistical analyses were performed using R software version 4.0.2 (R Core Team, 2019) with the *dlnm* package (Gasparrini, 2011).

3. Results

Table 1 summarizes the descriptive statistics of daily mortality and meteorological and air pollution data. Between 2006 and 2015, there were 151,001 deaths in São Paulo due to CVD and 64,778 deaths due to respiratory diseases. Of these, a total of 56,885 ischemic heart disease deaths were registered. Among them, 38,084 were overall cerebrovascular disease mortalities (ischemic stroke: 11,427; hemorrhagic stroke: 7,718), and 19,148 COPD mortalities.

During the study period, most of the heat wave events occurred in February, while cold spells events were registered in July. The annual mean number of cold spells on consecutive days for each definition ranged from 2 to 32 days, and that of heat waves on consecutive days for each definition ranged from 2 to 28 days. Detailed information on the descriptive statistics of heat waves and cold spell days for each definition is presented in Table 2.

Table 1
Descriptive statistics of daily mortality, meteorological, and air pollution data from 2006 to 2015.

Variables	Mean	SD	Min	Median	Max
Cardiovascular diseases	41.3	8.3	18	41	77
Respiratory diseases	17.7	5.3	3	17	44
Cerebrovascular diseases	10.4	3.4	1	10	26
Ischemic stroke	3.1	2.0	0	3	14
Hemorrhagic stroke	2.1	1.5	0	2	9
Ischemic heart diseases	15.6	4.6	3	15	35
Chronic obstructive pulmonary disease	5.2	2.4	0	5	17
Mean temperature (°C)	19.6	3.3	7.3	19.7	28.0
Relative humidity (%)	80.0	8.8	34.3	80.9	97.0
PM10 (μg/m^3)	35.5	17.1	7.4	31.6	132.4

SD: Standard deviation; Min: minimum; Max: maximum; PM_{10}: particulate matter with an aerodynamic diameter of <10 μm.

Table 2
Descriptive statistics of a heat wave and cold spell days for each definition in São Paulo, 2006–2015.

ETE model name	ETE definition	ETE days per year				
		Mean	SD	Min	Median	Max
HW_90P_2d	Heatwave >90th percentile with ≥2 days duration	28	13	9	25	55
HW_90P_3d	Heatwave >90th percentile with ≥3 days duration	20	12	3	15	43
HW_90P_4d	Heatwave >90th percentile with ≥4 days duration	14	12	0	8	34
HW_92.5P_2d	Heatwave >92.5th percentile with ≥2 days duration	19	13	4	16	48
HW_92.5P_3d	Heatwave >92.5th percentile with ≥3 days duration	12	10	0	9	34
HW_92.5P_4d	Heatwave >92.5th percentile with ≥4 days duration	9	9	0	6	28
HW_95P_2d	Heatwave >95th percentile with ≥2 days duration	12	10	0	8	34
HW_95P_3d	Heatwave >95th percentile with ≥3 days duration	8	8	0	6	24
HW_95P_4d	Heatwave >95th percentile with ≥4 days duration	5	7	0	3	21
HW_97.5P_2d	Heatwave >97.5th percentile with ≥2 days duration	5	6	0	3	18
HW_97.5P_3d	Heatwave >97.5th percentile with ≥3 days duration	3	5	0	0	16
HW_97.5P_4d	Heatwave >97.5th percentile with ≥4 days duration	2	5	0	0	16
CS_3P_2d	Cold spell <3rd percentile with ≥2 days duration	8	5	0	9	13
CS_3P_3d	Cold spell <3rd percentile with ≥3 days duration	4	4	0	5	11
CS_3P_4d	Cold spell <3rd percentile with ≥4 days duration	2	3	0	0	7
CS_5P_2d	Cold spell <5th percentile with ≥2 days duration	15	7	2	15	27
CS_5P_3d	Cold spell <5th percentile with ≥3 days duration	9	6	0	9	19
CS_5P_4d	Cold spell <5th percentile with ≥4 days duration	6	5	0	5	13
CS_10P_2d	Cold spell <10th percentile with ≥2 days duration	32	9	12	33	43
CS_10P_3d	Cold spell <10th percentile with ≥3 days duration	24	9	8	22	43
CS_10P_4d	Cold spell <10th percentile with ≥4 days duration	14	7	5	14	25

SD: Standard deviation; Min: minimum; Max: maximum.

Fig. 2 and Supplementary Table 1 illustrate the cumulative RRs of the association between heat waves under 12 definitions and cause-specific mortality at lag 0–10 days. In general, we found that a higher temperature threshold and duration (HW_95P_3d, HW_95P_4d, HW_97.5P_3d, and HW_97.5P_4d) had a higher significant risk, except for hemorrhagic stroke and COPD outcomes. The overall effects (without controlling for daily mean temperature) of heat waves were stronger on mortality due to ischemic stroke, especially in the HW_97.5P_3d and HW_97.5P_4d definitions with RR = 1.535 (95% CI: 1.103–2.135) and RR = 1.578 (95% CI: 1.088–2.289), respectively.

Fig. 3 displays the cumulative RRs of the impact of cold spells on mortality. The overall cold spell effects were significant in several outcomes and definitions. The effect estimates varied greatly according to the definition and outcome. The RRs of CVD, for instance, varied from 1.216 (95% CI: 1.026–1.442) in the CS_10P_2d definition to 2.484 (95% CI: 1.456–4.239) in the CS_3P_4d definition. In addition, the significant RR values for the cause-specific mortality of cerebrovascular diseases, ischemic stroke, and ischemic heart diseases were more pronounced in some cold spells than during heat waves.

The added effects in the heat waves and cold spell models were also significant for several definitions. The added effects of the heatwave models showed lower RRs compared to the overall effects in all cause-specific mortality. In addition, we observed a higher risk of death on the added effects in comparation with the overall effects for cold spell models, especially for CVD (CS_10P_2d), respiratory diseases (except the 10th percentile temperature threshold with ≥2 and ≥ 3 days), hemorrhagic stroke (CS_10P_4d, CS_5P_2d, CS_3P_3d, and CS_3P_4d), and for all statistically significant RRs of cerebrovascular diseases and ischemic stroke outcomes.

Fig. 4 and Supplementary Tables 3 and 4 show the RRs of the association between and the ETE and cause-specific mortality stratified by sex. The risk of death during heat waves was statistically significantly high in women for all overall CVD and respiratory outcomes. In addition, the results stratified by cause-specific mortality indicated that men presented a statistically significant high risk for cerebrovascular diseases and ischemic stroke in several heat waves and cold spell definitions. In contrast, the RR of mortality among women was high due to ischemic heart disease on cold events and only a few cases of ischemic heart disease and COPD during heat events. We did not find any statistically significant results for ischemic stroke in women on extremely cold and hot days.

During heat wave events, no higher RRs on added effects compared to the overall effects were detected in men on heat wave events, and we only observed a small increase in added effects in COPD outcomes in women for all temperature thresholds with ≥2 consecutive days. In addition, the results showed only a few higher added effects in women (CVD, respiratory disease, hemorrhagic stroke, and ischemic heart diseases) and men (respiratory, cerebrovascular diseases, and ischemic stroke) in some cold spell definitions. The added effects results for women and men can be checked on Supplementary Tables 3 and 4.

Supplementary Tables 5 and 6 show the RRR results of the differences between men and women. We identified that men were more vulnerable to die from cerebrovascular diseases and ischemic stroke during some ETEs definitions compared to women. The highest RRR values of the RRs differences among men and women due to ischemic stroke were found in two heatwaves definitions: HW_92.5P_3d (RRR: 1.510; 95% IC: 1.004–2.272) and HW_92.5P_4d (RRR: 1.531 95% IC: 1.003–2.337).

4. Discussion

This study assessed the risk of death among older adults (aged ≥65 years) due to CVD, respiratory diseases, cerebrovascular diseases, ischemic stroke, hemorrhagic stroke, ischemic heart disease, and COPD during the occurrence of ETEs from 2006 to 2015. To the best of our knowledge, this is the first study to quantify the impact of cold spells on mortality in Brazil and the first to estimate the association between heat waves and cold spells and cause-specific mortality in São Paulo under different definitions of ETEs.

Our results showed a significantly high risk of mortality associated with heat wave events in several definitions. The highest risk of death during heat waves was identified mostly in the higher temperature

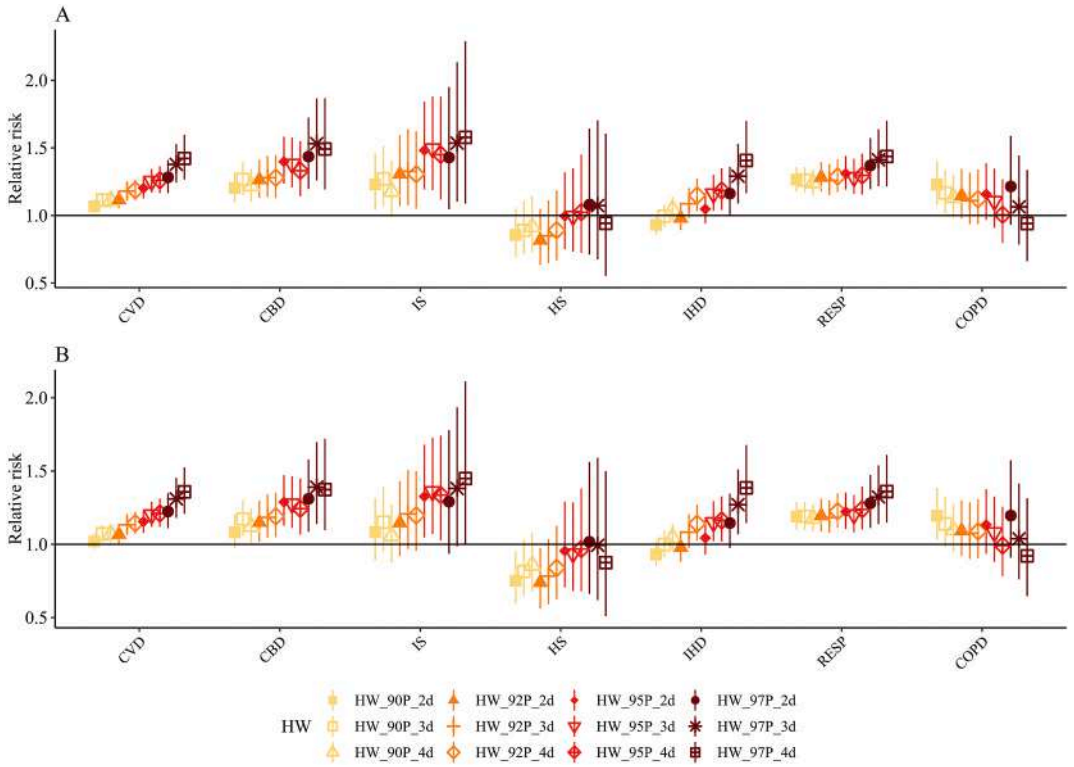

Fig. 2. Effects of heat waves under 12 definitions on mortality due to cardiovascular disease (CVD), cerebrovascular disease (CBD), ischemic stroke (IS), hemorrhagic stroke (HS), ischemic heart disease (IHD), respiratory disease (RESP), and chronic obstructive pulmonary disease (COPD) in people aged ≥65 years over lag 0–10 days in São Paulo. (A) Overall effects of heat waves without controlling for daily mean temperature (B) Added effects of heat waves after controlling for daily mean temperature.

threshold (95th and 97.5th percentile) with a duration of ≥3 and ≥ 4 consecutive days. Similar findings were found in a multi-community study of 400 communities in 18 countries. According to Guo et al. (2017), the higher temperature thresholds of the heat wave definitions (daily mean temperature, 95th and 97.5th percentile) presented a higher risk of all-cause and non-accidental mortality in most communities, including São Paulo and other cities in Brazil.

We observed an increase in deaths during cold spells compared to those on non-cold-spell days. Furthermore, the extremely cold spell threshold definition (percentile 3) presented the highest significant risk of mortality due to CVD, cerebrovascular diseases, and ischemic and hemorrhagic strokes among older adults. A Chinese study found a higher risk of mortality due to respiratory diseases and COPD during cold spells, and they also observed that older individuals were more vulnerable (Chen et al., 2019).

Older adults are particularly susceptible to extreme high and low temperatures compared to younger adults because of their lower thermoregulatory capacity to thermal variations and individual behaviors (such as social isolation, tobacco use, obesity, comorbidities, and frailty) (Balmain et al., 2018; Kenny et al., 2010; Tansey and Johnson, 2015). Physiological responses to high and low temperature exposure may induce changes in the metabolic rate, blood pressure, blood viscosity, cholesterol levels, cardiac output, thromboembolism, and bronchoconstriction (Keatinge et al., 1986; Koskela et al., 1996; Tansey and Johnson, 2015), which can lead to a higher risk of death and hospital admissions due to ischemic heart diseases, stroke, and COPD during ETEs (Gao et al., 2019; Monteiro et al., 2013; Yang et al., 2019; Yin et al., 2018). Medication use can also contribute to a reduction in thermoregulation capacity (Kenny et al., 2010).

Zhao et al. (2019) observed that the risk of CVD hospital admissions during heat wave days decreased in Brazil. However, our findings showed that ETEs significantly increased cardiovascular and respiratory mortality, which is consistent with the findings of previous studies (Anderson and Bell, 2009; Cheng et al., 2019; Fouillet et al., 2006; Yang et al., 2019). The differences in the risk of mortality and hospital admissions due to CVD may be associated with the heat effects on vulnerable individuals. People with comorbidities are more likely to die before receiving medical assistance or been able to be admitted to a hospital on heat wave events (Zhao et al., 2019).

Nevertheless, there are limited studies on the association between ETEs and cause-specific mortality, particularly the subtypes of stroke, ischemic heart disease, and COPD. This cause-specific death is a public health concern because of the high mortality rates worldwide, which can increase with the occurrence of ETEs. According to the World Health Organization (2021), approximately 3.17 million people die from COPD each year, and >15.2 million deaths occur globally due to stroke and heart attack. Calazans and Queiroz (2020) estimated that Brazil has the most significant impact on adult mortality due to cardiovascular diseases compared to 10 other Latin American countries. Another study reported that ischemic heart disease is the first cause of the years of life lost, among Brazilians, followed by stroke in the fourth, and COPD in the eighth position (Marinho et al., 2018). Therefore, it is extremely important to comprehend the cause-specific burden related to ETEs, and further studies should be conducted.

We found significant results and substantial variations in the RR associations between the overall effects of heat waves and cold spell events on cause-specific mortality in older adults. It was possible to identify that there was a high risk of death for all cerebrovascular diseases and ischemic stroke in almost all definitions of heat waves (except the HW_90P_4d classification of ischemic stroke). Statistically significant results were found only in two cold spell definitions for hemorrhagic stroke mortality (CS_3P_3d and CS_3P_4d), and no significant RR was observed during the occurrence of heat wave events. The ischemic heart disease and COPD results showed an increase in mortality only in a few definitions of heat wave events. Yin et al. (2018) found similar results in a heat wave study conducted in China (Yin et al., 2018).

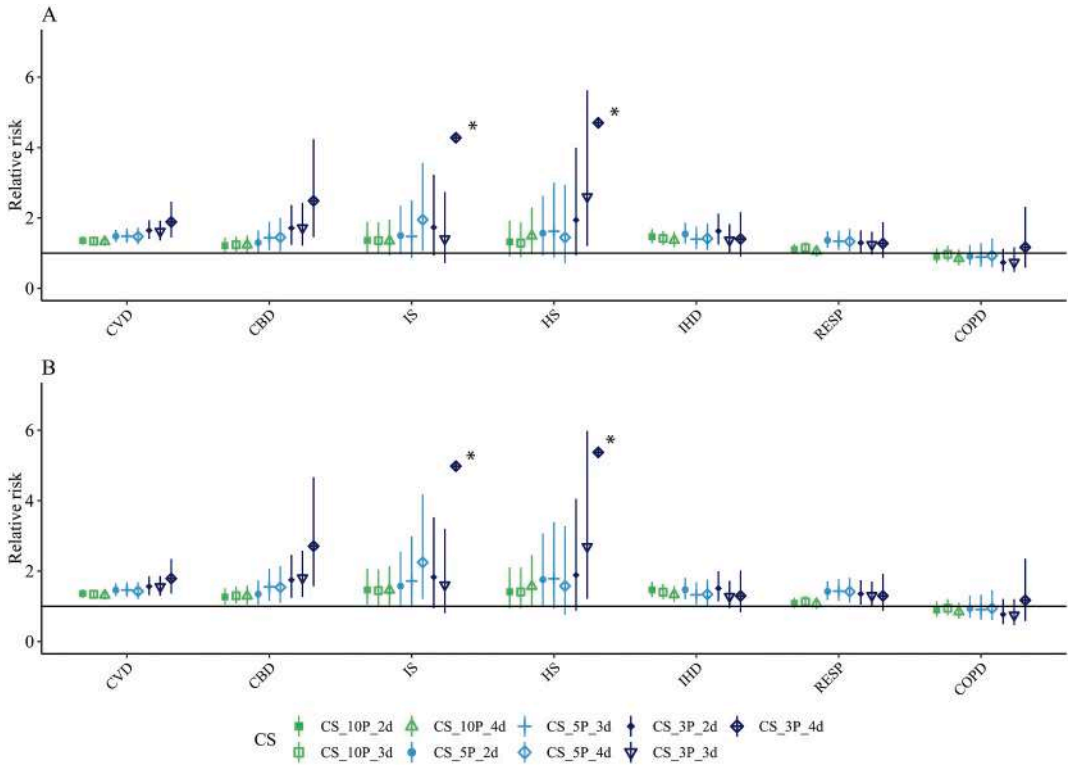

Fig. 3. Effects of cold spells under nine definitions on mortality due to cardiovascular disease (CVD), cerebrovascular disease (CBD), ischemic stroke (IS), hemorrhagic stroke (HS), ischemic heart disease (IHD), respiratory disease (RESP), and chronic obstructive pulmonary disease (COPD) in people aged ≥65 years over lag 0–21 days in São Paulo. (A) Overall effects of cold spells without controlling for daily mean temperature and (B) added effects of cold spells after controlling for daily mean temperature. * The confidence interval is not represented in the graph for better visualization of the other RRs. Confidence intervals are presented in Supplementary Table 1.

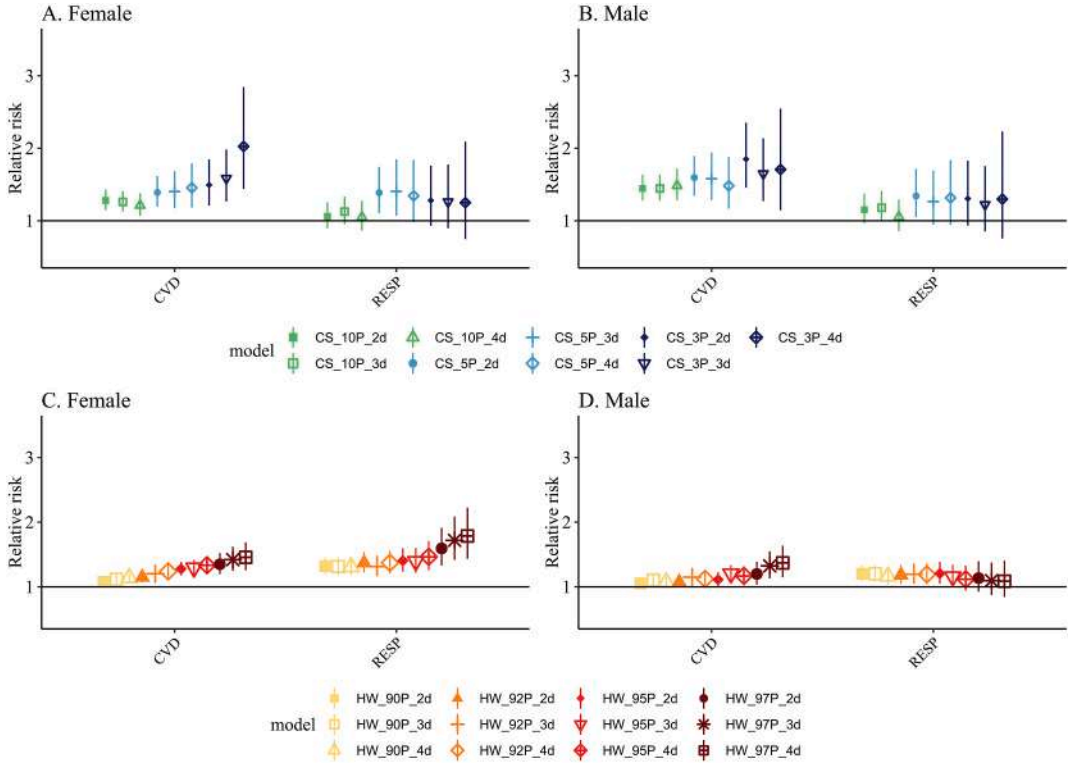

Fig. 4. Effects of cold spells (A and B) and heat waves (C and D) on cardiovascular diseases (CVD) and respiratory diseases (RESP) mortality stratified by sex (women and men).

Furthermore, they verified a higher risk of mortality due to ischemic stroke than that of hemorrhagic stroke on heat wave days.

In contrast, cold spell-related mortality was identified in all CVD categories and some ETE classifications of cerebrovascular diseases, ischemic stroke, hemorrhagic stroke (CS_10P_4d CS_5P_2d, CS_3P_3d, and CS_3P_4d), ischemic heart disease, and respiratory diseases outcomes. In contrast to the findings of other studies, no significant RR was found for COPD during cold spells (Chen et al., 2019; Han et al., 2017). The intensity and duration of the effects of heat waves and cold spells on mortality have also varied considerably in other studies (Chen et al., 2019; Yang et al., 2019).

Since few studies have investigated heat wave- and cold spell-related cause-specific mortality, especially stratified by sex, our study can provide substantially contributing data on this matter. We identified a significantly higher mortality risk in women than in men in a few heat waves definitions for overall cardiovascular and respiratory diseases. Recent studies have shown that women are more vulnerable to heat effects than men (Fouillet et al., 2006; van Steen et al., 2019; Yang et al., 2019). Nonetheless, the responses to extreme heat and cold event exposure in women and men are inconsistent in the literature and require further investigation.

Epidemiological investigations indicate that women may be more affected by high temperatures than men because of the changes in reproductive hormones, higher average life expectancy, and other physiological and thermoregulatory responses to heat stress (van Steen et al., 2019). In contrast, men could be at a higher risk of mortality due to some health outcomes during extreme temperature exposure because they have more cardiovascular diseases and unhealthy behaviors, and are less likely to undergo regular check-ups and seek health care for pre-existing health conditions than women (Crimmins et al., 2019; Rogers et al., 2010).

Our findings suggest a clear distinction in the risk of death stratified by cause-specific mortality and that stratified by sex. We verified that men are more vulnerable to die from cerebrovascular diseases and ischemic stroke during cold spells and heat waves, respectively, than women, while women presented a higher risk of dying from ischemic heart diseases during a cold spell and COPD in heat wave days, but only in a few ETEs definitions than men.

This study also investigated the added effects on mortality in older adults. We identified significant added effects of ETEs on cause-specific mortality and stratified them by sex. Compared to the overall effects models of ETEs, a higher RR of added effects was observed only in a few cold spell event definitions for the health outcomes and stratified by sex. We did not find an increase in the added effects on heat wave days, except for a small increase in the added effects in women due to COPD for all temperature thresholds with $\geq$2 consecutive days compared with the overall model results. The added effects on mortality remain inconclusive and controversial. Many studies (Gasparrini and Armstrong, 2011; Guo et al., 2017; Lee et al., 2018) have found significant results decomposing the main (independent effects of daily high temperature) and added effects on heat waves or cold spell days, while others have chosen modeling approaches without temperature adjustment or have reported inconsistent results of the added effects (Chen et al., 2019; Yang et al., 2019; Zhao et al., 2019).

In addition, our findings that the overall and added effects are higher on cold spell days than heat wave days can be partly explained by the hypothesis of the acclimatization of the population (Anderson and Bell, 2009). People living in warmer environmental conditions are more adapted to extreme heat events and are more vulnerable to extreme cold events. Guo et al. (2017) showed that heat wave-related mortality was higher in moderately hot and cold areas than in hot and cold areas.

Moreover, the effects of ETEs on mortality in older adults found in this study may also be related to the combination of physiological factors, individual behaviors, the urban environment, and socioeconomic status. Poor household conditions interfere directly and indirectly with thermal comfort (e.g., household quality, thermal building capacity, and lack of a heating and air conditioning system); lower levels of education, low income, and impact of the urban heat island intensity, especially in urbanized areas, are also potential risk factors for health outcomes (Almendra et al., 2017; Gao et al., 2019; Heaviside et al., 2016; Sera et al., 2019; Tan et al., 2010). In addition, future investigations are needed to better understand the higher risk of death during ETEs, particularly in the city of São Paulo, where about 2 million people live in slums (*favelas*) or under inadequate household and sanitation conditions (IBGE, 2020).

Although our study did not intend to identify the best predictor to quantify the impact of ETEs on human health, our results can support important future public health measures. For instance, we found that all the heat waves definitions (from the less intense with less duration to the more intense with longer duration) represent a high risk of cause-specific mortality for people aged $\geq$65 years. Public health measures and warnings should be considered from the most conservative approach based on the lower even though less impactful heatwave definitions to avoid as many deaths as possible related to the event. Nevertheless, further investigations should be conducted for the development of an ETE warning system in the city of São Paulo and planning measures to reduce the impact of heat waves and cold spells on the population health.

Finally, some limitations of this study need to be noted. We only obtained the temperature and humidity data from one meteorological station to represent the entire city. Furthermore, we did not address the association between the mortality burden during heat waves and cold spells with other risk factors, such as the built environment and socioeconomic status.

5. Conclusions

This study highlights the impact of heat waves and cold spell events on cause-specific mortality among older adults stratified by sex. Our findings allow us to advance the understanding of the relationship between climate and health in the city of São Paulo.

The results provide substantial evidence for public health managers and urban planners to implement and promote preventive measures to reduce the impact of heat wave and cold spell events. Development of strategies, such as the heat relief network with emergency cooling centers by the Canadian government during heat waves and expansion of shelters for the most vulnerable groups during cold events, are fundamental to mitigate the negative impacts on health outcomes. In addition, warning can be provided through the news and community health agents to educate and inform the population regarding the effects of ETEs, especially for people aged $\geq$65 years. Health units linked to the Brazilian Unified Health System as well as the private and supplementary systems must be prepared for immediate assistance in cases of hospital emergency due to myocardial infarction and stroke, for which prompt assistance can prevent death or sequelae.

Furthermore, improvements in the urban microclimate can be achieved through interventions in the built environment. The identification of urban heat islands can also allow urban planners to mitigate them by implementing green areas at strategic places of the city.

Authors contribution

Sara Lopes de Moraes: Conceptualization; Investigation; Data curation; Formal analysis; Methodology; Software; Writing - original draft; Writing - review & editing. **Ricardo Almendra:** Investigation; Methodology; Supervision; Validation; Visualization, Writing - original draft; Writing – review & editing. **Ligia Vizeu Barrozo:** Conceptualization; Investigation; Project administration; Supervision; Validation; Visualization; Writing – original draft; Writing - review & editing.

Declaration of competing interest

The authors declare that they have no known competing financial interests or personal relationships that could have appeared to influence the work reported in this paper.

Acknowledgements

This work was supported by São Paulo Research Foundation (FAPESP) [grant number 2018/25462–0] and the Coordenação de Aperfeiçoamento de Pessoal de Nível Superior (CAPES) – Financial code 001 and the. RA received support from the Centre of Studies in Geography and Spatial Planning (CEGOT), funded by national funds through the Foundation for Science and Technology (FCT) under the reference UIDB/04084/2020.

Appendix A. Supplementary data

Supplementary data to this article can be found online at https://doi.org/10.1016/j.ijheh.2021.113861.

References

Almendra, R., Santana, P., Vasconcelos, J., 2017. Evidence of social deprivation on the spatial patterns of excess winter mortality. Int. J. Publ. Health 62, 849–856. https://doi.org/10.1007/s00038-017-0964-7.

Altman, D.G., Bland, J.M., 2003. Interaction revisited: the difference between two estimates. BMJ 326 (7382), 219.

Anderson, B.G., Bell, M.L., 2009. Weather-related mortality: how heat, cold, and heat waves affect mortality in the United States. Epidemiology 20, 205–213. https://doi.org/10.1097/ede.0b013e318190ee08.

Balmain, B.N., Sabapathy, S., Louis, M., Morris, N.R., 2018. Aging and thermoregulatory control: the clinical implications of exercising under heat stress in older individuals. BioMed Res. Int. https://doi.org/10.1155/2018/8306154, 2018.

Calazans, J.A, Queiroz, B.L, 2020. The adult mortality profile by cause of death in 10 Latin American countries (2000–2016). Rev Panam Salud Publica 44. https://doi.org/10.26633/RPSP.2020.1.

Cecco, L., 2021. Record Heatwave May Have Killed 500 People in Western Canada. The Guardian. https://www.theguardian.com/world/2021/jul/02/canada-heatwave-500-deaths. (Accessed 4 July 2021).

Chen, J., Yang, J., Zhou, M., Yin, P., Wang, B., Liu, J., Chen, Z., Song, X., Ou, C.Q., Liu, Q., 2019. Cold spell and mortality in 31 Chinese capital cities: definitions, vulnerability and implications. Environ. Int. 128, 271–278. https://doi.org/10.1016/j.envint.2019.04.049.

Chen, J., Zhou, M., Yang, J., Yin, P., Wang, B., Ou, C.Q., Liu, Q., 2020. The modifying effects of heat and cold wave characteristics on cardiovascular mortality in 31 major Chinese cities. Environ. Res. Lett. 15 https://doi.org/10.1088/1748-9326/abaea0.

Cheng, J., Xu, Z., Bambrick, H., Prescott, V., Wang, N., Zhang, Y., Su, H., Tong, S., Hu, W., 2019. Cardiorespiratory effects of heatwaves : a systematic review and meta-analysis of global epidemiological evidence. Environ. Res. J. 177, 1–10. https://doi.org/10.1016/j.envres.2019.108610.

Crimmins, E.M., Shim, H., Zhang, Y.S., Kim, J.K., 2019. Differences between men and women in mortality and the health dimensions of the morbidity process. Clin. Chem. 65, 135–145. https://doi.org/10.1373/clinchem.2018.288332.

Fouillet, A., Rey, G., Laurent, F., Pavillon, G., Bellec, S., Guihenneuc-Jouyaux, C., Clavel, J., Jougla, E., Hémon, D., 2006. Excess mortality related to the August 2003 heat wave in France. Int. Arch. Occup. Environ. Health 80, 16–24. https://doi.org/10.1007/s00420-006-0089-4.

Gao, J., Yu, F., Xu, Z., Duan, J., Cheng, Q., Bai, L., Zhang, Y., Wei, Q., Yi, W., Pan, R., Su, H., 2019. The association between cold spells and admissions of ischemic stroke in Hefei, China: modified by gender and age. Sci. Total Environ. 669, 140–147. https://doi.org/10.1016/j.scitotenv.2019.02.452.

Gasparrini, A., 2011. Distributed lag linear and non-linear models in R: the package dlnm. J. Stat. Software 43, 1–20. https://doi.org/10.18637/jss.v043.i08.

Gasparrini, A., Armstrong, B., 2011. The impact of heat waves on mortality. Epidemiology 22, 68–73. https://doi.org/10.1097/EDE.0b013e3181fdcd99. The.

Gasparrini, A., Guo, Y., Hashizume, M., Lavigne, E., Zanobetti, A., Schwartz, J., Tobias, A., Tong, T., Rocklöv, J., Forsberg, B., Leone, M., Sario, M., Bell, M.L., Leon Guo, Y.L., Wu, C., Kan, H., Yi, S., Coelho, M.S.Z.S., Saldiva, P.H.N., Honda, Y., Armstrong, B., 2015. Mortality risk attributable to high and low ambient temperature: a multicountry observational study. Environnement, Risques & Santé 14, 464–465. https://doi.org/10.1016/S0140-6736(14)62114-0.

Gasparrini, A., Guo, Y., Sera, F., Vicedo-Cabrera, A.M., Huber, V., Tong, S., de Sousa Zanotti Stagliorio Coelho, M., Nascimento Saldiva, P.H., Lavigne, E., Matus Correa, P., Valdes Ortega, N., Kan, H., Osorio, S., Kyselý, J., Urban, A., Jaakkola, J.J.K., Ryti, N.R.I., Pascal, M., Goodman, P.G., Zeka, A., Michelozzi, P., Scortichini, M., Hashizume, M., Honda, Y., Hurtado-Diaz, M., Cesar Cruz, J., Seposo, X., Kim, H., Tobias, A., Iñiguez, C., Forsberg, B., Åström, D.O., Ragettli, M.S., Guo, Y.L., Wu, C. fu, Zanobetti, A., Schwartz, J., Bell, M.L., Dang, T.N., Van, D. Do, Heaviside, C., Vardoulakis, S., Hajat, S., Haines, A., Armstrong, B., 2017. Projections of temperature-related excess mortality under climate change scenarios. Lancet Planet. Heal. 1, e360–e367. https://doi.org/10.1016/S2542-5196(17)30156-0.

Guo, Y., Gasparrini, A., Armstrong, B.G., Tawatsupa, B., Tobias, A., Lavigne, E., Sousa, M. De, Stagliorio, Z., Pan, X., Kim, H., Hashizume, M., Honda, Y., Michelozzi, P., Punnasiri, K., Li, S., Tian, L., David, S., Garcia, O., Seposo, X., 2017. Heat wave and mortality : a multicountry , multicommunity study. Environ. Health Perspect. 1–11 https://doi.org/10.1289/EHP1026.

Guo, Y., Gasparrini, A., Li, S., Sera, F., Vicedo, A.M., Sousa, M. De, Stagliorio, Z., Hilario, P., Saldiva, N., Lavigne, E., Tawatsupa, B., Punnasiri, K., Overcenco, A., Correa, P.M., Ortega, N.V., Kan, H., Osorio, S., Jaakkola, J.J.K., Ryti, N.R.I., Goodman, P.G., Guo, Y.L., Chen, B., Forsberg, B., Å, D.O., 2018. Quantifying excess deaths related to heatwaves under climate change scenarios : a multicountry time series modelling study. PLoS Med. 15 (7), 1–17. https://doi.org/10.1371/journal.pmed.1002629 e10.

Han, J., Liu, S., Zhang, Jun, Zhou, L., Fang, Q., Zhang, Ji, Zhang, Y., 2017. The impact of temperature extremes on mortality: a time-series study in Jinan, China. BMJ Open 7, 1–8. https://doi.org/10.1136/bmjopen-2016-014741.

Heaviside, C., Vardoulakis, S., Cai, X.M., 2016. Attribution of mortality to the urban heat island during heatwaves in the West Midlands, UK. Environ. Heal. A Glob. Access Sci. Source 15. https://doi.org/10.1186/s12940-016-0100-9.

IBGE, 2020. Cidades@. URL https://www.ibge.gov.br/cidades-e-estados/sp/sao-paulo.html (accessed 8.8.20).

INMET, 2021a. BDMEP - Banco de Dados Meteorológicos para Ensino e Pesquisa. URL. https://bdmep.inmet.gov.br/ (accessed 7.6.21).

INMET, 2021b. Normais climatológicas do Brasil. URL. https://portal.inmet.gov.br/normais (accessed 2.14.21).

IPCC, 2014. In: Pachauri, R.K., Meyer, L.A. (Eds.), Climate Change 2014: Synthesis Report, Synthesis Report. Contribution of Working Groups I, II and III to the Fifth Assessment Report of the Intergovernmental Panel on Climate Change [Core Writing Team. Geneva, Switzerland.

Keatinge, W.R., Coleshaw, S.R.K., Easton, J.C., Cotter, F., Mattock, M.B., Chelliah, R., 1986. Increased platelet and red cell counts, blood viscosity, and plasma cholesterol levels during heat stress, and mortality from coronary and cerebral thrombosis. Am. J. Med. 81, 795–800. https://doi.org/10.1016/0002-9343(86)90348-7.

Kenny, G.P., Yardley, J., Brown, C., Mph, R.J.S., Jay, O., 2010. Heat stress in older individuals and patients with common chronic diseases. CMAJ (Can. Med. Assoc. J.) 182, 1053–1060. https://doi.org/10.1503/cmaj.081050.

Koskela, H.O., Koskela, A.K., Tukiainen, H.O., 1996. Bronchoconstriction due to cold weather in COPD * the roles of direct airway effects and cutaneous reflex mechanisms. Chest 110, 632–636. https://doi.org/10.1378/chest.110.3.632.

Lee, W., Choi, H.M., Lee, J.Y., Kim, D.H., Honda, Y., Kim, H., 2018. Temporal changes in mortality impacts of heat wave and cold spell in Korea and Japan. Environ. Int. 116, 136–146. https://doi.org/10.1016/j.envint.2018.04.017.

Marinho, F., de Azeredo Passos, V.M., Carvalho Malta, D., Barboza França, E., Abreu, D. M.X., Araújo, V.E.M., Bustamante-Teixeira, M.T., Camargos, P.A.M., da Cunha, C.C., Duncan, B.B., Felisbino-Mendes, M.S., Guerra, M.R., Guimaraes, M.D.C., Lotufo, P. A., Marcenes, W., Oliveira, P.P.V., de Moares Pedroso, M., Ribeiro, A.L., Schmidt, M. I., Teixeira, R.A., Vasconcelos, A.M.N., Barreto, M.L., Bensenor, I.M., Brant, L.C.C., Claro, R.M., Costa Pereira, A., Cousin, E., Curado, M.P., dos Santos, K.P.B., Faro, A., Ferri, C.P., Furtado, J.M., Gall, J., Glenn, S.D., Goulart, A.C., Ishitani, L.H., Kieling, C., Ladeira, R.M., Machado, I.E., Martins, S.C.O., Martins-Melo, F.R., Melo, A.P.S., Miller-Petrie, M.K., Mooney, M.D., Nunes, B.P., Palone, M.R.T., Pereira, C.C., Rasella, D., Ray, S.E., Roever, L., de Freitas Saldanha, R., Santos, I.S., Schneider, I.J.C., Santos Silva, D.A., Silveira, D.G.A., Soares Filho, A.M., Moraes Sousa, T.C., Szwarcwald, C.L., Traebert, J., Velasquez-Melendez, G., Wang, Y.P., Lozano, R., Murray, C.J.L., Naghavi, M., 2018. Burden of disease in Brazil, 1990–2016: a systematic subnational analysis for the global burden of disease study 2016. Lancet 392, 760–775. https://doi.org/10.1016/S0140-6736(18)31221-2.

Meehl, G.A., Tebaldi, C., 2004. More intense , more frequent , and longer lasting heat waves in the 21st century. Science 84 305, 994–998. https://doi.org/10.1126/science.1098704.

Monteiro, A., Carvalho, V., Góis, J., Sousa, C., 2013. Use of " Cold Spell " indices to quantify excess chronic obstructive pulmonary disease (COPD) morbidity during winter (November to March 2000 – 2007): case study in Porto. Int. J. Biometeorol. 857–870. https://doi.org/10.1007/s00484-012-0613-z.

Perkins, S.E., Alexander, L.V., Nairn, J.R., 2012. Increasing frequency, intensity and duration of observed global heatwaves and warm spells. Geophys. Res. Lett. 39, 1–5. https://doi.org/10.1029/2012GL053361.

R Core Team, 2019. R: A Language and Environment for Statistical Computing.

Robine, J.M., Cheung, S.L.K., Le Roy, S., Van Oyen, H., Griffiths, C., Michel, J.P., Herrmann, F.R., 2008. Death toll exceeded 70,000 in Europe during the summer of 2003. Comptes Rendus Biol. 331, 171–178. https://doi.org/10.1016/j.crvi.2007.12.001.

Robinson, P.J., 2001. On the definition of a heat wave. J. Appl. Meteorol. 40, 762–775. https://doi.org/10.1175/1520-0450(2001)040<0762:OTDOAH>2.0.CO;2.

Rogers, R.G., Everett, B.G., Onge, J.M.S., Krueger, P.M., 2010. Social, behavioral, and biological factors, and sex differences in mortality. Demography 47, 555–578. https://doi.org/10.1353/dem.0.0119.

Sera, F., Armstrong, B., Tobias, A., Vicedo-Cabrera, A.M., Åström, C., Bell, M.L., Chen, B. Y., De Sousa Zanotti Stagliorio Coelho, M., Correa, P.M., Cruz, J.C., Dang, T.N., Hurtado-Diaz, M., Do Van, D., Forsberg, B., Guo, Y.L., Guo, Y., Hashizume, M., Honda, Y., Iñiguez, C., Jaakkola, J.J.K., Kan, H., Kim, H., Lavigne, E., Michelozzi, P., Ortega, N.V., Osorio, S., Pascal, M., Ragettli, M.S., Ryti, N.R.I., Saldiva, P.H.N., Schwartz, J., Scortichini, M., Seposo, X., Tong, S., Zanobetti, A., Gasparrini, A., 2019. How urban characteristics affect vulnerability to heat and cold: a multi-

country analysis. Int. J. Epidemiol. 48, 1101–1112. https://doi.org/10.1093/ije/dyz008.

Song, X., Wang, S., Li, T., Tian, J., Ding, G., Wang, Jiaxin, Wang, Jiexin, Shang, K., 2018. The impact of heat waves and cold spells on respiratory emergency department visits in Beijing, China. Sci. Total Environ. 615, 1499–1505. https://doi.org/10.1016/j.scitotenv.2017.09.108.

Tan, J., Zheng, Y., Tang, X., Guo, C., Li, L., Song, G., Zhen, X., Yuan, D., Kalkstein, A.J., Li, F., Chen, H., 2010. The urban heat island and its impact on heat waves and human health in Shanghai. Int. J. Biometeorol. 54, 75–84. https://doi.org/10.1007/s00484-009-0256-x.

Tansey, E.A., Johnson, C.D., 2015. Recent advances in thermoregulation. Adv. Physiol. Educ. 39, 139–148. https://doi.org/10.1152/advan.00126.2014.

Tong, S., Wang, X.Y., Yu, W., Chen, D., Wang, X., 2013. The impact of heatwaves on mortality in Australia: a multicity study. BMJ Open 4, 1–6. https://doi.org/10.1136/bmjopen-2013-003579.

van Steen, Y., Ntarladima, A.M., Grobbee, R., Karssenberg, D., Vaartjes, I., 2019. Sex differences in mortality after heat waves: are elderly women at higher risk? Int. Arch. Occup. Environ. Health 92, 37–48. https://doi.org/10.1007/s00420-018-1360-1.

Vasconcelos, J., Freire, E., Almendra, R., Silva, G.L., Santana, P., 2013. The impact of winter cold weather on acute myocardial infarctions in Portugal. Environ. Pollut. 183, 14–18. https://doi.org/10.1016/j.envpol.2013.01.037.

Wang, L., Liu, T., Hu, M., Zeng, W., Zhang, Y., Rutherford, S., Lin, H., Xiao, J., Yin, P., Liu, J., Chu, C., Tong, S., Ma, W., Zhou, M., 2016. The impact of cold spells on mortality and effect modification by cold spell characteristics. Sci. Rep. 6, 1–10. https://doi.org/10.1038/srep38380.

WHO, 2021. Fact sheets - WHO. (Accessed 8 June 2021).

Yang, J., Yin, P., Sun, J., Wang, B., Zhou, M., Li, M., Tong, S., Meng, B., Guo, Y., Liu, Q., 2019. Heatwave and mortality in 31 major Chinese cities: definition, vulnerability and implications. Sci. Total Environ. 649, 695–702. https://doi.org/10.1016/j.scitotenv.2018.08.332.

Yin, P., Chen, R., Wang, L., Liu, C., Niu, Y., Wang, W., Jiang, Y., Liu, Y., Liu, J., Qi, J., You, J., Zhou, M., Kan, H., 2018. The added effects of heatwaves on cause-specific mortality: a nationwide analysis in 272 Chinese cities. Environ. Int. 121, 898–905. https://doi.org/10.1016/j.envint.2018.10.016.

Zhao, Q., Li, S., Coelho, M.S.Z.S., Saldiva, P.H.N., Hu, K., Huxley, R.R., Abramson, M.J., Guo, Y., 2019. The association between heatwaves and risk of hospitalization in Brazil: a nationwide time series study between 2000 and 2015. PLoS Med. 16, 1–16. https://doi.org/10.1371/journal.pmed.1002753.

Update

International Journal of Hygiene and Environmental Health
Volume 247, Issue , January 2023, Page

DOI: https://doi.org/10.1016/j.ijheh.2022.113952

International Journal of Hygiene and Environmental Health 247 (2023) 113952

Contents lists available at ScienceDirect

International Journal of Hygiene and Environmental Health

journal homepage: www.elsevier.com/locate/ijheh

Corrigendum to "Impact of heat waves and cold spells on cause specific mortality in the city of São Paulo, Brazil" [Int. J. Hyg. Environ. Health 239 (2022), 113861]

Sara Lopes de Moraes [a,b,*], Ricardo Almendra [c], Ligia Vizeu Barrozo [a,b]

[a] Department of Geography, School of Philosophy, Literature and Human Sciences, University of São Paulo, São Paulo, SP, Brazil
[b] Institute of Advanced Studies, University of São Paulo, São Paulo, SP, Brazil
[c] Centre of Studies on Geography and Spatial Planning (CEGOT), Department of Geography and Tourism, University of Coimbra, Coimbra, Portugal

The authors regret that in Fig. 3 title text "* The confidence interval is not represented in the graph for better visualization of the other RRs. Confidence intervals are presented in Supplementary Table 1." is incorrectly shown as Supplementary Table 1. It should be corrected to "* The confidence interval is not represented in the graph for better visualization of the other RRs. Confidence intervals are presented in **Supplementary Table 2**"

Figs. 2 and 4 legends indicate the heat wave models as HW_92P_2d, HW_92P_3d, HW_92P_4d, HW_97P_2d, HW_97P_3d, and HW_97P_4d. It should be updated to: **HW_92.5P_2d, HW_92.5P_3d, HW_92.5P_4d, HW_97.5P_2d, HW_97.5P_3d, and HW_97.5P_4d.**

Corrected figures (legends) as follows:

DOI of original article: https://doi.org/10.1016/j.ijheh.2021.113861.

* Corresponding author. Department of Geography, School of Philosophy, Literature and Human Sciences, University of São Paulo, Cidade Universitária, Avenida Professor Lineu Prestes, 338, 05508-000, São Paulo, SP, Brazil.
E-mail address: sara.moraes@usp.br (S.L. Moraes).

https://doi.org/10.1016/j.ijheh.2022.113952

Available online 15 March 2022

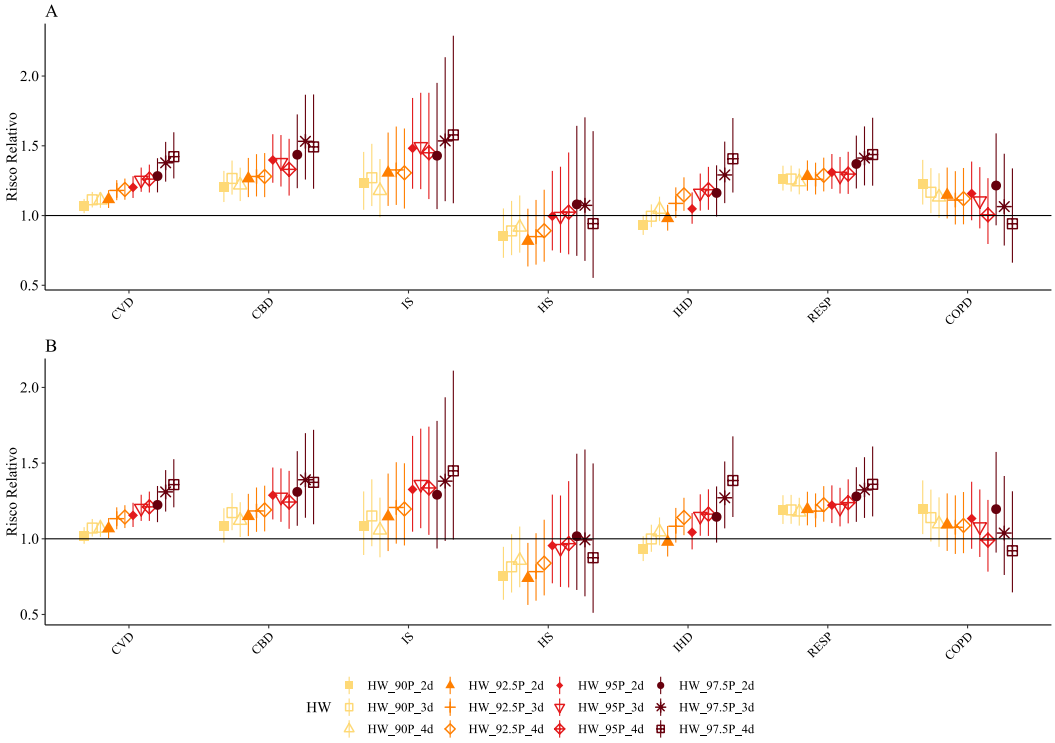

Fig. 2. Effects of heat waves under 12 definitions on mortality due to cardiovascular disease (CVD), cerebrovascular disease (CBD), ischemic stroke (IS), hemorrhagic stroke (HS), ischemic heart disease (IHD), respiratory disease (RESP), and chronic obstructive pulmonary disease (COPD) in people aged ≥65 years over lag 0–10 days in São Paulo. (A) Overall effects of heat waves without controlling for daily mean temperature (B) Added effects of heat waves after controlling for daily mean temperature.

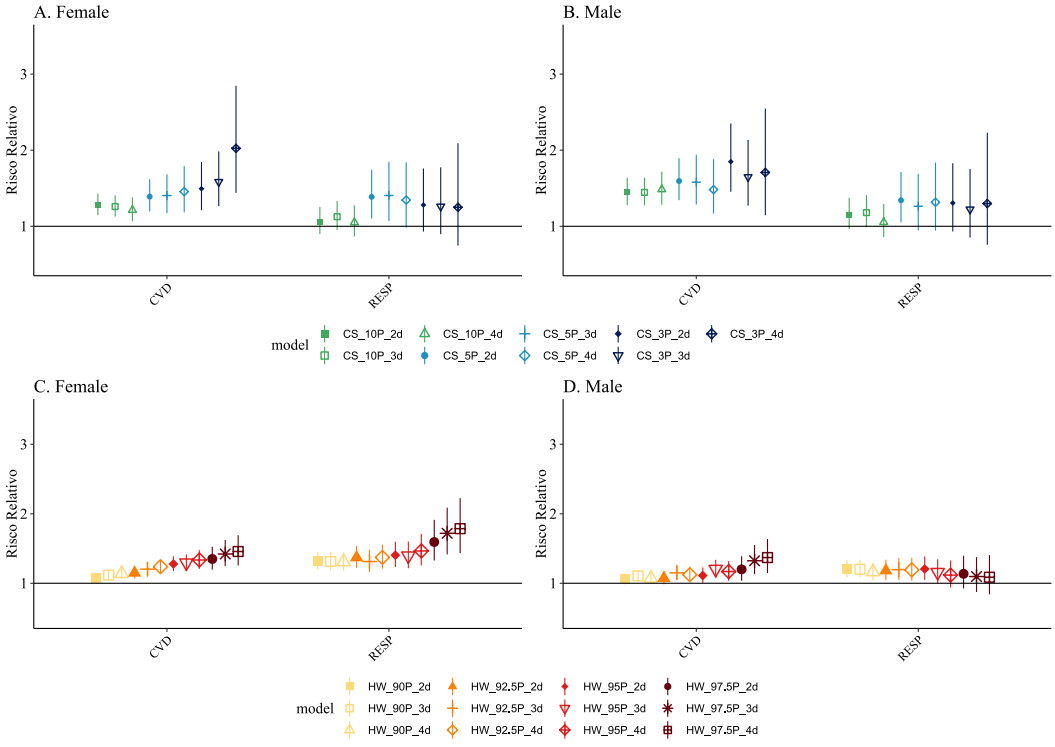

Fig. 4. Effects of cold spells (A and B) and heat waves (C and D) on cardiovascular diseases (CVD) and respiratory diseases (RESP) mortality stratified by sex (women and men).

The results were accurate in the original paper and were not affected by these corrections. The authors would like to apologise for any inconvenience caused.

International Journal of Hygiene and Environmental Health 239 (2022) 113883

Contents lists available at ScienceDirect

International Journal of Hygiene and Environmental Health

journal homepage: www.elsevier.com/locate/ijheh

Is living in a region with high groundwater arsenic contamination associated with adverse reproductive health outcomes? An analysis using nationally representative data from India

Jessie Pinchoff [a,*], Brent Monseur [b], Sapna Desai [c], Katelyn Koons [d], Ruben Alvero [b], Michelle J. Hindin [e]

[a] Population Council, One Dag Hammarskjold Plaza #3, New York, NY, 10017, USA
[b] Stanford University School of Medicine, 1195 W Fremont, Sunnyvale, CA, 94087, USA
[c] Population Council, Zone 5A, Ground Floor India Habitat Centre, Lodi Road, New Delhi, Delhi, 110003, India
[d] Sidney Kimmel Medical College, Thomas Jefferson University, Philadelphia, PA, 19107, USA
[e] Evidence 4 Global Impact, LLC, New Jersey, 07052, USA

ARTICLE INFO

Keywords:
Arsenic
Geospatial
India
Infertility
Reproductive health

ABSTRACT

Background: Exposure to groundwater arsenic via drinking water is common in certain geographies, such as parts of India, and causes a range of negative health effects, potentially including adverse reproductive health outcomes.

Methods: We conducted an ecological analysis of self-reported rates of stillbirth, recurrent pregnancy loss, and infertility in relation to groundwater arsenic levels in India. We used a gridded, modeled dataset of the probability of groundwater arsenic exceeding 10 μg/L (World Health Organization drinking water limit) to calculate mean probabilities at the district level (n = 599 districts). A spatial integration approach was used to merge these estimates with the third India District-Level Health Survey (DLHS-3) conducted in 2007-08 (n = 643,944 women of reproductive age). Maps of district level arsenic levels and rates of each of the three outcomes were created to visualize the patterns across India. To adjust for significant spatial autocorrelation, spatial error models were fit.

Findings: District-level analysis showed that the average level of stillbirth was 4.3%, recurrent pregnancy loss was 3.3%, and infertility was 8.1%. The average district-level probability of groundwater arsenic levels exceeding 10 μg/L was 42%. After adjustment for sociodemographic factors, and accounting for spatial dependence, at the district level, for each percentage point increase in predicted arsenic levels exceeding 10 μg/L increased, the rates of stillbirths was 4.5% higher (95% confidence interval (CI) 2.4–6.6, $p < 0.0001$), the rates of RPL are 4.2% higher (95% CI 2.5–5.9, $p < 0.0001$), and the rates of infertility are 4.4% higher (95% CI 1.2–7.7, p=<0.0001).).

Conclusions: While arsenic exposure has been implicated with a range of adverse health outcomes, this is one of the first population-level studies to document an association between arsenic and three adverse reproductive pregnancy outcomes. The high levels of spatial correlation suggest that further and targeted efforts to mitigate arsenic in groundwater are needed.

1. Background

Arsenic is a naturally occurring chemical element known to be highly toxic in its inorganic form. Natural arsenic contamination of water comes from rocks and sediments in the earth, and manmade contamination comes from industrial activities such as copper mining, when metal is extracted from the ground using heat. The general population is exposed to inorganic arsenic via drinking water and diet (Kumar et al., 2016; Pizent et al., 2012; Yan-Ping et al., 2017). Currently, the World Health Organization (WHO) guidelines on the limit of arsenic in drinking water is held at 10 parts per billion (ppb)(equivalent to 10 μg/L), even though a much lower level has been shown to cause adverse health effects (Lynch et al., 2017; Xu et al., 2020). Chronic arsenic exposure affects multiple organ systems and can be the cause of disorders of the skin and peripheral blood vessels, diabetes, hypertension and a variety of cancers: including skin, bladder, kidney, and lung cancers

* Corresponding author.
E-mail address: jpinchoff@popcouncil.org (J. Pinchoff).

https://doi.org/10.1016/j.ijheh.2021.113883
Received 23 June 2021; Received in revised form 8 November 2021; Accepted 17 November 2021
Available online 24 November 2021

Table 1
District level summary characteristics of survey participants (n = 599).

	Percent or mean	Std Dev	Min	Max
Any stillbirth, %	4.3	2.0	0.3	16.7
2 or more miscarriages, %	3.3	1.4	0	12.1
Any infertility, %	8.2	3.5	0.7	20.7
Arsenic >10 μg/L,%	0.42	0.12	0.18	0.74
Age, years	32.09	1.34	28.87	36.23
Rural, %	77.0	2.0	0	100
Wealth quintile (range 1–5 with 1 = poorest and 5 = richest))	3.2	0.8	1.3	4.9
Educational Attainment (range 0–3 with 0 = none and 3 = more than secondary)	1.2	0.5	0.2	2.5

(Lynch et al., 2017; Mink et al., 2008; Xu et al., 2020).

South and Southeast Asia are considered the most arsenic-polluted areas, including regions of India and Bangladesh (Ravenscroft et al., 2011). Other areas known to have high levels of arsenic contamination in drinking water include Chile, Mexico, China, Argentina, Pakistan, Cambodia, Vietnam, and regions across the United States of America (USA), affecting more than 150 million people worldwide Recent estimates suggest up to 220 million people (Podgorski and Berg, 2020) have exposure to arsenic contamination, with almost all (up to 95%) of residing in Asia. However, arsenic is not routinely included in water quality testing parameters and is not detected by human senses, making it challenging to understand the scale of the problem (Podgorski and Berg, 2020). While the presence of arsenic hazards in groundwater has been documented since the 1980s, it remains an understudied health issue in many regions.

Parts of India and Bangladesh have some of the highest levels of groundwater arsenic detected in drinking water, and a large population residing in these areas (Rahman et al., 2001). Communities rely on tube wells and hand pumps that access groundwater used for drinking and cooking. In India, more than 85% of drinking water comes from groundwater (Shrivastava, 2016). India's National Drinking Water Program aims to provide safe water to rural households by 2024; the program aims to improve quality in the long-term through piped water supply as well as technological interventions for potable water ("Jal Jeevan Mission," n.d.). In the short-term, central guidelines recommend installation of community water purification plants in arsenic-affected habitats for safe basic drinking and cooking water (National Water Quality Sub-Mission Revised Guidelines, n.d.). For example, West Bengal has invested in several water treatment plants over the past fifteen years, resulting in gradual improvements in the proportion of the population covered by piped water supply ("Public Health Engineering Department," n.d.).

Studies have suggested arsenic exposure is associated with a range of adverse reproductive health (RH) outcomes, and birth outcomes as inorganic arsenic can cross the placenta (Milton et al., 2017; Quansah et al., 2015). Documented adverse RH outcomes such as spontaneous abortion (<20 weeks gestational age), stillbirth (≥28 weeks gestational age, per WHO definition), low birthweight (<2500 g), and infant mortality suggesting multifactorial insults to the reproductive system (Milton et al., 2017; Mohammed Abdul et al., 2015; Quansah et al., 2015). For stillbirth, studies have found that even after adjustment for many socioeconomic characteristics, the risk of stillbirth is raised and increases with increasing levels of groundwater arsenic (Cherry et al., 2008; von Ehrenstein et al., 2006). Recurrent pregnancy loss (RPL), defined as two or more spontaneous abortions, affects ~5% of the population; however, clinical workups only uncovers a cause in about half of cases. Environmental exposures such as arsenic with its known association with any spontaneous abortion may have a causal role in cases of unknown etiology. More recently, some work has suggested arsenic exposure may be linked with infertility. Several small case control studies, particularly from China, have suggested an association between exposure to groundwater arsenic and infertility, potentially through oxidative stress and reported decreased sperm quality after arsenic exposure (Shen et al., 2013; Susko et al., 2017; Wang et al., 2016). Overall however the mechanisms for arsenic-induced adverse RH outcomes are not well known. In addition, most research on population-level variation in adverse RH outcomes has largely focused on demographic characteristics, with more recent recognition of the potential role of factors such as pollution, climate change, and other related environmental causes (Sorensen et al., 2018).

For this analysis, we examine adverse RH outcomes using data from the female respondents in India's nationally representative District Level Health Survey, Round 3 (DLHS=3). Modeled, gridded groundwater arsenic dataset to 1 km spatial resolution were joined with the DLHS-3 data to assess district-level associations. We hypothesized that we would find evidence in support of known associations between arsenic exposure and stillbirths, as well as with the more novel outcomes of RPL and infertility.

2. Methods

2.1. Surveys and populations

The District Level Household and Facility Survey (DLHS) is a nationally representative survey and one of the largest sources of health data in India. To date, there have been four 'waves' of data collection (first collected in 1998-99) (District Level Household and Facility Survey (DLHS-3) under Reproductive and Child Health Project (2007-08), n.d.). The DLHS collects data from households, ever married women as well as from villages (availability of services) and health facilities. The DLHS uses a multi-stage stratified sampling design, with 1000-1500 households per district (for more details on survey methodology, see the full report (International Institute for Population Sciences (IIPS), 2010). In the third wave (DLHS-3), from 2007 to 2008, the household response rate was 93% overall, and the ever-married woman response rate was 89%. All waves of the DLHS include a women's questionnaire that includes self-reported information on reproductive health, and maternal and child health, while only round 3 includes a module of questions regarding infertility.

2.2. Key measures

Three outcome variables comprise our analysis of "adverse reproductive health outcomes". From women's reports of their pregnancy histories, we created a variable indicating having had one or more stillbirth (defined as pregnancy ending at ≥28 weeks gestation), or recurrent pregnancy loss (RPL) (defined as two or more spontaneous abortions), and women's reports of experiencing any infertility, based on the question "In every place there are couples who want children but some women do not get pregnant. Did you face any such problem in getting pregnant?". Women who answered yes to this question were considered to have had experienced infertility. Each measure, when aggregated to the district level, is the proportion of women surveyed in that district that reported experiencing each outcome.

The key independent variable was a measure of groundwater arsenic. Groundwater arsenic measures are challenging particularly for a population-based study, since this would require many water samples over a very large geographic area. A recently published global analysis used data from over 80 previous studies (comprised of over 50,000 aggregated data points of measured groundwater arsenic concentration) and additional environmental variables (e.g., soil pH) to train a machine learning model using the random forest method to predict where groundwater arsenic exceeds 10 μg/L(Podgorski and Berg, n.d.) The prediction groundwater arsenic dataset is available at 1 km^2 grid cell resolution and freely available with the final dataset published in 2020. For India specifically, a total of 145,099 geographically distinct arsenic concentration measurements in groundwater were assembled from over

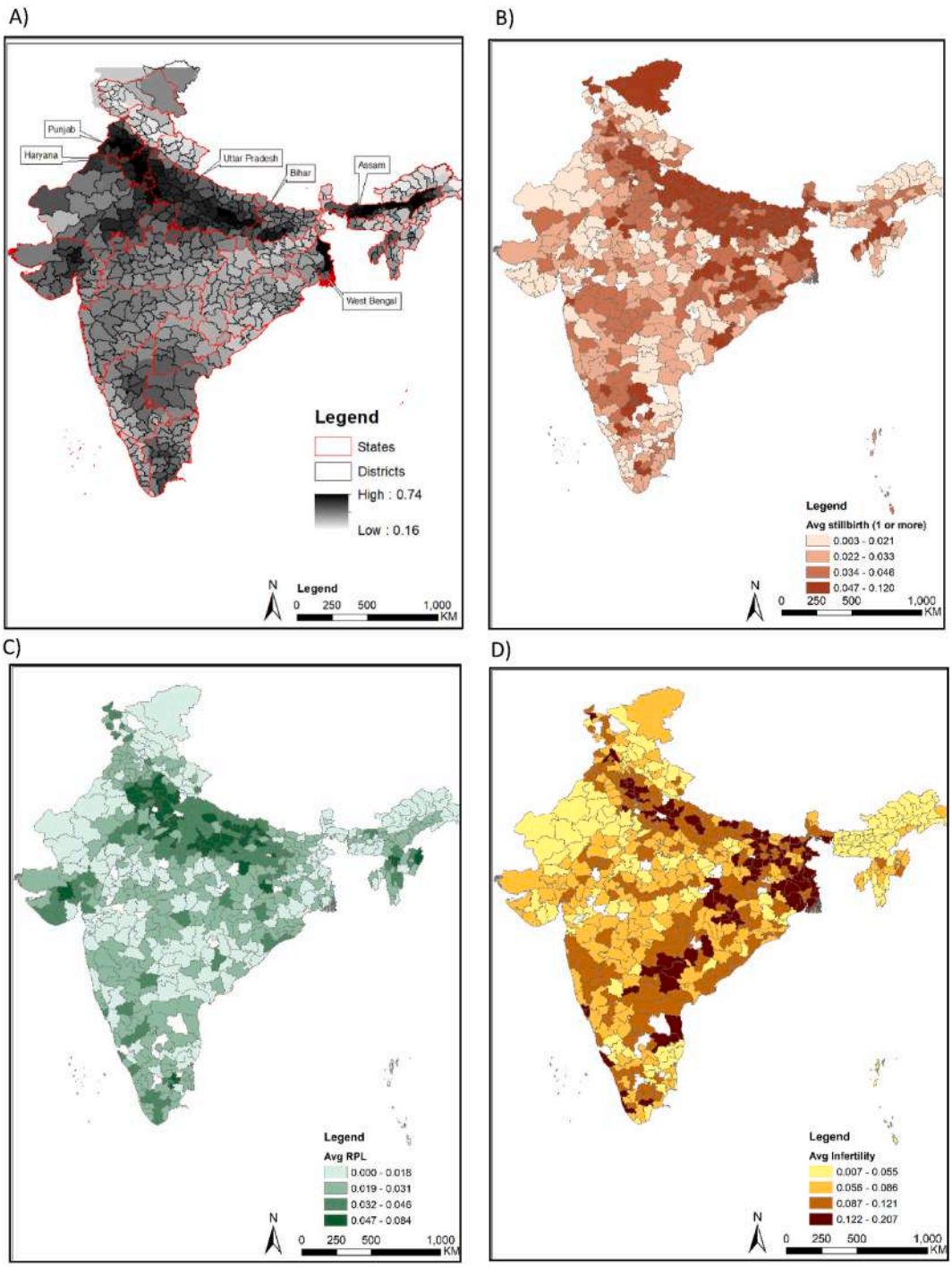

Fig. 1. Four panels showing district level: A) predicted probability groundwater arsenic levels>10 μg/L; B) average stillbirths (one or more); C) average RPL; and D) average infertility.

30 sources, mainly from India but also nearby Bangladesh, Nepal, and Pakistan (Podgorski et al., 2020). The underlying datasets for India range from 2005 to 2018. The arsenic modeled dataset is gridded, so these grid cells were overlaid with Indian district administrative boundaries from 2008 to match the DLHS-3 districts. The arsenic dataset was aggregated to the district level using the Zonal Statistics tool (extracting the average, minimum, maximum pixel values that cross each district polygon) in ArcGIS version 10.4.1 (ESRI, Redlands, CA).

2.3. Data analysis

First, we ran linear OLS regression models to explore the relationship between arsenic and the three RH outcomes, adjusting for sociodemographic variables. We adjusted models for covariates that were available in the DLHS-3, and known to be associated with adverse RH outcomes. These included age in years, educational attainment (0 = no formal schooling, 1 = some primary to completed primary, 2 = some secondary to completed secondary, 3 = greater than secondary), household wealth (categorized into quintiles from poorest to richest), and a variable for proportion rural (vs urban). We explored the data at the district level

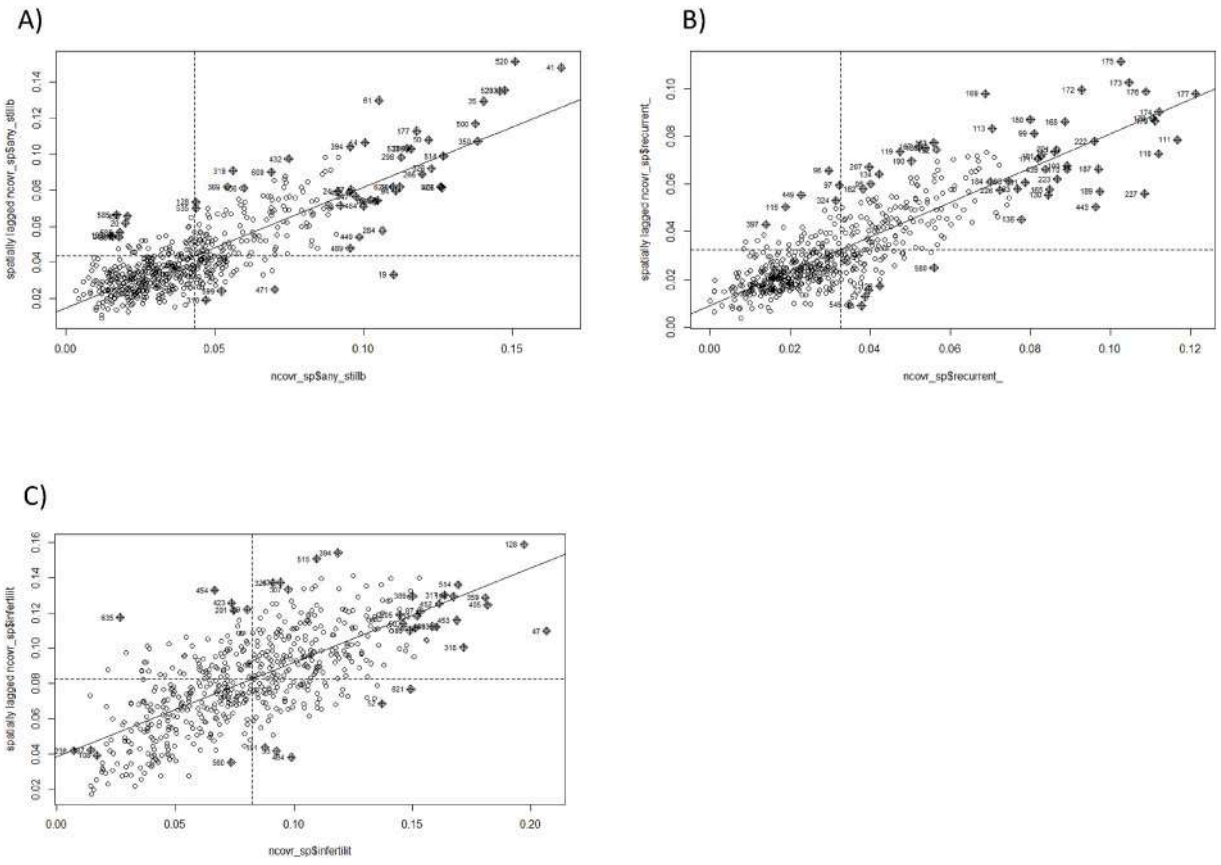

Fig. 2. Local Morans I scatterplots for each outcome: A) average stillbirths (one or more); B) average RPL, C) average infertility (primary or secondary).

across these characteristics.

Second, we took steps to determine the degree of spatial autocorrelation in the data. The dataset was exported to R for spatial analysis. Moran's I statistics were calculated to determine the degree of spatial autocorrelation in the outcomes of interest. A high degree of autocorrelation was detected, implying that neighboring districts are more similar to nearby districts, than would be expected at random. It is critical to account for spatial autocorrelation otherwise standard errors can be underestimated leading to inaccurate results due to underestimation of standard errors. Bivariate and adjusted models were constructed, and the global Moran's I implemented to detect the overall spatial clustering of the models (Moran, 1950). The local Moran's I statistics were then calculated, providing a clustering value for each individual district, by comparing each district to its neighboring districts. The results were plotted and mapped in local indicators of spatial association (LISA) maps to identify districts with clustering of high or low value districts for each outcome (high-high suggests the district has a higher than expected value, and its neighboring districts do also). Based on the significant spatial autocorrelation detected, the third and final step of data analysis was to fit spatial error models (SEM). SEMs are a linear regression model with a spatial autoregressive error term. The final models also adjust for all sociodemographic variables. We fit three separate SEMs for self-reported stillbirth, RPL and infertility as the outcomes and present both unadjusted and adjusted estimates.

3. Results

A total of 643,944 women ages 15–49 were included in the analysis, aggregated to the district level (n = 599). Table 1 shows the district-level range of key characteristics in the analysis. The average district proportion of women experiencing at least one stillbirth was 4.3% (range 0.3–16.7%), the average district proportion of women experiencing RPL was 3.3% (range 0.0–12.1%), and any infertility was 8.1% (range 0.7–20.7%). The predicted probability of arsenic >10 μg/L at the district level was 0.43, ranging from 0.18 to 74.0. Most of the women sampled in each district were rural (77%), the average district-level wealth was 3.2 (just over neither rich or poor), and the level of educational attainment was 1.2 (slightly more than some primary education).

The maps in Fig. 1 show the spatial distribution of the independent variable, the probability of arsenic in the groundwater above the WHO 10 μg/L cutoff (Panel A) and the average district-level rate of stillbirth (Panel B), RPL (Panel C), and infertility (Panel D). Panel A highlights the regions with the highest probability of groundwater arsenic above the 10 μg/L cutoff including in eastern (Bihar, Jharkand and West Bengal) and northern states (Uttar Pradesh, Haryana and Punjab). Panels B–D show the average district-level rates of any stillbirth, RPL, and infertility presented in quartiles. Any stillbirth and RPL follow a very similar pattern, with the highest district level rates reported in Bihar, Uttar Pradesh, and districts in Rajasthan. For infertility, rates were highest in West Bengal Bihar, Uttar Pradesh and Chhattisgarh, along with southern states of Andhra Pradesh and Telangana. The maps suggest a spatial pattern for both the RH outcomes and for arsenic.

To assess whether there was significant spatial autocorrelation of the outcomes, global and local Moran's I estimates were calculated. The global Moran's I value for stillbirth was 0.670 ($p < 0.0001$), for RPL was 0.719 ($p < 0.0001$), and for infertility was 0.536 ($p < 0.0001$) suggesting spatial autocorrelation. Fig. 2 presents local Moran's I scatterplots for stillbirth (Panel A), RPL (panel B), and infertility (panel C). While the global Moran's I shows significant spatial autocorrelation, it does not identify the location of clusters. Fig. 3 presents local indicator of spatial association (LISA) maps, depicting the degree of spatial clustering of local Moran's I values for each district. The LISA maps highlight the locations of clusters of districts that have higher or lower than expected rates of each outcome (compared to what would be expected at

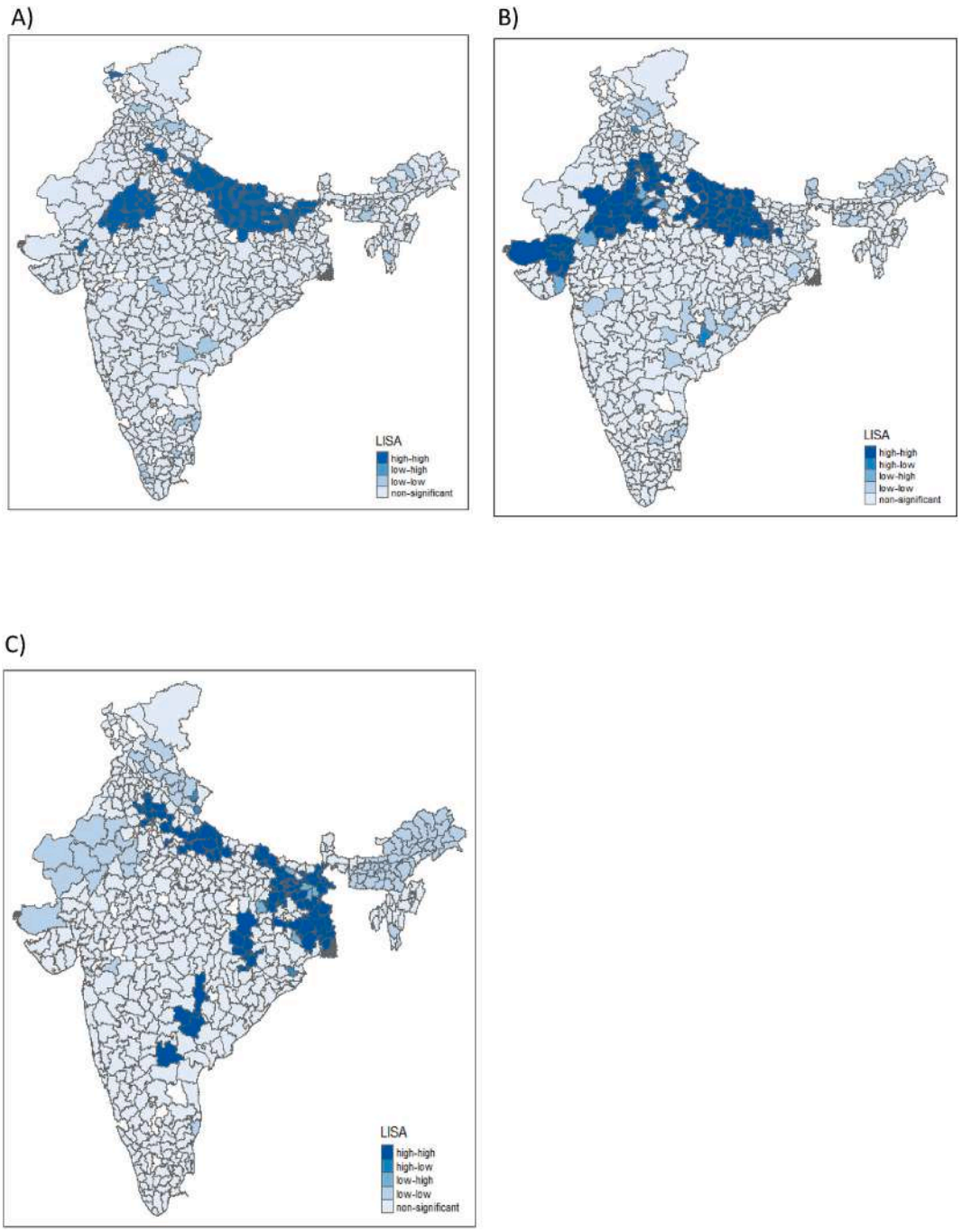

Fig. 3. Local indicators of spatial association (LISA) maps for each outcome highlighting clusters of higher than expected or lower than expected rates of the following outcomes: A) average stillbirths (one or more); B) average RPL, C) average infertility (primary or secondary).

random) to show regions with high or low values that are of interest.

Table 2 shows the unadjusted and adjusted spatial error model results which present the association between arsenic and each of the three adverse reproductive health outcomes. Adjusted models were adjusted for age, wealth quintile, educational attainment, and urban or rural residence. As there is no evidence of substantial attenuation or interactions, we focus on the adjusted models. We find that for all outcomes, in districts with a higher predicted level of arsenic in the groundwater, the average rate of adverse RH outcomes is statistically significantly higher. At the district level, for each percentage point increase in the predicted probability of arsenic in groundwater being greater than 10 μg/L, of the rates of stillbirths are 4.5% higher (95% confidence interval 2.4–6.6, $p < 0.0001$), the rates of RPL are 4.2% higher (95% CI 2.5–5.9, $p < 0.0001$), and the rates of infertility are 4.4% higher (95% CI 1.2–7.7, p=<0.0001). We also find that wealthier districts had a higher proportion of women reporting infertility (1.1%, 95% CI 0.4–1.8, $p = 0.002$) and that districts higher levels of educational attainment had significantly lower rates of stillbirth (−2.6%, 95 CI -4.1 to −1.2, $p < 0.0001$) and infertility (−3.8%, 95% CI -6.2 to −1.5, $p = 0.001$) (Table 2). The spatial autocorrelation coefficient (λ) for all three adjusted SEM models highlight the significant spatial variation in the models.

4. Discussion

Our study supports recent literature that has reported an association

Table 2
Unadjusted (bivariate) and adjusted spatial error model results for effects of district level groundwater arsenic probability of exceeding 10 μg/L on three RH outcomes of interest.

	Stillbirth		RPL		Infertility	
	Unadjusted SEM	Adjusted SEM	Unadjusted SEM	Adjusted SEM	Unadjusted SEM	Adjusted SEM
	β/(95% CI)	β/(95% CI)	β/(95% CI)	β/(95% CI)	β/(95% CI)	β/(95% CI)
Arsenic >10 μg/L	0.044***	0.045***	0.042***	0.042***	0.051**	0.044**
	(0.023, 0.066)	(0.024, 0.066)	(0.026, 0.059)	(0.025, 0.059)	(0.019, 0.083)	(0.012, 0.077)
Age	−0.003**	−0.001	0.001	0.001	−0.003*	−0.003
	(−0.005, −0.002)	(−0.003, 0.001)	(−0.001, 0.001)	(−0.002, 0.001)	(−0.006, 0.000)	(−0.006, 0.000)
Rural (vs Urban)	0.011*	−0.006	−0.001	0.001	0.005	0.004
	(0.003, 0.019)	(−0.017, 0.006)	(−0.007, 0.005)	(−0.008, 0.010)	(−0.008, 0.018)	(−0.014, 0.022)
Wealth	−0.005***	−0.001	0.002	0.002	0.011***	0.011**
	(−0.008, −0.002)	(−0.006, 0.003)	(−0.001, 0.004)	(−0.001, 0.006)	(0.004, 0.018)	(0.004, 0.018)
Educational attainment	−0.028***	−0.026**	0.001	−0.003	−0.02*	−0.038**
	(−0.038, −0.017)	(−0.041, −0.012)	(−0.007, 0.009)	(−0.014, 0.008)	(−0.036, −0.003)	(−0.062, −0.015)
Spatial Autocorrelation (λ)		0.81		0.81		0.71

Note: Adjusted models include all covariates shown in the table.
*p < 0.05; **p < 0.01; ***p < 0.001.

between arsenic exposure and stillbirth. Further, we identified a strong relationship between arsenic and RPL and infertility. While the link between arsenic and infertility has been suggested in rodent models and small case studies, this is the first documentation of this potential association using nationally representative data of women's reports of difficulty conceiving. Our findings highlight the strong spatial association in the adverse RH outcomes, aligned closely with the spatial distribution of arsenic at the district-level.

Our study is one of the first national and district-level analyses of the association between living in an area with high levels of groundwater arsenic contamination, and adverse RH outcomes. Our study is strengthened by a very large, nationally representative survey that measures multiple outcomes. While the DLHS-3 data was collected in 2007-08, it is one of the only large-scale surveys that asks women to directly report on their experiences in having had difficulty conceiving. This study also leverages a newly published model that predicts fine-scale geographic arsenic contamination in groundwater (Podgorski and Berg, n.d.). Our spatial integration approach is a unique approach to link datasets that capture silo-ed health or environment information. This spatial approach can be replicated in other settings, with available survey data using either GPS coordinates or matched administrative areas (e.g., districts).

Our findings suggest one possible explanation for previously established, yet puzzling geographic variation in infertility concentrated along parts of the Gangetic basin (Patra and Unisa, 2017). Geographic variation in adverse reproductive health outcomes warrants deeper examination of a wider range of environmental determinants at both the state and district level. Treatment for infertility, particularly assisted reproductive technology, is growing rapidly in India's private sector. In addition to policy efforts to regulate such services, heightened focus on identifying and addressing potential underlying determinants, such as arsenic, will be critical for prevention. Similarly, the uneven burden of adverse reproductive health outcomes requires targeted state-level public health responses, particularly strengthening resources in the district public health system (Patra and Unisa, 2017).

Rigorous data and evidence on environmental determinants of reproductive health are generally challenging to identify in low- and middle-income country settings. A population-based, prospective cohort study of almost 3000 women in Matlab, Bangladesh evaluated urinary arsenic levels and several adverse RH outcomes. They found an increased risk of infant mortality, spontaneous abortion, and stillbirth with increasing exposure to arsenic (Rahman et al., 2010). Several other studies from the region have also reported an association of arsenic exposure with spontaneous abortion and stillbirth, with about 2–3 times higher risks among women with high arsenic concentrations in their drinking water (>50 μg/L) (Cherry et al., 2008; Milton et al., 2005; von Ehrenstein et al., 2006). A recent publication on infertility in India highlights several potential causes, such as demographic characteristics and obesity, but did not explore arsenic or environmental toxins, and used a different dataset to estimate infertility using indirect methods (Naina Purkayastha and Sharma, 2021). Overall, the region has a high awareness of groundwater arsenic contamination, and several government-funded programs in place to reduce exposure, including increasing access to piped water. Since the 2007-08 DLHS survey used here, there have been improvements; conducting a future analysis with up-to-date information on both RH outcomes, infertility, and arsenic exposure (including drinking water sources) would provide additional insight into this issue, and whether it has resolved somewhat due to improved conditions.

This study has several limitations. First, it is an ecological analysis, which allows for presentation of associations but not causality. Second, the nature of our data sources require the unit of analysis to be districts, preventing the reporting of data at the individual level. Additionally, the DLHS-3 did not collect water samples, so we rely on the gridded groundwater arsenic dataset to approximate exposure. With only the single time point survey for the adverse RH outcomes, we cannot show temporality. Relatedly, we did not have information on how long the woman had resided in the district at the time of the survey, so it is not possible to measure duration of exposure. Third, while the RH outcomes reported in the DLHS-3 survey are comprehensive they are self-reported. The sociodemographic variables in our analyses are also limited and some individual level risk factors that may be associated with the outcomes, such as tobacco use, were not collected. Lastly, the survey data are older, but unique in their direct assessment of difficulty conceiving in a region that has not historically assessed this metric. And while the arsenic dataset is newer, it is based on estimates of groundwater arsenic, and does not account for interventions to treat water or close high risk tube wells; data collected from in-use water sources may provide better estimates of exposure.

Despite these limitations, we provide evidence for a strong association between arsenic exposure and adverse RH outcomes using a unique combination of datasets. Based on our results, we suggest furthering efforts to mitigate arsenic exposure, which remains high despite awareness of the multitude of health problems arsenic in drinking water is likely cause. Exposure to toxic environmental agents is nearly ubiquitous, however, some areas and populations face heightened exposure and risk ("Exposure to Toxic Environmental Agents," n.d.). Overall, vulnerable and underserved populations remain disproportionately affected. Our results find that even adjusting for income, or educational attainment, the effects of arsenic are still significant. Professional organizations such as the International Federation of Gynecology and Obstetrics have released statements advocating for policy to prevent

exposure to toxic environmental contaminants, and to ensure access to a healthy food system inclusive of drinking water free of toxic chemicals ("Exposure to Toxic Environmental Agents," n.d.). Numerous organizations in the field of reproductive medicine have called for action to achieve environmental justice by identifying and reducing exposure to environmental toxins while addressing the consequences of this exposure ("Exposure to Toxic Environmental Agents," n.d.). Climate change may exacerbate some of these exposures. Given the potential harm from environmental toxins, we hope this novel methodology will be replicated to explore associations between adverse health outcomes and environmental toxins broadly across the globe.

Declaration of interests

None declared.

Author contributions

JP conceptualized the study, designed and conducted the data analysis, and drafted the manuscript.

BM conceptualized the study, conducted review of the literature, and supported with drafting and revision of the manuscript.

KK conducted review of the literature and revision of the manuscript.

SD supported with review of the literature, study design, review of key literature, and supported with drafting and revision of the manuscript.

RA critically reviewed the drafting and revisions of the manuscript.

MJH conceptualized the study, informed the design and analysis of the data, and reviewed the manuscript.

JP and MJH verified the underlying data.

Data sharing

All data are publicly available; no primary data collection was collected for this analysis.

References

Cherry, N., Shaikh, K., McDonald, C., Chowdhury, Z., 2008. Stillbirth in rural Bangladesh: arsenic exposure and other etiological factors: a report from Gonoshasthaya Kendra. Bull. World Health Organ. 86, 172–177. https://doi.org/10.2471/blt.07.043083.

District Level Household And Facility Survey (DLHS-3) under Reproductive and Child Health Project (2007-08), n.d. . International Institute for Population Sciences (IIPS), Mumbai, India.

Exposure to Toxic Environmental Agents [WWW Document], n.d. URL. https://www.acog.org/en/clinical/clinical-guidance/committee-opinion/articles/2013/10/exposure-to-toxic-environmental-agents. accessed 3.23.21.

International Institute for Population Sciences (IIPS), 2010. District Level Household and Facility Survey 2007-08: India. IIPS, Mumbia, India.

Jal Jeevan Mission [WWW Document], n.d. URL. https://jaljeevanmission.gov.in/. accessed 1.22.21.

Kumar, M., Rahman, M.M., Ramanathan, A.L., Naidu, R., 2016. Arsenic and other elements in drinking water and dietary components from the middle Gangetic plain of Bihar, India: health risk index. Sci. Total Environ. 539, 125–134. https://doi.org/10.1016/j.scitotenv.2015.08.039.

Lynch, H.N., Zu, K., Kennedy, E.M., Lam, T., Liu, X., Pizzurro, D.M., Loftus, C.T., Rhomberg, L.R., 2017. Quantitative assessment of lung and bladder cancer risk and oral exposure to inorganic arsenic: meta-regression analyses of epidemiological data. Environ. Int. 106, 178–206. https://doi.org/10.1016/j.envint.2017.04.008.

Milton, A.H., Hussain, S., Akter, S., Rahman, M., Mouly, T.A., Mitchell, K., 2017. A review of the effects of chronic arsenic exposure on adverse pregnancy outcomes. Int. J. Environ. Res. Publ. Health 14. https://doi.org/10.3390/ijerph14060556.

Milton, A.H., Smith, W., Rahman, B., Hasan, Z., Kulsum, U., Dear, K., Rakibuddin, M., Ali, A., 2005. Chronic arsenic exposure and adverse pregnancy outcomes in Bangladesh. Epidemiology 16, 82–86. https://doi.org/10.1097/01.ede.0000147105.94041.e6.

Mink, P.J., Alexander, D.D., Barraj, L.M., Kelsh, M.A., Tsuji, J.S., 2008. Low-level arsenic exposure in drinking water and bladder cancer: a review and meta-analysis. Regul. Toxicol. Pharmacol. 52, 299–310. https://doi.org/10.1016/j.yrtph.2008.08.010.

Mohammed Abdul, K.S., Jayasinghe, S.S., Chandana, E.P.S., Jayasumana, C., De Silva, P. M.C.S., 2015. Arsenic and human health effects: a review. Environ. Toxicol. Pharmacol. 40, 828–846. https://doi.org/10.1016/j.etap.2015.09.016.

Moran, P.A.P., 1950. A test for the serial independence of residuals. Biometrika 37, 178–181. https://doi.org/10.2307/2332162.

Naina, Purkayastha, Sharma, H., 2021. Prevalence and potential determinants of primary infertility in India: evidence from Indian demographic health survey. Clin. Epidemiol. Glob. Health 9, 162–170. https://doi.org/10.1016/j.cegh.2020.08.008.

National Water Quality Sub-Mission Revised Guidelines, n.d.. Government of India, New Delhi, India.

Patra, S., Unisa, S., 2017. Female infertility in India: causes, treatment and impairment of fertility in selected districts with high prevalence. Global J. Med. Publ. Health 6, 1–11.

Pizent, A., Tariba, B., Zivkovic, T., 2012. Reproductive toxicity of metals in men. Arh. Hig. Rad. Toksikol. 63 (Suppl. 1), 35–46. https://doi.org/10.2478/10004-1254-63-2012-2151.

Podgorski, J., Berg, M., 2020. Global threat of arsenic in groundwater. Science 368, 845–850. https://doi.org/10.1126/science.aba1510.

Podgorski, J., Berg, M.. Data for: global threat of arsenic in groundwater. n.d, [WWW Document]. URL. https://opendata.eawag.ch/dataset/global-threat-of-arsenic-in-groundwater. accessed 11.19.20.

Podgorski, J., Wu, R., Chakravorty, B., Polya, D.A., 2020. Groundwater arsenic distribution in India by machine learning geospatial modeling. Int. J. Environ. Res. Publ. Health 17, 7119. https://doi.org/10.3390/ijerph17197119.

Public Health Engineering Department [WWW Document], n.d. URL. http://www.wbphed.gov.in/en/home. accessed 1.22.21.

Quansah, R., Armah, F.A., Essumang, D.K., Luginaah, I., Clarke, E., Marfoh, K., Cobbina, S.J., Nketiah-Amponsah, E., Namujju, P.B., Obiri, S., Dzodzomenyo, M., 2015. Association of arsenic with adverse pregnancy outcomes/infant mortality: a systematic review and meta-analysis. Environ. Health Perspect. 123, 412–421. https://doi.org/10.1289/ehp.1307894.

Rahman, A., Persson, L.-Å., Nermell, B., El Arifeen, S., Ekström, E.-C., Smith, A.H., Vahter, M., 2010. Arsenic exposure and risk of spontaneous abortion, stillbirth, and infant mortality. Epidemiology 21, 797–804. https://doi.org/10.1097/EDE.0b013e3181f56a0d.

Rahman, M.M., Chowdhury, U.K., Mukherjee, S.C., Mondal, B.K., Paul, K., Lodh, D., Biswas, B.K., Chanda, C.R., Basu, G.K., Saha, K.C., Roy, S., Das, R., Palit, S.K., Quamruzzaman, Q., Chakraborti, D.D., 2001. Chronic arsenic toxicity in Bangladesh and West Bengal, India—a review and commentary. J. Toxicol. Clin. Toxicol. 39, 683–700. https://doi.org/10.1081/CLT-100108509.

Ravenscroft, P., Brammer, H., Richards, K., 2011. Arsenic Pollution: A Global Synthesis. John Wiley & Sons.

Shen, H., Xu, W., Zhang, J., Chen, M., Martin, F.L., Xia, Y., Liu, L., Dong, S., Zhu, Y.G., 2013. Urinary metabolic biomarkers link oxidative stress indicators associated with general arsenic exposure to male infertility in a Han Chinese population. Environ. Sci. Technol. 47, 8843–8851. https://doi.org/10.1021/es402025n.

Shrivastava, B.K., 2016. Policy intervention for arsenic mitigation in drinking water in rural habitations in India: achievements and challenges. J. Water Health 14, 827–838. https://doi.org/10.2166/wh.2016.014.

Sorensen, C., Murray, V., Lemery, J., Balbus, J., 2018. Climate change and women's health: impacts and policy directions. PLoS Med. 15 https://doi.org/10.1371/journal.pmed.1002603.

Susko, M.L., Bloom, M.S., Neamtiu, I.A., Appleton, A.A., Surdu, S., Pop, C., Fitzgerald, E. F., Anastasiu, D., Gurzau, E.S., 2017. Low-level arsenic exposure via drinking water consumption and female fecundity - a preliminary investigation. Environ. Res. 154, 120–125. https://doi.org/10.1016/j.envres.2016.12.030.

von Ehrenstein, O.S., Guha Mazumder, D.N., Hira-Smith, M., Ghosh, N., Yuan, Y., Windham, G., Ghosh, A., Haque, R., Lahiri, S., Kalman, D., Das, S., Smith, A.H., 2006. Pregnancy outcomes, infant mortality, and arsenic in drinking water in West Bengal, India. Am. J. Epidemiol. 163, 662–669. https://doi.org/10.1093/aje/kwj089.

Wang, X., Zhang, J., Xu, W., Huang, Q., Liu, L., Tian, M., Xia, Y., Zhang, W., Shen, H., 2016. Low-level environmental arsenic exposure correlates with unexplained male infertility risk. Sci. Total Environ. 571, 307–313. https://doi.org/10.1016/j.scitotenv.2016.07.169.

Xu, L., Mondal, D., Polya, D.A., 2020. Positive association of cardiovascular disease (CVD) with chronic exposure to drinking water arsenic (as) at concentrations below the WHO provisional guideline value: a systematic review and meta-analysis. Int. J. Environ. Res. Publ. Health 17, E2536. https://doi.org/10.3390/ijerph17072536.

Yan-Ping, D., Xiao-Qin, G., Xiao Ping, M., Ying Quan, Y., 2017. Effects of chronic exposure to sodium arsenite on expressions of VEGF and VEGFR2 proteins in the epididymis of rats. BioMed Res. Int. https://doi.org/10.1155/2017/2597256, 2017, 2597256–2597256.

International Journal of Hygiene and Environmental Health 239 (2022) 113867

Contents lists available at ScienceDirect

International Journal of Hygiene and Environmental Health

journal homepage: www.elsevier.com/locate/ijheh

Long-term air pollution, noise, and structural measures of the Default Mode Network in the brain: Results from the 1000BRAINS cohort

Sarah Lucht [a,*], Lina Glaubitz [a], Susanne Moebus [b], Sara Schramm [c], Christiane Jockwitz [d,e], Svenja Caspers [d,e,f,1], Barbara Hoffmann [a,1]

[a] Environmental Epidemiology Group, Institute of Occupational, Social and Environmental Medicine, Centre for Health and Society, Medical Faculty and University Hospital Düsseldorf, Heinrich Heine University Düsseldorf, Düsseldorf, Germany
[b] Institute for Urban Public Health, University Hospital Essen, University of Duisburg-Essen, Essen, Germany
[c] Institute of Medical Informatics, Biometry and Epidemiology, University Hospital Essen, University of Duisburg-Essen, Essen, Germany
[d] Institute of Neuroscience and Medicine (INM-1), Research Centre Jülich, Jülich, Germany
[e] Institute for Anatomy I, Medical Faculty and University Hospital Düsseldorf, Heinrich Heine University Düsseldorf, Düsseldorf, Germany
[f] JARA-BRAIN, Jülich-Aachen Research Alliance, 52425, Jülich, Germany

ARTICLE INFO

Keywords:
Air pollution
Particulate matter
Brain imaging
Brain structure
Cognitive function

ABSTRACT

Background: While evidence suggests that long-term air pollution (AP) and noise may adversely affect cognitive function, little is known about whether environmental exposures also promote structural changes in underlying brain networks. We therefore investigated the associations between AP, traffic noise, and structural measures of the Default Mode Network (DMN), a functional brain network known to undergo specific changes with age.
Methods: We analyzed data from 579 participants (mean age at imaging: 66.5 years) of the German 1000BRAINS study. Long-term residential exposure to particulate matter (diameter ≤10 μm [PM_{10}]; diameter ≤2.5 μm [$PM_{2.5}$]), $PM_{2.5}$ absorbance ($PM_{2.5abs}$), nitrogen dioxide (NO_2), and accumulation mode particulate number concentration (PN_{AM}) was estimated using validated land use regression and chemistry transport models. Long-term outdoor traffic noise was modeled at participants' homes based on a European Union's Environmental Noise Directive. As measures of brain structure, cortical thickness and local gyrification index (lGI) values were calculated for DMN regions from T1-weighted structural brain images collected between 2011 and 2015. Associations between environmental exposures and brain structure measures were estimated using linear regression models, adjusting for demographic and lifestyle characteristics.
Results: AP exposures were below European Union standards but above World Health Organization guidelines (e.g., PM_{10} mean: 27.5 μg/m^3). A third of participants experienced outdoor 24-h noise above European recommendations. Exposures were not consistently associated with lGI values in the DMN. We observed weak inverse associations between AP and cortical thickness in the right anterior DMN (e.g., −0.010 mm [-0.022, 0.002] per 0.3 unit increase in $PM_{2.5abs}$) and lateral part of the posterior DMN.
Conclusion: Long-term AP and noise were not consistently associated with structural parameters of the DMN in the brain. While weak associations were present between AP exposure and cortical thinning of right hemispheric DMN regions, it remains unclear whether AP might influence DMN brain structure in a similar way as aging.

1. Introduction

Air pollution (AP), defined as a harmful mixture of gases and particles in the air, is a known risk factor for cardiovascular and respiratory diseases as well as mortality across the world (Schraufnagel et al., 2019; Thurston et al., 2017). Recent experimental and epidemiologic evidence suggests that AP exposure may also adversely affect the brain via systemic inflammation and direct translocation of small particles into the brain (Genc et al., 2012). Epidemiologic studies support that higher AP exposure is linked to decreases in cognitive function (Paul et al., 2019), including in memory function (e.g., Nuβbaum et al., 2020; Tonne et al., 2014; Tzivian et al., 2016b).

With growing evidence that AP exposure may accelerate cognitive

* Corresponding author. Universitätsklinikum Düsseldorf, AG Umweltepidemiologie, Postfach 101007, 40001, Düsseldorf, Germany.
E-mail address: sarah.lucht@uni-duesseldorf.de (S. Lucht).
[1] Contributed equally to this work.

https://doi.org/10.1016/j.ijheh.2021.113867
Received 2 August 2021; Received in revised form 15 October 2021; Accepted 18 October 2021
Available online 28 October 2021

Abbreviations

AD	Alzheimer's Disease
aDMN	anterior Default Mode Network
AP	air pollution
BMI	body mass index
DAG	directed acyclic graph
dB(A)	A-weighted decibels
DMN	Default Mode Network
ESCAPE	European Study of Cohorts for Air Pollution Effects
EURAD	European Air Pollution Dispersion
ETS	environmental tobacco smoke
GMV	gray matter volume
HNR	Heinz Nixdorf Recall
I-L_{den}	indoor 24-h weighted traffic noise
I-L_{night}	indoor nighttime traffic noise
IQR	interquartile range
iSES	individual socioeconomic status
L_{den}	outdoor 24-h weighted traffic noise
lGI	local gyrification index
L_{night}	outdoor nighttime traffic noise
LUR	land use regression
MP-RAGE	magnetization-prepared rapid acquisition gradient-echo
MRI	magnetic resonance imaging
NO_2	nitrogen dioxide
nSES	neighborhood socioeconomic status
PASA	posterior-anterior shift in aging
pDMN	posterior Default Mode Network
$M_{2.5}$	particulate matter with aerodynamic diameter $\leq$2.5 μm
$PM_{2.5abs}$	absorbance of particulate matter with aerodynamic diameter $\leq$2.5 μm
PM_{10}	particulate matter with aerodynamic diameter $\leq$10 μm
PN_{AM}	accumulation mode particle number concentration
ρ	Spearman correlation coefficient
SD	standard deviation
WMV	white matter volume

decline, several observational studies have investigated whether AP exposure is also associated with adult brain structure. Associations between AP exposure and lower brain volume have been observed in multiple studies (e.g., Erickson et al., 2020; Gale et al., 2020), but results are difficult to compare across differing brain regions. In studies all conducted in the UK Biobank cohort utilizing the same AP exposures ($PM_{2.5}$, PM_{10}, NO_x, NO_2, and PM_{coarse}), they observed inverse associations between $PM_{2.5}$, PM_{10}, NO_x and prefrontal volume (Gale et al., 2020), PM_{coarse} and volume in the left thalamus (Hedges et al., 2020), and $PM_{2.5}$ and left hippocampal volume (Hedges et al., 2019). Non-volumetric measures of brain structure, such as region-specific cortical thickness, have been studied less frequently than volumetric measures. Results from two cortical thickness studies suggest that AP may be associated with reduced cortical thickness in some areas (e.g., frontal and temporal cortices [Cho et al., 2020]; Alzheimer's associated areas [Crous-Bou et al., 2020]) but increased thickness in others (e.g., occipital and cingulate cortices [Cho et al., 2020])

Alongside AP, chronic noise exposure has emerged as an important environmental factor and co-exposure (e.g., through traffic) that also exerts adverse effects on human health. Long-term noise exposure has been linked to increased risk of non-auditory outcomes (e.g., cardiovascular disease, depression), with potential mechanisms including increased stress due to sleep disturbances and increased annoyance (Basner et al., 2014). Noise has also been linked to decreases in cognitive function, including poorer memory among children (Basner et al., 2014), increased risk of mild cognitive impairment (Tzivian et al., 2016b), and decreased memory function among adults (Tzivian et al., 2016a; Wright et al., 2014). At present, only three studies have examined how chronic noise exposure may influence adult brain structure with one showing adverse effects on gray matter volume (Cheng et al., 2019), one showing no effect on cortical thickness and regional volumes (Crous-Bou et al., 2020), and one showing null and positive associations with gyrification, a measure of brain folding (Nuβbaum et al., 2020).

While the study of long-term AP, noise, and brain health is relatively new, research supports that normal aging is consistently accompanied by global and region-specific changes in both brain function and structure. Structurally, old age is associated with decreased global cortical surface area as well as region-specific brain volume and cortical thickness, changes which have been linked to decreases in cognitive function (Gautam et al., 2015; Jockwitz et al., 2019; Tsapanou et al., 2019). Local Gyrification Index (lGI), a measure of local surface structure that is thought to be rather sensitive, is also known to decrease with age (Hogstrom et al., 2013). Likewise, age-related changes in functional brain networks, which are regions that show highly correlated activity levels, have also been identified using imaging studies (e.g., Davis et al., 2008; Jockwitz et al., 2017). To date, Nuβbaum et al. (2020)'s work in the fronto-parietal network is the only study to have looked at AP and brain structure in a functionally important brain network. They observed that AP exposures were inversely associated with lGI in the right hemisphere of the fronto-parietal network, results which are consistent with effects observed during aging. In conjunction with studies showing decreased cognitive function with higher AP exposure (Paul et al., 2019), this suggests that AP may accelerate or mimic the processes in the brain that occur with aging. Nevertheless, more work is needed before such conclusions can be made.

Composed of three bilateral regions in the brain, the Default Mode Network (DMN) is an important functional network that plays a large role in mental functions, such as self-referential thinking, and memory recall (Raichle, 2015). While the DMN is generally deactivated during externally-focused, attention-demanding activities, it is activated during the resting state (Raichle, 2015). Aging of this network is associated with changes in functional connectivity, including a posterior to anterior shift (PASA) where frontal brain regions take over additional functions to compensate for decreased activity in posterior regions (Davis et al., 2008). These changes in functional connectivity are reflected in structural changes locally, with greater relative decreases in lGI observable in posterior brain regions of the DMN than in the anterior regions (Jockwitz et al., 2017, 2019). Jockwitz et al. (2017) also observed larger age-associated structural differences in the right hemisphere of the DMN, consistent with the right hemi-aging theory that the right hemisphere is more susceptible to the effects of aging than the left (Brown and Jaffe, 1975; Dolcos et al., 2002). Nuβbaum et al. (2020) also observed that AP was more strongly associated with lower lGI in the right hemisphere of the fronto-parietal network compared to the left.

Despite the DMN's role in memory recall and previous studies linking AP and noise exposures to changes in memory-related brain functions, no studies have investigated how AP and noise exposures may influence brain structure in the DMN and whether these environmental exposures exert similar effects as observed with aging. We therefore investigated the associations between long-term ambient exposure to AP, road traffic noise, and structural measures of the DMN (cortical thickness, lGI) in the German 1000BRAINS study in order to evaluate the role these environmental exposures may have on brain structure. We hypothesized that higher exposure to AP and noise would be associated with decreased cortical thickness and lGI in the regions of the DMN, similar to what would be expected with aging.

2. Methods

2.1. Study population

This study was conducted using data from the 1000BRAINS Study, an epidemiologic population-based study designed to investigate the variability of brain structure, function, and connectivity during the normal aging process (Caspers et al., 2014). Participants of the 1000BRAINS study were recruited from the prospective Heinz Nixdorf Recall (HNR) study and the HNR MultiGeneration Study in the highly urbanized German Ruhr area (Essen, Bochum, Mülheim), but the current study includes only HNR participants of the 1000BRAINS participants, as no environmental exposure data is currently available for the HNR Multi-Generation Study. The HNR study has been described in detail previously (Schmermund et al., 2002; Stang et al., 2005). Briefly, middle-to older-aged participants (45–74 years) were randomly selected from city residential registries and recruited via mail (recruitment efficiency proportion: 55.8%; Stang et al., 2005). Participants completed baseline (2000–2003; n = 4,814), 5-year follow-up (2006–2008; n = 4,157), and 10-year follow-up (2011–2015; n = 3,087) examinations. At each examination, extensive sociodemographic, lifestyle, morbidity, and laboratory information was collected. HNR participants were approached about 1000BRAINS participation at the 10-year follow-up examination, with the requirement that they were willing to travel the 100–120 km distance to the MRI study and did not have debilitating diseases (Caspers et al., 2014). Subjects were also excluded from participation in the 1000BRAINS study if they were not eligible for having magnetic resonance imaging (MRI) measurements taken (i.e., claustrophobia, history of neurosurgery, presence of tattoos or permanent makeup on the head, cardiac pacemakers, surgical implants or prostheses in the trunk or head, coronary artery stents, and potentially dental implants and bridges producing artifacts in the images). Eligible and willing participants (n = 688) underwent MRI scans as well as neuropsychological and motor assessments between 2011 and 2015 (Fig. 1; more details in Caspers et al., 2014 and section 2.4). Any participants whose MRI showed conditions requiring immediate medical protocol (e.g., acute stroke, aneurysm) or medical referral (e.g., post-stroke status) were excluded from the study, but normal aging-associated brain changes were not considered criteria for exclusion. Protocols for both the HNR and 1000BRAINS studies were approved by the local Ethics Committee of the University of Essen. All participants gave written informed consent.

2.2. Air pollution exposures

Two air quality models were utilized for estimating long-term exposures in this study. Long-term exposure to particulate matter with aerodynamic diameter ≤2.5 μm ($PM_{2.5}$; μg/m^3), particulate matter with aerodynamic diameter ≤10 μm (PM_{10}; μg/m^3), $PM_{2.5}$ absorbance ($PM_{2.5abs}$; 0.0001/m), and nitrogen dioxide (NO_2; μg/m^3) was estimated using the European Study of Cohorts for Air Pollution Effects (ESCAPE) land use regression (LUR) model. This LUR model uses land use data to predict temporally-stable, point-specific AP exposures and was built following the standards of the European-wide ESCAPE project (more details provided in Cyrys et al., 2012; Eeftens et al., 2012). Briefly, the ESCAPE project was designed to investigate the effect of long-term air pollution on health using prospective cohort studies in 15 countries across Europe. LUR prediction models were built within each study according to common guidelines (Eeftens et al., 2012) using data from individual measurement campaigns and local geographic data (e.g., traffic density, population density). For the Ruhr area, PM (20 sites) and NO_2 (40 sites) data were collected between October 2008 and October 2009 (Hennig et al., 2016). Detailed information on the geographic data included in the specific AP models can be found in Eeftens et al. (2012) and Beelen et al. (2013). The ESCAPE models explained a large proportion of the variance in annual AP concentrations in the Ruhr area (69% for PM_{10}, 88% for $PM_{2.5}$, 97% for $PM_{2.5abs}$, and 89% for NO_2; Eeftens et al., 2012). Each participant of the HNR was assigned point-specific exposure estimates for their residence at the baseline examination (2001–2003). Residence at baseline was chosen for exposure estimation (approximately 10 years prior to MRI), because mechanistic hypotheses suggest that environmental effects on the brain likely accumulate over an extended period of time (Block and Calderón-Garcidueñas, 2009).

Particle number concentrations (PN_{AM}; n/mL) for the accumulation mode (mean diameter: 0.07 μm; 67% of particles with aerodynamic diameters between 0.035 and 0.14 μm) were estimated for all participants using the validated, time-dependent, three-dimensional EURopean Air pollution Dispersion (EURAD) chemistry transport model (Memmesheimer et al., 2004; Nonnemacher et al., 2014). Using multiple layers and grids, the EURAD model simulates the chemical transformation, deposition, and transport of AP on both local and regional levels (Memmesheimer et al., 2004). It uses four sequential nesting grids (125 km, 25 km, 5 km, and 1 km) to estimate hourly exposures for Europe, central Europe, the state of North Rhine-Westphalia in northwestern Germany, and the Ruhr Area, respectively. PN_{AM} exposure estimates have been validated against measurements taken using a TSI 3926 scanning mobility particle size spectrometer (size range: 0.014–0.750 μm; TSI Inc., Shoreview, MN, USA) at the Mülheim-Styrum monitoring station for the period 2011–2014 (Birmili et al., 2016). Pearson correlations were moderate (r = 0.57) for daily measurements,

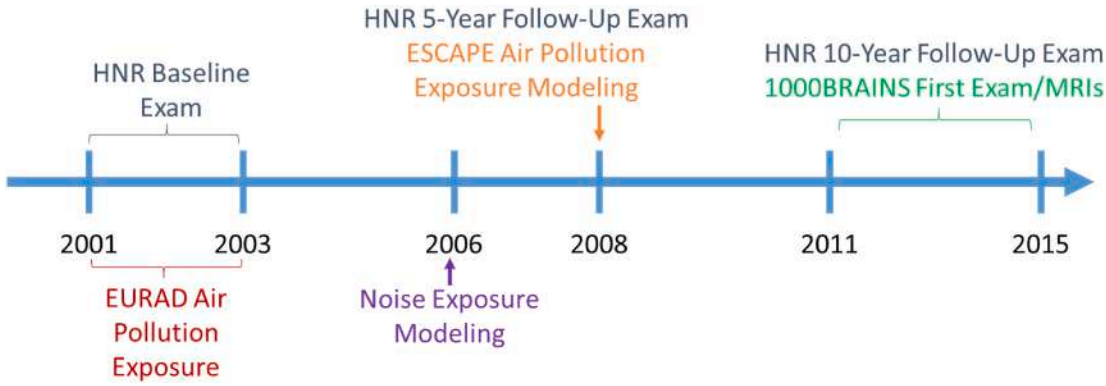

Fig. 1. Timeline showing when health examinations for the HNR as well as 1000BRAINS studies took place as well as when the air pollution and noise exposures were assessed. The ESCAPE and noise modeling estimates, while taking place later, were assigned to the residential addresses for HNR participants at baseline (2001–2003).

Abbreviations: ESCAPE, European Study of Cohorts for Air Pollution Effects; EURAD, European Air Pollution Dispersion; HNR, Heinz Nixdorf Recall; MRI, magnetic resonance imaging.

with strongest seasonal correlations seen during winter and fall (r = 0.61; Lucht et al., 2019). According to the 1 km^2 grid in which their residence was located, HNR participants were assigned mean PN_{AM} values for the baseline HNR period (2001–2003; ArcView, version 9.2, ESRI, Redlands, CA, USA).

2.3. Long-term traffic noise exposure

As required by the European Union Directive 2002/49/EC (European Environment Agency, 2002), long-term road traffic noise was modeled for the year 2006 on behalf of local city administrations, who supplied source-specific noise values from the VBUS/RLS-90 method (Bundesministerium der Justiz, 2006) using CadnaA software (DataKustik, 2018). Outdoor weighted 24-h noise (L_{den}; A-weighted decibels [dB(A)]) as well as outdoor nighttime noise (between 22:00 and 6:00; L_{night}) were modeled at façade points (height of 4 m ± 0.2 m) using small-scale topography, building dimensions, speed limit, street axis, noise barriers, type-specific vehicle traffic density, and road surface (Bundesministerium der Justiz, 2006). For L_{den}, daytime noise (6:00–18:00), evening noise (18:00–22:00), and nighttime noise (22:00–6:00) were weighted differently, under the assumption that excess noise in the evening and at night is more disturbing than daytime noise (WHO Regional Office for Europe, 2009). As such, penalties of 5 dB(A) and 10 dB(A) were added to evening and nighttime noise levels, respectively. Outdoor exposures were assigned to participants using the maximum estimated noise value in a 10-m buffer around each participant's address at baseline HNR examination. In analyses, outdoor L_{den} and L_{night} were modeled as a truncated continuous variables with lower thresholds of 45 dB(A) and 35 dB(A), respectively (Ohlwein et al., 2019). Participants were assigned noise values according to their baseline addresses.

Along with outdoor façade noise, we estimated indoor 24-h and nighttime noise levels using self-reported behavioral and apartment information based on a method by Foraster et al. (2014). It is described in detail for the HNR cohort in Ohlwein et al. (2019). Briefly, indoor L_{den} (I- L_{den}) was estimated in participants' living rooms whereas indoor L_{night} (I- L_{night}) estimates reflect bedroom levels. These estimates were derived from outdoor estimates, with various factors resulting in reduction of noise. If the room was orientated towards a direction other than the postal address street, 20 dB(A) were deducted. When persons reported usually having their windows closed, we subtracted 30 dB(A) if they had single-glazed windows and 40 dB(A) if they had double-glazed windows. For persons who often, seldom, and never closed their windows, we deducted 21 dB(A), 16 dB(A), and 15 dB(A) from outdoor levels, respectively, as described in Ohlwein et al. (2019). I-L_{den} and I-L_{night} were modeled with lower threshold values of 20 dB(A) and 10 dB(A), respectively, in the analyses.

2.4. Brain structure measures in regions of the DMN

Brain images were acquired for all participants included in 1000BRAINS using Magnetic Resonance Imaging on a 3T Siemens Tim-TRIO MR scanner (Erlangen, Germany), using a 32-channel head coil (Caspers et al., [2014]Caspers et al., [2014]). In order to examine brain structure, i.e., cortical thickness and lGI, a 3D high-resolution T1-weighted magnetization-prepared rapid acquisition gradient-echo (MP-RAGE) anatomical scan was acquired and used for subsequent surface reconstruction (176 slices, slice thickness: 1 mm, repetition time: 2250 ms, echo time: 3.03 ms, field of view: 256 × 256 mm^2, flip angle: 9°, voxel resolution: 1 mm^3).

The identification of the DMN was part of a previous study and has been described elsewhere in detail (Jockwitz et al., 2017). Briefly, 691 resting-state scans were preprocessed using the FMRIB Software Library processing pipeline (http://www.fmrib.ox.ac.uk/fsl; Jenkinson et al., 2012). Afterwards, common spatial patterns across subjects within the resting state data were identified using MELODIC (Beckmann et al., 2005). For reliability purposes, this procedure was repeated 100 times, with each sample consisting of 200 randomly selected subjects. For each group, the DMN was selected and all DMNs were superimposed onto each other resulting in a probability map, which was thresholded at 95% (using fslmaths, FSL) and binarized. Finally, the DMN was composed of six clusters: two anterior (left and right prefrontal cortex) and four posterior (left and right posterior cingulate cortex/precuneus; left and right angular gyrus; Jockwitz et al., 2017). In analyses, the prefrontal cortex region was denoted as the anterior DMN (aDMN) while the posterior parts were denoted as the medial (cingulate cortex/precuneus) and lateral (angular gyrus) pDMN (Fig. 2).

In order to calculate cortical thickness and local gyrification indices within all parts of the DMN (Jockwitz et al., 2019; Jockwitz et al., 2017), anatomical images were preprocessed using the automated surface-based processing stream implemented in FreeSurfer (version 6.0.0; for a detailed description of the surface reconstruction, see Dale et al., 1999; Fischl et al., 1999). Based on the reconstructed surfaces, LGI values were calculated according to Schaer et al. (2012) for each part of the DMN as the ratio between the total pial surface area (including sulci) to the outer hull surface area (excluding sulci). Mean cortical thickness (CT; for a detailed overview, see Fischl and Dale (2000)) was calculated for each DMN region as the shortest distance (mm) between a vertex on the white matter surface and the corresponding vertex on the pial surface.

2.5. Definition of covariates

Variables from the baseline HNR examination were used in all analyses, with the exception of age (years), where age at time of 1000BRAINS examination was used. Smoking status was defined as current, former (>1 year since quitting), or never smoker. Cumulative smoking exposure (pack-years) was assessed for former and current smokers and accounted for periods of non-smoking. Exposure to environmental tobacco smoke (ETS; Yes/No) was defined as regular passive exposure to smoke at home, work, or other location. Physical activity (Yes/No) was assessed as regular sporting activities at least once a week for a minimum of 30 min. Alcohol consumption was obtained through dietary questionnaire and divided into five categories (0, 1–3, 4–6, 6–14, and >14 drinks per week). Anthropometric measurements (height, weight) were measured at examinations according to standard protocols, and body mass index (BMI) was calculated as kilograms per meter squared. Quality of diet was assessed using a dietary pattern index, created by incorporating consumption frequency of 13 food items and diet quality classifications used in previous studies (Winkler and Döring, 1998, 1995). Possible scores ranged from 0 to 26 with 26 representing an ideal diet and were categorized into three categories (Unfavorable Diet, Normal Diet, Favorable Diet). Individual socioeconomic status (iSES) was defined as years of education, as classified by the International Standard Classification of Education (UNESCO, 1997), and divided into four categories (≤10, 11–13, 14–17, ≥18 years). For neighborhood SES (nSES), unemployment rates (units of percent) between 2001 and 2003 were obtained from local census authorities for each residential neighborhood according to administrative boundaries (median size: 11,263 inhabitants; Dragano et al., 2009). Nearness of a participant's residence to a major road (Yes/No), defined as ≤50 m from a main road or ≤100 m from a motorway, was calculated using official digitized maps with a precision of at least 0.5 m.

2.6. Statistical analysis

We investigated the association between long-term ambient AP and road traffic noise exposures and structural brain parameters (lGI; cortical thickness) in the DMN using linear regression models. Individual models were conducted for the aDMN, medial pDMN, lateral pDMN on both the right and left hemispheres. The normality of residuals was confirmed for the models using Q-Q plots, and the appropriateness of restricted cubic spline terms (knots = 4) for continuous variables was

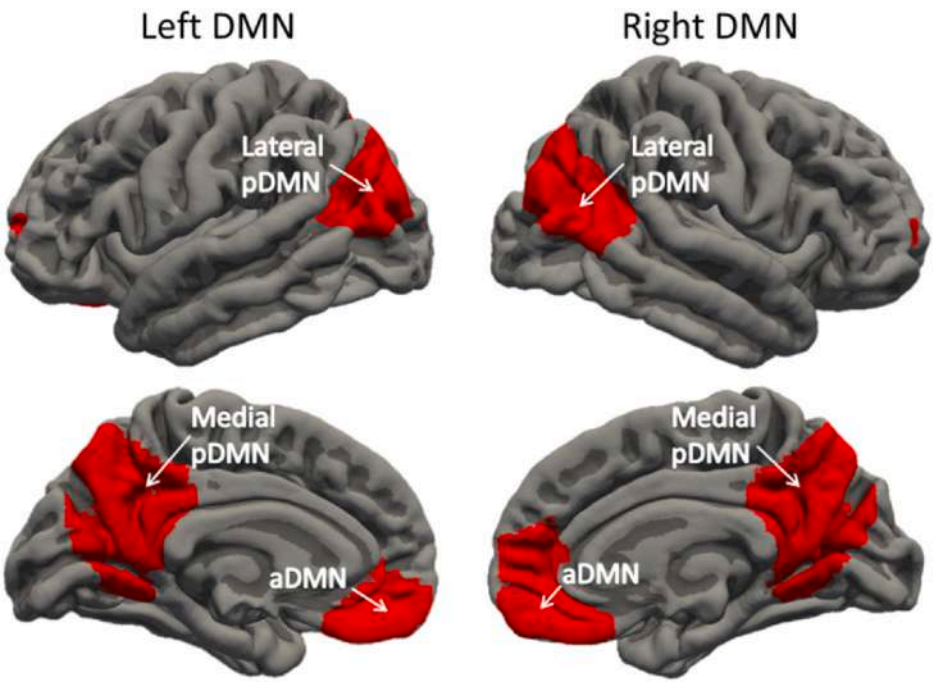

Fig. 2. The Default Mode Network (DMN) projected on the right and left hemispheres of a brain consisting of the lateral posterior DMN (pDMN), medial pDMN, and anterior DMN (aDMN).

assessed in exposure-free models. Associations were estimated as the absolute difference in the outcome per interquartile (IQR) increase for air pollutants or per 10 dB(A) increase for noise exposures and presented alongside 95% confidence intervals.

Three models of increasing covariate adjustment were conducted. Model 1 included the AP or noise exposure, age at MRI and sex. In addition to age and sex, variables in Model 2 were identified using a directed acyclic graph (DAG; Fig. S1) and included alcohol consumption, BMI, diet, physical activity, and smoking (status; cumulative; ETS). The DAG was built using DAGitty software, which outputs minimal sufficient adjustment sets (Textor et al., 2011), and included variables selected based on prior literature. For the Main Model (Model 3), all AP models were additionally adjusted for outdoor L_{den} whereas noise models were additionally adjusted for $PM_{2.5abs}$. Model 3 also included adjustment for all Model 2 variables.

Multipollutant models were conducted in order to investigate independence of effects by the various exposures. PM models were adjusted separately for NO_2 and PN_{AM}, NO_2 models were adjusted separately for $PM_{2.5}$ and PN_{AM}, and PN_{AM} models were adjusted separately for NO_2 and $PM_{2.5}$. In order to compare effect sizes between age and environmental exposures, we also conducted a secondary analysis examining the association between age and brain structure measures for DMN regions. Age models were adjusted for Main Model variables, with the addition of iSES and nSES, and associations were estimated per one-year increase in age at MRI. As indoor noise values were missing for approximately 10% of the analysis group (n = 61), we also conducted a secondary analysis for outdoor and indoor noise within this smaller group (n = 518) and using the Main Model adjustment set.

2.7. Effect modification & sensitivity analyses

We evaluated potential effect modification by age at MRI using the addition of an interaction term between the AP exposure and a binary categorization of age (<65 years vs. 65+ years). Several sensitivity analyses were also conducted to assess the robustness of our results. To assess sensitivity to socioeconomic variables, we conducted models including all Main Model variables plus iSES and nSES. As updated information on several HNR baseline lifestyle factors was also collected at the 1000BRAINS recruitment, we also conducted a model utilizing the updated data from the later examination. We restricted our population to participants who reported working less than 15 h per week, as we expected these participants to spend a greater proportion of their time at home and therefore errors in exposure estimates may be smaller. Additionally, we evaluated the associations using residential address at the 5-year follow-up HNR examination (2006–2008) and among participants who still resided at their baseline addresses at the 10-year follow-up examination (n = 442). As several previous studies have looked at residential distance to major roads as a proxy for traffic exposure (Kulick et al., 2017; Nuβbaum et al., 2020; Wilker et al., 2016; Wilker et al., 2015), we also evaluated this exposure (residence ≤50 m from a federal or main road or ≤ 100 m from a motorway) in a sensitivity analysis. Because some participants were excluded due to missing information, we compared those excluded with the participants included in the analysis as well as with all participants who attended the 10-year follow-up HNR examination.

3. Results

3.1. Study population

Overall, 688 participants of the 1000BRAINS study were recruited from the HNR study. Of these, participants were excluded from the analysis due to missing brain structure measures (n = 85), AP exposures (n = 5), outdoor noise levels (n = 2), or adjustment variables (n = 17; Fig. S2). The final study population therefore included 579 participants. In general, the study population was in late middle age at HNR baseline (mean age: 56.2 years [SD: 6.7], range: 45–74 years), approximately 10 years older at time of MRI (mean age: 66.5 years [SD 6.7], range: 56–85 years), slightly overweight (mean BMI: 27.3 kg/m^2 [SD: 4.1]), and had slightly more men than women (54.2% Male; Table 1). Most participants had at least 11 years of education and did not currently smoke. For observed time-varying lifestyle factors, participants had similar values at baseline and 1000BRAINS recruitment, with the exception of a shift from current smoking to former smoking and greater exposure to

Table 1
Demographic and lifestyle characteristics of the 1000BRAINS study participants (n = 579) at HNR baseline (2000–2003) and, when updated information was collected[a], at recruitment for 1000BRAINS (2011–2015).

	HNR Baseline	1000BRAINS Recruitment
Variable	Mean ± SD or Median [IQR] or n (%)	Mean ± SD or Median [IQR] or n (%)
Age (years)	56.2 ± 6.7	66.5 ± 6.7
BMI (kg/m^2)	27.3 ± 4.1	28.3 ± 4.4
Neighborhood Unemployment (%)	12.1 ± 3.3	–
Female	265 (45.8)	265 (45.8)
Formal Education		
≤10 years	32 (5.5)	32 (5.5)
11–13 years	302 (52.2)	302 (52.2)
14–17 years	143 (24.7)	143 (24.7)
≥18 years	102 (17.6)	102 (17.6)
Physical Activity, Yes	362 (62.5)	373 (64.5)
Smoking Status		
Never Smoker	250 (43.2)	250 (43.3)
Former Smoker	214 (37.0)	263 (45.5)
Current Smoker	115 (19.9)	65 (11.2)
Cumulative Smoking (pack-years)	18.8 [25.0]	–
Environmental Tobacco Smoke Exposure, Yes	225 (38.9)	380 (66.0)
Alcohol Consumption (Drinks/Week)		
Never	226 (39.0)	–
1 to 3	96 (16.6)	–
>3 to 6	80 (13.8)	–
>6 to 14	87 (15.0)	–
>14	90 (15.5)	–
Diet		
Unfavorable Diet	235 (40.6)	235 (40.9)
Normal Diet	209 (36.1)	192 (33.4)
Favorable Diet	135 (23.3)	147 (25.6)

Abbreviations: BMI, body mass index; HNR, Heinz Nixdorf Recall; IQR, interquartile range; MRI, magnetic resonance imaging; SD, standard deviation.
[a] Data available only at baseline examination for neighborhood unemployment, cumulative smoking, and alcohol consumption.

environmental tobacco smoke at the later time point (Table 1). Participants excluded from the analysis were very similar to those included (Table S1), with excluded participants slightly more likely to be male. On average, HNR participants who also took part in the 1000BRAINS study were slightly younger, more male, more likely to eat an unhealthy diet and drink more, and more highly educated than the average participant at the 10-year follow-up HNR examination (Table S1).

Air pollution levels at participants' homes were below the European Union Air Quality Standards for annual concentrations (40 μg/m^3 for NO_2 and PM_{10}, 25 μg/m^3 for $PM_{2.5}$; Table 2; European Parliament, Council of the European Union, 2008), but above the World Health Organization's Air Quality Guidelines for annual PM_{10} and $PM_{2.5}$ (20 μg/m^3 and 10 μg/m^3, respectively; World Health Organization [2006]). Mean 24-h outdoor noise levels were slightly below the European L_{den} guideline of 53 dB(A), with 203 participants (35.1%) exposed to noise levels above this recommendation (World Health Organization, 2018). AP exposures were moderately to highly correlated with each other (Spearman correlations [ρ]: 0.49–0.91) and weakly correlated with noise exposures (ρ: 0.08–0.41; Table S2). Outdoor L_{den} and L_{night} were highly correlated (ρ: 0.99), whereas outdoor and indoor noise exposures were only moderately correlated (ρ: 0.40–0.50; Table S2). LGI values were, on average, higher in the posterior regions of the DMN than in the anterior DMN, whereas cortical thickness was slightly lower in the medial pDMN compared to other regions (Table S3).

3.2. Model adjustment & main results

Only results from the Main Model (Model 3) will be presented in detail here, as increasing adjustment for potential confounders did not result in large changes in the estimated associations between AP, noise, and brain structure measures (Fig. S3). Interestingly, adjustment for co-exposures (i.e., L_{den} for AP exposures and $PM_{2.5abs}$ for noise exposures) did not result in qualitative changes in the estimated associations.

Table 2
Description of long-term air pollution and noise exposure levels at the baseline residential addresses of 1000BRAINS study participants.

Exposure	Mean ± SD or n (%)	Interquartile Range
Air Pollution		
PM_{10} (μg/m^3)	27.5 ± 1.8	2.1
$PM_{2.5}$ (μg/m^3)	18.2 ± 1.0	1.4
$PM_{2.5abs}$ (0.0001/m)	1.5 ± 0.4	0.3
NO_2 (μg/m^3)	29.5 ± 4.6	5.2
PN_{AM} (n/mL)	3,725 ± 435	612
Near Major Road (Yes)	109 (18.8)	–
Noise		
Outdoor L_{den} (dB[A])	53.4 ± 8.4	13.1
Outdoor L_{night} (dB[A])	44.4 ± 8.3	12.7
Indoor L_{den} (dB[A])	35.1 ± 12.5	20.6
Indoor L_{night} (dB[A])	27.3 ± 13.8	24.1

Abbreviations: dB(A), A-weighted decibels; L_{den}, outdoor 24-h weighted noise; L_{night}, outdoor nighttime noise; NO_2, nitrogen dioxide; PM_{10}, particulate matter with diameter ≤10 μm; $PM_{2.5}$, particulate matter with diameter ≤2.5 μm; $PM_{2.5abs}$, $PM_{2.5}$ absorbance; PN_{AM}, accumulation mode particle number concentration; SD, standard deviation.

For lGI, no consistent associations were observable with AP and noise exposures across the various regions and two hemispheres (Fig. 3; AP estimates in Table S4). Point estimates for AP exposures were all associated with slightly lower lGI in the left aDMN, whereas several AP exposures were associated with slightly higher lGI in the lateral pDMN and medial pDMN. Results for outdoor noise exposures were similarly mixed (Fig. 3). Age at MRI was inversely associated with lGI in the lateral pDMN regions (Fig. 3).

Higher AP exposure was weakly associated with lower cortical thickness in the right aDMN and lateral pDMN for all air pollutants (Fig. 4; AP estimates in Table S5). In the left aDMN, results were more inconsistent, with some negative and null associations present. In contrast, increases in outdoor 24-h and nighttime noise exposure were associated with higher cortical thickness in the right aDMN. Age at MRI was inversely associated with cortical thickness in all regions, with strongest associations apparent in the pDMN regions (Fig. 4). In the right aDMN, AP exposures were more inversely associated with cortical thickness (e.g., −0.010 [95% CI: 0.022, 0.002] per IQR increase in $PM_{2.5abs}$) than a 1-year increase in age (−0.001 mm [95% CI: 0.003, 0.001] per 1-year increase).

In the multipollutant models, associations for lGI (Table S4) and cortical thickness (Table S5) were similar to those estimated in the single pollutant models, with the exception of lGI in the lateral pDMN. When restricting the analyses to the smaller group with complete indoor noise exposure data, we observed similar associations for both outdoor and indoor noise exposures (Fig. S4). Positive associations between outdoor noise and cortical thickness in the right aDMN were also reflected in the indoor estimates. For lGI in the aDMN as well as for cortical thickness in the left lateral pDMN, indoor noise associations were attenuated compared to the positive associations observed for outdoor exposures.

3.3. Effect modification

For age, no consistent differences were apparent for lGI in the aDMN and medial pDMN (Fig. S5a). In the right lateral pDMN, most AP exposures were weakly positively associated with lGI among older participants but not younger participants. There were no clear variations in the association between AP and cortical thickness by age, though inverse associations with AP were observed only for younger participants in the left aDMN (Fig. S5b). For noise, we observed that increased outdoor

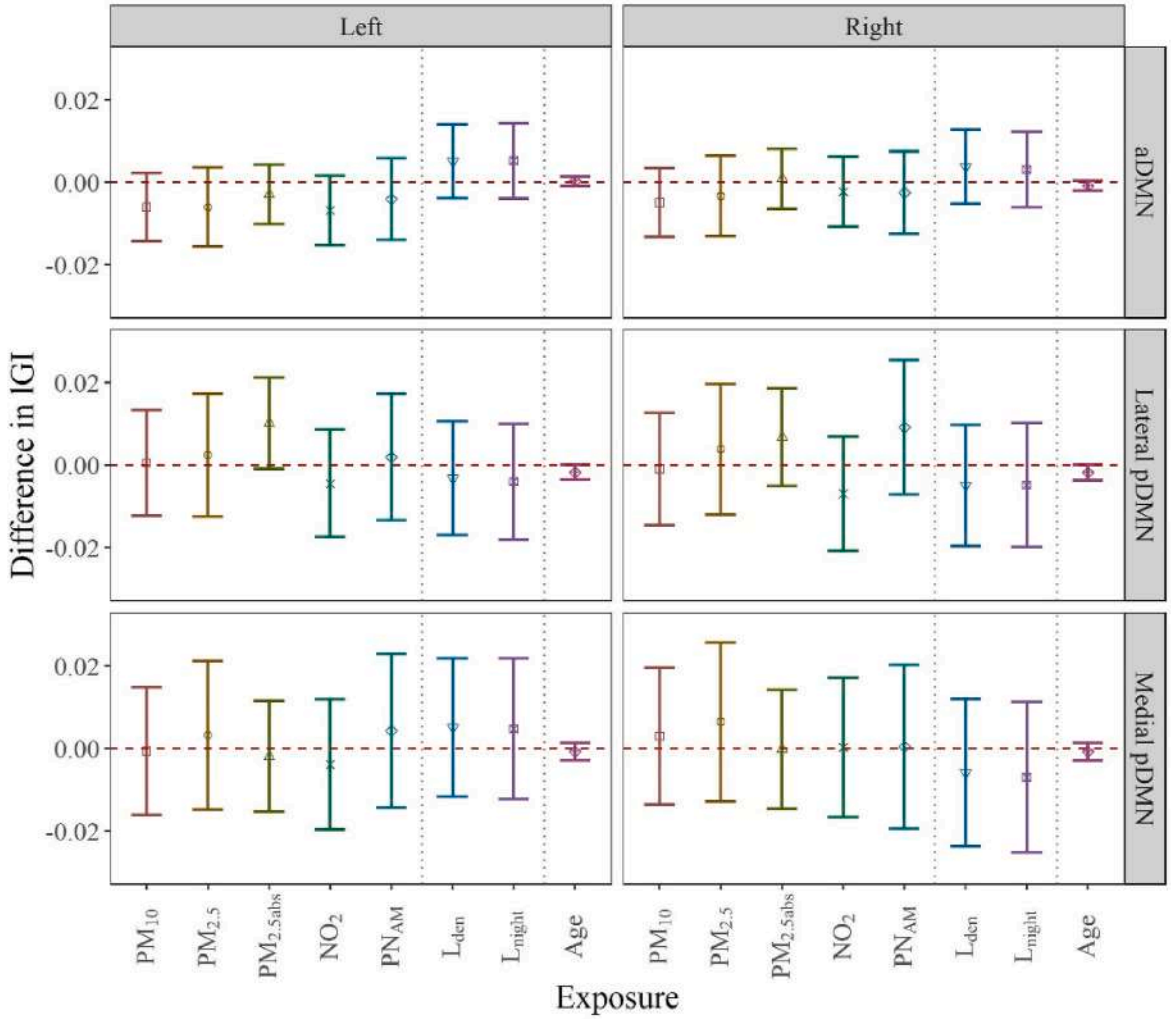

Fig. 3. Associations between AP, noise, and lGI within regions of the DMN in the right and left hemispheres of the brain. AP and noise estimates were calculated per IQR increase and per 10 dB(A), respectively, and are shown with 95% confidence intervals. Models were adjusted for age at MRI, sex, alcohol consumption, body mass index, diet, physical activity, smoking status, cumulative smoking, and environmental tobacco smoke exposure. AP models were additionally adjusted for 24-h outdoor noise and noise models were adjusted for $PM_{2.5abs}$. For reference, age at MRI and lGI was also modeled per 1-year increase and adjusting for sociodemographic variables included in the AP models as well as iSES and nSES.

Abbreviations: aDMN, anterior Default Mode Network; AP, air pollution; DMN, Default Mode Network; pDMN, posterior Default Mode Network; iSES, individual socioeconomic status; L_{den}, outdoor 24-h weighted noise; lGI, local gyrification index; L_{night}, outdoor nighttime noise; MRI, magnetic resonance imaging; NO_2, nitrogen dioxide; nSES, neighborhood socioeconomic status; PM_{10}, particulate matter with diameter ≤10 μm; $PM_{2.5}$, particulate matter with diameter ≤2.5 μm; $PM_{2.5abs}$, $PM_{2.5}$ absorbance; PN_{AM}, accumulation mode particle number concentration.

noise was positively associated with cortical thickness in the lateral pDMN among younger participants whereas estimates were null or slightly negative for older participants.

3.4. Sensitivity analyses

Addition of individual and neighborhood SES did not qualitatively alter the associations we estimated for lGI or cortical thickness (Fig. S3). Use of updated lifestyle variable data also did not affect the estimated associations (Table S6). When updating analyses to use exposures from participants' addresses at the 5-year HNR follow-up examination, we observed very similar estimates of association for lGI and cortical thickness as in the main analysis (Fig. S6). Similarly, restriction of the study population to those who did not move between baseline and 10-year HNR follow-up (n = 442) or to only those working less than 15 h per week (n = 429) did not result in large changes in the associations for lGI or cortical thickness (Fig. S6). Models using residential nearness to a major road (yes/no) broadly yielded weak negative associations with lGI and cortical thickness for those living close to major roads (Table S7).

4. Discussion

In a study of older adults within the 1000BRAINS study, we observed no strong associations between air pollution, noise, and brain structure measures of the DMN. Nevertheless, higher AP exposures were weakly associated with cortical thinning in the right aDMN and lateral pDMN with mixed results for noise. These results contribute to a small but growing literature investigating ambient environmental exposures and brain structure, while simultaneously confirming that connections between these exposures and the brain are complex and poorly understood at present.

4.1. Comparison to prior studies on AP and brain structure

Most studies connecting air pollution to brain health have focused primarily on measures of cognitive function. AP exposure has been

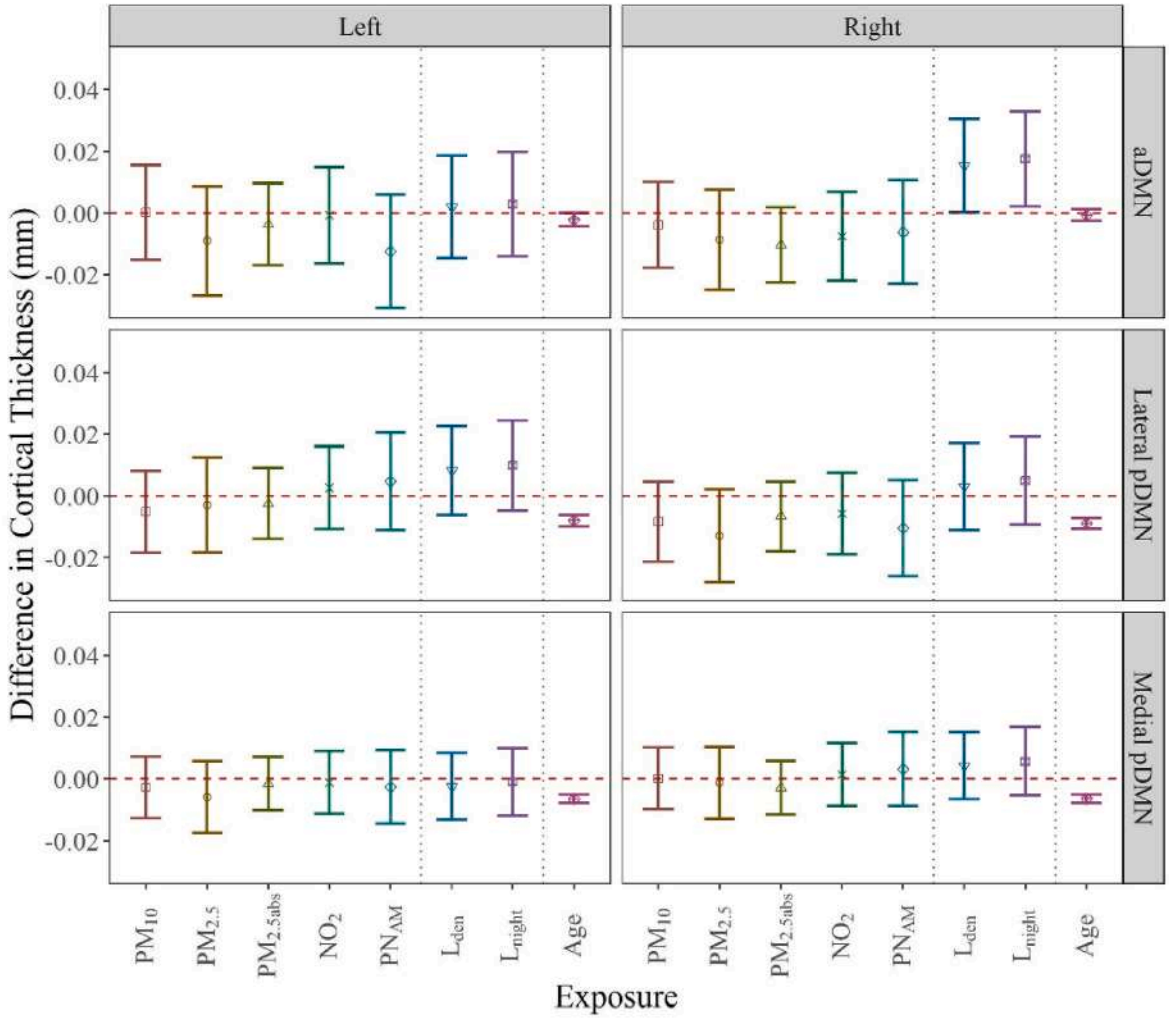

Fig. 4. Associations between AP, noise, and change in cortical thickness (mm) within regions of the DMN in the right and left hemispheres of the brain. AP and noise estimates were calculated per IQR increase and per 10 dB(A), respectively, and are shown with 95% confidence intervals. Models were adjusted for age at MRI, sex, alcohol consumption, body mass index, diet, physical activity, smoking status, cumulative smoking, and environmental tobacco smoke exposure. AP models were additionally adjusted for 24-h outdoor noise and noise models were adjusted for $PM_{2.5abs}$. For reference, age at MRI and cortical thickness was also modeled, with associations estimated per 1-year increase and adjusted for sociodemographic variables included in the AP models as well as iSES and nSES.
Abbreviations: aDMN, anterior Default Mode Network; AP, air pollution; DMN, Default Mode Network; pDMN, posterior Default Mode Network; iSES, individual socioeconomic status; L_{den}, outdoor 24-h weighted noise; L_{night}, outdoor nighttime noise; MRI, magnetic resonance imaging; NO_2, nitrogen dioxide; nSES, neighborhood socioeconomic status; PM_{10}, particulate matter with diameter ≤10 μm; $PM_{2.5}$, particulate matter with diameter ≤2.5 μm; $PM_{2.5abs}$, $PM_{2.5}$ absorbance; PN_{AM}, accumulation mode particle number concentration.

linked to impaired cognitive development among children (D'Angiulli, 2018) as well as faster cognitive decline among adults (e.g., Kulick et al., 2020; Tzivian et al., 2015; Weuve et al., 2012). Additionally, epidemiologic studies have shown associations between AP and increased risk of neurodegenerative diseases such as Alzheimer's and dementia (Carey et al., 2018; Chen et al., 2017; Oudin et al., 2018). At present, studies on AP exposures and structural parameters of the brain are limited and have focused predominantly on volumetric measures (e.g., white matter volume [WMV], gray matter volume [GMV], total volume) or white matter hyperintensities. Most studies have observed decreases in one or more measures of brain volume with increased AP exposure (e.g., lower GMV and WMV in Casanova et al., 2016, lower WMV in Chen et al., 2015), with some variability by exposure and brain region. For example, in four studies within the UK Biobank, NO_2 exposure was associated with lower total GMV (Erickson et al., 2020) and prefrontal cortex volume (Gale et al., 2020), but not with GMV in the hippocampus (Hedges et al., 2019) or thalamus (Hedges et al., 2020). Windows of exposure also ranged from 2-year (Kulick et al., 2017) up to 17-year cumulative average exposure prior to MRI (Power et al., 2018).

To our knowledge, the only prior study to investigate AP and lGI was also conducted within the 1000BRAINS study and observed weak negative associations between AP exposures and lGI in the posterior regions of the fronto-parietal network (Nuβbaum et al., 2020). AP and cortical thickness has been investigated in two recent studies on adults (Cho et al., 2020; Crous-Bou et al., 2020). In 957 adults, Cho et al. (2020) found that AP was associated with cortical thinning in frontal and temporal brain regions together with cortical thickening in occipital and cingulate brain regions. Within a cohort of healthy middle-aged adults with increased risk of Alzheimer's Disease (AD), Crous-Bou et al. (2020) observed associations between AP and cortical thinning in most AD-associated brain areas. Our results support these results that AP may be linked to cortical thinning in certain regions of the brain, but future studies investigating AP and brain structure using longitudinal data are needed to evaluate whether these associations represent true AP-induced changes in brain structures over time.

Unlike most prior studies, we focused on a specific functionally-

defined network rather than using a whole-brain or anatomically-defined approach. The Default Mode Network is one of the most studied functional brain networks and plays an important role in memory recall as well as self-referential thought (Raichle, 2015). Within aging research, typical age-related changes in the deactivation of the DMN have been observed (Hafkemeijer et al., 2012). Additionally, the DMN is of particular interest in aging research because it is known to undergo atrophy, changes in functional connectivity (e.g., the PASA theory), and amyloid deposition with increasing age (Hafkemeijer et al., 2012).

When comparing our lGI results to patterns observed with aging, we observed no clear associations between AP, noise, and lGI as well as no evidence supporting a PASA pattern in the associations, which had been observed for AP and lGI levels in the fronto-parietal network (Nuβbaum et al., 2020). This may be due to differences in the activation patterns of the two networks, as the DMN is most active during resting states whereas the fronto-parietal network is most active during externally-focused tasks. When considering our cortical thickness results and aging, the inverse associations between AP and cortical thickness in several regions of the right aDMN align with the right hemi-aging model (Brown and Jaffe, 1975; Dolcos et al., 2002). Nevertheless, like with lGI, we observed no pattern of association consistent with the PASA theory for cortical thickness.

While changes in cortical thickness and lGI can both be used to assess brain atrophy and both decrease with age (Hogstrom et al., 2013), it is not entirely surprising that we observed different patterns of associations between the two, as prior studies have shown them to be uncorrelated or weakly negatively correlated (Gautam et al., 2015). This may be due to the fact that while cortical thickness reflects gray matter, lGI is a measure dependent on both gray and white matter. While it is not fully clear what AP-induced decreases in one measure but not in the other means for cognition or brain function, future studies should use several measures of brain structure in order to better understand how AP and noise may be influencing both white and gray matter in the brain (Hogstrom et al., 2013). Furthermore, few studies have analyzed how AP exposure may influence the patterns of functional communication in the brain (Pujol et al., 2016a; Pujol et al., 2016b). As brain signaling occurs both within networks as well as between networks, further studies are needed on how environmental exposures may affect both types of communication and whether AP-induced changes in brain structure are also reflected in changes in functional connectivity.

4.2. Noise

Chronic noise is an important environmental exposure that is known to cause adverse health effects, including increased risk of cardiovascular disease (Münzel et al., 2018), sleep disturbances (Basner et al., 2014), and depression (Hegewald et al., 2020; Orban et al., 2016). Nevertheless, very few epidemiologic studies have evaluated how long-term noise exposures may influence adult brain structure (Cheng et al., 2019; Crous-Bou et al., 2020; Nuβbaum et al., 2020). In Cheng et al. (2019), fighter jet pilots had lower hippocampal GMV and worse working memory compared to matched controls. Using data from a healthy middle-aged cohort with increased AD risk, Crous-Bou et al. (2020) observed no statistically significant associations between noise and hippocampal volume, ventricle volume, or cortical thickness in brain regions vulnerable to AD. Contrary to expected, Nussbaum et al. (2020) observed positive associations between chronic outdoor noise and lGI in some regions of the fronto-parietal network. Nevertheless, indoor noise was not considered in the Nussbaum et al. (2020) study.

We observed positive associations between outdoor noise exposures and structural brain measures in several areas of the brain, with the strongest associations present for the aDMN. These results align with those seen by Nussbaum et al. (2020), where the positive associations were also observed primarily in the frontal regions of the brain. Nevertheless, in most cases, the positive associations we observed for outdoor noise exposures were attenuated for indoor exposures. Differences between outdoor and indoor noise estimates may also be due to systematic differences in window type and use for persons with high noise exposure (e.g., more noise-proof windows and less time with windows open for highly exposed participants) that are only accounted for in the indoor noise estimates.

While little is known about noise and brain structure, some evidence exists showing that higher noise levels may be associated with decreased cognitive function, particularly among children (Clark and Paunovic, 2018). Studies on adults are more limited, particularly investigating long-term noise exposures, but the evidence seems to support that chronic noise exposure is associated with decreased cognitive function (Cheng et al., 2019; Fuks et al., 2019; Nuβbaum et al., 2020; Tzivian et al., 2016b). While these studies do not provide evidence for direct comparison to our results on brain structure, they do support the hypothesis that environmental noise exposures may be important determinants of brain health and therefore influential in shaping morphological parameters.

4.3. Potential mechanisms

Air pollution is hypothesized to influence health through several main pathways: first, by initiating local inflammatory processes in the lungs that can spawn systemic inflammation under chronic exposure; secondly, by direct translocation of small particles across the alveoli and into the blood stream, where they can travel and damage organs across the body; and thirdly, through activation and dysregulation of the autonomic nervous system (Block and Calderón-Garcidueñas, 2009). In recent years, evidence has emerged that small particles may also be able to enter into the brain directly via the olfactory bulb (Oberdörster et al., 2004). Systemic inflammation and circulating air pollutants are known to interact with the blood brain barrier, including the diffusion of cytokines across it and the initiation of neuroinflammatory cascades (Genc et al., 2012). Neuroinflammation is a hallmark of several neurologic diseases (e.g., Alzheimer's disease, Parkinson's Disease) as well as being associated with neuronal damage and decreases in white matter volume (Allen et al., 2017; Block and Calderón-Garcidueñas, 2009). Direct deposition of AP particles in the brain via the olfactory bulb may also result in the chronic activation of microglial cells and subsequently chronic production of pro-inflammatory species and oxidative stress (Block and Calderón-Garcidueñas, 2009; Block and Hong, 2005). With chronic AP exposure, these mechanisms may lead to structural changes in the brain. At present, it remains unclear as to why AP exposure may affect certain regions but not others in the brain. One possible explanation for effects in frontal regions is through the direct deposition of particles via the olfactory bulb pathway.

Noise exposure is hypothesized to adversely influence human health through somewhat different pathways than AP. It is known that chronic noise exposure increases levels of annoyance and stress, which can activate the autonomic nervous system/hypothalamus-pituitary-adrenal axis (Jafari et al., 2019). Noise may also influence health by decreasing sleep quality and subsequently negatively affecting metabolism (Basner et al., 2014). At present, the ways by which noise exposure may influence brain structure remains unknown. Some possibilities include the induction of persistent tau pathology and altered auditory input that may cause changes in the hippocampus and cortex (Paul et al., 2019); increases in stress-induced free radicals, which may go on to affect cell morphology; increased glucocorticoids that can alter synaptic terminal structures and inhibit neuronal regeneration in some regions; and alterations in neurotransmitters that may affect synaptic plasticity (Arjunan and Rajan, 2020). Chronic noise has also been linked to increased risk of cardiovascular disease, which is associated with decreased cognitive function (Barnes, 2015). Lower cardiorespiratory fitness, which may result from disease, has also been associated with faster rates of brain atrophy (Barnes, 2015). As mentioned above, the mixed associations we observed for noise exposures, lGI, and cortical thickness may be due to error in exposure estimation, but it may also

reflect compensatory mechanisms in certain areas of the brain. Should noise adversely affect other areas that have not been investigated up to this point, increased or non-changing lGI values in certain areas may reflect compensatory mechanisms on the part of the brain in order to offset the damage elsewhere. Further studies are needed looking at long-term effects of noise, particularly low-level chronic noise, on the brain in order to better understand the mix of positive and negative associations we observed in our study.

4.4. Study strengths and weaknesses

There are several limitations to our study. While the exposures were modeled for periods prior to the MRI examinations and ought to represent long-term exposures, we cannot draw longitudinal, causal conclusions as we do not have MRI data at baseline and therefore cannot identify exactly when any AP-associated structural changes may have occurred. Exposure misclassification in our exposures also exists, as they are modeled exposures and participants spent time other places than their home address. Nevertheless, sensitivity analyses restricted to those who did not move over the study period or were not working showed no qualitative change in our results. Some of the AP exposures are highly correlated and, even after conducting multipollutant models, it is difficult to tease out which air pollutant may have be most strongly associated with brain structure. Future analyses including greenspace may also be of interest. Our indoor noise estimates were calculated based on behavior and window information collected via questionnaire and therefore have not been validated with on-site measurements. The study population in this study is also small and it is likely that we are somewhat underpowered to fully evaluate potential associations, particularly in the effect modification analyses. Nevertheless, efforts to obtain AP and noise exposure information for the HNR MultiGeneration Study participants in the 1000BRAINS Study are currently being planned and would result in an almost doubling of available participants for analysis. The results from this study should also be considered in the context participants' air pollution exposure levels, which while higher than recommended by the 2005 WHO guidelines (World Health Organization Occupational and Environmental Health Team, 2006), are lower than those observed in other regions of the world, including much of Asia and the Middle East. Establishment of cohorts with AP, noise, and MRI data in areas with higher exposure levels would provide insight whether and what kind of dose-response relationship may exist between AP and structural brain measures.

Our study also has several strengths. First, the 1000BRAINS study includes rich demographic and lifestyle data, which allowed us to adjust for many potential confounders. We were also able to leverage extensive exposure data to evaluate several novel exposures, including PN_{AM}. Few prior studies have investigated whether chronic noise exposures influence brain structure or whether quasi-ultrafine particles may be particularly influential due to their ability to pass through the olfactory bulb. This is also one of the first studies to adjust for chronic noise, a potentially important co-exposure from traffic, when estimating the association between AP and brain structure. Finally, we focused in this study on brain structural measures within an important functional network of the brain, a strategy which has not been employed in many prior studies and will hopefully inform future studies on environmental exposures and functional connectivity in the brain. As mentioned previously, future studies with long-term follow-up periods are needed to better understand how long-term AP may influence brain health over the lifespan and help elucidate potential causal pathways. There also remains a need for studies with information on several aspects of brain health, such that the interplay between air pollution, structural measures, functional connectivity, and neurological diseases (e.g., Alzheimer's disease) can be examined together within the same participants.

4.5. Conclusion

Overall, long-term air pollution and noise exposures were not consistently associated with the structural brain measures of lGI and cortical thickness within the DMN, with the exception of weak negative associations between AP and cortical thickness in the right hemisphere. As few prior studies exist on environmental exposures and brain structure within functional networks, further studies into how AP and noise may alter both brain structure as well as brain signaling are needed to better understand the role the environment plays in affecting human health across the whole body.

Declaration of competing interest

The authors declare they have no actual or potential competing financial interests.

Acknowledgements

We thank the North Rhine-Westphalia State Agency for Nature, Environment and Consumer Protection (LANUV) for providing emission and land use data for North Rhine-Westphalia. We are indebted to the investigative group and the study personnel of the Heinz Nixdorf Recall (HNR) study and the 1000BRAINS study. We also thank the Heinz Nixdorf Foundation for the generous support of this study. The HNR study was supported by grants from the German Research Council (Deutsche Forschungsgemeinschaft; grants ER 155/6-1, ER 155/6-2, SI 236/8-1, and SI 236/9-1) and the Kulturstiftung Essen, Germany. The exposure assessment was funded through the European Community's Seventh Framework Program (FP7/2007–2011; grant 211250) and by the German Research Council (DFG; HO 3314/4-3). Further, this project was partially funded by the 1000BRAINS-Study of the Institute of Neuroscience and Medicine, Research Centre Jülich, Germany, and has received funding from the European Union's Horizon 2020 Research and Innovation Programme under grant agreement no. 945539 (HBP SGA3; S.C.) as well as from the Initiative and Networking Fund of the Helmholtz Association (S.C.).

Appendix A. Supplementary data

Supplementary data to this article can be found online at https://doi.org/10.1016/j.ijheh.2021.113867.

References

Allen, J.L., Klocke, C., Morris-Schaffer, K., Conrad, K., Sobolewski, M., Cory-Slechta, D. A., 2017. Cognitive effects of air pollution exposures and potential mechanistic underpinnings. Current Environ. Health Rep. 4, 180–191. https://doi.org/10.1007/s40572-017-0134-3.

Arjunan, A., Rajan, R., 2020. Noise and brain. Physiol. Behav. 227, 113136 https://doi.org/10.1016/j.physbeh.2020.113136.

Barnes, J.N., 2015. Exercise, cognitive function, and aging. Adv. Physiol. Educ. 39, 55–62. https://doi.org/10.1152/advan.00101.2014.

Basner, M., Babisch, W., Davis, A., Brink, M., Clark, C., Janssen, S., Stansfeld, S., 2014. Auditory and non-auditory effects of noise on health. Lancet 383, 1325–1332. https://doi.org/10.1016/S0140-6736(13)61613-X.

Beckmann, C.F., DeLuca, M., Devlin, J.T., Smith, S.M., 2005. Investigations into resting-state connectivity using independent component analysis. Phil. Trans. Roy. Soc. Lond. B Biol. Sci. 360, 1001–1013. https://doi.org/10.1098/rstb.2005.1634.

Beelen, R., Hoek, G., Vienneau, D., Eeftens, M., Dimakopoulou, K., Pedeli, X., Tsai, M.-Y., Künzli, N., Schikowski, T., Marcon, A., Eriksen, K.T., Raaschou-Nielsen, O., Stephanou, E., Patelarou, E., Lanki, T., Yli-Tuomi, T., Declercq, C., Falq, G., Stempfelet, M., Birk, M., Cyrys, J., Klot, S.v., Nádor, G., Varró, M.J., Dėdelė, A., Gražulevičienė, R., Mölter, A., Lindley, S., Madsen, C., Cesaroni, G., Ranzi, A., Badaloni, C., Hoffmann, B., Nonnemacher, M., Krämer, U., Kuhlbusch, T., Cirach, M., Nazelle, A. de, Nieuwenhuijsen, M., Bellander, T., Korek, M., Olsson, D., Strömgren, M., Dons, E., Jerrett, M., Fischer, P., Wang, M., Brunekreef, B., Hoogh, K. de, 2013. Development of NO2 and NOx land use regression models for estimating air pollution exposure in 36 study areas in Europe – the ESCAPE project. Atmos. Environ. 72, 10–23. https://doi.org/10.1016/j.atmosenv.2013.02.037.

Birmili, W., Weinhold, K., Rasch, F., Sonntag, A., Sun, J., Merkel, M., Wiedensohler, A., Bastian, S., Schladitz, A., Löschau, G., Cyrys, J., Pitz, M., Gu, J., Kusch, T.,

Flentje, H., Quass, U., Kaminski, H., Kuhlbusch, T.A.J., Meinhardt, F., Schwerin, A., Bath, O., Ries, L., Gerwig, H., Wirtz, K., Fiebig, M., 2016. Long-term observations of tropospheric particle number size distributions and equivalent black carbon mass concentrations in the German Ultrafine Aerosol Network (GUAN). Earth Syst. Sci. Data 8, 355–382. https://doi.org/10.5194/essd-8-355-2016.

Block, M.L., Calderón-Garcidueñas, L., 2009. Air pollution: mechanisms of neuroinflammation and CNS disease. Trends Neurosci. 32, 506–516. https://doi.org/10.1016/j.tins.2009.05.009.

Block, M.L., Hong, J.-S., 2005. Microglia and inflammation-mediated neurodegeneration: multiple triggers with a common mechanism. Prog. Neurobiol. 76, 77–98. https://doi.org/10.1016/j.pneurobio.2005.06.004.

Brown, J.W., Jaffe, J., 1975. Hypothesis on cerebral dominance. Neuropsychologia 13, 107–110. https://doi.org/10.1016/0028-3932(75)90054-8.

Bundesministerium der Justiz, 2006. Vorläufige berechnungsmethode Für den umgebungslärm an StraBen (VBUS). In: Bundesanzeiger, vol. 154a, pp. 30–49.

Carey, I.M., Anderson, H.R., Atkinson, R.W., Beevers, S.D., Cook, D.G., Strachan, D.P., Dajnak, D., Gulliver, J., Kelly, F.J., 2018. Are noise and air pollution related to the incidence of dementia? A cohort study in London, England. BMJ open 8, e022404. https://doi.org/10.1136/bmjopen-2018-022404.

Casanova, R., Wang, X., Reyes, J., Akita, Y., Serre, M.L., Vizuete, W., Chui, H.C., Driscoll, I., Resnick, S.M., Espeland, M.A., Chen, J.-C., 2016. A voxel-based morphometry study reveals local brain structural alterations associated with ambient fine particles in older women. Front. Hum. Neurosci. 10, 495. https://doi.org/10.3389/fnhum.2016.00495.

Caspers, S., Moebus, S., Lux, S., Pundt, N., Schütz, H., Mühleisen, T.W., Gras, V., Eickhoff, S.B., Romanzetti, S., Stöcker, T., Stirnberg, R., Kirlangic, M.E., Minnerop, M., Pieperhoff, P., Mödder, U., Das, S., Evans, A.C., Jöckel, K.-H., Erbel, R., Cichon, S., Nöthen, M.M., Sturma, D., Bauer, A., Jon Shah, N., Zilles, K., Amunts, K., 2014. Studying variability in human brain aging in a population-based German cohort-rationale and design of 1000BRAINS. Front. Aging Neurosci. 6, 149. https://doi.org/10.3389/fnagi.2014.00149.

Chen, H., Kwong, J.C., Copes, R., Hystad, P., van Donkelaar, A., Tu, K., Brook, J.R., Goldberg, M.S., Martin, R.V., Murray, B.J., Wilton, A.S., Kopp, A., Burnett, R.T., 2017. Exposure to ambient air pollution and the incidence of dementia: a population-based cohort study. Environ. Int. 108, 271–277. https://doi.org/10.1016/j.envint.2017.08.020.

Chen, J.-C., Wang, X., Wellenius, G.A., Serre, M.L., Driscoll, I., Casanova, R., McArdle, J. J., Manson, J.E., Chui, H.C., Espeland, M.A., 2015. Ambient air pollution and neurotoxicity on brain structure: evidence from women's health initiative memory study. Ann. Neurol. 78, 466–476. https://doi.org/10.1002/ana.24460.

Cheng, H., Sun, G., Li, M., Yin, M., Chen, H., 2019. Neuron loss and dysfunctionality in hippocampus explain aircraft noise induced working memory impairment: a resting-state fMRI study on military pilots. Biosci. Trends 13, 430–440. https://doi.org/10.5582/bst.2019.01190.

Cho, J., Noh, Y., Kim, S.Y., Sohn, J., Noh, J., Kim, W., Cho, S.-K., Seo, H., Seo, G., Lee, S.-K., Seo, S., Koh, S.-B., Oh, S.S., Kim, H.J., Seo, S.W., Shin, D.-S., Kim, N., Kim, H.H., Lee, J.I., Kim, C., 2020. Long-term ambient air pollution exposures and brain imaging markers in Korean adults: the environmental pollution-induced neurological EFfects (EPINEF) study. Environ. Health Perspect. 128, 117006 https://doi.org/10.1289/EHP7133.

Clark, C., Paunovic, K., 2018. WHO environmental noise guidelines for the European region: a systematic review on environmental noise and cognition. Int. J. Environ. Res. Publ. Health 15. https://doi.org/10.3390/ijerph15020285.

Crous-Bou, M., Gascon, M., Gispert, J.D., Cirach, M., Sánchez-Benavides, G., Falcon, C., Arenaza-Urquijo, E.M., Gotsens, X., Fauria, K., Sunyer, J., Nieuwenhuijsen, M.J., Luis Molinuevo, J., 2020. Impact of urban environmental exposures on cognitive performance and brain structure of healthy individuals at risk for Alzheimer's dementia. Environ. Int. 138, 105546 https://doi.org/10.1016/j.envint.2020.105546.

Cyrys, J., Eeftens, M., Heinrich, J., Ampe, C., Armengaud, A., Beelen, R., Bellander, T., Beregszaszi, T., Birk, M., Cesaroni, G., Cirach, M., Hoogh, K. de, Nazelle, A. de, Vocht, F. de, Declercq, C., Dėdelė, A., Dimakopoulou, K., Eriksen, K., Galassi, C., Grąulevičienė, R., Grivas, G., Gruzieva, O., Gustafsson, A.H., Hoffmann, B., Iakovides, M., Ineichen, A., Krämer, U., Lanki, T., Lozano, P., Madsen, C., Meliefste, K., Modig, L., Mölter, A., Mosler, G., Nieuwenhuijsen, M., Nonnemacher, M., Oldenwening, M., Peters, A., Pontet, S., Probst-Hensch, N., Quass, U., Raaschou-Nielsen, O., Ranzi, A., Sugiri, D., Stephanou, E.G., Taimisto, P., Tsai, M.-Y., Vaskövi, É., Villani, S., Wang, M., Brunekreef, B., Hoek, G., 2012. Variation of NO2 and NOx concentrations between and within 36 European study areas: results from the ESCAPE study. Atmos. Environ. 62, 374–390. https://doi.org/10.1016/j.atmosenv.2012.07.080.

Dale, A.M., Fischl, B., Sereno, M.I., 1999. Cortical surface-based analysis: I. Segmentation and surface reconstruction. Neuroimage 9, 179–194. https://doi.org/10.1006/nimg.1998.0395.

D'Angiulli, A., 2018. Severe urban outdoor air pollution and children's structural and functional brain development, from evidence to precautionary strategic action. Front. Publ. Health 6, 95. https://doi.org/10.3389/fpubh.2018.00095.

DataKustik, GmbH. CadnaA.. https://www.datakustik.com/produkte/cadnaa/warum-cadnaa/.

Davis, S.W., Dennis, N.A., Daselaar, S.M., Fleck, M.S., Cabeza, R., 2008. Que PASA? The posterior-anterior shift in aging (New York, N.Y. : 1991). Cerebr. Cortex 18, 1201–1209. https://doi.org/10.1093/cercor/bhm155.

Dolcos, F., Rice, H.J., Cabeza, R., 2002. Hemispheric asymmetry and aging: right hemisphere decline or asymmetry reduction. Neurosci. Biobehav. Rev. 26, 819–825. https://doi.org/10.1016/S0149-7634(02)00068-4.

Dragano, N., Hoffmann, B., Stang, A., Moebus, S., Verde, P.E., Weyers, S., Möhlenkamp, S., Schmermund, A., Mann, K., Jöckel, K.-H., Erbel, R., Siegrist, J., 2009. Subclinical coronary atherosclerosis and neighbourhood deprivation in an urban region. Eur. J. Epidemiol. 24, 25–35. https://doi.org/10.1007/s10654-008-9292-9.

Eeftens, M., Beelen, R., Hoogh, K. de, Bellander, T., Cesaroni, G., Cirach, M., Declercq, C., Dėdelė, A., Dons, E., Nazelle, A. de, Dimakopoulou, K., Eriksen, K., Falq, G., Fischer, P., Galassi, C., Gražulevičienė, R., Heinrich, J., Hoffmann, B., Jerrett, M., Keidel, D., Korek, M., Lanki, T., Lindley, S., Madsen, C., Mölter, A., Nádor, G., Nieuwenhuijsen, M., Nonnemacher, M., Pedeli, X., Raaschou-Nielsen, O., Patelarou, E., Quass, U., Ranzi, A., Schindler, C., Stempfelet, M., Stephanou, E., Sugiri, D., Tsai, M.-Y., Yli-Tuomi, T., Varró, M.J., Vienneau, D., Klot, S.v., Wolf, K., Brunekreef, B., Hoek, G., 2012. Development of Land Use Regression models for PM (2.5), PM(2.5) absorbance, PM(10) and PM(coarse) in 20 European study areas; results of the ESCAPE project. Environ. Sci. Technol. 46, 11195–11205. https://doi.org/10.1021/es301948k.

Erickson, L.D., Gale, S.D., Anderson, J.E., Brown, B.L., Hedges, D.W., 2020. Association between exposure to air pollution and total gray matter and total white matter volumes in adults: a cross-sectional study. Brain Sci. 10 https://doi.org/10.3390/brainsci10030164.

European Environment Agency, 2002. Directive 2002/49/EC of the European Parliament and of the Council of 25 June 2002 relating to the assessment and management of environmental noise. Off. J. Euro. Commun. 12–25.

European Parliament, Council of the European Union, 2008. Directive 2008/50/EC of the European Parliament and of the Council of 21 May 2008 on ambient air quality and cleaner air for Europe. Off. J. Euro. Union L152, 1–44.

Fischl, B., Dale, A.M., 2000. Measuring the thickness of the human cerebral cortex from magnetic resonance images. Proc. Natl. Acad. Sci. U.S.A. 97, 11050–11055. https://doi.org/10.1073/pnas.200033797.

Fischl, B., Sereno, M.I., Dale, A.M., 1999. Cortical surface-based analysis. II: inflation, flattening, and a surface-based coordinate system. Neuroimage 9, 195–207. https://doi.org/10.1006/nimg.1998.0396.

Foraster, M., Künzli, N., Aguilera, I., Rivera, M., Agis, D., Vila, J., Bouso, L., Deltell, A., Marrugat, J., Ramos, R., Sunyer, J., Elosua, R., Basagaña, X., 2014. High blood pressure and long-term exposure to indoor noise and air pollution from road traffic. Environ. Health Perspect. 122, 1193–1200. https://doi.org/10.1289/ehp.1307156.

Fuks, K.B., Wigmann, C., Altug, H., Schikowski, T., 2019. Road traffic noise at the residence, annoyance, and cognitive function in elderly women. Int. J. Environ. Res. Publ. Health 16. https://doi.org/10.3390/ijerph16101790.

Gale, S.D., Erickson, L.D., Anderson, J.E., Brown, B.L., Hedges, D.W., 2020. Association between exposure to air pollution and prefrontal cortical volume in adults: a cross-sectional study from the UK biobank. Environ. Res. 185, 109365. https://doi.org/10.1016/j.envres.2020.109365.

Gautam, P., Anstey, K.J., Wen, W., Sachdev, P.S., Cherbuin, N., 2015. Cortical gyrification and its relationships with cortical volume, cortical thickness, and cognitive performance in healthy mid-life adults. Behav. Brain Res. 287, 331–339. https://doi.org/10.1016/j.bbr.2015.03.018.

Genc, S., Zadeoglulari, Z., Fuss, S.H., Genc, K., 2012. The adverse effects of air pollution on the nervous system. J. Toxicol., 782462 https://doi.org/10.1155/2012/782462, 2012.

Hafkemeijer, A., van der Grond, J., Rombouts, S.A.R.B., 2012. Imaging the default mode network in aging and dementia. Biochim. Biophys. Acta 1822, 431–441. https://doi.org/10.1016/j.bbadis.2011.07.008.

Hedges, D.W., Erickson, L.D., Gale, S.D., Anderson, J.E., Brown, B.L., 2020. Association between exposure to air pollution and thalamus volume in adults: a cross-sectional study. PLoS One 15, e0230829. https://doi.org/10.1371/journal.pone.0230829.

Hedges, D.W., Erickson, L.D., Kunzelman, J., Brown, B.L., Gale, S.D., 2019. Association between exposure to air pollution and hippocampal volume in adults in the UK Biobank. Neurotoxicology 74, 108–120. https://doi.org/10.1016/j.neuro.2019.06.005.

Hegewald, J., Schubert, M., Freiberg, A., Romero Starke, K., Augustin, F., Riedel-Heller, S.G., Zeeb, H., Seidler, A., 2020. Traffic noise and mental health: a systematic review and meta-analysis. Int. J. Environ. Res. Publ. Health 17. https://doi.org/10.3390/ijerph17176175.

Hennig, F., Sugiri, D., Tzivian, L., Fuks, K., Moebus, S., Jöckel, K.-H., Vienneau, D., Kuhlbusch, T., Hoogh, K. de, Memmesheimer, M., Jakobs, H., Quass, U., Hoffmann, B., 2016. Comparison of land-use regression modeling with dispersion and chemistry transport modeling to assign air pollution concentrations within the Ruhr area. Atmosphere 7, 48. https://doi.org/10.3390/atmos7030048.

Hogstrom, L.J., Westlye, L.T., Walhovd, K.B., Fjell, A.M., 2013. The structure of the cerebral cortex across adult life: age-related patterns of surface area, thickness, and gyrification (New York, N.Y. : 1991). Cerebr. Cortex 23, 2521–2530. https://doi.org/10.1093/cercor/bhs231.

Jafari, Z., Kolb, B.E., Mohajerani, M.H., 2019. Noise exposure accelerates the risk of cognitive impairment and Alzheimer's disease: adulthood, gestational, and prenatal mechanistic evidence from animal studies. Neurosci. Biobehav. Rev. 117, 110–128. https://doi.org/10.1016/j.neubiorev.2019.04.001.

Jenkinson, M., Beckmann, C.F., Behrens, T.E.J., Woolrich, M.W., Smith, S.M., 2012. FSL. NeuroImag. 62, 782–790. https://doi.org/10.1016/j.neuroimage.2011.09.015.

Jockwitz, C., Caspers, S., Lux, S., Jütten, K., Schleicher, A., Eickhoff, S.B., Amunts, K., Zilles, K., 2017. Age- and function-related regional changes in cortical folding of the default mode network in older adults. Brain Struct. Funct. 222, 83–99. https://doi.org/10.1007/s00429-016-1202-4.

Jockwitz, C., Mérillat, S., Liem, F., Oschwald, J., Amunts, K., Caspers, S., Jäncke, L., 2019. Generalizing age effects on brain structure and cognition: a two-study

comparison approach. Hum. Brain Mapp. 40 (8), 2305–2319. https://doi.org/10.1002/hbm.24524.
Kulick, E.R., Elkind, M.S., Boehme, A.K., Joyce, N.R., Schupf, N., Kaufman, J.D., Mayeux, R., Manly, J.J., Wellenius, G.A., 2020. Long-term exposure to ambient air pollution, APOE-ε4 status, and cognitive decline in a cohort of older adults in northern Manhattan. Environ. Int. 136, 105440 https://doi.org/10.1016/j.envint.2019.105440.
Kulick, E.R., Wellenius, G.A., Kaufman, J.D., DeRosa, J.T., Kinney, P.L., Cheung, Y.K., Wright, C.B., Sacco, R.L., Elkind, M.S., 2017. Long-term exposure to ambient air pollution and subclinical cerebrovascular disease in NOMAS (the northern manhattan study). Stroke 48. https://doi.org/10.1161/STROKEAHA.117.016672, 1966–1968.
Lucht, S., Hennig, F., Moebus, S., Führer-Sakel, D., Herder, C., Jöckel, K.-H., Hoffmann, B., 2019. Air pollution and diabetes-related biomarkers in non-diabetic adults: a pathway to impaired glucose metabolism? Environ. Int. 124, 370–392. https://doi.org/10.1016/j.envint.2019.01.005.
Memmesheimer, M., Friese, E., Ebel, A., Jakobs, H.J., Feldmann, H., Kessler, C., Piekorz, G., 2004. Long-term simulations of particulate matter in Europe on different scales using sequential nesting of a regional model. Int. J. E Polit. 22 https://doi.org/10.1504/IJEP.2004.005530, 5530, 108.
Münzel, T., Schmidt, F.P., Steven, S., Herzog, J., Daiber, A., Sørensen, M., 2018. Environmental noise and the cardiovascular system. J. Am. Coll. Cardiol. 71, 688–697. https://doi.org/10.1016/j.jacc.2017.12.015.
Nonnemacher, M., Jakobs, H., Viehmann, A., Vanberg, I., Kessler, C., Moebus, S., Möhlenkamp, S., Erbel, R., Hoffmann, B., Memmesheimer, M., 2014. Spatio-temporal modelling of residential exposure to particulate matter and gaseous pollutants for the Heinz Nixdorf Recall Cohort. Atmos. Environ. 91, 15–23. https://doi.org/10.1016/j.atmosenv.2014.03.052.
Nußbaum, R., Lucht, S., Jockwitz, C., Moebus, S., Engel, M., Jöckel, K.-H., Caspers, S., Hoffmann, B., 2020. Associations of air pollution and noise with local brain structure in a cohort of older adults. Environ. Health Perspect. 128, 67012 https://doi.org/10.1289/EHP5859.
Oberdörster, G., Sharp, Z., Atudorei, V., Elder, A., Gelein, R., Kreyling, W., Cox, C., 2004. Translocation of inhaled ultrafine particles to the brain. Inhal. Toxicol. 16, 437–445. https://doi.org/10.1080/08958370490439597.
Ohlwein, S., Hennig, F., Lucht, S., Matthiessen, C., Pundt, N., Moebus, S., Jöckel, K.-H., Hoffmann, B., 2019. Indoor and outdoor road traffic noise and incident diabetes mellitus. Environ. Epidemiol. 3, e037 https://doi.org/10.1097/EE9.0000000000000037.
Orban, E., McDonald, K., Sutcliffe, R., Hoffmann, B., Fuks, K.B., Dragano, N., Viehmann, A., Erbel, R., Jöckel, K.-H., Pundt, N., Moebus, S., 2016. Residential road traffic noise and high depressive symptoms after five years of follow-up: results from the Heinz Nixdorf recall study. Environ. Health Perspect. 124, 578–585. https://doi.org/10.1289/ehp.1409400.
Oudin, A., Segersson, D., Adolfsson, R., Forsberg, B., 2018. Association between air pollution from residential wood burning and dementia incidence in a longitudinal study in Northern Sweden. PLoS One 13, e0198283. https://doi.org/10.1371/journal.pone.0198283.
Paul, K.C., Haan, M., Mayeda, E.R., Ritz, B.R., 2019. Ambient air pollution, noise, and late-life cognitive decline and dementia risk. Annu. Rev. Publ. Health 40, 203–220. https://doi.org/10.1146/annurev-publhealth-040218-044058.
Power, M.C., Lamichhane, A.P., Liao, D., Xu, X., Jack, C.R., Gottesman, R.F., Mosley, T., Stewart, J.D., Yanosky, J.D., Whitsel, E.A., 2018. The association of long-term exposure to particulate matter air pollution with brain MRI findings: the ARIC study. Environ. Health Perspect. 126, 27009 https://doi.org/10.1289/EHP2152.
Pujol, J., Fenoll, R., Macià, D., Martínez-Vilavella, G., Alvarez-Pedrerol, M., Rivas, I., Forns, J., Deus, J., Blanco-Hinojo, L., Querol, X., Sunyer, J., 2016a. Airborne copper exposure in school environments associated with poorer motor performance and altered basal ganglia. Brain Behav. 6, e00467 https://doi.org/10.1002/brb3.467.
Pujol, J., Martínez-Vilavella, G., Macià, D., Fenoll, R., Alvarez-Pedrerol, M., Rivas, I., Forns, J., Blanco-Hinojo, L., Capellades, J., Querol, X., Deus, J., Sunyer, J., 2016b. Traffic pollution exposure is associated with altered brain connectivity in school children. Neuroimage 129, 175–184. https://doi.org/10.1016/j.neuroimage.2016.01.036.
Raichle, M.E., 2015. The brain's default mode network. Annu. Rev. Neurosci. 38, 433–447. https://doi.org/10.1146/annurev-neuro-071013-014030.
Schaer, M., Cuadra, M.B., Schmansky, N., Fischl, B., Thiran, J.-P., Eliez, S., 2012. How to measure cortical folding from MR images: a step-by-step tutorial to compute local gyrification index. JoVE : JoVE 59, e3417. https://doi.org/10.3791/3417.
Schmermund, A., Möhlenkamp, S., Stang, A., Grönemeyer, D., Seibel, R., Hirche, H., Mann, K., Siffert, W., Lauterbach, K., Siegrist, J., Jöckel, K.-H., Erbel, R., 2002. Assessment of clinically silent atherosclerotic disease and established and novel risk factors for predicting myocardial infarction and cardiac death in healthy middle-aged subjects: rationale and design of the Heinz Nixdorf RECALL Study. Am. Heart J. 144, 212–218. https://doi.org/10.1067/mhj.2002.123579.
Schraufnagel, D.E., Balmes, J.R., Cowl, C.T., Matteis, S. de, Jung, S.-H., Mortimer, K., Perez-Padilla, R., Rice, M.B., Riojas-Rodriguez, H., Sood, A., Thurston, G.D., To, T., Vanker, A., Wuebbles, D.J., 2019. Air pollution and noncommunicable diseases: a review by the forum of international respiratory societies' environmental committee, Part 2: air pollution and organ systems. Chest 155, 417–426. https://doi.org/10.1016/j.chest.2018.10.041.
Stang, A., Moebus, S., Dragano, N., Beck, E.M., Möhlenkamp, S., Schmermund, A., Siegrist, J., Erbel, R., Jöckel, K.H., 2005. Baseline recruitment and analyses of nonresponse of the Heinz Nixdorf recall study: identifiability of phone numbers as the major determinant of response. Eur. J. Epidemiol. 20, 489–496. https://doi.org/10.1007/s10654-005-5529-z.
Textor, J., Hardt, J., Knüppel, S., 2011. DAGitty: a graphical tool for analyzing causal diagrams. Epidemiology (Cambridge, Mass.) 22, 745. https://doi.org/10.1097/EDE.0b013e318225c2be.
Thurston, G.D., Kipen, H., Annesi-Maesano, I., Balmes, J., Brook, R.D., Cromar, K., Matteis, S. de, Forastiere, F., Forsberg, B., Frampton, M.W., Grigg, J., Heederik, D., Kelly, F.J., Kuenzli, N., Laumbach, R., Peters, A., Rajagopalan, S.T., Rich, D., Ritz, B., Samet, J.M., Sandstrom, T., Sigsgaard, T., Sunyer, J., Brunekreef, B., 2017. A joint ERS/ATS policy statement: what constitutes an adverse health effect of air pollution? An analytical framework. Eur. Respir. J. 49 https://doi.org/10.1183/13993003.00419-2016.
Tonne, C., Elbaz, A., Beevers, S., Singh-Manoux, A., 2014. Traffic-related air pollution in relation to cognitive function in older adults. Epidemiology (Cambridge, Mass.) 25, 674–681. https://doi.org/10.1097/EDE.0000000000000144.
Tsapanou, A., Habeck, C., Gazes, Y., Razlighi, Q., Sakhardande, J., Stern, Y., Salthouse, T. A., 2019. Brain biomarkers and cognition across adulthood. Hum. Brain Mapp. 40, 3832–3842. https://doi.org/10.1002/hbm.24634.
Tzivian, L., Dlugaj, M., Winkler, A., Hennig, F., Fuks, K., Sugiri, D., Schikowski, T., Jakobs, H., Erbel, R., Jöckel, K.-H., Moebus, S., Hoffmann, B., Weimar, C., 2016a. Long-term air pollution and traffic noise exposures and cognitive function:A cross-sectional analysis of the Heinz Nixdorf Recall study. J. Toxicol. Environ. Health Part A 79, 1057–1069. https://doi.org/10.1080/15287394.2016.1219570.
Tzivian, L., Dlugaj, M., Winkler, A., Weinmayr, G., Hennig, F., Fuks, K.B., Vossoughi, M., Schikowski, T., Weimar, C., Erbel, R., Jöckel, K.-H., Moebus, S., Hoffmann, B., 2016b. Long-term air pollution and traffic noise exposures and mild cognitive impairment in older adults: a cross-sectional analysis of the Heinz Nixdorf recall study. Environ. Health Perspect. 124, 1361–1368. https://doi.org/10.1289/ehp.1509824.
Tzivian, L., Winkler, A., Dlugaj, M., Schikowski, T., Vossoughi, M., Fuks, K., Weinmayr, G., Hoffmann, B., 2015. Effect of long-term outdoor air pollution and noise on cognitive and psychological functions in adults. Int. J. Hyg Environ. Health 218, 1–11. https://doi.org/10.1016/j.ijheh.2014.08.002.
UNESCO, 1997. International Standard Classification of Education ISCED 1997. UNITED NATIONS EDUCATIONAL, SCIENTIFIC AND CULTURAL ORGANIZATION, p. 49.
Weuve, J., Puett, R.C., Schwartz, J., Yanosky, J.D., Laden, F., Grodstein, F., 2012. Exposure to particulate air pollution and cognitive decline in older women. Arch. Intern. Med. 172, 219–227. https://doi.org/10.1001/archinternmed.2011.683.
WHO Regional Office for Europe, 2009. Night Noise Guidelines for Europe. World Health Organization, Copenhagen, p. 162. https://www.euro.who.int/en/health-topics/environment-and-health/noise/publications/2009/night-noise-guidelines-for-europe.
Wilker, E.H., Martinez-Ramirez, S., Kloog, I., Schwartz, J., Mostofsky, E., Koutrakis, P., Mittleman, M.A., Viswanathan, A., 2016. Fine particulate matter, residential proximity to major roads, and markers of small vessel disease in a memory study population. J. Alzheim. Dis. : JAD 53, 1315–1323. https://doi.org/10.3233/JAD-151143.
Wilker, E.H., Preis, S.R., Beiser, A.S., Wolf, P.A., Au, R., Kloog, I., Li, W., Schwartz, J., Koutrakis, P., DeCarli, C., Seshadri, S., Mittleman, M.A., 2015. Long-term exposure to fine particulate matter, residential proximity to major roads and measures of brain structure. Stroke 46, 1161–1166. https://doi.org/10.1161/STROKEAHA.114.008348.
Winkler, G., Döring, A., 1995. Kurzmethoden zur Charakterisierung des Ernährungsmusters: einsatz und Auswertung eines Food-Frequency-Fragebogens. Ernahrungs Umsch. 42, 289–291.
Winkler, G., Döring, A., 1998. Validation of a short qualitative food frequency list used in several German large scale surveys. Zeitschrift fur Ernahrungswissenschaft 37, 234–241.
World Health Organization, 2018. Environmental Noise Guidelines for the European Region. World Health Organization, Copenhagen, p. 181. https://www.euro.who.int/_data/assets/pdf_file/0008/383921/noise-guidelines-eng.pdf. (Accessed 2 August 2021).
World Health Organization Occupational and Environmental Health Team, 2006. WHO Air Quality Guidelines for Particulate Matter, Ozone, Nitrogen Dioxide and Sulfur Dioxide: Global Update 2005. World Health Organization, Geneva, Switzerland, p. 22. https://apps.who.int/iris/handle/10665/69477. (Accessed 7 March 2019).
Wright, B., Peters, E., Ettinger, U., Kuipers, E., Kumari, V., 2014. Understanding noise stress-induced cognitive impairment in healthy adults and its implications for schizophrenia. Noise Health 16, 166–176. https://doi.org/10.4103/1463-1741.134917.

International Journal of Hygiene and Environmental Health 239 (2022) 113875

Contents lists available at ScienceDirect

International Journal of Hygiene and Environmental Health

journal homepage: www.elsevier.com/locate/ijheh

Long-term exposure to ambient nitrogen dioxide and ozone modifies systematic low-grade inflammation: The CHCN-BTH study

Kuo Liu [a], Han Cao [a], Bingxiao Li [a], Chunyue Guo [a], Wei Zhao [b], Xiaoyan Han [b], Han Zhang [c], Zhengfang Wang [c], Naijun Tang [d], Kaijun Niu [e], Li Pan [f], Huijing He [f], Ze Cui [g], Jixin Sun [g], Guangliang Shan [f], Ling Zhang [a,*]

[a] Department of Epidemiology and Health Statistics, School of Public Health, Capital Medical University, Beijing Municipal Key Laboratory of Clinical Epidemiology, Beijing, China
[b] Department of Chronic and Noncommunicable Disease Prevention and Control, Chaoyang District Center for Disease Prevention and Control, Beijing, China
[c] Health Management Center, Beijing Aerospace General Hospital, Beijing, China
[d] Department of Occupational and Environmental Health, School of Public Health, Tianjin Medical University, Tianjin, China
[e] Nutritional Epidemiology Institute and School of Public Health, Tianjin Medical University, Tianjin, China
[f] Department of Epidemiology and Statistics, Institute of Basic Medical Sciences, Chinese Academy of Medical Sciences, School of Basic Medicine, Peking Union Medical College, Beijing, China
[g] Department of Chronic and Noncommunicable Disease Prevention and Control, Hebei Provincial Center for Disease Prevention and Control, Shijiazhuang, Hebei, China

ARTICLE INFO

Keywords:
Long-term gaseous pollutant
Nitrogen dioxide
Ozone
Low-grade systematic inflammation

ABSTRACT

The potential effect of long-term exposure to ambient air pollutants on low-grade systematic inflammation has seldom been evaluated taking indoor air pollution and self-protection behaviors on smog days into account. A total of 24,346 participants at baseline were included to conduct a cross-sectional study. The annual (2016) average pollutant concentrations were assessed by air monitoring stations for $PM_{2.5}$, PM_{10}, SO_2, NO_2, O_3 and CO. Associations between annual ambient air pollution and low-grade systematic inflammation (hsCRP>3 mg/L) were estimated by generalized linear mixed models. Stratification analysis was also performed based on demographic characteristics, health-related behaviors and disease status. Annual ambient NO_2 and O_3 were all associated with low-grade systematic inflammation in single-pollutant models after adjusting for age, sex, blood lipids, blood pressure, lifestyle risk factors, cooking fuel, heating fuel and habits during smog days (NO_2 per 10 $\mu g/m^3$: OR = 1.057, $P = 0.018$; O_3 per 10 $\mu g/m^3$: OR = 0.953, $P = 0.012$). The 2-year and 3-year ozone concentrations were consistently associated with lower systematic inflammation (2-year O_3 per 10 $\mu g/m^3$: OR = 0.959, $P = 0.004$; 3-year O_3 per 10 $\mu g/m^3$: OR = 0.961, $P = 0.014$). In two-pollutant models, the estimated effects of annual NO_2 and O_3 on low-grade systematic inflammation remained stable. The effect size of annual pollutants on inflammation increased in participants without air-purifier usage (NO_2 per 10 $\mu g/m^3$: OR = 1.079, $P = 0.009$; O_3 per 10 $\mu g/m^3$: OR = 0.925, $P = 0.001$), while the association was null in the air-purifier usage group. Thus, long-term exposure to ambient NO_2 and O_3 was associated with low-grade systemic inflammation, and the results were generally stable after sensitivity analysis. The usage of air purifiers on smog days can modify the association between gaseous pollutants and systematic inflammation.

1. Introduction

Air pollution is a complex mixture of particulate and gaseous materials and has become a serious public health problem in developing countries (WHO (World Health Organization), 2016). Ambient particulate matter air pollution and ozone contributed approximately 90 million DALYs (Disability Adjusted of Life Years) in 2017 (GBD 2017 Risk Factor Collaborators, 2018). Major pathophysiological pathways through which air pollution may promote the development of cardiometabolic disorders are increased oxidative stress and inflammation (Li et al., 2020; Pope et al., 2016). C-reactive protein (CRP) is a biomarker of inflammatory reactions and is an important mediator of

* Corresponding author. Department of Epidemiology and Health Statistics, School of Public Health, Capital Medical University, No. 10, Xi Toutiao You Anmenwai, Fengtai District, Beijing, 100069, China.
E-mail address: zlilyepi@ccmu.edu.cn (L. Zhang).

https://doi.org/10.1016/j.ijheh.2021.113875
Received 22 July 2021; Received in revised form 19 October 2021; Accepted 20 October 2021
Available online 29 October 2021

atherosclerosis (Libby and Ridker, 2014). High-sensitivity CRP (hsCRP) is more precise (detection range 0.01–10 mg/L) than traditional CRP measurements (detection range 1–10 mg/L) (Kamath et al., 2015), and this improved sensitivity makes hsCRP suitable for detecting low-grade inflammation and the risk of cardiometabolic disorders among the general population (Blaha et al., 2011).

Long-term gaseous pollutant exposure has been demonstrated to induce pulmonary inflammation in mice (Wegmann et al., 2003); however, there is few epidemiological evidence on the potential effect of long-term exposure to gaseous pollutants on low-grade systemic inflammation, which is represented by hsCRP. Many studies have demonstrated an association between long-term particulate matter exposure, especially fine particulate matter (particles less than 2.5 μm in diameter, or $PM_{2.5}$) and hsCRP, but the results are not consistent (Liu et al., 2019).

There are several reasons that epidemiological studies of the long-term estimated effects of air pollution on inflammatory markers are inconsistent. First, the use of cooking and heating fuel will produce high levels of nitrogen dioxide (NO_2) and sulfur dioxide (SO_2), and indoor air pollution (IAP) from household cooking and space heating causes substantial adverse health effects in developing countries (Seow et al., 2016). Previous studies that focused on demonstrating the potential effects of ambient air pollution seldom considered the confounding caused by IAP. Moreover, self-protection behaviors on smog or haze days, such as wearing face masks, using air purifiers or reducing outdoor activities, can also modify the estimated effects of ambient air pollutant exposure. These self-protection behaviors are rarely considered in previous studies that aimed to demonstrate the adverse health effects of ambient air pollution.

The CoHort study on CHronic disease of Community Natural population in Beijing-Tianjin-Hebei region (CHCN-BTH) collected residential location, information related to IAP, self-protection behaviors on smog days and measurements of high-sensitivity CRP (hsCRP). In our analysis, we examined the relationship between inflammatory marker and long-term exposure to particulate and gaseous pollutants with consideration of IAP and self-protection behaviors on smog days.

2. Materials and methods

2.1. Study population

The CoHort study on CHronic disease of Community Natural population in the Beijing-Tianjin-Hebei region (CHCN-BTH) is a longitudinal cohort study that aimed to explore the environmental and genetic determinants of noncommunicable diseases (NCDs) in BTH areas with varying air quality and urbanization levels. Details of this study have been described in our previous research article (Liu et al., 2021). Briefly, the current community-based study recruited participants using a multistage, stratified cluster sampling method. Participants older than 18 who had been living in the local area for more than 3 years without pregnancy or major physical or mental disability were recruited for this study.

A total of 33,391 participants were recruited for the baseline survey in 2017. Among these participants, 24,346 subjects who had hsCRP measurements less than 10 mg/L and with completed IAP information and self-protection habits on smog days were included in the current analysis to conduct a cross-sectional study. Face-to-face interviews were performed to collect sociodemographic characteristics, a familial and personal medical history, lifestyle behaviors (including drinking, smoking, physical exercise), and pollutant exposure (passive smoking condition, cooking habits, cooking fuels, heating fuels, and self-protection habits on smog days) by using uniform questionnaires. To ensure the accuracy of the questionnaire information, all questionnaires were verified by the inspectors. This study was approved by the ethics committees of the Center for Disease Control (IRB2017–003, CYCDPCIRB-20170830–1) and Capital Medical University (2018SY81). Written informed consents were obtained from all participants prior to the baseline survey.

2.2. Air pollution exposure assessment

Concentrations of fine particles of pollutants ($PM_{2.5}$), particles of no greater than 10 μm in aerodynamic diameter (PM_{10}), NO_2, SO_2, carbonic oxide (CO) and ozone (O_3) were collected using district-specific air monitoring stations, as detailed previously (Liu et al., 2021). Data from the air monitoring site were used to calculate daily mean concentrations of $PM_{2.5}$, PM_{10}, SO_2, NO_2, CO and daily 8-h maximum O_3 observations. The annual (2016), 2-year (2015–2016), and 3-year (2014–2016) mean concentrations of the six air pollutants were calculated and assigned to each individual living in the corresponding village or community as the surrogates of exposure. Potential indoor pollution, including cooking fuel, heating fuel and cooking habits, were assessed by face-to-face interviews. The types of cooking fuel included no cooking habits, electricity, natural gas, coal gas, coal and crop straw fuel. Heating fuel types included no heating in winter, electricity, natural gas, coal gas, coal, crop straw fuel and central heating. Cooking habits included kitchen ventilator usage, kitchen door closure during cooking and bedroom separation from the kitchen.

2.3. Serum markers

Fasting blood samples were collected and stored in a 2% EDTA vacutainer, and plasma samples were separated after centrifugation and aliquoting. Samples were kept in an insulated box with ice packs to maintain their temperature at 0–4 °C and transported with dry-ice to Beijing Hepingli Hospital to test for serum markers. Highly sensitive C-reactive protein, fasting plasma glucose (FPG), triglyceride (TG), low-density lipoprotein cholesterol (LDLC), high-density lipoprotein cholesterol (HDLC), and total cholesterol (TC) were assessed using a Beckman Coulter chemistry analyzer AU5800. In the current study, hsCRP was treated as a dichotomous variable that reflected systematic inflammation. Low-grade inflammation was defined as hsCRP >3 mg/L.

2.4. Covariates

The potential confounders included age, sex, health status, biomarkers, lifestyle risk factors, indoor pollution and self-protection-related habits on smog days; the details are shown in the Supplemental file. Hypertension was defined as having self-reported physician-diagnosed hypertension or taking antihypertensive medication according to the Chinese Guidelines for the Management of Hypertension (Joint Committee for Guideline Revision, 2019) or having an SBP ≥140 mmHg or DBP ≥90 mmHg at the baseline measurement. Hyperlipidemia was defined according to the Chinese Guideline for the Management of Dyslipidemia in Adults (LDLC ≥4.1 mmol/L, TG ≥ 2.3 mmol/L, TC ≥ 6.2 mmol/L, or HDLC ≤1 mmol/L) (Joint Committee for Guideline Revision, 2018). Participants with a BMI ≥28 were defined as obese according to the Chinese BMI classification standard (Wang et al., 2007). Diabetes was defined as having a fasting plasma glucose (FPG) ≥ 7.0 mmol/L and/or a diagnosis of diabetes by a physician and/or taking antidiabetic medication (American Diabetes Association, 2020).

2.5. Statistical analysis

The mean (standard deviation, SD) was used to describe continuous variables with a normal distribution, and the median (interquartile range, IQR) was used to represent continuous variables with a non-normal distribution. The *t*-test and Mann–Whitney *U* test were used to test for the differences in normally distributed variables and non-normally distributed variables between the two groups, respectively. Counts (percentages) were used to characterize the distribution of the categorical variables. Spearman rank correlation coefficients were used

to determine the relationships among the different air pollutants. Generalized linear mixed models (GLMMs) were used to demonstrate the association between air pollutants and low-grade systematic inflammation with a logit link function. Cities were incorporated as a random effect.

Three single pollutant models were first used to evaluate the potential effects of exposure and low-grade system inflammation. Model 1 is a crude model without adjusting for any covariates. In Model 2, age, sex, smoking, alcohol consumption, passive smoking, BMI, exercise frequency, blood pressure and blood lipids were adjusted. In Model 3, cooking habits, cooking and heating fuel, and self-protection habits on smog days were further adjusted. The pollutants significantly associated with systemic inflammation in the above analysis were further tested in the two-pollutant model with full adjustments (Model 3), and the concentration of PM_{10} was additionally adjusted in each two-pollutant model. Moreover, we performed a stratified analysis according to different disease statuses and potential confounders, such as age group, sex, cooking (yes/no), exercise (never/regular), air purifier usage (yes/no), and mask-wearing habit (yes/no).

3. Result

3.1. General characteristics of the study participants

A total of 24,346 participants with baseline data on cooking habits and self-protection habits during smog were analyzed. The characteristics of the current study participants and all CHCN-BTH participants are shown in Supplementary Table A.1. The participants' mean (SD) age was 50.8 (14.4) years; 11036 (45.3%) were men. More than 30% were smokers, 43.6% were passive smokers, 80% used natural gas as cooking fuel, and 66.9% had central heating in the winter. Most of the participants (71%) reduced their outdoor activities during smog days, 31.7% used air purifiers, and 54.2% had mask-wearing habits during smog or haze days. Approximately 10.5% were diagnosed with diabetes, and 7.4% had self-reported cardiovascular disease. The details are shown in Table 1.

The mean age of the participants who used air purifiers was younger than those who did not use air purifiers (49.3 vs. 51.6, $P < 0.001$). In addition, participants with air purifier usage habits had a lower BMI and blood pressure and a lower proportion of diabetes and hyperlipidemia. Moreover, those who used air purifiers on smog days had healthier habits, including less smoking and more physical activity ($P < 0.001$). However, a higher percentage of people who used air purifiers drank alcohol than those who did not. Moreover, the proportion of participants who reduced outdoor activity and wore masks on smog or haze days was higher among air purifier users than among those who did not ($P < 0.001$). The details are shown in Table 1.

3.2. Associations between air pollutants and hsCRP

The annual NO_2 and O_3 concentrations were negatively correlated with each other (correlation coefficient = - 0.71, $P < 0.001$), and the Spearman's correlation coefficients for each pollutant are shown in Fig. 1 and Supplementary Figure A.1. In univariate analysis, the associations between the annual average concentrations of ambient pollutants and low-grade systematic inflammation were null. Annual ambient NO_2 and the O_3 concentrations were associated with low-grade systematic inflammation in the single-pollutant models after adjusting for age, sex, blood lipids, blood pressure, and lifestyle risk factors (Model 2: NO_2 per 10 μg/m^3: OR = 1.055, $P = 0.016$; O_3 per 10 μg/m^3: OR = 0.960, $P = 0.027$). The associations between annual NO_2 and O_3 concentrations were consistently significant after further adjusting for cooking fuel, heating fuel and habits during smog days (Model 3: NO_2 per 10 μg/m^3: OR = 1.057, $P = 0.018$; O_3 per 10 μg/m^3: OR = 0.953, $P = 0.012$). After further adjusting for distance to the main road, the association between one-year ozone and systematic inflammation became

Table 1
General characteristics of the study population.

	CHCN-BTH cohort		Without air purifier usage	With air purifier usage	*P* value**
	n = 24,346	*P* value*	n = 7726	n = 16,620	
Age, mean (SD), y	50.8 (14.4)	<0.001	51.6 (14.3)	49.3 (14.7)	<0.001
Male, number (%)	11,036 (45.3)	0.131	7525 (45.3)	3511 (45.4)	0.807
BMI, mean (SD), kg/m^2	25.3 (3.7)	<0.001	25.5 (3.8)	24.9 (3.7)	<0.001
SBP, mean (SD), mmHg	130.2 (19.3)	<0.001	131.8 (19.5)	127.0 (18.6)	<0.001
DBP, mean (SD), mmHg	77.4 (12.6)	<0.001	78.1 (13.0)	75.9 (11.6)	<0.001
TC, mean (SD), mmol/L	5.1 (1.0)	<0.001	5.1 (1.1)	5.1 (1.0)	0.522
TG, mean (SD), mmol/L	1.6 (1.2)	<0.001	1.6 (1.2)	1.6 (1.1)	0.056
LDLC, mean (SD), mmol/L	3.0 (0.9)	<0.001	3.0 (1.0)	3.0 (0.8)	0.429
HDLC, mean (SD), mmol/L	1.4 (0.4)	<0.001	1.4 (0.4)	1.4 (0.4)	0.038
Hyperlipidemia, number (%)	8494 (34.9)	<0.001	5906 (35.5)	2592 (33.5)	0.002
FPG, mean (SD), mmol/L	5.9 (1.7)	<0.001	5.8 (1.8)	5.9 (1.5)	0.173
Diabetes, number (%)	2549 (10.5)	<0.001	1856 (11.2)	693 (9.0)	<0.001
Passive smoking, number (%), days per/week		0.089			<0.001
Seldom/Never	13,411 (56.4)	NA	8860 (53.3)	4551 (59.4)	NA
<1	2189 (9.2)	NA	1434 (8.6)	755 (9.9)	NA
1-2	836 (3.5)	NA	552 (3.3)	284 (3.7)	NA
3-5	1264 (5.3)	NA	830 (5.0)	434 (5.7)	NA
>5	6086 (25.6)	NA	4454 (26.8)	1632 (21.3)	NA
Cooking (yes), number (%)	17,090 (70.2)	0.092	11,797 (71.8)	5293 (69.0)	<0.001
Kitchen door (closed during cooking), number (%)	13,222 (54.3)	0.106	8636 (54.8)	4586 (59.4)	<0.001
Cook fuel, number (%)		NA			<0.001
No cooking	235 (1.0)	ref	199 (1.2)	36 (0.5)	NA
Electricity	1145 (4.7)	0.699	1023 (6.2)	122 (1.6)	NA
Natural gas	19,359 (80.0)	0.600	12,304 (74.6)	7055 (91.3)	NA
Coal gas	3090 (12.8)	0.111	2622 (15.9)	468 (6.1)	NA
Coal	266 (1.1)	0.395	250 (1.5)	16 (0.2)	NA
Crop straw fuel	96 (0.4)	0.154	94 (0.6)	2 (0.0)	NA
Kitchen ventilator (yes), number (%)	22,314 (91.7)	0.704	14,800 (91.7)	7514 (98.7)	<0.001
Heating fuel, number (%)					<0.001
No heating	72 (0.3)	ref	72 (0.4)	0 (0.0)	NA
Electricity	1890 (7.8)	0.464	1587 (9.6)	303 (3.9)	NA
Natural gas	4166 (17.2)	0.244	2733 (16.6)	1433 (18.5)	NA
Coal gas	440 (1.8)	0.412	335 (2.0)	105 (1.4)	NA
Coal	1.034 (4.3)	0.464	999 (6.1)	35 (0.5)	NA

(continued on next page)

Table 1 (*continued*)

	CHCN-BTH cohort		Without air purifier usage	With air purifier usage	*P* value**
	n = 24,346	*P* value*	n = 7726	n = 16,620	
Crop straw fuel	393 (1.6)	0.153	333 (2.0)	60 (0.8)	NA
Central heating	16,184 (66.9)	0.433	10,436 (63.3)	5748 (74.8)	NA
Smoking, number (%)	7450 (30.6)	<0.001	5293 (31.8)	2157 (27.9)	<0.001
Alcohol Drinking, number (%)	9735 (40.0)	0.010	6522 (39.2)	3213 (41.6)	0.001
Exercise, number (%), times per/ week		0.360			<0.001
5-7	11,172 (45.9)	NA	7585 (45.6)	3587 (46.4)	NA
3-4	2641 (10.8)	NA	1735 (10.4)	906 (11.7)	NA
1-2	3723 (15.3)	NA	2303 (13.9)	1420 (18.4)	NA
<1	1731 (7.1)	NA	1070 (6.4)	661 (8.6)	NA
Seldom/Never	5079 (20.9)	NA	3927 (23.6)	1152 (14.9)	NA
Habits during smog or haze, number (%)					
Reduce outdoor activity	17,276 (71.0)	0.373	11,231 (67.6)	6045 (78.2)	<0.001
Mask wearing	13,200 (54.2)	<0.001	8368 (50.3)	4832 (62.5)	<0.001
Air purifier usage	7726 (31.7)	0.393	NA	NA	
$PM_{2.5}$[a], median (IQR), μg/m^3	77.8 (9.5)	0.004	75.0 (9.3)	77.8 (5.9)	<0.001[b]
PM_{10}[a], median (IQR), μg/m^3	102.8 (10.6)	<0.001	102.8 (11.6)	103.5 (9.3)	<0.001[b]
SO_2[a], median (IQR), μg/m^3	11.3 (0.7)	0.103	11.2 (1.3)	11.4 (0.3)	<0.001[b]
NO_2[a], median (IQR), μg/m^3	51.8 (7.6)	0.924	51.8 (7.6)	51.8 (16.7)	<0.001[b]
CO[a], median (IQR), μg/m^3	1.2 (0.1)	0.012	1.2 (0.1)	1.2 (0.1)	<0.001[b]
O3[a], median (IQR), μg/m^3	96.9 (19.8)	NA	96.9 (15.7)	100.4 (27.7)	<0.001[b]

TC, total cholesterol, *TG,* triglyceride, *LDLC,* low density lipoprotein cholesterol, *HDLC,* high density lipoprotein cholesterol, *FPG,* fasting plasma glucose.

**P* values for univariate logistic regression, the dependent variable was systematic low-grade inflammation.

***P* values for tests between participants with and without air purifier usage habit, *t* tests for normal distributed continuous variables and chi-square tests for categorical variables.

[a] Annual concentration of each pollutant.

[b] Variables with non-normal distribution were represented as median (IQR), and were tested by Mann-Whitney *U* test.

null. The details are shown in Table 2. The 2-year or 3-year average concentrations of O_3 were significantly associated with low-grade systematic inflammation (2 years per 10 μg/m^3: OR = 0.959, $P = 0.004$; 3 years per 10 μg/m^3: OR = 0.961, $P = 0.014$). After further adjusting for the distance to the main road, the association between 2-year or 3-year average concentrations of ozone and low-grade systematic inflammation was still significant. However, the associations between 2-year or 3-year average NO_2 and low-grade systematic inflammation were null (2 years per 10 μg/m^3: OR = 1.045, $P = 0.064$; 3 years per 10 μg/m^3: OR = 1.083, $P = 0.055$). The details are shown in Supplementary Table A.2.

Among participants who did not use air purifiers on smog days, concentrations of NO_2 were consistently associated with elevated hsCRP (1-year NO_2 per 10 μg/m^3: OR = 1.079, $P = 0.009$; 2-year NO_2 per 10 μg/m^3: OR = 1.067, $P = 0.027$; 3-year NO_2 per 10 μg/m^3: OR = 1.125, $P = 0.024$). The average concentration of O_3 was consistently associated with a reduced hsCRP (1-year O_3 per 10 μg/m^3: OR = 0.925, $P = 0.001$; 2-year O_3 per 10 μg/m^3: OR = 0.952, $P = 0.006$; 3-year O_3 per 10 μg/m^3: OR = 0.946, $P = 0.008$). After further adjusting for the distance to the main road, the association between the concentrations of ozone and low-grade systematic inflammation among participants who did not use air purifiers on smog days was stable. Neither NO_2 nor O_3 was significantly associated with low-grade systematic inflammation among participants who used air purifiers on smog days (see Supplementary Table A.2).

3.3. Sensitivity analysis

To verify the potential effect of gaseous pollutants, models were built by further adjusting for particulate matter. The Spearman's correlation coefficient between PM_{10} and $PM_{2.5}$ was 0.604 ($P < 0.05$, see Fig. 1), so only one particulate matter was included in the gaseous-particulate pollutant joint model to avoid collinearity. In participants without air purifier use habits, concentrations of 3-year average PM_{10} were significantly associated with low-grade systematic inflammation (PM_{10} per 10 μg/m^3: OR = 1.050, $P = 0.036$); see Supplementary Table A.2. Thus, the models were further adjusted for gaseous particulate pollutants.

In the gaseous particulate pollutant models, annual ambient NO_2 and O_3 were still significantly associated with low-grade systematic inflammation after adjusting for PM_{10} (NO_2 per 10 μg/m^3: OR = 1.057, $P = 0.018$; O_3 per 10 μg/m^3: OR = 0.961, $P = 0.031$). In the 2-year and 3-year pollutant models, only the average O_3 concentration was still associated with low-grade systematic inflammation (2-year O_3 per 10 μg/m^3: OR = 0.964, $P = 0.014$; 3-year O_3 per 10 μg/m^3: OR = 0.968, $P = 0.055$). In participants without air purifier usage habits, the results were consistent with the results from the entire population, while the association turned to be null in participants who used air purifiers on smog days. The details are shown in Table 3.

In gaseous-particulate pollutant models, ambient NO_2 (annual) and O_3 (2 years, 3 years) were significantly associated with low-grade systematic inflammation after adjusting for $PM_{2.5}$ (annual NO_2 per 10 μg/m^3: OR = 1.059, $P = 0.017$; 2-year O_3 per 10 μg/m^3: OR = 0.961, $P = 0.010$; 3-year O_3 per 10 μg/m^3: OR = 0.961, $P = 0.020$). In participants with or without air purifier usage habits, the results were consistent with the results from the entire population. The details are shown in Table A.3.

We also treated hsCRP as a continuous variable to perform the above analysis. The results showed that the association between NO_2 and hsCRP was still significant, but the association between O_3 and hsCRP became null. The details are shown in Table A.4.

3.4. Stratification analysis

After stratification by different disease statuses, annual NO_2 and O_3 concentrations were significantly associated with low-grade systemic inflammation among nonobese participants and participants without diabetes. The largest estimated harmful effect of NO_2 on low-grade systematic inflammation was among participants with hyperlipidemia (1-year per 10 μg/m^3: OR = 1.097, $P = 0.006$). The largest estimated protective effect of O_3 on systemic inflammation was among nonobese participants (1-year per 10 μg/m^3: OR = 0.937, $P = 0.007$). The details are shown in Supplementary Figure A.2.

In the younger population (age<65), women, people who exercised less than once per week and non-obese people, ambient NO_2 was positively associated with elevated systematic inflammation, while O_3 was significantly associated with reduced systematic inflammation in the above populations. In the elderly population, men, people who exercised more than once per week and obese people, the associations between gaseous pollutants and low-grade systematic inflammation were null (see Figure A.2). After stratification by cooking behavior, a significant association between air pollutants and systematic inflammation could only be observed in people with cooking behaviors (NO_2 per 10 μg/m^3: OR = 1.085, $P = 0.003$; O_3 per 10 μg/m^3: OR = 0.942, $P = 0.006$),

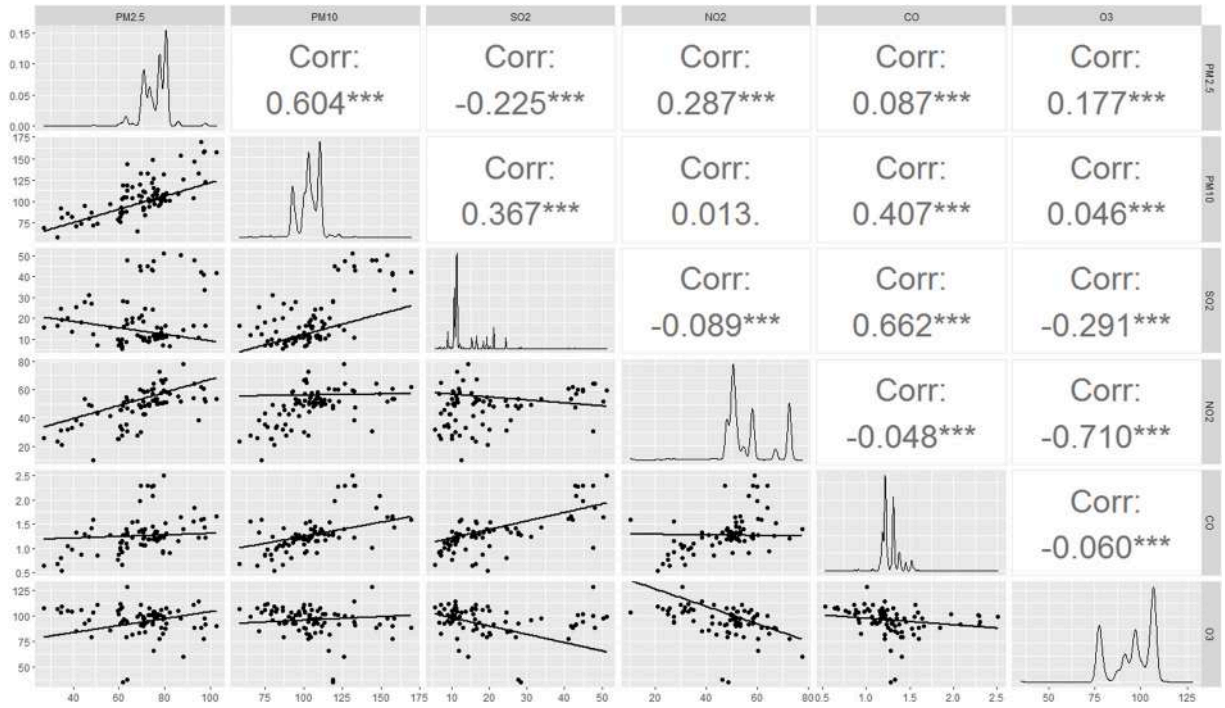

Fig. 1. The spearman correlation efficient for annual ambient air pollutants. ***, $P<0.001$.

Table 2
The effect of annual ambient pollutant concentration on systematic low-grade inflammation.

	Model 1[a]		Model 2[b]		Model 3[c]	
	OR (95% CI)	*P* value	OR (95% CI)	*P* value	OR (95% CI)	*P* value
$PM_{2.5}$ (10 μg/m^3)	1.044 (0.969, 1.125)	0.253	0.942 (0.880, 1.009)	0.089	0.980 (0.902, 1.065)	0.636
PM_{10} (10 μg/m^3)	1.041 (0.983, 1.101)	0.173	0.966 (0.907, 1.028)	0.274	1.013 (0.949, 1.080)	0.700
NO_2 (10 μg/m^3)	0.984 (0.946, 1.024)	0.434	1.055 (1.010, 1.103)	0.016	1.057 (1.009, 1.105)	0.018
O_3 (10 μg/m^3)	1.000 (0.968, 1.034)	0.997	0.960 (0.926, 0.995)	0.027	0.953 (0.919, 0.989)	0.012
O_3_mainroad (10 μg/m^3)[d]	1.003 (0.970, 1.037)	0.860	0.982 (0.950, 1.015)	0.287	0.955 (0.920, 0.991)	0.015
SO_2 (10 μg/m^3)	1.035 (0.892, 1.200)	0.649	1.050 (0.931, 1.184)	0.424	1.078 (0.962, 1.208)	0.200
CO (mg/m^3)	1.241 (0.848, 1.817)	0.266	1.069 (0.707, 1.616)	0.752	1.226 (0.827, 1.818)	0.310

[a] No covariates were adjusted in model 1.
[b] Model 2 adjusted for: age, gender, smoking, alcohol drinking, passive smoking, BMI, exercise, systolic blood pressure, diastolic blood pressure, triglyceride, high density lipoprotein cholesterol, low density lipoprotein cholesterol, cholesterol, fasting glucose.
[c] Model 3 additionally adjusted for: Cooking behavior, cooking fuel, kitchen ventilator usage during cooking, kitchen door closed during cooking, bedroom separated from kitchen, heating fuel, reduced outdoor activities in smog days, air purifier usage in smog days, mask-wearing habits in smog days.
[d] The distance to main road was adjusted in all the three models.

Supplementary Figure A.2. However, among cooks that used air purifiers on smog days, the association became null. Among cooks without air purifier usage habits on smog days, ambient air pollutants were still significantly associated with systematic inflammation (NO_2 per 10 μg/m^3: OR = 1.102, $P = 0.006$; O_3 per 10 μg/m^3: OR = 0.914, $P = 0.001$), see Table A.5.

4. Discussion

Our findings showed that long-term exposure to ambient NO_2 and O_3 were risk factors and protective factors against low-grade systemic inflammation, respectively. The results were generally stable after sensitivity analysis. The usage of air purifiers on hazy days could attenuate the impact of ambient gaseous pollutants on systematic inflammation. These results were generally stable after sensitivity analysis.

In the current study, we found that the annual NO_2 concentration was associated with elevated systemic inflammation, which was represented as hsCRP, and our results were consistent when we treated hsCRP as a continuous variable. Another study from Sweden also demonstrated that long-term exposure to traffic NO_2 in outdoor residential air was associated with increased IL-6 and CRP levels (Panasevich et al., 2009; Hajat et al., 2015) analyzed data from the Multi-Ethnic Study of Atherosclerosis (MESA) cohort and found that annual NO_2 exposure was not significantly associated with CRP. However, NO_2 in the MESA cohort was not measured directly and was calculated by the difference between the concentrations of NO and NO_x. Because of the fewer air quality system sites for NO compared with NO_2, the precision of the NO_2 estimation was slightly inaccurate. In addition, there were only 805 (11%) Chinese participants in the MESA study, and the different ethnic compositions might explain its inconsistent result with ours.

A study conducted in Taiwan also found that increased 1-year averaged NO_2 was associated with elevated neutrophils, which could represent systematic inflammation (Chuang et al., 2011). In people with diabetes and/or hypertension, the association of long-term NO_2 exposure with systematic inflammation was null in the current study. The hsCRP level, which is used to reflect the chronic systematic

Table 3
The effect of gaseous pollutant on systematic low-grad inflammation after adjusted for particulate matter.

Pollutants (10 μg/m^3)	Overall		Without air purifier usage habit		With air purifier usage habit	
	OR (95%CI)	*P* value	OR (95%CI)	*P* value	OR (95%CI)	*P* value
1-year						
NO_2[a]	1.057 (1.009, 1.105)	0.018	1.081 (1.020, 1.146)	0.008	1.022 (0.951, 1.099)	0.549
O_3[a]	0.961 (0.927, 0.996)	0.031	0.938 (0.896, 0.982)	0.007	0.996 (0.939, 1.057)	0.888
O_3_mainroad[b]	0.962 (0.928, 0.997)	0.034	0.938 (0.896, 0.983)	0.007	0.997 (0.940, 1.059)	0.933
SO_2[a]	1.054 (0.936, 1.017)	0.386	0.964 (0.784, 1.184)	0.727	1.038 (0.822, 1.310)	0.757
2-years						
NO_2[a]	1.031 (0.983, 1.081)	0.211	1.053 (0.992, 1.119)	0.088	0.992 (0.919, 1.073)	0.846
O_3[a]	0.964 (0.935, 0.993)	0.014	0.958 (0.924, 0.994)	0.022	0.975 (0.926, 1.027)	0.341
O_3_mainroad[a]	0.964 (0.935, 0.993)	0.015	0.958 (0.924, 0.994)	0.022	0.975 (0.927, 1.027)	0.347
SO_2[a]	1.061 (0.977, 1.153)	0.16	1.043 (0.947, 1.147)	0.391	1.120 (0.940, 1.335)	0.205
3-years						
NO_2[a]	1.055 (0.981, 1.137)	0.148	1.082 (0.988, 1.185)	0.087	1.008 (0.887, 1.146)	0.904
O_3[a]	0.968 (0.935, 1.001)	0.055	0.957 (0.917, 0.998)	0.041	0.986 (0.932, 1.043)	0.629
O_3_mainroad[a]	0.969 (0.936, 1.001)	0.059	0.957 (0.917, 0.998)	0.042	0.988 (0.933, 1.045)	0.663
SO_2[a]	0.996 (0.918, 1.081)	0.924	0.959 (0.869, 1.058)	0.398	1.271 (0.969, 1.669)	0.083

[a] Covariates in model 3 and annual PM_{10} were adjusted.
[b] Covariates in model 3, distance to main road and annual PM_{10} were adjusted.

inflammation status, was significantly elevated in participants with cardiometabolic disease (Castro et al., 2018; Carbone et al., 2019; Xiao et al., 2019). These patients might take medication that has anti-inflammatory functions and thus weaken the potential effect of air pollutants on the inflammatory response (Miller et al., 2019; Zheng et al., 2019).

Researchers have demonstrated that potential indoor NO_2 sources are linked to cooking activities, representing adverse health effects among cooks (IIelpo et al., 2019). In the current study, 80% of participants reported using natural gas stoves, and previous researches showed that the indoor NO_2 concentration mainly depended on the gas stoves used in the kitchen (Dėdelė and Miškinytė, 2016; Dennekamp et al., 2001; Paulin et al., 2017). Since indoor exposure was not measured separately in this study, we performed a stratified analysis to avoid the confounding caused by pollutants from cooking behavior. First, we concluded that in people who use air purifiers on haze days, regardless of whether they have cooking behavior, outdoor NO_2 does not affect systematic inflammation (see Supplementary Table A.5). In participants who were not accustomed to using air purifiers, the estimated effect of outdoor NO_2 on systematic inflammation was higher in people who cooked (OR = 1.097; 95% CI, 1.023 to 1.176; P = 0.009) than in people who did not cook (OR = 1.013, 95% CI, 0.915 to 1.123; P = 0.801). Experiments with C57BL/6 mice showed that NO_2 exposure could cause progressive airway inflammation together with focal inflammation of the lung parenchyma, and the induction of a significant inflammatory response began at a dose of 20 ppm NO_2 (Wegmann et al., 2005). Cooking behavior increases the accumulation of NO_2 exposure (Good et al., 1982), leading to a significant association between ambient NO_2 concentration and inflammation in these specific participants. Although the nonlinear association between ambient NO_2 and hsCRP concentration was not significant in the current study, we found that the association between ambient NO_2 and low-grade systematic inflammation was null in participants with the lowest 10% ambient NO_2 concentration, while NO_2 could significantly increase low-grade inflammation in the other participants. Moreover, in addition to the estimated harmful effects of NO_2 from fuel combustion, cooking behavior may affect systematic inflammation through other pathways, such as harmful substances in oil fumes (e.g., benzo[a]pyrene). More researches are necessary to further demonstrate the effects of indoor gaseous pollution and systematic inflammation. It is worth mentioning that the estimated harmful effect of NO_2 on systematic inflammation would become null in participants with air purifier usage habits. Our findings provide evidence to support interventions for the prevention and control of potential adverse health outcomes caused by air pollution.

Epidemiological evidence of the association of long-term exposure to ozone is remarkably limited compared to its association with short-term exposure (Kim et al., 2020). Our study results showed that long-term low ozone concentrations (<120 μg/m^3) could reduce systematic inflammation, but the association became null when we treated hsCRP as a continuous variable. The current study used data from air monitoring stations. However, O_3 is scavenged rapidly by nitric oxide near roadways and therefore varies substantially at the local scale. Considering that some of our residential survey sites were near roadways, we further adjusted our models by the distance to the main roadway and found that the association between ambient O_3 and systematic inflammation was stable (see Table 3 and Table A.2). Wang et al. analyzed MESA data and found that O_3 exposure could affect both diffuse carotid arterial injury and focal lesions of carotid atherosclerosis (Wang et al., 2019). Chuang KJ et al. found an association of increased 1-year averaged O_3 with elevated neutrophils (Chuang et al., 2011). However, another cohort study from the UK suggested that long-term exposure to higher levels of outdoor ozone was not associated with C-reactive protein concentrations (Forbes et al., 2009), which is consistent with our results (Table A.4). Because of the limited and inconsistent epidemiological evidence, the causal association of long-term exposure to ozone is only suggestive according to the Environmental Protection Agency (U.S. EPA) (U.S. Environmental Protection Agency, 2016).

There have been few studies on the mechanism of how ozone exposure affects systemic inflammation, but a number of animal experiments have shown that ozone therapy can be used to control local inflammatory responses. Ozone therapy is based on high doses to stimulate the immune system. The mechanism of ozone therapy is based on the formation of reactive oxygen species (ROS) and lipid oxidation products (LOPs), which disappear quickly. These particles stimulate antioxidant defense and modify the immune system without causing harmful effects (Juchniewicz and Lubkowska, 2020). For instance, researchers found that ozone therapy could suppress the inflammatory state of LPS-induced endotoxic shock (Alvarez et al., 2009) and could generate an anti-inflammatory effect against peptidoglycan-polysaccharide-induced arthritis in rats (Vaillant et al., 2013). Chen et al. also revealed that ozone therapy could attenuate tubulointerstitial inflammation injury in chronic kidney disease rats by mediating TLR4 (Chen et al., 2016). The alleviating effect of O_3 therapy on inflammation involves several pathways. O_3 exposure causes an increase in adenosine triphosphate (ATP) and the 2,3-diphosphoglycerate content in red blood cells. Ozone also promotes pentose phosphate pathway reactions that upregulate tricarboxylic acid and stimulate fat

catabolism. As a result, fatty materials on the vessel wall may be removed, which would reduce vascular endothelial inflammation (Juchniewicz and Lubkowska, 2020). However, the anti-inflammatory mechanism of long-term environmental ozone exposure still needs to be further revealed.

Moreover, the hypothesis that exposure to short-term ozone exposure causes inflammation is controversial. A cross-sectional study in Germany demonstrated that the relationship between hsCRP levels and short-term ozone exposure was J-shaped. Low ozone concentrations ($<$120 μg/m^3) tended to be negatively associated with hsCRP levels, while high concentrations ($\geq$120 μg/m^3) were associated with elevated levels (Zhao et al., 2019). In the current study, nearly all of the study subjects had ozone exposure levels below 120 μg/m^3, except for 3 participants. Balmes et al. showed that 4-h ozone exposure could not increase the hsCRP levels in healthy older adults (Balmes et al., 2019). Other studies showed that short-term exposure to 100–300 ppb ozone caused adverse changes in the markers of inflammation (hsCRP) in young healthy subjects (Devlin et al., 2012; Arjomandi et al., 2015). In the current study, the estimated protective effect of long-term ozone on low-grade systematic inflammation was only observed in participants under 65 years old, while the association was null in older adults. The conflicting results between our study and other randomized trials might indicate that the mechanisms of long-term ozone exposure on systematic inflammation may be different from those of short-term exposure.

Previous studies have demonstrated that air pollutants can influence blood lipid metabolism and glucose homeostasis. We performed additional analysis and found that NO_2 was positively associated with FPG, LDLC, HDLC and TC, while O_3 was negatively associated with the above biomarkers (see Supplementary Table A.6). Our results suggested that NO_2 has a potential harmful effect on multiple metabolic abnormalities, while O_3 has an estimated protective effect on multiple metabolic indicators, including FPG, blood lipid biomarkers and inflammation markers. Our findings are consistent with other evidence in the Chinese population that long-term exposure to NO_2 is significantly related to increased FPG (Yang et al., 2018a,b; Hou et al., 2021), TC, TG, and LDL-C (Gui et al., 2020; Zhang et al., 2021). The biological mechanisms underlying the links between gaseous pollutants and glucose/lipid metabolism are not fully understood. One hypothesis showed that air pollution could induce adverse lipid metabolism and lipid oxidation (Byun et al., 1999) through systemic inflammation (Krishna et al., 1996), which could explain our results. Moreover, the estimated beneficial effects for O_3 in TC, TG, and LDL-C are also consistent with previous studies (Yang et al., 2018a,b). Researchers have shown that through proper administration of precise and high doses, ozone decreases cholesterol, improves the glycemic index and induces antioxidant defenses (Elvis and Ekta, 2011), but the mechanisms of environmental ozone exposure on blood lipid and glucose homeostasis have not been well demonstrated.

The strength of the current study is as follows: First, the relatively large population would provide robust statistical estimates for the potential effect of ambient air pollution on systematic inflammation. Second, the current study chose stable communities in different geographical locations with environmental characteristics as study sites. Significant spatial differentiation is well suited to demonstrate the potential effects of air pollutants on health status. Third, self-protection behaviors on smog days, individual cooking habits, cooking and heating fuel were also considered as potential confounders, which would improve the accuracy of estimating the potential effect of ambient air pollution.

Our study also had the following limitations. First, information about cooking behavior, cooking habits, cooking fuel types, and heating fuel types was collected to reflect indoor air pollution. However, the information we collected could only partially reflect indoor air pollution. The time spent indoors and ventilation indoors are also closely related to indoor air pollution. Unfortunately, the current research design could not accurately evaluate indoor pollution exposure but could only collect behaviors that affect indoor pollution and adjust its possible influence on the association between ambient air pollutants and health effects. More research focusing on the health effect of indoor gaseous pollutants is still necessary with accurate measurements of the pollutants. Additionally, the exposure assessment used in the current study was tied to residence, and it did not account for exposures away from home. Accurate assessment of individual environmental exposure is crucial for the accuracy of environmental epidemiological studies. Precise environmental exposure assessment methods that can be applied to large epidemiological studies still need to be explored in the future. Moreover, the air pollutant concentration assessment was based on the data from monitoring stations instead of the exact individual pollutant exposure. The following research will use a machine learning method, combined with remote sensing data for more accurate individual exposure assessment, to verify the results of this study. Finally, the cross-sectional study design limited the ability to infer the causal effects of air pollutants and low-grade systematic inflammation

5. Conclusions

Long-term exposure to ambient NO_2 and O_3 were risk factors and protective factors against low-grade systemic inflammation, respectively. The usage of air purifiers on hazy days could attenuate the impact of ambient gaseous pollutants on systematic inflammation. The results were generally stable after sensitivity analysis.

Funding

This work was supported by The National Key Research and Development Program of China (grant number 2016YFC0900600/2016YFC0900603).

Declaration of competing interest

The authors report no conflicts of interest.

Acknowledgements

We thank all colleagues in the CHCN-BTH for their efforts in data collection.

Appendix A. Supplementary data

Supplementary data to this article can be found online at https://doi.org/10.1016/j.ijheh.2021.113875.

References

American Diabetes Association, 2020. Improving care and promoting health in populations: standards of medical care in diabetes-2020. Diabetes Care 43, S7–S13. https://doi.org/10.2337/dc20-S001.

Arjomandi, M., Wong, H., Donde, A., Frelinger, J., Dalton, S., Ching, W., Power, K., Balmes, J.R., 2015. Exposure to medium and high ambient levels of ozone causes adverse systemic inflammatory and cardiac autonomic effects. Am. J. Physiol. Heart Circ. Physiol. 308, H1499–H1509. https://doi.org/10.1152/ajpheart.00849.2014.

Alvarez, R.G., Zamora, Z.B., Borrego, A., Delgado, R., Schulz, S., Alonso, Y., 2009. Ozone oxidative preconditioning reduces nitrite levels in blood serum in LPS: induced endotoxic shock in mice. Inflamm. Res. 58, 441–443. https://doi.org/10.1007/s00011-009-0055-1.

Balmes, J.R., Arjomandi, M., Bromberg, P.A., Costantini, M.G., Dagincourt, N., Hazucha, M.J., Hollenbeck-Pringle, D., Rich, D.Q., Stark, P., Frampton, M.W., 2019. Ozone effects on blood biomarkers of systemic inflammation, oxidative stress, endothelial function, and thrombosis: the Multicenter Ozone Study in oldEr Subjects (MOSES). PLoS One 14, e0222601. https://doi.org/10.1371/journal.pone.0222601.

Blaha, M.J., Rivera, J.J., Budoff, M.J., Blankstein, R., Agatston, A., O'Leary, D.H., Cushman, M., Lakoski, S., Criqui, M.H., Szklo, M., Blumenthal, R.S., Nasir, K., 2011. Association between obesity, high-sensitivity C-reactive protein $\geq$2 mg/L, and subclinical atherosclerosis: implications of JUPITER from the Multi-Ethnic Study of Atherosclerosis. Arterioscler. Thromb. Vasc. Biol. 31, 1430–1438. https://doi.org/10.1161/ATVBAHA.111.223768.

Byun, J., Mueller, D.M., Fabjan, J.S., Heinecke, J.W., 1999. Nitrogen dioxide radical generated by the myeloperoxidase-hydrogen peroxide-nitrite system promotes lipid peroxidation of low density lipoprotein. FEBS Lett. 455, 243–246. https://doi.org/10.1016/s0014-5793(99)00893-5.

Carbone, F., Elia, E., Casula, M., Bonaventura, A., Liberale, L., Bertolotto, M., Artom, N., Minetti, S., Dallegri, F., Contini, P., Verzola, D., Pontremoli, R., Viazzi, F., Viviani, G. L., Bertolini, S., Pende, A., Pisciotta, L., Montecucco, F., 2019. Baseline hs-CRP predicts hypertension remission in metabolic syndrome. Eur. J. Clin. Invest. 49, e13128 https://doi.org/10.1111/eci.13128.

Castro, A.R., Silva, S.O., Soares, S.C., 2018. The use of high sensitivity C-reactive protein in cardiovascular disease detection. J. Pharm. Pharmaceut. Sci. 21, 496–503. https://doi.org/10.18433/jpps29872.

Chen, Z., Liu, X., Yu, G., Chen, H., Wang, L., Wang, Z., Qiu, T., Weng, X., 2016. Ozone therapy ameliorates tubulointerstitial inflammation by regulating TLR4 in adenine-induced CKD rats. Ren. Fail. 38, 822–830. https://doi.org/10.3109/0886022X.2016.1143757.

Chuang, K.J., Yan, Y.H., Chiu, S.Y., Cheng, T.J., 2011. Long-term air pollution exposure and risk factors for cardiovascular diseases among the elderly in Taiwan. Occup. Environ. Med. 68, 64–68. https://doi.org/10.1136/oem.2009.052704.

Dėdelė, A., Miškinytė, A., 2016. Seasonal variation of indoor and outdoor air quality of nitrogen dioxide in homes with gas and electric stoves. Environ. Sci. Pollut. Res. Int. 23, 17784–17792. https://doi.org/10.1007/s11356-016-6978-5.

Dennekamp, M., Howarth, S., Dick, C.A., Cherrie, J.W., Donaldson, K., Seaton, A., 2001. Ultrafine particles and nitrogen oxides generated by gas and electric cooking. Occup. Environ. Med. 58, 511–516. https://doi.org/10.1136/oem.58.8.511.

Devlin, R.B., Duncan, K.E., Jardim, M., Schmitt, M.T., Rappold, A.G., Diaz-Sanchez, D., 2012. Controlled exposure of healthy young volunteers to ozone causes cardiovascular effects. Circulation 126, 104–111. https://doi.org/10.1161/CIRCULATIONAHA.112.094359.

Elvis, A.M., Ekta, J.S., 2011. Ozone therapy: a clinical review. J. Nat. Sci. Biol. Med. 2, 66–70. https://doi.org/10.4103/0976-9668.82319.

Forbes, L.J., Patel, M.D., Rudnicka, A.R., Cook, D.G., Bush, T., Stedman, J.R., Whincup, P.H., Strachan, D.P., Anderson, R.H., 2009. Chronic exposure to outdoor air pollution and markers of systemic inflammation. Epidemiology 20, 245–253. https://doi.org/10.1097/EDE.0b013e318190ea3f.

GBD 2017 Risk Factor Collaborators, 2018. Global, regional, and national comparative risk assessment of 84 behavioural, environmental and occupational, and metabolic risks or clusters of risks for 195 countries and territories, 1990-2017: a systematic analysis for the Global Burden of Disease Study 2017. Lancet 392, 1923–1994. https://doi.org/10.1016/S0140-6736(18)32225-6.

Good, B.W., Vilcins, G., Harvey, W.R., Lewis, A.L., 1982. Effect of cigarette smoking on residential NO2 levels. Environ. Int. 8, 167–175. https://doi.org/10.1016/0160-4120(82)90025-3.

Gui, Z.H., Yang, B.Y., Zou, Z.Y., Ma, J., Jing, J., Wang, H.J., Dong, G.H., Ma, Y.H., Guo, Y.M., Chen, Y.J., 2020. Exposure to ambient air pollution and blood lipids in children and adolescents: a national population based study in China. Environ. Pollut. 266, 115422. https://doi.org/10.1016/j.envpol.2020.115422.

Hajat, A., Allison, M., Diez-Roux, A.V., Jenny, N.S., Jorgensen, N.W., Szpiro, A.A., Vedal, S., Kaufman, J.D., 2015. Long-term exposure to air pollution and markers of inflammation, coagulation, and endothelial activation: a repeat-measures analysis in the Multi-Ethnic Study of Atherosclerosis (MESA). Epidemiology 26, 310–320. https://doi.org/10.1097/EDE.0000000000000267.

Hou, J., Tu, R., Dong, Y., Liu, X., Dong, X., Li, R., Pan, M., Yin, S., Hu, K., Mao, Z., Huo, W., Guo, Y., Li, S., Chen, G., Wang, C., 2021. Associations of residing greenness and long-term exposure to air pollution with glucose homeostasis markers. Sci. Total Environ. 776, 145834. https://doi.org/10.1016/j.scitotenv.2021.145834.

IIelpo, P., Mangia, C., Marra, G.P., Comite, V., Rizza, U., Uricchio, V.F., Fermo, P., 2019. Outdoor spatial distribution and indoor levels of NO2 and SO2 in a high environmental risk site of the South Italy. Sci. Total Environ. 648, 787–797. https://doi.org/10.1016/j.scitotenv.2018.08.159.

Joint Committee for Guideline Revision, 2018. 2016 Chinese guidelines for the management of dyslipidemia in adults. J Geriatr Cardiol 15, 1–29. https://doi.org/10.11909/j.issn.1671-5411.2018.01.011.

Joint Committee for Guideline Revision, 2019. 2018 Chinese guidelines for prevention and treatment of hypertension-A report of the revision committee of Chinese guidelines for prevention and treatment of hypertension. J. Geriatr. Cardiol. 16, 182–241. https://doi.org/10.11909/j.issn.1671-5411.2019.03.014.

Juchniewicz, H., Lubkowska, A., 2020. Oxygen-ozone (O_2-O_3) therapy in peripheral arterial disease (PAD): a review study. Therapeut. Clin. Risk Manag. 16, 579–594. https://doi.org/10.2147/TCRM.S255247.

Kamath, D.Y., Xavier, D., Sigamani, A., Pais, P., 2015. High sensitivity C-reactive protein (hsCRP) & cardiovascular disease: an Indian perspective. Indian J. Med. Res. 142, 261–268. https://doi.org/10.4103/0971-5916.166582.

Kim, S.Y., Kim, E., Kim, W.J., 2020. Health effects of ozone on respiratory diseases. Tuberc. Respir. Dis. 83, S6–S11. https://doi.org/10.4046/trd.2020.0154.

Krishna, M.T., Springall, D.R., Frew, A.J., Polak, J.M., Holgate, S.T., 1996. Mediators of inflammation in response to air pollution: a focus on ozone and nitrogen dioxide. J R Coll Physicians Lond. 30, 61–66. https://doi.org/10.1016/0885-3924(95)00137-9.

Li, Z., Liu, Q., Xu, Z., Guo, X., Wu, S., 2020. Association between short-term exposure to ambient particulate air pollution and biomarkers of oxidative stress: a meta-analysis. Environ. Res. 191, 110105. https://doi.org/10.1016/j.envres.2020.110105.

Libby, P., Ridker, P.M., 2014. Inflammation and atherosclerosis: role of C-reactive protein in risk assessment. Am. J. Med. Suppl 6A, 9S–16S. https://doi.org/10.1016/j.amjmed.2004.02.006.

Liu, K., Cao, H., Guo, C., Pan, L., Cui, Z., Sun, J., Zhao, W., Han, X., Zhang, H., Wang, Z., Niu, K., Tang, N., Shan, G., Zhang, L., 2021. Environmental and genetic determinants of major chronic disease in Beijing-Tianjin-Hebei region: protocol for a community-based cohort study. Front. Publ. Health 9, 659701.

Liu, Q., Gu, X., Deng, F., Mu, L., Baccarelli, A.A., Guo, X., Wu, S., 2019. Ambient particulate air pollution and circulating C-reactive protein level: a systematic review and meta-analysis. Int. J. Hyg Environ. Health 222, 756–764. https://doi.org/10.1016/j.ijheh.2019.05.005.

Miller, M., Ballantyne, C.M., Bays, H.E., Granowitz, C., Doyle, R.T., Juliano, R.A., Philip, S., 2019. Effects of icosapent ethyl (eicosapentaenoic acid ethyl ester) on atherogenic lipid/lipoprotein, apolipoprotein, and inflammatory parameters in patients with elevated high-sensitivity C - reactive protein (from the ANCHOR study). Am. J. Cardiol. 124, 696–701. https://doi.org/10.1016/j.amjcard.2019.05.057.

Panasevich, S., Leander, K., Rosenlund, M., Ljungman, P., Bellander, T., de Faire, U., Pershagen, G., Nyberg, F., 2009. Associations of long- and short-term air pollution exposure with markers of inflammation and coagulation in a population sample. Occup. Environ. Med. 66, 747–753. https://doi.org/10.1136/oem.2008.043471.

Paulin, L.M., Williams, D.L., Peng, R., Diette, G.B., McCormack, M.C., Breysse, P., Hansel, N.N., 2017. 24-h Nitrogen dioxide concentration is associated with cooking behaviors and an increase in rescue medication use in children with asthma. Environ. Res. 159, 118–123. https://doi.org/10.1016/j.envres.2017.07.052.

Pope 3rd, C.A., Bhatnagar, A., McCracken, J.P., Abplanalp, W., Conklin, D.J., O'Toole, T., 2016. Exposure to fine particulate air pollution is associated with endothelial injury and systemic inflammation. Circ. Res. 119, 1204–1214. https://doi.org/10.1161/CIRCRESAHA.116.309279.

Seow, W.J., Downward, G.S., Wei, H., Rothman, N., Reiss, B., Xu, J., Bassig, B.A., Li, J., He, J., Hosgood, H.D., Wu, G., Chapman, R.S., Tian, L., Wei, F., Caporaso, N.E., Vermeulen, R., Lan, Q., 2016. Indoor concentrations of nitrogen dioxide and sulfur dioxide from burning solid fuels for cooking and heating in Yunnan Province, China. Indoor Air 26, 776–783. https://doi.org/10.1111/ina.12251.

U.S. Environmental Protection Agency, 2016. Integrated science assessment (ISA) for oxides of nitrogen: health criteria. Retrieved Dec 2, 2020 from. https://cfpub.epa.gov/ncea/isa/recordisplay.cfm?deid=310879.

Vaillant, J.D., Fraga, A., Díaz, M.T., Mallok, A., Viebahn-Hänsler, R., Fahmy, Z., Barberá, A., Delgado, L., Menéndez, S., Fernández, O.S., 2013. Ozone oxidative postconditioning ameliorates joint damage and decreases pro-inflammatory cytokine levels and oxidative stress in PG/PS-induced arthritis in rats. Eur. J. Pharmacol. 714, 318–324. https://doi.org/10.1016/j.ejphar.2013.07.034.

Wang, M., Sampson, P.D., Sheppard, L.E., Stein, J.H., Vedal, S., Kaufman, J.D., 2019. Long-term exposure to ambient ozone and progression of subclinical arterial disease: the multi-ethnic study of atherosclerosis and air pollution. Environ. Health Perspect. 127, 57001. https://doi.org/10.1289/EHP3325.

Wang, Y., Mi, J., Shan, X.Y., Wang, Q.J., Ge, K.Y., 2007. Is China facing an obesity epidemic and the consequences? The trends in obesity and chronic disease in China. Int. J. Obes. 31, 177–188. https://doi.org/10.1038/sj.ijo.0803354.

Wegmann, M., Fehrenbach, A., Heimann, S., Fehrenbach, H., Renz, H., Garn, H., Herz, U., 2005. NO2-induced airway inflammation is associated with progressive airflow limitation and development of emphysema-like lesions in C57bl/6 mice. Exp. Toxicol. Pathol. 56, 341–350. https://doi.org/10.1016/j.etp.2004.12.004.

Wegmann, M., Renz, H., Herz, U., 2003. Long-term NO2 exposure induces pulmonary inflammation and progressive development of airflow obstruction in C57BL/6 mice: a mouse model for chronic obstructive pulmonary disease? Pathobiology 70, 284–286. https://doi.org/10.1159/000070743.

WHO (World Health Organization), 2016. Ambient Air Pollution: a Global Assessment of Exposure and Burden of Disease. World Health Organization. Retrieved. http://www.who.int/phe/publications/airpollution-global-assessment/en/. (Accessed 4 October 2018).

Xiao, L., Zhou, Y., Ma, J., Cao, L., Zhu, C., Li, W., Wang, D., Fan, L., Ye, Z., Chen, W., 2019. Roles of C-reactive protein on the association between urinary cadmium and type 2 diabetes. Environ. Pollut. 255, 113341. https://doi.org/10.1016/j.envpol.2019.113341.

Yang, B.Y., Bloom, M.S., Markevych, I., Qian, Z.M., Vaughn, M.G., Cummings-Vaughn, L. A., Li, S., Chen, G., Bowatte, G., Perret, J.L., Dharmage, S.C., Heinrich, J., Yim, S.H., Lin, S., Tian, L., Yang, M., Liu, K.K., Zeng, X.W., Hu, L.W., Guo, Y., Dong, G.H., 2018a. Exposure to ambient air pollution and blood lipids in adults: the 33 Communities Chinese Health Study. Environ. Int. 119, 485–492. https://doi.org/10.1016/j.envint.2018.07.016.

Yang, B.Y., Qian, Z.M., Li, S., Chen, G., Bloom, M.S., Elliott, M., Syberg, K.W., Heinrich, J., Markevych, I., Wang, S.Q., Chen, D., Ma, H., Chen, D.H., Liu, Y., Komppula, M., Leskinen, A., Liu, K.K., Zeng, X.W., Hu, L.W., Guo, Y., Dong, G.H., 2018b. Ambient air pollution in relation to diabetes and glucose-homoeostasis markers in China: a cross-sectional study with findings from the 33 Communities Chinese Health Study. Lancet Planet Health 2, e64–e73. https://doi.org/10.1016/S2542-5196(18)30001-9.

Zhang, K., Wang, H., He, W., Chen, G., Lu, P., Xu, R., Yu, P., Ye, T., Guo, S., Li, S., Xie, Y., Hao, Z., Wang, H., Guo, Y., 2021. The association between ambient air pollution and blood lipids: a longitudinal study in Shijiazhuang, China. Sci. Total Environ. 752. https://doi.org/10.1016/j.scitotenv.2020.141648. Jan 15, 141648.

Zhao, T., Markevych, I., Standl, M., Schikowski, T., Berdel, D., Koletzko, S., Jörres, R.A., Nowak, D., Heinrich, J., 2019. Short-term exposure to ambient ozone and inflammatory biomarkers in cross-sectional studies of children and adolescents: results of the GINIplus and LISA birth cohorts. Environ. Pollut. 255, 113264. https://doi.org/10.1016/j.envpol.2019.113264.

Zheng, H.J., Guo, J., Jia, Q., Huang, Y.S., Huang, W.J., Zhang, W., Zhang, F., Liu, W.J., Wang, Y., 2019. The effect of probiotic and synbiotic supplementation on biomarkers of inflammation and oxidative stress in diabetic patients: a systematic review and

meta-analysis of randomized controlled trials. Pharmacol. Res. 142, 303–313. https://doi.org/10.1016/j.phrs.2019.02.016.

International Journal of Hygiene and Environmental Health 239 (2022) 113881

Contents lists available at ScienceDirect

International Journal of Hygiene and Environmental Health

journal homepage: www.elsevier.com/locate/ijheh

Proximity to endocrine-disrupting pesticides and risk of testicular germ cell tumors (TGCT) among adolescents: A population-based case-control study in California

Scott J. Swartz [a,b], Libby M. Morimoto [c], Todd P. Whitehead [c], Mindy C. DeRouen [d,e], Xiaomei Ma [f], Rong Wang [f], Joseph L. Wiemels [g], Katherine A. McGlynn [h], Robert Gunier [c], Catherine Metayer [c,*]

[a] Joint Medical Program, University of California, Berkeley/San Francisco, Berkeley, CA, USA
[b] School of Medicine, University of California, San Francisco, San Francisco, CA, USA
[c] Division of Epidemiology, School of Public Health, University of California, Berkeley, CA, USA
[d] Department of Epidemiology and Biostatistics, University of California, San Francisco, San Francisco, CA, USA
[e] Helen Diller Family Comprehensive Cancer Center, University of California, San Francisco, San Francisco, CA, USA
[f] Department of Chronic Disease Epidemiology, Yale School of Public Health, New Haven, CT, USA
[g] Center for Genetic Epidemiology, Department of Preventive Medicine, Keck School of Medicine of the University of Southern California, Los Angeles, CA, USA
[h] Division of Cancer Epidemiology and Genetics, National Cancer Institute, Bethesda, MD, USA

ARTICLE INFO

Keywords:
Testicular cancer
Adolescent and young adults
Testicular dysgenesis syndrome
Pesticides
Endocrine disruptors
Epidemiology

Background: The incidence of testicular germ cell tumors (TGCT) is increasing steadily in the United States, particularly among Latinos. TGCT is thought to be initiated *in utero* and exposure to endocrine-disrupting chemicals, suspected contributors to TGCT pathogenesis, during this critical developmental period may contribute to the rise.
Objectives: To assess the relationship between fetal exposure to agricultural endocrine-disrupting pesticides (EDPs) and TGCT risk among adolescents in a diverse population in California.
Methods: We conducted a registry-based case-control study of TGCT. Cases, diagnosed between 1997 and 2011, were 15–19 years of age (n = 381). Controls were matched on birth year and race/ethnicity (n = 762). Quantities (kilograms) of 33 pesticides applied within 3 km and 1 km radii of each individual's address before birth were estimated using the Pesticide Use Reporting database. Odds ratios (OR), 95% confidence intervals (CI), and population attributable risk (PAR) were calculated for each EDP (using log-2 transformed values). Risk models considered race/ethnicity, birth year, and neighborhood socioeconomic status.
Results: A doubling of nearby acephate applications (3 km and 1 km radii) and malathion applications (1 km radius) was associated with increased risks of TGCT among Latinos only (OR = 1.09; 95% CI:1.01–1.17; 1.30; 95% CI:1.08–1.57, and 1.19; 95% CI:1.01–1.39, respectively), whereas application of carbaryl within a 3 km radius increased TGCT risk in non-Latinos only (OR = 1.14, 95% CI:1.01–1.28). We estimate that acephate was associated with approximately 10% of the TGCT PAR, malathion with 3% and carbaryl with 1%.
Conclusions: TGCT among adolescents in California was associated with prenatal residential proximity to acephate and malathion among Latinos, and with carbaryl among non-Latinos. These results suggest that the rise in TGCT risk among Latinos may be associated with exposure to these pesticides.

Abbreviations: APC, Annual percent change; CCR, California Cancer Registry; CCRLP, Childhood Cancer Record Linkage Project; CDPH-VR, California Department of Public Health Vital Records; CI, Confidence interval; COMTRS, County, meridian, township, range, section; EDP, Endocrine-disrupting pesticide; GCNIS, Germ cell neoplasia in situ; OR, Odds ratio; PAR, Population attributable risk; PUR, Pesticide Use Reporting; SEER, Surveillance, Epidemiology, and End Results Program; TDS, Testicular dysgenesis syndrome; TGCT, Testicular germ cell tumor; US, United States.

* Corresponding author. School of Public Health, University of California, Berkeley, 1995 University Avenue, Suite 265, Berkeley, CA, 94704, USA.
E-mail address: cmetayer@berkeley.edu (C. Metayer).

https://doi.org/10.1016/j.ijheh.2021.113881
Received 20 August 2021; Received in revised form 28 October 2021; Accepted 8 November 2021
Available online 25 November 2021

1. Introduction

Testicular cancer is the most common malignancy in adolescent and young adult males (Gurney et al., 2019). In 2016, there were an estimated 66,833 new testicular cancer cases and 8,651 testicular cancer deaths globally (Pishgar et al., 2019). Testicular germ cell tumors (TGCTs) are the predominant histologic type, comprising about 98% of all testicular cancers (Znaor et al., 2014). In recent decades, TGCT incidence has been rising steadily in the United States (US). Using combined cancer surveillance data from the Centers for Disease Control and Prevention (CDC), National Cancer Institute (NCI), and the US Cancer Statistics (USCS) public use databases (United States Department of Health and Human Services 2019), the annual percent change (APC) in TGCT incidence was estimated to have risen modestly (+0.41%) from 2001 to 2016 (Ghazarian and McGlynn 2020), although subgroup analyses revealed more striking increases in some racial/ethnic groups, including Latinos (APC: +2.10%) during this time period. Incidence rose more than 30% from 2001 to 2016 among Latino males vs. 6% among non-Latino white males (Ghazarian and McGlynn 2020). California-specific data show a similar incidence trend by race/ethnicity (Morris et al., 2010). Though racial/ethnic differences in TGCT susceptibility may have some genetic origins (Litchfield et al., 2017; Wang et al., 2017), the rapid change in incidence over time points to an environmental cause. Furthermore, while first-generation migrant populations show incidence rates similar to those in their native countries, incidence in later generations increasingly resemble rates in the adoptive country, supporting a role for environmental risk factors (Beiki et al., 2010; Hemminki et al., 2010; Myrup et al., 2008; NCI 2003; Parkin and Iscovich 1997; Schmiedel et al., 2010).

Testicular dysgenesis syndrome (TDS), first hypothesized in 2001, attempts to tie TGCT and three other conditions (hypospadias, cryptorchidism, and poor semen quality) to a common etiology of Sertoli and/or Leydig cell dysfunction leading to abnormal germ cell development (Sharpe and Skakkebaek 1993; Skakkebaek et al., 2001). The fetal origin of TGCT is supported by the finding that the precursor lesions of TGCT, germ cell neoplasia in situ (GCNIS), resemble pluripotent fetal gonocytes (Jorgensen et al., 2015). Endocrine disruption is thought to underlie TDS pathogenesis (Baroni et al., 2019; Sharpe and Skakkebaek 1993; Xing and Bai 2018). *In utero* estrogen exposure is specifically named as a potential cause, owing partly to early epidemiologic evidence linking exposure to the synthetic estrogen diethylsilbestrol (DES) during pregnancy to TGCT and cryptorchidism (Depue et al., 1983; Henderson et al., 1979). Androgen dysfunction may also be involved in the pathogenesis of TGCT (Sharpe and Skakkebaek 2008), as supported by animal models of TDS (Xing and Bai 2018). In human studies, high androgen levels measured during pregnancy and at birth have been shown to be associated with TGCT risk (Holl et al., 2009; Morimoto et al., 2018). The carcinogenicity of pesticides has been well reviewed in the literature, with several organophosphates, carbamates, and pyrethroids found to be probable or possible carcinogens (Guyton et al., 2015; U.S. Environmental Protection Agency Office of Pesticide Programs). Epidemiologic studies have observed elevated risks of several cancer types including leukemias, soft-tissue sarcomas, multiple myeloma, non-Hodgkin lymphoma, and breast cancer associated with agricultural/occupational (Curl et al., 2020; de Graaf et al., 2021) and residential (Teitelbaum et al., 2007) exposures to pesticides. In addition, testicular cancer specifically has been associated with living in areas with high environmental exposure to pesticides (Requena-Mullor et al., 2021), and specific endocrine-disrupting pesticides (EDPs), such as chlordane and DDE, have been associated with TGCT risk (Giannandrea and Fargnoli 2017; McGlynn and Trabert 2012). Although animal models have provided evidence for the role of *in utero* endocrine disruption in some TDS disorders (Toppari et al., 2010), there is sparse evidence for TGCT, especially in epidemiologic studies. This is likely due to the difficulty of studying early-life exposures and their effect on testicular dysgenesis, and connecting them to development of TGCT later in life: fetal testes are unavailable for study at the stage dysgenesis may occur, the many-decade gap between exposure and outcome is longer than the duration of most research studies, and data on exposures from the distant past are often unavailable or susceptible to recall bias (Sharpe and Skakkebaek 2008).

This study addresses these issues, as the availability of historic pesticide use data from the California's Pesticide Use Reporting (PUR) database provides an estimate of prenatal exposure to EDPs, the use of which has been increasing since the 20th century, especially in California (Mnif et al., 2011; Wilhoit 2016). Using a population-based sample of adolescents diagnosed with TGCT identified through the California Cancer Registry (CCR), this is the first study to assess the role of *in utero* EDP exposure with risk of developing TGCT 15–19 years later.

2. Methods

2.1. Study population and geolocation

TGCT cases and cancer-free controls were selected from the Childhood Cancer Record Linkage Project (CCRLP), details of which have been described elsewhere (Morimoto et al., 2016). In short, the CCRLP consists of a probabilistic linkage of CCR records to birth certificate records maintained by the California Department of Public Health Vital Records (CDPH-VR) unit. Eligibility criteria for cases and controls are shown in Table 1. Eligible cases for this analysis were males born in or after 1982 (the earliest year when California birth records with zip code data were available) and diagnosed during adolescence (age 15–19 years) during 1997–2011 (2011 is the terminal year included in the CCRLP). Only malignant testicular germ cell tumors that were patients' first or only tumors were included. Cases were diagnosed with TGCT per International Classification of Diseases for Oncology, 3rd edition (ICD-O-3) codes [Topography codes: C620, C621, and 629. Morphology codes: 9060–9062, 9064 (seminomas); 9065–9084, 9100–9102 (non-seminomas); and 9085 (mixed germ cell tumors)]. Controls were cancer-free by age 19 or by the year 2011, whichever came first. Controls were drawn at random from statewide birth records and matched to TGCT cases at a 2:1 ratio on year and month of birth and race/ethnicity (categorized as Latino, non-Latino white, non-Latino black, non-Latino Asian/Pacific Islander, and other). In total, 381 TGCT cases and 762 matched controls were selected for the analysis.

The most granular geographic data available in California electronic birth records prior to 1997 was the home zip code at birth (available

Table 1
Inclusion/exclusion criteria for eligible cases and controls.

Cases	Controls
Inclusion Criteria	
Male sex	Male sex
Born 1982 or later in California	Born 1982 or later in California
Diagnosed with cancer between years 1997–2001, reported to California Cancer Registry (CCR)	No recorded cancer in CCR by age 19 or by year 2011 (whichever came first)
ICD-O-3 morphology codes: 9060–9062, 9064-9102	
ICD-O-3 topography codes: C62.0, C62.1, C62.9	
ICD-O-3 behavior code: 3 (malignant)	
First or only primary cancer recorded in CCR	
Diagnosed age 15–19 years	
Diagnosed in California	
Exclusion Criteria	
Maternal residential address on birth certificate could not be mapped to latitude/longitude (e.g., no listed address, P.O. Box only, nonexistent street name, etc.)	

Note: individuals born in California but diagnosed after 2011 or outside of California are not captured in this linkage. However, due to the rarity of TGCT, this is anticipated to be a very small number of total California-born cases.

beginning in 1982). To ascertain precise home addresses, individuals' paper birth certificates were ordered from CDPH-VR only for those individuals suspected to have non-negligible nearby EDP exposure in the year before their birth (n = 207 cases and 410 controls). This was determined by calculating the total quantity of known or suspected EDPs in each individual's zip code (based on PUR records), divided by the area of the zip code in square kilometers. Individuals with less than 0.1 kg/km^2 of EDP application in their zip code in either the year before or the year of their birth were deemed to have negligible nearby EDP application and nearby application values were coded as zero for all EDPs for such individuals. For individuals whose birth certificates were ordered, the precise latitude/longitude coordinates of their mother's listed address were ascertained. Birth certificates were digitized and home addresses were manually abstracted and reviewed by two independent reviewers for quality control. Addresses were converted to latitude/longitude coordinates using ESRI's ArcGIS Business Analyst software; 540 addresses (87.5%) were successfully geolocated on the first attempt. Fifty-two additional addresses (8.4%) were successfully geolocated following manual data cleaning (e.g. including adding street labels ["AVE", "DR", etc.], correcting apparent typographical errors, removing apartment numbers, etc.). Twenty-five addresses were unable to be matched (4.1%) (reasons include: no listed address, only P.O. Box listed, nonexistent street names, and multiple possible addresses based on the birth certificate address). These 25 individuals (n = 4 cases, 21 controls) were removed from the analysis, leading to a final sample size of 377 cases and 741 controls.

Median neighborhood household income, a proxy for neighborhood socioeconomic status, was linked to CCRLP records via census block group identifiers associated with individuals' geocoded home address at birth (also available in the CCRLP dataset). Census block group-level household income measures were used from the census in 1990, the census year most proximal and central to individuals' birth years (1982–1995). These data were linked using the census block group of each individual's home address at birth, which was also available in the CCRLP dataset.

2.2. Nearby EDP application assessment

Pesticide application data were obtained from California's PUR database. The PUR data include the amount of active ingredient applied in kilograms, application date, and location, which is defined as a one-square mile section defined by the Public Land Survey System as the county, meridian, township, range, section (COMTRS). Since 1970, California state law has required reporting of all commercial agricultural applications of "restricted use" pesticides to each county's agricultural commissioner, who performs quality control checks before sending these data to the statewide PUR system (California Department of Pesticide Regulation, 2017). PUR records have an estimated 0.5% error rate, and its administrators estimate 80–90% reporting completeness (California Department of Pesticide Regulation 2017). The PUR system was updated beginning in 1990 from "restricted use" to "full use" reporting of all commercial agricultural pesticide applications (California Department of Pesticide Regulation 2017), resulting in more comprehensive records of pesticide applications.

Full PUR application datasets were downloaded for all birth years (1982–1995) and subset to include only our pesticides of interest. Included were 33 pesticides that had reported use in California PUR during our study period with known or suspected estrogenic or anti-androgenic effects (Mnif et al., 2011). We calculated the total kilograms of each EDP agriculturally applied in each COMTRS for each month of the study period.

EDP application quantities within 1 km and 3 km radii of each geolocated home address were estimated (Fig. 1). A 1 km buffer was used for increased specificity of exposure, while a 3 km buffer was included to increase sensitivity and power while retaining a realistic distance of pesticide dispersion; these two distances were most strongly associated with measured concentrations of pesticides in house dust and outdoor air in previous studies (Deziel et al., 2017; Gunier et al., 2011; Harnly et al. 2005, 2009). Using ESRI's ArcMap software, latitude and longitude coordinates were overlaid onto the Public Land Survey System grid of COMTRS units used by PUR across California. One and 3 km buffers were created around each address, and the intersections of residential buffers and COMTRS grid areas were found. The area (in square

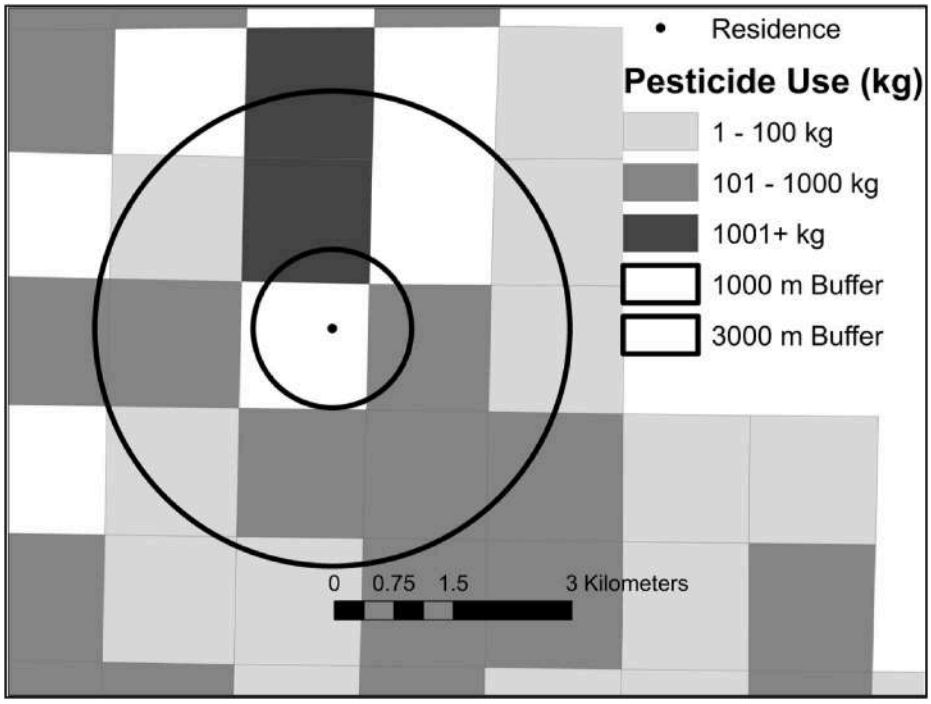

Fig. 1. Example of Pesticide Use Reporting data, residential locations, and buffer distances. Each shaded grid square represents the quantity of EDP application in a single COMTRS (county, meridian, township, range, section) unit.

meters) of each COMTRS section's overlap with a residential buffer was calculated and used to calculate the proportion of each COMTRS area that overlapped with the buffer. The total number of kilograms of each EDP used in each COMTRS area overall was multiplied by this proportional area to approximate the application within the address buffer area (i.e. uniform pesticide application across each COMTRS area was assumed). For each COMTRS area-address buffer overlap, only the application records from the 12 months prior to the individual's birth were retained. For each individual EDP and all EDPs combined, the total number of kilograms applied was calculated for five time periods: 1) the full 12 months before birth, 2) the 3-month preconception period [40–52 weeks before birth], 3) the first trimester [27–39 weeks before birth], 4) the second trimester [14–26 weeks before birth], and 5) the third trimester [0–13 weeks before birth].

2.3. Preparation for analysis

We restricted both 1 km and 3 km radii analyses to include only the most commonly-used EDPs – those applied near the homes of 50 or more individuals. Of the 33 EDPs listed in the PUR database, 16 met this criterion at 1 km and 24 met it at 3 km. The EDPs excluded from the 3 km radii analyses were bifenthrin, cypermethrin esfenvalerate, ethalfluralin, linuron, myclobutanil, nitralin, phorate, and profluralin. Copper sulfate, dicofol, mancozeb, methyl parathion, oryzalin, pendimethalin, trifluralin, and vinclozolin were additionally excluded from the 1 km radius analyses. The three copper sulfate compounds present in the dataset (copper sulfate [basic], copper sulfate [pentahydrate], and copper sulfate [monohydrate]) were grouped together for all analyses. For both 1 km and 3 km radii, overall application of each EDP in the year before birth was compared for 1) cases vs. controls, 2) Latinos vs. non-Latinos (all races; non-Latino whites comprised the more than 83% of non-Latinos), and 3) those born in 1990 (the year reporting for all commercial agricultural pesticide applications was fully implemented) and earlier ("pre-1990") vs. after 1990 ("post-1990"). Based only on individuals with non-zero application values, the arithmetic mean, standard deviation, median, and inter-quartile range were tabulated for each compound. Correlation between the application of different EDPs in each measured time period (3 months before conception and each trimester of the pregnancy) was assessed.

To normalize EDP application data for parametric regression and reduce the influence of outliers, all values were log-2 transformed (after adding 1 to each value) before analysis. In addition to EDP application, other covariates included in all regressions were 1) median household income in 1990 of the census block group at birth, 2) an indicator for ethnicity (Latino vs. non-Latino), and 3) an indicator birth year (pre- vs. post-1990) (unless regressions were stratified on these variables). Though block group household income values were missing for a small number (~5%) of individuals, these values were replaced with the median household income for the overall study population. Regressions stratified by Latino vs. non-Latino and pre -vs. post-1990 birth year were performed to assess whether effects of nearby EDP application differed between these groups of interest. While regressions stratified by histologic subtype (seminoma/nonseminoma) were performed, the large majority of tumors (89%) were nonseminomatous and results were not meaningfully different from those seen in the overall study population; therefore, these results are not included here.

2.4. Statistical modeling

Unconditional multivariable logistic regressions with case-control status as the outcome were performed to estimate the odds ratios (ORs) and 95% confidence intervals (CIs) using two methods of classifying EDP application: continuous and categorized. Continuous application models used the log2-transformed kilograms of each EDP applied in the time period of interest. Categorized application models classified each individual as being exposed to none/low vs. high EDP application, with low and high categories defined as either below or above the median application quantity among control individuals with non-zero exposure.

Similar regression models (all individuals, stratified by Latino vs. non-Latino, and stratified by pre- vs. post-1990) were also used to estimate the population attributable risk (PAR) percentage for each EDP that showed a statistically significant result in the continuous or categorized regression models for the full year time period. For interpretability of these statistics, EDP application was dichotomized into high vs. low and zero application (categories as described above). PAR percentage was calculated according to the formula:

$$PAR\ \% = 100\% \times \frac{P(high\ application)^*(OR-1)}{(P(high\ application)^*(OR-1))+1}$$

where *P(high application)* represents the proportion of control subjects with greater than the median non-zero pesticide application quantity, and *OR* represents the odds ratio of a subject developing TGCT given high nearby application (versus low or zero application), adjusted for ethnicity, household income, and birth year pre- or post-1990.

We also performed formal Wald tests for interaction for each EDP with race/ethnicity and period of PUR reporting, using a p-value of 0.1 as a threshold for statistical significance. Lastly, possible nonlinearity was assessed by generating plots of TGCT risk by decile of nearby EDP application, with deciles defined by percentiles of application in controls only and zero application included as a baseline category.

R software (version 3.6.1) was used for all data processing and statistical analyses. Institutional Review Board approval was granted by the Committees for the Protection of Human Subjects for both the California Health and Human Services Agency and the University of California, Berkeley.

3. Results

The majority of individuals in our study were Latino (54.9%), followed by non-Latino white (37.7%) (Table 2). The median neighborhood household income was higher among cases than controls ($p = 0.02$). The EDPs were typically weakly correlated (correlation coefficients less than 0.25); the strongest correlations (coefficients above 0.6) were found between copper sulfate/chlorpyrifos, diazinon/iprodione, methomyl/acephate, diuron/simazine, diuron/copper sulfate, dicofol/pendimethalin, and methyl bromide/iprodione at 3 km, and carbaryl/chlorpyrifos, diuron/simazine, and methyl bromide/iprodione at 1 km (Supplemental Figs. S1 and S2). Application of at least one EDP within a 3 km radius was found for almost half of cases and controls; nearby application of individual EDPs ranged from about one in twenty subjects (pendimethalin) to greater than one in four (methyl bromide) (Table 3). The proportions of exposed individuals were similar for Latinos and non-Latinos; however, mean EDP applications (combined or individual) were generally higher in proximity to Latino homes than non-Latino homes (Table 4). The proportion of individuals with nearby EDP application, as well as the quantity of pesticides applied, at the 1 km radius were less than those observed at 3 km, yet the overall distribution by various characteristics was similar (Tables 5 and 6). Only 23% of individuals were born after the PUR expanded its reporting requirements in 1990, and those persons were more likely to be Latino (64.1% after 1990 vs. 52.2% before 1990), and to have greater reported quantities of nearby EDP applications (median total EDP application within 3 km was 143.4 kg after 1990 vs. 42.5 kg before 1990) (Supplemental Tables S1 and S2).

Odds ratios for TGCT risk associated with each doubling of EDP application within 3 km during the year prior to birth are shown in Table 7. A doubling of acephate was associated with increased risks in the overall study population (OR: 1.09; 95% CI: 1.02–1.16) and in the Latino group (OR: 1.09; 95% CI: 1.01–1.17). Additionally, carbaryl was associated with increased TGCT risk only in the non-Latino group (OR:

Table 2
Characteristics of the study population by case-control status (1997–2011).

Variable	Category	Overall (n = 1118)	Cases (%) (n = 377)	Controls (%) (n = 741)
Histologic subtype	Non-seminoma		336 (89.1%)	
	Seminoma		41 (10.9%)	
Age at diagnosis	15		52 (13.8%)	
	16		64 (17.0%)	
	17		81 (21.5%)	
	18		86 (22.8%)	
	19		94 (24.9%)	
Race/Ethnicity	Latino	614 (54.9%)	207 (54.9%)	407 (54.9%)
	Non-Latino white	421 (37.7%)	143 (37.9%)	278 (37.5%)
	Non-Latino Asian/Pacific Islander	47 (4.2%)	15 (4%)	32 (4.3%)
	Non-Latino black	21 (1.9%)	7 (1.9%)	14 (1.9%)
	Other/unknown	15 (1.3%)	5 (1.3%)	10 (1.3%)
Birth year	1982–1985	351 (31.4%)	118 (31.3%)	233 (31.4%)
	1986–1990	508 (45.4%)	172 (45.6%)	336 (45.3%)
	1991–1995	259 (23.2%)	87 (23.1%)	172 (23.2%)
Household income	<$20,000	237 (21.2%)	72 (19.1%)	165 (22.3%)
	$20,000-$40,000	568 (50.8%)	194 (51.5%)	374 (50.5%)
	>$40,000	263 (23.5%)	95 (25.2%)	168 (22.7%)
	Missing	50 (4.5%)	16 (4.2%)	34 (4.6%)

Note: 25 subjects (4 cases, 21 controls) for whom birth certificates were ordered were unable to be located, and were dropped from the analysis.

1.14; 95% CI: 1.01–1.28). Odds ratios for TGCT risk associated with each doubling of EDP application within 1 km in the year before birth are shown in Table 8. Acephate was associated with increased risk in the overall study population (OR: 1.25; 95% CI: 1.06–1.47) and in the Latino group (OR: 1.30; 95% CI: 1.09–1.57). Additionally, malathion was associated with increased TGCT risk in the overall population (OR: 1.14; 95% CI: 1.00–1.30) and in the Latino group (OR: 1.19; 95% CI: 1.01–1.39). No other ORs were statistically significant. Analyses during the period after PUR instituted "full use" reporting (after 1990) showed associations with acephate within 3 km radius (OR: 1.11; 95% CI: 1.02–1.20) and methomyl within 1 km radius (OR: 1.22; 95% CI: 1.01–1.48), although based on a limited sample size (Supplemental Tables S3 and S4). A model including both acephate and methomyl (found to be correlated) showed similar ORs for both 3 km and 1 km radii (data not shown).

In formal tests for interaction of the pesticides with significant main effects, the association between carbaryl and TGCT risk differed by ethnicity (p-value for interaction = 0.006) at the 3 km radius. There were no other statistically significant interactions between other pesticides and ethnicity and PUR reporting period. The ORs and 95% CIs for EDP applications at 3 km and 1 km radii did not show differences by time window of exposure (trimester-specific ORs for EDP applications within 3 km and 1 km can be found in Supplemental Tables S5 and S6, respectively). Additionally, nonlinearity of the relationship between EDP application and TGCT risk was assessed for two EDPs of interest: acephate and carbaryl. Visualizations of nonlinearity are provided in Supplemental Figs. S3 and S4 for acephate and carbaryl, respectively, at a 3 km application radius. No evidence of nonlinearity is present for

Table 3
Characteristics of nearby application of EDPs within 3 km of an individual's home address in the year before birth in cases vs. controls.

Pesticide	Cases			Controls		
	# exposed (%)	Mean (SD)	Median (IQR)	# exposed (%)	Mean (SD)	Median (IQR)
Total EDP application	184 (48.8%)	970.3 (4140.8)	50.3 (9.0, 435.0)	348 (47.0%)	856.9 (3015.9)	70.2 (10.4, 324.9)
Acephate	88 (23.3%)	31 (79.4)	3 (0.1, 18.3)	174 (23.5%)	13.4 (43.9)	0.8 (0.0, 5.6)
Carbaryl	90 (23.9%)	22.7 (90)	0.6 (0.1, 6.9)	166 (22.4%)	18.5 (68.4)	0.6 (0.0, 8.8)
Chlorpyrifos	85 (22.5%)	88.5 (170.2)	8.4 (0.9, 94.2)	158 (21.3%)	89.6 (239.9)	12.3 (2.0, 62.3)
Copper sulfate	34 (9.0%)	184.3 (738.3)	4.5 (0.3, 28.1)	58 (7.8%)	299.2 (913.9)	2 (0.6, 25.3)
Diazinon	99 (26.3%)	51.8 (162.7)	3.8 (0.4, 18.0)	192 (25.9%)	37.3 (96.0)	2.2 (0.1, 18.9)
Dicofol	55 (14.6%)	40.8 (114.9)	1.7 (0.2, 15.4)	87 (11.7%)	31.4 (113.6)	1.8 (0.3, 11.6)
Dimethoate	78 (20.7%)	79.1 (157.9)	9.5 (0.5, 68.7)	162 (21.9%)	64.1 (190.3)	9.2 (0.9, 34.6)
Diuron	50 (13.3%)	24.5 (50.6)	0.7 (0.0, 23.6)	84 (11.3%)	52.3 (190.9)	0.9 (0.0, 26)
Endosulfan	61 (16.2%)	30.7 (78.6)	2.4 (0.0, 17.9)	131 (17.7%)	32.3 (86.5)	0.4 (0.0, 9.9)
Iprodione	59 (15.6%)	28 (71.7)	3.4 (0.2, 17.9)	122 (16.5%)	27.2 (68.2)	2 (0.1, 16.4)
Malathion	75 (19.9%)	37.1 (78.0)	5.4 (0.6, 28.8)	124 (16.7%)	35.2 (84.8)	7.9 (1.1, 24.4)
Mancozeb	46 (12.2%)	30.8 (88.2)	2.6 (0.1, 20.3)	94 (12.7%)	52.0 (176.0)	0.4 (0.0, 9.4)
Methomyl	110 (29.2%)	24 (62.2)	0.8 (0.1, 11.3)	208 (28.1%)	23.8 (67.2)	1.1 (0.1, 12.8)
Methyl bromide	114 (30.2%)	906.8 (4661.2)	12.3 (1.3, 108.5)	216 (29.1%)	720.6 (2865.5)	9.2 (1.0, 48.5)
Methyl parathion	35 (9.3%)	15 (27.4)	6.8 (1.0, 13.8)	66 (8.9%)	64.3 (115.6)	13.3 (4.2, 79.1)
Oryzalin	41 (10.9%)	37.6 (100.2)	13.1 (1.4, 26.7)	81 (10.9%)	41.4 (78.7)	5.4 (0.4, 30.4)
Oxyfluorfen	46 (12.2%)	24.3 (30.3)	9.1 (1.3, 40.5)	79 (10.7%)	38.4 (70.3)	9.9 (2.0, 32.4)
Paraquat dichloride	68 (18.0%)	59.1 (109.2)	19 (3.2, 56.6)	149 (20.1%)	60.4 (99.6)	14.2 (2.7, 78.3)
Parathion	45 (11.9%)	60.3 (124.2)	9 (3.5, 52.4)	94 (12.7%)	79.3 (249.5)	9.8 (2.4, 39.6)
Pendimethalin	19 (5.0%)	28.7 (53.3)	6.1 (2.4, 22.6)	31 (4.2%)	15.8 (19.7)	8.4 (2.2, 18.4)
Permethrin	65 (17.2%)	205.7 (584.3)	9.2 (0.4, 83.2)	126 (17.0%)	79.2 (205.5)	9.5 (1.5, 44.1)
Simazine	49 (13.0%)	51.2 (100.5)	4.7 (0.1, 54.5)	105 (14.2%)	103.6 (370.3)	3.1 (0.0, 43.0)
Trifluralin	39 (10.3%)	92.7 (184.1)	6.2 (0.2, 89.4)	74 (10.0%)	94.3 (241.4)	8.4 (0.7, 34.0)
Vinclozolin	59 (15.6%)	6.6 (21.1)	0.4 (0.1, 4.8)	79 (10.7%)	16.6 (56.4)	0.5 (0.0, 9.7)

Note: Only those EDPs applied near >50 individuals are listed; arithmetic mean, standard deviation, medium, and interquartile range (in kilograms) represent only those individuals with any nearby EDP application (i.e., zero values are excluded).

Table 4
Characteristics of nearby application of EDPs within 3 km of an individual's home address in the year before birth in Latinos vs. non-Latinos.

Pesticide	Latinos			Non-Latinos		
	# exposed (%)	Mean (SD)	Median (IQR)	# exposed (%)	Mean (SD)	Median (IQR)
Total EDP application	291 (47.4%)	1132.3 (4100.8)	77 (15.4, 543.9)	241 (47.8%)	610.9 (2400.5)	38.4 (4.8, 225.8)
Acephate	157 (25.6%)	24.9 (69.8)	2.6 (0.1, 17.4)	105 (20.8%)	11 (35.1)	0.5 (0.0, 4.9)
Carbaryl	137 (22.3%)	25.6 (79.1)	2.4 (0.1, 11.0)	119 (23.6%)	13.5 (73.2)	0.2 (0.0, 3.8)
Chlorpyrifos	144 (23.5%)	108.9 (266.2)	9.4 (1.1, 98.8)	99 (19.6%)	60.6 (110.8)	13.4 (1.6, 53.0)
Copper sulfate	53 (8.6%)	342.3 (957.6)	3.8 (0.8, 28.9)	39 (7.7%)	140.4 (674.2)	2 (0.2, 17.1)
Diazinon	176 (28.7%)	45.6 (125.8)	4.6 (0.8, 25.5)	115 (22.8%)	37.1 (118.2)	1.3 (0.1, 9.8)
Dicofol	86 (14%)	33.3 (103.8)	1.7 (0.2, 12.3)	56 (11.1%)	37.7 (128.6)	2.7 (0.3, 13.7)
Dimethoate	137 (22.3%)	93.2 (224.5)	9.9 (0.7, 55.3)	103 (20.4%)	36.8 (84.3)	8.7 (0.7, 23.8)
Diuron	74 (12.1%)	57 (202.2)	1.7 (0.0, 33.6)	60 (11.9%)	23.3 (50.8)	0.3 (0.0, 10.4)
Endosulfan	110 (17.9%)	43 (100)	3 (0.0, 33.4)	82 (16.3%)	16.7 (52.3)	0.2 (0.0, 6.6)
Iprodione	113 (18.4%)	28.2 (75.2)	4 (0.5, 19.5)	68 (13.5%)	26.3 (58.2)	0.5 (0.0, 15.8)
Malathion	127 (20.7%)	36.1 (86.5)	7.9 (1.5, 24.0)	72 (14.3%)	35.6 (74.3)	6.2 (0.4, 26.8)
Mancozeb	91 (14.8%)	27.9 (85.6)	1.1 (0.1, 10.8)	49 (9.7%)	76.8 (228.6)	0.3 (0.0, 5.5)
Methomyl	182 (29.6%)	28.4 (69.9)	2.6 (0.2, 26.9)	136 (27%)	17.9 (58.6)	0.4 (0.0, 4.7)
Methyl bromide	183 (29.8%)	985 (4228.9)	17 (2.7, 143.8)	147 (29.2%)	535.9 (2553.3)	6.9 (0.7, 21.2)
Methyl parathion	64 (10.4%)	39.2 (62.5)	10.7 (2.5, 43.5)	37 (7.3%)	61 (138.7)	9.6 (4.2, 39.4)
Oryzalin	76 (12.4%)	47.3 (99.8)	10.2 (0.8, 34.9)	46 (9.1%)	28.2 (55.8)	6.5 (0.8, 25.0)
Oxyfluorfen	76 (12.4%)	36 (68.4)	9.1 (1.5, 33.9)	49 (9.7%)	28.9 (40.8)	12.6 (2.1, 35.8)
Paraquat dichloride	113 (18.4%)	67.4 (117.6)	17.2 (4.8, 79.4)	104 (20.6%)	51.9 (82.8)	14.2 (1.6, 73.5)
Parathion	72 (11.7%)	97.4 (235.5)	11.7 (3.3, 65.6)	67 (13.3%)	47.1 (192.8)	9.1 (2.1, 33.5)
Pendimethalin	28 (4.6%)	19.3 (44.4)	3.1 (1.3, 16.6)	22 (4.4%)	22.4 (23.2)	12.9 (7.5, 32.3)
Permethrin	115 (18.7%)	144.3 (458.3)	10 (0.5, 66.8)	76 (15.1%)	88.9 (222.8)	7.3 (1.0, 54.0)
Simazine	86 (14%)	100.7 (381.1)	5.6 (0.2, 62.4)	68 (13.5%)	69.5 (191.6)	0.2 (0.0, 31.2)
Trifluralin	63 (10.3%)	110.5 (242.5)	11.8 (1.3, 57.0)	50 (9.9%)	72.7 (194.7)	2.7 (0.1, 25.2)
Vinclozolin	88 (14.3%)	10.1 (26.4)	0.4 (0.1, 7.5)	50 (9.9%)	16.3 (66.3)	0.5 (0.0, 5.3)

Note: Only those EDPs applied near >50 individuals are listed; arithmetic mean, standard deviation, medium, and interquartile range (in kilograms) represent only those individuals with any nearby EDP application (i.e., zero values are excluded). Non-Latino group includes all races (>83% white).

Table 5
Characteristics of nearby application of EDPs within 1 km of an individual's home address in the year before birth in cases vs. controls.

Pesticide	Cases			Controls		
	# exposed (%)	Mean (SD)	Median (IQR)	# exposed (%)	Mean (SD)	Median (IQR)
Total EDP application	134 (35.5%)	94.3 (446.3)	5 (0.4, 50.4)	257 (34.7%)	128.3 (559.1)	7.4 (0.8, 40.1)
Acephate	42 (11.1%)	5.4 (13.7)	0.7 (0.1, 5.1)	67 (9%)	1.9 (5.7)	0.2 (0.0, 1.0)
Carbaryl	37 (9.8%)	1.9 (5.6)	0 (0.0, 0.2)	67 (9%)	4.1 (9.9)	0.2 (0.0, 3.0)
Chlorpyrifos	35 (9.3%)	19 (33.4)	7.9 (1.6, 17.7)	81 (10.9%)	16.3 (41.4)	2.8 (0.4, 15.0)
Diazinon	52 (13.8%)	8.1 (19.3)	0.3 (0.0, 2.9)	94 (12.7%)	6.2 (15.5)	0.4 (0.0, 3.0)
Dimethoate	40 (10.6%)	10.1 (14.5)	2.4 (0.0, 15.1)	81 (10.9%)	12.1 (51.5)	1.5 (0.2, 6.4)
Diuron	24 (6.4%)	5.1 (16.9)	0 (0.0, 1.4)	35 (4.7%)	8.2 (27.9)	0.8 (0.0, 3.7)
Endosulfan	29 (7.7%)	3.9 (10.7)	0.2 (0.0, 2.2)	50 (6.7%)	3.9 (7.7)	0.5 (0.0, 4.2)
Iprodione	28 (7.4%)	5 (10.6)	0.3 (0.0, 3.1)	55 (7.4%)	4.7 (8.2)	0.4 (0.0, 4.7)
Malathion	29 (7.7%)	14.5 (30.3)	1.4 (0.2, 16.9)	55 (7.4%)	3.9 (9.6)	0.6 (0.1, 2.1)
Methomyl	53 (14.1%)	4.9 (10.3)	0.1 (0.0, 2.8)	99 (13.4%)	2.9 (6.7)	0.1 (0.0, 1.6)
Methyl bromide	48 (12.7%)	164.2 (699.3)	0.8 (0.2, 6.8)	101 (13.6%)	217.6 (762.7)	2.6 (0.3, 12.0)
Oxyfluorfen	23 (6.1%)	3.9 (4.6)	1.6 (1.0, 5.2)	32 (4.3%)	9.3 (13.9)	4.2 (1.2, 11.6)
Paraquat dichloride	32 (8.5%)	9.3 (17.3)	4.4 (1.4, 11.2)	86 (11.6%)	9.8 (23.8)	2.3 (0.3, 8.6)
Parathion	21 (5.6%)	7.1 (13.7)	2.3 (0.5, 6.7)	46 (6.2%)	8.5 (16.1)	2.1 (0.2, 7.4)
Permethrin	31 (8.2%)	20.4 (37.7)	5.7 (0.3, 18.6)	50 (6.7%)	14.2 (35.9)	3.5 (0.3, 9.6)
Simazine	24 (6.4%)	2.3 (4)	0.3 (0.0, 2.5)	52 (7%)	13.6 (35)	1.9 (0.0, 9.6)

Note: Only those EDPs applied near >50 individuals are listed; arithmetic mean, standard deviation, medium, and interquartile range (in kilograms) represent only those individuals with any nearby EDP application (i.e., zero values are excluded).

acephate in either the Latino or non-Latino group, though carbaryl does show an increase in risk at low application quantities, followed by a decrease in risk with greater application, in both ethnic groups (data not shown).

Although this was the first study to examine this relationship, the potential contribution of EDP application to overall TGCT burden in California was estimated by calculating the PAR percentages using ORs for categorized EDP application (zero/low vs. high levels) within 3 km and 1 km using PUR data to estimate prevalence of exposure (Table 9). Results are shown for the population overall and by ethnic group and year of PUR reporting. At the 3 km radius, 2.9% (95% CI: 0.0%–7.0%) of TGCTs could be associated with application of high levels of acephate in the year before birth in the overall population; this number increases to 5.3% (95% CI: 0.3%–11.6%) in the Latino group, and 10.2% (95% CI: 0.8%–21.3%) in the post-1990 era. When limited to applications within a 1 km radius, acephate could be associated with 2.1% of TGCTs in the overall population (95% CI: 0.1%–4.9%), and 4.2% in the Latino group (95% CI: 0.9%–9.0%). The PAR percentage associated with carbaryl (3 km radius) was 5.5% (95% CI: 0.4%–12.2%) in non-Latinos and mostly concentrated after 1990, and 2.9% (95% CI: 0.0%–10.3%) for malathion (1 km radius) in the post 1990.

4. Discussion

This population-based study is the first to show that application of several agricultural EDPs near individuals' residences before birth is associated with an increased risk of TGCT in adolescence (15–19 years of age). Our observations could explain a substantive proportion of TGCT

Table 6
Characteristics of nearby application of EDPs within 1 km of an individual's home address in the year before birth in Latinos vs. non-Latinos.

Pesticide	Latinos			Non-Latinos		
	# exposed (%)	Mean (SD)	Median (IQR)	# exposed (%)	Mean (SD)	Median (IQR)
Total EDP application	219 (35.7%)	158.1 (596)	9.4 (0.8, 60.9)	172 (34.1%)	63.9 (406.9)	4.7 (0.6, 21.9)
Acephate	70 (11.4%)	4.5 (11.8)	0.5 (0.1, 3.0)	39 (7.7%)	1.1 (2.5)	0.1 (0.0, 0.6)
Carbaryl	60 (9.8%)	4.9 (10.7)	0.2 (0.0, 3.4)	44 (8.7%)	1.1 (3.8)	0.0 (0.0, 0.3)
Chlorpyrifos	72 (11.7%)	20.2 (47.2)	4.7 (0.4, 20.1)	44 (8.7%)	12.1 (19.0)	3.6 (1.1, 13.7)
Diazinon	90 (14.7%)	7.6 (19.2)	0.5 (0.0, 3.3)	56 (11.1%)	5.6 (12.2)	0.2 (0.0, 1.6)
Dimethoate	72 (11.7%)	15.8 (54.6)	2.1 (0.1, 14.4)	49 (9.7%)	5.1 (10.7)	1.0 (0.2, 5.2)
Diuron	31 (5.0%)	11.1 (32.3)	1 (0.0, 3.4)	28 (5.6%)	2.4 (5.6)	0.0 (0.0, 1.9)
Endosulfan	48 (7.8%)	5.2 (10.8)	0.4 (0.0, 4.6)	31 (6.2%)	1.8 (3.5)	0.2 (0.0, 2.4)
Iprodione	55 (9.0%)	5.2 (9.3)	1.1 (0.1, 4.8)	28 (5.6%)	4 (8.6)	0.2 (0.0–2.1)
Malathion	53 (8.6%)	9.0 (23.3)	0.7 (0.2, 5.2)	31 (6.2%)	5.1 (12.1)	0.6 (0.1, 2.9)
Methomyl	98 (16.0%)	3.9 (8.3)	0.2 (0.0, 2.7)	54 (10.7%)	3.1 (8)	0.1 (0.0, 0.6)
Methyl bromide	84 (13.7%)	274.3 (816.3)	4.4 (0.5, 27.1)	65 (12.9%)	104.8 (623.5)	0.4 (0.1, 5.4)
Oxyfluorfen	35 (5.7%)	7.6 (13.5)	2.6 (1.2, 6.1)	20 (4.0%)	6 (5.9)	2.8 (1.1, 10.8)
Paraquat dichloride	56 (9.1%)	14.3 (30.7)	5.1 (1.2, 10.5)	62 (12.3%)	5.5 (7.4)	1.3 (0.1, 8.8)
Parathion	36 (5.9%)	11.8 (18.6)	5.1 (1.0, 9.6)	31 (6.2%)	3.7 (8.7)	1.5 (0.0, 3.2)
Permethrin	49 (8.0%)	17.1 (37.7)	5.1 (0.4, 16.3)	32 (6.3%)	15.8 (35.2)	1.3 (0.2, 9.9)
Simazine	42 (6.8%)	12.4 (35.4)	1.6 (0.0, 8.6)	34 (6.7%)	7.1 (19.8)	0.1 (0.0–4.0)

Note: Only those EDPs applied near >50 individuals are listed; arithmetic mean, standard deviation, medium, and interquartile range (in kilograms) represent only those individuals with any nearby EDP application (i.e., zero values are excluded). Non-Latino group includes all races (>83% white).

Table 7
Odds ratios (ORs) and 95% confidence intervals (CIs) for the change in TGCT risk associated with a doubling of kg of EDPs applied within 3 km in the full year before birth.

Pesticide	Overall OR[a] (95% CI)	Latinos OR[a] (95% CI)	Non-Latinos OR[a] (95% CI)
Acephate	1.09 (1.02, 1.16)	1.09 (1.01, 1.17)	1.08 (0.96, 1.22)
Carbaryl	1.01 (0.94, 1.09)	0.94 (0.85, 1.05)	1.14 (1.01, 1.28)
Chlorpyrifos	1.00 (0.96, 1.05)	1.00 (0.95, 1.06)	1 .00 (0.94, 1.08)
Copper sulfate	1.01 (0.94, 1.09)	1.00 (0.90, 1.11)	1.09 (0.96, 1.23)
Diazinon	1.02 (0.97, 1.07)	1.01 (0.94, 1.07)	1.05 (0.97, 1.14)
Dicofol	1.05 (0.98, 1.12)	1.09 (0.99, 1.2)	0.99 (0.88, 1.11)
Dimethoate	1.01 (0.96, 1.05)	1.00 (0.94, 1.06)	1.02 (0.95, 1.10)
Diuron	1.02 (0.95, 1.09)	0.97(0.88, 1.06)	1.10 (0.98, 1.23)
Endosulfan	1.01 (0.95, 1.08)	1.00 (0.93, 1.08)	1.05 (0.93, 1.17)
Iprodione	1.01 (0.94, 1.08)	0.97(0.89, 1.07)	1.06 (0.95, 1.19)
Malathion	1.03 (0.97, 1.09)	1.02 (0.95, 1.10)	1.04 (0.95, 1.14)
Mancozeb	1.02 (0.95, 1.10)	1.01 (0.91, 1.11)	1.04 (0.93, 1.17)
Methomyl	1.01 (0.95, 1.06)	1.01 (0.94, 1.08)	1.01 (0.91, 1.11)
Methyl bromide	1.02 (0.99, 1.05)	1.01 (0.97, 1.05)	1.05 (0.99, 1.11)
Methyl parathion	0.94 (0.88, 1.02)	0.93 (0.84, 1.02)	0.97(0.87, 1.09)
Oryzalin	1.02 (0.95, 1.09)	1.01 (0.93, 1.09)	1.04 (0.93, 1.17)
Oxyfluorfen	1.02 (0.95, 1.09)	0.99 (0.91, 1.08)	1.06 (0.96, 1.18)
Paraquat dichloride	1.00 (0.95, 1.04)	0.98 (0.93, 1.05)	1.01 (0.94, 1.08)
Parathion	1.00 (0.95, 1.06)	0.98 (0.91, 1.06)	1.04 (0.95, 1.14)
Pendimethalin	1.04 (0.94, 1.17)	1.14 (0.97, 1.34)	0.96 (0.81, 1.13)
Permethrin	1.00 (0.96, 1.05)	1.01 (0.95, 1.07)	0.99 (0.92, 1.07)
Simazine	1.00 (0.95, 1.06)	0.97 (0.9, 1.05)	1.05 (0.96, 1.15)
Trifluralin	1.01 (0.95, 1.07)	1.02 (0.95, 1.10)	0.99 (0.89, 1.1)
Vinclozolin	1.03 (0.93, 1.13)	1.02 (0.90, 1.16)	1.04 (0.89, 1.21)

Note: Non-Latino group includes all races (>83% white) [a] Adjusted for median neighborhood household income, birth pre-/post-1990, and ethnicity (when not already stratified upon).

Table 8
Odds ratios (ORs) and 95% confidence intervals (CIs) for the change in TGCT risk associated with a doubling of kg of EDPs applied within 1 km in the full year before birth.

Pesticide	Overall OR[a] (95% CI)	Latinos OR[a] (95% CI)	Non-Latinos OR[a] (95% CI)
Acephate	1.25 (1.06, 1.47)	1.30 (1.08, 1.57)	1.04 (0.69, 1.57)
Carbaryl	0.91 (0.75, 1.10)	0.83 (0.65, 1.06)	1.19 (0.81, 1.73)
Chlorpyrifos	1.01 (0.93, 1.10)	0.98 (0.88, 1.09)	1.08 (0.94, 1.24)
Diazinon	1.03 (0.92, 1.14)	1.00 (0.87, 1.14)	1.09 (0.91, 1.29)
Dimethoate	1.03 (0.93, 1.14)	1.04 (0.93, 1.17)	0.99 (0.81, 1.20)
Diuron	0.98 (0.82, 1.18)	0.96 (0.77, 1.20)	1.04 (0.74, 1.46)
Endosulfan	0.98 (0.83, 1.17)	0.93 (0.75, 1.15)	1.16 (0.83, 1.63)
Iprodione	0.99 (0.84, 1.15)	0.98 (0.82, 1.18)	1.00 (0.75, 1.32)
Malathion	1.14 (1.00, 1.30)	1.19 (1.01, 1.39)	1.04 (0.81, 1.33)
Methomyl	1.08 (0.96, 1.23)	1.05 (0.90, 1.22)	1.18 (0.94, 1.48)
Methyl bromide	0.96 (0.90, 1.03)	0.95 (0.88, 1.03)	1.00 (0.90, 1.12)
Oxyfluorfen	1.01 (0.87, 1.17)	0.90 (0.72, 1.11)	1.21 (0.95, 1.54)
Paraquat dichloride	0.98 (0.89, 1.09)	0.96 (0.84, 1.10)	1.02 (0.87, 1.19)
Parathion	0.99 (0.86, 1.14)	0.92 (0.77, 1.11)	1.18 (0.91, 1.54)
Permethrin	1.06 (0.96, 1.17)	1.08 (0.96, 1.22)	1.04 (0.88, 1.22)
Simazine	0.88 (0.74, 1.03)	0.77 (0.59, 1.01)	1.01 (0.80, 1.27)

Note: Non-Latino group includes all races (>83% white).
[a] Adjusted for median neighborhood household income, birth pre-/post-1990, and ethnicity (when not already stratified upon).

cases diagnosed in California, especially among Latinos born in areas where pesticides have been used.

The effect of prenatal exposure to endocrine-disrupting chemicals on the development of TGCT has been difficult to study in humans, and evidence in the literature is mixed. Self-reported exogenous estrogen exposure during pregnancy has been reported to be associated with elevated risk (Depue et al., 1983; Weir et al., 2000), while biomarker studies suggest that high perinatal serum androgen levels may also play a role (Holl et al., 2009; Morimoto et al., 2018). Also, some studies have found an association between serum EDP levels and TGCT (McGlynn et al., 2008; Purdue et al., 2009), while others find no association (Biggs et al., 2008; Hardell et al., 2006). Both of the published quantitative meta-analyses that synthesized findings on perinatal EDC exposure and TGCT found elevated risks (Bonde et al., 2016; Martin et al., 2008), though the relationship was only statistically significant in one of them. The link between EDCs and other TDS-related outcomes has been more widely studied, with several reporting positive associations between parental occupational (Jorgensen et al., 2014) and residential (Agopian et al., 2013; Bougneres et al., 2021; Cognez et al., 2019) exposure to pesticides and increased risks of hypospadias and cryptorchidism in the offspring. Studies measuring endocrine disrupting chemicals in biological specimens (maternal and offspring), however, have been equivocal, suggesting that association of these compounds, should they exist, exhibit significant heterogeneity across male reproductive outcomes (Bonde et al., 2016). While the role that EDCs play in these TDS associated outcomes remains suggestive, the difficulty in obtaining appropriate biospecimens during the relevant time periods, in large enough sample sizes, make a more definitive conclusion elusive.

The most robust finding from our study was the association between nearby acephate application at both 3 km and 1 km radii in the year

Table 9
Population risk percentage attributable to application of selected EDPs within 3 km and 1 km in the year before birth.

Pesticide	Group	Categorical OR (95% CI)		Population attributable risk %	
		3 km	1 km	3 km	1 km
Acephate	Overall	1.26 (0.96, 1.64)	1.47 (1.01, 2.13)	2.9 (0.0, 7.0)	2.1 (0.1, 4.9)
	Latinos	1.44 (1.02, 2.03)	1.90 (1.19, 3.01)	5.3 (0.3, 11.6)	4.2 (0.9, 9.0)
	Non-Latinos	1.10 (0.72, 1.69)	0.89 (0.45, 1.75)	1.0 (0.0, 6.7)	0.0 (0.0, 3.1)
	Pre-1990	1.06 (0.76, 1.48)	1.45 (0.89, 2.35)	0.6 (0.0, 4.3)	1.4 (0.0, 4.1)
	Post-1990	1.57 (1.04, 2.37)	1.27 (0.71, 2.25)	10.2 (0.8, 21.3)	2.4 (0.0, 10.4)
Carbaryl	Overall	1.05 (0.78, 1.40)	0.73 (0.45, 1.19)	0.5 (0.0, 4.3)	0.0 (0.0, 0.9)
	Latinos	0.63 (0.39, 1.02)	0.50 (0.24, 1.07)	0.0 (0.0, 0.2)	0.0 (0.0, 0.4)
	Non-Latinos	1.53 (1.04, 2.25)	1.29 (0.71, 2.38)	5.5 (0.4, 12.2)	1.1 (0.0, 5.1)
	Pre-1990	1.00 (0.72, 1.39)	0.85 (0.51, 1.43)	0.0 (0.0, 4.3)	0.0 (0.0, 1.9)
	Post-1990	1.12 (0.61, 2.05)	0.81 (0.31, 2.07)	1.2 (0.0, 9.9)	0.0 (0.0, 4.7)
Malathion	Overall	1.13 (0.83, 1.54)	1.26 (0.83, 1.92)	1.1 (0.0, 4.3)	1.0 (0.0, 3.4)
	Latinos	1.17 (0.79, 1.72)	1.31 (0.78, 2.20)	1.6 (0.0, 6.6)	1.4 (0.0, 5.0)
	Non-Latinos	1.07 (0.63, 1.80)	1.16 (0.56, 2.39)	0.4 (0.0, 5.0)	0.5 (0.0, 4.0)
	Pre-1990	0.95 (0.61, 1.47)	0.95 (0.53, 1.73)	0.0 (0.0, 2.6)	0.0 (0.0, 2.1)
	Post-1990	1.18 (0.75, 1.85)	1.47 (0.77-, 2.79)	3.0 (0.0, 12.9)	2.9 (0.0, 10.3)

Note: Both the categorical OR and population attributable risk percentage calculations used a dichotomous measure of EDP application, comparing "zero" + "low" categories to the "high" category. Model covariates included median neighborhood household income, and ethnicity and birth pre-/post-1990 when not already stratified upon. Non-Latino group includes all races (>83% white).

before birth and TGCT risk, particularly among Latinos. In persons born after 1990 (which likely have a more accurate representation of nearby acephate exposure due to the expansion of the PUR system) the corresponding estimated attributable risk reached 10.2% in the overall population in California. The Latinx community is subject to disproportionate pesticide exposure in the US (Brulle and Pellow 2006; Carter-Pokras et al., 2007). For acephate specifically, one study of predominately Latinx pregnant individuals in the Salinas Valley of California found acephate in 3.1% of urine samples (Montesano et al., 2007). Acephate is a commonly used organophosphate insecticide that acts as a cholinesterase inhibitor and can cause acute cholinergic symptoms; in addition, it is considered a "possible human carcinogen" by the US Environmental Protection Agency (US Environmental Protection Agency National Center for Environmental Assessment 1988). Numerous studies in animal models have supported its endocrine-disrupting effects. Most relevant to this study, acephate has been found to impair testicular development in the offspring of rats exposed to acephate during gestation (Sampaio et al., 2020). Additionally, in rats it has been found to inhibit androgen synthesis (Joshi and Sharma 2011; Wang et al., 2020), decrease fertility in males (Farag et al., 2000a; Jasuja et al., 2013), and decrease pregnancy viability in females (Farag et al., 2000b). Though one study showed cytotoxic and genotoxic effects on human sperm (Dhanushka and Peiris 2017), human studies are lacking. Malathion, another wide-spectrum organophosphate insecticide linked to decreased sperm count, lowered androgen levels, and degeneration of the seminiferous tubules (Joshi and Sharma 2011), was associated with increased TGCT risk in our study.

We also found associations between TGCT risk and carbaryl, a commonly used carbamate insecticide that has been associated with disruption of the pituitary-gonad axis and spermatotoxic effects in rats (Fattahi et al., 2012; Pant et al., 1996; Shtenberg and Rybakova 1968), as well as decreased sperm motility and increased sperm abnormality and DNA fragmentation in humans (Dziewirska et al., 2019; Xia et al., 2005). We reported an isolated association with methomyl (1 km radius in the post-1990 subgroup only) which is another carbamate insecticide connected to seminiferous tubule degeneration, decreased testosterone, and decreased fertility in male rats (Mahgoub and El-Medany 2001; Shalaby et al., 2010).

Despite having assessed application of 24 EDPs at 3 km and 16 EDPs at 1 km, only the four EDPs listed above showed statistically significant associations with TGCT risk. The lack of correlation between nearby application of individual EDPs allowed independent assessment of individual EDP impact. The statistically significant results represent a small percentage of associations tested; other pesticides included are also known or suspected endocrine disruptors, with findings in the literature similar to those cited above to support this designation. Overall, acephate demonstrated the most consistent association with TGCT risk, with statistical significance among all participants and the Latino group at both 3 km and 1 km application radii. It is unclear why ethnicity-specific trends, such as a stronger association with carbaryl among non-Latino males, were seen, though possibilities include differential real-life exposure associated with socioeconomic factors such as agricultural occupation, more intensive exposure associated with use of specific pesticides, or household pesticide use.

Our ability to identify trimester-specific associations may have been partially hampered by the lack of statistical power. There is, however, reason to believe that critical periods of testicular development, in which the testes are particularly sensitive to endocrine disruption, may exist. Germ cell development meets key, timed milestones throughout gestation, as primordial germ cells begin to form as early as 3–4 gestational weeks and mature into pre-spermatogonia at approximately 17–20 gestational weeks (Jorgensen et al., 2015). Endocrine disruption can also have persistent effects, theoretically altering the gestational hormonal milieu even when exposure occurs prior to conception. Rat models support the existence of a fetal programming window during which masculinization of reproductive tissues occurs at a time period corresponding to about 8–14 gestational weeks in humans (Welsh et al., 2008).

Strengths of this study include its status as the first to geospatially assess the proximity to EDPs during the prenatal period and its association with TGCT risk, using an exposure measure free of recall bias. The study was also carried out using a statewide population-based cancer registry, which minimized selection bias. While the validity of birth certificate data has been shown to vary considerably, with some items (e.g. insurance, birthweight, Apgar score, delivery type) being more reliable than others (e.g., prenatal visits, maternal complications and comorbidities) (DiGiuseppe et al., 2002; Northam and Knapp 2006), race and ethnicity from California birth certificate data was found to have very high agreement to self-reported race and Hispanic ethnicity for most race groups (Baumeister et al., 2000). The California Department of Pesticide Regulation has made great efforts to minimize errors and improve the quality of the data in PUR by incorporating rigorous error-checking procedures to confirm active ingredients are registered to be applied to the crops reported with approved application rates and also by assessing the quality of the spatial data provided. Although there is no way to definitively confirm all pesticide applications are reported

in PUR, growers and applicators in California are required by law to report all pesticide applications on commodities grown for commercial purposes and compliance is considered to be very high (Wilhoit et al., 2001). Therefore, while having some limitations, registry data remains the best source of large, diverse information collected with no selection, especially for a relatively rare cancer like testicular cancer.

Most of the study's limitations relate to difficulties in precisely assessing time- and location-specific pesticide exposure years before diagnosis. Most notably, nearby pesticide application is not necessarily equivalent to pesticide exposure. Though application within a 1 km or 3 km radius of residential address provides a proxy for exposure, unmeasured factors such as residential mobility in the year before birth, wind patterns, variable amount of time spent at home/outdoors, and occupational and other non-agricultural pesticide exposure limit our ability to precisely infer exposure. In our data, pesticide application quantities are greater for individuals born in 1990 or later mostly due to the change to full-use reporting, although an actual increase in application of some pesticides cannot be ruled out. This was addressed in our analyses by adjusting our models and/or stratifying individuals based on birth pre- or post-1990. Additionally, the difference in PUR standards between pre- and post-1990 data signifies known under-reporting before 1990, though we have no reason to believe this under-reporting was biased in a particular direction or differential between cases and controls. While we tested the hypothesis that prenatal exposure to EDPs increases the risk of TGCT, we did not attempt to assess individuals' pesticide exposure after birth, which could affect TGCT risk as well. Our analysis may have also been impacted by inability to assess and adjust for risk factors associated with pesticide exposure, such as parental occupation. However, to date there have been no strong environmental or lifestyle risk factors (beyond family history and cryptorchidism) associated with TGCT risk; therefore, we do not have reasons to believe this omission would affect our risk estimates. Additionally, given the design of the study, our study did not include TGCT cases that were diagnosed in California but born elsewhere. It is possible that some of the controls could have moved from California prior to a diagnosis of TGCT, and therefore not linked to the CCR. Given the rarity of TGCT, and childhood and adolescent cancer overall, however, this is anticipated to be a very small proportion of total cases occurring among California born subjects. Other limitations unrelated to exposure assessment include multiple comparisons, although we selected the EDPs based on *a priori* hypothesis.

In conclusion, this study conducted in California suggests associations between TGCT risk in adolescents and prenatal proximity to acephate applications and, to a lesser extent, to carbaryl and malathion. The impact of these risks varied by Latino vs. non-Latino ethnicity.

Declaration of competing interest

None declared.

Appendix A. Supplementary data

Supplementary data to this article can be found online at https://doi.org/10.1016/j.ijheh.2021.113881.

Funding

This work was funded by Alex's Lemonade Stand Foundation (ALSF) Award #044782 and by the University of California, Berkeley/University of California, San Francisco Joint Medical Program.

References

Agopian, A.J., Cai, Y., Langlois, P.H., Canfield, M.A., Lupo, P.J., 2013. Maternal residential atrazine exposure and risk for choanal atresia and stenosis in offspring. J. Pediatr. 162, 581–586.

Baroni, T., Arato, I., Mancuso, F., Calafiore, R., Luca, G., 2019. On the origin of testicular germ cell tumors: from gonocytes to testicular cancer. Front. Endocrinol. 10, 343.

Baumeister, L., Marchi, K., Pearl, M., Williams, R., Braveman, P., 2000. The validity of information on "race" and "hispanic ethnicity" in California birth certificate data. Health Serv. Res. 35, 869–883.

Beiki, O., Granath, F., Allebeck, P., Akre, O., Moradi, T., 2010. Subtype-specific risk of testicular tumors among immigrants and their descendants in Sweden, 1960 to 2007. Cancer Epidemiol. Biomarkers Prev. 19, 1053–1065.

Biggs, M.L., Davis, M.D., Eaton, D.L., Weiss, N.S., Barr, D.B., Doody, D.R., et al., 2008. Serum organochlorine pesticide residues and risk of testicular germ cell carcinoma: a population-based case-control study. Cancer Epidemiol. Biomarkers Prev. 17, 2012–2018.

Bonde, J.P., Flachs, E.M., Rimborg, S., Glazer, C.H., Giwercman, A., Ramlau-Hansen, C. H., et al., 2016. The epidemiologic evidence linking prenatal and postnatal exposure to endocrine disrupting chemicals with male reproductive disorders: a systematic review and meta-analysis. Hum. Reprod. Update 23, 104–125.

Bougneres, P., Porcher, R., Esterle, L., Baker, D., de la Vaissiere, A., Meurisse, S., et al., 2021. Exploring the risk of hypospadias in children born from mothers living close to a vineyard. PLoS One 16, e0249800.

Brulle, R.J., Pellow, D.N., 2006. Environmental justice: human health and environmental inequalities. Annu. Rev. Publ. Health 27, 103–124.

California Department of Pesticide Regulation, 2017. Summary of pesticide use report (PUR) data. Available: https://www.cdpr.ca.gov/docs/pur/pur17rep/17sum.htm#trends. (Accessed 8 February 2021).

Carter-Pokras, O., Zambrana, R.E., Poppell, C.F., Logie, L.A., Guerrero-Preston, R., 2007. The environmental health of latino children. J. Pediatr. Health Care 21, 307–314.

Cognez, N., Warembourg, C., Zaros, C., Metten, M.A., Bouvier, G., Garlantezec, R., et al., 2019. Residential sources of pesticide exposure during pregnancy and the risks of hypospadias and cryptorchidism: the French elfe birth cohort. Occup. Environ. Med. 76, 672–679.

Curl, C.L., Spivak, M., Phinney, R., Montrose, L., 2020. Synthetic pesticides and health in vulnerable populations: agricultural workers. Curr Environ Health Rep 7, 13–29.

de Graaf, L., Boulanger, M., Bureau, M., Bouvier, G., Meryet-Figuiere, M., Tual, S., et al., 2021. Occupational pesticide exposure, cancer and chronic neurological disorders: a systematic review of epidemiological studies in greenspace workers. Environ. Res. 203, 111822.

Depue, R.H., Pike, M.C., Henderson, B.E., 1983. Estrogen exposure during gestation and risk of testicular cancer. J. Natl. Cancer Inst. 71, 1151–1155.

Deziel, N.C., Freeman, L.E., Graubard, B.I., Jones, R.R., Hoppin, J.A., Thomas, K., et al., 2017. Relative contributions of agricultural drift, para-occupational, and residential use exposure pathways to house dust pesticide concentrations: meta-regression of published data. Environ. Health Perspect. 125, 296–305.

Dhanushka, M.A., Peiris, L.D., 2017. Cytotoxic and genotoxic effects of acephate on human sperm. J. Toxicol. 2017:3874817.

DiGiuseppe, D.L., Aron, D.C., Ranbom, L., Harper, D.L., Rosenthal, G.E., 2002. Reliability of birth certificate data: a multi-hospital comparison to medical records information. Matern. Child Health J. 6, 169–179.

Dziewirska, E., Radwan, M., Wielgomas, B., Klimowska, A., Radwan, P., Kaluzny, P., et al., 2019. Human semen quality, sperm DNA damage, and the level of urinary concentrations of 1N and TCPY, the biomarkers of nonpersistent insecticides. Am. J. Men's Health 13, 1557988318816598.

Farag, A.T., Eweidah, M.H., El-Okazy, A.M., 2000a. Reproductive toxicology of acephate in male mice. Reprod. Toxicol. 14, 457–462.

Farag, A.T., Eweidah, M.H., Tayel, S.M., El-Sebae, A.H., 2000b. Developmental toxicity of acephate by gavage in mice. Reprod. Toxicol. 14, 241–245.

Fattahi, E., Jorsaraei, S.G., Gardaneh, M., 2012. The effect of carbaryl on the pituitary-gonad axis in male rats. Iran. J. Reproductive Med. 10, 419–424.

Ghazarian, A.A., McGlynn, K.A., 2020. Increasing incidence of testicular germ cell tumors among racial/ethnic minorities in the United States. Cancer Epidemiol. Biomarkers Prev. 29, 1237–1245.

Giannandrea, F., Fargnoli, S., 2017. Environmental factors affecting growth and occurrence of testicular cancer in childhood: an overview of the current epidemiological evidence. Children 4.

Gunier, R.B., Ward, M.H., Airola, M., Bell, E.M., Colt, J., Nishioka, M., et al., 2011. Determinants of agricultural pesticide concentrations in carpet dust. Environ. Health Perspect. 119, 970–976.

Gurney, J.K., Florio, A.A., Znaor, A., Ferlay, J., Laversanne, M., Sarfati, D., et al., 2019. International trends in the incidence of testicular cancer: lessons from 35 years and 41 countries. Eur. Urol. 76, 615–623.

Guyton, K.Z., Loomis, D., Grosse, Y., El Ghissassi, F., Benbrahim-Tallaa, L., Guha, N., et al., 2015. Carcinogenicity of tetrachlorvinphos, parathion, malathion, diazinon, and glyphosate. Lancet Oncol. 16, 490–491.

Hardell, L., Bavel, B., Lindstrom, G., Eriksson, M., Carlberg, M., 2006. In utero exposure to persistent organic pollutants in relation to testicular cancer risk. Int. J. Androl. 29, 228–234.

Harnly, M., McLaughlin, R., Bradman, A., Anderson, M., Gunier, R., 2005. Correlating agricultural use of organophosphates with outdoor air concentrations: a particular concern for children. Environ. Health Perspect. 113, 1184–1189.

Harnly, M.E., Bradman, A., Nishioka, M., McKone, T.E., Smith, D., McLaughlin, R., et al., 2009. Pesticides in dust from homes in an agricultural area. Environ. Sci. Technol. 43, 8767–8774.

Hemminki, K., Mousavi, S.M., Brandt, A., Ji, J., Sundquist, J., 2010. Histology-specific risks in testicular cancer in immigrants to Sweden. Endocr. Relat. Cancer 17, 329–334.

Henderson, B.E., Benton, B., Jing, J., Yu, M.C., Pike, M.C., 1979. Risk factors for cancer of the testis in young men. International journal of cancer Journal international du cancer 23, 598–602.
Holl, K., Lundin, E., Surcel, H.M., Grankvist, K., Koskela, P., Dillner, J., et al., 2009. Endogenous steroid hormone levels in early pregnancy and risk of testicular cancer in the offspring: a nested case-referent study. International journal of cancer Journal international du cancer 124, 2923–2928.
Jasuja, N.D., Sharma, P., Joshi, S.C., 2013. A comprehensive effect of acephate on cauda epididmis and accessory sex organs of male rats. African Journal of Pharmacy and Pharmacology 7, 1560–1567.
Jorgensen, A., Lindhardt Johansen, M., Juul, A., Skakkebaek, N.E., Main, K.M., Rajpert-De Meyts, E., 2015. Pathogenesis of germ cell neoplasia in testicular dysgenesis and disorders of sex development. Semin. Cell Dev. Biol. 45, 124–137.
Jorgensen, K.T., Jensen, M.S., Toft, G.V., Larsen, A.D., Bonde, J.P., Hougaard, K.S., 2014. Risk of cryptorchidism among sons of horticultural workers and farmers in Denmark. Scand. J. Work. Environ. Health 40, 323–330.
Joshi, S.C., Sharma, P., 2011. Male reproductive toxicity or organophosphorous compounds: a review. Toxicol. Environ. Chem. 93, 1486–1507.
Litchfield, K., Levy, M., Orlando, G., Loveday, C., Law, P.J., Migliorini, G., et al., 2017. Identification of 19 new risk loci and potential regulatory mechanisms influencing susceptibility to testicular germ cell tumor. Nat. Genet. 49, 1133–1140.
Mahgoub, A.A., El-Medany, A.H., 2001. Evaluation of chronic exposure of the male rat reproductive system to the insecticide methomyl. Pharmacol. Res. 44, 73–80.
Martin, O., Shialis, T., Lester, J., Scrimshaw, M., Boobis, A., Voulvoulis, N., 2008. Testicular dysgenesis syndrome and the estrogen hypothesis: a quantitative meta-analysis. Ciência Saúde Coletiva 13, 1601–1618.
McGlynn, K.A., Quraishi, S.M., Graubard, B.I., Weber, J.P., Rubertone, M.V., Erickson, R. L., 2008. Persistent organochlorine pesticides and risk of testicular germ cell tumors. J. Natl. Cancer Inst. 100, 663–671.
McGlynn, K.A., Trabert, B., 2012. Adolescent and adult risk factors for testicular cancer. Nat. Rev. Urol. 9, 339–349.
Mnif, W., Hassine, A.I., Bouaziz, A., Bartegi, A., Thomas, O., Roig, B., 2011. Effect of endocrine disruptor pesticides: a review. Int. J. Environ. Res. Publ. Health 8, 2265–2303.
Montesano, M.A., Olsson, A.O., Kuklenyik, P., Needham, L.L., Bradman, A.S., Barr, D.B., 2007. Method for determination of acephate, methamidophos, omethoate, dimethoate, ethylenethiourea and propylenethiourea in human urine using high-performance liquid chromatography-atmospheric pressure chemical ionization tandem mass spectrometry. J. Expo. Sci. Environ. Epidemiol. 17, 321–330.
Morimoto, L.M., McCauley, K., Ma, X., Wiemels, J.L., Chokkalingam, A.P., Metayer, C., 2016. Birth weight, fetal growth, and risk of pediatric rhabdomyosarcoma: an updated record linkage study in California. Ann. Epidemiol. 26, 141–145.
Morimoto, L.M., Zava, D., McGlynn, K.A., Stanczyk, F.Z., Kang, A.Y., Ma, X., et al., 2018. Neonatal Hormone Concentrations and Risk of Testicular Germ Cell Tumors (TGCT). Cancer Epidemiol Biomarkers Prev.
Morris, C.R., Epstein, J., Nassere, K., Hofer, B.M., Rico, J., Bates, J.H., Snipes, K.P., 2010. Trends in Cancer Incidence, Mortality, Risk Factors, and Health Behaviors in California. California Department of Public Health, Cancer Surveillance Section, Sacramento, CA.
Myrup, C., Westergaard, T., Schnack, T., Oudin, A., Ritz, C., Wohlfahrt, J., et al., 2008. Testicular cancer risk in first- and second-generation immigrants to Denmark. J. Natl. Cancer Inst. 100, 41–47.
National Cancer Institute, 2003. Surveillance Epidemiology and End Results Program. Cancer Incidence in U.S. Immigrant Populations - Landmark Studies. Available: https://seer.cancer.gov/archive/studies/surveillance/study5.html. (Accessed 8 February 2021). accessed.
Northam, S., Knapp, T.R., 2006. The reliability and validity of birth certificates. J. Obstet. Gynecol. Neonatal Nurs. 35, 3–12.
Pant, N., Shankar, R., Srivastava, S.P., 1996. Spermatotoxic effects of carbaryl in rats. Hum. Exp. Toxicol. 15, 736–738.
Parkin, D.M., Iscovich, J., 1997. Risk of cancer in migrants and their descendants in Israel: Ii. Carcinomas and germ-cell tumours. International journal of cancer Journal international du cancer 70, 654–660.
Pishgar, F., Haj-Mirzaian, A., Ebrahimi, H., Saeedi Moghaddam, S., Mohajer, B., Nowroozi, M.R., et al., 2019. Global, regional and national burden of testicular cancer, 1990-2016: results from the global burden of disease study 2016. BJU Int. 124, 386–394.
Purdue, M.P., Engel, L.S., Langseth, H., Needham, L.L., Andersen, A., Barr, D.B., et al., 2009. Prediagnostic serum concentrations of organochlorine compounds and risk of testicular germ cell tumors. Environ. Health Perspect. 117, 1514–1519.
Requena-Mullor, M., Navarro-Mena, A., Wei, R., Lopez-Guarnido, O., Lozano-Paniagua, D., Alarcon-Rodriguez, R., 2021. Evaluation of gonadal alterations in a population environmentally exposed to a mixture of endocrine active pesticides. Int. J. Environ. Res. Publ. Health 18.
Sampaio, C.F., Prates, K.V., Siervo, G., Mathias, P.C.F., Fernandes, G.S.A., 2020. Impairment of testicular development in rats exposed to acephate during maternal gestation and lactation. Environ. Sci. Pollut. Res. Int. 27, 5482–5488.
Schmiedel, S., Schuz, J., Skakkebaek, N.E., Johansen, C., 2010. Testicular germ cell cancer incidence in an immigration perspective, Denmark, 1978 to 2003. J. Urol. 183, 1378–1382.
Shalaby, M.A., El Zorba, H.Y., Ziada, R.M., 2010. Reproductive toxicity of methomyl insecticide in male rats and protective effect of folic acid. Food Chem. Toxicol. 48, 3221–3226.
Sharpe, R.M., Skakkebaek, N.E., 1993. Are oestrogens involved in falling sperm counts and disorders of the male reproductive tract? Lancet 341, 1392–1395.
Sharpe, R.M., Skakkebaek, N.E., 2008. Testicular dysgenesis syndrome: mechanistic insights and potential new downstream effects. Fertil. Steril. 89, e33–38.
Shtenberg, A.I., Rybakova, M.N., 1968. Effect of carbaryl on the neuroendocrine system of rats. Food Chem. Toxicol. 6, 461–467.
Skakkebaek, N.E., Rajpert-De Meyts, E., Main, K.M., 2001. Testicular dysgenesis syndrome: an increasingly common developmental disorder with environmental aspects. Hum. Reprod. 16, 972–978.
Teitelbaum, S.L., Gammon, M.D., Britton, J.A., Neugut, A.I., Levin, B., Stellman, S.D., 2007. Reported residential pesticide use and breast cancer risk on long island, New York. Am. J. Epidemiol. 165, 643–651.
Toppari, J., Virtanen, H.E., Main, K.M., Skakkebaek, N.E., 2010. Cryptorchidism and hypospadias as a sign of testicular dysgenesis syndrome (tds): environmental connection. Birth Defects Res A Clin Mol Teratol 88, 910–919.
U.S. Environmental Protection Agency, 2020. Office of Pesticide Programs. Chemicals Evaluated For Carcinogenic Potential: Annual Cancer Report. Available: https://apublica.org/wp-content/uploads/2020/05/chemicals-evaluated.pdf. (Accessed 25 October 2021).
Surveillance, Epidemiology, and End Results (SEER) Program (https://www.seer.cancer.gov) SEER*Stat Database: Incidence - SEER Research Data, 18Registries, Nov 2020 Sub (2000-2018) - Linked To County Attributes - Time Dependent (1990-2018) Income/Rurality, 1969-2019 Counties, National CancerInstitute, DCCPS, Surveillance Research Program, released April 2021, based on the November 2020 submission.
US Environmental Protection Agency National Center for Environmental Assessment, 1988. Integrated risk information system (iris) chemical assessment summary: Acephate; casrn 30560-19-1. Available: https://iris.epa.gov/static/pdfs/0354_summary.pdf, 1988. (Accessed 8 February 2021).
Wang, Y., Dong, Y., Wu, S., Zhu, Q., Li, X., Liu, S., et al., 2020. Acephate interferes with androgen synthesis in rat immature leydig cells. Chemosphere 245, 125597.
Wang, Z., McGlynn, K.A., Rajpert-De Meyts, E., Bishop, D.T., Chung, C.C., Dalgaard, M. D., et al., 2017. Meta-analysis of five genome-wide association studies identifies multiple new loci associated with testicular germ cell tumor. Nat. Genet. 49, 1141–1147.
Weir, H.K., Marrett, L.D., Kreiger, N., Darlington, G.A., Sugar, L., 2000. Pre-natal and peri-natal exposures and risk of testicular germ-cell cancer. International journal of cancer Journal international du cancer 87, 438–443.
Welsh, M., Saunders, P.T., Fisken, M., Scott, H.M., Hutchison, G.R., Smith, L.B., et al., 2008. Identification in rats of a programming window for reproductive tract masculinization, disruption of which leads to hypospadias and cryptorchidism. J. Clin. Invest. 118, 1479–1490.
Wilhoit, L., Zhang, M., Ross, L., 2001. Data quality of California's pesticide use report. Pm, pp. 01–02. Available. http://agis.ucdavis.edu/pur/Papers/dataq_rpt.pdf, 2001.
Wilhoit, L., 2016. The history of california's pesticide use reporting system (PUR). Available: http://agis.ucdavis.edu/pur/pdf/2016/7-Wilhoit.pdf.
Xia, Y., Cheng, S., Bian, Q., Xu, L., Collins, M.D., Chang, H.C., et al., 2005. Genotoxic effects on spermatozoa of carbaryl-exposed workers. Toxicol. Sci. : an official journal of the Society of Toxicology 85, 615–623.
Xing, J.S., Bai, Z.M., 2018. Is testicular dysgenesis syndrome a genetic, endocrine, or environmental disease, or an unexplained reproductive disorder? Life Sci. 194, 120–129.
Znaor, A., Lortet-Tieulent, J., Jemal, A., Bray, F., 2014. International variations and trends in testicular cancer incidence and mortality. Eur. Urol. 65, 1095–1106.

International Journal of Hygiene and Environmental Health 239 (2022) 113868

Contents lists available at ScienceDirect

International Journal of Hygiene and Environmental Health

journal homepage: www.elsevier.com/locate/ijheh

Stress hormone biosynthesis-based genes and lifestyle moderated the association of noise exposure with blood pressure in a cohort of Chinese tobacco factory workers: A cross-sectional analysis

Luoyao Yang [b,c,1], Xiayun Dai [a,1], Lisha Wu [a,1], Tian Xu [a], Zhuowang Chen [a], Zhiteng Min [a], Yonggang Liao [a], Lei Ni [a], Yong Yao [a], Guilin Yi [a], Zhenlong Chen [a,*], Wenjun Yin [a,d,**]

[a] Wuhan Prevention and Treatment Center for Occupational Diseases, Jianghan Bei Lu 18, Wuhan, 430015, Hubei, PR China
[b] Department of Occupational and Environmental Health, School of Public Health, Tongji Medical College, Huazhong University of Science and Technology, Hangkong Road 13, Wuhan, 430030, Hubei, PR China
[c] Key Laboratory of Environment and Health, Ministry of Education & Ministry of Environmental Protection, and State Key Laboratory of Environmental Health (Incubating), School of Public Health, Tongji Medical College, Huazhong University of Science and Technology, Hangkong Road 13, Wuhan, 430030, Hubei, PR China
[d] Hubei Province Key Laboratory of Occupational Hazard Identification and Control, Wuhan University of Science and Technology, Wuhan, 430065, Hubei, PR China

ARTICLE INFO

Keywords:
Noise exposure
Genetic polymorphism
Lifestyles
Blood pressure
Moderated moderation analysis

ABSTRACT

When evaluating noise-related cardiovascular risk, noise is generally solely assessed as the major stressor. However, cardiovascular effect of other simultaneous exposure events, such as unhealthy lifestyle and genetic variation, is easily neglected. The aim of this study is to estimate the combined effect of noise and lifestyle on blood pressure alteration, particularly under different genetic background. This study included 536 workers from a tobacco factory in Wuhan, China, who were divided into high exposure group and low exposure group according to noise measurement in their working area. All participants took annual physical examination and questionnaire survey to provide information on individual systolic and diastolic blood pressure (SBP and DBP) and lifestyle (smoking, drinking and physical activity). Single nucleotide polymorphism at genes related to stress hormone production were determined. Moderated moderation models were constructed to investigate the interaction effect of noise exposure and lifestyle factors on blood pressure with regard to different genetic background. We identified an expected trend in association between noise exposure and SBP among active smokers ($P = 0.086$). The moderated moderation analysis showed significant three-way interaction effect (*COMT* rs4680 × smoking status × noise exposure levels) on SBP or DBP (both $P < 0.05$). For *COMT* rs4680 GA+AA genotype carriers, active smoking significantly moderated the association between noise exposure and SBP or DBP (both $P < 0.05$). The results indicated that for *COMT* rs4680 A allele carriers, tobacco and noise exposure contribute collectively to blood pressure alteration, supporting that stress hormone production may play a certain role in the smoke-and-noise-induced cardiovascular effect.

1. Introduction

Noise is a common occupational hazard worldwide (Basner et al., 2014). In China, over ten million workers suffer from occupational noise exposure exceeding permissible limit. The high intensity and continuity of occupational noise particularly underline the vulnerability of cardiovascular system to noise-induced adverse health effects, where the abnormal regulation of blood pressure has been highlighted and intensively studied (Lang et al., 1992; Oliveira and Arenas 2012; Yang et al., 2018). A series of epidemiological studies have reported increased blood pressure under occupational noise exposure, especially when over 85 dB (A) (Gan et al., 2011; Talbott et al., 1985; Tomei et al., 2000). However,

Abbreviations: BMI, body mass index; CVD, cardiovascular diseases; DBP, diastolic blood pressure; SBP, systolic blood pressure; SNP, single nucleotide polymorphism.

* Corresponding author.
** Corresponding author. Wuhan Prevention and Treatment Center for Occupational Diseases, Jianghan Bei Lu 18, Wuhan, 430015, Hubei, PR China.
E-mail address: ywjyjs@foxmail.com (W. Yin).

[1] These authors contributed equally to this study.

https://doi.org/10.1016/j.ijheh.2021.113868
Received 19 April 2021; Received in revised form 21 September 2021; Accepted 18 October 2021
Available online 23 October 2021

the finding is still inconclusive due to the complexity of noise-induced health effect and disability to rule out confounding factors (Babisch 2002; van Kempen et al., 2002).

Several exposures events, including environmental pollutants and lifestyle factors could potentially modify the adverse effect of noise exposure (Lang et al., 1992; Passchier et al., 2000). Given that certain unhealthy lifestyle, such as active smoking and excessive alcohol drinking, is well-acknowledged risk factor of cardiovascular diseases (CVD), it is necessary to investigate their combined effect with noise exposure on blood pressure (Laonigro et al., 2009; Virdis et al., 2010).

Other than environmental factors, genetic factors are also regarded as determinants of high blood pressure (Kurland et al., 2005). A treasure of linkage studies revealed hypertension-associated genetic variation, uncovering the underling biological mechanism, namely the regulation of sodium homeostasis, sympathetic pathways, etc (Akther et al., 2021; Htun et al., 2011; Padmanabhan and Dominiczak 2021). Genetic background related to stress hormone production has been pointed out to potentially alter the susceptibility to CVD (Burrello et al., 2017). For example, it is reported that Met allele of the *COMT* rs4680 is positively correlated with higher blood pressure in 214 middle-aged Swedish males (Annerbrink et al., 2008). The activation of sympathetic nervous system and disturbance of endocrine function caused by long-term noise exposure, leading to elevated stress hormone secretion was also suggested to facilitate the progression of CVD (Babisch 2003; Babisch et al., 2001; Schmidt et al., 2013). However, limited data was available concerning stress hormone related genetic variants in noise-induced CVD. Investigating the cardiovascular effect of noise and lifestyle in different genetic background may reveal the underlying biological pathway and help understand detailed mechanism.

The aim of this study is to explore the role of lifestyle factors and genetic susceptibility in noise-induced cardiovascular effect. We first investigated the combined effect of occupational noise exposure and unhealthy lifestyle on blood pressure. Additionally, we sought to determine whether genetic variants related to stress hormone production would modify noise-related blood pressure alteration. Finally, we speculate that the interaction effect of noise and lifestyle factors on blood pressure varies in different genetic background. Moderated moderation models were constructed to test our hypothesis (Fig. 1).

2. Materials and methods

2.1. Study population

All participants were recruited from three different workshops in a tobacco factory in Wuhan city, China in 2019, using stratified random cluster sampling method. According to the average noise exposure levels during 8h standard working time ($L_{ex,8h}$) limit in China (GBZ2.2-2007), the participants were categorized into two groups (i.e., low exposure group: < 85 dB(A) and high exposure group: ≥ 85 dB(A)). The endpoint of this cohort study is CVD (coronary heart disease, myocardial infarction, peripheral vascular diseases, ischaemic stroke, ischaemic heart disease, angina, heart failure, etc.).

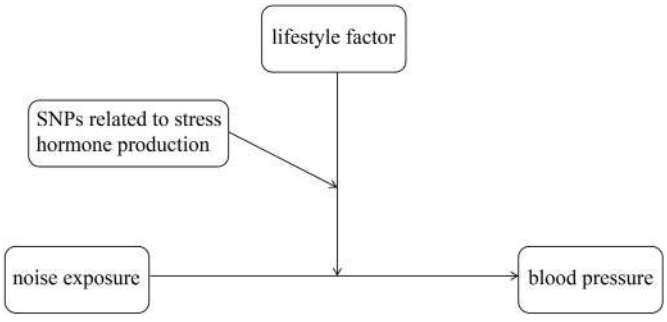

Fig. 1. Conceptual diagram of moderated moderation model: three-way interaction of noise exposure, lifestyle factor and SNP genotype on blood pressure. Age, gender, BMI, lifestyle factors (active smoking, alcohol use and physical exercise), and antihypertensive medication use were included as covariants.

To the best of our knowledge, the prevalence of CVD is about 20.7% in Chinese population aged ≥15 years in 2016 (Joint Task Force for Guideline on the and Management of Cardiovascular Risk in 2019). Exposure to high occupational noise (generally measured as ≥ 85 dB(A)) was associated with a large, clinically meaningful increase in the incidence of CVD (hazard ratio = 1.34, 95% confidence interval: 1.15–1.56) (Teixeira et al., 2019). Compared with participants without occupational noise exposure, the association of CVD risk with noise exposure was higher in males (odds ratio = 1.86, 95% confidence interval: 1.12–3.14) (Wang et al., 2021). In three different workshops of the tobacco factory, the ratio of male to female is about 3 : 1, and the average age exceeds 45 years old.

In addition, the statistical power value (1-β) and type I error rate (α) were set at 0.8 and 0.05 respectively. We used the Epi info version.7.0 software (Centers for Disease Control and Prevention, Georgia USA) to calculate the minimum sample size for the cohort study, which was about 512. Given that the expected rate of loss to follow-up was estimated at 20%, about 614 participants needed to be included in the cohort study.

Finally, a total of 627 participants were recruited. All of them provided written informed consents before the study enrollment. Each participant finished physical examination and face-to-face questionnaire survey and provided blood samples for single nucleotide polymorphism (SNP) determination. They were free from CVD (including coronary heart disease, myocardial infarction, peripheral vascular diseases, ischaemic stroke, ischaemic heart disease, angina, heart failure) and cancer. Participants will be visited every 2 years to complete the questionnaire survey. The physical examination will be conducted annually. The current analysis only includes the baseline data of this cohort. After excluding those with missing data on blood pressure (n = 54), body mass index (BMI) (n = 37), routine blood indices (n = 4) and noise exposure levels (n = 14) at baseline, 536 participants were finally included in current analysis. This study is approved by the Medical Research Ethics Committee of Wuhan Prevention and Treatment Center for Occupational Diseases.

2.2. Physical examination and questionnaire survey

All participants underwent a physical examination and were face-to-face interviewed by trained staff to acquire socio-demographic characteristics using questionnaires. Active smokers are defined as those who smoke at least one cigarette per day during the past 6 months. Alcohol use is defined as drinking alcohol beverage at least once per week during the past 6 months. Physical exercise is defined as regularly taking at least 20 min leisure-time exercise during the past 6 months (Yang et al., 2014). Hypertension is defined as systolic blood pressure (SBP) ≥ 140 mmHg and/or diastolic blood pressure (DBP) ≥ 90 mmHg, or self-reported doctor-diagnosed hypertension or taking antihypertensive medication (Chalmers et al., 1999).

The physical examination is comprised of determination of anthropometric parameters (weight, height and waist circumference), blood pressure (DBP and SBP), routine blood indices and blood biochemical indices. BMI was calculated as body weight (in kilograms) divided by height (in meters squared). A fasting blood sample was collected for examination of white blood cell count, lymphocyte count, platelets, glucose, alanine transaminase, aspartate transaminase, creatine kinase and creatine kinase MB.

2.3. Noise exposure measurement

The noise exposure measurement was conducted in working area using sound level meters (3M, SP-DL). The instrument was placed in the

hearing zone near the noisy machine where workers performed their jobs. All measurements were taken on the same day in the period of actual working time (T_e) corresponding to each job group. The output was A-weighted equivalent noise levels in designated T_e ($L_{Aeq,Te}$). $L_{ex,8h}$ were calculated as follows:

$$L_{ex,8h} = L_{Aeq,\ Te} + 10\lg(T_e/T_0)\ \mathrm{dB(A)}$$

Where T_0 = 8h. The noise exposure data was matched to individuals according to their working places and working time.

2.4. SNP selection and genotyping

Genes associated with stress hormone production, including *PAH*, *TH*, *DDC*, *DBH*, *PNMT*, *CYP17A1*, *HSD3B2*, *CYP21A2*, *CYP11B2*, *CYP4F2*, *CYP11A1*, and *COMT* were determined according to Ensemble database (http://www.ensembl.org/index.html). A total of 1389 SNPs located on genes mentioned above based on human genome version GRCh37/hg19 were obtained from UCSC Table Browser (http://genome.ucsc.edu/cgi-bin/hgTables). SNPs were screened according to: minimum allele frequency >0.05; showing evidence of function and being bi-allelic. The remaining SNPs were evaluated for their RegulomeDB score (http://www.regulomedb.org/index) according to their functional location and consequence, and were put into SNPinfo software (http://snpinfo.niehs.nih.gov/snpinfo/snpfunc.htm) to predict the most potentially functional SNPs. The SNPs in the ten top-ranked loci were selected for genotyping. After excluding those with high linkage disequilibrium with each other ($r^2 \geq 0.8$), 9 SNPs locus were included in current study.

Each participant underwent a venipuncture to collect 2 ml of blood. The blood samples were stored in cryotubes at −80 °C. DNA was extracted using Whole Blood Genomic DNA Extraction kit (DP1102, BioTekeCorp., China) following the manufacturer's protocol and was normalized to a concentration of 10–30 ng/μL. SNPs were typed using the mass spectroscopy-based technique, Mass ARRAY (Sequenom, San Diego, USA).

We selected SNPs with minimum allele frequency > 0.05, Hardy–Weinberg equilibrium > 0.05 and genotyping success rate > 95%, leaving 5 SNPs locus finally included in further analyses (Table 1).

2.5. Statistical analysis

To increase statistical stability, we applied dominant risk allele models to categorize SNP into two groups: common (homozygous wild type) and variant group (heterozygous/homozygous variant). Categorical variables were presented as number (percentage). Normally distributed variables were described as mean ± standard deviation. Non-normally distributed continuous variables were expressed as medians with inter quartile range.

To study the moderating effect of genotype and lifestyle factors on the association of noise exposure with blood pressure, interaction term (noise exposure level × mediators) was constructed in multiple linear regression models. Analyses were carried out with R 3.5.2 software. We further established moderated moderation models with bootstrapping strategy (N = 1,000), utilizing PROCESS macro v3.0 (Hayes 2017) for SPSS v25.0. The PROCESS macro is a modeling tool to construct models with simultaneous multiple mediators or moderators, based on ordinary least squares regression and logistic regression using Bootstrap method (Hayes 2012). The moderated moderation model is to test the influence of secondary moderator on the moderating effect of primary moderator, that is, to answer in what condition, primary moderator would alter the relation between independent variable and outcome variable (Hayes and Rockwood 2017). The moderated moderation model by PROCESS macro estimates the interaction effect of primary moderator and dependent variable conditioned by secondary moderator. As requested, a slope difference test was conducted to visualize the moderated moderation effect (Dawson and Richter 2006). As shown in Fig. 1 (conceptual diagram), SNP genotype was added to the model as the moderator of moderation of the association between noise exposure and blood pressure by lifestyle factors. All models were adjusted for age, gender, BMI, lifestyle factors (active smoking, alcohol use and physical exercise), and antihypertensive medication use. A *P*-value of < 0.05 was considered as a statistically significant (two-tailed).

3. Results

3.1. Characteristics of participants

Table 2 demonstrated selected variables in study population at baseline (n = 536) according to noise exposure levels. Age and glucose levels are significantly higher in low noise exposure group (both $P < 0.05$). While lymphocyte count, red blood cell count and creatine kinase levels are higher in high noise exposure group (all $P < 0.05$). SBP and DBP exhibited no statistically significant difference between two groups.

3.2. Simple moderation

As shown in Fig. 2, the interaction of lifestyle factors (active smoking, alcohol use and physical exercise) and noise exposure levels on SBP or DBP was not statistically significant ($P > 0.05$). In different lifestyle subgroups, we found a nearly significant association between noise exposure and SBP among smokers ($\beta = 3.154$, $P = 0.086$). We also investigated the gene-environment interaction effect on SBP and DBP (Fig. 3). Different genotype of *COMT* rs4680 showed no significant moderating effect on association between noise exposure and SBP or DBP. The effect of noise exposure on SBP is moderated by different groups of *DDC* rs11978267. Specifically, among participants carrying *DDC* rs11978267 AA, noise exposure was positively associated with SBP increase ($\beta = 3.119$, $P = 0.039$). Among participants carrying *COMT* rs4680 GA + AA, the association between noise exposure and SBP nearly reached a significant level ($P = 0.068$).

Table 1
Selected SNPs and genotyping distribution in study population.

Gene	SNP	Strand	Alleles (risk/other)	MAF	HWE	Genotype	Genotype frequency (%)
COMT	rs165815	+	T/C	0.50	0.275	CC	118 (22.0)
						CT + TT	407 (75.9)
	rs4680	+	A/G	0.50	0.976	GG	130 (24.3)
						GA + AA	389 (72.6)
PAH	rs10860869	+	T/A	0.42	0.975	AA	174 (32.5)
						AT + TT	350 (65.3)
DDC	rs11978267	+	G/A	0.12	0.447	AA	399 (74.4)
						AG + GG	121 (22.6)
DBH	rs4740203	+	T/C	0.25	0.613	CC	283 (52.8)
						CC + TC	234 (43.7)

MAF: minor allele frequency; HWE: Hardy-Weinberg equilibrium.

Table 2
Distributions of selected variables by noise exposure levels at baseline.

Characteristics	Low noise exposure[a] (n = 271)	High noise exposure[a] (n = 265)	*P*-value
Age (year, mean ± S.D.)	44.03 ± 9.53	40.26 ± 8.52	0.000[b]
Gender (male/female, n, %)	196/75 (72.3/27.7)	212/53 (76.1/23.9)	0.037[c]
Active smoking (yes/no, n, %)	121/150 (44.6/55.4)	134/131/(50.6/49.4)	0.170[c]
Alcohol use (yes/no, n, %)	66/205 (24.4/75.6)	63/203 (23.4/76.6)	0.795[c]
Physical exercise (yes/no, n, %)	147/124 (54.2/45.8)	136/129 (51.3/48.7)	0.498[c]
Antihypertensive medication (yes/no, n, %)	33/238 (12.2/87.8)	34/231 (12.8/87.2)	0.819[c]
Hypertension (yes/no, n, %)	59/212 (21.8/78.2)	59/206 (22.3/77.7)	0.890[c]
BMI (kg/m^2, mean ± S.D.)	23.76 ± 3.59	23.66 ± 3.39	0.752[b]
Blood pressure			
SBP (mm Hg, mean ± S.D.)	118.96 ± 16.43	119.38 ± 14.81	0.757[b]
DBP (mm Hg, mean ± S.D.)	73.79 ± 10.71	73.44 ± 11.12	0.706[b]
Routine blood indices			
WBC (10^9/L, median, IQR)	5.83 ± 1.50	5.76 ± 1.43	0.567[b]
LYM (10^9/L, median, IQR)	1.87 ± 0.48	1.94 ± 0.51	0.072[b]
PLT (10^9/L, mean ± S.D.)	211.03 ± 46.43	214.60 ± 47.02	0.376[b]
RBC (10^{12}/L, mean ± S.D.)	4.69 ± 0.43	4.80 ± 0.44	0.004[b]
Blood biochemical indices			
GLU (mol/L, mean ± S.D.)	5.39 ± 1.43	5.13 ± 0.95	0.014[b]
ALT (U/L, median, IQR)	19.10 (14.50, 27.80)	19.30 (14.20, 30.45)	0.526[d]
AST (U/L, median, IQR)	19.70 (17.20, 24.00)	20.00 (17.40, 24.10)	0.526[d]
CK (IU/L, median, IQR)	103.2 (77.00, 135.90)	115.60 (88.55, 161.60)	0.000[d]
CKMB (IU/L, median, IQR)	11.30 (9.10, 13.80)	11.40 (9.35, 14.10)	0.535[d]

IQR: interquartile range; S.D.: standard deviation; BMI: body mass index; SBP: systolic blood pressure; DBP: diastolic blood pressure; WBC: white blood cell count; LYM: lymphocyte count; PLT: platelets; RBC: red blood cell count; GLU: glucose; ALT: alaninetransaminase; AST: aspartatetransaminase; CK: creatine kinase; CKMB: creatine kinase MB.

[a] The noise exposure is classified into high (≥ 85 dB(A)) and low (< 85 dB(A)) levels.

[b] Student's t-test was used to compare means of the continuous variables between the two groups.

[c] Chi-square test was used to compare categorical variables.

[d] Mann-Whitney test was used to compare differences in non-normal variable distributions between the two groups.

3.3. Moderated moderation analysis

In the moderated moderation analysis, SNP genotype was set as the secondary moderator to test whether it altered the two-way interaction of lifestyle factor on the association of noise exposure levels with blood pressure. No significant three-way interaction was found in explorations of SNP genotype × alcohol use × noise exposure levels or SNP genotype × physical exercises × noise exposure levels (see Tables S1–4 in Supplementary Materials). As shown in Fig. 4, when smoking status was considered as the first moderator, the three-way interaction effect on SBP (*COMT* rs4680 × smoking status × noise exposure levels) was found significant (β = 12.853, $P = 0.026$). For *COMT* rs4680 GA+AA group possessing active smoking habit, noise exposure level was positively associated with SBP increase (β = 4.748, $P = 0.024$), and marginally significantly associated with DBP (β = 2.583, $P = 0.084$). After identifying the significant three-way interaction, we further visualize the model in Fig. 5A. For *COMT* rs4680 GA+AA, active smoking significantly moderated the association between noise exposure and SBP (β = 8.66, $P = 0.018$).

Fig. 4 also shows results when outcome variable is DBP. The three-way interaction was statistically significant when *COMT* rs4680 (β = 8.207, $P = 0.046$) and *PAH* rs10860869 (β = −8.776, $P = 0.019$) were put in the model as the secondary moderator. For *PAH* rs10860869 AA group possessing active smoking habit, noise exposure level was positively associated with DBP increase (β = 5.083 $P = 0.023$). As shown in Fig. 5B, for *COMT* rs4680 GA+AA, active smoking significantly moderated the association between noise exposure and DBP (β = 5.159, $P = 0.012$). Fig. 5C demonstrated that for *PAH* rs10860869 AA, the moderation effect of active smoking on the association between noise exposure and DBP was also observed (β = 8.858, $P = 0.004$). The moderated moderation analysis was also conducted using additive models (see Table S5 in Supplementary Materials).

4. Discussion

The current study did not determine a significant effect of occupational noise exposure on blood pressure change in the study population. By stratifying participants into subgroups according to lifestyle factors, we identified an expected trend in association between noise exposure and SBP among active smokers. We also included determination of SNPs in genes associated with stress hormone production and observed a nearly significant positive association between noise exposure and DBP for *CMOT* rs4680 A allele carriers. To further investigate whether the moderation effect of lifestyle factor on the association between noise exposure and blood pressure varies in different genetic background, we constructed moderated moderation models. The moderation effect of smoking status on association between noise exposure and blood

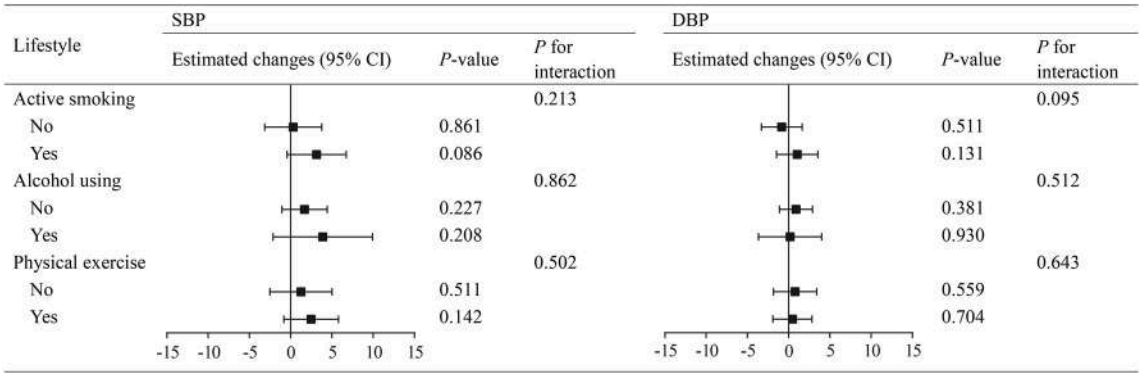

Fig. 2. The association between noise exposure and blood pressure in different lifestyle subgroups. Multiple linear regression model was adjusted for age, gender, BMI, alcohol drinking status, physical exercise, and antihypertensive medication use. The solid squares and horizontal error bars correspond to the unstandardized regression coefficient (β) and the 95% confidence intervals. Two-side *P*-values < 0.05 were considered as significant.

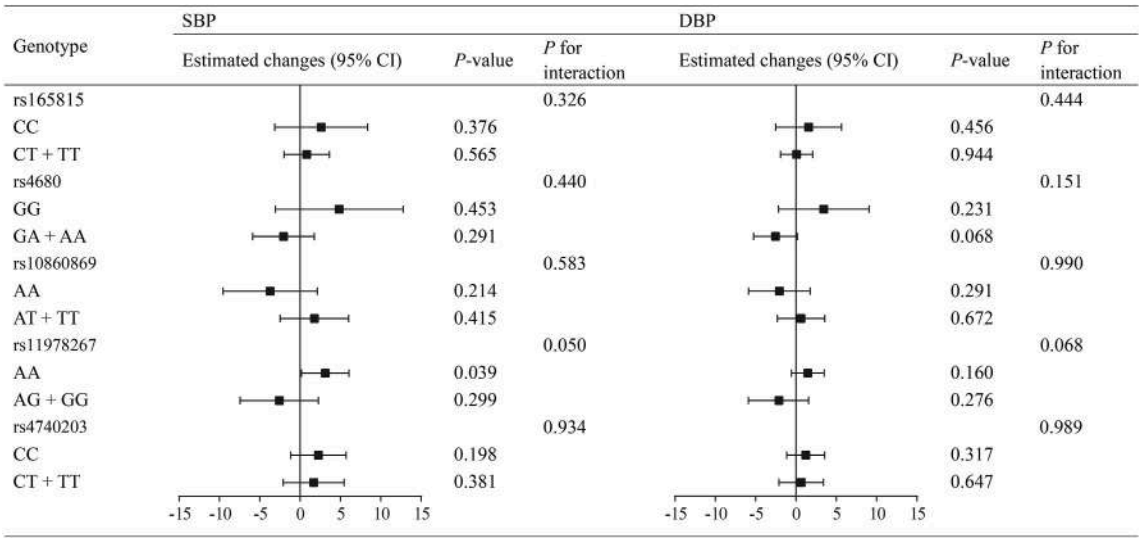

Fig. 3. The association between noise exposure and blood pressure in different SNP genotype subgroups. Multiple linear regression model was adjusted for age, gender, BMI, alcohol drinking status, physical exercise, and antihypertensive medication use. The solid squares and horizontal error bars correspond to the unstandardized regression coefficient (β) and the 95% confidence intervals. Two-side *P*-values < 0.05 were considered as significant.

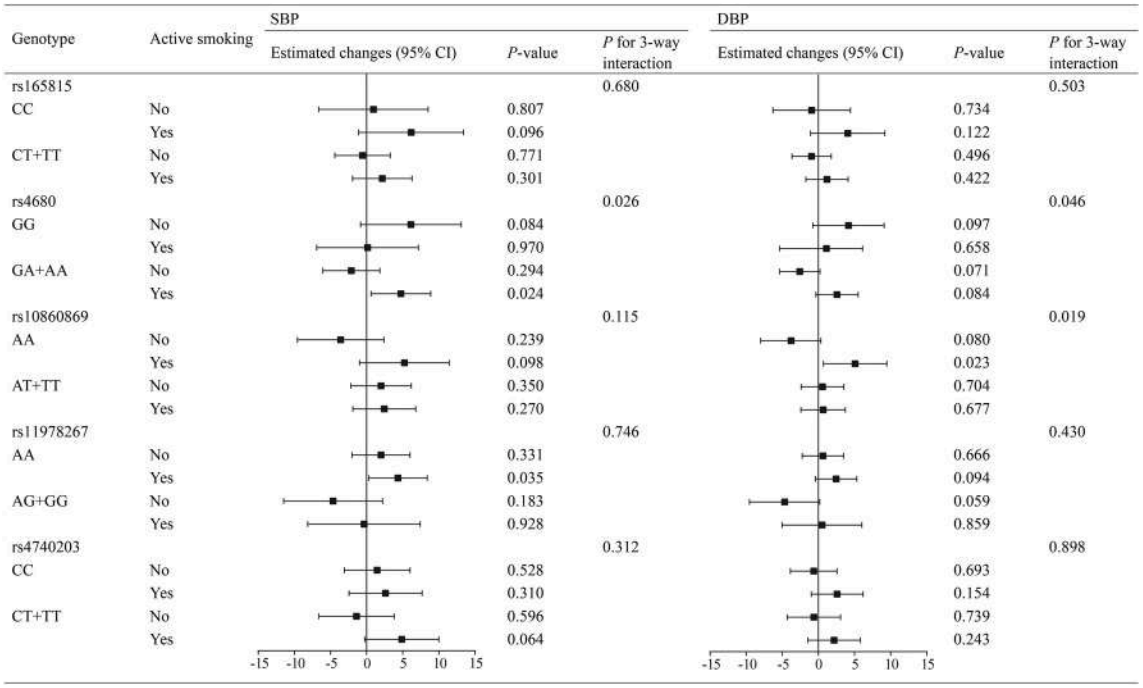

Fig. 4. Conditional effect of noise exposure on blood pressure at levels of smoking status and SNP genotypes. The moderated moderation model was adjusted for age, gender, BMI, alcohol drinking status, physical exercise, and antihypertensive medication use. The solid squares and horizontal error bars correspond to the unstandardized regression coefficient (β) and the 95% confidence intervals. Two-side *P*-values < 0.05 were considered as significant.

pressure was significantly different in SNP genotyping group (rs4680 in *COMT* and rs10860869 in *PAH*).

Occupational noise exposure has been reported to elevate the risk of CVD, for example, increasing blood pressure and altering electrocardiograph (Yang et al., 2018). However, in current study, we did not observe a significant association between noise exposure and SBP or DBP in study population. The inconsistent conclusion of noise-induced adverse effect may be due to the existence of confounding factors, especially concurrent exposure events (Babisch 2002). It is generally acknowledged that various risk factors promote the progression of CVD, such as environmental pollutants, genetic predisposition and unhealthy lifestyle (Cosselman et al., 2015; Yu et al., 2016). Previous studies determined that some of the mentioned factors might also facilitate noise-triggered stress, collectively exerting cardiovascular effect (Golmohammadi and Darvishi 2019). Identifying these factors might help unmask the contribution of noise exposure to blood pressure alteration.

The current study took lifestyle factors into consideration. By stratifying participants into different groups according to lifestyle factors, we observed a possibly statistically significant association between noise exposure and blood pressure among workers with smoking habit. It has been widely investigated on the health risk of occupational noise exposure on CVD, especially the increase of blood pressure. However, research involving both noise exposure and lifestyle factors is scarce. In a cross-sectional study including 6307 employed workers, a significant

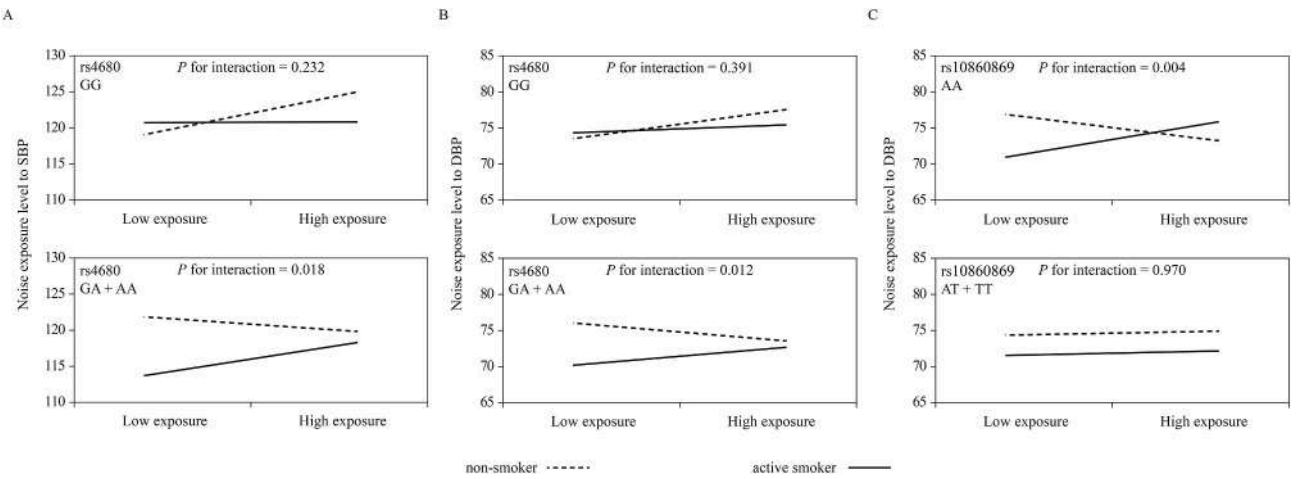

Fig. 5. The interaction of active smoking and noise exposure on blood pressure for *COMT* rs4680 genotype (A & B) and *PAH* rs10860869 genotype (C). The moderated moderation model was adjusted for age, gender, BMI, alcohol drinking status, physical exercise, and antihypertensive medication use. Simple slope represents the linear relationship of noise exposure on blood pressure with active smoking habit (solid line) or without active smoking habit (dashed line).

association between self-reported occupational noise exposure and coronary heart disease was demonstrated among current smokers (Gan et al., 2011). The tobacco toxins, mainly nicotine contents, are known to stimulate sympathetic nervous system, leading to vasoconstriction and increased cardiac output (Omvik 1996). High noise level also causes sympathetic activation and adrenaline secretion, leading to vascular oxidative stress (Babisch 2002; Hahad et al., 2019). Previous studies focused on the synergistic effects of noise and tobacco exposure, suggesting that both share common pathway leading to pathophysiological consequence, via vascular reactive oxygen species production and endothelial dysfunction (Ahn et al., 2011; Ferrite et al., 2013; Munzel et al., 2020). With regard to hematological parameters, prior research recruiting 50 male workers from a food manufacturing plant demonstrated elevated red blood cells count under simultaneous exposure to noise and smoking, indicating increased blood viscosity, which contribute to the development of hypertension (Alimohammadi and Danesh, 2014; Raine 1988). These findings support that smoking and noise contribute collectively to elevated risk of cardiovascular events. For those frequently exposed to occupational noise, it is necessary to reduce tobacco use to avoid exacerbating noise-induced adverse cardiovascular effect.

In addition to behavior factors, genetic variation is also regarded as essential risk factors for CVD. Considering activation of both sympathetic nervous system and neuroendocrine system induced by noise was proposed to make notable contribution to adverse cardiovascular effect of noise exposure. It is reasonable to conjecture that secretion of stress hormone triggered by noise potentially served as a pathway leading blood pressure alteration, and that genetic background with regard to stress hormone may be determined as a risk factor. By investigating the genetic variation related to stress hormone production, we observed a significant trend in positive association between noise exposure level and DBP for *COMT* rs4680 GA+AA, which means workers suffered from high noise exposure tend to exhibit higher levels of DBP for A allele carriers. COMT is an enzyme participating in the degradation of catecholamines, including dopamine, epinephrine, and norepinephrine, all of which are essential to cardiovascular control (Mannisto and Kaakkola 1999). The Val allele (G) of *COMT* rs4680 exhibits increased enzymatic activity of COMT compared to Met allele (A), leading to higher degradation of dopamine (Chen et al., 2004). The role of *COMT* and its polymorphism in regulation of blood pressure has been studied. Higher level of blood pressure in those with Met allele has been demonstrated among middle-aged Japanese and Swedish men (Annerbrink et al., 2008; Htun et al., 2011). The COMT inhibitor, entacapone, increased SBP and DBP in patients with multiple system atrophy (Jordan et al., 2002). It is suggested that reduced COMT activity resulted in peripheral dopamine elevation, leading to increased blood pressure (Ge et al., 2015).

We wanted to further test whether genetic variation would alter the moderation effect of smoking on association between noise exposure and blood pressure. The moderated moderation analysis showed that active smoking positively moderated the association between noise exposure and SBP or DBP for *COMT* rs4680 Met (A) allele carriers, who suffered from relatively blunted COMT activity. Prior studies focused on the gene-environment interaction effect of *COMT*, reporting that those who carried Met allele showed higher sensitivity to stress (Collip et al., 2011; He et al., 2012). In panic disorder patients, *COMT* rs4680 Met allele is reported to be associated with enhanced sympathetic activity (Kang et al., 2010). It is possible that this group of people have higher level of catecholamines and sympathetic activity, which contribute to increased reactivity to noise and tobacco exposure. To our knowledge, this is the first study to investigate the modifying effect of variants in gene related to stress hormone production on noise-induced cardiovascular effect. Future studies should include more polymorphines in genes involved in related biological pathways to identify genetic determinants in noise-impaired blood pressure regulation. The mechanism of combination effect of genotype, tobacco and noise exposure exerting on blood pressure regulation may be better clarified by in vivo experimental studies.

The current study has several limitations. Firstly, the study participants are workers with different length of service: from 5 to 42 years. Since we detected a high correlation between age and length of service ($r = 0.955$, $P < 0.001$), to avoid collinearity problem, we did not adjust length of service in the models. However, a previous study reported elevated SBP and DBP, together with altered electrocardiograph, particularly among factory workers who were exposed to noise over 10 years compared to control groups (Sancini et al., 2014). It is suggested that noise exposure exerts different effect, depending on exposure intensity and length (Lang et al., 1992; Sancini et al., 2014). Future studies investigating the adverse effect of noise exposure on cardiovascular health should take length of service into consideration. Secondly, we applied moderated moderation analysis to estimate the association between noise exposure and blood pressure regarding genetic background and lifestyle. The estimation error is more likely to occur due to the limited sample size. Future studies should include a larger population to further validate the hypothesis. Thirdly, many results of this study only reached marginal significance. Though similar tendency was detected by other studies, the results of this exploratory study still was interpreted with caution. Finally, workers recruited in this study were from a

tobacco factory, where other exposure events, such as tobacco dust, secondhand smoking and unhealthy diet habits, are also worth noting. The concentrations of tobacco dust were measured for future analysis concerning simultaneous exposure to noise and tobacco dust. To precisely evaluate secondhand smoke exposure, the determination of urinary nicotine and metabolites is requisite, rather than traditional questionnaire survey. Meanwhile, the detection of genetic background to reveal hypertension disposition of this population is also essential, which should be included in our future analysis.

5. Conclusions

The current study identified a suggestive association between occupational noise exposure and SBP among active smokers. Genetic variation relating to stress hormone production possibly modified the association between noise exposure and blood pressure. For *COMT* rs4680 A allele carriers, active smoking may modify the association between noise exposure and blood pressure elevation. Our study suggests that workers in noisy working environment should prevent cigarette smoking to mitigate noise-induced CVD risk. Future studies should make efforts to identify related genetic determinants and to protect high-risk population. In the field of occupational health surveillance, it is essential that genetic susceptibility be screened and that healthy lifestyle be advocated.

Declaration of competing interest

The authors declare no competing financial interests.

Acknowledgements

This study was supported by research funds from the National Natural Science Foundation of China [grant number 81703203]; Hubei Province Health and Family Planning Scientific Research Project [grant number WJ2017M203, WJ2018H0101]; Health Commission of Hubei Province Scientific Research Project [grant number WJ2019M025] and the Wuhan Municipal Health and Family Planning Scientific Research Project [grant number WG16B08]. The authors are grateful to all volunteers who participated in this study.

Appendix A. Supplementary data

Supplementary data to this article can be found online at https://doi.org/10.1016/j.ijheh.2021.113868.

References

Ahn, J.H., Joo, H.S., Suh, J.K., Kim, H., So, H.S., Chung, J.W., 2011. Effects of cigarette smoking on hearing recovery from noise-induced temporary hearing threshold shifts in mice. Otol. Neurotol. 32 (6), 926–932.

Akther, J., Das, A., Rahman, M.A., Saha, S.K., Hosen, M.I., Ebihara, A., Nakagawa, T., Suzuki, F., Nabi, A., 2021. Non-coding single nucleotide variants of renin and the (pro)renin receptor are associated with polygenic diseases in a bangladeshi population. Biochem. Genet. 59 (5), 1116–1145.

Alimohammadi, I., Danesh, F.J., 2014. Combined effect of workplace noise and smoking on some hematological parameters on workers in a food manufacturing plant. Iran J. Health Saf. Environ. 1 (4), 151–158.

Annerbrink, K., Westberg, L., Nilsson, S., Rosmond, R., Holm, G., Eriksson, E., 2008. Catechol o-methyltransferase val158-met polymorphism is associated with abdominal obesity and blood pressure in men. Metabolism 57 (5), 708–711.

Babisch, W., 2002. The noise/stress concept, risk assessment and research needs. Noise Health 4 (16), 1–11.

Babisch, W., 2003. Stress hormones in the research on cardiovascular effects of noise. Noise Health 5 (18), 1–11.

Babisch, W., Fromme, H., Beyer, A., Ising, H., 2001. Increased catecholamine levels in urine in subjects exposed to road traffic noise: the role of stress hormones in noise research. Environ. Int. 26 (7–8), 475–481.

Basner, M., Babisch, W., Davis, A., Brink, M., Clark, C., Janssen, S., Stansfeld, S., 2014. Auditory and non-auditory effects of noise on health. Lancet 383 (9925), 1325–1332.

Burrello, J., Monticone, S., Buffolo, F., Tetti, M., Veglio, F., Williams, T.A., Mulatero, P., 2017. Is there a role for genomics in the management of hypertension? Int. J. Mol. Sci. 18 (6).

Chalmers, J., MacMahon, S., Mancia, G., Whitworth, J., Beilin, L., Hansson, L., Neal, B., Rodgers, A., Ni, C.M., Clark, T.J.C., et al., 1999. 1999 world health organization-international society of hypertension guidelines for the management of hypertension. guidelines sub-committee of the world health organization, 21 (5–6), 1009–1060.

Chen, J., Lipska, B.K., Halim, N., Ma, Q.D., Matsumoto, M., Melhem, S., Kolachana, B.S., Hyde, T.M., Herman, M.M., Apud, J., et al., 2004. Functional analysis of genetic variation in catechol-o-methyltransferase (comt): effects on mrna, protein, and enzyme activity in postmortem human brain. Am. J. Hum. Genet. 75 (5), 807–821.

Collip, D., van Winkel, R., Peerbooms, O., Lataster, T., Thewissen, V., Lardinois, M., Drukker, M., Rutten, B.P., Van Os, J., Myin-Germeys, I., 2011. Comt val158met-stress interaction in psychosis: role of background psychosis risk. CNS Neurosci. Ther. 17 (6), 612–619.

Cosselman, K.E., Navas-Acien, A., Kaufman, J.D., 2015. Environmental factors in cardiovascular disease. Nat. Rev. Cardiol. 12 (11), 627–642.

Dawson, J.F., Richter, A.W., 2006. Probing three-way interactions in moderated multiple regression: development and application of a slope difference test. J. Appl. Psychol. 91 (4), 917–926.

Ferrite, S., Santana, V.S., Marshall, S.W., 2013. Interaction between noise and cigarette smoking for the outcome of hearing loss among women: a population-based study. Am. J. Ind. Med. 56 (10), 1213–1220.

Gan, W.Q., Davies, H.W., Demers, P.A., 2011. Exposure to occupational noise and cardiovascular disease in the United States: the national health and nutrition examination survey 1999-2004. Occup. Environ. Med. 68 (3), 183–190.

GBZ2.2-, 2007. Occupational Exposure Limits for Hazardous Factors in the Workplace Part 2: Physical Factors.

Ge, L., Wu, H.Y., Pan, S.L., Huang, L., Sun, P., Liang, Q.H., Pang, G.F., Lv, Z.P., Hu, C.Y., Liu, C.W., et al., 2015. Comt val158met polymorphism is associated with blood pressure and lipid levels in general families of bama longevous area in China. Int. J. Clin. Exp. Pathol. 8 (11), 15055–15064.

Golmohammadi, R., Darvishi, E., 2019. The combined effects of occupational exposure to noise and other risk factors - a systematic review. Noise Health 21 (101), 125–141.

Hahad, O., Kroller-Schon, S., Daiber, A., Munzel, T., 2019. The cardiovascular effects of noise. Dtsch Arztebl Int 116 (14), 245–250.

Hayes, A.F., 2012. Process: A Versatile Computational Tool for Observed Variable Mediation, Moderation, and Conditional Process Modeling. University of Kansas, KS.

Hayes, A.F., 2017. Introduction to Mediation, Moderation, and Conditional Process Analysis: A Regression-Based Approach. Guilford publications.

Hayes, A.F., Rockwood, N.J., 2017. Regression-based statistical mediation and moderation analysis in clinical research: observations, recommendations, and implementation. Behav. Res. Ther. 98, 39–57.

He, Q., Xue, G., Chen, C., Lu, Z.L., Chen, C., Lei, X., Liu, Y., Li, J., Zhu, B., Moyzis, R.K., et al., 2012. Comt val158met polymorphism interacts with stressful life events and parental warmth to influence decision making. Sci. Rep. 2, 677.

Htun, N.C., Miyaki, K., Song, Y., Ikeda, S., Shimbo, T., Muramatsu, M., 2011. Association of the catechol-o-methyl transferase gene val158met polymorphism with blood pressure and prevalence of hypertension: interaction with dietary energy intake. Am. J. Hypertens. 24 (9), 1022–1026.

Joint Task Force for Guideline on the A, Management of Cardiovascular Risk in C, 2019. [guideline on the assessment and management of cardiovascular risk in China]. Zhonghua Yufang Yixue Zazhi 53 (1), 13–35.

Jordan, J., Lipp, A., Tank, J., Schroder, C., Stoffels, M., Franke, G., Diedrich, A., Arnold, G., Goldstein, D.S., Sharma, A.M., et al., 2002. Catechol-o-methyltransferase and blood pressure in humans. Circulation 106 (4), 460–465.

Kang, E.H., Song, Y.J., Kim, K.J., Shim, H.B., Park, J.E., Yu, B.H., 2010. Sympathetic nervous function and the effect of the catechol-o-methyltransferase val(158)met polymorphism in patients with panic disorder. J. Affect. Disord. 123 (1–3), 337–340.

Kurland, L., Liljedahl, U., Lind, L., 2005. Hypertension and snp genotyping in antihypertensive treatment. Cardiovasc. Toxicol. 5 (2), 133–142.

Lang, T., Fouriaud, C., Jacquinet-Salord, M.C., 1992. Length of occupational noise exposure and blood pressure. Int. Arch. Occup. Environ. Health 63 (6), 369–372.

Laonigro, I., Correale, M., Di Biase, M., Altomare, E., 2009. Alcohol abuse and heart failure. Eur. J. Heart Fail. 11 (5), 453–462.

Mannisto, P.T., Kaakkola, S., 1999. Catechol-o-methyltransferase (comt): biochemistry, molecular biology, pharmacology, and clinical efficacy of the new selective comt inhibitors. Pharmacol. Rev. 51 (4), 593–628.

Munzel, T., Miller, M.R., Sorensen, M., Lelieveld, J., Daiber, A., Rajagopalan, S., 2020. Reduction of environmental pollutants for prevention of cardiovascular disease: it's time to act. Eur. Heart J. 41 (41), 3989–3997.

Oliveira, C.R., Arenas, G.W., 2012. Occupational exposure to noise pollution in anesthesiology. Rev. Bras. Anestesiol. 62 (2), 253–261.

Omvik, P., 1996. How smoking affects blood pressure. Blood Pres. 5 (2), 71–77.

Padmanabhan, S., Dominiczak, A.F., 2021. Genomics of hypertension: the road to precision medicine. Nat. Rev. Cardiol. 18 (4), 235–250.

Passchier, W., Knottnerus, A., Albering, H., Walda, I., 2000. Public health impact of large airports. Rev. Environ. Health 15 (1–2), 83–96.

Raine, A.E., 1988. Hypertension, blood viscosity, and cardiovascular morbidity in renal failure: implications of erythropoietin therapy. Lancet 1 (8577), 97–100.

Sancini, A., Caciari, T., Rosati, M.V., Samperi, I., Iannattone, G., Massimi, R., Loreti, B., Scala, B., Sacco, C., Tomei, F., et al., 2014. Can noise cause high blood pressure? Occupational risk in paper industry. Clin. Ter. 165 (4), e304–311.

Schmidt, F.P., Basner, M., Kroger, G., Weck, S., Schnorbus, B., Muttray, A., Sariyar, M., Binder, H., Gori, T., Warnholtz, A., et al., 2013. Effect of nighttime aircraft noise

exposure on endothelial function and stress hormone release in healthy adults. Eur. Heart J. 34 (45), 3508–3514a.
Talbott, E., Helmkamp, J., Matthews, K., Kuller, L., Cottington, E., Redmond, G., 1985. Occupational noise exposure, noise-induced hearing loss, and the epidemiology of high blood pressure. Am. J. Epidemiol. 121 (4), 501–514.
Teixeira, L.R., Azevedo, T.M., Bortkiewicz, A., Correa da Silva, D.T., de Abreu, W., de Almeida, M.S., de Araujo, M.A.N., Gadzicka, E., Ivanov, I.D., Leppink, N., et al., 2019. Who/ilo work-related burden of disease and injury: protocol for systematic reviews of exposure to occupational noise and of the effect of exposure to occupational noise on cardiovascular disease. Environ. Int. 125, 567–578.
Tomei, F., Fantini, S., Tomao, E., Baccolo, T.P., Rosati, M.V., 2000. Hypertension and chronic exposure to noise. Arch. Environ. Health 55 (5), 319–325.
van Kempen, E.E., Kruize, H., Boshuizen, H.C., Ameling, C.B., Staatsen, B.A., de Hollander, A.E., 2002. The association between noise exposure and blood pressure and ischemic heart disease: a meta-analysis. Environ. Health Perspect. 110 (3), 307–317.
Virdis, A., Giannarelli, C., Neves, M.F., Taddei, S., Ghiadoni, L., 2010. Cigarette smoking and hypertension. Curr. Pharmaceut. Des. 16 (23), 2518–2525.
Wang, D., Xiao, Y., Feng, X., Wang, B., Li, W., He, M., Zhang, X., Yuan, J., Yi, G., Chen, Z., et al., 2021. Association of occupational noise exposure, bilateral hearing loss with atherosclerotic cardiovascular disease risk in Chinese adults. Int. J. Hyg Environ. Health 235, 113776.
Yang, L., Zhou, Y., Sun, H., Lai, H., Liu, C., Yan, K., Yuan, J., Wu, T., Chen, W., Zhang, X., 2014. Dose-response relationship between polycyclic aromatic hydrocarbon metabolites and risk of diabetes in the general Chinese population. Environ. Pollut. 195, 24–30.
Yang, Y., Zhang, E., Zhang, J., Chen, S., Yu, G., Liu, X., Peng, C., Lavin, M.F., Du, Z., Shao, H., 2018. Relationship between occupational noise exposure and the risk factors of cardiovascular disease in China: a meta-analysis. Medicine (Baltim.) 97 (30), e11720.
Yu, E., Rimm, E., Qi, L., Rexrode, K., Albert, C.M., Sun, Q., Willett, W.C., Hu, F.B., Manson, J.E., 2016. Diet, lifestyle, biomarkers, genetic factors, and risk of cardiovascular disease in the nurses' health studies. Am. J. Publ. Health 106 (9), 1616–1623.

International Journal of Hygiene and Environmental Health 239 (2022) 113878

Contents lists available at ScienceDirect

International Journal of Hygiene and Environmental Health

journal homepage: www.elsevier.com/locate/ijheh

The mediating role of vascular inflammation in traffic-related air pollution associated changes in insulin resistance in healthy adults

Hongbing Xu [a,i,1], Shengcong Liu [b,i,1], Yang Wang [c,1], Rongshan Wu [a,d], Tieci Yi [b,i], Tong Wang [a,i], Yutong Zhu [a,i], Jiakun Fang [a,i], Yunfei Xie [a,i], Qian Zhao [a,i], Xiaoming Song [a,i], Jie Chen [a,e], Sanjay Rajagopaplan [f], Robert D. Brook [g], Jianping Li [b,i], Junji Cao [h,**], Wei Huang [a,i,*]

[a] Department of Occupational and Environmental Health Sciences, Peking University School of Public Health, And Peking University Institute of Environmental Medicine, Beijing, China
[b] Division of Cardiology, Peking University First Hospital, Beijing, China
[c] Department of Prevention and Health Care, Hospital of Health Science Center, Peking University, Beijing, China
[d] State Key Laboratory of Environmental Criteria and Risk Assessment, State Environmental Protection Key Laboratory of Ecological Effect and Risk Assessment of Chemicals, Chinese Research Academy of Environmental Sciences, Beijing, China
[e] Institute for Risk Assessment Sciences, University Medical Centre Utrecht, University of Utrecht, the Netherlands
[f] Division of Cardiovascular Medicine, Case Western Reserve University, Ohio, USA
[g] Division of Cardiovascular Medicine, University of Michigan, Michigan, USA
[h] Institute of Atmospheric Physics Chinese Academy of Sciences, Beijing, China
[i] Key Laboratory of Molecular Cardiovascular Sciences of the Ministry of Education, Beijing, China

ARTICLE INFO

Keywords:
Traffic-related air pollution
Insulin resistance
Vascular inflammation
Biomarkers

ABSTRACT

Aim: The precise pathophysiologic pathway linking traffic-related air pollution (TRAP) to diabetes mellitus is not well elucidated. We aimed to investigate whether activation of vascular inflammation can be a mechanistic linkage between ambient TRAP and insulin resistance.

Methods: Study outcomes were determined by assessing a series of circulating biomarkers indicative of insulin resistance and vascular inflammation among 73 healthy adults who underwent repeated clinical visits in Beijing, China, 2014–2016. Concomitantly, concentrations of ambient TRAP indices, including particulate matter in diameter <2.5 μm ($PM_{2.5}$), particles in size fractions of 5–560 nm, black carbon, carbon monoxide, nitrogen dioxide, and oxides of nitrogen, were continuously monitored.

Results: Participants experienced extremely high levels of TRAP exposures, with mean (standard deviation) $PM_{2.5}$ concentrations of 91.8 (48.3) $\mu g/m^3$, throughout the study. We found that interquartile range increases in exposure to moving average concentrations of various TRAP indices at prior up to 7 days were associated with significant elevations of 8.9–49.6% in insulin levels. Higher pollutant levels were also related to worsening metrics of insulin resistance (soluble insulin receptor ectodomain, adipokines, and homeostasis model assessment of insulin resistance) and heightened vascular inflammatory responses, particularly disruptions of the receptor activator of nuclear factor κB ligand/osteoprotegerin system balance and elevations of monocyte/macrophage and T cell activation markers. Mediation analyses showed that activation of vascular inflammation could explain up to 66% of the alterations in metrics of insulin resistance attributable to air pollution.

Conclusion: Our results suggest that ambient traffic pollution exposure was capable of promoting insulin resistance possibly via generating vascular inflammation.

* Corresponding author. Department of Occupational and Environmental Health, Peking University School of Public Health, No. 38 Xueyuan Rd, Haidian District, Beijing, 100191, China.
** Corresponding author. Institute of Atmospheric Physics Chinese Academy of Sciences, No. 40 Huayanli, Beichen West Road, Chaoyang District, Beijing, 100029, China.
E-mail addresses: jjcao@mail.iap.ac.cn (J. Cao), whuang@bjmu.edu.cn (W. Huang).
[1] These authors are equally contributing to this work.

https://doi.org/10.1016/j.ijheh.2021.113878
Received 10 June 2021; Received in revised form 22 October 2021; Accepted 25 October 2021
Available online 30 October 2021

1. Introduction

Anthropogenic air pollution, consisting of a mixture of particulate matter (PM) and gaseous air pollution from various fossil fuel combustion sources, poses an enormous risk to global public health (Al-Kindi et al., 2020). More recently, traffic-related air pollution (TRAP), a crucial source of environmental exposure in urban areas, has become of significant health concerns due to their toxic properties that can potentiate various cardiometabolic disorders such as diabetes mellitus (DM) (Al-Kindi et al., 2020). Indeed, numerous studies support the linkages between ambient TRAP and clinically overt DM and diabetes-related mortality (Bowe et al., 2018). Population studies have shown that TRAP exposures over a few days are capable of prompting insulin resistance, which is fundamentally implicated in the pathogenesis of DM (Rao et al., 2015). Despite extensive investigations, it remains poorly understood the impacts of air pollution mixtures, particularly TRAP, on the progression of DM.

To date, the immunological and inflammatory dysfunctions in the vasculature that have been hypothesized in association with air pollution might heighten inflammatory state in various insulin-sensitive tissues (e.g., liver), thereby worsening insulin resistance systemically (Rao et al., 2015). Emerging evidence has shown that disrupting the balance of receptor activator of nuclear factor κB (NF-κB) ligand (RANKL)/osteoprotegerin (OPG) system-induced NF-κB signaling activation plays a crucial role in the etiology of insulin resistance (Cai et al., 2005; Catrysse and van Loo, 2017; Walsh and Choi, 2014). As a potent stimulator of NF-κB, binding of RANKL to its receptor (RANK) is capable of activating NF-κB and downstream inflammatory cascades, as well as amplifying inflammatory responses via interactions with immune cells (e.g., T cells and macrophages) (Walsh and Choi, 2014). The biological actions of RANKL can be directly inhibited by its soluble decoy receptor OPG, and the RANKL/OPG system imbalance is closely linked to an array of metabolic disorders, including insulin resistance, DM, and diabetic vascular complications (Pieralice et al., 2018). Under normal conditions, NF-κB is maintained inactive status by the inhibitory subunit IκB, whereas phosphorylation of IκB by IκB kinases (IKKs) promotes NF-κB translocation into the nucleus and consequently up-regulates transcription of genes relevant to encoding inflammatory mediators (Barnabei et al., 2021). Studies in animals indicated that blockade of the RANKL signaling significantly suppressed phosphorylation of IKKs, decreased production of inflammatory cytokines, and improved insulin sensitivity in liver and skeletal muscle (Bonnet et al., 2019; Kiechl et al., 2013). Thus far, an increasing number of experimental studies suggested that exposure to concentrated ambient PM may cause insulin resistance via activation of NF-κB pathways-mediated vascular inflammation in mice (Haberzettl et al., 2016; Zheng et al., 2013). Further, central inhibition of IKKβ could exert potent protection against insulin resistance and inflammation caused by ambient PM collected from urban environments (Liu et al., 2014). Also, exposure to air pollution has shown to trigger the RANKL/OPG system imbalance, along with elevated levels of inflammatory indicators in human (Saha et al., 2016; Wang et al., 2021; Yamawaki and Iwai, 2006) Nevertheless, it remains unclear whether the changes in balance of RANKL/OPG system and its individual components posed by air pollution inhalation may potentiate vascular inflammatory responses, and thereby prompt the genesis of insulin resistance that could occur before developing clinically overt DM.

In this context, here we hypothesized that recent air pollution exposure during the prior days would worsen insulin resistance, potentially due to activation of vascular inflammation. We first assessed the impacts of a variety of ambient pollutants, particularly TRAP indices, on biomarkers indicative of insulin resistance and various metrics of immune and inflammatory biomarkers. We further evaluated to which extent the alterations in metrics of insulin resistance could be explained by air pollution-associated heightened vascular inflammatory responses, focusing on the mediating role of the RANKL/OPG system.

Abbreviations

DM	diabetes mellitus
OPG	osteoprotegerin
sRANKL	soluble receptor activator of nuclear factor-κB ligand;
sIRα	soluble insulin receptor ectodomain
HOMA-IR	homeostasis model assessment of insulin resistance
BTC	betacellulin
CNTF	ciliary neurotrophic factor
HGF	hepatocyte growth factor
IL	interleukin
sIL1RA	soluble IL-1 receptor antagonist
CCL	C–C chemokine ligand;
CXCL-8	C-X-C chemokine motif ligand-8
sCD163	soluble CD163
$PM_{2.5}$	particulate matter in diameter <2.5 μm
PNC	particulate number concentration
PSC	particulate surface area concentration
BC	black carbon
CO	carbon monoxide
NO_2	nitrogen dioxide
NO_X	oxides of nitrogen

2. Subjects and methods

2.1. Study participants

The Beijing AIRCHD study (Air Pollution and Cardiovascular Dysfunctions in Healthy Adults Living in Beijing) was a prospective follow-up of 73 non-smoking healthy adults with repeated measurements (the baseline examination and subsequent 4 clinical visits) in 2014–2016. Detailed design and selection criteria of this project have been described previously (Xu et al., 2019). Briefly, participants with pre-existing cardiometabolic disorders (e.g., pre-diabetes, diabetes, and hypertension) or taking any medications (e.g., glucose/blood pressure-lowering medication, and antioxidant) were excluded from enrollment. The baseline examination was performed in November 1, 2014, to November 5, 2014, and 4 rounds of follow-ups with 3–4 months apart were conducted in November 24, 2014, to January 8, 2014 (visit 1), April 22, 2015, to June 1, 2015 (visit 2), September 20, 2015, to November 9, 2015 (visit 3), and December 27, 2015, to January 18, 2016 (visit 4), respectively. All participants were scheduled to undergo clinical examinations during weekdays, and blood and urine samples, participants' information on demographic characteristics, smoking status, medical history, and residential address were collected following standardized protocols. All participants provided written informed consent, and the Institutional Review Board of Peking University Health Science Center (PKUHSC) approved the study.

2.2. Biomarker assessment

Serum samples were taken between 8 a.m. and 10 a.m. after an overnight fasting and stored at −80 °C upon collection. Multiplex bead-based flow cytometry assays were used to simultaneously detect biomarkers implicating in the insulin signaling pathways (insulin, adiponectin, leptin, resistin, betacellulin [BTC], ciliary neurotrophic factor [CNTF], and hepatocyte growth factor [HGF]), and indicators relevant to vascular inflammation including OPG, soluble RANKL (sRANKL), T-cell/interleukin-1 (IL-1) family-related indicators (IL-2, 10, 22, and soluble IL-1 receptor antagonist [sIL1RA]), and monocyte/macrophage activation indicators (C–C chemokine ligand-2 [CCL-2], CCL-5, C-X-C chemokine motif ligand-8 [CXCL-8], soluble CD163 [sCD163]). Serum

concentrations of soluble insulin receptor ectodomain (sIRα) were determined by an enzyme-linked immunosorbent assay (ELISA) approach (BioVendor, Brno, Czech Republic). The ratio between sRANKL and OPG (sRANKL/OPG ratio) was calculated reflecting the overall biological activity and balance of the RANKL/OPG system (Ndip et al., 2014). Elevated sRANKL/OPG ratio may also reflect an insufficient compensatory self-defensive mechanism against immune inflammation (Gümüş et al., 2013; Hofbauer and Schoppet, 2001). Further, blood glucose was measured, and the homeostasis model assessment of insulin resistance (HOMA-IR) was calculated using the formula of (insulin [μU/mL] × glucose [mmol/L]/22.5) (Dang et al., 2018). In this study, we evaluated insulin resistance status using multiple metrics of circulating indicators, including insulin, adiponectin, leptin, resistin, BTC, CNTF, HGF, sIRα, and HOMA-IR, because worsening of these indicators has shown associations with developing metabolic insulin resistance and DM (Funcke and Scherer, 2019; Hiriart et al., 2014; Oliveira et al., 2018; Rezende et al., 2012). Detailed information on the biological action for each measured biomarker was summarized in Supplementary Table 1. Given that potential environmental tobacco smoking exposure and stress response of human body might affect the ability to capture cardiometabolic effects attributable to air pollution exposure (Śliwińska-Mossoń and Milnerowicz, 2017), spot urine samples were analyzed for urinary concentrations of cotinine (IMMUNAL YSIS, Pomona, CA) and cortisol (LIUHEBIO, Wuhan, China) using ELISA approaches for further analyses.

2.3. Ambient air pollution and meteorology assessment

Hourly measures of PM in diameter <2.5 μm ($PM_{2.5}$), temperature and relative humidity, minute-to-minute measures of black carbon (BC), carbon monoxide (CO), nitrogen dioxide (NO_2), and oxides of nitrogen (NO_X), as well as 5-min number and surface area concentrations of particles with sizes of 5–560 nm were monitored continuously throughout the study. To assess the health impacts of size-fractioned particles, particle number concentrations (PNCs) and particle surface area concentrations (PSCs) were grouped into 5–100 nm and 100–560 nm for further analysis, respectively (Hennig et al., 2018). All environmental factors were measured at a fixed monitoring station, which was located within 1 km in distance to the vast majority (93%) of study participants. Previous studies have shown that air pollution-associated insulin resistance could likely occur within several days of exposure (Rajagopalan et al., 2018). Thus, 1- to 7-day moving average (MA) concentrations of air pollutants before each participant's clinic visit were calculated as exposure metrics, including pollutant-specific averaged levels over the last 24 h (MA day 1 [1 MA day]), 1–2 days (2 MA days), and so on up to 7 MA days. Daily averages of all environmental factors were computed from 9 a.m. to 9 a.m. the next day because blood samples were obtained from participants at approximately 9 a.m. during the study period.

2.4. Statistical analysis

Summary statistics were computed for all measurements of study outcomes and environmental exposures, including means (standard deviation), medians (range), and interquartile range (IQR). Spearman correlations between pollutants were performed.

Linear mixed-effects (LME) models were conducted to characterize associations between ambient air pollutants and outcome measures. Outcome variables with skewed distributions were log-transformed for further analysis. A backward stepwise model selection procedure was operated to discern the key covariates for each outcome measure, including age, sex, body mass index, waist-to-hip ratio, day of week of clinical visit, month of blood withdrawal, creatinine-corrected urinary cotinine and cortisol. To control potential impacts of meteorological parameters, 24-h averages (1 MA day) of temperature and relative humidity were included in all LME models using natural splines with degrees of freedom (≤3) based on the minimizing Akaike's Information Criterion. Seasonality was explained by adding sine and cosine terms of calendar dates of blood withdrawal. The identified covariates in final LME models are summarized in Supplementary Table 2.

In exploratory analyses, we firstly performed mediation analyses with a single mediator to examine the potential mechanisms responsible for insulin resistance attributable to air pollution, focusing on activation of vascular inflammation (Xu et al., 2019). We also assessed the mediating roles of the RANKL/OPG system in pollutant-associated heightened immune inflammatory responses. Further, considering significant correlations observed among measured study biomarkers (Supplementary Table 3), multiple-mediator models were further developed by including all potential mediators with statistical significance (p-value <0.05) in the single-mediator model (VanderWeele and Vansteelandt, 2014; Xu et al., 2019). Moreover, two-pollutant models were performed to assess if single-pollutant effects could be confounded by co-exposure ambient pollutants (Supplementary Table 4). To reduce potential collinearity, two-pollutant models were only fitted in this study when the correlation coefficient of pairwise pollutants was <0.60 (Rückerl et al., 2016). Lastly, several sensitivity analyses were conducted by: (1) excluding individuals with urinary cortisol levels >75th percentile (2.2 ng/mg Cr) to assess whether the observed associations could be partially affected by the stress response of human body; (2) excluding individuals that had urinary levels of cotinine >150 ng/mg Cr to reduce the potential impact of environmental tobacco smoking exposure (Riboli et al., 1995); (3) restricting the analysis to those who lived within 1 km from the ambient air monitoring station.

All estimates are presented as percent changes with 95% confidence intervals (CIs) associated with IQR increases in air pollutant concentrations. Statistical significance was determined at p-value <0.05. To control for potential type I error rate, we considered a p-value <0.0025 (0.05/20) as significant after a Bonferroni correction for multiple comparisons among outcome variables. All analyses were conducted using R, version 3.4.3 with "nlme" (Pinheiro et al., 2021) and "mediation" packages (Tingley et al., 2014) (R Project for Statistical Computing).

3. Results

3.1. Participant characteristics and air pollution exposure

Descriptive characteristics of study participants, outcome measurements, and environmental factors are summarized in Table 1 and Supplementary Table 5. As expected, large day-to-day variations in TRAP concentrations were found across the entire study period, which were reflected by large IQRs and wide ranges for measured pollutants. For instance, the mean 7 MA days of BC and NO_X exposures were 5.9 $\mu g/m^3$ and 124.8 $\mu g/m^3$, respectively.

3.2. Association between air pollution and the metrics of insulin resistance

Based on LME models, the adjusted changes in multiple metrics of insulin resistance in relation to air pollutants are shown in Fig. 1. We found increases in circulating insulin of 8.9% (95% CI, 0.4–17.3) to 49.6% (95% CI, 20.2–79.1) associated with IQR increases in most air pollutants (except for $PSC_{100\text{-}560}$). For soluble form of the receptor for insulin, significant reductions of sIRα levels were observed in association with a variety of air pollutants (Fig. 1). Among the examined exposure periods, the largest reductions in sIRα levels, ranging from 8.9% (95% CI, −17.7 to −0.1) to 13.8% (95% CI, −21.4 to −6.2), were associated with IQR increases in $PM_{2.5}$, BC and CO at prior 5 MA days. Additionally, positive associations of HOMA-IR, adiponectin, and leptin with air pollutants were found at prior 1–7 MA days, but inverse associations were found for resistin (Figs. 1 and 2). For growth factors, significant reductions of CNTF levels were associated with air pollutants, with estimate effects ranging from 4.9% (95% CI, −9.3 to −0.5) to 22.2% (95%

Table 1
Descriptive statistics of study participants (N = 73), outcome measurements, and environmental factors during the study period.

	Mean ± SD	Median	IQR	N (%)
Age, years	23.3 ± 5.4	23.0	4.0	
Females				48 (66)
Body mass index, kg/m^2	22.5 ± 3.5	21.5	5.8	
Waist-to-hip ratio	0.80 ± 0.07	0.80	0.10	
Urinary cotinine, ng/mg Cr	20.8 ± 102.7	2.6	3.4	
Urinary cortisol, ng/mg Cr	2.1 ± 2.7	1.1	1.9	
Health outcomes				
Insulin resistance				
Insulin, μU/mL	2.35 ± 2.84	1.39	2.52	
sIRα, ng/mL	32.5 ± 21.6	26.6	14.0	
HOMA-IR	0.59 ± 0.67	0.46	0.57	
Adiponectin, ng/mL	635.1 ± 519.8	475.2	477.7	
Leptin, ng/mL	2.05 ± 1.69	1.66	2.07	
Resistin, ng/mL	21.1 ± 9.1	19.4	11.5	
BTC, pg/mL	64.4 ± 148.8	28.5	31.7	
CNTF, pg/mL	314.6 ± 601.7	134.5	151.6	
HGF, pg/mL	347.8 ± 148.0	341.6	202.5	
Vascular inflammation				
RANKL/OPG system				
OPG, pg/mL	176.9 ± 150.7	145.8	106.7	
sRANKL, pg/mL	132.6 ± 460.8	41.1	42.6	
sRANKL/OPG ratio	1.07 ± 2.90	0.30	0.50	
Immune Inflammation				
IL-2, pg/mL	21.0 ± 59.5	4.2	11.7	
IL-10, pg/mL	7.9 ± 29.3	3.2	2.0	
IL-22, pg/mL	8.2 ± 29.8	2.6	2.3	
sIL1RA, pg/mL	82.2 ± 98.2	51.9	50.2	
CCL-2, pg/mL	159.1 ± 87.4	136.6	79.1	
CCL-5, ng/mL	5.9 ± 2.7	5.2	2.5	
CXCL-8, pg/mL	9.8 ± 9.7	7.8	5.2	
sCD163, ng/mL	23.5 ± 11.8	20.7	7.9	
Environmental measurements				
Air pollutants				
$PM_{2.5}$, μg/m^3	91.8 ± 48.3	85.6	63.8	
$PNC_{5\text{-}100}$, × 10^3 particles/cm^3	18.8 ± 4.1	19.2	3.2	
$PNC_{100\text{-}560}$, × 10^3 particles/cm^3	4.5 ± 1.9	4.6	3.0	
$PSC_{5\text{-}100}$, cm^2/m^3	1.8 ± 0.8	1.5	1.6	
$PSC_{100\text{-}560}$, cm^2/m^3	5.3 ± 4.3	4.9	3.8	
BC, μg/m^3	5.9 ± 2.9	5.6	4.0	
CO, ppm	1.16 ± 0.60	1.04	0.68	
NO_2, μg/m^3	70.3 ± 15.4	68.8	16.9	
NO_X, μg/m^3	124.8 ± 43.3	123.0	48.7	
Meteorological parameters				
Temperature,°C	14.6 ± 12.0	17.4	22.3	
Relative humidity, %	33.1 ± 10.6	29.3	15.4	

Results of health outcomes represent the values averaged from each clinical visit for all study participants. Environmental measurements levels were averaged separate 7-day moving average periods before clinical visits. Abbreviations: OPG, osteoprotegerin; sRANKL, soluble receptor activator of NF-κB ligand; sIRα, soluble insulin receptor ectodomain; HOMA-IR, homeostasis model assessment of insulin resistance; BTC, betacellulin; CNTF, ciliary neurotrophic factor; HGF, hepatocyte growth factor; IL, interleukin; sIL1RA, soluble IL-1 receptor antagonist; CXCL-8, C-X-C chemokine motif ligand-8; CCL, C–C chemokine ligand; sCD163, soluble CD163; $PM_{2.5}$, particulate matter in diameter <2.5 μm; PNC_X, number concentration of particles in given size ranges (nm); PSC_X, surface area concentration of particles in given size ranges (nm); BC, black carbon; CO, carbon monoxide; NO_2, nitrogen dioxide; NOx, oxides of nitrogen.

CI, −39.2 to −5.1; Fig. 2). Concomitantly, elevations of BTC and HGF levels were found for exposure to $PM_{2.5}$, CO, and NO_X.

3.3. Association between air pollution and vascular inflammation

In line with the hypothesized mechanism that air pollution exposure may disrupt RANKL/OPG system imbalance, as shown in Fig. 3, we found significant increases in OPG of 9.7% (95% CI, 3.2–16.2) to 34.1% (95% CI, 22.9–45.2) associated with IQR increases in $PM_{2.5}$, $PNC_{100\text{-}560}$, $PSC_{100\text{-}560}$, CO, NO_2 and NO_X at prior 2–7 MA days. The estimated effects were greater when the exposure periods were extended, suggesting that accumulative exposure to air pollution may exert prominent effects on disruption of the RANKL/OPG system balance. Inverse associations with OPG were also observed for $PNC_{5\text{-}100}$ exposures. Further, significant increases in sRANKL of 22.7% (95% CI, 3.3–58.1) to 30.6% (95% CI, 3.3–42.0) associated with IQR increases in $PM_{2.5}$, BC, CO, NO_2 and NO_X at prior 2 MA days. For the biological activity of the RANKL/OPG system, with IQR increases in exposure to all measured pollutants (except for $PSC_{100\text{-}560}$) at prior 2–7 MA days, the sRANKL/OPG ratio were significantly increased by 78.2% (95% CI, 1.3–155.0) to 322.2% (95% CI, 109.4–535.0).

Additionally, we found significant changes in a suite of biomarkers indicative of immune inflammation associated with air pollutants exposures (Figs. 4 and 5). As shown in Fig. 4, significant increases in T cell-related cytokines (IL-2, 10, 22) of 7.6% (95% CI, 0.8–14.5) to 42.5% (95% CI, 7.2–77.8) and IL-1 family mediator (sIL1RA) of 13.3% (95% CI, 1.9–24.6) to 32.0% (95% CI, 14.3–49.7), were observed in association with IQR increases in $PM_{2.5}$, CO, and NO_X at prior 1–7 MA days. For chemokines, significant increases in CCL-2 were related to $PM_{2.5}$, $PNC_{100\text{-}560}$, $PSC_{100\text{-}560}$, BC, CO, NO_2, and NO_X, with the stronger effects observed at prior 5–7 MA days of exposure (Fig. 5). Similar association patterns and the magnitude of effect estimates were also observed for CCL-5. As expected, significant elevations of 7.8% (95% CI, 0.9–14.8) to 20.4% (95% CI, 10.3–30.5) in macrophage activation marker sCD163 were observed in association with IQR increases in exposure to air pollutants at prior 1–7 days. In addition, greater magnitude of elevated CXCL-8 levels was found ranging from 12.4% (95% CI, 0.3–24.6) to 31.5% (95% CI, 12.1–50.9, Fig. 5). As shown in Supplementary Fig. 1, results of single-pollutant models were also scaled to 10 μg/m^3 for $PM_{2.5}$, NO_2, and NO_X exposures, as well as 1 μg/m^3 for BC exposures.

3.4. Mediation analyses

In mediation analyses, single-mediator models showed that heightened immune and inflammatory responses, particularly alterations in the biological activity and balance of the RANKL/OPG system, could mediate up to 66% of the effects of selected pollutants (e.g., $PM_{2.5}$ and CO) on various metrics of insulin resistance (Supplementary Table 6). Further, air pollutants-associated increases in products of inflammatory mediators could be mediated via disruption of the RANKL/OPG system balance (Supplementary Table 7). Results obtained from multiple-mediator models were in line with those observed in single-mediator models (Supplementary Table 8).

3.5. Sensitivity analyses

As shown in Supplementary Fig. 2 and Fig. 3, the main findings and the study conclusions remained unchanged when sensitivity analyses were performed, including two-pollutant models, excluding individuals with urinary cotinine levels >150 ng/mg Cr or cortisol levels >2.2 ng/mg Cr, and excluding individuals who lived beyond 1 km from the air monitoring station.

4. Discussion

As graphically depicted in the Graphic Abstract, we have shown here that short-term exposure to various ambient air pollutants, particularly TRAP, can significantly prompt the genesis of insulin resistance. Higher levels of air pollutants were also associated with heightened vascular inflammation (e.g., worsening of the RANKL/OPG system imbalance). The alterations in metrics of insulin resistance attributable to air pollution might be partially mediated via disruption of the RANKL/OPG system. Our findings unveil air pollution-associated alterations in a suite of metabolic biomarkers that are potentially implicated in the pathogenesis of DM. Though the relatively modest changes in metabolic homeostasis could be transient or reversible; however, persistent air pollution exposure, especially for individuals residing in urban

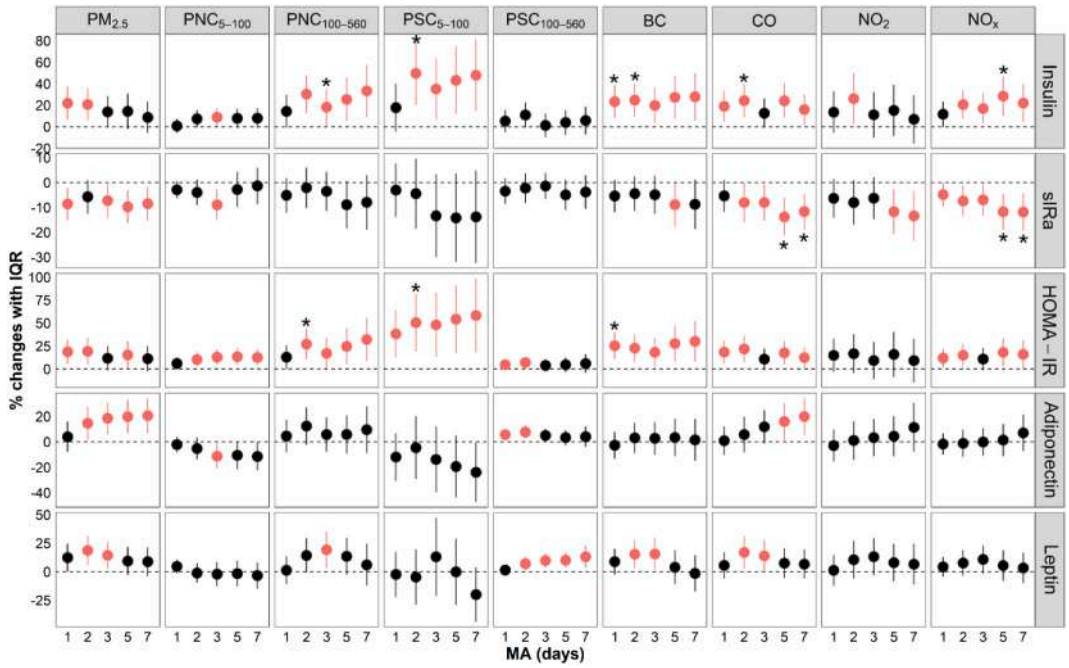

Fig. 1. Percent changes in metrics of insulin resistance associated with IQR increases in pollutant concentrations. Error bars indicate 95% confidence intervals. Significant associations (p-value <0.05) are shown in red; Bonferroni corrections with significance (p-value <0.0025) are indicated by asterisks. Moving average concentrations of air pollutants over the last 24 h prior to each participant's clinic visit are presented as 1 MA day, 1–2 days as 2 MA days, 1–3 days as 3 MA days and up to 7 MA days. Abbreviations: IQR, interquartile range; MA, moving average; $PM_{2.5}$, particulate matter in diameter <2.5 μm; PNC_X, number concentration of particles in given size ranges (nm); PSC_X, surface area concentration of particles in given size ranges (nm); BC, black carbon; CO, carbon monoxide; NO_2, nitrogen dioxide; NOx, oxides of nitrogen; sIRα, soluble insulin receptor ectodomain; HOMA-IR, homeostasis model assessment of insulin resistance. (For interpretation of the references to colour in this figure legend, the reader is referred to the Web version of this article.)

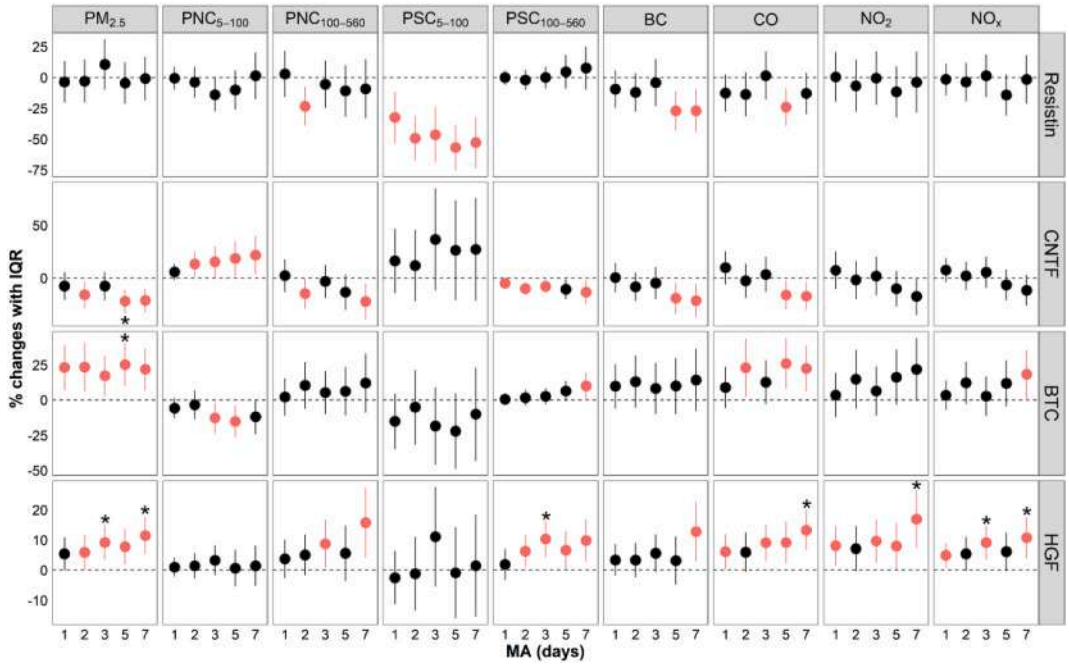

Fig. 2. Percent changes in metrics of insulin resistance associated with IQR increases in pollutant concentrations. Error bars indicate 95% confidence intervals. Significant associations (p-value <0.05) are shown in red; Bonferroni corrections with significance (p-value <0.0025) are indicated by asterisks. Moving average concentrations of air pollutants over the last 24 h prior to each participant's clinic visit are presented as 1 MA day, 1–2 days as 2 MA days, 1–3 days as 3 MA days and up to 7 MA days. Abbreviations: IQR, interquartile range; MA, moving average; $PM_{2.5}$, particulate matter in diameter <2.5 μm; PNC_X, number concentration of particles in given size ranges (nm); PSC_X, surface area concentration of particles in given size ranges (nm); BC, black carbon; CO, carbon monoxide; NO_2, nitrogen dioxide; NOx, oxides of nitrogen; BTC, betacellulin; CNTF, ciliary neurotrophic factor; HGF, hepatocyte growth factor. (For interpretation of the references to colour in this figure legend, the reader is referred to the Web version of this article.)

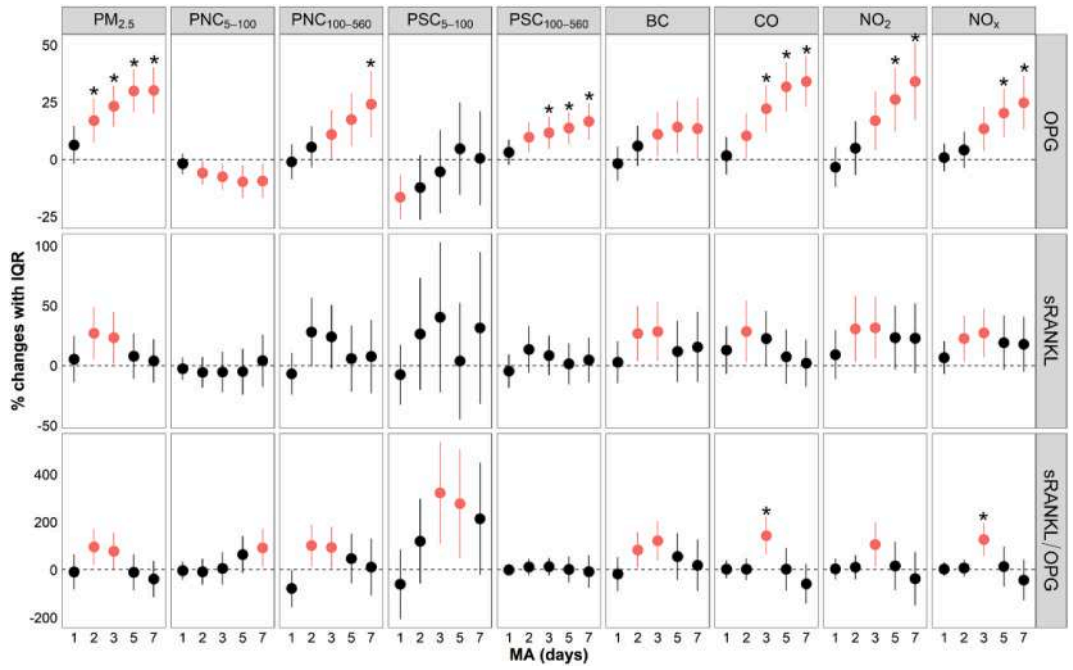

Fig. 3. Percent changes in the RANKL/OPG system balance associated with IQR increases in pollutant concentrations. Error bars indicate 95% confidence intervals. Significant associations (p-value <0.05) are shown in red; Bonferroni corrections with significance (p-value <0.0025) are indicated by asterisks. Moving average concentrations of air pollutants over the last 24 h prior to each participant's clinic visit are presented as 1 MA day, 1–2 days as 2 MA days, 1–3 days as 3 MA days and up to 7 MA days. Abbreviations: IQR, interquartile range; MA, moving average; $PM_{2.5}$, particulate matter in diameter <2.5 μm; PNC_X, number concentration of particles in given size ranges (nm); PSC_X, surface area concentration of particles in given size ranges (nm); BC, black carbon; CO, carbon monoxide; NO_2, nitrogen dioxide; NOx, oxides of nitrogen; OPG, osteoprotegerin; sRANKL, soluble receptor activator of NF-κB ligand. (For interpretation of the references to colour in this figure legend, the reader is referred to the Web version of this article.)

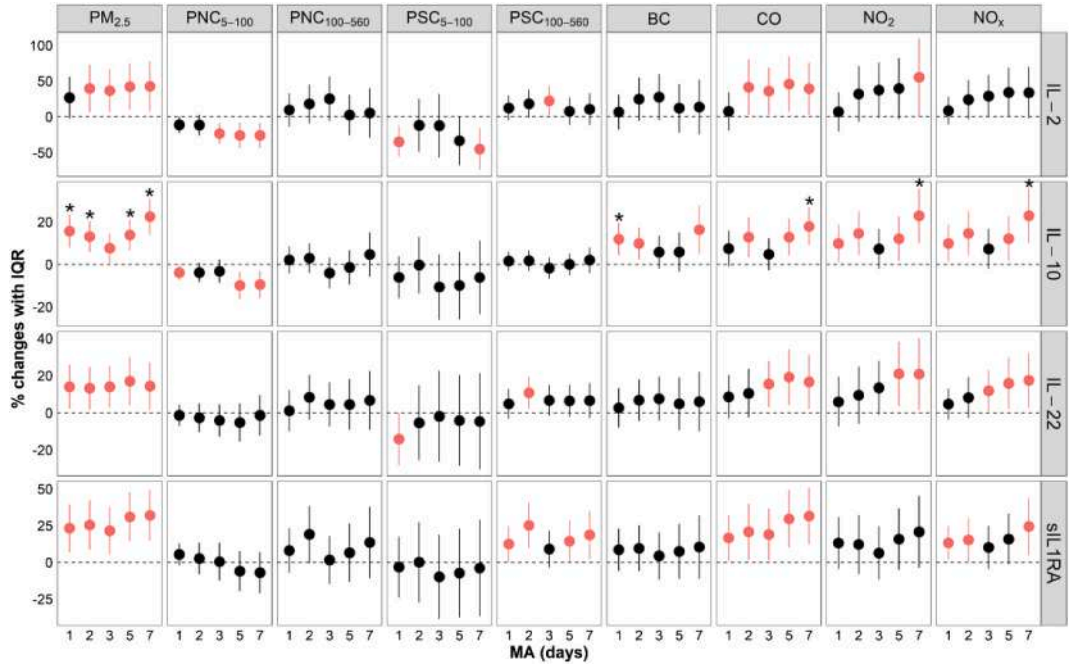

Fig. 4. Percent changes in IL-1 family/T-cell related cytokines associated with IQR increases in pollutant concentrations. Error bars indicate 95% confidence intervals. Significant associations (p-value <0.05) are shown in red; Bonferroni corrections with significance (p-value <0.0025) are indicated by asterisks. Moving average concentrations of air pollutants over the last 24 h prior to each participant's clinic visit are presented as 1 MA day, 1–2 days as 2 MA days, 1–3 days as 3 MA days and up to 7 MA days. Abbreviations: IQR, interquartile range; MA, moving average; $PM_{2.5}$, particulate matter in diameter <2.5 μm; PNC_X, number concentration of particles in given size ranges (nm); PSC_X, surface area concentration of particles in given size ranges (nm); BC, black carbon; CO, carbon monoxide; NO_2, nitrogen dioxide; NOx, oxides of nitrogen; IL, interleukin; sIL1RA, soluble IL-1 receptor antagonist. (For interpretation of the references to colour in this figure legend, the reader is referred to the Web version of this article.)

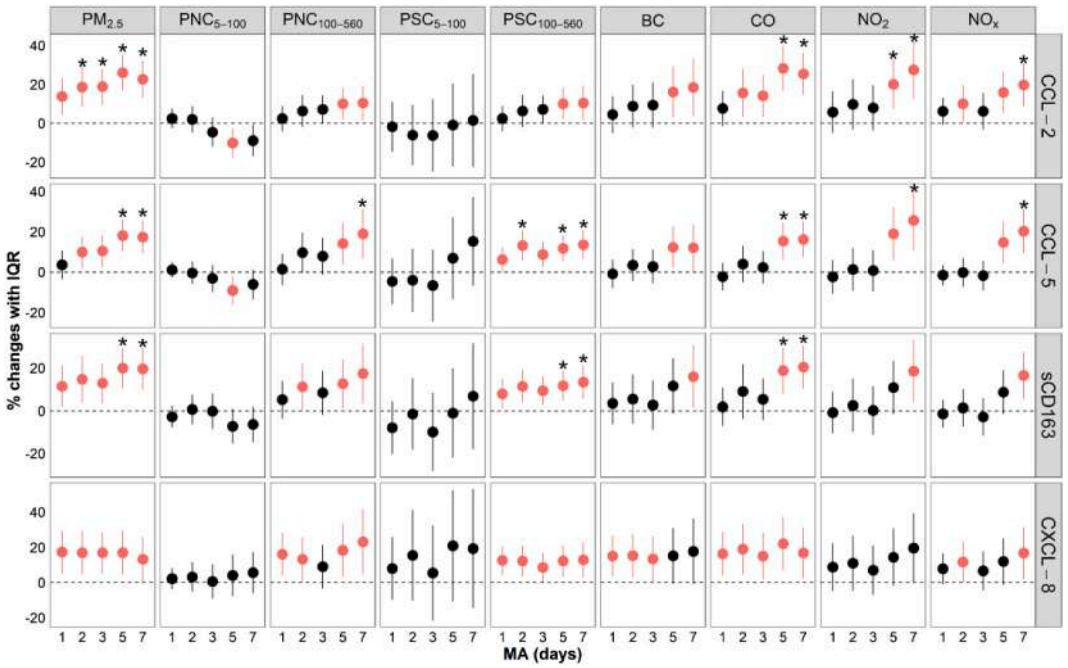

Fig. 5. Percent changes in macrophage/monocyte activation markers associated with IQR increases in pollutant concentrations. Error bars indicate 95% confidence intervals. Significant associations (p-value <0.05) are shown in red; Bonferroni corrections with significance (p-value <0.0025) are indicated by asterisks. Moving average concentrations of air pollutants over the last 24 h prior to each participant's clinic visit are presented as 1 MA day, 1–2 days as 2 MA days, 1–3 days as 3 MA days and up to 7 MA days. Abbreviations: IQR, interquartile range; MA, moving average; $PM_{2.5}$, particulate matter in diameter <2.5 μm; PNC_X, number concentration of particles in given size ranges (nm); PSC_X, surface area concentration of particles in given size ranges (nm); BC, black carbon; CO, carbon monoxide; NO_2, nitrogen dioxide; NOx, oxides of nitrogen; CCL, C–C chemokine ligand; sCD163, soluble CD163; CXCL-8, C-X-C chemokine motif ligand-8. (For interpretation of the references to colour in this figure legend, the reader is referred to the Web version of this article.)

environments with high TRAP levels, may potentially convey the risk burden of metabolic disorders at older ages and heighten future cardiometabolic events (Johnson et al., 2020; Pope et al., 2015).

Limited epidemiological studies assessed the associations of PM originating from biomass burning and fossil fuel combustion with circulating OPG levels, and have yielded mixed results (Li et al., 2019; Saha et al., 2016; Wang et al., 2021). In this study, we observed elevations of OPG and sRANKL levels in relation to a variety of ambient TRAP among exposed healthy individuals. Changes in the circulating levels of OPG and the sRANKL/OPG ratio are indicators of the altered biological activity and imbalance of the RANKL/OPG system (Ndip et al., 2014). Growing evidence has shown that worsening of the RANKL/OPG system imbalance is likely responsible for the increased risk of insulin resistance state and developing DM (Duan et al., 2017). Mechanistically, it has been reported that OPG and RANKL appear to be highly expressed in immune and vascular cells (e.g., T cells and endothelial cells), following cellular activation by inflammatory stimuli (Grgurevic et al., 2016; Walsh and Choi, 2014). Addition of inflammatory cytokines, such as IL-22 and CCL-2, is capable of promoting RANKL and OPG expressions in vitro and vivo, which can in turn activate RANK singling and further trigger inflammatory cascades (Andoh et al., 2000; Liu et al., 2013; Monasterio et al., 2018). In this study, we extended the existing evidence to suggest that TRAP exposures are associated with the imbalance of RANKL/OPG system in a real-world setting with higher levels of exposure.

To our knowledge, the Beijing AIRCHD study is the first to assess the mediating roles of vascular inflammation in air pollution-associated various metrics of insulin resistance and to gain insight into potential interlinked mechanisms in human. Few observational studies have examined associations of ambient air pollution exposure with metabolic and inflammatory indicators (Brook et al., 2013; Wolf et al., 2016). Evidence from a large cross-sectional analysis showed positive associations of annual average TRAP exposure metrics (e.g., NO_X, NO_2) with insulin and leptin levels but no association with pro-inflammatory acute-phase proteins such as high-sensitivity C-reactive protein among non-diabetic participants (Wolf et al., 2016). Further, reduced insulin sensitivity has shown an association with 5-day average $PM_{2.5}$ exposures in healthy adults, whereas no significant effect was found for systemic inflammatory cytokines (e.g., IL-6, tumor necrosis factor-α) (Brook et al., 2013). However, prior epidemiological studies mainly focused on the impacts of air pollution on biomarker indicative of systemic inflammation. In this study, we found that exposure to air pollutants was significantly associated with worsening multiple metrics of insulin resistance and elevations of various monocyte/macrophage and T cell activation markers. Both immunological dysfunctions and inflammatory processes driven by circulating activated T cells and monocytes/macrophages have been demonstrated to be important contributors involving in the pathogenesis of insulin resistance and DM (Donath and Shoelson, 2011). An experimental study showed increases in adipose tissue macrophages and impairments in insulin sensitivity following exposure to ambient $PM_{2.5}$ (Sun et al., 2009). Interestingly, the impacts of air pollution on inflammation and different metrics of insulin resistance observed in this study were not always consistent. For instance, significant increases in insulin and leptin levels were associated with $PNC_{5\text{-}100}$ and $PSC_{5\text{-}100}$ exposures, whereas null or inverse associations were found for immune-inflammatory mediators. These disparate findings suggested that insulin resistance attributable to air pollution exposure might not be exclusively mediated via immune-inflammatory pathways. Indeed, prior studies showed that significant activation of the RANKL/OPG system was observed in diabetic patients but not elevated levels of pro-inflammatory cytokines (O'Sullivan et al., 2010). Genetic disruption of the RANKL singing pathway in mouse liver has shown resulting in suppressed phosphorylation of IKKs and improving insulin sensitivity (Kiechl et al., 2013). Inhibition of IKKβ protects against ambient $PM_{2.5}$-induced insulin resistance and inflammation (Liu et al., 2014). A mechanistic study reported that insulin sensitivity was reduced in the

liver of mice exposed to ambient $PM_{2.5}$ via activation of NF-κB pathways-mediated inflammation (Zheng et al., 2013). Collectively, our results indicated that ambient air pollution-associated metabolic insulin resistance might be potentially mediated via worsening of the RANK/OPG system imbalance, given that the RANK/OPG system can be a crucial contributor implicating in modulating vascular inflammation.

Besides, our study revealed that air pollution-associated changes in components of the insulin signaling pathways might be mediated via activation of vascular inflammation. A critical step in the cascade of insulin action is that insulin binding to α-subunits of insulin receptor (IR-α) actives the tyrosine kinase of β subunits (IR-β) and recruits IR substrates (e.g., IRS1) for tyrosine phosphorylation (Yaribeygi et al., 2019). Down-regulation of the density of cell surface IR can lead to hyperinsulinemia and peripheral insulin resistance (Guo, 2014; Yaribeygi et al., 2019). Circulating sIRα, which contains one of the IR-α and a part of the IR-β, is primarily shed from the cell surface IR in hepatocytes, and altered sIRα levels may reflect the expression of cellular membrane-bound IR (Group, 2007; Hiriart et al., 2014). Prior mechanistic studies showed that significant reductions of IR expressions were caused by concentrated ambient PM from vehicular traffic, and the phosphorylation levels of IRS1 were also inhibited by PM-induced inflammation (Rao et al., 2015; Woodward et al., 2019). In addition, sIRα can bind a larger proportion of insulin in the circulation system and thereby buffer the amount of insulin available to exert biological effects (Hiriart et al., 2014). Further, CNTF can improve insulin sensitivity via regulation of the metabolic clearance rate of insulin from circulation (Rezende et al., 2012). More recently, modulation of IR by HGF has been found to alter IR response to insulin, and higher serum levels of HGF have been linked to NO_2 exposures (Dadvand et al., 2014; Oliveira et al., 2018). Considering all these evidence, our results indicated that generating vascular inflammation could be partially responsible for ambient air pollution-associated insulin resistance.

Our study has several strengths. The Beijing AIRCHD study was conducted in a real-world scenario with a wide spectrum of TRAP concentrations and over an extended follow-up period, making our findings of critical implications for reducing the global burden of cardiometabolic diseases attributable to air pollution. Further, there was minimal potential for confounding by environmental tobacco smoke exposure or the stress response of human body because urinary cotinine and cortisol levels were both assessed in this healthy population and controlled in the analyses. Moreover, mediation analysis was conducted to examine potential mediators of interest on the associations between air pollutants and metabolic responses, which allowed to explore the pathophysiologic mechanisms linking air pollution exposure to insulin resistance. Concomitantly, several limitations should also be merited in discussion. First, although mediation analyses were conducted according to plausible hypotheses and existing experimental evidence, further mechanistic studies are needed to validate our observational findings. Second, the fixed-location monitoring data as a surrogate for individual exposure may introduce non-differential exposure error that may bias effect estimates toward the null (e.g., underestimates of effect). However, higher correlations between ambient and personal pollutant data (e.g., $PM_{2.5}$ and BC) within individuals indicated the reliability of using ambient air pollution monitoring data as individual exposure metrics in this study population (Xu et al., 2019). Also, results from sensitivity analyses suggested that the findings remained robust after excluding participants living beyond 1 km from our fixed monitoring station. Third, the enrollment of a homogenous group of healthy and young adults with similar demographic characteristics and the relative uniformity of lifestyle patterns might have limited the generalizability of our findings to a broader clinical setting. Despite these, the study design also allowed to reduce potential confounders from medication use, age-related susceptibility, indoor sources of air pollution, and lifestyle related factors.

5. Conclusions

We have shown that short-term exposure to TRAP is significantly associated with elevations of insulin resistance, which might be partially mediated via prompting the genesis of vascular inflammation. These findings provide novel insights into pathophysiologic interlinks between air pollution and developing DM, and highlight the importance to mitigate the health risk from reducing air pollution exposure during early life stage.

Declaration of competing interest

The authors declare that they have no competing interests.

Acknowledgements

We would like to thank all study participants.

Appendix A. Supplementary data

Supplementary data to this article can be found online at https://doi.org/10.1016/j.ijheh.2021.113878.

Funding

This work was supported by China National Key Research and Development Projects, China (2017YFC0211701), National Natural Science Foundation of China (81773381), and Michigan Medicine-PKUHSC Joint Institute for Translational and Clinical Research (BMU20140467).

References

Al-Kindi, S.G., Brook, R.D., Biswal, S., Rajagopalan, S., 2020. Environmental determinants of cardiovascular disease: lessons learned from air pollution. Nat. Rev. Cardiol. 17, 656–672.

Andoh, A., Takaya, H., Saotome, T., Shimada, M., Hata, K., Araki, Y., Nakamura, F., Shintani, Y., Fujiyama, Y., Bamba, T., 2000. Cytokine regulation of chemokine (IL-8, MCP-1, and RANTES) gene expression in human pancreatic periacinar myofibroblasts. Gastroenterology 119, 211–219.

Barnabei, L., Laplantine, E., Mbongo, W., Rieux-Laucat, F., Weil, R., 2021. NF-κB: at the borders of autoimmunity and inflammation. Front. Immunol. 12, 716469.

Bonnet, N., Bourgoin, L., Biver, E., Douni, E., Ferrari, S., 2019. RANKL inhibition improves muscle strength and insulin sensitivity and restores bone mass. J. Clin. Invest. 129, 3214–3223.

Bowe, B., Xie, Y., Li, T., Yan, Y., Xian, H., Al-Aly, Z., 2018. The 2016 global and national burden of diabetes mellitus attributable to $PM_{2.5}$ air pollution. Lancet Planet Health 2, e301–e312.

Brook, R.D., Xu, X., Bard, R.L., Dvonch, J.T., Morishita, M., Kaciroti, N., Sun, Q., Harkema, J., Rajagopalan, S., 2013. Reduced metabolic insulin sensitivity following sub-acute exposures to low levels of ambient fine particulate matter air pollution. Sci. Total Environ. 448, 66–71.

Cai, D., Yuan, M., Frantz, D.F., Melendez, P.A., Hansen, L., Lee, J., Shoelson, S.E., 2005. Local and systemic insulin resistance resulting from hepatic activation of IKK-beta and NF-kappaB. Nat. Med. 11, 183–190.

Catrysse, L., van Loo, G., 2017. Inflammation and the metabolic syndrome: the tissue-specific functions of NF-kappaB. Trends Cell Biol. 27, 417–429.

Dadvand, P., Nieuwenhuijsen, M.J., Agusti, A., de Batlle, J., Benet, M., Beelen, R., Cirach, M., Martinez, D., Hoek, G., Basagana, X., Ferrer, A., Ferrer, J., Rodriguez-Roisin, R., Sauleda, J., Guerra, S., Anto, J.M., Garcia-Aymerich, J., 2014. Air pollution and biomarkers of systemic inflammation and tissue repair in COPD patients. Eur. Respir. J. 44, 603–613.

Dang, J., Yang, M., Zhang, X., Ruan, H., Qin, G., Fu, J., Shen, Z., Tan, A., Li, R., Moore, J., 2018. Associations of exposure to air pollution with insulin resistance: a systematic Review and meta-analysis. Int. J. Environ. Res. Publ. Health 20 (11), 2593, 15.

Donath, M.Y., Shoelson, S.E., 2011. Type 2 diabetes as an inflammatory disease. Nat. Rev. Immunol. 11, 98–107.

Duan, P., Yang, M., Wei, M., Liu, J., Tu, P., 2017. Serum osteoprotegerin is a potential biomarker of insulin resistance in Chinese postmenopausal women with prediabetes and type 2 diabetes. Internet J. Endocrinol. 2017, 8724869.

Funcke, J.B., Scherer, P.E., 2019. Beyond adiponectin and leptin: adipose tissue-derived mediators of inter-organ communication. J. Lipid Res. 60, 1648–1684.

Grgurevic, L., Christensen, G.L., Schulz, T.J., Vukicevic, S., 2016. Bone morphogenetic proteins in inflammation, glucose homeostasis and adipose tissue energy metabolism. Cytokine Growth Factor Rev. 27, 105–118.

Group, S.I.R.S., 2007. Soluble insulin receptor ectodomain is elevated in the plasma of patients with diabetes. Diabetes 56, 2028–2035.
Gümüş, P., Buduneli, E., Bıyıkoğlu, B., Aksu, K., Saraç, F., Nile, C., Lappin, D., Buduneli, N., 2013. Gingival crevicular fluid, serum levels of receptor activator of nuclear factor-κB ligand, osteoprotegerin, and interleukin-17 in patients with rheumatoid arthritis and osteoporosis and with periodontal disease. J. Periodontol. 84, 1627–1637.
Guo, S., 2014. Insulin signaling, resistance, and the metabolic syndrome: insights from mouse models into disease mechanisms. J. Endocrinol. 220, T1–t23.
Haberzettl, P., McCracken, J.P., Bhatnagar, A., Conklin, D.J., 2016. Insulin sensitizers prevent fine particulate matter-induced vascular insulin resistance and changes in endothelial progenitor cell homeostasis. Am. J. Physiol. Heart Circ. Physiol. 310, H1423–H1438.
Hennig, F., Quass, U., Hellack, B., Küpper, M., Kuhlbusch, T.A.J., Stafoggia, M., Hoffmann, B., 2018. Ultrafine and fine particle number and surface area concentrations and daily cause-specific mortality in the Ruhr area, Germany, 2009-2014. Environ. Health Perspect. 126, 027008.
Hiriart, M., Sanchez-Soto, C., Diaz-Garcia, C.M., Castanares, D.T., Avitia, M., Velasco, M., Mas-Oliva, J., Macias-Silva, M., González-Villalpando, C., Delgado-Coello, B., Sosa-Garrocho, M., Vidaltamayo, R., Fuentes-Silva, D., 2014. Hyperinsulinemia is associated with increased soluble insulin receptors Release from hepatocytes. Front. Endocrinol. 5, 95.
Hofbauer, L.C., Schoppet, M., 2001. Osteoprotegerin: a link between osteoporosis and arterial calcification? Lancet 358, 257–259.
Johnson, M., Brook, J.R., Brook, R.D., Oiamo, T.H., Luginaah, I., Peters, P.A., Spence, J. D., 2020. Traffic-related air pollution and carotid plaque burden in a Canadian city with low-level ambient pollution. J Am Heart Assoc 9, e013400.
Kiechl, S., Wittmann, J., Giaccari, A., Knoflach, M., Willeit, P., Bozec, A., Moschen, A.R., Muscogiuri, G., Sorice, G.P., Kireva, T., Summerer, M., Wirtz, S., Luther, J., Mielenz, D., Billmeier, U., Egger, G., Mayr, A., Oberhollenzer, F., Kronenberg, F., Orthofer, M., Penninger, J.M., Meigs, J.B., Bonora, E., Tilg, H., Willeit, J., Schett, G., 2013. Blockade of receptor activator of nuclear factor-κB (RANKL) signaling improves hepatic insulin resistance and prevents development of diabetes mellitus. Nat. Med. 19, 358–363.
Li, W., Dorans, K.S., Wilker, E.H., Rice, M.B., Ljungman, P.L., Schwartz, J.D., Coull, B.A., Koutrakis, P., Gold, D.R., Keaney Jr., J.F., Vasan, R.S., Benjamin, E.J., Mittleman, M. A., 2019. Short-term exposure to ambient air pollution and circulating biomarkers of endothelial cell activation: the Framingham Heart Study. Environ. Res. 171, 36–43.
Liu, C., Fonken, L.K., Wang, A., Maiseyeu, A., Bai, Y., Wang, T.Y., Maurya, S., Ko, Y.A., Periasamy, M., Dvonch, T., Morishita, M., Brook, R.D., Harkema, J., Ying, Z., Mukherjee, B., Sun, Q., Nelson, R.J., Rajagopalan, S., 2014. Central IKKbeta inhibition prevents air pollution mediated peripheral inflammation and exaggeration of type II diabetes. Part. Fibre Toxicol. 11, 53.
Liu, Z., Xu, J., Li, H., Zheng, Y., He, J., Liu, H., Zhong, Y., Lu, Y., Hong, B., Zhang, M., Lin, P., Du, J., Hou, J., Qian, J., Kwak, L.W., Yi, Q., Yang, J., 2013. Bone marrow stromal cells derived MCP-1 reverses the inhibitory effects of multiple myeloma cells on osteoclastogenesis by upregulating the RANK expression. PLoS One 8, e82453.
Monasterio, G., Castillo, F., Rojas, L., Cafferata, E.A., Alvarez, C., Carvajal, P., Nunez, C., Flores, G., Diaz, W., Vernal, R., 2018. Th1/Th17/Th22 immune response and their association with joint pain, imagenological bone loss, RANKL expression and osteoclast activity in temporomandibular joint osteoarthritis: a preliminary report. J. Oral Rehabil. 45, 589–597.
Ndip, A., Wilkinson, F.L., Jude, E.B., Boulton, A.J., Alexander, M.Y., 2014. RANKL-OPG and RAGE modulation in vascular calcification and diabetes: novel targets for therapy. Diabetologia 57, 2251–2260.
O'Sullivan, E.P., Ashley, D.T., Davenport, C., Devlin, N., Crowley, R., Agha, A., Thompson, C.J., O'Gorman, D., Smith, D., 2010. Osteoprotegerin and biomarkers of vascular inflammation in type 2 diabetes. Diabetes Metab Res Rev 26, 496–502.
Oliveira, A.G., Araújo, T.G., Carvalho, B.M., Rocha, G.Z., Santos, A., Saad, M.J.A., 2018. The role of hepatocyte growth factor (HGF) in insulin resistance and diabetes. Front. Endocrinol. 9, 503.
Pieralice, S., Vigevano, F., Del Toro, R., Napoli, N., Maddaloni, E., 2018. Lifestyle management of diabetes: implications for the bone-vascular Axis. Curr. Diabetes Rep. 18, 84.
Pinheiro, J., B, D., DebRoy, S., Sarkar, D., R Core Team, 2021. Nlme: Linear and Nonlinear Mixed Effects Models. R package version 3.1-153. https://CRAN.R-project.org/package=nlme.
Pope 3rd, C.A., Turner, M.C., Burnett, R.T., Jerrett, M., Gapstur, S.M., Diver, W.R., Krewski, D., Brook, R.D., 2015. Relationships between fine particulate air pollution, cardiometabolic disorders, and cardiovascular mortality. Circ. Res. 116, 108–115.
Rajagopalan, S., Al-Kindi, S.G., Brook, R.D., 2018. Air pollution and cardiovascular disease: JACC state-of-the-art Review. J. Am. Coll. Cardiol. 72, 2054–2070.
Rao, X., Patel, P., Puett, R., Rajagopalan, S., 2015. Air pollution as a risk factor for type 2 diabetes. Toxicol. Sci. 143, 231–241.
Rezende, L.F., Santos, G.J., Santos-Silva, J.C., Carneiro, E.M., Boschero, A.C., 2012. Ciliary neurotrophic factor (CNTF) protects non-obese Swiss mice against type 2 diabetes by increasing beta cell mass and reducing insulin clearance. Diabetologia 55, 1495–1504.
Riboli, E., Haley, N.J., Trédaniel, J., Saracci, R., Preston-Martin, S., Trichopoulos, D., 1995. Misclassification of smoking status among women in relation to exposure to environmental tobacco smoke. Eur. Respir. J. 8, 285–290.
Rückerl, R., Schneider, A., Hampel, R., Breitner, S., Cyrys, J., Kraus, U., Gu, J., Soentgen, J., Koenig, W., Peters, A., 2016. Association of novel metrics of particulate matter with vascular markers of inflammation and coagulation in susceptible populations -results from a panel study. Environ. Res. 150, 337–347.
Saha, H., Mukherjee, B., Bindhani, B., Ray, M.R., 2016. Changes in RANKL and osteoprotegerin expression after chronic exposure to indoor air pollution as a result of cooking with biomass fuel. J. Appl. Toxicol. 36, 969–976.
Śliwińska-Mossoń, M., Milnerowicz, H., 2017. The impact of smoking on the development of diabetes and its complications. Diabetes Vasc. Dis. Res. 14, 265–276.
Sun, Q., Yue, P., Deiuliis, J.A., Lumeng, C.N., Kampfrath, T., Mikolaj, M.B., Cai, Y., Ostrowski, M.C., Lu, B., Parthasarathy, S., Brook, R.D., Moffatt-Bruce, S.D., Chen, L. C., Rajagopalan, S., 2009. Ambient air pollution exaggerates adipose inflammation and insulin resistance in a mouse model of diet-induced obesity. Circulation 119, 538–546.
Tingley, D., Yamamoto, T., Hirose, K., Keele, L., Imai, K., 2014. Mediation: R package for causal mediation analysis. J. Stat. Software 59, 1–38.
VanderWeele, T.J., Vansteelandt, S., 2014. Mediation analysis with multiple mediators. Epidemiol. Methods 2, 95–115.
Walsh, M.C., Choi, Y., 2014. Biology of the RANKL-RANK-OPG system in immunity, bone, and beyond. Front. Immunol. 5, 511.
Wang, T., Xu, H., Zhu, Y., Sun, X., Chen, J., Liu, B., Zhao, Q., Zhang, Y., Liu, L., Fang, J., Xie, Y., Liu, S., Wu, R., Song, X., He, B., Huang, W., 2021. Traffic-related air pollution associated pulmonary pathophysiologic changes and cardiac injury in elderly patients with COPD. J. Hazard Mater. 424, 127463.
Wolf, K., Popp, A., Schneider, A., Breitner, S., Hampel, R., Rathmann, W., Herder, C., Roden, M., Koenig, W., Meisinger, C., Peters, A., 2016. Association between long-term exposure to air pollution and biomarkers related to insulin resistance, subclinical inflammation, and adipokines. Diabetes 65, 3314–3326.
Woodward, N.C., Crow, A.L., Zhang, Y., Epstein, S., Hartiala, J., Johnson, R., Kocalis, H., Saffari, A., Sankaranarayanan, I., Akbari, O., Ramanathan, G., Araujo, J.A., Finch, C. E., Bouret, S.G., Sioutas, C., Morgan, T.E., Allayee, H., 2019. Exposure to nanoscale particulate matter from gestation to adulthood impairs metabolic homeostasis in mice. Sci. Rep. 9, 1816.
Xu, H., Wang, T., Liu, S., Brook, R.D., Feng, B., Zhao, Q., Song, X., Yi, T., Chen, J., Zhang, Y., Wang, Y., Zheng, L., Rajagopalan, S., Li, J., Huang, W., 2019. Extreme levels of air pollution associated with changes in biomarkers of atherosclerotic plaque vulnerability and thrombogenicity in healthy adults. Circ. Res. 124, e30–e43.
Yamawaki, H., Iwai, N., 2006. Mechanisms underlying nano-sized air-pollution-mediated progression of atherosclerosis: carbon black causes cytotoxic injury/inflammation and inhibits cell growth in vascular endothelial cells. Circ. J. 70, 129–140.
Yaribeygi, H., Farrokhi, F.R., Butler, A.E., Sahebkar, A., 2019. Insulin resistance: Review of the underlying molecular mechanisms. J. Cell. Physiol. 234, 8152–8161.
Zheng, Z., Xu, X., Zhang, X., Wang, A., Zhang, C., Hüttemann, M., Grossman, L.I., Chen, L.C., Rajagopalan, S., Sun, Q., Zhang, K., 2013. Exposure to ambient particulate matter induces a NASH-like phenotype and impairs hepatic glucose metabolism in an animal model. J. Hepatol. 58, 148–154.

International Journal of Hygiene and Environmental Health 239 (2022) 113880

Contents lists available at ScienceDirect

International Journal of Hygiene and Environmental Health

journal homepage: www.elsevier.com/locate/ijheh

Time trend of the exposure to geraniol in 24-h urine samples derived from the German Environmental Specimen Bank from 2004 to 2018

Nikola Pluym [a], Markus Stöckelhuber [a], Till Weber [b], Gerhard Scherer [a], Max Scherer [a,*], Marike Kolossa-Gehring [b]

[a] ABF Analytisch-Biologisches Forschungslabor GmbH, Semmelweisstr. 5, 82152, Planegg, Germany
[b] German Environment Agency (UBA), Corrensplatz 1, 14195, Berlin, Germany

ARTICLE INFO

Keywords:
Geraniol
8-Carboxygeraniol
LC-MS/MS
Human biomonitoring (HBM)
Time trend
Environmental specimen bank

ABSTRACT

Geraniol (*trans*-3,7-dimethyl-2,6-octadiene-1-ol) is an acyclic isoprenoid monoterpene with a widespread use as fragrance in consumer products, agrochemicals and pharmaceuticals. The class of terpene chemicals has been associated with varying sensitizing potencies. A recently developed sensitive LC- MS/MS method for the analysis of geraniol metabolites was further improved and validated for the two metabolites, 8-carboxygeraniol and Hildebrandt acid. The successfully validated method was applied to 250 urine samples derived from the Environmental Specimen Bank (ESB) collected between 2004 and 2018. Both metabolites of this allergen of special concern were quantified in all urine samples of this study. Correlation analysis revealed that 8-carboxygeraniol appears to be the sole specific biomarker in urine for geraniol exposure. Overall, the excreted amounts of 8-carboxygeraniol remained unchanged in urine samples collected from 2004 to 2018. However, a significantly higher 8-carboxygeraniol excretion per 24 h was observed in females compared to males across the sampling years from 2004 to 2012. This trend equalized in the years 2015 and 2018. We could demonstrate that 8-carboxygeraniol may be a suited biomarker for assessing the geraniol exposure in the general population. Regardless of the fact that additional, preferably population representative studies combining HBM and health examination were helpful to further elucidate the risks of a geraniol exposure, the current study adds important data for identifying time trends and body burden of geraniol in the environment and shows the ubiquitous exposure towards mixtures of sensitizing chemicals.

1. Introduction

Geraniol (*trans*-3,7-dimethyl-2,6-octadiene-1-ol) is an acyclic isoprenoid monoterpene with a fresh flowery smell. Geraniol possesses versatile applications across various industries and products including fragrances, flavors, agrochemicals (biocides) and pharmaceuticals (Cantrell et al., 2001; Carnesecchi et al., 2001, 2002; Duncan et al., 2004; Hagvall et al., 2007). It is a common constituent of several essential oils, however the diverse uses and the great demand of geraniol require additional production capacities, which are covered mainly through biotechnological processes (Zhao et al., 2016; Zhou et al., 2014).

Fragrance contact allergy is perceived as a primarily consumer product related health impact (Johansen and Werfel, 2019). In particular, the chemical class of terpenes, such as limonene, linalool and geraniol are prone to autoxidation, forming oxidation products with varying sensitizing potencies (Karlberg et al., 1992, 1994; Skold et al., 2004). Geraniol is one of 26 fragrance chemicals listed as contact allergens due to their skin sensitizing properties (Uter et al., 2013) by the Scientific Committee on Consumer Safety (SCCS). Since 2005, it is mandatory in the EU for these 26 chemicals to be listed as an ingredient when present at or above 10 ppm in leave-on cosmetics and at or above 100 ppm in wash-off products (Scientific Committee on Consumer Safety (SCCS), 2012). Furthermore, geraniol has been classified as an allergen of special concern for which between 100 and 1000 cases have been published (Uter et al., 2013).

Despite its use as cosmetic product, geraniol was also shown to possess various physiological properties including antioxidant, anti-inflammatory, anti-microbial and anti-tumor activities (Lei et al., 2019). However, the underlying biochemical mechanisms are currently not fully understood and require further research. Moreover, essential oils containing geraniol among other compounds have been suggested to

* Corresponding author.
E-mail address: max.scherer@abf-lab.com (M. Scherer).

https://doi.org/10.1016/j.ijheh.2021.113880
Received 27 August 2021; Received in revised form 3 November 2021; Accepted 4 November 2021
Available online 10 November 2021

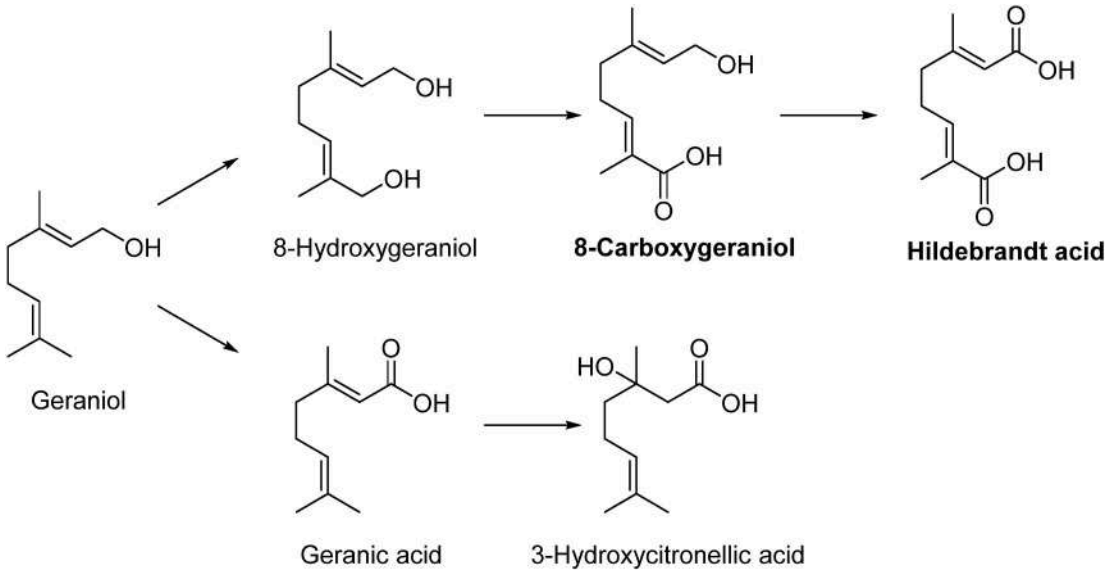

Fig. 1. Human metabolism of geraniol according to (Chadha and Madyastha, 1984). Metabolites investigated in this study are highlighted in bold.

be used in eco-friendly and safe control programs against mosquitos (Tabari et al., 2017). Although geraniol can be found in different consumer products, pharmaceuticals and agrochemicals, information on the exposure and the human metabolism are very limited up to now. Human biomonitoring (HBM) has been shown as the gold standard for the exposure assessment to emerging chemicals (Kolossa-Gehring et al., 2017). Hence, geraniol, amongst other frequently used fragrances such as 7-hydroxycitronellal, lysmeral or rose oxide, was targeted for the development of a suitable HBM method within the frame of a collaboration between the German Federal Ministry for the Environment, Nature Conservation and Nuclear Safety (BMU) and the German Chemical Industry Association (VCI).

For this study a recently developed biomonitoring method for geraniol (Jäger et al., 2020) was further optimized. In total, the four metabolites 2,6-octadienedioic acid (Hildebrandt acid), 9-hydroxy-3, 7-dimethylnona-3,7-dienoic acid (8-carboxygeraniol), 3,7-dimethyl-2, 6-octadienoic acid (Geranic acid), and 3-hydroxy-3,7-dimethyloct-6-enoic acid (3-hydroxycitronellic acid) were identified (Jäger et al., 2020). Hildebrandt acid appears to be the most abundant metabolite since it is a terminal metabolite of several oxidation pathways of geraniol (Jäger et al., 2020). However, Hildebrandt acid is not specific to geraniol as it is also a metabolite of another industrially important terpene, namely the aldehyde citral (Diliberto et al., 1990). The same applies to geranic acid and 3-hydroxycitronellic acid, that were originally included in the method described by (Jäger et al., 2020). Consequently, Hildebrandt acid and 8-carboxygeraniol were selected as suitable biomarkers for the current HBM study (see Fig. 1). The criteria for the selection were the specificity (8-carboxygeraniol appears to be the sole specific metabolite with no other precursor than geraniol), the analytical robustness (significantly improved by the availability of labeled authentic internal standards) and the sensitivity (important for a sufficiently high rate of quantifiable urine samples in the general population). In addition, the method was improved in terms of the sample throughput for application in large HBM studies.

Besides the German Environmental Surveys, which are based on subjects representative for the people living in Germany, the German Environmental Specimen Bank (ESB), coordinated by the German Environment Agency (UBA), is the second main pillar in the German HBM system at federal level (Kolossa-Gehring et al., 2012). The ESB archives biological samples (blood, blood plasma and urine from 20 to 29 year old students collected at four different locations in Germany; cryo-stored over liquid nitrogen) with the aim of monitoring the time trend of human exposure towards environmental pollutants. The archived samples are very well characterized with respect to general information such as sex, body weight, height, and age of the donors but also regarding important normalization parameters like 24h-urine volumes and creatinine concentrations. Hence, these samples allow for the retrospective investigation of time trends of internal exposure to toxicants and environmental chemicals in Germany (Kolossa-Gehring et al., 2017).

In this study, we improved and applied a recently developed biomonitoring method for geraniol (Jäger et al., 2020) to 250 24h-urine samples collected over a time span of 14 years from 2004 to 2018 and stored in the ESB. This manuscript adds important information for the monoterpene geraniol to a series of publications identifying time trends and body burden for risk assessment of different emerging chemicals, such as phthalates (Koch et al., 2017), glyphosate (Conrad et al., 2017), the fragrance chemical 7-hydroxycitronellal (7-HC) (Pluym et al., 2020) and lysmeral (Scherer et al., 2021), the biocides and methylisothiazolinone, methylchloroisothiazolinone (Schettgen et al., 2020) and the antioxidant BHT (Schmidtkunz et al., 2020).

Table 1
MS parameters (Quan = Quantifier, Qual = Qualifier, IS = internal standard, DP = declustering potential, CE = collision energy, RT = retention time) and limits of detection (LOD) and quantification (LLOQ) for 8-carboxygeraniol and Hildebrandt acid.

Analyte/IS	MRM [m/z]	DP [V]	CE [V]	RT [min]	LLOQ (LOD) [ng/mL]
8-Carboxygeraniol	167.0 → 93.0 (Quan) 167.0 → 121.1 (Qual)	86 86	23 29	10.0	0.50 (0.15)
d_5-8-Carboxygeraniol	172.0 → 97.0	86	21	9.9	–
Hildebrandt acid	181.0 → 163.0 (Quan) 181.0 → 135.0 (Qual)	51 51	9 15	9.7	0.50 (0.15)
d_5-Hildebrandt acid	186.0 → 168.2	51	9	9.6	–

Table 2
Characteristics of the study population by sampling year.

Year of sampling	N (m/f)	Age [years] mean (min-max)	BMI [kg/m^2] mean (min-max)	24-h urine volume [mL] mean (min-max)	Creatinine concentration [g/L] mean (min-max)
2004	50 (25/25)	23.4 (20–29)	22.2 (18.7–30.4)	1759 (601–2789)	0.849 (0.345–1.75)
2008	50 (25/25)	25.2 (20–29)	22.1 (18.0–28.7)	1780 (473–3141)	1.01 (0.275–2.83)
2012	50 (25/25)	24.7 (20–29)	22.8 (17.6–32.0)	1815 (586–3799)	0.861 (0.159–2.50)
2015	50 (25/25)	24.3 (20–28)	23.4 (18.6–31.6)	1985 (645–3057)	0.769 (0.297–1.79)
2018	50 (25/25)	24.6 (20–29)	22.8 (18.0–41.4)	1964 (606–2993)	0.814 (0.298–2.51)
∑ all	250	24.1 (20–29)	22.5 (17.4–41.4)	1865 (473–3799)	0.978 (0.159–4.26)
∑ male	125	24.6 (20–29)	23.4 (18.1–32.0)	1895 (473–3141)	1.17 (0.305–4.26)
∑ female	125	23.6 (20–29)	21.6 (17.4–41.4)	1113 (528–3799)	0.815 (0.298–2.51)

2. Materials and methods

2.1. Analytical method

Urine sample analysis for the two geraniol metabolites 8-caboxygeraniol and Hildebrandt acid was carried out according to Jäger et al. (2020) with modifications. Briefly, 1 mL of urine was spiked with 10 μL of an internal standard mix (IS-mix *containing* d_5-8-carboxygeraniol and d_5-Hildebrandt acid at a concentration of 10 μg/mL), 0.5 mL of acetate buffer (pH = 5.1) and 10 μL enzyme suspension (β-glucuronidase, 30 units/μL + arylsulfatase 60 units/μL). After incubation at 37 °C for 3 h, liquid-liquid extraction (LLE) was performed with 50 μL of phosphoric acid (4 M) and 2 mL of diethyl ether. The organic phase was evaporated to dryness and reconstituted in water with 0.033% of formic acid. 20 μL were injected into the LC-MS/MS system consisting of a U(H)PLC Nexera X2 (Shimadzu, Duisburg, Germany) coupled to an MS 6500+ QTRAP (Sciex, Darmstadt, Germany). Chromatographic separation was achieved by gradient elution on an ACQUITY UPLC HSS T3 column (1.8 μm; 2.1 × 100 mm, Waters, Eschborn, Germany) with 0.033% formic acid in water (solvent A) and acetonitrile (solvent B). The column was maintained at 40 °C with a flow rate of 600 μL/min throughout the entire analytical run. Gradient elution started with 10% B and a linear increase until 10 min to 20% B, a step to 90% B at 11 min followed by a step back to 10% B at 13 min, and re-equilibration until a total run time of 15 min.

MS/MS analysis was performed with a turbo ion spray source in multiple-reaction monitoring mode (MRM) with positive electrospray ionization (ESI). Two fragment ions for each compound were taken into account, using the MRM transition with the highest signal-to-noise ratio as quantifier and the MRM transition with the second highest intensity as qualifier. MS/MS parameters, quantifier and qualifier mass transitions, retention times and the achieved limits of detection and quantification are shown in Table 1.

The method was fully validated according to the US Food and Drug Administration (FDA) guidelines (Food and Drug Administration (FDA), 2018). Intra- and inter-day precisions were found to be <9% (CV) and the method accuracy rates were between 89 and 113% for both analytes throughout the calibration range. The mean recovery rates were 60% for both 8-caboxygeraniol and Hildebrandt acid. We did not observe any matrix suppression for the Hildebrandt acid, whereas for 8-caboxygeraniol, a mean matrix suppression of 20% was observed, which was fully compensated by the stable-isotope labeled IS. No carryover was observed and the method was linear over the range of 0.5–100 ng/mL for 8-carboxygeraniol. For Hildebrandt acid, a quadratic regression between 0.5 and 800 ng/mL was obtained. Analytes in urine samples were proven to be stable for at least six freeze-thaw cycles, 24 h at room temperature, 6 months at < -20 °C (longer storage periods are currently under investigation) and for storing the sample extracts for at least eight days in the autosampler at 10 °C. The stock solutions of the reference standards were stable for at least 26 months at 4 °C.

Since no analyte-free urine samples were available for Hildebrandt acid, quantification of the study samples was performed by using water as surrogate matrix. Applicability of water as calibration matrix was proven during the validation experiments by comparing the slopes of urine against water. In-house quality control (QC) samples were prepared by pooling spot urine samples in order to get three different concentration levels (low, medium, high), reflecting the expected concentration range of the study samples. QC samples were randomly interspersed across the analytical batches. Acceptance criteria as set forth in the FDA Guidance for Bioanalytical Method Validation (Food and Drug Administration (FDA), 2018) were used to monitor the validity of the measurement. Mean accuracies were found to be 103% for 8-carboxygeraniol and 95% for Hildebrandt acid. The sample-to-sample carry over was monitored by wash injections and potential contaminations were determined with reagent blanks. No contaminations or carryover above LLOQ were identified for this study.

2.1.1. Study population

The analyzed 24-h urine samples were collected and stored in the ESB in the years 2004, 2008, 2012, 2015, and 2018. Samples were provided by the German Environmental Agency (Umweltbundesamt, UBA) for analysis. In total, 250 urine samples (male to female split 50/50; 50 samples per year investigated) were analyzed in this study. HBM samples were derived from students from the University of Halle-Wittenberg, aged between 20 and 29 years. Details about the samples, sampling procedures and storage conditions are described elsewhere (Kolossa-Gehring et al., 2012; Pluym et al., 2020; Schettgen et al., 2020). The study protocol of the ESB has been approved by the ethics committee of the Medical Association Westfalen-Lippe, the Medical Faculty of the University of Münster and (since 2012) by the ethical committee of the Medical Association of the Saarland. Information on 24-h urine volume, urinary creatinine concentration, BMI, age and sex is summarized in Table 2.

2.2. Data evaluation

Urinary levels of the geraniol metabolites were expressed as μg excreted in 24 h (for creatinine-adjusted concentrations expressed as μg/g creatinine, see Supplementary Information). Where appropriate, means, standard deviations (SD) and medians were calculated. Since the concentrations were not normally distributed (according to the D'Agostino-Pearson and Shapiro-Wilk tests), statistical significance of the differences between males and females as well as that of time trends were tested by applying the non-parametric Mann-Whitney *U* test. Time trends were evaluated for each consecutive collection year (e.g., 2004 vs. 2008) and over all sampling years from 2004 to 2018 for their statistical significance using the Mann-Whitney *U* test (comparison of two time points) and the Kruskal-Wallis test over all years. Correlations between the different metabolites were evaluated computing the non-parametric Spearman rank correlation analysis. All statistical analyses were carried out using Prism 9.0.2 (GraphPad Software, LaJolla, CA, USA).

3. Results and discussion

We modified and successfully validated an existing method from Jaeger et al. (Jäger et al., 2020) for the human biomonitoring of geraniol. Method validation was performed according to FDA guidelines (Food and Drug Administration (FDA), 2018). The method showed excellent performance with regard to precision, accuracy and LLOQ/-LOD. From the four metabolites initially included in the method, specificity was only given for 8-carboxygeraniol, although this metabolite accounts only for a minor fraction of the four metabolites. Thus, the method was further optimized with the premise of improving the sample throughput by reducing the consumption of the organic solvent for extraction (2 mL instead of 25 mL diethyl ether) and an accelerated chromatographic separation, a prerequisite for the application of the method for large human biomonitoring studies encompassing hundreds or thousands of samples. In addition, we were able to improve the sensitivity by a factor of 3 and 5 for 8-carboxygeraniol (LLOQ of 0.5 μg/L in the current method vs. 1.5 μg/mL according to Jaeger et al.) and Hildebrandt acid (LLOQ of 0.5 μg/L in the current method vs. 2.7 μg/mL according to Jaeger et al.), respectively. Ultimately, our optimized method included two metabolites, that have been initially selected due to their specificity (8-carboxygeraniol) and abundance (Hildebrandt acid).

All statistical analyses were performed for the total amount excreted in urine based on the 24-h urine volumes and expressed as μg per 24 h (μg/24h) (Table 3). In addition, creatinine-normalized concentrations (μg/g_{crea}) were assessed and are presented in Supplementary Tables S1 and S2 for 8-carboxygeraniol and Hildebrandt acid, respectively. In analogy to (Scherer et al., 2021), we focused on the evaluation of the 24h-urine adjusted data since creatinine concentrations may add more variability because of several confounding factors such as body weight, sex or age (Barr et al., 2005; Lermen et al., 2019). The absolute excretion amounts per 24 h are summarized in Tables 3 and 4 according to sex and collection year for 8-carboxygeraniol and Hildebrandt acid, respectively. However, creatinine-normalized results shall provide suitable information with respect to the comparison to a previous study reporting creatinine-adjusted data (Jäger et al., 2020).

The two geraniol metabolites 8-carboxygeraniol and Hildebrandt acid were determined in 250 samples from the ESB from 2004 to 2018. The concentrations were evaluated for each sampling year (2004, 2008, 2012, 2015 and 2018) and sex. 8-Carboxygeraniol and Hildebrandt acid could be detected in all samples above the LLOQ (0.5 ng/mL). This is in good agreement with the results reported by (Jäger et al., 2020), which showed a background excretion in 41 spot urine samples of the general population, quantifiable in 83% for 8-carboxygeraniol and 100% of the samples for Hildebrandt acid (Jäger et al., 2020). The higher detection rate for 8-carboxygeraniol in the current study might be due to the improved sensitivity of our method (LLOQ = 0.5 μg/L). We found an average urinary level for Hildebrandt acid of 604.0 μg/24h (453.5 μg/g_{crea}) and for 8-carboxygeraniol of 23.99 μg/24h (19.17 μg/g_{crea}), which is in accordance with the data presented by Jaeger et al. (Hildebrandt acid: 443 μg/g_{crea}, 8-carboxygeraniol: 15 μg/g_{crea}) (Jäger et al.,

Table 3
Summary statistics for urinary excretion (μg/24h) of 8-carboxygeraniol by sampling year and sex.

	Sampling year	2004	2008	2012	2015	2018	∑2004–2018
All subjects (N = 50 per year)	Mean	25.36	28.49	22.85	26.21	22.82	25.15
8-carboxygeraniol [μg/24 h]	GM	21.15	23.70	18.68	22.84	19.65	21.12
	Median	21.20	25.00	18.45	23.60	19.55	20.90
	P95	72.37	58.94	69.12	58.86	49.86	58.95
	Min-Max	6.40–74.10	4.30–62.90	6.00–83.60	4.70-62.10	6.90-61.70	4.30–83.60
	N > LLOQ	50 (100%)	50 (100%)	50 (100%)	50 (100%)	50 (100%)	250
Male subjects (N = 25 per year)	Mean	23.11	23.03	20.03	27.28	23.13	23.31
8-carboxygeraniol [μg/24 h]	GM	19.74	19.40	16.60	23.43	19.18	19.55
	Median	19.20	19.40	17.00	26.30	16.00	18.80
	P95	63.52	55.76	69.86	61.47	57.77	55.76
	Min-Max	6.40–73.30	7.00–56.30	6.00–83.60	4.70-62.10	6.90-61.70	4.70–83.60
	N > LLOQ	25 (100%)	25 (100%)	25 (100%)	25 (100%)	25 (100%)	125
Female subjects (N = 25 per year)	Mean	27.62	33.95*	25.67	25.14	22.53	26.98
8-carboxygeraniol [μg/24 h]	GM	22.66	28.94*	21.03	22.27	20.13	22.81
	Median	22.70	29.60*	21.40	22.80	20.20	22.60
	P95	73.35	61.76*	71.02	54.60	47.20	60.99
	Min-Max	7.80-74.10	4.30–62.90	6.10–74.50	5.50–56.10	8.60-51.40	4.30–74.50
	N > LLOQ	25 (100%)	25 (100%)	25 (100%)	25 (100%)	25 (100%)	125

GM: geometric mean; P95: 95th percentile; Min: minimum; Max: Maximum.
*Statistically significant difference between males and females (Mann-Whitney-U test, $p < 0.05$).

Table 4
Summary statistics for urinary excretion (μg/24h) of Hildebrandt acid by sampling year and sex.

	Sampling year	2004	2008	2012	2015	2018	∑2004–2018
All subjects (N = 50 per year)	Mean	708.4	845.9	609.7	692.5	653.1	701.9
Hildebrandt acid [μg/24 h]	GM	534.8	656.7	498.7	573.7	478.3	544.9
	Median	585.4	621.3	521.0	575.0	427.3	539.5
	P95	1446.0	2443.0	1633.0	1760.0	2581.0	1706.0
	Min-Max	145.7–5953.0	190.8–3695.0	71.3–1723.0	181.9–2533.0	78.5–3293.0	71.3–5953.0
	N > LLOQ	50 (100%)	50 (100%)	50 (100%)	50 (100%)	50 (100%)	250
Male subjects (N = 25 per year)	Mean	640.0	873.8	609.7	778.3	621.3	704.6
Hildebrandt acid [μg/24 h]	GM	575.0	689.5	689.5	619.3	490.4	575.2
	Median	607.8	740.3	740.3	569.2	446.3	569.2
	P95	1158.0	2478.0	2478.0	2449.0	2322.0	1662.0
	Min-Max	145.7–1101.0	203.7–2521.0	184.8–1692.0	197.1–2533.0	78.50–2716.0	78.5–2716.0
	N > LLOQ	25 (100%)	25 (100%)	25 (100%)	25 (100%)	25 (100%)	125
Female subjects (N = 25 per year)	Mean	776.7	817.9	609.8	606.8	621.3	684.8
Hildebrandt acid [μg/24 h]	GM	497.3	625.4	475.7	531.4	466.5	466.5
	Median	441.9	596.5	493.0	580.7	402.9	402.9
	P95	4658.0	3283.0	1681.0	1279.0	3046.0	3046.0
	Min-Max	155.7–5953.0	190.8–3695.0	71.3–1723.0	181.9–1302.0	112.2–3293.0	112.2–3293.0
	N > LLOQ	25 (100%)	25 (100%)	25 (100%)	25 (100%)	25 (100%)	125

GM: geometric mean; P95: 95th percentile; Min: minimum; Max: Maximum.

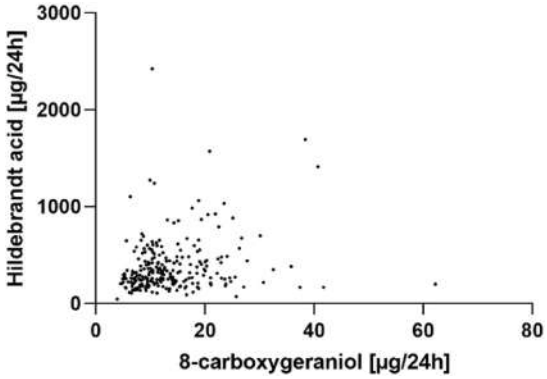

Fig. 2. Correlation between 8-carboxygeraniol and Hildebrandt acid. r (Spearman) = 0.2028 (p = 0.0013); y = 7.632 x + 272.6.

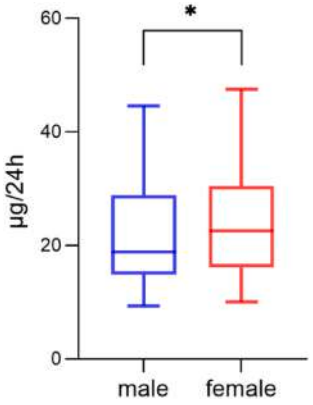

Fig. 3. Boxplot of the excreted amount of 8-carboxygeraniol in 24 h for males and females over all sampling years. The boxes and whiskers represent the 75th/25th and the 95th/5th percentiles, respectively. The horizontal line in the box indicates the median. *: p < 0.05 (Mann-Whitney *U* test).

2020). The poor correlation (r (Spearman) = 0.2028) between 8-carboxygeraniol and Hildebrandt acid, as shown in Fig. 2, may be regarded as an indicator for an additional source of exposure (citral) as reported previously (Diliberto et al., 1990). Hence, further data evaluation was focused solely on the specific biomarker 8-carboxygeraniol.

For the entire study population, the daily excretion of 8-carboxygeraniol showed a moderate but significant difference (Mann-Whitney-U test, p = 0.029) between males and females as shown in the boxplots of Fig. 3. This difference was even more pronounced in the creatinine adjusted concentrations (Mann-Whitney-U test, p < 0.0001) as highlighted in Supplementary Fig. 1. This observation can be explained by the fact that female subjects showed higher 8-carboxygeraniol concentrations and simultaneously significantly lower creatinine concentrations due to the different physiology (particularly muscle mass) and metabolism (Lermen et al., 2019).

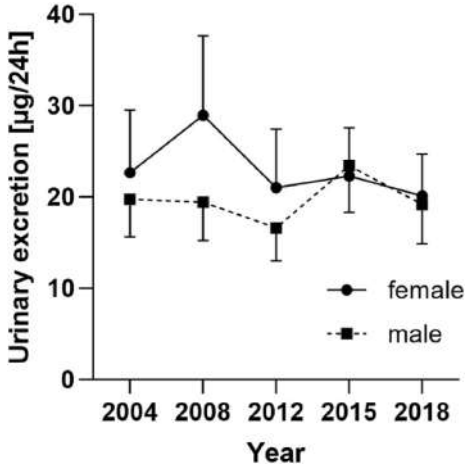

Fig. 4. Time course of the urinary excretion (μg/24h) of 8-carboxygeraniol in female and male participants (geometric mean ± 95% CI).

The average excreted amounts in 24 h were found to be 22.27 μg (respectively a concentration of 14.19 $\mu g/g_{crea}$) in males as compared to 25.70 μg (23.14 $\mu g/g_{crea}$) in females.

The sex-specific excretion of 8-carboxygeraniol over 24 h are shown in Fig. 4 for the collection years from 2004 to 2018. Overall, the excreted amount of 8-carboxygeraniol from 2004 to 2018 did not show a significant change (Kruskal-Wallis test). This finding was confirmed with the logarithm-transformed 8-carboxygeraniol results over time (data not shown). However, we observed a higher excretion in female subjects for the years 2004–2012, which was statistically significant only in 2008 (Table 3). As expected, this was even more pronounced in the creatinine adjusted concentrations for the reasons discussed previously (Table S1). The highest amounts of 8-carboxygeraniol were found in urine samples of females in the year 2008. In addition, a decline of 8-carboxygeraniol excretion, even though non-significant, was observed in females from

2008 to 2012 which remained unchanged until 2018. Due to the widespread use of geraniol in consumer products, in particular cosmetic products, a higher exposure in women can be expected in analogy to previous findings for the 7-hydroxycitronellal exposure in the same cohort (Pluym et al., 2020). In parallel to the decline of excretion in women, 8-carboxygeraniol excretion in male subjects showed a non-significant increase from 2012 to 2015 leading to equal amounts of excretion between males and females in the years 2015 and 2018, respectively. This observation is in line with the data from Jaeger et al. (Jäger et al., 2020), who did not find a sex-specific difference in a small cohort of 41 subjects, collected at the time of the study conduct (2019–2020, 26 males vs. 15 females). This is possibly an indication that geraniol-containing consumer products are nowadays used in similar proportions by men and women. A similar trend was observed for 7-hydroxycitronellal (Pluym et al., 2020) and the specific lysmeral metabolite hydroxy-lysmerylic acid (M-11) (Scherer et al., 2021) in the same population, for which the exposure differences between sexes also appear to level off from the year 2000–2015/2018. Unfortunately, information on the production and the exact usage in different products is not publicly available, so the reason for this trend cannot be finally deduced.

Health based guidance values such as the DNEL (derived no effect level) are usually expressed per body weight. The repeated dose toxicity values for oral and dermal administration of the general population from the ECHA dossier (EC number: 203-377-1) are 13.75 mg/kg bw/d and 7.5 mg/kg bw/d, respectively (European Chemicals Agency (ECHA), 2021). However, the most prominent effect of geraniol is skin sensitization, an endpoint related with a high individual variability. The established DNEL for geraniol by the ECHA is 11,800 μg/cm^2 (European Chemicals Agency (ECHA), 2021). In comparison to the fragrance chemicals lysmeral and 7-hydroxycitronellal, for which the DNELs from the exposure via the dermal route are considerably lower (lysmeral: 890 μg/kg bw/d; 7-Hydrocycitronellal: 600 μg/kg bw/d) (Pluym et al., 2020; Scherer et al., 2021). Furthermore, we could show an ubiquitous exposure to 7-hydroxycitronellal (Pluym et al., 2020) and lysmeral (Scherer et al., 2021) by measuring suitable biomarkers for both chemicals in the same cohort. Although, a decreasing trend from 2000 to 2018 was observed, the data still calls for efforts to reduce the exposure, especially considering that with this dataset we show ubiquitous exposure to the third consecutive fragrance with skin sensitizing properties. Over the last years the exposure to chemical mixtures is increasingly recognized as relevant, especially if the toxicological endpoint is the same. As exposure to sensitizing agents is related to the probable development of allergies and allergic symptoms, a general reduction of exposure towards all sensitizing agents is warranted.

A clear strength of the current study is the very well characterized and controlled study population along with a standardized sample collection over a time span of more than a decade, which should allow to decipher time trends (Kolossa-Gehring et al., 2012). In addition, the analysis of 24 h urine samples is advantageous compared to spot urines with regard to the interpretation of human exposure to specific chemicals (Lermen et al., 2019). Another strength is the sensitivity of the method which allowed for the quantification of the specific biomarker 8-carboxygeraniol across all study samples demonstrating the widespread exposure of the general population. Furthermore, this study represents the first systematic assessment of the exposure to geraniol in a particular German subpopulation (students) over a time-span of 14 years.

A risk assessment for the dose-related systemic effects of the exposure levels is not possible as information on human conversion factors, needed for their derivation for example from daily intakes (Apel et al., 2017) is lacking. Since geraniol is mainly used in products for dermal application, the risk of dermal geraniol exposure should also be evaluated. The systemic, internal levels do not necessarily reflect the exposure derived from skin contact of the chemical, which is usually expressed as mass per square cm skin and is more important for the development of skin sensitization compared to an oral administration. A qunatiative risk assessment (QRA) was established for setting maximum limits for fragrance materials in consumer products. This effort was driven to establish safe levels for sensitizing fragrance materials, such as geraniol, in multiple products in order to limit the risk of induction of contact allergy (Api et al., 2020). The Scientific Committee on Cosumer Saftey (SCCS) provided valuable comments on the refined version of the QRA (named QRA2) in their opinion in 2018 (Scientific Committee on Consumer Safety (SCCS), 2018). However, areas of uncertainty were identified when assessing the risk of induction of skin sensitization which includes those associated with the use of non-animal methods, better understanding of the impact of exposure variables such as frequency and duration, and the role of inflammation. There is still work to be done and ultimately, only longitudinal studies can verify the utility of a QRA for the prevention of contact allergy to fragrance materials.

One limitation for the interpretation is that no information on the geraniol production over the time-span of interest are publicly accessible, therefore a correlation to the internal exposure to the production volume of this chemical is not possible. The investigated subpopulation (students) is not representative for the German population and while cryostorage of the ESB urine samples above liquid nitrogen is taken as granted to minimize the risk of major degradation processes over time to the greatest possible extent, it can not be excluded. In addition, we did not observe a correlation between older samples and a decline in the analyte concentrations, which is at least a hint that the analytes of interest are stable over the time period of the study under the described storage conditions.

4. Summary and conclusion

To the best of our knowledge, this is the first systematic investigation of geraniol exposure in a larger population (N = 250) over a long time-span of 14 years. All study participants were exposed to geraniol, proven by the 100% detection rate in the ESB samples. The inevitable contact to a sensitizing chemical, which has to be declared on cosmetic products due to the sensitization potential, can be clearly classified as undesirable. Furthermore, our data shows that 8-carboxygeraniol, other than Hildebrandt acid, is a specific biomarker for geraniol exposure applicable for larger HBM campaigns. Data evaluation revealed a sex-specific difference based on female subjects showing higher concentrations in the sampling years between 2004 and 2012, whereby the overall excretion remained unchanged throughout the investigated time span. Excretion levels of 8-carboxygeraniol between men and women appear to converge in the years 2015–2018. There was no clear time-trend (either increase or decrease) observed for the study period investigated, neither for men nor for women.

In summary, we could show that 8-carboxygeraniol is a suitable biomarker for geraniol exposure. Women tended to excrete higher amounts than men. For bother sexes, no systematic trend (either increase or decrease) over the complete study period of 14 years (2004–2018) was observed.

Declaration of competing interest

The authors declare that they have no conflict of interest.

Acknowledgments

This study was funded by the Federal Ministry for the Environment, Nature Conservation, and Nuclear Safety (BMU). We would like to acknowledge the work of the ESB teams of Fraunhofer IBMT and the University Hospital Münster for their work in acquiring, handling and storing of human samples and measuring of the physiological parameters for the German ESB. We would also like to thank T. Jaeger (BASF SE) for providing the internal standards.

The development of the analytical method and its application in a

population study are part of a large-scale 15-year cooperation project on the advancement of human biomonitoring in Germany. This project is a cooperation agreed in 2010 between the German Federal Ministry for the Environment, Nature Conservation and Nuclear Safety (BMU) and the Verband der Chemischen Industrie e.V. (German Chemical Industry Association – VCI); it is administered by the German Environment Agency (UBA). In this cooperation project, the analytical method development is financed by the Chemie Wirtschaftsförderungsgesellschaft GmbH, while the first application of the novel methodology in a population study was realized by the German Environment Agency. Experts from governmental authorities, industry and science accompany and advise the project in selecting substances and developing methods.

Appendix A. Supplementary data

Supplementary data to this article can be found online at https://doi.org/10.1016/j.ijheh.2021.113880.

References

Apel, P., Angerer, J., Wilhelm, M., Kolossa-Gehring, M., 2017. New HBM values for emerging substances, inventory of reference and HBM values in force, and working principles of the German Human Biomonitoring Commission. Int. J. Hyg Environ. Health 220, 152–166.

Api, A.M., Basketter, D., Bridges, J., Cadby, P., Ellis, G., Gilmour, N., Greim, H., Griem, P., Kern, P., Khaiat, A., O'Brien, J., Rustemeyer, T., Ryan, C., Safford, B., Smith, B., Vey, M., White, I.R., 2020. Updating exposure assessment for skin sensitization quantitative risk assessment for fragrance materials. Regul. Toxicol. Pharmacol. : RTP (Regul. Toxicol. Pharmacol.) 118, 104805.

Barr, D.B., Wilder, L.C., Caudill, S.P., Gonzalez, A.J., Needham, L.L., Pirkle, J.L., 2005. Urinary Creatinine Concentrations in the US Population: Implications for Urinary Biologic Monitoring Measurements. Environmental health perspectives, pp. 192–200.

Cantrell, C.L., Franzblau, S.G., Fischer, N.H., 2001. Antimycobacterial plant terpenoids. Planta Med. 67, 685–694.

Carnesecchi, S., Bradaia, A., Fischer, B., Coelho, D., Scholler-Guinard, M., Gosse, F., Raul, F., 2002. Perturbation by geraniol of cell membrane permeability and signal transduction pathways in human colon cancer cells. J. Pharmacol. Exp. Therapeut. 303, 711–715.

Carnesecchi, S., Schneider, Y., Ceraline, J., Duranton, B., Gosse, F., Seiler, N., Raul, F., 2001. Geraniol, a component of plant essential oils, inhibits growth and polyamine biosynthesis in human colon cancer cells. J. Pharmacol. Exp. Therapeut. 298, 197–200.

Chadha, A., Madyastha, K.M., 1984. Metabolism of geraniol and linalool in the rat and effects on liver and lung microsomal enzymes. Xenobiotica; the fate of foreign compounds in biological systems, 14, 365–374.

Conrad, A., Schröter-Kermani, C., Hoppe, H.W., Rüther, M., Pieper, S., Kolossa-Gehring, M., 2017. Glyphosate in German adults - time trend (2001 to 2015) of human exposure to a widely used herbicide. Int. J. Hyg Environ. Health 220, 8–16.

Diliberto, J.J., Srinivas, P., Overstreet, D., Usha, G., Burka, L.T., Birnbaum, L.S., 1990. Metabolism of citral, an alpha,beta-unsaturated aldehyde, in male F344 rats. Drug Metab. Dispos. 18, 866–875.

Duncan, R.E., Lau, D., El-Sohemy, A., Archer, M.C., 2004. Geraniol and beta-ionone inhibit proliferation, cell cycle progression, and cyclin-dependent kinase 2 activity in MCF-7 breast cancer cells independent of effects on HMG-CoA reductase activity. Biochem. Pharmacol. 68, 1739–1747.

European Chemicals Agency (ECHA), 2021. Substance Information Geraniol. https://echa.europa.eu/en/registration-dossier/-/registered-dossier/14184/7/1.

Food and Drug Administration (FDA), 2018. Bioanalytical Method Validation - Guidance for Industry. https://www.fda.gov/downloads/Drugs/GuidanceComplianceRegulatoryInformation/Guidances/UCM070107.pdf.

Hagvall, L., Backtorp, C., Svensson, S., Nyman, G., Borje, A., Karlberg, A.T., 2007. Fragrance compound geraniol forms contact allergens on air exposure. Identification and quantification of oxidation products and effect on skin sensitization. Chem. Res. Toxicol. 20, 807–814.

Jäger, T., Backer, S., Brodbeck, T., Leibold, E., Bader, M., 2020. Quantitative determination of urinary metabolites of geraniol by ultra-performance liquid chromatography-tandem mass spectrometry (UPLC-MS/MS). Anal Methods 12, 5718–5728.

Johansen, J.D., Werfel, T., 2019. Highlights in allergic contact dermatitis 2018/2019. Curr. Opin. Allergy Clin. Immunol. 19, 334–340.

Karlberg, A.T., Magnusson, K., Nilsson, U., 1992. Air oxidation of d-limonene (the citrus solvent) creates potent allergens. Contact Dermatitis 26, 332–340.

Karlberg, A.T., Shao, L.P., Nilsson, U., Gafvert, E., Nilsson, J.L., 1994. Hydroperoxides in oxidized d-limonene identified as potent contact allergens. Arch. Dermatol. Res. 286, 97–103.

Koch, H.M., Ruther, M., Schutze, A., Conrad, A., Palmke, C., Apel, P., Bruning, T., Kolossa-Gehring, M., 2017. Phthalate metabolites in 24-h urine samples of the German Environmental Specimen Bank (ESB) from 1988 to 2015 and a comparison with US NHANES data from 1999 to 2012. Int. J. Hyg Environ. Health 220, 130–141.

Kolossa-Gehring, M., Becker, K., Conrad, A., Schroter-Kermani, C., Schulz, C., Seiwert, M., 2012. Environmental surveys, specimen bank and health related environmental monitoring in Germany. Int. J. Hyg Environ. Health 215, 120–126.

Kolossa-Gehring, M., Fiddicke, U., Leng, G., Angerer, J., Wolz, B., 2017. New human biomonitoring methods for chemicals of concern—the German approach to enhance relevance. Int. J. Hyg Environ. Health 220, 103–112.

Lei, Y., Fu, P., Jun, X., Cheng, P., 2019. Pharmacological properties of geraniol - a review. Planta Med. 85, 48–55.

Lermen, D., Bartel-Steinbach, M., Gwinner, F., Conrad, A., Weber, T., von Briesen, H., Kolossa-Gehring, M., 2019. Trends in characteristics of 24-h urine samples and their relevance for human biomonitoring studies - 20years of experience in the German Environmental Specimen Bank. Int. J. Hyg Environ. Health 222, 831–839.

Pluym, N., Petreanu, W., Weber, T., Scherer, G., Scherer, M., Kolossa-Gehring, M., 2020. Biomonitoring data on young adults from the Environmental Specimen Bank suggest a decrease in the exposure to the fragrance chemical 7-hydroxycitronellal in Germany from 2000 to 2018. Int. J. Hyg Environ. Health 227, 113508.

Scherer, M., Petreanu, W., Weber, T., Scherer, G., Pluym, N., Kolossa-Gehring, M., 2021. Human biomonitoring in urine samples from the Environmental Specimen Bank reveals a decreasing trend over time in the exposure to the fragrance chemical lysmeral from 2000 to 2018. Chemosphere 265, 128955.

Schettgen, T., Ruther, M., Weber, T., Kraus, T., Kolossa-Gehring, M., 2020. N-methylmalonamic acid (NMMA) as metabolite of methylisothiazolinone and methylchloroisothiazolinone in 24-h urine samples of the German Environmental Specimen Bank from 2000 to 2017 - exposure and time trends. Chemosphere 246, 125743.

Schmidtkunz, C., Küpper, K., Weber, T., Leng, G., Kolossa-Gehring, M., 2020. A biomonitoring study assessing the exposure of young German adults to butylated hydroxytoluene (BHT). Int. J. Hyg Environ. Health 228, 113541.

Scientific Committee on Consumer Safety (SCCS), 2012. Opinion on Fragrance Allergens in Cosmetic Products.

Scientific Committee on Consumer Safety (SCCS), 2018. Opinion on Skin Sensitisation Quantitative Risk Assessment for Fragrance Ingredients (QRA2). Submission I.

Skold, M., Borje, A., Harambasic, E., Karlberg, A.T., 2004. Contact allergens formed on air exposure of linalool. Identification and quantification of primary and secondary oxidation products and the effect on skin sensitization. Chem. Res. Toxicol. 17, 1697–1705.

Tabari, M.A., Youssefi, M.R., Esfandiari, A., Benelli, G., 2017. Toxicity of beta-citronellol, geraniol and linalool from Pelargonium roseum essential oil against the West Nile and filariasis vector Culex pipiens (Diptera: Culicidae). Res. Vet. Sci. 114, 36–40.

Uter, W., Johansen, J.D., Börje, A., Karlberg, A.T., Lidén, C., Rastogi, S., Roberts, D., White, I.R., 2013. Categorization of fragrance contact allergens for prioritization of preventive measures: clinical and experimental data and consideration of structure-activity relationships. Contact Dermatitis 69, 196–230.

Zhao, J., Bao, X., Li, C., Shen, Y., Hou, J., 2016. Improving monoterpene geraniol production through geranyl diphosphate synthesis regulation in Saccharomyces cerevisiae. Appl. Microbiol. Biotechnol. 100, 4561–4571.

Zhou, J., Wang, C., Yoon, S.H., Jang, H.J., Choi, E.S., Kim, S.W., 2014. Engineering Escherichia coli for selective geraniol production with minimized endogenous dehydrogenation. J. Biotechnol. 169, 42–50.